IMPACTS OF TRANSPORTATION, LAND USES, AND METEOROLOGY ON URBAN AIR QUALITY

Dissertation

Presented in Partial Fulfillment of the Requirements for the Degree Doctor of Philosophy

in the Graduate School of The Ohio State University

By

Youngkook Kim

Graduate Program in City and Regional Planning

The Ohio State University

2010

Dissertation Committee:

Jean-Michel Guldmann, Adviser

Steven I. Gordon

Philip A. Viton

Gulsah Akar

Copyright by

Youngkook Kim

2010

ABSTRACT

Criteria air pollutants, such as nitrogen oxides (NO_x), carbon monoxide (CO), sulfur dioxide (SO_2), particulate matter (PM), and ozone (O_3), are characterized by temporal and locational hot spots in urban areas, frequently violating pollution standards, and, as a result, threatening the health and well-being of the population. Several factors, such as the intensity and duration of emissions, the chemical reactions among pollutants, the uptake and assimilation of pollutants by urban vegetation, and the meteorological factors that induce chemical reactions and atmospheric dispersion, have been considered as explanatory variables in air quality models. Among them, emissions from motor vehicles turn out to be a key determinant of the spatial and temporal patterns of ambient pollution concentrations.

The purpose of this research is to formulate and estimate (1) metropolitan-wide time-series air quality models and (2) land-use regression (LUR) air quality panel models, in order to explain spatio-temporal variations in pollution concentrations. Using the Seoul Metropolitan Area as a case study, traffic counts, vehicle-kilometers-traveled (VKT), land uses, and meteorological factors, such as solar radiation, temperature, humidity, wind speed and wind direction, are used as explanatory variables. An extensive understanding of atmospheric pollutants chemistry is reflected in the formulation of these models. Differences in concentrations measured at air quality monitoring stations (AQMs) across the week (weekdays vs. Sunday) and geographical locations (roadside vs. background), are also investigated using dummy variables and the product of these variables with the original variables.

The results of the time-series models and panel regression models indicate that traffic counts and VKT are significant in explaining the concentrations of both directly emitted

pollutants, such as NO_2, CO, SO_2, and PM, and O_3, a secondary pollutant. The concentrations of the directly emitted pollutants are positively correlated with vehicle flows. In the case of O_3, however, vehicle emissions have a negative impact on O_3 concentrations. Since solar radiation, temperature, humidity, and wind speed influence both chemical reactions and physical dispersion, these factors are closely correlated with pollution concentrations. In particular, solar radiation plays a critical role regarding NO_2 and O_3 concentrations. Ultraviolet (UV) radiation causes the photodissociation of NO_2, providing favorable conditions for the generation of O_3 in the troposphere. The estimated models confirm that solar radiation have a positive effect in the O_3 models, and a negative one in the NO_2 models.

Reduced traffic flows on Sunday increase the ratio of volatile organic compounds (VOC) to NO_x and, consequently, lead to favorable conditions for O_3 generation. Less O_3 titration and less HNO_3 formation occur on Sunday as compared to weekdays, resulting in higher O_3 concentrations on Sunday. For directly emitted pollutants, reduced traffic flows on Sunday induce a decrease in concentrations. The locations of the AQMs turn out to be critical. Traffic flows closer to AQMs have larger impacts on pollution concentrations. The product terms between VKT and roadside dummy variable display the expected results: for directly emitted pollutants, the coefficients are significant and positive, suggesting that the impacts of roadside VKT are greater than those of background VKT. In the case of O_3, the estimated coefficients are negative, indicating that the negative impacts of VKT on O_3 concentrations are increased at roadside areas. Nitric oxide emissions from commercial and residential areas have a negative impact on O_3 concentrations. Plants have an O_3 assimilation capacity, but also emit biogenic VOC during the growing seasons, generating simultaneous negative and positive impacts. The overall vegetative areas impact on O_3 concentrations is positive. For directly emitted pollutants, however, vegetative areas have a negative impact. Since residential, commercial, and industrial areas generate anthropogenic emissions, the coefficients of these land uses are positive.

DEDICATION

Dedicated to my brother, Yeongho Kim

ACKNOWLEDGMENTS

All theory, dear friend, is grey, but the golden tree of life springs ever green.

- *Faust: The First Part of the Tragedy*, Johann Wolfgang von Goethe -

I am indebted to many people for enabling me to complete this dissertation. Thank you to all of you. Most of all, my wife Somyeng deserves my praise. I will remember your love, patience, and encouragement. Several people ought to receive a special acknowledgment for helping me start and finish my studies at The Ohio State University. Yeongho Kim, my brother, who passed away in 2003, for encouraging me to study abroad. Professor Jean-Michel Guldmann, my PhD advisor, for pushing me to broaden my knowledge and thinking beyond my limits. Professors Steven Gordon, Philip Viton, and Gulsah Akar, my committee members, for helpful comments on earlier dissertation drafts. Particularly, Professor Steven Gordon allowed me to work as his TA in the Department of City and Regional Planning and RA at the Ohio Supercomputer Center. Without their assistance, this work would not have been possible. To my parents, friends, and fellow students, especially In-Kwon: you all helped and assisted me in your own ways. I will always keep in mind your help.

VITA

February, 1991	B.S., Architectural Engineering, Yonsei University, Seoul, Republic of Korea
August, 1993	M.E., Urban and Regional Planning, Yonsei University, Seoul, Republic of Korea
September, 1993 ~ February 1996	Researcher, Urban & Transportation Research Institute, Yonsei University, Seoul, Republic of Korea
March, 1996 ~ January 2000	Assistant Manager, LG Chairman's office and LG Construction Co. Ltd. Seoul, Republic of Korea
February 2000 ~ December 2002	Co-founder & Manager, Digital Names Co. Seoul, Republic of Korea
January 2003 ~ August 2003	Researcher, Korea Research Institute for Local Administration, Seoul, Republic of Korea
September 2003 ~ December 2004	Research Assistant, Urban Modeling Laboratory, Louisiana State University, Baton Rouge, Louisiana
January 2005 ~ August 2005	Researcher, Korea Research Institute for Local Administration, Seoul, Republic of Korea
September 2005 ~ March 2007	Teaching Associate, City and Regional Planning, The Ohio State University, Columbus, Ohio
April 2007	Environmental Policy Fellowship, School of Environment and Natural Resources, The Ohio State University, Columbus, Ohio
November 2007	1st Prize of GRI Paper Competition, Gyeonggi Research Institute, Gyeonggi-do, Republic of Korea
August 2009	M.C.R.P, City and Regional Planning, The Ohio State University, Columbus, Ohio
October 2009	ACSP Student Travel Award, 50th Anniversary ACSP Conference, Crystal City, Virginia
July 2007 ~ March 2010	Graduate Research Associate, Ohio Supercomputer Center, The Ohio State University, Columbus, Ohio

PUBLICATIONS

Peer-reviewed articles

W. Yu, I.H. Kim, and Youngkook Kim, (1992) *The Method of Housing Choice by Household Characteristics*, Journal of the Korea Planners Association, Vol. 27, No. 4, 27-36.

Presentations (published in the form of abstract, extended abstract, or article in CD-ROM)

Youngkook Kim and J.M. Guldmann (2007) 48th Annual Meeting of the Association of Collegiate Schools of Planning (ACSP), Milwaukee, WI, October 2007. Presentation: *Urban Air Pollution, Traffic Volumes, and Road Congestion*

Youngkook Kim and J.M. Guldmann (2008) Annual Meeting of the Association of American Geographers (AAG), Boston, MA, April 2008. Presentation: *Urban Vegetation: Is It Really Helpful for Air Pollution Mitigation?*

Youngkook Kim and J.M. Guldmann (2008) 4th ACSP-AESOP 2008 Joint Congress, Chicago, IL, July 2008. Presentation: *No Driving for a Day per Week: Collective Actions for Urban Traffic Congestion*

Youngkook Kim, H.M. Ra and J.M. Guldmann (2008) 7th Annual Community Modeling and Analysis System (CMAS) Conference, UNC, Chapel Hill, NC, October 2008. Oral Presentation: *Traffic volumes and wind directions impacts on air pollution concentrations in Seoul, Korea*

Youngkook Kim (2009) Communicative Cities: Integrating Technology and Place Conference, Columbus, Ohio, June 25~26, 2009. Presentation: *Radio Frequency Identification (RFID), a Cutting-Edge Technology to Enforce Communications for Relieving Traffic Congestion*

Youngkook Kim and J.M. Guldmann (2009) 50th ACSP 2009 Congress, Crystal City, VA, October 2009. Presentation: *Reduced Traffic During the Weekend: Is It Good For Urban Air Quality?*

FIELD OF STUDY

Major Field: City and Regional Planning

Minor Field: Environmental Modeling, Geographic Information Systems, Transportation Planning, Environmental Science, Computer Simulation

TABLE OF CONTENTS

Page

ABSTRACT ..... **ii**

DEDICATION ..... **iv**

ACKNOWLEDGMENTS ..... **v**

VITA ..... **vi**

LIST OF TABLES ..... **xiii**

LIST OF FIGURES ..... **xv**

CHAPTRES:

1. INTRODUCTION **1**

2. LITERATURE REVIEW **5**

2.1 CHEMISTRY OF POLLUTANTS 5

2.1.1 Nitrogen Oxides (NO_x) 5

2.1.1.1 Source of NO_x 5

2.1.2.2 Chemical Reactions of NO_2 6

2.1.2 Carbon Monoxide (CO) 9

2.1.2.1 Source and Health Impacts of CO 9

2.1.2.2 Chemical Reactions of CO 10

2.1.3 Ozone (O_3) 14

2.1.3.1 Chemistry of O_3 15

2.1.3.2 Biogenic VOCs and O_3 18

2.1.3.3 Roles of VOC and NO_x in O_3 Formation: The O_3 Isopleth Plot 19

2.1.4 Sulfur Dioxide (SO_2) 22

2.1.4.1 Source and Health Impacts of SO_2 22

2.1.4.2 Chemical Reactions of SO_2 23

2.1.5 Particulate Matter 24
2.1.5.1 Sources of Particulate Matter 24
2.1.5.2 Chemistry of Secondary Particles 25
2.2 REVIEW OF AIR POLLUTION MODELING STUDIES 27
2.2.1 Overview 27
2.2.2 Air Quality Models Based on Emission Inventory and Dispersion Methods 31
2.2.3 Air Quality Models Based on Land Use Regression Methods 36
2.2.4 Other Statistical Air Quality Models 41
2.3 SUMMARY 44

3. METHODOLOGY 45

3.1 CONCEPTUAL FRAMEWORK 45
3.2 EXPLORATORY ANALYSIS 47
3.3 STATISTICAL MODELING 48
3.3.1 General Models 48
3.3.2 Time-Series Air Quality Models 52
3.3.3 Panel Air Quality Models 55

4. DATA SOURCES AND PROCESSING 58

4.1 OVERVIEW 58
4.2 AIR POLLUTION CONCENTRATIONS 60
4.3 TRANSPORTATION NETWORK AND ORIGIN/DESTINATION (OD) TRAFFIC FLOWS 67
4.4 VEHICLE-KILOMETERS-TRAVELED (VKT) 69
4.4.1 Overview of Traffic Assignment 69
4.4.2 Comparison of Traffic Assignment Methods 71
4.4.3 Calculations of Vehicle-Kilometers-Traveled (VKT) and Wind-Direction Weighted VKT (WVKT) 75
4.4.4 Traffi Counts 78
4.5 LAND USES 82
4.5.1 Vegetative and Non-vegetative Classification using Satellite Imagery 82
4.5.2 Biotope Map 83
4.6 METEOROLOGY 86

5. EXPLORATORY ANALYSIS 93

5.1 TRAFFIC VOLUMES AND NO_2 CONCENTRATIONS 93

5.1.1 Temporal Variations of NO_2 Concentrations 93

5.1.2 NO_2 Concentration Difference between Roadside and Background AQMs 96

5.1.3 Hourly Traffic and NO_2 Concentrations 100

5.1.4 Comparison between Weekdays and Weekend 102

5.2 TRAFFIC VOLUMES AND CO CONCENTRATIONS 104

5.2.1 Temporal Variations of CO Concentrations 104

5.2.2 CO Concentration Differences between Roadside and Background AQMs 107

5.2.3 Hourly Traffic and CO Concentrations 111

5.2.4 Comparison between Weekdays and Weekend 113

5.3 TRAFFIC VOLUMES AND O_3 CONCENTRATIONS 115

5.3.1 Temporal Variations of O_3 Concentrations 115

5.3.2 O_3 Concentration Differences between Roadside and Background AQMs 118

5.3.3 Hourly Traffic and O_3 Concentrations 122

5.3.4 Comparison between Weekdays and Weekend 124

5.4 TRAFFIC VOLUMES AND SO_2 CONCENTRATIONS 126

5.4.1 Temporal Variations of SO_2 Concentrations 126

5.4.2 SO_2 Concentration Differences between Roadside and background AQMs 128

5.4.3 Hourly traffic and SO_2 concentration 132

5.4.4 Comparison between Weekdays and Weekend 134

5.5 TRAFFIC VOLUMES AND PM10 CONCENTRATIONS 136

5.5.1 Temporal variations of PM10 Concentrations 136

5.5.2 PM10 Concentration Differences between Roadside and background AQMs 138

5.5.3 Hourly traffic and PM10 Concentrations 142

5.5.4 Comparison between Weekdays and Weekend 144

5.6 SUMMARY ANALYSIS 146

5.6.1 Descriptive Statistics 146

5.6.2 Correlation Analysis 151

5.6.3 Solar Radiation vs. O_3 Concentrations 154

6. TIME-SERIES ANALYSES OF AIR QUALITY 155

6.1 OVERVIEW 155

6.2 TIME SERIES MODELING 163
6.2.1 Data 163
6.2.2 Model Specifications 166
6.3 ESTIMATION RESULTS 169
6.3.1 Results for O_3 169
6.3.2 Results for NO_2 180
6.3.3 Results for CO 190
6.3.4 Results for SO_2 201
6.3.5 Results for PM10 212
6.4 SUMMARY 223

7. PANEL AIR QUALITY MODELS 224

7.1 GENERAL PROCESS 224
7.2 AIR QUALITY MODELING METHOD 228
6.2.1 Data 228
6.2.2 Model Specifications 232
7.3 ESTIMATION RESULTS 238
7.3.1 Results for O_3 panel models 239
7.3.2 Results for NO_2 panel models 246
7.3.3 Results for CO panel models 252
7.3.4 Results for SO_2 panel models 258
7.3.5 Results for PM10 panel models 263
7.4 SUMMARY 269

8. CONCLUSIONS 271

REFERENCES 276

APPENDICES 285

APPENDIX A: MATRIX OF DISTANCES BETWEEN AQMS. 285
APPENDIX B: ANNUAL, SEASONAL, AND HOURLY AVERAGE CONCENTRATIONS. 287

APPENDIX C: HOURLY CONCENTRATIONS ACROSS FOUR SEASONS. . 298

APPENDIX D: VEHICLE-KILOMETERS-TRAVELED (VKT) AND WIND-DIRECTION WEIGHTED VKT. 300

APPENDIX E: TRAFFIC COUNTS. 303

APPENDIX F: SUB-CLASSIFICATION OF LAND USES IN THE SEOUL METROPOLITAN AREA. 307

APPENDIX G: CORRELATION ANALYSIS. 309

APPENDIX H: DESCRIPTIVE STATISTICS OF ELASTICITIES: TIME-SERIES AIR QUALITY MODELS. 313

APPENDIX I: RESULTS OF FIXED EFFECTS REGRESSION MODELS. 339

APPENDIX J: FIRST-ORDER AUTOREGRESSIVE PARAMETERS IN PANEL MODELS. 341

APPENDIX K: DESCRIPTIVE STATISTICS OF ELASTICITIES: AIR QUALITY PANEL MODELS. 347

APPENDIX L: SPECIFICATIONS OF THE TOTAL R^2 AND THE REGRESSION R^2 IN AUTOREGRESSIVE TIME-SERIES MODELS. 370

LIST OF TABLES

Table Page

2.1 Comparison of urban air quality models based on emission inventory and dispersion modules 34

2.2 Comparison of urban air quality models based on land use regression method 39

4.1 Comparisons between monitored and assigned traffic flows for the selected links.....74

4.2 Monthly traffic factors 80

4.3 Comparisons of land use change in Seoul (2000 ~ 2005).....85

5.1 Temporal variations and exceedances of NO_2 standards at background AQMs in 2003.....95

5.2 Temporal variations of CO concentrations at both background and roadside AQMs in 2003 106

5.3 Temporal variations of O_3 at both background and roadside AQMs in 2003.....117

5.4 Temporal variations of SO_2 at both background and roadside AQMs in 2003.....123

5.5 Temporal variations of PM10 at both background and roadside AQMs in 2003 137

5.6 Descriptive statistics for the dependent variables 147

5.7 Descriptive statistics for VKT and land use variables 148

5.8 Descriptive statistics for of meteorological factors.....150

5.9 Pearson correlation coefficients between pollutant concentrations, VKT, and land use variables.....153

5.10 Pearson correlation coefficients between pollutant concentrations and meteorological variables.....153

6.1 Descriptive statistics for the dependent variables on weekdays, Saturday, and Sunday.....164

6.2 Descriptive statistics for the explanatory variables on weekdays, Saturday and Sunday 165

6.3 Results of time series regression for O_3 models.....170

6.4 Derivative functions of O_3 models with regard to each explanatory variable.....172

6.5 Summary statistics for the derivatives with regard to the explanatory variables in the O_3 models.....173

6.6 Summary statistics for the elasticities w.r.t. explanatory variables in the O_3 models.....176

6.7 Results of time series regression for NO_2 models.....182

6.8 Derivative functions of NO_2 models w.r.t. each explanatory variable.....183

6.9 Summary statistics for the derivatives w.r.t. the explanatory variable in the NO_2 models...184

6.10 Summary statistics for the elasticities w.r.t. the explanatory variables in the NO_2 models 186
6.11 Results of time series regression for CO models 192
6.12 Derivative functions of the CO models w.r.t. each explanatory variable 194
6.13 Summary statistics for the derivatives w.r.t. each explanatory variable in the CO models 195
6.14 Summary statistics for the elasticities w.r.t. each explanatory variable in the CO models.197
6.15 Results of time series regression for SO_2 models 203
6.16 Derivative functions of SO_2 models w.r.t. each explanatory variable 205
6.17 Summary statistics for the derivatives w.r.t. each explanatory variables in the SO_2 models 206
6.18 Summary statistics for elasticities for each explanatory variable in the SO_2 models 208
6.19 Results of time series regression for PM10 models.....214
6.20 Derivative functions of PM10 models w.r.t. each explanatory variable.....215
6.21 Summary statistics for the derivatives w.r.t. each explanatory variables in the PM10 models 216
6.22 Summary statistics for elasticities for each explanatory variable in the PM10 models.....218
7.1 Descriptive statistics for seasonally-summarized hourly concentrations.....230
7.2 Descriptive statistics of seasonally-summarized hourly meteorological factors 231
7.3 Moran's I for the annual average pollution concentrations 232
7.4 Parameters of distance decay functions 238
7.5 Results of O_3 panel regression models estimation 241
7.6 Summary statistics for the elasticities w.r.t. WVKT and solar radiation in the O_3 models...243
7.7 Results of NO_2 panel regression models estimation 248
7.8 Summary statistics for the elasticities w.r.t. WVKT and solar radiation in the NO_2 models249
7.9 Results of CO panel regression models estimation.....254
7.10 Summary statistics for the elasticities w.r.t. WVKT and solar radiation in the CO models255
7.11 Results of SO_2 panel regression models estimation.....259
7.12 Summary statistics for the elasticities w.r.t. WVKT, solar radiation, and humidity in the SO_2 models.....260
7.13 Results of PM10 panel regression models estimation.....265
7.14 Summary statistics for the elasticities w.r.t. WVKT and solar radiation in the PM10 models 266

LIST OF FIGURES

Table Page

2.1 Ozone isopleth diagram based on the simulation of the Empirical Kinetics Modeling Approach (EKMA) 24

2.2 Concentrations in an urban street canyon with a line source placed halfway between two buildings 38

2.3 Examples of estimated pollution maps 43

3.1 Generalized components of a metropolitan air quality system 49

3.2 Land uses and transportation network in the Seoul Metropolitan area 51

3.3 Location of AQM and surrounding buffers and sectors 55

4.1 Locations of AQMs on the topographic map of the Seoul Metropolitan area 61

4.2 Spatial variations of annual average pollution concentrations 64

4.3 Temporal variations of hourly average NO_2 concentrations 65

4.4 Temporal variations of hourly average CO concentrations 65

4.5 Temporal variations of hourly average SO_2 concentrations 65

4.6 Temporal variations of hourly average O_3 concentrations 66

4.7 Temporal variations of hourly average PM10 concentrations 66

4.8 Transportation network, locations of AQMs, and samples of circular buffers in the Seoul Metropolitan Area 67

4.9 Location of traffic flows monitoring links 69

4.10 Traffic assignment with the user equilibrium method 70

4.11 Eight-Sector buffer 76

4.12 Hourly traffic counts of CBD, Han River bridge, arterial roads, and cordon lines during weekday, Saturday, and Sunday 79

4.13 Comparing hourly traffic counts on weekdays and Sunday 81

4.14 Classification of land surface into vegetative and non-vegetative area 83

4.15 Land use classification in Seoul, Korea, 2005 84

4.16 Variations of average daily concentrations of pollution during weekday 88

4.17 Intra-daily and seasonal variations of solar radiation 90

4.18 Intra-daily and seasonal variations of humidity 90

4.19 Wind rose and wind direction frequency 91

4.20 Intra-daily and seasonal variations of wind speed 92
4.21 Intra-daily and seasonal variations of temperatures 92
4.22 Variations of daily high, average, and low temperatures 92
5.1 Seasonal variations of NO_2 concentrations 97
5.2 Monthly variations of NO_2 concentrations 98
5.3 Hourly variations of NO_2 concentrations 99
5.4 Variations of hourly traffic volumes and hourly NO_2 average concentrations at roadside and background AQMs in the four seasons 101
5.5 Weekday, Saturday, and Sunday hourly NO_2 concentrations and traffic flows at roadside and background AQMs in 2003 103
5.6 Seasonal variations of CO concentrations 108
5.7 Monthly variations of CO concentrations 109
5.8 Hourly variations of CO concentrations 110
5.9 Variations of traffic volumes and hourly CO averages at roadside and background AQMs in the four seasons 112
5.10 Weekday, Saturday, and Sunday hourly CO concentrations and traffic flows at roadside and background AQMs in 2003 114
5.11 Seasonal variations of O_3 concentrations 119
5.12 Monthly variations of O_3 concentrations 120
5.13 Hourly variations of O_3 concentrations 121
5.14 Variations of traffic volumes and hourly O_3 averages at roadside and background AQMs in the four seasons 123
5.15 Weekday, Saturday, and Sunday hourly O_3 concentrations and traffic flows at roadside and background AQMs during May, 2003 125
5.16 Seasonal variations of SO_2 concentrations 129
5.17 Monthly variations of SO_2 concentrations 130
5.18 Hourly variations of SO_2 concentrations 131
5.19 Variations of hourly traffic volumes and SO_2 concentrations at roadside and background AQMs in the four seasons 133
5.20 Weekday, Saturday, and Sunday hourly SO_2 concentrations and traffic flows at roadside and background AQMs in 2003 135
5.21 Seasonal variations of PM10 concentrations 139
5.22 Monthly variations of PM10 concentrations 140
5.23 Hourly variations of PM10 concentrations 141
5.24 Variations of traffic volumes and hourly PM10 averages in roadside and background AQMs in the four seasons 143

5.25 Weekday, Saturday, and Sunday hourly PM10 concentrations and traffic flows at roadside and background AQMs in 2003 145
5.26 Comparison between O_3 concentrations and UV radiation during May 2003 154
6.1 Hourly O_3 concentrations for weekdays, Saturday, and Sunday 157
6.2 Hourly NO_2 concentrations for weekdays, Saturday, and Sunday 157
6.3 Hourly CO concentrations for weekdays, Saturday, and Sunday 157
6.4 Hourly SO_2 concentrations for weekdays, Saturday, and Sunday 158
6.5 Hourly PM10 concentrations for weekdays, Saturday, and Sunday 158
6.6 Box plots of O_3 concentrations among the four data sets 159
6.7 Box plots of NO_2 concentrations among the four data sets 160
6.8 Box plots of CO concentrations among the four data sets 160
6.9 Box plots of SO_2 concentrations among the four data sets 161
6.10 Box plots of PM10 concentrations among the four data sets 161
6.11 Comparison between hourly O_3 concentration and 6 hour-averaged UV radiation 166
6.12 Average hourly derivatives w.r.t. traffic in the O_3 models 174
6.13 Average hourly derivatives w.r.t. solar radiation in the O_3 models 175
6.14 Average hourly elasticities w.r.t. traffic in the O_3 models 178
6.15 Average hourly elasticities w.r.t. solar radiation in the O_3 models 178
6.16 Average hourly elasticities w.r.t. wind speed in the O_3 models 179
6.17 Average hourly elasticities w.r.t. temperature in the O_3 models 179
6.18 Average hourly elasticities w.r.t. humidity in the O_3 models 180
6.19 Average hourly derivatives w.r.t. traffic in the NO_2 models 185
6.20 Average hourly derivatives w.r.t. solar radiation in the NO_2 models 185
6.21 Average hourly elasticities w.r.t. traffic in the NO_2 models 188
6.22 Average hourly elasticities w.r.t. solar radiation in the NO_2 models 188
6.23 Average hourly elasticities w.r.t. wind speed in the NO_2 models 189
6.24 Average hourly elasticities w.r.t. temperature in the NO_2 models 189
6.25 Average hourly elasticities w.r.t. humidity in the NO_2 models 190
6.26 Average hourly derivatives w.r.t. traffic in the CO models 196
6.27 Average hourly derivatives w.r.t. solar radiation in the CO models 196
6.28 Average hourly elasticities w.r.t. traffic in the CO models 199
6.29 Average hourly elasticities w.r.t. solar radiation in the CO models 199
6.30 Average hourly elasticities w.r.t. wind speed in the CO models 200
6.31 Average hourly elasticities w.r.t. temperature in the CO models 200
6.32 Average hourly elasticities w.r.t. humidity in the CO models 201

6.33 Average hourly derivatives w.r.t. traffic in the SO_2 models 207
6.34 Average hourly derivatives w.r.t. humidity in the SO_2 models..... 207
6.35 Average hourly elasticities w.r.t. traffic in the SO_2 models..... 210
6.36 Average hourly elasticities w.r.t. solar radiation in the SO_2 models..... 210
6.37 Average hourly elasticities w.r.t. wind speed in the SO_2 models..... 211
6.38 Average hourly elasticities w.r.t. temperature in the SO_2 models..... 211
6.39 Average hourly elasticities w.r.t. humidity in the SO_2 models 212
6.40 Average hourly derivatives w.r.t. traffic in the PM10 models..... 217
6.41 Average hourly derivatives w.r.t. solar radiation in the PM10 models..... 217
6.42 Average hourly elasticities w.r.t. traffic in the PM10 models 220
6.43 Average hourly elasticities w.r.t. solar radiation in the PM10 models 220
6.44 Average hourly elasticities w.r.t. wind speed in the PM10 models 221
6.45 Average hourly elasticities w.r.t. temperature in the PM10 models 221
6.46 Average hourly elasticities w.r.t. humidity in the PM10 models..... 222
7.1 Components of a LUR model: AQMs, buffers, traffic flows, and land uses 225
7.2 Research process for air quality panel models..... 227
7.3 Average hourly-seasonal elasticities w.r.t. WVKT in the O_3 models 245
7.4 Average hourly-seasonal elasticities w.r.t. solar radiation in the O_3 models 245
7.5 Average hourly-seasonal elasticities w.r.t. VKT in the NO_2 models..... 251
7.6 Average hourly-seasonal elasticities w.r.t. solar radiation in the NO_2 models 251
7.7 Average hourly-seasonal elasticities w.r.t. VKT in the CO models 257
7.8 Average hourly-seasonal elasticities w.r.t. solar radiation in the CO models..... 257
7.9 Average hourly-seasonal elasticities w.r.t. VKT in the SO_2 models..... 262
7.10 Average hourly-seasonal elasticities w.r.t. solar radiation in the SO_2 models..... 262
7.11 Average hourly-seasonal elasticities w.r.t. humidity in the SO_2 models 263
7.12 Average hourly-seasonal elasticities w.r.t. VKT in the PM10 models 267
7.13 Average hourly-seasonal elasticities w.r.t. solar radiation in the PM10 models 268

CHAPTER 1

INTRODUCTION

Criteria air pollutants[1] are ubiquitous in urban areas, with temporal and locational hot spots that threaten the health of urban residents, the natural environment, and properties. Understanding the spatial and temporal patterns of pollution concentrations is important not only for modeling urban air pollution, but also for developing and evaluating air quality-related policies. Reliable air quality models can help delineate various management systems and policy options for maintaining desirable air quality in urban regions.

Transportation is responsible for a substantial share of air pollutant emissions, including carbon monoxide (CO), nitrogen oxides (NO_x), volatile organic compounds (VOC), and suspended particulate matters (PM). Emissions from motor vehicles are key determinants of the spatial and temporal patterns of ambient pollution concentrations. Generally, these concentrations are related to the intensity and duration of emissions, the topographical variations of sources and receptors, the uptake and assimilation of pollutants by urban vegetation, the chemical reactions among pollutants, and the meteorological factors that induce chemical reactions and atmospheric dispersion (Derwent & Hertel, 1998; Harrison, 2001; Seinfeld & Pandis, 2006; Takahashi et al., 2005; US EPA, 2000; WHO, 2006). Among these factors, vehicle emissions are considered a key determinant. Despite improvements in vehicle emission control technology, the growth in vehicle ownership and average trip length in recent decades has led to unhealthy air quality in urbanized areas. It is reasonable to expect that, as vehicle-kilometers-traveled (VKT) increase, ambient air pollution concentrations will also increase (Kim, 2007; Kim & Guldmann, 2008; Lau, Hung, Cheung, & Yuen, 2008; Roorda-Knape et al., 1999).

Integrated air quality modeling systems have been developed in several countries for dense urban regions, where pollutants generated by road traffic tend to be present at high concentrations. These systems include both emission inventories and dispersion models. To

[1] According to the U.S. EPA, criteria pollutants include ozone, particulate matter, carbon monoxide, nitrogen oxides, sulfur dioxide, and lead. http://www.epa.gov/air/urbanair/

enhance the credibility of emission inventories, it is necessary to develop up-to-date emission factors and data on actual traffic flows, vehicle speeds, fleet composition, and weather conditions. Dispersion models require significant computational resources to calculate high-resolution air pollution concentrations from both geographical and temporal perspectives. Other approaches to explain the relationships between air pollution concentrations and urban land uses have taken advantage of improvements in geographic information systems (GIS). To explain observed spatial variations in pollution concentrations, land uses identified and measured with GIS procedures are inputs into land-use regression (LUR) models. Pioneering LUR research was initiated in the EU-funded SAVIAH (Small Area Variations in Air Quality and Health) project (Briggs et al., 1997). The pollution maps predicted with LUR models have been used for epidemiological studies, assessment of long-term exposure to traffic-related pollution, and scenario-based land-use impacts on air quality. Since observed concentrations at air quality monitoring stations (AQMs) and measured land uses around AQMs are used as dependent and independent variables, LUR models are regarded as primarily empirical models. Despite developments in conventional air quality modeling systems and in recent LUR models, the complex interactions between pollution concentrations, traffic flows, land uses, meteorological factors, and chemical reactions have not been satisfactorily investigated. As the spatial and temporal variations in vehicle emissions are expected to significantly impact pollution concentrations, LUR models must be expanded to incorporate traffic flows over both space and time.

Emitted pollutants undergo chemical reactions under specific meteorological conditions. Humidity, temperature, and solar radiation influence pollution concentrations as follows: (1) as humidity increases, pollution concentrations decrease, because water vapor or rain drops scavenge air pollutants; (2) as temperature increases, the concentrations of directly emitted pollutants decrease, because the use of fossil fuels for space heating decreases; (3) solar radiation has a positive impact on ozone (O_3) concentration, but a negative one on nitrogen dioxide (NO_2) concentration, because ultraviolet (UV) rays are indispensible to generate tropospheric O_3 but lead to the photodissociation of NO_2. It is therefore necessary to understand and account for all the factors and processes of pollutants chemistry when air quality models are being formulated.

Since traffic flows are closely related to the concentrations of directly emitted pollutants, it is commonly observed that decreased vehicle flows during the weekend result in decreased concentrations of directly emitted pollutants. In contrast, the concentrations of O_3, a secondary product, increase during weekends in urban regions. The reduced traffic emissions change the ratio of VOC to NO_x, and hence induce less formation of nitric acid (HNO_3), and less O_3 titration.

Consequently, urban regions during weekends produce favorable conditions for O_3 generation (Fujita et al., 2003; Heuss, Kahlbaum, & Wolff, 2003; Seinfeld, 1989). As O_3 is the most toxic of the ambient oxidants and weekends overlap with the outdoor activities of urban residents, it is necessary to further investigate the differences in O_3 generation between weekdays and weekends.

Sustainable development is important to ensure and maintain the current and future quality of life of urban residents. As Paul Farmer, the CEO of the American Planning Association, points out, sustainability issues have a high priority in the planning process. Environmentally sound, economically resilient, and equitable communities are necessary to advance public health and wellness.[2] The above mentioned LUR models have the potential to become critical components of urban air quality management systems. LUR models can be used to delineate fine-resolution air quality maps, both over space and time. These maps can help identify where and when hot spots occur, streamline epidemiological studies, design air pollution mitigation plans, and evaluate land-use and transportation policies in terms of their air quality impacts.

The purpose of this research is to: (1) better understand the system of air pollution concentrations, with a particular focus on the chemistry of air pollutants and meteorological factors; (2) analyze the temporal variations (seasonal, monthly, and hourly) of concentrations, compare concentrations at roadside and non-roadside (urban background) AQMs, and examine the variations in pollution concentrations and traffic flows over weekdays and weekend; (3) formulate and estimate metropolitan-wide time-series air quality models to assess the differences in concentrations observed across the week (weekdays vs. Sunday) and over broad geographical areas (roadside AQMs and background AQMs); (4) develop and estimate air quality panel models based on the LUR framework, accounting for the impacts of VKT, land uses, and meteorological factors on pollution concentrations.

Five air pollutants – NO_2, CO, O_3, sulfur dioxide (SO_2), and particulate matter with a diameter less than 10μm (PM10) – have had their concentrations monitored on an hourly basis in the Seoul Metropolitan Area in 2003. Traffic counts and meteorological factors, including solar radiation, temperature, wind direction, wind speed, and humidity, have also been measured along the same time dimension. Since transportation and land uses explain a large share of the spatial and temporal variations of pollution concentrations, VKT and land uses around AQMs are considered as independent variables for explaining pollution concentrations. To assess VKTs, a

[2] Farmer, Paul (2008) Sustainability: Planning's Search for the Holy Grail (Perspectives from APA Executive Director and CEO), *Planning,* 74 (7), July.

Farmer, Paul (2009) Change (Perspectives from APA Executive Director and CEO), *Planning,* 75 (1), January.

traffic assignment model is implemented, with an origin-destination (OD) table and the Seoul transportation network. Distances between emission sources and receptors play a key role in determining concentrations at receptors. Recently developed LUR models have established relationships between monitored pollution concentrations at AQMs and surrounding land uses, with buffer sizes varying from a few hundred to several thousand meters. To evaluate the impacts of population and building density on pollution concentrations, larger radii (up to 10 km) have been considered in LUR models. Despite these endeavors, there is little empirical research on the systemic relationship between traffic flows and pollution concentrations variations in terms of buffer size. This relationship is to be further investigated. Also, since wind is a determinant of the impacts of emission sources on receptors, accounting for wind fields should improve air pollution predictions. Wind-direction weighted VKT is to be used as an explanatory variable, together with solar radiation, wind speed, humidity, and temperature.

The remainder of this dissertation is organized as follows. Chapter 2 consists of a literature review, including the sources, regulatory standards, health impacts, and chemical interactions of all five criteria pollutants. The strengths and weaknesses of conventional air quality models and LUR approaches are also assessed. Chapter 3 presents the general modeling framework. Data sources and processing are discussed in Chapter 4. Exploratory analyses of the air pollution concentrations are presented in Chapter 5. Time-series air quality models are discussed in Chapter 6. Estimation results of LUR air quality models based on panel data are presented in Chapter 7. Chapter 8 concludes and outlines areas for further research.

CHAPTER 2

LITERATURE REVIEW

This chapter reviews two general literature streams: (1) the chemistry of air pollutants, including nitrogen oxides (NO_x), carbon monoxide (CO), ozone (O_3), sulfur dioxide (SO_2), and particulate matter with diameter less than 10μm (PM10), and (2) air pollution modeling studies. The latter are classified into three categories: models based on emissions inventory and dispersion models, land-use regression (LUR) models, and time-series regression models. Understanding pollutants sources and their chemistry provides the theoretical background to formulate air quality models. The significant impacts of meteorological factors on chemical reactions and pollution concentrations are reviewed. Recently developed air pollution maps based on LUR models are introduced. The chapter reviews how pollutants are created and destroyed, and what are the strengths and weaknesses of the different modeling approaches. This review culminates in an assessment of research gaps in air pollution modeling.

2.1 CHEMISTRY OF POLLUTANTS

2.1.1 Nitrogen Oxides (NO_x)

2.1.1.1 Sources of NO_x

When fossil fuels (coal, gasoline, diesel, and natural gas) are burned, nitrogen monoxide (NO) and nitrogen dioxide (NO_2) gases are released into the atmosphere. Oxides of nitrogen (NO_x) are defined as the sum of both NO and NO_2. Due to the increase in fossil fuel use, such as road transport, power plants, combustion in industrial and commercial uses, and residential heating, NO_x is a common pollutant (Air Quality Expert Group, 2004). The US EPA (2000) estimates that, in 1998, U.S. on-road and off-road sources contributed 53% of nitrogen oxides, and the EU reports that road transport and other mobile sources account for 57% of NO_x, based on CORINAIR (The Core Inventory of Air Emissions in Europe) 1990 inventory (CORINAIR, 2003). In 2000, road transport in the United Kingdom was found to be the largest contributor of NO_x emissions (Air Quality Expert Group, 2004). Because of NO_x emissions, it is expected that

urbanized regions are more vulnerable to vehicle emissions than rural ones. According to the Korea Ministry of Environment (2005), the contributions of on-road vehicles to both the national and Seoul Metropolitan region NO_2 concentrations are 42.2% and 61.1%, respectively.

NO is derived from nitrogen (N_2) in high-temperature combustion processes, such as internal combustion engines, and NO_x emissions released from these engines contain over 90% of NO, which is relatively unstable when compared to oxygen (O_2) and N_2. The main fate of NO is to react with ozone (O_3) in the ambient atmosphere and to be converted into NO_2 (Derwent & Hertel, 1998). Typically, directly emitted NO_2 (hereafter primary NO_2) represents 5% of emissions by both gasoline and diesel vehicles. However, Carslaw & Beevers (2004) assert that diesel vehicles are responsible for higher primary NO_2 emissions (12.7%) than gasoline vehicles (0.6%), based on monitoring results in London. Nonetheless, it is certain that the share of primary NO_2 is far smaller than that of directly emitted NO. In urban regions, relatively abundant ozone (O_3) reacts rapidly with NO to generate NO_2. This reaction is investigated in the following section in detail.

2.1.1.2 Chemical Reactions of NO_2

In order to understand the temporal variations of air pollutant concentrations, it is necessary to understand and quantify how different emission sources vary across geographic locations, how meteorological factors influence the dispersion of air pollutants, and how chemical reactions among air pollutants are taking place. In particular, the chemical reactions leading to the creation and removal of secondary pollutants, such as NO_2 and O_3, are important, because their concentrations are primarily affected by these creation and removal processes.

1) Creation of NO_2

NO, created by combustion processes at high temperatures, undergoes a reaction with O_3, and is converted into NO_2 (Seinfeld, 1989; Derwent & Hertel, 1998). Since NO is primarily generated by motor vehicles in urban regions and the reaction (Eq. 2.1) requires only a few seconds, the ambient O_3 near the NO emission sources tends to be rapidly depleted:

$$\mathrm{NO} + \mathrm{O_3} \rightarrow \mathrm{NO_2} + \mathrm{O_2} \tag{2.1}$$

Another chemical reaction creating NO_2 is the interaction of NO and organic peroxy radicals ($RO_2\cdot$), where R is an alkyl radical.[1] In this reaction (Eq. 2.2) an abundance of peroxy radicals in the atmophere stimulates the accumulation of O_3, because O_3 molecules are no longer required to generate NO_2 (Seinfeld, 1989):

$$NO + RO_2\cdot \rightarrow NO_2 + RO\cdot \tag{2.2}$$

Oxidations of hydrocarbons (HC) are important, because these processes impact NO_2 creation as well as the accumulation of O_3. Methane (CH_4) is the most abundant HC in the troposphere, and, during daytime, the presence of a hydroxyl radical ($OH\cdot$) drives CH_4 into a methyl radical ($CH_3\cdot$). Then, the radical quickly combines with O_2 to form a methyl peroxy radical ($CH_3O_2\cdot$), where M is the third body, such as N_2 or O_2 molecules, which absorb the extra energy and stabilizes the reaction process (Eqs. 2.3 and 2.4).

$$CH_4 + OH\cdot \rightarrow CH_3\cdot + H_2O \tag{2.3}$$

$$CH_3\cdot + O_2 + M \rightarrow CH_3O_2\cdot + M \tag{2.4}$$

As noted in Eq. (2.2), the methyl radical produced in Eq. (2.4) reacts with NO and creates NO_2 (Eq. 2.5). Subsequently, the remaining alkoxy radical ($RO\cdot$; $CH_3O\cdot$) reacts with oxygen molecules, converting them into hydroperoxy radicals ($HO_2\cdot$) and formaldehyde (HCHO) (Eq. 2.6). Then, the highly reactive $HO_2\cdot$ plays a role in converting another NO molecule into NO_2 (Eq. 2.7) (Derwent & Hertel, 1998, p.144-145). Since the processes of HC oxidation include conversions of two molecules of NO in NO_2 and the highly reactive $OH\cdot$ radical recycled, substantial amounts of HC can react and are degraded to generate NO_2. As a result, the potential of O_3 creation increases (Seinfeld & Pandis, 1998, p.246).

$$NO + CH_3O_2\cdot \rightarrow NO_2 + CH_3O\cdot \tag{2.5}$$

$$CH_3O\cdot + O_2 \rightarrow HO_2\cdot + HCHO \tag{2.6}$$

$$NO + HO_2\cdot \rightarrow NO_2 + OH\cdot \tag{2.7}$$

---

1 Alkyl radicals are generally designated R·, where R represents the chemical formula for alkyl group. The chemical formula of alkanes is C_nH_{2n+2}. Once a hydrogen atom is removed from the alkane, the involved carbon atom has an unpaired electron and the molecule becomes a highly reactive free radical. Examples of alkyl radicals include the following: methyl ($CH_3\cdot$), ethyl ($CH_3–CH_2\cdot$), n-Propyl ($CH_3–CH_2–CH_2\cdot$), isopropyl ($CH_3–\dot{C}H–CH_3$), n-Butyl($CH_3–CH_2–CH_2–CH_2\cdot$) (Seinfeld & Pandis, 1998, pp.76, 240).

Since vehicles are the major sources of NO_x emissions in urban regions, it is reasonable to expect that roadside AQMs record higher NO_2 concentrations than urban background AQMs (Jo & Park, 2005; Lewné et al., 2004; Nguyen & Kim, 2006; Pandey et al., 2008). Similarly, it is expected that weekday concentrations are higher than weekend ones, because, generally, weekend traffic is less intense than the weekday one (Fujita, Stockwell, Campbell, Keislar, & Lawson, 2003; Sullivan et al., 2004).

2) Removal of NO_2

The main fate of NO_2 during daylight is photodissociation with ultraviolet (UV) rays and reforming NO and a ground-state oxygen atom, $O(^3P)$. The oxygen atom produced in the photolysis of NO_2 reacts with O_2, producing O_3 (National Research Council, 1991), a reaction that will be explained in detail in the ozone section (2.1.3). The range of UV wavelength in the photolysis process is known as 200 to 400 nm (nanometers, 10^{-9} meters) (Derwent & Hertel, 1998, p.139) and 280 to 430 nm (Seinfeld, 1989, p.745).

$$NO_2 + hv \rightarrow NO + O(^3P) \tag{2.8}$$

The other chemical removal of NO_2 is the reaction with OH·, forming nitric acid (HNO_3). Since the hydroxyl radical is created with electronically excited oxygen atoms, $O(^1D)$, and water vapor (Eq. 2.13), the presence of short wavelength UV (less than 320 nm) is required (Eq. 2.14). Under usual daytime conditions, the reaction of NO_2 and OH· converts around 5% of NO_2 per hour (Derwent & Hertel, 1998, p.141). The produced HNO_3 reacts with ammonia (NH_3) to form particulate nitrate (NO_3^-).

$$NO_2 + OH\cdot + M \rightarrow HNO_3 + M \tag{2.9}$$

Understanding the creation and removal processes of NO_2 helps explain the hourly variations of NO_2 concentrations. Roadside concentrations of NO_2 are relatively high as compared to urban background concentrations, because of the primary NO_2 emissions from tail pipes and the conversions of NO to NO_2 with O_3.

2.1.2 Carbon Monoxide (CO)

2.1.2.1 Sources and Health Impacts of CO

Carbon monoxide results from the incomplete combustion of carbon-containing materials, such as gas, oil, kerosene, wood, or charcoal. It is a colorless, practically odorless, and tasteless gas, or liquid classified as an inorganic compound (Hawley & Lewis, 2002). CORINAIR (2003) reports that road transport is responsible 56% of CO emissions in the EU's 28 countries. In the US, the main contributor to CO emissions is on-road vehicles, making up 57% of total national CO emissions in 1998 (US EPA, 2000). It is reasonable to expect that heavily urbanized regions have a higher likelihood to be affected by emissions from motor vehicles than rural or suburban areas. California's South Coast Air Basin (SoCAB) includes portions of Los Angeles, Riverside and San Bernardino counties and all of Orange county, with a population of 14.6 million.[2] The estimated CO contribution of on-road vehicles accounts for 80% of CO emissions in the summer 2000 in the SoCAB (Chinkin et al., 2003). According to the Korea Ministry of Environment (2005), the on-road vehicles shares of CO emissions are reported to be 78.9% and 90.1%, in the nation and Seoul Metropolitan region, respectively, in 2003.

Inhaled CO penetrates the blood through alveoli, and then binds to hemoglobin (Hb) to create carboxyhemoglobin (COHb). The affinity of CO for Hb is much greater than that of O_2 for Hb, which hinders O_2 transport throughout the human body, causing tissue hypoxia (Federal Register, 1994). Normally, COHb levels in the non-smoking population range from 0.5% to 2.0%. It is recommended that COHb level should not exceed 2.5%, to protect from CO poisoning, ischemic heart attacks, and hypoxic effects on fetuses (Raub et al., 1999). CO has been reported as the cause of fatal poisoning, so proper prevention and control measures are required to protect public health. Most industrialized countries have CO regulations, because CO is ubiquitous in the ambient air, with possible harmful effects for the public. To protect susceptible people and typical outdoor workers, 1- and 8-hour standards have to be established (Raub, Mathieu-Nolf, Hampson, & Thom, 2000). The US EPA (2000) suggests that the 1-hour standard is necessary for protecting people from acute exposures in the urban environment, and the 8-hour standard serves as a tracking indicator for measuring continuous exposure during 24-hour.

The WHO (World Health Organization) has established guidelines for CO concentrations in ambient air: 100 mg/m^3 (87 ppm)[3] for a 15-min average, 60 mg/m^3 (52 ppm) for a 30-min average, 30 mg/m^3 (26 ppm) for a 1-hour average, and 10 mg/m^3 (9 ppm) for an 8-hour average.

---

[2] http://www.aqmd.gov/map/MapAQMD1.pdf

[3] 1 ppm = 1.145 mg/m^3, 1 mg/m^3 = 0.873 ppm at 25˚C, 760 mm Hg

These guidelines have been determined to ensure that the level of COHb does not exceed 2.5% (Raub et al., 1999). The US EPA has promulgated National Ambient Air Quality Standard (NAAQS) for CO: 40 mg/m^3 (35 ppm) for a 1-hour average and 10 mg/m^3 (9 ppm) for an 8-hour average. These standards should not be exceeded more than once per year (Federal Register, 1994). Korean Ambient Air Quality Standards (KAAQS) for CO are 25 ppm for a 1-hour average and 9 ppm for an 8-hour average (Korea Ministry of Environment, 2003).

Although fixed-site air quality monitoring stations may report less than 10 mg/m^3 (9 ppm for annual average), CO concentrations from personal-level monitoring data, such as pedestrians or street workers, have reached 10~16 mg/m^3 (9~14 ppm) and 11~57 mg/m^3 (10~50 ppm), respectively. Workers in certain occupations, such as taxi, bus, and truck drivers, garage and tunnel workers, policemen, firemen, street workers, and mechanics, are exposed to high CO concentrations (Raub et al., 1999). In addition, the general public, such as residents, pedestrian near heavy traffic roadways, and passengers of buses and taxis, are likely to be involuntarily exposed to elevated CO concentrations.

2.1.2.2 Chemical Reactions of CO

In contrast to other carbon-containing molecules, CO does not react with oxygen, but it does with the hydroxyl radical (OH·) (Equation 2.10), and then the hydrogen atom generated in this reaction quickly combines with oxygen to form a hydroperoxyl radical (HO_2·) (Eq. 2.11). These two reactions are summarized by Eq. (2.12). As discussed earlier in the case of NO_2 creation, the reactive HO_2· radical plays an important role in converting NO to NO_2 (Eq. 2.7), and then, ultimately, the photolysis of NO_2 under UV rays at wavelengths < 424 nm is the primary source of troposphere ozone creation (Seinfeld and Pandis, 1998, p.235-240). Thus, the co-presence of CO and OH· is one of the bases for O_3 creation. Since CO is relatively abundant[4], the existence of OH· is a key to understanding the oxidation of CO. Ozone creation will be investigated in detail in the O_3 chemical reaction section.

$$\mathrm{CO} + \mathrm{OH}\cdot \rightarrow \mathrm{CO_2} + \mathrm{H}\cdot \tag{2.10}$$

$$\mathrm{H}\cdot + \mathrm{O_2} \rightarrow \mathrm{HO_2}\cdot + \mathrm{M} \tag{2.11}$$

$$\mathrm{CO} + \mathrm{OH}\cdot \xrightarrow{\mathrm{O_2}} \mathrm{CO_2} + \mathrm{HO_2}\cdot \tag{2.12}$$

[4] In 2003, the annual average CO concentration in Seoul was 0.7ppm. On the other hand, concentrations of NO_2, O_3, and SO_2 were 0.024ppm, 0.021ppm, and 0.006ppm,respectively(Korea Ministry of Environment, 2003).

1) Creation of OH·

Although the concentration of OH· is relatively low[5], the OH radical has a key role in the chemistry of the troposphere during daytime, because of its high reactivity and its reactions with trace gases (Eq. 2.3 OH· + CH_4; Eq. 2.9 OH· + NO_2; Eq. 2.10 OH· + CO; Eq. 2.24 OH· + SO_2). There are three ways to produce OH· in the troposphere: photolysis of O_3, photolysis of nitrous acid (HONO), and the reaction between HO_2· and NO.

On a global scale, the OH· radical in the troposphere is generated by the photolysis of O_3, which produces both ground-state atomic oxygen, $O(^3P)$, (Eq. 2.13) and an electronically excited oxygen atom, $O(^1D)$ (Eq. 2.14). UV wavelengths of less than 1180 nm and 320 nm produce the ground-state $O(^3P)$ and the electronically excited oxygen atom $O(^1D)$, respectively. The ground-state $O(^3P)$ rapidly combines with O_2 to reform ozone, thus Equation (2.13) does not yield any net chemical effect. The extremely reactive $O(^1D)$ collides with a third body (M: N_2 or O_2) and returns back to the ground-state oxygen (Eq. 2.15). 90% of $O(^1D)$ returns to $O(^3P)$ and around 10% of $O(^1D)$ produced in Eq. (2.14) reacts with water vapor (H_2O) to create OH· (Eq. 2.13). Thus, each $O(^1D)$ molecule generated by Equation (2.14) yields 0.2 molecule of OH· (Seinfeld & Pandis, 1998, p.172-173).

$$O_3 + h\nu \rightarrow O(^3P) + O_2 \tag{2.13}$$

$$O_3 + h\nu \rightarrow O(^1D) + O_2 \tag{2.14}$$

$$O(^1D) + M \rightarrow O(^3P) + M \tag{2.15}$$

$$O(^1D) + H_2O \rightarrow 2OH\cdot \tag{2.16}$$

The photolysis of HONO is the second way to produce OH·. HONO plays the role of a reservoir of NO and OH· at nighttime. In the morning and with sunlight, HONO is rapidly photodissociated back to the reactants (NO and OH·). The third process to create OH· takes place during hydrocarbon (HC) oxidations. As reviewed in the previous section on NO_2 creation, the oxidations of HC is initiated by OH· (Eq. 2.3) and produce HO_2· (Eq. 2.6). The generated HO_2· in Equation (2.6) reacts with NO to produce the OH· (Eq. 2.7). Since freshly emitted NO from the tail pipe is abundant in the urban atmosphere, HC oxidation ends up with the creation of OH·.

---

[5] 1 ~ 10×10^6 molecules/cm^3 (0.05 ~ 0.5 ppt) (Derwent & Hertel, 1998, p.142), Daytime (summer): 5 ~ 10×10^6 molecules/cm^3, Daytime (winter): 1 ~ 5×10^6 molecules/cm^3, Nighttime: ≤ 2×10^5 molecules/cm^3 (Seinfeld & Pandis, 1998, p.250)

Several studies have measured and estimated $HO_2\cdot$ concentrations. At noontime, $HO_2\cdot$ concentration is estimated at 3.2×10^8 molecules/cm^3 (Madronich & Calvert, 1990). Hard et al. (1992) measured $HO_2\cdot$ concentrations in downtown Portland and Lincoln City, Oregon. The daily maximum was in the range of $1\sim2\times10^8$ molecules/cm^3 at both sites. Seinfeld & Pandis (1998, p.253) simulated the concentrations of OH· created by the above three paths under the following conditions: noontime at 298K (≈ 25°C); O_3 = 50 ppb; $HO_2\cdot = 4 \times 10^{-3}$ ppb (1×10^8 molecules/cm^3); NO = 40 ppb (9.8×10^{11} molecules/cm^3); HONO = 1 ppb. Under these conditions, the OH· concentrations generated by the photolysis of ozone, the photolysis of HONO, and the reaction between $HO_2\cdot$ and NO are 0.22, 0.097, and 2.36 ppb/min, respectively. Adding the three generated OH· concentrations yields 2.677 ppb/min, and, converting minutes to hour, 0.16 ppm of OH· generation per hour. Since the conditions in the simulations are common in the urban atmosphere, it is logical to conclude that the reaction between $HO_2\cdot$ and NO is a major contributor of OH· concentration among three processes. In urban regions, it is expected that some portion of the generated OH· reacts with CO, influencing its concentration. As discussed above, under a typical urban atmosphere at noon time, the generated OH· per hour can reach 0.16 ppm. As relatively stable traffic flows are maintained after the morning rush hour, an accumulation of CO can be expected. However, the measured data do not support this theory. Thus, it is reasonable to assume that the reactive OH· radical has a role in decreasing CO concentrations during daytime.

2) Chain reaction of CO and NO_x via OH·

The only reaction producing ozone in the atmosphere occurs between atomic and molecular oxygen (Eq. 2.17). Since the photolysis of O_2 requires solar radiation with less than 290 nm wavelength, and sunlight with wavelength below 290 nm cannot reach ground level, the photolysis of NO_2 (Eq. 2.8) is the sole source of atomic oxygen to create O_3 in the troposphere (Seinfeld & Pandis, 1998, p.234). As discussed in the case of NO_x, ambient ozone reacts with NO to form NO_2 (Eq. 2.1). Without O_2 inclusion on both sides, the three reactions (Eqs. 2.17, 2.8 and 2.1) can be roughly represented by Equation (2.18).

$$O(^3P) + O_2 + M \rightarrow O_3 + M \tag{2.17}$$

$$NO_2 + hv \rightarrow NO + O(^3P) \tag{2.8}$$

$$NO + O_3 \rightarrow NO_2 + O_2 \tag{2.1}$$

$$NO_2 \overset{hv}{\Leftrightarrow} NO + O_3 \tag{2.18}$$

When CO is present, the OH· radical reacts with CO to produce the hydroperoxyl radical (Eq. 2.12), and then the HO_2· radical reacts with NO to regenerate NO_2 and OH· (Eq. 2.7). Thus, in the presence of CO, Equation (2.18) is accompanied by two interwoven cycles (Eqs. 2.7 and 2.12) (Seinfeld & Pandis, 1998, p.243).

$$\mathrm{CO} + \mathrm{OH}\cdot \xrightarrow{\mathrm{O_2}} \mathrm{CO_2} + \mathrm{HO_2}\cdot \tag{2.12}$$

$$\mathrm{NO} + \mathrm{HO_2}\cdot \rightarrow \mathrm{NO_2} + \mathrm{OH}\cdot \tag{2.7}$$

The chain reaction of CO and OH· with NO provides an explanation for how O_3 can accumulate and why CO concentrations in daytime are decreasing. There are competing reactions (Eqs. 2.1 and 2.7) to convert NO to NO_2. In the presence of NO and HO_2·, the reaction between O_3 and NO (Eq. 2.1) is inhibited and, as a result, ozone has a chance to accumulate. CO reacts with the OH· radical to be converted to CO_2 and HO_2·. Under relatively abundant NO concentrations, most of HO_2· reacts with NO to generate OH·. The recycled OH· in Equation (2.7) reacts again with CO, stimulating the reduction of CO concentrations. The co-presence of CO, OH·, and NO makes these reactions iterative. The coefficients of these recursive reactions would help to estimate the concentration of each pollutant.

2.1.3 Ozone (O_3)

Around 90% of atmospheric O_3 is found in the stratosphere, absorbing hazardous UV rays from the sun. It is known to have been seriously depleted by diverse CFCs (chlorofluorocarbons) anthropogenic emissions. In the troposphere, the observed concentrations of O_3 over remote tropical forests and sea water bodies range from 20 ~ 40 ppb as summertime daily maximum, and therefore O_3 concentrations under natural conditions are not a cause for concern (National Research Council, 1991). Tropospheric O_3 is produced by photochemical reactions, which include the following forerunner chemicals: VOCs, NO_x, and CO. These pollutants are emitted by both anthropogenic activities and biological processes. Due to the increased emissions from traffic and fuel combustion, it is generally accepted that O_3 concentrations are significantly high in urban regions and in areas downwind from highly polluted regions (Intergovernmental Panel on Climate Change, 2007). Contrary to common sense, however, it is not uncommon to find studies reporting that heavily traveled roadside areas are less polluted by O_3 than urban background regions (Jo & Park, 2005; Kim, 2007; Kim & Guldmann, 2008), and that average concentrations of O_3 at rural and non-urban sites are higher than those at urban sites (Gregg, Jones, & Dawson, 2003; Yang & Miller, 2002). Average O_3 concentrations over 2003 ~ 2006 at urban, suburban and rural sites in central Taiwan were equal to 24 ppb, 27 ppb, and 29 ppb, respectively (Tsai, Wang, Wang, & Chan, 2008). A comparison of daily maximum O_3 concentrations in urban (Bridgeport and New Heaven), suburban (Danbury, East Hartford, Greenwich, Middletown, Madison, and Stratford), and rural (Stafford) areas in Connecticut indicates a difference of 10 ppb or more between non-urban and urban sites (Yang & Miller, 2002). The annual average O_3 concentrations at sites in New York City and surrounding rural areas also support these results: O_3 concentrations in rural areas are significantly higher (28 ppb) than those at urban sites (16 ppb). On the other hand, the concentrations of SO_2, NO_x, and CO_2 are characterized by the opposite spatial pattern (Gregg, Jones, & Dawson, 2003).

The reason for this counterintuitive phenomenon can be explained by Eq. (2.1). The roadside area has relatively high NO concentrations due to traffic emissions. The freshly emitted NO reacts with ambient O_3 to be converted into NO_2. This reaction is quick and complete, thus the concentrations of O_3 near the roadside are scavenged and NO_2 accumulates. Comparing O_3 concentrations at roadside and urban background monitoring stations, it is possible to investigate the magnitude and timing of the concentration difference. The intrusion of stratospheric O_3 can also influence the concentrations of O_3 in the middle and upper troposphere. The transported O_3 from the stratosphere may affect surface concentrations through boundary layer mixing mechanism (US EPA, 2006).

Sections 108 and 109 of the US Clean Air Act delineate the establishment, review, and revision of NAAQS. The NAAQS for photochemical oxidants were promulgated by the US EPA in 1971: the concentrations of photochemical oxidants should not exceed 0.08 ppm/hour. After several revisions of the NAAQS, the up-to-date O_3 standards for one hour and 8-hour are 0.12 ppm (235 μg/m^3)[6] and 0.075 ppm (147 μg/m^3)[7], respectively. A significant number of epidemiological studies support a positive relationship between daily mortality and O_3 concentrations (Bell, McDermott, Zeger, Samet, & Dominici, 2004; Bell & Dominici, 2008; Gryparis et al., 2004; Zanobetti & Schwartz, 2008). Considering O_3 health impacts studies, the WHO guideline for O_3 changed from 120 μg/m^3 (0.061 ppm) to 100 μg/m^3 (0.051 ppm) for a maximum 8-h mean concentration (WHO, 2006). According to the annual Korean Environmental White Book, KAAQS for O_3 was promulgated in 1983 and revised in 1995, representing 0.1 ppm/h and 0.06 ppm/8-h[8].

2.1.3.1 Chemistry of O_3

Ozone in the stratosphere absorbs UV waves with less than 290 nm wavelength. Thus, sunlight with wavelengths less than 290 nm cannot reach the earth surface (National Research Council, 1991). As discussed earlier regarding the chain reactions of CO and NO_x via OH radicals, the formation of O_3 in the troposphere depends upon the creation of ground-state atomic oxygen, $O(^3P)$ (Eq. 2.8). Ozone in the troposphere is generated by combining $O(^3P)$ with O_2 (Eq. 2.17). In Eq. (2.17), M is a third body absorbing excessive energy and stabilizing the formed O_3 molecule. This is the only significant source of O_3 formation in the troposphere. Since sunlight with wavelengths exceeding 290 nm can reach the ground, $O(^3P)$ is produced only by the photolysis of NO_2 at wavelengths in the range [290 nm ~ 424 nm] (Eq. 2.8) (Derwent & Hertel, 1998; Seinfeld & Pandis, 2006):

$$NO_2 + hv \rightarrow NO + O(^3P) \tag{2.8}$$

$$O(^3P) + O_2 + M \rightarrow O_3 + M \tag{2.17}$$

---

[6] 1 ppm = 1,962 μg/m^3, 1 μg/m^3 = 5.097×10^{-4} ppm at 25 °C and 760 mm Hg

[7] Effective May 27, 2008. According to the 1997 NAAQS, the 8-hour standard was 0.08ppm/8-h (157 μg/m^3). The standard requires that 3-year average of the fourth-highest daily maximum 8-hour average should not exceed 0.075 ppm. http://www.epa.gov/air/ozonepollution/standards.html

[8] The values above the 99.9 percentile and 99.0 percentile should not exceed the 1-hour and 8-hour standards, respectively.

As soon as the formation of O_3 is completed, the regeneration of NO_2 occurs through the reaction of NO with O_3 (Eq. 2.1), called ozone titration (Yarwood, Grant, Koo, & Dunker, 2008):

$$NO + O_3 \rightarrow NO_2 + O_2 \tag{2.1}$$

Since there is a cycle for NO, O_3, and NO_2, one can deduce dynamic equations for this cycle.[9] The rates of change for NO_2 and $O(^3P)$ can be represented by the following equations:

$$\frac{d[NO_2]}{dt} = -j_{2.8}[NO_2] + k_{2.1}[NO][O_3] \tag{2.19}$$

$$\frac{d[O(^3P)]}{dt} = j_{2.8}[NO_2] - l_{2.14}[O(^3P)][O_2][M] \tag{2.20}$$

where $j_{2.8}$ is the photolysis rate of Eq. (2.8), $k_{2.1}$ is the reaction rate coefficient in Eq. (2.1), and $l_{2.14}$ is the reaction rate of Eq. (2.17). The ground-state atomic oxygen, $O(^3P)$, is so reactive that its residence time in the air is very short. The rate of formation (Eq. 2.8) is considered equal to the rate of disappearance (Eq. 2.17), leading to a pseudo-steady state, with:

$$j_{2.8}[NO_2] = l_{2.14}[O(^3P)][O_2][M] \tag{2.21}$$

Similarly, the cyclic system including the reaction of NO and O_3 (Eq. 2.1) and the photolysis of NO_2 (Eq. 2.8) lasts a few minutes under sunlight. NO_2 is destroyed and reformed in a cyclic manner and a steady state is established:

$$\frac{[NO][O_3]}{[NO_2]} = \frac{j_{2.8}}{k_{2.1}} \tag{2.22}$$

Equation (2.22) leads to the steady state concentration of O_3, with:

$$[O_3] = \frac{j_{2.8}[NO_2]}{k_{2.1}[NO]} \tag{2.23}$$

The ratio of NO_2 and NO determines the concentration of O_3. In the summer afternoon at mid-latitudes with a clear sky, the photolysis rate of Eq. (2.8), $j_{2.8}$, is 7×10^{-3} ppb^{-1} s^{-1} and the

[9] Assuming that the system is a reactor with a constant volume of components and the temperature and solar radiation are not changed.

reaction rate of Eq. (2.1), $k_{2.1}$, is 4×10^{-4} ppb^{-1} s^{-1}, which leads to the ratio of 17.5 in Eq. (2.19). If the ratio of NO_2 to NO is 2, we can expect an O_3 concentration of about 35 ppb. If it is 5, a concentration of 88 ppb can be expected. In addition to Eqs. (2.1), (2.8), and (2.17), there are other reactions, such as the oxidations of VOCs and CO, that play important roles in determining O_3 concentrations in the atmosphere (Leighton, 1961; Derwent & Hertel, 1998; Seinfeld & Pandis, 2006).

Since the photolysis of NO_2 is the only source of O_3 creation in the atmosphere, it is necessary to understand when and how NO_2 is formed. As discussed earlier, in the presence of NO, there are three reaction paths to the formation of NO_2 (Eqs. 2.1, 2.2, and 2.7). In these equations, $RO_2\cdot$, and $HO_2\cdot$ react with NO to generate NO_2, without consumption of O_3. Conditions favorable to the reactions represented by Eq. (2.2) and (2.7) provide an opportunity for O_3 accumulation (Seinfeld, 1989).

$$\mathrm{NO} + \mathrm{RO_2}\cdot \rightarrow \mathrm{NO_2} + \mathrm{RO}\cdot \tag{2.2}$$

$$\mathrm{NO} + \mathrm{HO_2}\cdot \rightarrow \mathrm{NO_2} + \mathrm{OH}\cdot \tag{2.7}$$

Organic peroxy radicals ($RO_2\cdot$) and hydroperoxy radical ($HO_2\cdot$) are produced in the oxidation processes of VOCs and CO. All carbon containing compounds, except CO and CO_2, are classified as VOCs, originating from both anthropogenic and biogenic sources. VOCs include alkanes, alkenes (olefins), aromatic compounds, carbonyl compounds (e.g. aldehydes and ketones), and alcohols. The simplest chemical structure of VOC is methane (CH_4) and its oxidation process is reviewed in Section 2.1.1 (NO_x chemical reactions). VOCs oxidation processes have not all been clearly investigated, and therefore their reaction times and rates are not all available. Additionally, in the oxidation process of alkanes, the formation of alkyl nitrate is uncertain, so the amount of NO to NO_2 conversion is not exactly known. Consequently, the amount of O_3 formation in the processes of alkanes oxidation is imprecise. Uncertainties are also found in the chemistry of alkenes and aromatic compounds. The yields of radicals in the oxidation process of alkenes are not available. Aromatic carbon compounds make up approximately 30% of the total carbon of VOCs in urban areas, but the products and reaction mechanisms producing free radicals are not clearly understood (US EPA, 2006). Generally, the formation of O_3 is considered a complex and nonlinear function of many factors, including concentrations, mixing ratios, reaction rates of precursors, and meteorological factors (sunlight intensity, wind, temperature, and humidity). The uncertainties in the chemistry of VOCs add to the difficulties in estimating O_3 concentrations, which is more complex in urban regions, where

complicated anthropogenic and biogenic VOCs, such as aromatics and naturally emitted VOCs, co-exist.

The OH radical plays a key role in the chemistry of the troposphere. The oxidation processes of CO and VOCs are initiated by OH·, and these processes are iterative, because OH· is recycled. Favorable conditions for reactions (2.2) and (2.7) inhibit the consumption of O_3 in the conversion process of NO to NO_2. Places where VOCs and CO are abundant are more likely to have O_3 accumulation. It logically follows that roadside areas have higher concentrations of O_3 than urban background regions. As mentioned earlier, however, empirical studies present counter-intuitive results. The conversion of NO to NO_2 with O_3 (Eq. 2.1) is much faster (less than 5 min) than the organic oxidation processes (Eqs. 2.2 and 2.7; one to several hours). Therefore, in heavily traveled areas, reaction (2.1) is dominant in converting NO to NO_2 among the three competing reactions. Consequently, areas with abundant fresh NO emissions have lower O_3 concentrations. The formation of O_3 is influenced by not only the amounts of precursors but also the mixing ratios of these components. The impact of the VOC/NO_x ratio will be discussed in the O_3 isopleth plot in Figure 2.1, providing a clue to why the weekend O_3 concentrations are higher than the weekdays ones.

2.1.3.2 Biogenic VOCs and O_3

It has been known that episodes of high O_3 concentration occur in late spring and summer under specific meteorological conditions, such as high pressure, warm temperature, low cloud cover, and light wind. Temperature has direct and indirect impacts on O_3 creation. A high temperature can directly enhance O_3 concentrations by facilitating the photochemistry of O_3 and increasing the emission rates of O_3 precursors. During the growing seasons (spring and summer), plants emit highly reactive hydrocarbons, including isoprene (C_5H_8), primarily from deciduous trees, and α-pinene ($C_{10}H_{16}$), primarily from coniferous trees. Since the biogenic VOCs (BVOCs) are sensitive to temperature, the enhanced BVOC emissions due to higher temperatures can be expected to increase O_3 formation (Sanderson, Jones, Collins, Johnson, & Derwent, 2003). The estimate emission rate of isoprene at 25˚C is 8.5 $\mu g\ g^{-1}\ h^{-1}$, but, as the temperature increases to 30˚C, the rate jumps to 35 $\mu g\ g^{-1}\ h^{-1}$ (Lamb, Guenther, Gay, & Westberg, 1987)[10]. The natural sources of VOCs include vegetation, soil microbes, biomass burning, and lightning. Vegetation makes up most of the total annual biogenic emissions (98%). Isoprene is the major component of BVOCs emitted by plants (35%). In addition, nineteen terpenoid compounds and seventeen non-

[10] $\mu g\ g^{-1}\ h^{-1}$: micrograms of carbon per gram foliar dry mass per hour

terpenoid compounds make up 25% and 40% of BVOCs, respectively (Guenther et al., 2000). Since the emission activities of isoprene and α-pinene depend on light and temperature, these BVOCs present diurnal cycles in their mixing ratio (Rinne, Guenther, Greenberg, & Harley, 2002).

Urbanization is inevitably accompanied by the loss of green areas due to the construction of urban infrastructures, such as roads, buildings, parking spaces, etc. The materials used in urban structures have different thermal properties in terms of heat capacity, albedo, and emissivity, as compared to those in rural areas. Urban facilities increase surface roughness and decrease wind velocity. Therefore, an increasing number of calm days inhibits the cooling process due to horizontal air movements, and the materials used in urban structures, such as asphalt and concrete, absorb more heat than they re-radiate. In addition, the waste heat produced by air conditioners and industrial processes also contributes to the urban heat island. According to a study of the Atlanta metropolitan area over 1974 ~ 1988, about 20% of forests have been converted into urban surfaces, with a resulting reduction of BVOC emissions. Because of the urban heat island, however, the temperature of the Atlanta area increased by 2 degrees centigrade, and the warmer temperatures resulted in a significant increase in the net emissions of BVOCs. The phenomenon of the urban heat island may negate the impacts of reduced BVOC emissions caused by decreased vegetative areas. The urban heat island may also cancel out the policy impacts of anthropogenic VOC emission reduction (Cardelino & Chameides, 1990). A simulation study of O_3 concentrations in California indicates that increasing temperatures induce increased BVOC emissions and, as a result, the increased BVOC emissions in NO_x-abundant areas, such as urban regions, cause an increase in O_3 formation (Steiner et al., 2006).

2.1.3.3 Roles of VOC and NO_x in O_3 Formation: The O_3 Isopleth Plot

The OH· radical has a key role in initiating the oxidations of VOCs and CO, leading to the formation of O_3. OH· also reacts with NO_2, forming nitric acid (HNO_3) and removing both OH· and NO_x from the system (Eq. 2.9). Thus, increasing the reaction between OH· and NO_2 limits the recycling of OH· and HO_2·, decreasing the rate of O_3 formation[11]:

$$NO_2 + OH\cdot + M \rightarrow HNO_3 + M \tag{2.9}$$

[11] In addition, the following three reactions terminate the recycling process of radicals, leading to the inhibition of ozone formation: (1) the reaction of alkyl peroxy radical (RO_2·) and NO to form alkyl nitrates; $RO_2\cdot + NO + M = RONO_2 + M$, self-reaction between peroxy radicals to form peroxides; (2) $HO_2\cdot + HO_2\cdot = H_2O_2 + O_2$, (3) $RO_2\cdot + HO_2\cdot = ROOH + O_2$ (Seinfeld & Pandis, 2006; Steiner, Tonse, Cohen, Goldstein, & Harley, 2006)

Under an average urban atmosphere, the rate constants for the VOC + OH· reaction[12] and the NO_2 + OH· reaction are 3.1×10^3 $ppmC^{-1}min^{-1}$ and 1.7×10^4 $ppm^{-1}min^{-1}$, respectively. Since the ratio of the (NO_2 + OH·) to (VOC + OH·) rates is around 5.5, the rates of the two reactions are equal only when the concentration ratio of VOC to NO_2 reaches 5.5 : 1. If the VOC ratio is less than 5.5, the reaction of NO_2 + OH· dominates the system and results in slowing down the formation of O_3. Conversely, when the VOC ratio exceeds 5.5, the reaction between VOC and the OH· radical generates more intermediate products, such as NO_2, peroxy radicals, and recycled OH· radicals, speeding up the formation of O_3. As reviewed above, there is an optimal ratio of VOC to NO_x concentrations, leading to a maximum amount of O_3 formation. Using an ozone isopleth plot, one can clearly understand the mechanism of O_3 production in terms of the ratio of VOC to NO_x (Derwent & Hertel, 1998; Seinfeld & Pandis, 2006).

The ozone isopleth is illustrated by contour plotting of the predicted O_3 maxima calculated with different VOC/ NO_x ratios. An example of an ozone isopleth plot is illustrated in Figure 2.1, which was obtained from the Ozone Isopleth Plotting Program Web Interface[13] and modified by the author. The ridge (solid green line) in Figure 2.1 separates the region of low VOC/NO_x ratio (region A), above the ridge, and high VOC/NO_x ratio, below the ridge (region B). The ridge represents the maximum O_3 concentration that can be calculated at a given NO_x and VOC levels.

Region A has low VOC/NO_x ratios, and it is called NO_x-saturated. On the other hand, region B has high VOC/NO_x ratios, and is called NO_x-limited. Note that the same changes in VOC and NO_x concentrations in both regions lead to significantly different results in terms of O_3 generation. In the NO_x-saturated region (A), an increase in the initial VOC concentrations (solid red arrow) induces an increase in peak O_3 concentrations. At high VOC/NO_x ratios (region B), an increase or decrease in VOC (solid blue arrow) has little impact on O_3 generation. When VOC is abundant relative to NO_x, O_3 formation is limited by the available NO_x. Therefore, decreasing NO_x (dotted blue arrow) induces a decrease in O_3 formation. In contrast, in the VOC-limited region (A), O_3 formation is limited by the available VOC. As discussed earlier, the reaction of NO_2 + OH· dominates under VOC-limited conditions, thereby inhibiting the oxidation of VOC. Decreasing NO_x under VOC-limited condition (dotted red line) produces an increase in O_3 formation, because decreased NO_x decelerates the formation of HNO_3 and, consequently, more

[12] The rate constant of the VOC + OH reaction is represented as parts per million by volume of carbon atoms (ppmC).

[13] http://www.shodor.org/ekma/model/ozipform.html

OH· is available, expediting the rate of the VOC + OH· reaction, leading to favorable conditions to generate O_3 (Fujita et al., 2003; Heuss, Kahlbaum, & Wolff, 2003; Seinfeld, 1989).

Under comparable meteorological conditions, the hourly average concentrations of O_3 during the weekend are higher than those during weekdays in California's South Coast Air Basin (SoCAB). Emission activity data, including various mobile, point, and area sources, have been collected in the SoCAB and the emission patterns of VOCs and NO_x during weekdays and weekends have been assessed. Since the reduction rate of NO_x is around three times greater than that of VOCs, leading to a 30% increase in the VOC/NO_x ratio, lower NO_x emissions in the weekend induce less O_3 titration and less (NO_2+OH·) inhibition of O_3 production, and consequently, result in higher O_3 concentrations (Chinkin et al., 2003; Yarwood, Stoeckenius, Heiken, & Dunker, 2003; Yarwood et al., 2008).

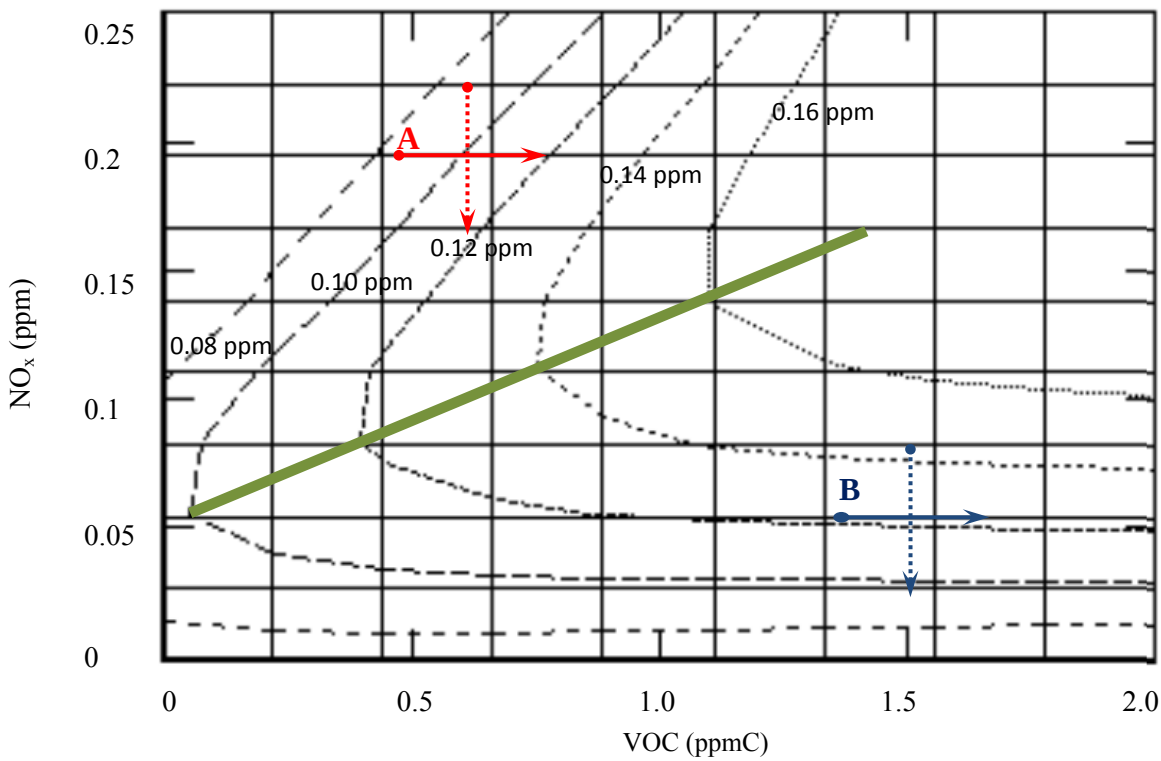

Figure 2.1 Ozone isopleth diagram based on the simulation of the Empirical Kinetics Modeling Approach (EKMA)[14]

[14] Detail information regarding the ozone isopleth plotting program can be found at the following website: http://www.shodor.org/ekma/

2.1.4 Sulfur Dioxide (SO_2)

2.1.4.1 Sources and Health Impacts of SO_2

Sulfur-containing fossil fuels, such as coal and petroleum, have been widely used for industrial, heating, and transportation uses, and therefore SO_2 has been commonly observed in both developed and developing countries. Since SO_2 has water-soluble characteristics, sulfur trioxide (SO_3) reacts with water vapor to form sulfuric acid (H_2SO_4). H_2SO_4 is a strongly hygroscopic acid, thus vapors condense on the surface of H_2SO_4, leading to the growth of composite particles, and resulting in small droplets of sulfuric acid (acid rain). The declining use of coal for domestic heating and the tall stacks of power plants and industrial factories have led to lower concentrations in the surrounding regions. According to the EPA (2002) National Emissions Inventory Data, a major source of SO_2 emissions in the U.S. is electric generations (66%), and industry use makes up for 30% of SO_2 emissions. Since gasoline has been de-sulfurized, diesel vehicles are the only source of SO_2 in vehicle emissions; transportation-related emissions contribute to around 5% of total SO_2 emissions. Recently, ultra-low sulfur diesel (ULSD) has become available in many countries. In Korea, the allowable sulfur content of diesel has been restricted from 430 ppm to 30 ppm since 2005.

In 2006, the WHO regional office for Europe established new guidelines for SO_2 concentrations: 20 μg/m^3 (7.5 ppb)[15] for a daily average and 500 μg/m^3 (0.19 ppm) for a 10-minutes average (WHO, 2006). The US NAAQS for SO_2 are at 0.03 ppm (79.8 μg/m^3) for an annual average, and 0.14 ppm (372.4 μg/m^3) for a daily average. The daily average should not be exceeded more than once a year.[16] Korean Ambient Air Quality Standards for SO_2 are 0.02 ppm for an annual average, 0.05 ppm for a daily average, and 0.15 ppm for a 1-hour average (Korea Ministry of Environment, 2003).

The only exposure to SO_2 is through inhalation. As discussed earlier, SO_2 is highly water-soluble, and therefore inhaled SO_2 is absorbed in the upper respiratory tract. Consequently, SO_2 exposure has negative effects mainly on pulmonary functions, such as severe broncho-constriction. Sensitive groups, such as asthmatic people, tend to be easily affected (WHO, 2006). In the Seoul Metropolitan Area, SO_2 concentrations are closely correlated with other pollutants (NO_x, CO, VOCs, and PM), hence traffic flows are major source of these pollutants. In addition, SO_2, NO_x, and VOCs have a strong potential to be converted into fine particles. There are several ways to evaluate the contribution of co-present pollutants to adverse health effects; (1) an

---

[15] 1 ppm = 2660 μg/m^3, 1 mg/m^3 = 0.3759 ppm at 20˚C, 1013 hPa

[16] http://www.epa.gov/air/criteria.html

individual pollutant has an independent effect on respiratory functions, (2) a certain pollutant may be serving as a surrogate of other pollutants and has no confounding effects, and (3) joint risks from co-present pollutants might be expected. Besides the above mentioned pollutants, other hazardous pollutants might be mingled in these multi-factorial causations (US EPA, 2008).

2.1.4.2 Chemical Reactions of SO_2

As discussed in the section on OH· creation, hydroxyl radicals (OH·) are initiated with sunlight, and OH· is recycled in the co-presence of VOCs, CO, and NO (Eqs. 2.3 ~ 2.7, 2.10). The OH· radical in the ambient atmosphere reacts with SO_2 (Eq. 2.24):

$$SO_2 + OH\cdot + M \rightarrow HOSO_2\cdot + M \tag{2.24}$$

Then sulfur trioxide (SO_3) and hydroperoxyl radical (HO_2·) are generated as follows:

$$HOSO_2\cdot + O_2 \rightarrow HO_2\cdot + SO_3 \tag{2.25}$$

The above two reactions are similar to the oxidation process of CO (Eqs. 2.10 and 2.11). Sulfuric acid (H_2SO_4) is generated by the reaction of SO_3 with water vapor (Eq. 2.26) (Seinfeld & Pandis, 2006):

$$SO_3 + H_2O + M \rightarrow H_2SO_4 + M \tag{2.26}$$

H_2SO_4 nucleates with other H_2SO_4 or with water vapor, and then, through coagulation and coalescence with other sulfuric droplets and suspended particulates, the gas-phase SO_2 is converted into particle-phase sulfuric acid, with size from a few nanometers to several μm (Derwent & Hertel, 1998).

2.1.5 Particulate Matters

2.1.5.1 Sources of Particulate Matters

The size of particulate matters (PM) in the atmosphere varies from ultrafine (a few nanometers, slightly larger than molecules) to several millimeters (lapilli and hailstones). The pollutants discussed in the earlier sections (NO_2, CO, O_3, and SO_2) have their own chemical signature, but PM have no specific chemical compounds. Since PM are a mixture of particles, their origins, sizes, and properties vary. Initial regulations of PM were directed at general particles concentrations, including total suspended particulate in the US and black smoke in Europe (WHO Regional Office for Europe, 2006). The US EPA established a standard for PM10 (particulate matter with a diameter less than 10 μm) in 1987 (US EPA, 1987), and then a standard for PM2.5 (particulate matter with a diameter less than 2.5 μm) in 1997 (US EPA, 1997). The US NAAQS for PM10 are 150 $\mu g/m^3$ for a 24-h average and 50 $\mu g/m^3$ for an annual average. Two PM2.5 standards are set: a 24-h standard of 65 $\mu g/m^3$ and an annual standard of 15 $\mu g/m^3$. The WHO has also established short-term (24-h average) and long-term (annual average) guidelines for PM10 and PM2.5 concentrations: 20 $\mu g/m^3$ and 50 $\mu g/m^3$ were suggested for PM10 annual mean and 24-h average, and 10 $\mu g/m^3$ and 25 $\mu g/m^3$ for PM2.5 annual mean and 24-h average. Since the WHO goals for PM10 and PM2.5 are hard to achieve in both developed and developing countries, three interim targets have also been proposed, and are expected to be achievable with the consecutive implementation of interim abatement policies (WHO, 2006). A 0.62% increase in mortality has been observed for each 10 $\mu g/m^3$ increment of short-term (24-h) PM10 exposure in 29 cities in Europe (Katsouyanni et al., 2001), and a 0.46% increase in 20 cities in the US (Samet et al., 2000). In addition, strong associations have been consistently reported regarding PM exposure and adverse health effects, including mortality increase, increased hospital and emergency visits, chronic obstructive pulmonary disease, asthma, heart disease, etc. The adverse health effects, ranging from death to reduced quality of life, are also divided into short-term and long-term effects. Long-term exposure causes chronic diseases such as asthma, lung cancer, cardiovascular disease, and obstructive pulmonary disease, and acute short-term exposure increases sudden mortality, hospital and emergency room visits, and work and school absenteeism (World Health Organization, 2000; American Thoracic Society, 2000). Reports from the WHO and the US EPA provide well-organized extensive research reviews for these health-related studies (World Health Organization, 2004; National Center for Environmental Assessment, 2004; WHO Regional Office for Europe, 2006).

The sources of PM vary widely, from human activities to natural sources, including dusts from roads, construction sites, and agricultural land, combustion of fossil fuels (electric

generation and internal combustion engines), ammonia from agriculture, marine aerosols, pollen, biomass burning, wind blowing from China (yellow sand phenomenon), and secondary particles, such as ammonium sulfate and ammonium nitrate. A major source of fine PM emissions in urban regions is diesel vehicles. With advances in catalytic converter technology, gasoline vehicles with converters emit far less PM than those without and than diesel vehicles. Therefore, directly emitted elemental carbon soot from diesel vehicles, re-suspended dust from roads, and secondary acidic particles are major contributors of PM at urban roadside areas. Biological emissions are also known as sources of PM, including BVOC, such as terpene, pollen, moulds, spores, and bacterial endotoxin. The oxidation of BVOCs produces fine particles, such as organonitrates and amines (WHO Regional Office for Europe, 2006).

2.1.5.2 Chemistry of Secondary Particles

Depending on their source, PM are classified into primary and secondary particles. Primary particles are emitted directly from sources and secondary particles are formed from natural and anthropogenic gases, such as SO_2, NO_2, and VOCs, through chemical reactions. Generally, secondary particles have a variable composition, and their main particle components include sulfuric acid (H_2SO_4; Eq. 2.26), ammonium sulfate ($(NH_4)_2SO_4$; Eq. 2.27), ammonium nitrate (NH_4NO_3; Eq. 2.28), ammonium chloride (NH_4CL; Eq. 2.29), sodium chloride, sodium nitrate, etc. Among these compounds, $(NH_4)_2SO_4$ accounts for the largest fraction of secondary particles (Derwent & Hertel, 1998). $(NH_4)_2SO_4$, NH_4NO_3, and traffic emissions explain 50 ~ 70 % of PM2.5 concentrations at six sites in the California San Joaquin Valley (Chow et al. 1992). The reactions are:

$$2NH_3 + H_2SO_4 \rightarrow (NH_4)_2SO_4 \tag{2.27}$$

$$NH_3 + HNO_3 \leftrightarrow NH_4NO_3 \tag{2.28}$$

$$NH_3 + HCL \leftrightarrow NH_4CL \tag{2.29}$$

Ammonia (NH_3) is a commonly observed alkaline gas in the atmosphere, and is emitted from animal waste, nitrogenous fertilizers, soils, and industrial processes. As discussed above, NH_3 has reactions with acidic gases and hydrogen chloride, forming fine particles with diameters less than 2.5 μm. As indicated in the above three equations, the reaction of NH_3 and H_2SO_4 is irreversible (Eq. 2.27), but the other two reactions are reversible (Eqs. 2.28 and 2.29). Depending

on the relative humidity in the ambient atmosphere, ammonium compounds may exist in a solid or aqueous phase (solution of NH_4^+, HSO_4^- , SO_4^{2-}, and NO_3^-) (Seinfeld & Pandis, 2006).

2.2 REVIEW OF AIR POLLUTION MODELING STUDIES

2.2.1 Overview

There is much empirical evidence regarding the positive association between traffic flows and air pollutant concentrations. Since transportation is known to be responsible for a substantial share of urban air pollution emissions, it is reasonable to expect that the contribution of on-road vehicles to the air pollution of urbanized regions is greater than to that of rural areas. In a spatial perspective, the areas adjacent to heavily travelled roads are more susceptible to vehicular emissions than remote areas. The spatial and temporal exceedances of air pollution standards must be examined and estimated, because these hotspots of spatiotemporal exceedances can lead to harmful impacts on human health and natural and man-made environments. There are many studies reviewing the consequences of air pollution, including hedonic models of housing values (C. W. Kim, Phipps, & Anselin, 2003), benefit-cost assessment of urban air pollution (Krupnick & Portney, 1991), spatial property assessment (Setton, Hystad, & Keller, 2005), valuing health benefits of clean air (Hall et al., 1992), particulate matter and health outcomes (Dockery et al., 1993; Dominici & Burnett, 2003), PM2.5 and mortality (Franklin, Zeka, & Schwartz, 2007), NO_2 and human health (Kraft et al., 2005), air pollution and mortality (Schwartz & Zanobetti, 2000), and epidemiology of traffic-related pollution and asthma (Zmirou et al., 2002).

Pollutants emitted by motor vehicles influence the spatial and temporal variations of ambient pollution concentrations, which depend upon such diverse factors as the strength and location of emission sources, meteorological variables, chemical reactions, topographic variations, and mitigation by vegetation. Since air pollution in urban regions has induced considerable attention from scholars and public administrators, air quality models have been developed while considering the above-mentioned factors in modeling processes. Most of these studies have adopted dispersion methods as key modeling modules, with extensive emission inventories. The air quality models based on dispersion methods developed in many countries are presented in Table 2.1 and their purposes, components, and major results will be reviewed. The assessment of air pollution exposure is one of the major applications of air quality models. Danish exposure assessment research (Berkowicz, Winther, & Ketzel, 2006; Berkowicz, 1998; Berkowicz, 2000) will be summarized.

Air quality models based on dispersion methods require many input data and much computing power to generate acceptable results over both space and time. As an alternative to these models, land use regression (LUR) models have been recently developed and applied to high-resolution pollution mapping. Generally, traffic related variables are considered as major

and significant predictors in LUR equations. In addition, many land uses have been tested as explanatory variables for pollution concentrations. Generally, LUR studies present reliable coefficients of determination (R^2), with a range of 0.5 to 0.8, using monitored data (Hoek et al., 2008). With the development of GIS technology, variables potentially related to air pollution concentrations can be obtained in much less time and at lower costs, as compared to dispersion-based approaches, including measures of traffic, land uses, density, and meteorological factors. These variables are assessed for various buffers and used as explanatory variables. In addition, measuring explanatory variables at unsampled sites allows for predicting pollution concentrations, resulting in air pollution maps, one of the major applications of the LUR approach. The air quality models based on LUR methods and their applications will also be reviewed.

2.2.2 Air Quality Models Based on Emissions Inventory and Dispersion Methods

One of the fundamental goals in predicting urban air quality is to provide decision support with regard to reducing the negative impacts of air pollution. The decision support system can be used to assess air pollution exposure, develop least-cost emission control methods, and evaluate air pollution reduction policies. In 1998, a decision support system of urban traffic air pollution for local administrators was developed in Florence, Italy. This system is composed of three sub-modules, including a traffic model, an emission model, and a dispersion model. The three sub-modules are integrated into a GIS program, allowing for the mapping of traffic flows, emissions, and concentrations (Gualtieri & Tartaglia, 1998).

IMULATE (Integrated Model of Urban LAnd-use and Transportation for Environmental analysis) was developed to simulate and map air pollution in the Metropolitan Area of Hamilton, Canada, utilizing a vehicle emission model (MOBILE5C[17]), a dispersion model (CALINE4[18]), and spatial mapping, using universal kriging interpolation methods. Since the emissions of motor vehicles are the major source of CO in urban regions, IMULATE shows that the maximum CO concentrations occur along major roads in the Hamilton Metropolitan area (Potoglou & Kanaroglou, 2005).

---

[17] MOBILE is a vehicle emission factor model developed by the US EPA. The most recently released version is MOBILE6, which is used to predict gram per mile emissions of HC, CO, NO_x, CO_2, PM, and other air toxics. http://epa.gov/OMS/mobile.htm

[18] CALINE4 (CAlifornia LINE Source Dispersion Model, Version 4) is used to assess CO impacts by transportation, which is the standard modeling program of the California Department of Transportation. The software and user's guide are downloadable. (http://www.dot.ca.gov/hq/env/air/index.htm) The California Air Resources Board provides links of diverse air quality models and documents at the following website: http://www.arb.ca.gov/HTML/Soft.htm

TEMMS (Traffic Emission Modelling and Mapping Suite) has been developed to estimate vehicle emissions in urban road networks, and is one of the sub-programs of the Quantifiable City Model, a strategic model of urban sustainability (May, Mitchell, & Kupiszewska, 1997). The Quantifiable City Model has been developed under a program of the UK Research Council, "Towards the Sustainable City". TEMMS includes SATURN (Simulation and Assignment of Traffic to Urban Road Networks), a traffic modeling program, ROADFAC (calculating emission rates for a road link), an emission model, and Airviro (SMHI, 2006)[19] or ADMS (Atmospheric Dispersion Modelling System)[20], a dispersion model. TEMMS has been applied to Leeds, UK, and the model performance has been assessed by using monitored NO_2, CO, PM10, and SO_2 concentrations. The deviations of the calibrated values from the monitored ones are -3.8 % for NO_2, 12.1 % for CO, 16.1 % for PM10, and -0.6 % for SO_2 (Namdeo, Mitchell, & Dixon, 2002).

In general, traffic-induced pollutants are highly concentrated in street canyons, in which the dilution of traffic emissions is limited by the buildings flanking both sides of the street. As seen in Figure 2.2, when wind is blowing in a direction perpendicular to the street, the vortex inside the street canyon is clearly observable (middle picture), and the canyon wall at the upwind (leeward side) building has the highest pollution concentration (bottom picture) (Schatzmann et al., 1998). OSPM (Danish Operational Street Pollution Model) has been developed based on CAR (Calculation of Air Pollution from Road traffic), a Dutch traffic pollution model. In the OSPM, a plume model, for direct impacts of traffic emissions, and a box model, for pollutants recirculated within the street canyon by the vortex flow, are combined. The OSPM estimates hourly concentrations of CO, NO_2, NO_x, O_3, and benzene with the input data of street configurations, hourly traffic flows, meteorological factors, and background concentrations. The hourly modeled and monitored NO_x concentrations are well correlated ($R^2 = 0.89$, N = 4,275) at Jagtvey street in Copenhagen, Denmark. The street is busy (22,000 vehicles/day), has a 25 m width, and is flanked on both sides by 18-meter buildings (4~5 stories) (Berkowicz, 1998). To improve model estimation, especially for irregular street configurations and a variety of metrological conditions, two more sets of monitored data for NO_2 concentrations have been tested, including the streets of Albanigade in Odense, Denmark, and Schildhorstrasse in Berlin, Germany. The fit between measured and modeled NO_2 is very good for Albanigade ($R^2 = 0.90$, N = 2,368), but larger scatters between monitored and modeled values are observed for Schildhornstrasse ($R^2 = 0.52$, N

[19] http://www.indic-airviro.smhi.se/

[20] http://www.cerc.co.uk/software/pubs/ADMS%204%20User%20Guide.pdf

= 3,275) (Berkowicz, 2000). As discussed in the section on the chemical reactions of NO_x and O_3, NO_2 concentrations are directly influenced by nearby O_3 concentrations, because freshly emitted NO from motor vehicles reacts with O_3 to be converted into NO_2 (Eq. 2.1). Thus, a pollution estimation model, such as OSPM, that includes chemical reactions in the modeling process, must incorporate the correct concentrations of reactants. In the Schildhornstrasse case, the concentration of O_3 used in the OSPM model is an average measure from 3 monitoring stations located in the suburbs of Berlin. As discussed in the review of the empirical evidence on monitored O_3, the O_3 concentrations at roadside AQMs are significantly lower than those at background AQMs. This may be a possible reason for the lesser fit between monitored and modeled values in the Berlin case.

TEIS (Traffic Emission Information System) has been developed to predict traffic induced air pollution in Hong Kong. TEIS is composed of three modules: traffic flow model, traffic emission model, and atmospheric dispersion model. A GIS framework is applied to visualize and analyze the results of these sub-models. A dynamic traffic assignment with three travel options (random turning trip, preferred turning trip, and shortest path) is simulated, and the assignment results are in good agreement with six traffic counting data sets (three tunnels and three counting stations). Hong Kong had adopted the EU emission standards since 1995, and the COPERT II[21] emission factor program developed by the European Environmental Agency (EEA) is used to calculate emission rates. Comparing the estimated hourly emission rates of CO, NO_x, and PM10 with the corresponding monitored pollution concentrations provides good correlation coefficients (R^2 = 0.80 ~ 0.84 for CO, R^2 = 0.74 ~ 0.86 for NO_x, and R^2 =0.82 ~ 0.85 for PM10) (Xia & Shao, 2005).

A GIS-based decision support system has been developed for big cities in Turkey, and is used by government agencies to control local air quality and analyze the impacts of pollution abatement policies. The system is composed of an emission factor model and a dispersion model (CALPUFF[22]). Emission inventories are categorized as point, line, and area sources, representing industrial, traffic, and domestic heating sources, respectively. Because of the lack of a transportation planning process, this study includes traffic emissions from seven major roads only.

---

[21]COPERT II (Computer programme to Calculate Emissions from Road Transport) has been developed by EEA and a new version, COPERT III, has been released in 2000. http://reports.eea.europa.eu/TEC05/en

[22]CALPUFF is an air quality modeling system considering non-steady-state meteorological conditions, which has been adopted by US EPA's Guidelines on Air Quality Models (*ibid.*). The system is composed of three parts: CALMET (a meteorological model), CALPUFF (an air quality dispersion model), and CALPOST (a post-processing package). http://www.src.com/calpuff/calpuff1.htm

Comparisons between average modeled concentrations and monitored concentrations at four AQMs provide an overall accuracy of 68% for SO_2 and 52% for PM (Elbir, 2004).

Another air quality model utilizing a GIS to estimate the spatial distribution of traffic-related emissions has been developed for Taichung city, Taiwan. This model includes an emission factor module to calculate traffic emissions based on vehicle kilometers traveled (VKT), and emission factors of nine types of vehicles. The length of a road segment within a gridded cell (0.5 km × 0.5 km), monitored traffic counts, and fleet composition data are used to compute VKT. CALINE4 is a simple line source Gaussian dispersion model adopted to simulate receptor concentrations. This study evaluates two traffic management policies in terms of air quality enhancement: (1) upgrading 2-stroke motorcycles (MC) to 4-stroke ones, and (2) increasing average vehicle speed by 5 km/h. The air quality model results indicate that MC upgrading reduces by 10% total suspended particulates, and increasing travel speed reduces by 14% CO emissions (Lin & Lin, 2002).

The Finnish Meteorological Institute (FMI) has developed an integrated air quality modeling system, including two dispersion models, the UDM-FMI (urban dispersion model) and CAR-FMI (road network dispersion model), and a Meteorological Pre-Processing model (MPP-FMI) (Karppinen et al., 1997). The integrated air quality model also combines EMME/2[23], a transportation planning program, and LIISA[24], a traffic emission calculation software. Stationary sources, including power generation, industry, and residential areas, are considered in the integrated model. The CAR-FMI is based on the Gaussian diffusion model for a finite line source, using meteorological parameters calculated from the MPP-FMI. As discussed in the review of the O_3 empirical evidence, O_3 near the road network is quickly scavenged by the oxidation of NO to NO_2. Therefore, the concentrations of background O_3 are higher than those of roadside O_3. This is commonly observed in modern cities, such as Daegu Metropolitan Area, South Korea (Jo & Park, 2005), New York, US (Gregg et al., 2003), Birmingham, UK (Coyle, Smith, Stedman, Weston, & Fowler, 2002), and Connecticut (Yang & Miller, 2002). The integrated model takes into account the chemical interdependence between O_3 and NO_x. To illustrate the predicted distribution of pollution, concentrations have been calculated at 10,000 grid receptors covering the entire Helsinki area, with spacing of 50 meters in the vicinity of major roads, 100 meters for downtown, and 500 meters in other areas (Karppinen, Kukkonen, Elolähde, Konttinen, & Koskentalo, 2000).

---

[23]Travel demand forecasting software. http://www.inro.ca/en/products/emme/index.php

[24]LIISA is developed by Technical Research Centre of Finland to calculate vehicle-induced emission gas. http://lipasto.vtt.fi/liisae/index.htm

To assess the performance of the integrated air quality model, four monitoring stations in the Helsinki metropolitan area have been selected, and various statistics, such as the index of agreement, the correlation coefficient, the normalized mean square error, and the fraction bias, are calculated. Since the correlation coefficients vary between 0.5 and 0.65 (N = 8,760, hourly NO_2 concentrations in 1993), the results of the integrated air quality model can be used in the decision support system.

As discussed above, air quality models have been developed all over the world, and three sub-modules -transportation planning, emissions calculation, and dispersion process- are common in most of these models. Some air quality systems use traffic counts data as direct input (Turkey and Taiwan), and therefore transportation planning is not integrated into the modeling process. Otherwise, either by developing new transportation models (Canada and UK) or by using commercial software (Italy, Hong Kong, and Finland), traffic assignment, with an origin/ destination matrix (O/D) and a network, is a key module to simulate urban traffic. While traffic assignment is an important starting point for air quality modeling, the validation of assignment results is rarely discussed.

An emission factor-based approach is widely accepted for the estimation of traffic-generated pollution. The reliability of the emission factor model, however, depends upon the fit between assigned and real traffic volumes, the estimated vehicle speeds, fleet composition, temperature conditions (hot or cold-start), Reid vapor pressure of gasoline, and the accuracy of the applied emission factors. Emission factors have a direct influence on the credibility of emission calculations. Therefore, it is necessary to develop state-of-the-art emission factors covering all types of vehicles currently operating in the study areas. CORINAIR (The Core Inventory of Air Emissions in Europe) was updated in 2006[25], and MOBILE, a vehicle emission modeling software developed by the US EPA, had a new version, MOBILE 6.2, released in 2003.

Dispersion models calculate the final outcomes of the air quality modeling process, the concentrations of traffic-related pollutants at receptor locations. Depending on their purposes, dispersion models can cover diverse study areas, from the street to the region. Combining GIS with the outcomes of dispersion models allows for mapping concentrations in the study areas. Because of the exponential decrease in traffic-related concentrations with distance from the road (Roorda-Knape et al., 1998), the resolution of air pollution maps must be high enough to identify concentrations decreasing away from the roads. The air quality model developed in Finland

[25] http://www.eea.europa.eu/publications/EMEPCORINAIR4

produces a fine resolution of receptor concentrations to represent these pollution gradients, but a Cray C94 super-computer is used for the calculations.

AirGIS is a Danish decision support GIS tool to manage urban air quality and assess human exposure. The OSPM (Danish Operational Street Pollution Model) reviewed earlier is combined with cadastral databases to create AirGIS. To estimate ambient air quality levels and human exposures at residences and workplaces, the numbers of families living at residences and the numbers of employees working at companies are identified, with addresses, and a geocoding process[26] is applied to identify geographic locations. Assessing exposure with only outdoor air quality and the spatial distribution of the population is a crude process, because it does not consider individual activities over space and time (Briggs, 2005). Detailed exposure assessment should include air quality levels both indoor and outdoor, with individual activity profiles (Jensen, Berkowicz, Sten Hansen, & Hertel, 2001). Nonetheless, AirGIS can be used as a decision support tool for the locations of new kindergartens, elementary schools, or hospital. The selected locations for these facilities minimize users' exposure to air pollution. In addition, AirGIS can help to design land-use regulations that guarantee that pollution exposure is within the air quality standards. Finally, diverse pollution-related policies, such as subsidy of catalytic converters, strict emission standards, alternative fuels, and transportation demand management, can be evaluated using AirGIS.

[26] Process of assigning coordinates according to addresses (Cameron & Environmental Systems Research Institute, 2005)

Program	Purpose	Modules	Study region	References
Predicting urban traffic air pollution	Develop a decision support system to reduce air pollution impacts caused by traffic.	Traffic: user equilibrium assignment with O/D and network Emission: emission factor model w/ traffic flow and average speed Dispersion: street canyon model and Gaussian dispersion model	Florence Italy	Gualtieri & Tartaglia, 1998
IMULATE (Integrated Model of Urban Land-use and Transportation for Environmental analysis)	Impact assessment of land-use and transport policies on traffic flows and emissions. Evaluation of population exposure to traffic-related pollution.	Traffic : IMULATE Emission: MOBILE5.C Dispersion: CALINE4 Mapping: Interpolation (Universal Krigging)	Hamilton Canada	Potoglou & Kanaroglou, 2005
TEMMS (Traffic Emission Modelling and Mapping Suite)	Estimates of vehicle emissions, air quality mapping, evaluation of transportation policies, and inputs to other (e.g., epidemiological) models.	Traffic: SATURN Emission: ROADFAC Dispersion: Airviro or ADMS Mapping: MapInfo w/ VB	Leeds UK	Namdeo & Colls, 1996; Namdeo et al., 2002
OSPM (Danish Operational Street Pollution Model)	Development of a mathematical model for street scale, considering vortex flows caused by winds and turbulence generated by traffic flows.	Traffic emission: CAR (Calculation of Air Pollution from Road Traffic) Dispersion: Simplified Canyon Plume and Box Model	Copenhagen Denmark	R. Berkowicz, Winther, & Ketzel, 2006; R. Berkowicz, 1998; R. Berkowicz, 2000
TEIS (Traffic Emission Information System)	Establish a traffic information database for Hong Kong, considering traffic flow simulation and traffic induced air pollution.	Traffic: revised dynamic traffic assignment with O/D and network Emission: emission factor model w/ traffic flow and fraction of vehicle	Hong Kong	Xia & Shao, 2005
A GIS based decision support system for estimation of air pollution	Develop air quality management system to support local government agencies. Mapping of air pollution at high temporal and spatial resolutions.	Emission source: Industry, domestic heating, traffic Emission inventory: Emission Factor Model Dispersion: CALPUFF	Izmir Turkey	Elbir & Muezzinoglu, 2004; Elbir, 2004
Air quality analysis	Estimate traffic emission inventory and spatial distributions of pollutants. Predict emission changes due to traffic management policies.	Traffic: traffic counts Emission: Emission Factor Model Dispersion: CALINE4	Taichung Taiwan	Lin & Lin, 2002
UDM-FMI (Urban Dispersion Modelling - Finnish Meteorological Institute) CAR-FMI (road network dispersion model)	Develop UDM-FMI and CAR-FMI. Compare modeled and monitored concentrations	Traffic: EMME/2 Emission: LIISA Dispersion: MPP-FMI, UDM-FMI and CAR-FMI Post-processing: statistical and graphical analysis	Helsinki Finland	Karppinen et al., 2000; Karppinen, Kukkonen, Elolähde, Konttinen, & Koskentalo, 2000; Kukkonen, Härkönen, Walden, Karppinen, & Lusa, 2001

Table 2.1 Comparison of urban air quality models based on emission inventory and dispersion modules

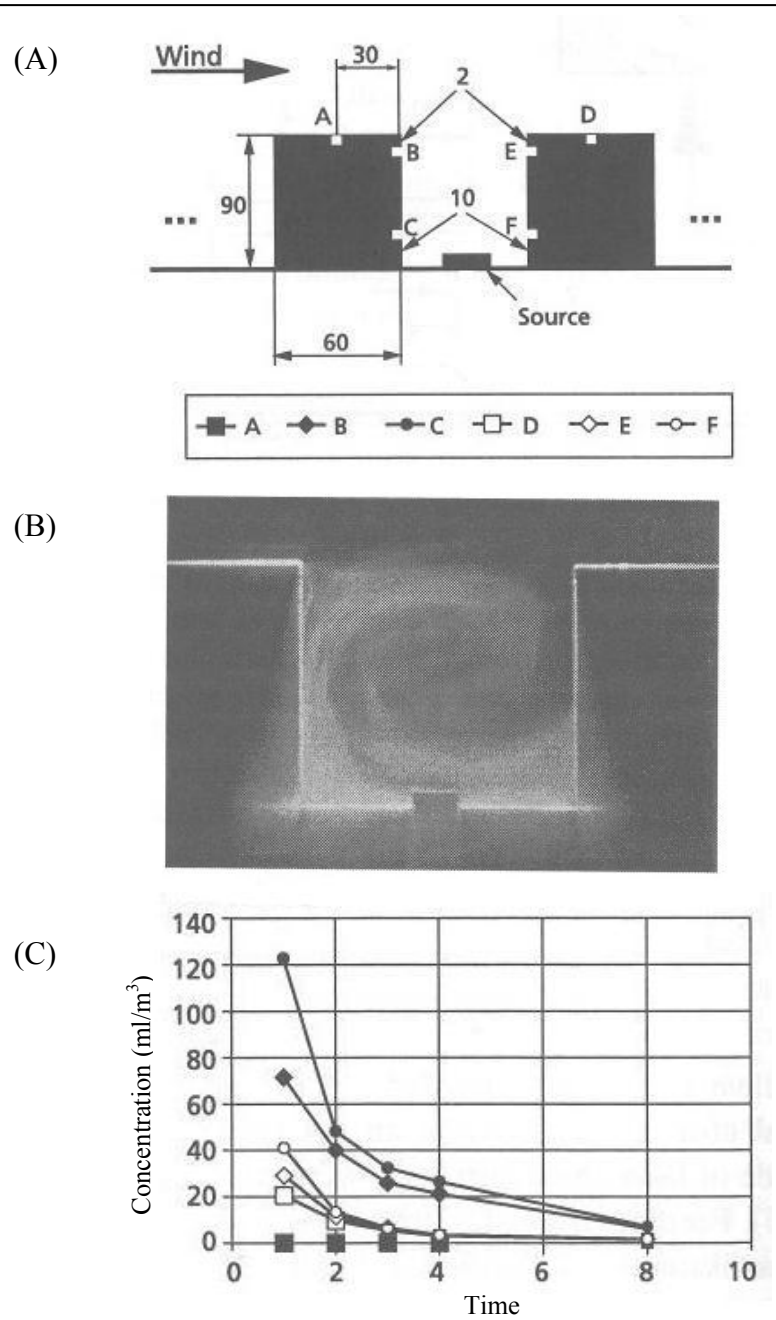

(A) Design of experiment and positions of concentrations measuring points

(B) Observed vortex in street canyon

(C) Concentrations at the measuring points

Figure 2.2 Concentrations in an urban street canyon with a line source placed halfway between two buildings[27]

[27] Adopted from Figures 14.11 and 14.13 in (Schatzmann, Rafailidis, & Duum, 1998).

2.2.3 Air Quality Models Based on Land Use Regression Methods

Attempts to explain the relationships between monitored air pollution concentrations and land uses have expanded with the improvement of Geographic Information System (GIS) techniques. Data on diverse land uses, identified and calculated for various buffers using GIS, have been used in linear regression models to explain the observed spatial variability of pollution concentrations. Pioneering research for land use regression (LUR) was initiated in the SAVIAH (Small Area Variations In Air Quality and Health) study sponsored by the European Union (Briggs et al., 1997). Since the explanatory variables used in the regression model are obtained through GIS, it is possible to calculate the values of the explanatory variables for the entire study region. Therefore, prediction of the air quality in unsampled areas and the mapping of air pollution based on this prediction have been implemented in several LUR studies. NO_2 maps have been estimated in Huddersfield, UK, and Amsterdam, Netherlands (Briggs et al., 1997), Toronto, Canada (Kanaroglou et al., 2005), Hamilton, Canada (Sahsuvaroglu et al., 2006), San Diego, CA (Ross et al., 2006), and Oslo, Norway (Madsen et al., 2007). Air pollution maps for particulate matters (PM) are also been generated in several studies, including New York City and adjacent counties (Ross, Jerrett, Ito, Tempalski, & Thurston, 2007) and on the European continent (Beelen et al., 2009). Based on the predicted pollution map, an epidemiological study has been implemented in Sadabell, Spain (Aguilera et al., 2008), and long-term exposure to traffic-related pollution has been assessed in the Netherlands (Beelen, Hoek, Fischer, Brandt, & Brunekreef, 2007). Since land uses in urban areas determine movements of freight and passengers, poorly designed urban development plans can increase the levels of vehicle emissions, resulting in temporal and spatial pollution hotspots. Scenario-based future land-use plans were introduced to evaluate impacts on air quality in Southwest California (Kahyaoğlu-Koračin, Bassett, Mouat, & Gertler, 2009). As expected, traffic-related variables, such as traffic density, traffic volume, VKT, distance from highway, and length of highway, high density residential areas (population density), commercial areas, and industrial land uses, are all positively correlated with NO_2 concentrations (Aguilera et al., 2008; Beelen et al., 2007; Briggs et al., 1997; Gilbert, Goldberg, Beckerman, Brook, & Jerrett, 2005; Kahyaoğlu-Koračin et al., 2009; Ross et al., 2006; Sahsuvaroglu et al., 2006; Smith et al., 2006). On the other hand, open space, including urban forests, parks, and water bodies, is negatively correlated with NO_2 concentrations (Henderson, Beckerman, Jerrett, & Brauer, 2007; Kanaroglou et al., 2005).

The SAVIAH project is known as the first attempt to model air quality using a land use regression approach. LUR models are developed with measured NO_2 concentrations and explanatory variables, including land cover (high density residential and industrial uses), traffic

flows (monitored and estimated flows), and altitude. Annual NO_2 concentration maps are generated for two regions, Huddersfield, UK and Amsterdam, Netherlands. The R^2 values of the regressions are 0.82 for Huddersfield, and 0.87 for Amsterdam. There are comparable to the reported performances of other dispersion-based approaches (Briggs et al., 1997). In terms of performance, LUR approaches have generally displayed relatively good outputs, with R^2 ranging from 0.6 to 0.8, as illustrated in Table 2.2. Briggs et al. (2000) compare the performance of three types air quality modeling approaches, including a dispersion model (CALINE-3), three interpolation methods (contouring, kriging, and trend surface analysis), and LUR modeling, all applied to Huddersfield, UK. The results indicate that the LUR model generates the highest R^2.

Since the EU-funded SAVIAH project, several LUR-based air quality models have been implemented in European countries, including NO_x analysis in Oslo, Norway (Madsen et al., 2007), NO_2 and PM2.5 analyses in North-Rhine Westphalia, Germany (Hochadel et al., 2006), and NO_2 and BTEX[28] analyses in Sabadell, Spain (Aguilera et al., 2008). As expected traffic-related variables, such as road length, traffic flows, and distance to nearest road, are selected as key explanatory variables. In addition, land uses around air quality monitoring stations and altitude are also used as predictor variables, resulting in good performance of model outputs (R^2 range 0.66 ~ 0.90).

For epidemiologic purpose, air quality models have been estimated in three Canadian cities: Montreal (Gilbert et al., 2005), Hamilton (Sahsuvaroglu et al., 2006), and Vancouver (Henderson et al., 2007). Traffic variables, population density, and land uses, such as residential, commercial, and industrial areas, are positively associated with NO_2 and PM2.5 concentrations, whereas open space and distance to Lake Ontario have negative relationships with pollutants. Updatable and high-resolution air pollution maps are made possible with LUR approaches with less input data and computational requirements as compared to conventional air quality models based on emission inventories and dispersion modeling. The explanatory variables used in LUR models are transportation-related variables, land uses, and demographic variables, which can be simply assessed with GIS. Therefore, the air pollution maps based on LUR models can be generated with less expenses and labor inputs. Samples of estimated pollution maps are displayed in Figure 2.3.

Since air quality models based on LUR approaches are empirical models, derived from monitored air pollution concentrations and explanatory variables, the transferability of the estimated coefficients to other locations is inevitably problematic. Metropolitan areas have their

[28] BTEX: benzene, toluene, ethylbenzene, and xylene

own patterns of pollution concentrations, traffic flows, and land uses, thus the LUR models need to be estimated case by case. PM2.5 land use regression models for New York City and surrounding regions are estimated with travel demand forecast and land use data. Five circular buffers with radii of 50, 100, 300, 500, and 1000 m are delineated around air quality monitoring stations and explanatory variables inside these buffers are calculated and used as explanatory variables. Total traffic flows in the 500 m buffer, population in the 1000 m buffer, and industrial area in the 300 m buffer are selected in final model, with $R^2 = 0.64$ (Ross et al., 2007).

Recently, EU-wide air pollution maps, including NO_2, O_3, and PM10 have been generated at a 1 km resolution. Ordinary kriging[29], LUR models, and universal kriging[30] have been developed for three different spatial scales: global, rural, and urban. An EU-wide (1-km resolution) GIS database has been prepared to estimate LUR models at the three spatial scales. Explanatory variables used in the LUR models are land cover data, road with 5 classifications, meteorological factors, and population. The R^2 of LUR models are rather low (0.4 ~ 0.6), because coarser information is used to construct the LUR models. Universal kriging generates better pollution map estimation than other methods, and the R^2 between measured and predicted concentrations are 0.61 for NO_2, 0.70 for O_3, and 0.45 for PM10. The estimated EU-wide O_3 map is presented in Figure 2.3.

The previously discussed LUR models are estimated with air quality data from a given urban region. Shen (2004) and Guldmann and Kim (2001) develop and estimate statistical models with air quality data from large samples of US cities. These models have structures similar to LUR models, where pollution concentrations (SO_2 for Shen, O_3 and CO for Guldmann and Kim) are regressed on land uses, meteorological factors, and socioeconomic variables. Both approaches consider the contributions to pollution concentrations of both local effects (pollution factors around the air quality monitoring station) and regional effects (pollution transported from outside the local area). The regional effects are accounted for by using the observed pollution concentrations at monitoring stations that make up a ring around the central monitoring station.

---

[29] Kriging is advanced geostatistical technique to interpolate the values of unobserved locations from nearby measured values when data is spatially correlated or biased (Environmental Systems Research Institute, 2006).

[30] Universal kriging interpolates unobserved random value variations with regression relationships of predictor variables (Beelen et al., 2009).

Study regions	Pollutants	Predictor Variables	R^2 of Model	References
Huddersfield (UK) Amsterdam (Netherlands) Prague (Czech)	NO_2	Traffic volume with buffer 60 and 60~120 m, Land cover factor w/ buffer 60 m, Altitude, Distance to the nearest road	0.82 0.87 0.79	Briggs et al., 1997
Huddersfield (UK) Northampton (UK) Sheffield (UK)	NO_2	Traffic density in two circular buffers (~40 & 40~300 m), High density housing in a circular buffer (0–300 m), Altitude	0.76 0.58 0.73	Briggs et al., 2000
Oslo (Norway)	NO NO_2 NO_x	Elevation, Length high traffic flow roads within 100 m, Length medium traffic flow roads within 250 m, Length small traffic flow roads within 1000 m	0.66 0.77 0.73	Madsen et al., 2007
North-Rhine Westphalia (Germany)	NO_2	Heavy vehicle traffic 250m, Total traffic 250 m, Maximum traffic 100 m, Building Density	0.90	Hochadel et al., 2006
	PM2.5	Heavy vehicle traffic 100m, Total traffic 100 m, Maximum traffic 100 m, Distance to highway	0.82	
Sabadell (Spain)	NO_x	Altitude, Land cover factor (500 m), Major roads length (50 m), Secondary roads length (500 m)	0.68	Aguilera et al., 2008
	NO_2	Altitude, Land cover factor (500 m), Major roads length (50 m), Secondary roads length (500 m)	0.69	
	BTEX*	Altitude, Distance to nearest major road, Distance to nearest secondary road, Distance to nearest parking lot	0.74	
Montreal (Canada)	NO_2	Distance highway, Traffic count, Length highways within 100 m, Length major roads within 100 m, Length minor roads within 500 m, Open space within 100 m, Population	0.52	Gilbert et al., 2005
Hamilton (Canada)	NO_2	Traffic density 300 m, Industrial 200 m, Open space 500 m, 1500 m downwind highway 403, 50 m from highways, Distance from Lake, Downtown industrial core 1000 m	0.76	Sahsuvaroglu et al., 2006
Vancouver (Canada)	NO	Length of major roads, Population	0.62	Henderson et al., 2007
	NO_2	Highways, Roads, Commercial, Elevation, Population	0.56	
	PM2.5	Elevation, Commercial, Residential ,Industrial area	0.52	
New York city (US)	PM2.5	Traffic within 500 m, Population within 1000 m, Industrial land use within 300 m	0.64	Ross et al., 2007
EU wide	NO_2	High density residential, Major road, Minor road	0.49	Beelen et al., 2009
	PM10	Residential, Altitude, Agriculture, Meteorology	0.41	
	O_3	Altitude, Distance to sea, Residential, Major road	0.62	

* BTEX: benzene, toluene, ethylbenzene, and xylene

Table 2.2 Comparison of urban air quality models based on land use regression method

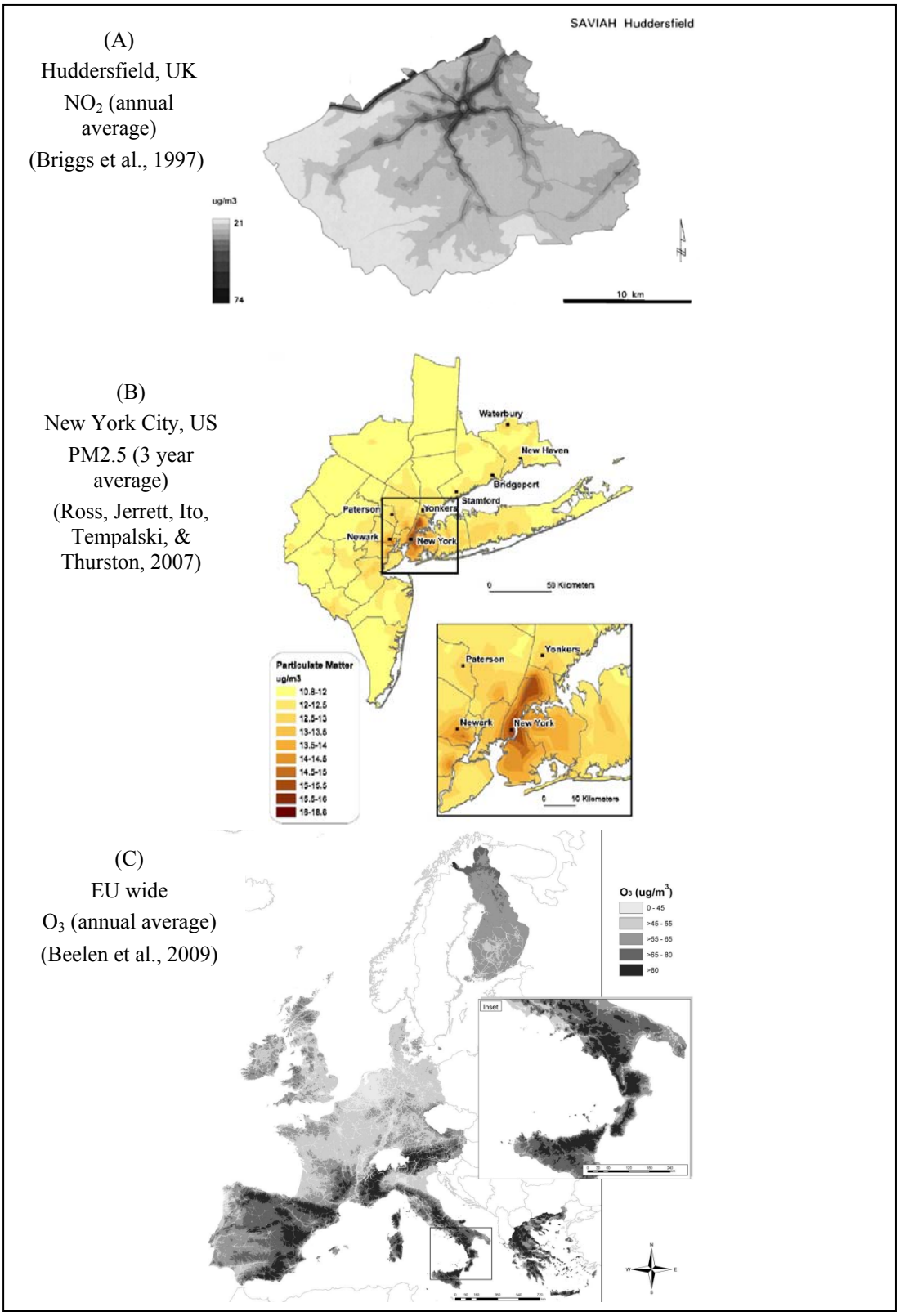

Figure 2.3 Examples of estimated pollution maps

2.2.4 Other Statistical Air Quality Models

Besides LUR regression models, other statistical regression models making use of time-series data have been developed. Because of serial correlations among pollution concentrations, the assumptions of ordinary least squares (OLS) regression are violated. Autoregressive integrated moving average (ARIMA) models relax the assumptions of the OLS error term, and thus have been used to investigate the relationships between serially measured pollution concentrations and meteorological factors.

The general form of a regression model explaining the relationships between the pollutant concentration, *C*, and *K* explanatory variables is expressed as follows:

$$C_j = \alpha + \sum_{i=1}^{K} \beta_i X_{ij} + u_j \qquad j = 1, \cdots, \mathrm{N} \tag{2.30}$$

where $X_1, \ldots, X_K$ are the explanatory variables, including generally emission sources, meteorological factors, socio-economic variables, lags of the dependent variable, and seasonal dummy variables; N is the total number of observations; the β_i's are the coefficients to be estimated; and u_j is the stochastic error term. If the error term follows the assumptions of the classic linear regression model, one can apply OLS estimation. Chock et al. (1975) discuss the problem of OLS with serially correlated air quality data. Milionis and Davies (1994) review diverse methods to correct for the autocorrelated disturbances, including the autoregressive process of order p [AR(p)], the moving average process of order q [MA(q)], the mixed autoregressive moving average process of order p, q [ARMA(p,q)], the lag-dependent variable(s) among the regressors, and Box-Jenkins (ARIMA) models.

Shi and Harrison (1997) develop a first-order autocorrelation model with hourly-measured NO_x and NO_2 concentrations. Meteorological factors, such as wind speed, boundary layer depth, temperature, Pasquill stability category, relative humidity, and solar radiation, are used as explanatory variables. The first-order time-series error model yields better results than the ordinary regression model. However, Durbin-Watson (DW) statistics are not provided with the results of the time-series model, and it is not possible to confirm if possible serial correlation has been corrected. The first-order time-series model used in this study is:

$$\ln(C_j) = B_1 + \sum_{i=2}^{k} B_i \ln(X_{ij}) + u_j \tag{2.31}$$

$$u_j = \emptyset u_{j-1} + \varepsilon_j, \quad j = 1, \cdots, N \tag{2.32}$$

where B_i and $\emptyset$ are parameters, C_j are hourly measured NO_x and NO_2 concentrations, and X_{ij} are hourly measured meteorological factors. Diverse meteorological factors, such as wind speed, boundary layer depth, temperature, Pasquill stability category, relative humidity, and solar radiation, are included in the model, but the theoretical rationale is not sufficiently discussed, and it is therefore difficult to understand why these variables have positive or negative impacts on NO_x and NO_2 concentrations.

Daily average PM2.5 concentrations measured over 2000 ~ 2002 in Steubenville, OH, are modeled using an ARIMA model with several explanatory variables, including gaseous pollutants (CO, NO_x, SO_2, and O_3) and meteorological factors (temperature, wind speed, relative humidity) (Connell et. al, 2005). The autoregressive model is:

$$\begin{aligned}\ln(PM_{2.5}) = {} & \omega_0 + (\omega_1 + \omega_2 S)\ln(NO_x) + \omega_3 \ln(CO + 0.1) + \omega_4 \ln(SO_2) + \omega_5\sqrt{O_3} \\ & + (\omega_6 + \omega_7 S)Temp + \omega_8 \ln(WS) + \omega_9 RH^{1.5} + \frac{\varepsilon}{1-\varphi B}\end{aligned} \tag{2.33}$$

where ω_i and φ are parameters to be estimated, and S is equal to 1 in Summer and 0 all other days. All estimated parameters are statistically significant, at the 0.05 level. As expected, the concentrations of NO_x and SO_2 are positively correlated with PM2.5 concentrations, because NO_x and SO_2 have the strong potential to be converted into fine particulate matters. Although linear combinations of the Summer dummy variable are introduced in the coefficients of NO_x and temperature, the interpretations of these parameters are missing. Intuitively, NO_x emissions are smaller in Summer than in the other seasons, but temperature in Summer is higher, and therefore ω_2 is expected to be negative and ω_7 positive. The results support these expectations.

Peak daily 1-hr O_3 concentrations are analyzed with a regression of time-series error (RTSE) model in Milwaukee, WI (Liu and Johnson, 2002). The RTSE model includes a principal component (PC) trigger to predict O_3 concentrations when the level of O_3 is above 100 ppb. During regular days, the model forecasts O_3 concentrations without the PC trigger, but, for high-ozone days, the PC trigger is included in the RTSE model to correctly predict high episode of O_3 concentrations. The RTSE model with the PC trigger is:

$$\ln(O_3) = \omega_0 + \omega_1 Temp + \omega_2 WindDir + \omega_3 PC + \frac{a_t}{1 - \varphi_1 B - \varphi_2 B^2} \quad (2.34)$$

$$PC = \gamma_1 Temp + \gamma_2 NO_x + \gamma_3 WindDir \quad (2.35)$$

where the error term follows an AR(2) time-series model and B is a backward shift operator, thus $\varphi_1 B Y_t = \varphi_1 Y_{t-1}$ and $\varphi_2 B^2 Y_t = \varphi_2 Y_{t-2}$. Since the PC trigger is applied to account for the high concentrations of O_3, the estimated results reduce the under-prediction of high O_3 concentrations. The inclusion of the PC trigger increases the R^2 from 0.68 to 0.81. Despite the fact that UV rays are essential in the creation of O_3, solar radiation is not selected in the final model represented by Eqs. (2.34) and (2.35).

2.3 SUMMARY

Conventional air quality models based on emission inventories and dispersion processes have limitations that prevent their implementation, including large data requirements and computational burdens. In contrast, as an alternative approach, LUR modeling, displays potential for future implementations. Traffic-related data represent significantly good explanatory variables in LUR models. Hence, as most metropolitan areas use traditional transportation planning for traffic flow estimation, these estimated traffic flows can be validated with monitored flows and used as input data in LUR models (Briggs, 2007). There is not much empirical research examining the temporal and spatial relationships between pollution concentrations and estimated traffic flows. Since concentrations of air pollutants vary widely, depending on the hour of the day, and these variations are closely associated with traffic flows, it is technically possible to generate dynamic maps of pollution concentrations with LUR models and hourly traffic flows.

Distances between emission sources and receptors play key roles in determining concentrations at receptors. Since little is known about the size of the area affected by emission sources, it is necessary to identify the buffer size appropriate to explain these relationships. Recently developed LUR models have tried to establish relationships between monitored pollution concentrations at AQMs and surrounding land uses. Generally, buffer size in LUR models varies from a few hundred to several thousand meters (Briggs et al., 1997; Carr et al., 2002; Gilbert, Goldberg, Beckerman, Brook, & Jerrett, 2005; Jerrett et al., 2007; Ross et al., 2006; Sahsuvaroglu et al., 2006). Systematic investigations of the impacts of buffer sizes are, however, rare in LUR models.

As discussed earlier in Section 2.2.4, diverse time-series regression models have been developed to deal with serially-correlated air quality data. Although pollution concentrations and explanatory variables, such as VKT, are measured over both time-series and cross-sections, combined time-series cross-sectional regression models have rarely been implemented. In addition, significant chemical interactions between pollutants (e.g. NO_2 vs. O_3) have been reviewed, that would require a simultaneous equations model approach. This is also a gap in the existing literature.

CHAPTER 3

METHODOLOGY

This chapter presents a framework for the estimation of statistical air quality models for a metropolitan area with clearly delineated boundaries. These models are grouped in two categories: aggregate temporal models and cross-sectional models. Aggregate temporal models focus on the variations in city-wide pollutant concentrations across the week (weekdays vs. Sunday) and over broad geographical areas (roadside vs. urban background). Cross-sectional models focus on the local impacts of traffic flows, land uses and meteorological factors on pollution concentrations as measured at a large sample of air quality monitoring stations (AQMs). Regression models for pollution concentrations are developed for NO_2, CO, O_3, SO_2, and PM10.

3.1 CONCEPTUAL FRAMEWORK

Population growth, land-use changes, and increases in traffic flows and vehicle-kilometers-travelled (VKT), all affect the air quality of metropolitan regions. Transportation is a major air pollution contributor. In addition, land uses, such as residential, commercial, industrial, and green areas, also influence urban air quality. Since the shares of emissions from traffic and land uses vary across space, air pollution concentrations are also likely to vary across geographic locations. The intensity of traffic flows, anthropogenic activities taking place in different land uses, and variations in meteorological factors, such as solar radiation, wind speed, temperature, and humidity, have also a temporal pattern, hence pollution concentrations vary over both time and space. Since emitted pollutants undergo chemical reactions under specific meteorological conditions, air quality models must consider these chemical interactions, in addition to emission intensities and meteorological factors.

Traffic flows are closely correlated with the concentrations of several directly emitted pollutants (NO_2, CO, SO_2, and PM10) and a secondary pollutant (O_3). It has been demonstrated that heavy traffic flows lead to higher pollution concentrations of directly emitted pollutants. However, in the case of O_3, concentrations on weekends are higher than those on weekdays. As

discussed in the O_3 chemistry section in Chapter 2, decreased vehicle emissions in NO_x-saturated regions provide better conditions for the creation of O_3. This counterintuitive phenomenon is observed when comparing O_3 concentrations on weekdays and Sunday, as well as at roadside AQMs and urban background AQMs. To measure the different spatio-temporal impacts of traffic flows and meteorological factors on directly emitted and secondary pollutant concentrations, concentrations averaged out along four groups – weekday-background, Sunday-background, weekday-roadside, and Sunday-roadside – will be examined.

As discussed in Chapter 2, air quality modeling research can be classified into two broad streams: (1) dispersion models with pollution inventory and (2) land-use regression (LUR) models. Air pollution inventory and dispersion models are costly in terms of input data and computation. In contrast, LUR models have become more attractive because improvements in GIS techniques allow for the easy collection of the needed land-use and transportation-related data. The LUR model relating monitored pollution concentrations and potential explanatory variables, including VKT and land uses, provides a basis for predicting pollution concentrations at a high level of spatial resolution. In addition, dependent (pollution concentrations) and independent (VKT) variables can be measured over both time and space, and hence diverse time-space models can be formulated and estimated, depending on the research purposes.

This chapter outlines the proposed research methodology. First, exploratory analyses of the dependent and independent variables (VKT, land uses, and meteorological factors) are to be conducted, in order to uncover basic spatial and temporal patterns in these variables. These patterns are to generate fundamental hypotheses on causal relationships, including the impacts of traffic flows and meteorological factors on pollution concentrations, and chemical reactions among pollutants. In order to test the hypothesis that reduced traffic flows impact pollution concentrations, aggregate temporal models are proposed and estimated. Finally, based on LUR approaches, cross-sectional regression models are considered to explain the pollution concentrations observed across all AQMs within a metropolitan area.

3.2 EXPLORATORY ANALYSES

The concentrations of five air pollutants, NO_2, CO, O_3, SO_2, and PM10, monitored at both roadside and urban background air quality monitoring stations (AQMs), are available on an hourly basis. These concentrations vary both spatially and temporally. Annual, seasonal, monthly, and hourly concentrations patterns are to be analyzed, using descriptive statistics, Box plots[1], and line graphs. Geographical differences can be analyzed by considering the dichotomy between roadside and background AQMs.

Vehicle emissions contribute a major share of urban air pollution. Urban traffic flows generally display two peaks, in the morning and evening, and this pattern is expected to be reflected in significant differences in hourly pollution concentrations. By comparing hourly-measured traffic flows with pollution concentrations, it is possible to assess simultaneity and/or lag between these variables. Since meteorological conditions vary both in the short term (hour of day) and long term (season), and anthropogenic emissions also vary over time, descriptive statistics of hourly concentration patterns are to be provided over the four seasons. Similar analyses are to be conducted on comparing the temporal variations of concentrations at roadside and background AQMs.

Differences in traffic flows between weekdays and weekend contribute to differences in pollution concentrations. In the case of directly emitted pollutants, such as CO, NO_x, and SO_2, smaller traffic flows during the weekend are expected to produce lower pollution concentrations. However, in the case of O_3, as discussed earlier, reduced traffic causes less O_3 titration and less inhibition for O_3 creation, resulting in increased O_3 concentrations during the weekend, especially on Sunday and in urban roadside areas. By comparing measured hourly O_3 concentrations on weekdays, Saturday, and Sunday, it is possible to observe when and why this phenomenon occurs.

[1] Box plots are also useful to identify outliers and display data skewness.

3.3 STATISTICAL MODELING

3.3.1 General Model

Different factors, such as mobile and stationary air pollution emissions and meteorological conditions, impact air pollution concentrations at AQMs in a metropolitan area. The general components of a metropolitan air quality system are illustrated in Figure 3.1. Emission sources include all transportation network links and stationary residential, commercial, and industrial sources. Green areas can act as both generators of biogenic volatile organic compounds (VOCs) and as pollution filters. In addition, the whole metropolitan area is subject to background pollution originating beyond its boundary. It is necessary to define the following indices and basic variables:

i: AQM station ($1 \rightarrow N$),

l: Elementary transportation link ($1 \rightarrow L$),

k: Stationary pollution source ($1 \rightarrow K$),

p: Pollutant ($1 \rightarrow P$),

g: Green space ($1 \rightarrow G$),

t: Time ($1 \rightarrow T$),

m: Meteorological factors ($1 \rightarrow M$),

C_{pit}: Concentration of pollutant p at AQM i at time t,

E_{plt}: Emission of pollutant p from transportation link l at time t,

E_{pkt}: Emission of pollutant p from fixed source k at time t,

B_{pt}: Background pollution for pollutant p at time t,

G_{gt}: Green area at location g at time t,

MET_{mt}: Meteorological factor m at time t (assumed spatially uniform).

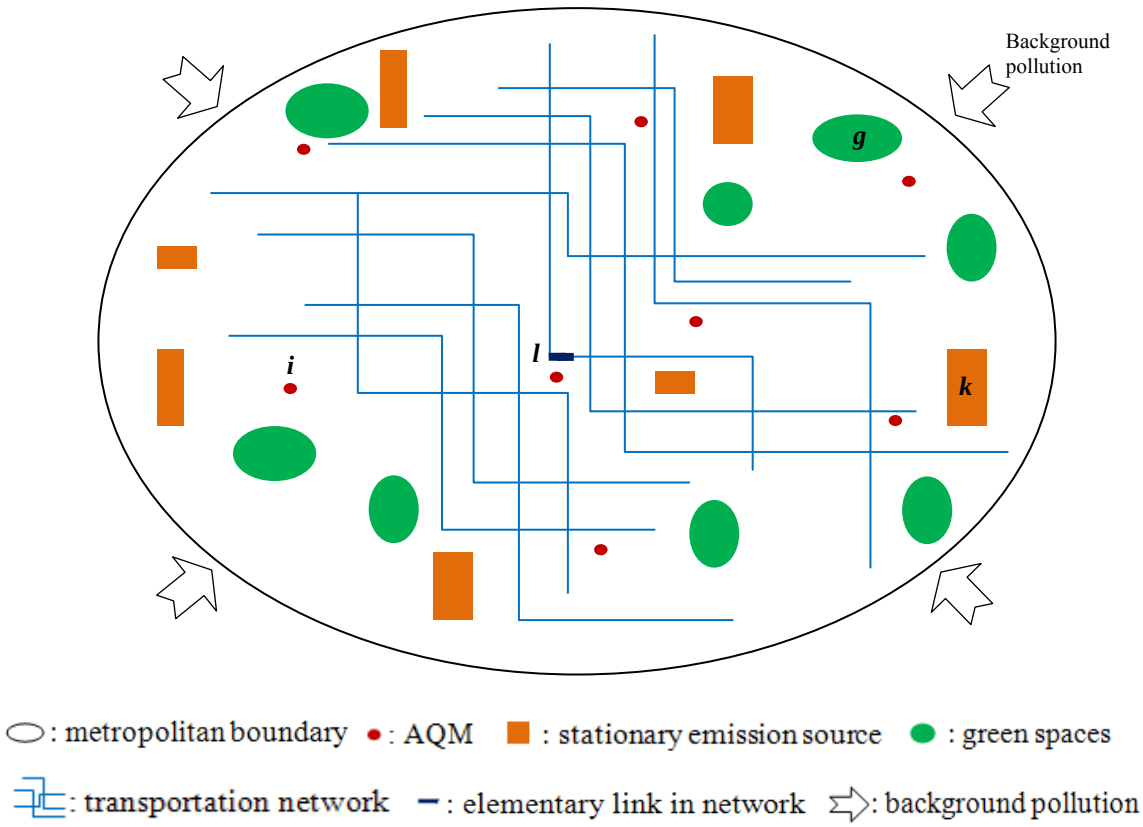

Figure 3.1 Generalized components of a metropolitan air quality system

Given geographical and temporal data on air pollution concentrations and the explanatory variables, a general air quality model linking concentrations to emission sources, background pollution, green areas, and meteorological variables, can be expressed as:

$$\boldsymbol{C}_{pit} = F_i(\boldsymbol{E}_t^T, \boldsymbol{E}_{t-1}^T, \cdots, \boldsymbol{E}_{t-\tau_1}^T;\ \boldsymbol{E}_t^S, \boldsymbol{E}_{t-1}^S, \cdots, \boldsymbol{E}_{t-\tau_2}^S;\ \boldsymbol{B}_t, \boldsymbol{B}_{t-1}, \cdots, \boldsymbol{B}_{t-\tau_3};$$
$$\boldsymbol{G}_t, \boldsymbol{G}_{t-1}, \cdots, \boldsymbol{G}_{t-\tau_4};\ \boldsymbol{MET}_t, \boldsymbol{MET}_{t-1}, \cdots, \boldsymbol{MET}_{t-\tau_5}) \tag{3.1}$$

where:

$\boldsymbol{E}_t^T$: Vector of emissions from transportation links $\boldsymbol{E}_t^T = (\boldsymbol{E}_{plt} \mid p = 1 \to P,\ l = 1 \to L)$,

$\boldsymbol{E}_t^S$: Vector of emissions from stationary sources $\boldsymbol{E}_t^S = (\boldsymbol{E}_{pkt} \mid p = 1 \to P,\ k = 1 \to K)$,

$\boldsymbol{B}_t$: Vector of background pollution $\boldsymbol{B}_t = (\boldsymbol{B}_{pt} \mid p = 1 \to P)$,

$\boldsymbol{G_t}$: Vector of green areas $\boldsymbol{G_t} = (\boldsymbol{G_{gt}} \mid \mathrm{g} = 1 \rightarrow G)$,

$\boldsymbol{MET_t}$: Vector of meteorological variables $\boldsymbol{MET_t} = (\boldsymbol{SOL_t}, \boldsymbol{TEM_t}, \boldsymbol{HUM_t}, \boldsymbol{WS_t}, \boldsymbol{WD_t})$,

$\boldsymbol{SOL_t}$: Solar radiation at time *t*,

$\boldsymbol{TEM_t}$: Temperature at time *t*,

$\boldsymbol{HUM_t}$: Humidity at time *t*,

$\boldsymbol{WS_t}$: Wind speed at time *t*,

$\boldsymbol{WD_t}$: Wind direction at time *t*.

Emissions from transportation (E_{plt}) are a function of the traffic flow on link *l* at time *t* and the length of link *l*. The *VKT* (vehicle-kilometers-travelled) variable is calculated by multiplying the traffic flow over link *l* at time *t*, V_{lt}, by the length of link *l*, d_l, with:

$$VKT_{lt} = V_{lt} \times d_l \tag{3.2}$$

E_{plt} is computed by multiplying pollutant *p* emission factor (e_p) by VKT_{lt}, with:

$$E_{plt} = e_p \times VKT_{lt} \tag{3.3}$$

Since emissions from stationary activities (E_{pkt}) sited at location *j* (1 → *J*) are related to the amount and type of land use *a* (1 → *A*: residential, commercial, industrial, etc.) at location *j* and time *t* (LU_{ajt}), it is assumed that E_{pkt} can be proxied by the land-use area variable, LU_{ajt}, which represents the level of activity related to pollutant emissions (product outputs, energy consumption), with:

$$\boldsymbol{LU}_{ajt} = f(\boldsymbol{E}_{pkt} \mid k \in \text{location } j) \tag{3.4}$$

Green areas play a dual role, emitting biogenic VOCs and filtering anthropogenic pollutants. Plant metabolism is generally correlated with solar radiation intensity, and thus biogenic emissions (or filtering) are a function of the amount of green areas at location *j* and time *t*. The corresponding land-use relationship is presented by:

$$\boldsymbol{LU}_{gjt} = h\left(\boldsymbol{G}_{gt} \mid g \in \text{location } j\right) \tag{3.5}$$

As an illustration of the above discussion, the land uses and transportation network of the Seoul Metropolitan Area are presented in Figure 3.2.

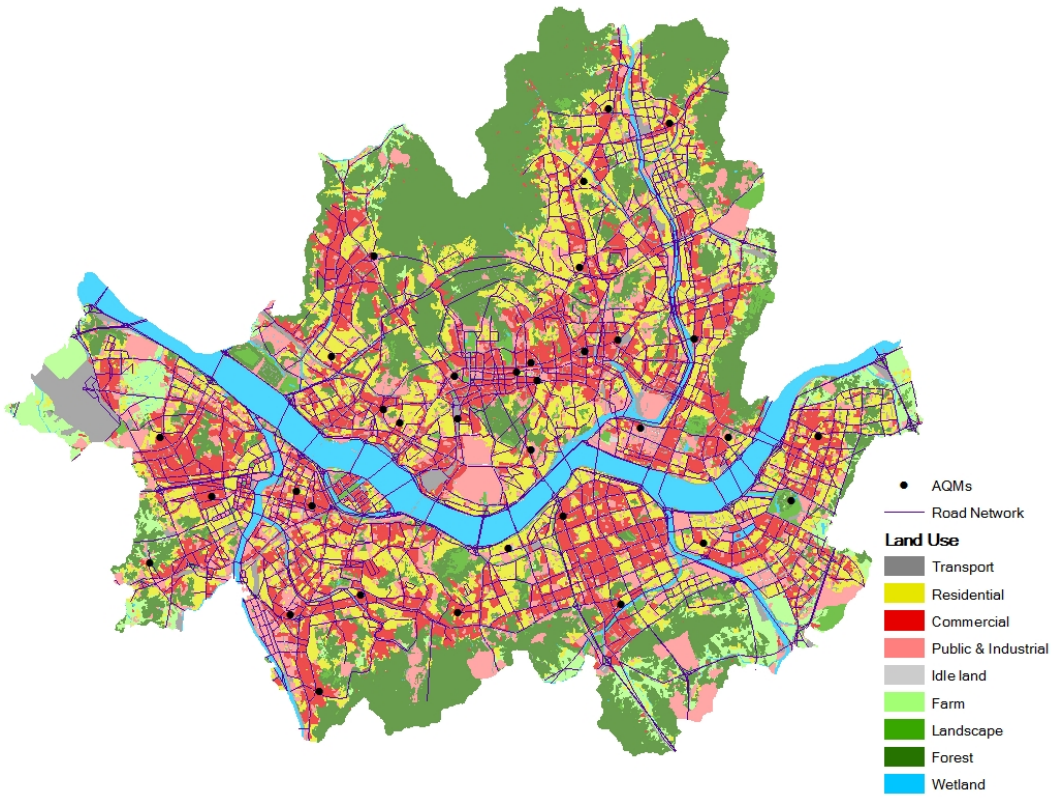

Figure 3.2 Land uses and transportation network in the Seoul Metropolitan area

Since emissions from transportation and stationary sources can be proxied by *VKT* and *LU*, the emission-related explanatory variables in Eq. (3.1) can be replaced by these variables. In addition, Eq. (3.1) implicitly represents interactions between emissions and meteorological factors. Solar radiations are indispensible conditions to generate O_3, thus the varying intensity of solar radiations across hours of day and seasons induces different impacts on pollution concentrations. Lower temperature not only causes a direct increase of fossil fuel burning for building heating, but is also a factor in incomplete fuel burning, leading to higher emission rates.

Hence, interaction terms between emission proxy variables and meteorological factors must be introduced into air quality models.

The spatial and temporal dimensions may vary, depending on the variables of interest and research purposes. For example, air quality models focused on inter-regional comparisons need only use city-wide average pollution concentrations. In contrast, in the case of intra-city models, concentrations at each AQM located within the city of interest should be used for model estimation. Similarly, the temporal dimension varies from hourly average to annual average. In this research, the spatial dimension is limited to intra-city variations, and hourly measured concentrations are averaged over months, seasons, and the whole year, depending on the research questions.

Some explanatory variables have measurement limitations, either spatially or temporally. For example, if temporal activity profiles are not surveyed, it may not be possible to investigate the impacts of time-varying land-use emissions. The two transportation-related variables used in this research, traffic counts and VKT, have different spatial and temporal scopes. Since VKT is measured based on the estimated network flows within circular buffers around AQMs, its spatial dimension is similar to the dependent variable. In contrast, the locations of traffic count stations and AQMs do not match, and it is therefore difficult to directly introduce traffic counts into cross-sectional models based on individual AQM data. However, traffic counts are measured hourly across the entire year, and therefore these data can be used to differentiate the weekdays/weekend impacts of traffic flows on air quality. In contrast, VKT is calculated based on assigned traffic flows, which are the results of a transportation planning model applied with an origin/destination (OD) table and a given network. Generally, an OD table is constructed based on individual travel patterns, such as work trips, shopping trips, leisure trips, etc. These patterns are expected to be significantly different between weekdays and weekend. However, without a weekend OD table, it is not possible to estimate weekend traffic flows on the network. Finally, the effects of background pollution external to the metropolitan area are very difficult to measure. It is assumed that these effects are uniform over the area, and are captured by the error terms of the estimated regression models.

3.3.2 Time-Series Air Quality Models

Traffic flows are closely correlated with the concentrations of directly emitted and secondary pollutants. It is logical to infer that decreased vehicle flows lead to decreased direct emissions, and thus concentrations monitored during weekdays are expected to be higher than

those during weekend. In addition, concentrations measured at roadside AQMs are substantially higher than those at background AQMs. To investigate these different spatiotemporal impacts of traffic on pollution concentrations, hourly measured concentrations across all AQMs during a year are averaged out as follows:

$$\boldsymbol{C}_{ph}^{RS} = \frac{1}{\mathrm{N}} \sum_{i=1}^{N} \boldsymbol{C}_{phi}^{RS} \tag{3.6}$$

$$\boldsymbol{C}_{ph}^{BG} = \frac{1}{\mathrm{K}} \sum_{i=1}^{K} \boldsymbol{C}_{phi}^{BG} \tag{3.7}$$

where:

$\boldsymbol{C}_{phi}^{RS}$: Concentration of pollutant *p* at roadside (RS) AQM *i* on hour *h*,

$\boldsymbol{C}_{phi}^{BG}$: Concentration of pollutant *p* at background (BG) AQM *i* on hour *h*,

$\boldsymbol{C}_{ph}^{RS}$: Concentration of pollutant *p* averaged out for hour *h* across roadside AQMs,

$\boldsymbol{C}_{ph}^{BG}$: Concentration of pollutant *p* averaged out for hour *h* across background AQMs,

RS: Roadside AQMs,

BG: Background AQMs,

N: number of roadside AQMs,

K: number of background AQMs,

h: hour of the day for 365 days (1 → 8,760).

Since hourly concentrations are averaged over both roadside and background AQMs, there are two sets of hourly averaged data. A total of 8,760 observations (24 hours × 365 days) are generated for an each set.

As pollution concentrations are aggregated over space, explanatory variables also need to be similarly aggregated. A proxy for the aggregate emissions from traffic flows would be the sum of VKT over all links, with:

$$TR_t = \sum_{l=1}^{L} VKT_{lt} \tag{3.8}$$

As discussed in the Section 3.3.1, the OD table used to calculate VKT is based on weekdays only. Since VKTs on weekends are not available, Eq. (3.8) cannot be used. However, traffic counts are available over the whole week, and they can be used as proxy for aggregate traffic emissions. Let *TC* represent the traffic counts variable.

The averaged concentrations along the distinctions between roadside AQMs and background AQMs can be represented as a function of the average traffic count $\boldsymbol{TC}_h$ and meteorological vector $\boldsymbol{MET}_h$. The dichotomy between weekdays and Sunday can be represented by a dummy variable $\boldsymbol{D}_{ws}$. Since interactions between explanatory and dummy variable are expected, interaction terms can also be introduced. Finally, it is assumed that the time-linked effects of aggregated stationary sources emissions (i.e., land uses) are captured by the meteorological variables (e.g., temperature) as well as by the weekday-weekend dichotomy (less production on weekends). If there is no lag effect, Eq. (3.1) then becomes:

$$\boldsymbol{C}_{ph}^{Loc} = F(\boldsymbol{TC}_h, \boldsymbol{MET}_h, \boldsymbol{TC}_h \times \boldsymbol{D}_{ws}, \boldsymbol{MET}_h \times \boldsymbol{D}_{ws}, \boldsymbol{D}_{ws}) \tag{3.9}$$

where *Loc* = *RS* or *BG*.

3.3.3 Air Quality Panel Models

Several studies have demonstrated significant variations in air pollution concentrations at the intra-urban spatial scale (Fischer et al., 2000; Kingham, Briggs, Elliott, Fischer, & Erik, 2000; Lebret et al., 2000; Wilson, Kingham, Pearce, & Sturman, 2005). Since LUR approaches combine air pollution concentrations monitored within an urban area with predictor variables, such as traffic-related variables and land-use shares measured around AQMs, most LUR models use standard regression techniques. Some stochastic models use a logarithmic transformation of pollutant concentration as the dependent variable to normalize the distribution of the error terms (Beelen et al., 2009; Madsen et al., 2007; Moore, Jerrett, Mack, & Künzli, 2007; Ryan et al., 2007).

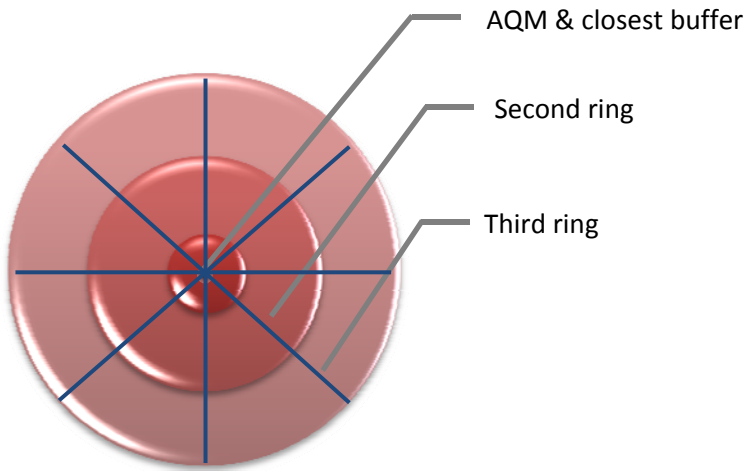

Figure 3.3 Location of AQM and surrounding buffers and sectors

LUR models have been constructed based on the buffer system. The basic concept of this approach is illustrated in Figure 3.3. A buffer is made of successive rings $r = 1 \rightarrow R$, and is subdivided into sectors $s = 1 \rightarrow S$. Although all AQMs used in this study are located within the Seoul municipal boundary,[2] their concentrations vary significantly, due to variations in the intensity of traffic emissions and activities/land uses inside the buffers. To uncover the separate impacts of transportation and land uses on pollution concentrations, VKT and land-use areas are used as explanatory variables. Since VKT is calculated based on a weekday OD table, only the pollution concentrations measured on weekdays should be used to compute average values over time.

For a general cross-sectional model using the LUR approach, pollution concentrations are averaged over for a certain period, with:

$$\boldsymbol{C}_{pi} = \frac{1}{N_h} \times \sum_t \boldsymbol{C}_{pit} \tag{3.10}$$

where N_h is number of hours used to calculate the average pollution concentrations. Since concentrations are averaged over the study period, the time-linked effects of meteorological

[2] The matrix of distances between AQMs is presented in Appendix A.

factors vanish, except for wind directions. Let FWD_s present the frequency of wind direction into sector s. Explanatory variables, such as VKT and LU, can be weighted using FWD_s, with:

$$\boldsymbol{VKT}_{ir} = \sum \boldsymbol{FWD}_s \times \boldsymbol{VKT}_{irs} \tag{3.11}$$

$$\boldsymbol{LU}_{iar} = \sum \boldsymbol{FWD}_s \times \boldsymbol{LU}_{iars} \tag{3.12}$$

where:

$\boldsymbol{VKT}_{irs}$: Aggregated VKT measured in ring r and sector s around AQM i,

$\boldsymbol{LU}_{iars}$: Area of land-use a measured in ring r and sector s around AQM i.

Then, a cross-sectional model can be formulated as:

$$\boldsymbol{C}_{pi} = F_p(\boldsymbol{VKT}_{ir}, \boldsymbol{LU}_{iar} \mid r = 1 \rightarrow R, a = 1 \rightarrow A) \tag{3.13}$$

It is reasonable to assume that there are additive effects across buffer rings in terms of the impacts of VKT and LU on pollution concentrations. Equation (3.13) can then be formulated as:

$$\boldsymbol{C}_{pi} = \alpha + \sum_{r=1}^{R} \beta_r \ \boldsymbol{VKT}_{ir} + \sum_{a=1}^{A} \sum_{r=1}^{R} \gamma_{ar} \ \boldsymbol{LU}_{iar} + \varepsilon_{pi} \tag{3.14}$$

As discussed in Chapter 2, meteorological factors have significant impacts on pollution concentrations. The model represented by Eq. (3.14) can be extended into a seasonal time-series cross-sectional (panel) air quality model, where $\boldsymbol{C}_{pi}^{h}$ represent the average hourly concentration over a season. The VKT and LU vectors can be recomputed to account for wind direction frequencies in each season. To formulate the seasonal-hourly panel model, concentrations are averaged over each season for a given hour h. Meteorological factors are also averaged in the same way. For the calculation of hourly VKT, the estimated daily VKT is apportioned using traffic counts information. The panel data set for each season includes 816 observations (34 AQMs × 24 hours). Since activity profiles are not available for land uses, LU does not vary across the 24 hours of the day. A seasonal/hourly air quality panel model can be formulated as follows:

$$\boldsymbol{C}_{pi}^{h} = F_p\left(\boldsymbol{VKT}_{ir}^{h}, \boldsymbol{MET}^{h}, \boldsymbol{LU}_{iar} \mid\ r = 1 \rightarrow R, a = 1 \rightarrow A\right) \tag{3.15}$$

Using locational dummy variables (background AQMs vs. roadside AQMs), the model can be re-formulated as Eq. (3.16), that can measure the different impacts of the explanatory variables on pollution concentrations under different general locational conditions, with:

$$\boldsymbol{C}_{pi}^{h} = \alpha_0 + \sum_{r=1}^{R}(\beta_r + \mu_r\, \boldsymbol{D}_i^h)\boldsymbol{VKT}_{ir}^{h} + \sum_{a=1}^{A}\sum_{r=1}^{R}(\gamma_{ar} + \rho_{ar}\, \boldsymbol{D}_i^h)\boldsymbol{LU}_{iar} + \sum_{f=1}^{F}(\omega_f + \delta_f \boldsymbol{D}_i^h)\boldsymbol{MET}_f^h + \varepsilon_i^h \tag{3.16}$$

CHAPTER 4

DATA SOURCES AND PROCESSING

This chapter provides an overview of the study area, and a detailed description of data sources and processing methods. Various data are used to formulate air quality models, including origin-destination (OD) traffic flows, traffic counts, vehicle-kilometers-traveled (VKT), land uses (residential, commercial, industrial, transportation, and green areas), and meteorological factors (solar radiation, temperature, humidity, wind speed, and wind direction). A particular focus is set on the transportation network and the assignment of OD flows on its links.

4.1 OVERVIEW

The Seoul Metropolitan area is located on the west side of the Korean peninsula (37˚ 33´ N latitude and 126˚ 59´ E longitude). The area of the city is 605.41 km^2 (233.7 sq. mi., East-West distance: 36.78 km, South-North distance: 30.30 km), roughly divided into northern (298 km^2) and southern (307 km^2) halves by the Han River. The 2003 population was 10,276,968[1]. The city is surrounded by mountains 600 ~ 800 meters high, with its western part bordering close to the Yellow Sea. The geographic location and topography of Seoul is illustrated in Figure 4.1. The climate of the Korean peninsula is classified as mostly humid continental, with hot summer. Meteorological factors, such as wind direction, wind speed, temperature, solar radiation, and humidity will be analyzed in the following sections.

Transportation is responsible for a substantial share of pollution emissions in the Seoul Metropolitan area, such as CO, NO_2, VOC, PM10 and SO_2. According to the 2003 annual report of the Korea Ministry of Environment, the contribution of transportation to air pollution in the Seoul Metropolitan area is greater than at the national level. Specifically, the shares of pollution due to transportation in the Seoul region are 90.1%, 60.6%, 31.9%, 73.3%, and 11.0%, for CO, NO_2, VOC, PM10 and SO_2, respectively. On the other hand, the same shares at the national level

[1] http://www.seoul.go.kr/v2007/publicinfo/statistics/data/4_02.html

are 78.9%, 40.9%, 16.5%, 43.3%, and 1.3% (Korea Ministry of Environment, 2006, 2003). As expected, urbanized regions are more vulnerable to vehicle emissions than rural ones. Since the pollutants emitted by motor vehicles tend to be distributed in close proximity to people's breathing level, dwellers, pedestrians and passengers close to high traffic flows and congested roads are exposed to greater health risks. Vehicle-kilometers-traveled (VKTs) estimated with traffic assignment models and GIS manipulations are used as proxy variables for transportation emissions. The required data, process and results of the traffic assignment are introduced in the following sections. Since pollution concentrations are measured hourly, the assigned daily traffic flows are broken down by hour, using monitored traffic counts. The hourly traffic counts data were collected over a week at 4 different types of roads: cordon lines (39 locations), the Han river bridges (18 locations), arterial roads (34 locations), and central business districts (CBD) roads (26 locations) (Seoul Metropolitan Police Agency, 2003).

4.2 AIR POLLUTION CONCENTRATIONS

Air pollution concentrations in 2003 have been measured at 34 AQMs and are reported in both the Seoul Metropolitan government website (Seoul Metropolitan Government, 2008) and in the Annual Report of Air Quality in Korea (National Institute of Environmental Research, 2004). As illustrated in Figure 4.1, AQMs are distributed over the Seoul Metropolitan area, with at least one AQM in each district. Out of the 34 AQMs, 27 are classified as urban background AQMs, monitoring the average air quality and assessing whether air quality standards are attained. The other 7 AQMs are located near crowded traffic links to measure the air quality of roadsides. The hourly-averaged pollution concentrations of NO_2, CO, O_3, SO_2, and PM10 are used. Pollution concentrations are measured in ppb (parts per billion) units for NO_2, CO, O_3, and SO_2. In the case of PM10, the unit is $\mu g/m^3$ (microgram per cubic meter). An exploratory analysis of five pollutants will be presented in Chapter 5, including the temporal variations of concentrations, comparisons between roadside and urban background AQMs, hourly variations of traffic flows and pollution concentrations, and comparisons between weekdays and weekend concentrations.

The roadside AQMs are located a few meters from the curbside of major roads or junctions, including Euljiro-7ga, Seoul Station, Cheongge-4ga Rotary, Cheongnyangni Rotary, Shinchon Rotary, Yeongdeungpo Rotary, and Sinsa Rotary. The junctions are intersecting arterial roads, and heavy traffic volumes and congestion are commonly observed. Pollutant sampling tools are set up at a height of around 2.5 meter above the level of each road. In contrast, urban background AQMs are located away from major roadways, on the roofs of two- or three-story public buildings, such as elementary schools and public office buildings. One-hour average concentrations are calculated based on one measurement every five minutes (12 readings per hour) (Korea Ministry of Environment, 2003). The geographic locations of AQMs and the map of the Seoul Metropolitan area are presented in Figure 4.1.

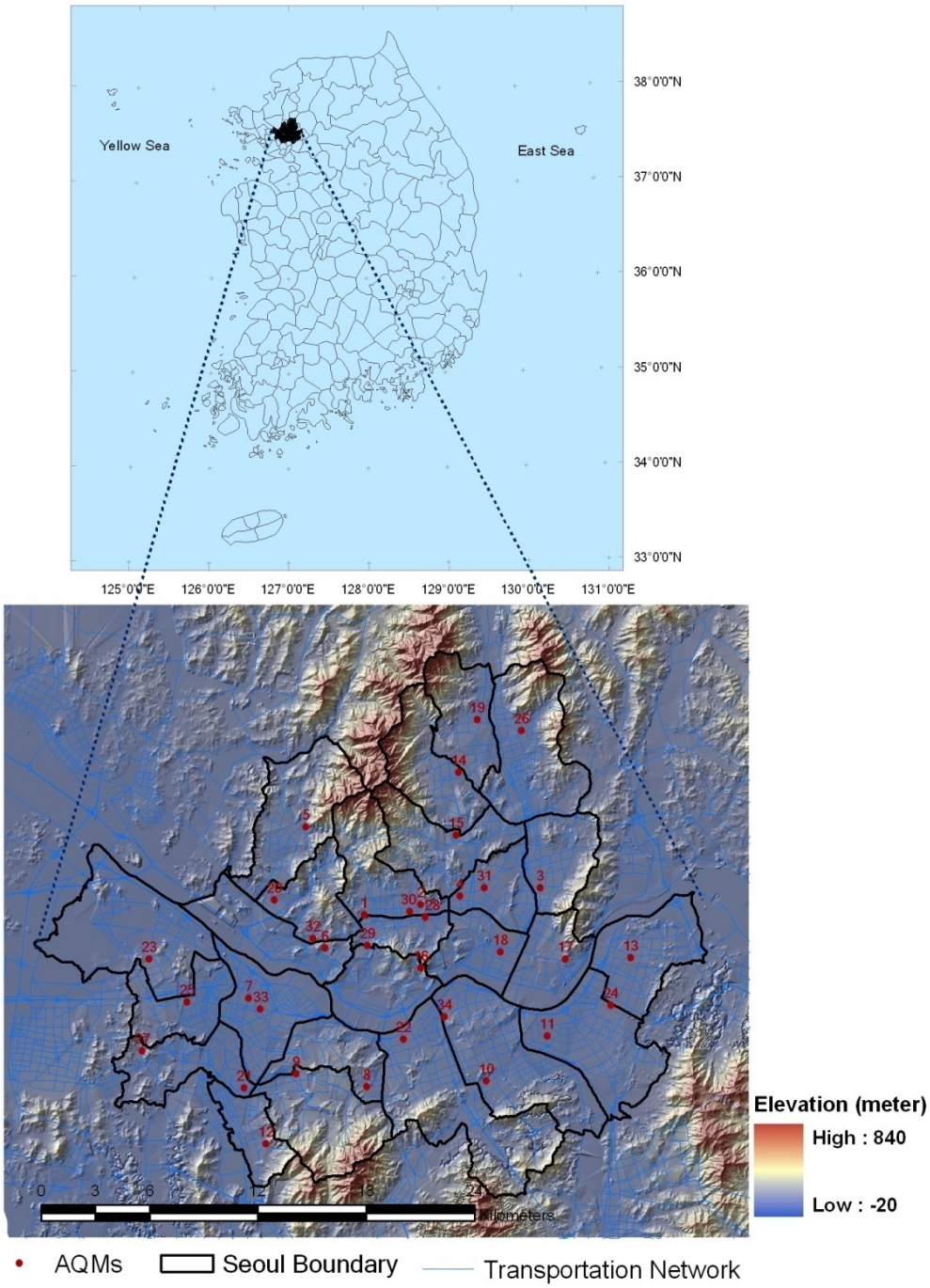

Figure 4.1 Locations of AQMs on the topographic map of the Seoul Metropolitan area

As shown in Figure 4.2 and Appendix B[2], the annual average concentrations at the 34 air quality monitoring stations (AQMs) of the Seoul metropolitan area display significant variations across geographic locations. The annual average concentration of NO_2 is 40.2 ppb, with minimum and maximum of 28.3 ppb and 55.8 ppb, respectively. The other four pollutants also display large variations: CO varies from 358 ppb to 1,391 ppb, O_3 from 7.8 ppb to 19.9 ppb, SO_2 from 3.2 ppb to 7.9 ppb, and PM10 from 58 $\mu g/m^3$ to 88 $\mu g/m^3$. Although all AQMs are located within the same municipal boundaries[3] and same local climate shed, their concentrations vary significantly, due to variation in the intensity of traffic emissions and nearby activities/land uses.

As shown in Figure 4.3 through Figure 4.7,[4] the hourly average concentrations of the five air pollutants during the four seasons display significant temporal variations with the time of day. NO_2 hourly concentrations display two troughs within the day across all four seasons. The other pollutants also display specific temporal concentration patterns. As discussed in Chapter 2, mobile emissions account for the major share of pollution concentrations (US EPA, 2000; AQEG, 2004; CORINAIR, 2003; Korea Ministry of Environment; 2005). Since traffic volumes change significantly during the day, it is reasonable to hypothesize that hourly pollution concentrations are affected by hourly traffic flows.

In the case of hourly NO_2 concentrations (Figure 4.3), the first (and lowest) trough occurs early in the morning, and then a steep increase starts around 6 AM. The first peak coincides with the morning traffic peak. The second trough takes place at mid-day, and the daily peak after 7 PM. The hourly NO_2 concentration during the summer is lower than those in the other seasons. The highest concentrations are observed during the late evening in spring, but winter concentrations are higher than those in daytime (6AM ~ 7PM) spring. Given NO_x chemistry, the photolysis of NO_2 is closely related to the intensity of UV radiation. Therefore, it is possible that UV radiation in daytime causes a decrease in NO_2 concentrations and, as a result, the daytime trough. Similarly, hourly CO and SO_2 concentrations during the four seasons can be explained by the sources of emissions and the impacts of UV radiation. As expected, lower temperatures during the cold seasons increase the consumption of fossil fuels, leading to higher concentrations of directly emitted pollutants, such as NO_2, CO and SO_2. As seen in Figures 4.3 ~ 4.5, the hourly concentrations in winter are generally the highest, while those in summer are the lowest. CO is oxidized with hydroxyl radical (OH·) and converted into CO_2 (Eq. 2.12), and SO_2 reacts with OH· and is

[2] The concentrations in Appendix B are calculated with based weekday monitoring data.

[3] The matrix of distances between AQMs is presented in Appendix A.

[4] The hourly average concentrations used in these graphs do not include weekend and national holiday data.

converted into sulfuric acid (H_2SO_4) (Eqs. 2.24 ~ 2.26). As OH· is generated under UV radiation, troughs are observed during afternoon (1 PM ~ 5 PM) across all seasons except for winter SO_2 concentrations. Unlike the directly emitted pollutants, O_3, a secondary pollutant, displays a different concentration pattern. As seen in Figure 4.6, the hourly concentration of O_3 has a peak during the period 3 PM ~ 4 PM across the four seasons, because UV radiation is a key determinant to generate O_3 (Eq. 2.18). The accumulation of O_3 reaches its highest point at 3 PM in winter and autumn. During spring and summer, sunlight lasts longer, and therefore the accumulation peaks at 4 PM.

The hourly concentrations of the five air pollutants averaged across 34 AQMs are represented in Appendix C. Across all seasons the daily NO_2 concentration varies from 30.3 ppb and 51.3 ppb; the concentration of CO varies from 5.6 ppm to 13.6 ppm; the concentration of O_3 from 3.4 ppb to 33.2 ppb; the concentration of SO_2 from 3.7 ppb to 9.0 ppb; and the concentration of PM10 from 52.7μg/m^3 to 98.1μg/m^3. These variations suggest that the hourly variations of traffic emissions and meteorological factors have an influence on the variations of hourly pollution concentrations.

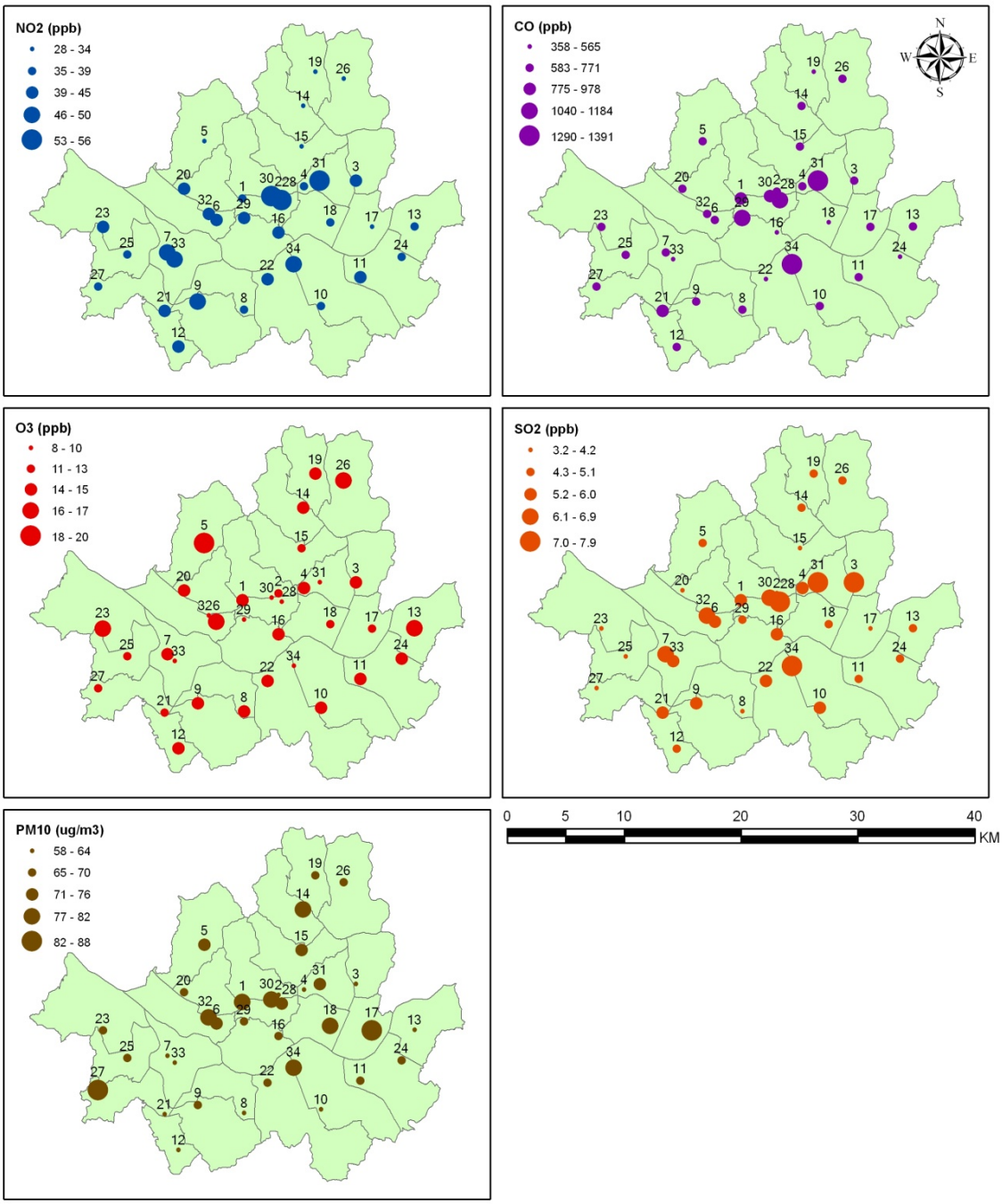

Figure 4.2 Spatial variations of annual average pollution concentrations

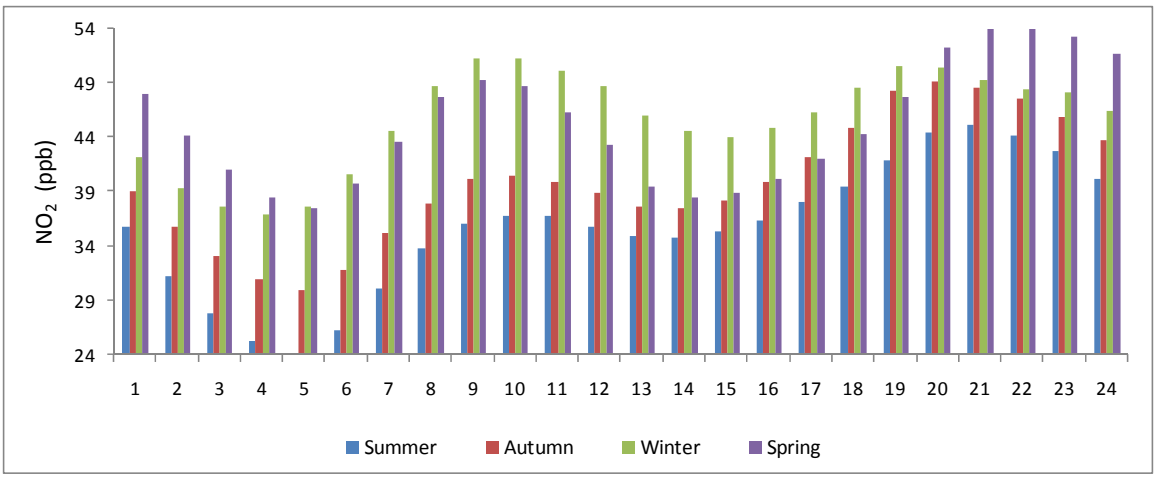

Figure 4.3 Seasonal variations of hourly average NO_2 concentrations

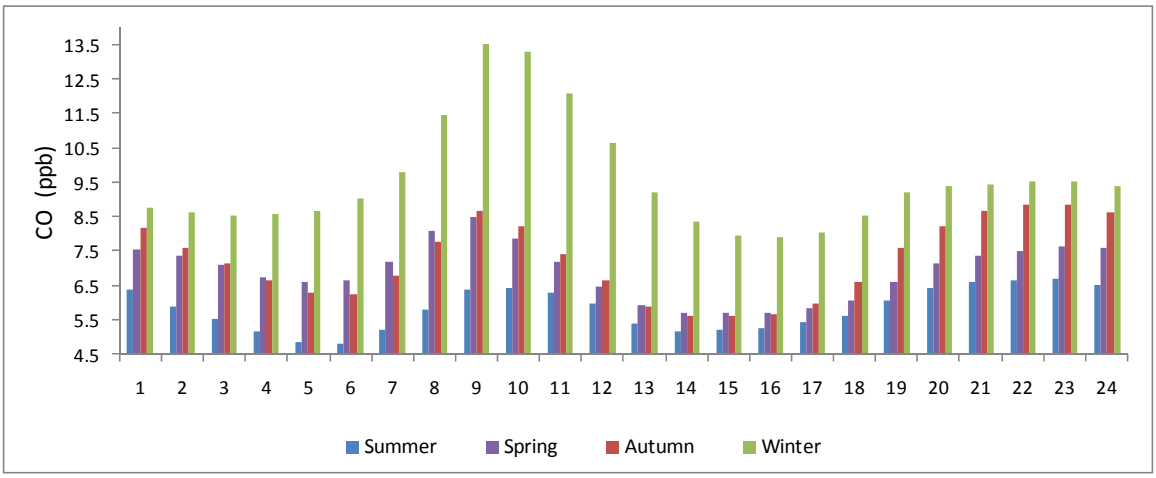

Figure 4.4 Seasonal variations of hourly average CO concentrations

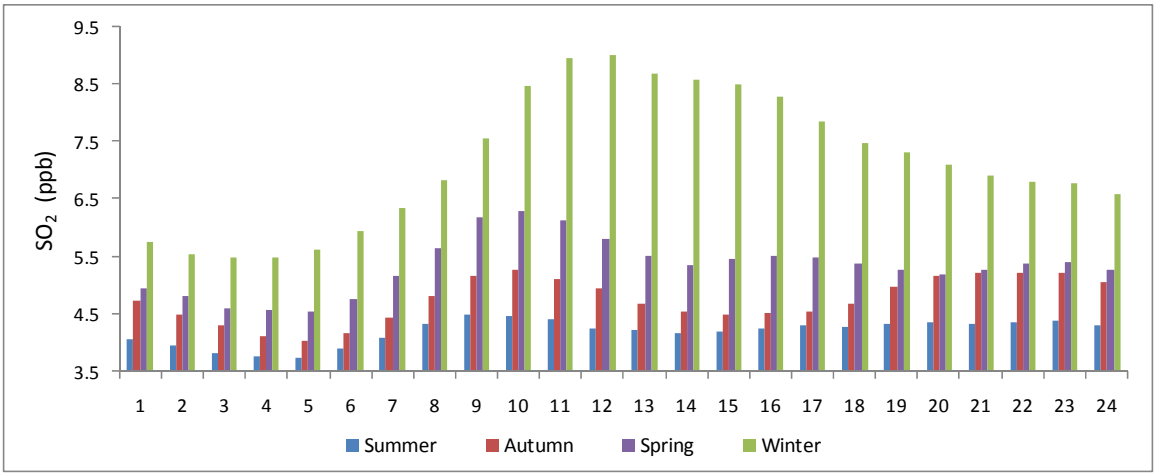

Figure 4.5 Seasonal variations of hourly average SO_2 concentrations

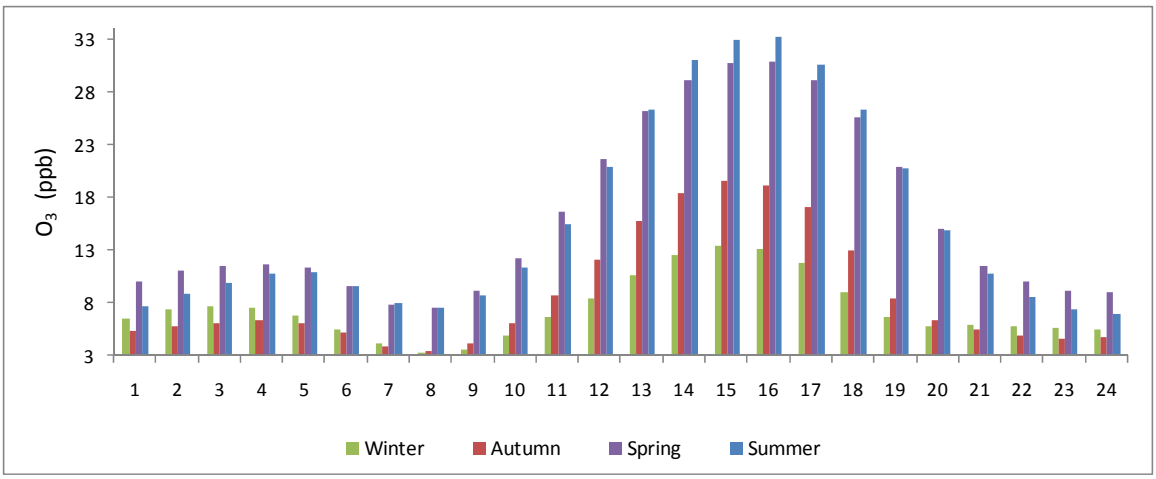

Figure 4.6 Seasonal variations of hourly average O_3 concentrations

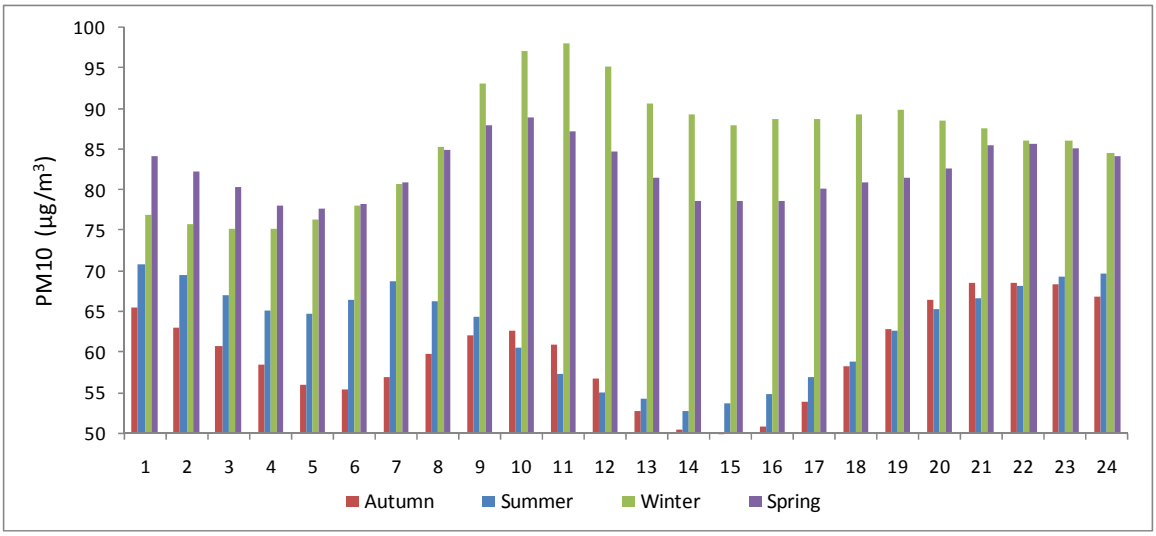

Figure 4.7 Seasonal variations of hourly average PM10 concentrations

4.3 TRANSPORTATION NETWORK AND ORIGIN/DESTINATION (OD) TRAFFIC FLOWS

The Seoul Development Institute releases transportation network and OD matrix data for the Capital region of Korea every year. The network and OD data cover the Seoul, Incheon, and Gyeonggi regions. The transportation network and the locations of the AQMs are illustrated at Figure 4.8. These OD and network data are used in traffic assignment models. The OD table and network involve 1,142 traffic zones, divided into 1,129 internal and 13 external zones. The OD system includes auto, taxi, and bus OD tables. According to the report, "The Standard Guideline of Pre-feasibility Study for Road and Railroad Sectors" (Korea Development Institute, 2004), the surveyed average numbers of people per vehicle are 1.46 and 14.99 for automobile and bus, respectively. These values are used to convert person trip to vehicle trip. As freight OD data are not available in 2003, freight flows are not included in the traffic assignment process. Therefore, the assigned volumes on each link can be expected to be less than the actual traffic flows.

Figure 4.8 Transportation network, locations of AQMs, and samples of circular buffers in the Seoul Metropolitan Area

The distances between traffic emissions and receptors are important in determining the concentrations at receptors. To identify the impacts of traffic emissions on the concentrations at AQMs, several circular buffers with a radius varying from 500 meters to 5,500 meters are delineated around each AQM. The VKTs on the transportation links within the circular buffers are estimated as follows: (1) the traffic flow of each transportation link is estimated with a traffic assignment model; (2) the buffers are intersected[5] onto the traffic network; (3) the attributes of the intersected links are calculated using ArcGIS® and Python® scripts. To account for the wind-direction (WD) effects on traffic emissions, the circular buffer is subdivided into eight sectors, each sector is overlaid onto the assigned network, and then the VKTs for each sector are computed using the above process, and then weighted by the WD frequency. WD-weighted VKT (WVKT) is calculated as the sum of the eight sectors' VKT. Using available hourly traffic counts data, the estimated daily VKTs are divided into hourly VKTs. Detailed information regarding the traffic assignment method and results are represented in the following section.

[5] The intersecting process divides a transportation link crossing over a buffer boundary into two split links. The split links have the same attribute data, in this case the same VKT, because the geo-processing process only changes the physical feature. To adjust the attribute data of the split links, it is necessary to apply the ratio of length between the original and split links to the attribute data.

4.4 VEHICLE-KILOMETERS-TRAVELED (VKT)

4.4.1 Overview of Traffic Assignment

TransCAD® is widely used by public agencies and private planning firms as the tool for the transportation planning process[6]. Traditional 4-step models can be implemented with TransCAD®, and six assignment methods are available in the traffic assignment process, including all-or- nothing, capacity restraint, incremental, stochastic, system optimum, and user equilibrium (UE). To select the appropriate traffic assignment method, 56 links are chosen for comparing actual (monitored) vehicle counts and estimated (assigned) traffic flows. These 56 links include 18 Han-river bridges and 38 cordon line locations, as illustrated in Figure 4.9. Since the selected links constitute major roads in the network and the locations of these links are distributed over the entire study region, it is expected that the comparison of monitored and assigned traffic flows will provide a comprehensive assessment of the six assignment methods.

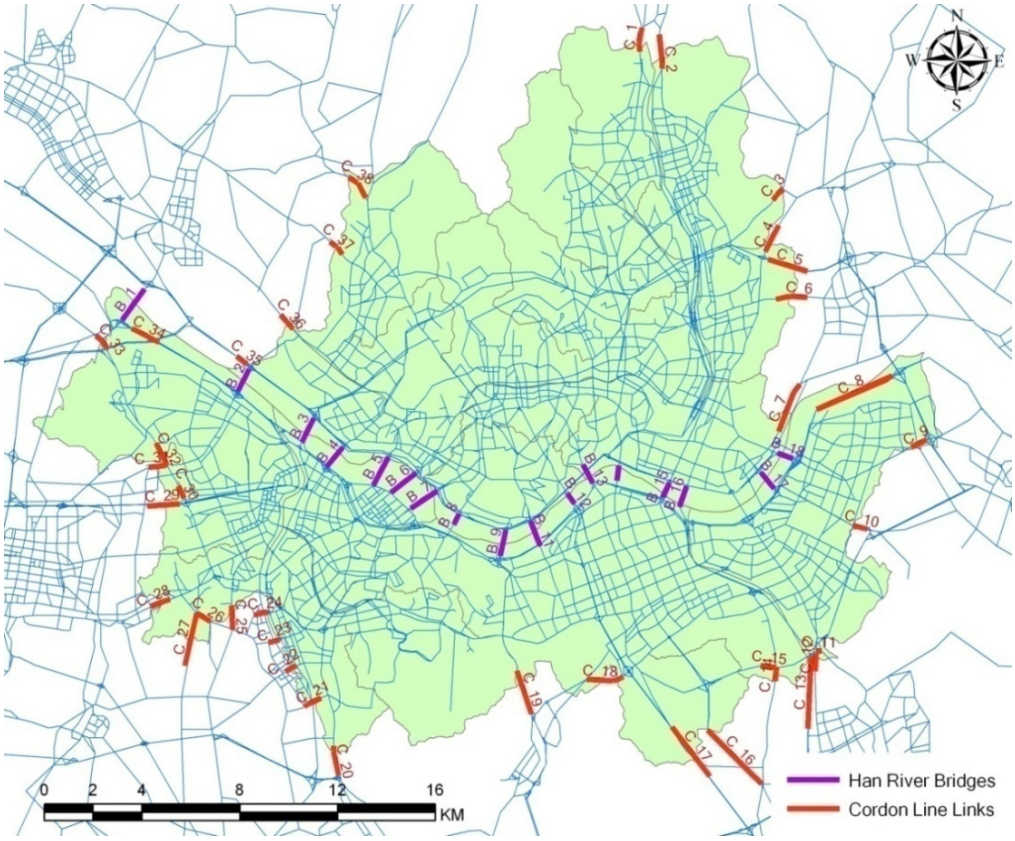

Figure 4.9 Location of traffic flows monitoring links

[6] http://www.caliper.com/TransCAD/ApplicationModules.htm#Transportation%20Planning

The origin-destination (OD) system included of two types of OD tables: passenger car and bus. A passenger OD table is derived by summing auto and taxi OD tables. Because highway capacity is measured in passenger car equivalent (PCE), the PCE is applied to bus OD flows. Since public transit has fixed routes, it is reasonable to assign bus OD flows with the all-or-nothing method prior to the assignment of passenger OD flows. After the assignment of bus OD flows, the passenger OD table is assigned onto the pre-bus-loaded network using the six assignment methods. After the traffic assignment process, the traffic volume for each link in the whole network is identified. The traffic assigned with the UE method is illustrated in Figure 4.10. The calculations of VKTs and WVKTs are followed by the traffic assignment process, which will be described in the next section.

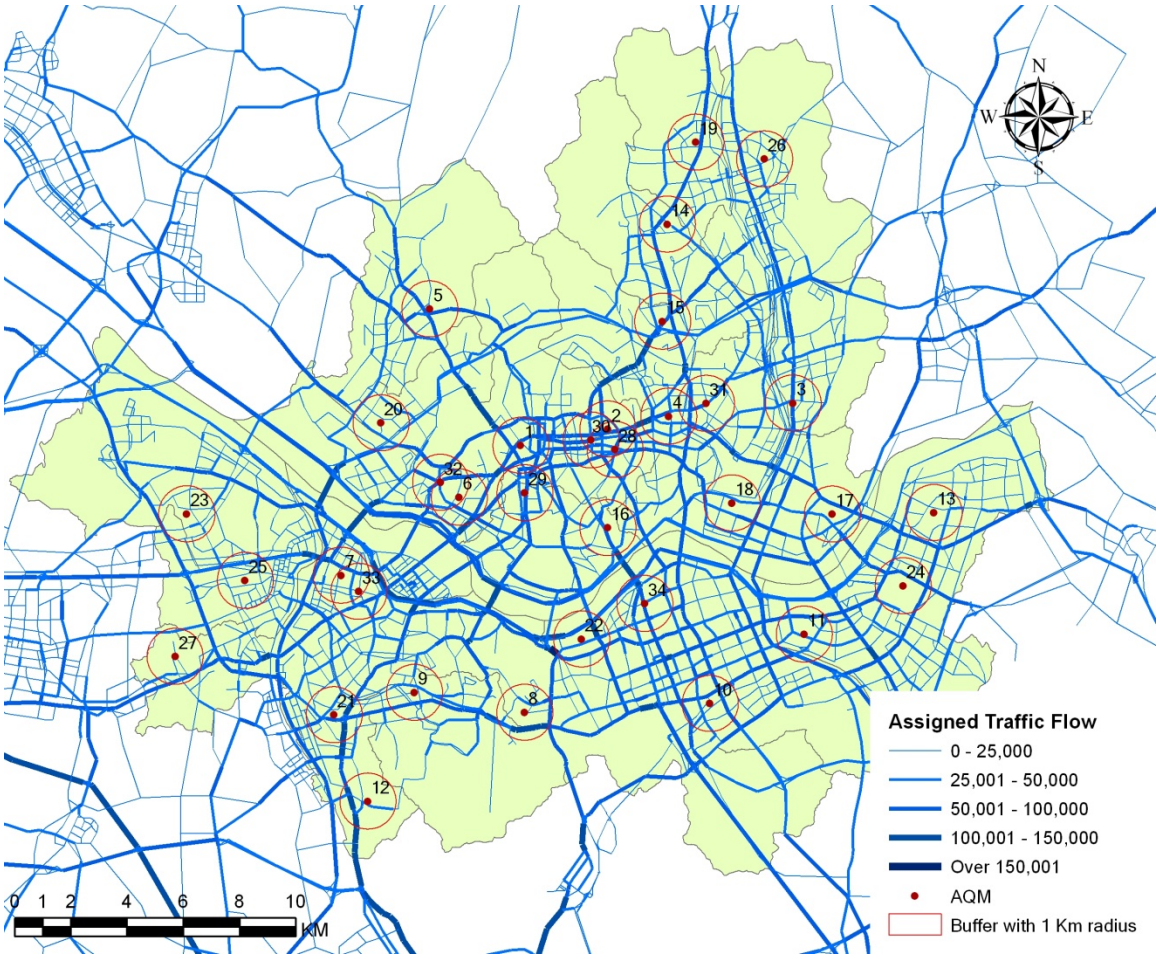

Figure 4.10 Traffic assignment with the user equilibrium method

4.4.2 Comparison of Traffic Assignment Methods

In order to select the best method of traffic assignment, the monitored traffic counts and the estimated traffic flows are compared for the 56 links. The results are presented in Table 4.1. As discussed earlier, the flows on these links are predicted using six assignment methods, with passenger car OD flows loaded onto the pre-bus-loaded network. Quantitative measures of agreement between observed (*O*) and model-predicted (*P*) values are calculated to evaluate the performance of the traffic assignment methods. Seven measures are used, as described by the following equations:

$$\mathrm{RMSE} = \sqrt{\frac{\sum_{i=1}^{N}(P_i - O_i)^{\,2}}{N}} \tag{4.1}$$

$$\mathrm{NMSE} = \frac{\mathrm{RMSE}}{O_{max} - O_{min}} \tag{4.2}$$

$$r = \frac{1}{N-1}\sum_{i=1}^{N}\left(\frac{P_i - \overline{P}}{\sigma_P}\right)\left(\frac{O_i - \overline{O}}{\sigma_O}\right) \tag{4.3}$$

$$\text{Index of Agreement} = 1 - \left[\frac{\sum_{i=1}^{N}(P_i - O_i)^2}{\sum_{i=1}^{N}(|P_i - \overline{O}| + |O_i - \overline{O}|)^2}\right] \tag{4.4}$$

$$\text{Average Difference} = \frac{1}{N}\sum_{i=1}^{N}\frac{|O_i - P_i|}{O_i} \tag{4.5}$$

$$\text{Maximum Difference} = \mathrm{Max}\left(\frac{|O_i - P_i|}{O_i}\right) \tag{4.6}$$

$$\text{Minimum Difference} = \mathrm{Min}\left(\frac{|O_i - P_i|}{O_i}\right) \tag{4.7}$$

The root mean square error (RMSE) is used to measure the difference between predicted and actual values (Eq. 4.1). The normalized RMSE (NMSE) is equal to the RMSE divided by the range of monitored values (Eq. 4.2). Since both measures are calculated based on the magnitude of the differences between the predicted and monitored values, the smaller their values the better the result. Pearson correlation coefficient (r) has been used to measure the linear dependence between the predicted and the observed values (Eq. 4.3). Willmott (1982) suggests that the

correlation coefficient is not sufficient to quantify the accuracy of predictions, and proposes an index of agreement (IOA, Eq. 4.4) as an alternative. The higher r and IOA, the better the fit between the predicted and observed values. In addition, three simple difference measures are also calculated and their functional forms are presented in Eqs (4.5) ~ (4.7). The above general approaches to evaluate model performance have been suggested by Fox (1980) and Willmott (1982). They have been applied in air pollution modeling studies, including the assessment of urban air pollution modeling in Helsinki, Finland (Karppinen, Kukkonen, Elolähde, Konttinen, & Koskentalo, 2000), the evaluation of industrial pollution modeling in Jamshedpur, India (Sivacoumar, Bhanarkar, Goyal, Gadkari, & Aggarwal, 2001), and the evaluation of a neural network model for the prediction of urban NO_2 and PM10 concentrations (Kukkonen et al., 2003).

Among the six assignment methods, the system optimum and user equilibrium (UE) ones are characterized by good performance measures, as reported in Table 4.1. Since the basic assumptions of the UE assignment are generally considered as most appropriate to simulate real-world driver behavior, the UE method is selected to calculate the VKT.

Drivers on the road network will try to minimize their travel time when they select their routes (set of links) from origin to destination. The travel times of links and routes will change, depending on the flow on each link, because travel time is determined as a function of traffic volume and link capacity. The widely accepted link performance function (delay function) developed by the U.S. Bureau of Public Roads is:

$$t = t_0 \left[1 + \alpha \left(\frac{volume}{capacity} \right)^{\beta} \right] \tag{4.8}$$

where t is the travel time on the link, t_0 is the free flow time, and α and β are parameters that vary with road hierarchy (Horowitz, 1991). As the travel time on each link changes, the travel times on potentially possible paths for each trip also change. The assumption of UE assignment is that an equilibrium condition can be obtained when no driver can reduce her/his travel time by unilateral route change. Therefore, at equilibrium, the travel times for all the paths connecting any given OD pair would be the same. The UE model is mathematically defined as follows:

$$Min: z(x) = \sum_{a} \int_{0}^{x_a} t_a(w)\, dw \tag{4.9}$$

s.t. $$\sum f_k^{rs} = q_{rs} \qquad \forall\ r,\ s \tag{4.10}$$

$$f_k^{rs} \geq 0 \qquad \forall\ k,\ r,\ s \tag{4.11}$$

$$x_a = \sum_r \sum_s \sum_k f_k^{rs} \delta_{a,\,k}^{rs} \quad \forall\ a \in A \quad \text{(Incidence relations)} \tag{4.12}$$

The travel time on a particular path k between node r and s, c_k^{rs}, is the sum of the travel times on all the links comprising this path, with:

$$c_k^{rs} = \sum_a t_a \delta_{a,\,k}^{rs} \quad \forall\ k \in K_{rs},\ \forall\ r \in R,\ \forall\ s \in S \tag{4.13}$$

Notations :

N	Node set
A	link set
R	Set of origin nodes: $R \subseteq N$
S	Set of destination nodes; $S \subseteq N$
K_{rs}	Set of paths connecting OD pair *r-s*: $r \in R,\ s \in S$
x_a	Flow on link *a*
t_a	Travel time on link *a*: $t_a = t_a(x_a)$
f_k^{rs}	Flow on path (route) *k* connecting OD pair *r-s*
c_k^{rs}	Travel time on path (route) *k* connecting OD pair *r-s*
q_{rs}	Trip rate between origin *r* and destination *s*
$\delta_{a,\,k}^{rs}$	$\begin{cases} 1, \text{if link } a \text{ is on path } k \text{ between } r \text{ and } s \\ 0, \text{if link } a \text{ is not on path } k \text{ between } r \text{ and } s \end{cases}$

Constraint 4.10 stipulates that the sum of the flows on all paths connecting each OD pair (*r, s*) has to be equal to the original OD trip rate (q_{rs}). The non-negativity condition (4.11) ensures non-negative flows. Constraint (4.12) states that the flow on each link is the sum of the flows on all paths going through that link, and is known as the incidence relation equation (Sheffi, 1984; 1985).

	Link Name	Monitored Traffic	All or Nothing	Capacity Restraint	Incremental	Stochastic	System Optimum	User Equilibrium
Han River Bridges	B_01.Hangjoo Brdg	93,668	65,112	27,941	46,765	63,471	38,310	38,243
	B_02.Gayang Brdg	71,735	20,835	41,133	39,928	19,297	46,228	46,452
	B_03.Sungsan Brdg	182,139	142,621	132,162	117,840	142,533	118,538	117,606
	B_04.Yanghwa Brdg	127,063	92,033	141,961	110,349	91,150	120,398	120,687
	B_05.Seogang Brdg	69,584	39,851	74,104	71,601	46,029	68,427	67,674
	B_06.Mapo Brdg	138,375	175,724	60,877	92,915	173,404	87,046	85,452
	B_07.Wonhyo Brdg	83,774	79,591	66,499	97,077	82,105	86,350	87,397
	B_08.Hangang Brdg	127,942	86,685	116,837	122,356	85,687	109,392	108,591
	B_09.Dongjak Brdg	77,434	73,398	65,062	71,117	75,838	65,762	66,961
	B_10.Banpo Brdg	94,012	91,554	60,093	73,687	84,795	69,145	65,922
	B_11.Jamsu Brdg	55,388	0	38,518	11,126	11,686	29,081	28,872
	B_12.Hannam Brdg	172,976	144,151	120,233	145,784	146,328	127,683	128,366
	B_13.Dongho Brdg	103,551	70,046	64,296	86,004	67,954	77,098	77,135
	B_14.Sungsoo Brdg	82,382	119,144	84,733	90,008	110,092	90,664	90,686
	B_15.Youngdong Brdg	175,399	59,768	81,020	87,930	58,949	80,394	78,319
	B_16.Cheongdam Brdg	106,139	82,675	75,177	64,757	91,231	65,770	65,647
	B_17.Olympic Brdg	87,444	59,473	67,744	65,365	57,425	73,508	72,388
	B_18.Cheonho Brdg	101,888	75,687	66,329	77,425	82,715	69,075	69,714
Cordon Line	C_01.Dobongro	84,251	144,303	96,292	106,890	144,150	90,155	89,996
	C_02.Dongilro	102,599	8,892	48,256	29,116	8,922	34,286	33,614
	C_03.Samyook Univ.	39,161	14,397	17,684	15,029	13,090	16,379	16,508
	C_04.Saewoojae	26,888	19,549	25,973	27,256	24,001	28,784	29,091
	C_05.Sinnae I.C.	118,897	62,637	57,333	53,447	65,962	53,171	53,035
	C_06.Mangwoori	62,925	56,342	56,980	55,943	53,290	53,379	53,216
	C_07.Kwangjang	71,886	55,098	46,916	57,513	54,729	50,704	50,258
	C_08.Gangil I.C.	115,847	22,424	40,445	21,457	21,282	33,496	33,622
	C_09.Sangil I.C.	79,732	124,068	106,561	122,075	125,288	109,386	109,633
	C_10.Seohanam I.C.	98,195	57,761	58,339	55,792	60,907	63,979	64,331
	C_11.Namsungdae	48,635	83,412	83,841	78,240	80,573	72,714	71,641
	C_12.Bokjung	79,602	49,711	57,450	75,718	51,039	73,990	74,693
	C_13.Jangj-Bundang	151,962	95,063	90,503	79,003	90,531	76,920	77,315
	C_14.Segok_Bamgogae	37,019	4,593	16,290	16,393	4,224	29,976	30,359
	C_15.Segok_Hunrung	49,073	12,610	30,387	17,721	11,934	25,901	25,798
	C_16.Bundang-Naegok	93,832	42,744	91,388	97,763	43,895	82,924	83,059
	C_17.Yangjae_Kyungbu	162,149	216,959	153,578	148,813	215,858	141,325	141,906
	C_18.Yangjaedaero	135,139	51,311	51,832	70,566	53,832	64,237	64,346
	C_19.Namtaeryung	102,894	97,451	56,480	86,069	100,778	63,926	64,855
	C_20.Sihung boundary	119,875	124,713	132,658	142,844	117,774	129,695	129,011
	C_21.Siheung Brdg.	27,959	49,830	20,289	30,921	41,624	31,847	32,148
	C_22.Geumchen	65,305	34,476	44,033	56,506	39,896	59,161	58,564
	C_23.Cheolsan Brdg.	104,066	42,457	46,660	44,254	42,931	42,446	41,695
	C_24.Kwangmyung	49,828	59,305	40,919	45,142	63,232	39,930	38,590
	C_25.Gaebong	43,663	13,313	21,228	20,075	15,282	25,906	25,545
	C_26.Cheonwang_Gwangduk	31,018	15,506	28,340	26,261	16,775	29,905	29,711
	C_27.Cheonwang_local	11,004	1,398	16,087	9,951	1,429	12,431	12,740
	C_28.Yoohan	53,781	111,552	54,158	66,334	109,510	59,400	59,191
	C_29.Shinwal I.C._express	214,657	166,425	130,381	142,848	170,930	131,463	130,719
	C_30.Shinwal_nambu	115,787	88,587	82,069	89,076	86,324	77,666	77,510
	C_31.Gongsu_hwagok	43,693	19,185	42,483	24,726	25,854	35,041	35,148
	C_32.Gongsu_nambu	72,558	62,662	76,784	64,599	61,229	68,495	68,444
	C_33.Gaehwa Brdg	80,553	32,818	38,653	26,712	32,237	35,217	34,170
	C_34.Nangido	253,090	235,247	148,444	187,082	238,510	164,532	163,545
	C_35.Kukbang Univ.	80,951	34,982	31,796	49,730	34,135	56,631	56,341
	C_36.Seoneung	42,662	45,265	61,563	53,238	43,104	55,675	55,902
	C_37.Gaehwa I.C	139,113	46,069	48,474	46,076	43,865	45,666	46,988
	C_38.Gupabal	74,589	49,697	43,492	51,196	50,281	50,229	50,237
RMSE			44105	42433	**39746**	43338	40680	40896
NMSE			18%	17%	**16%**	17%	**16%**	**16%**
Correlation Coefficient			0.72	0.74	0.76	0.73	**0.77**	**0.77**
Index of Agreement			0.78	0.73	0.78	**0.79**	0.75	0.75
Average Difference			44%	34%	32%	41%	**30%**	**30%**
Maximum Difference			107%	72%	81%	104%	**71%**	**71%**
Minimum Difference			3%	**1%**	**1%**	**1%**	2%	3%

Table 4.1 Comparisons between monitored and assigned traffic flows for the selected links

4.4.3 Calculations of Vehicle-Kilometers-Traveled (VKT) and Wind-Direction Weighted VKT (WVKT)

To measure the impacts of traffic intensity on air pollution concentrations, the sums of VKTs over circular buffers around AQMs are calculated using GIS functions, such as buffering, intersecting, and database calculations. Generally, geo-processing GIS tools only change the physical feature of an entity, so that it is necessary to reassess the attribute data of geo-processed features. In the case of VKT, the attribute data of a splint link must be recalculated, and a new column is added in the attribute table: the length of split links. After adjusting for road length, the VKT of each link can be obtained by multiplying the assigned traffic flow by the new link length.

Air movements are key determinants of pollution concentrations because horizontal and vertical air movements influence the mixing and transport of air pollutants. The former are called wind and the latter turbulence (Seaman, 2000). Recently, land use regression (LUR) studies have been conducted to establish the relationships between monitored pollution concentrations (mostly NO_2) at AQMs and the surrounding physical environment (Jerrett et al., 2007). Hoek et al. (2008) have critically reviewed 25 LUR studies, with the concentrations of the pollutants of interest as dependent variables, and diverse land uses as predictor variables. In general, transportation related variables, such as traffic counts, road length, and inverse distance to highway, have strong positive relationships with NO_2 concentrations. The conclusion is that LUR models have a substantial potential to explain pollution concentrations in European and North-American cities, with better or equivalent performance when compared to conventional dispersion models. Despite the importance of wind impacts on pollution concentrations, wind variables are rarely included in LUR models. Arain et al. (2007) have tried to include wind effects in LUR models, using estimated wind field data interpolated from observed wind direction data. Using the estimated wind field and the highway network, they calculate whether the monitoring point is located up- or down-wind of emission sources (e.g., expressways). The inclusion of wind variables has enhanced the performance of the models.

To account for wind direction (WD) impacts on pollution concentrations, eight-sector[7] wind directions are considered for each AQM and the estimated VKTs for different buffer radii are also sub-divided into eight sectors. Figure 4.11 illustrates an eight-sector, 1,500 meter radius buffer around AQM No.10. By combining wind direction frequencies and the corresponding sub-divided VKTs, a WD-weighted VKT (WVKT) variable is calculated. Monitored hourly WD data

[7] Eight-sector includes N-NNE, NE-ENE, E-ESE, SE-SSE, S-SSW, SW-WSW, W-WNW, and NW-NNW.

have been downloaded from the website of the Korea Meteorological Administration (2008)[8]. WD data are originally measured for 16 directions, and if wind speed is less than 0.2 m/s then the WD is recorded as CALM. The detailed description of wind data is presented in Section 4.6.

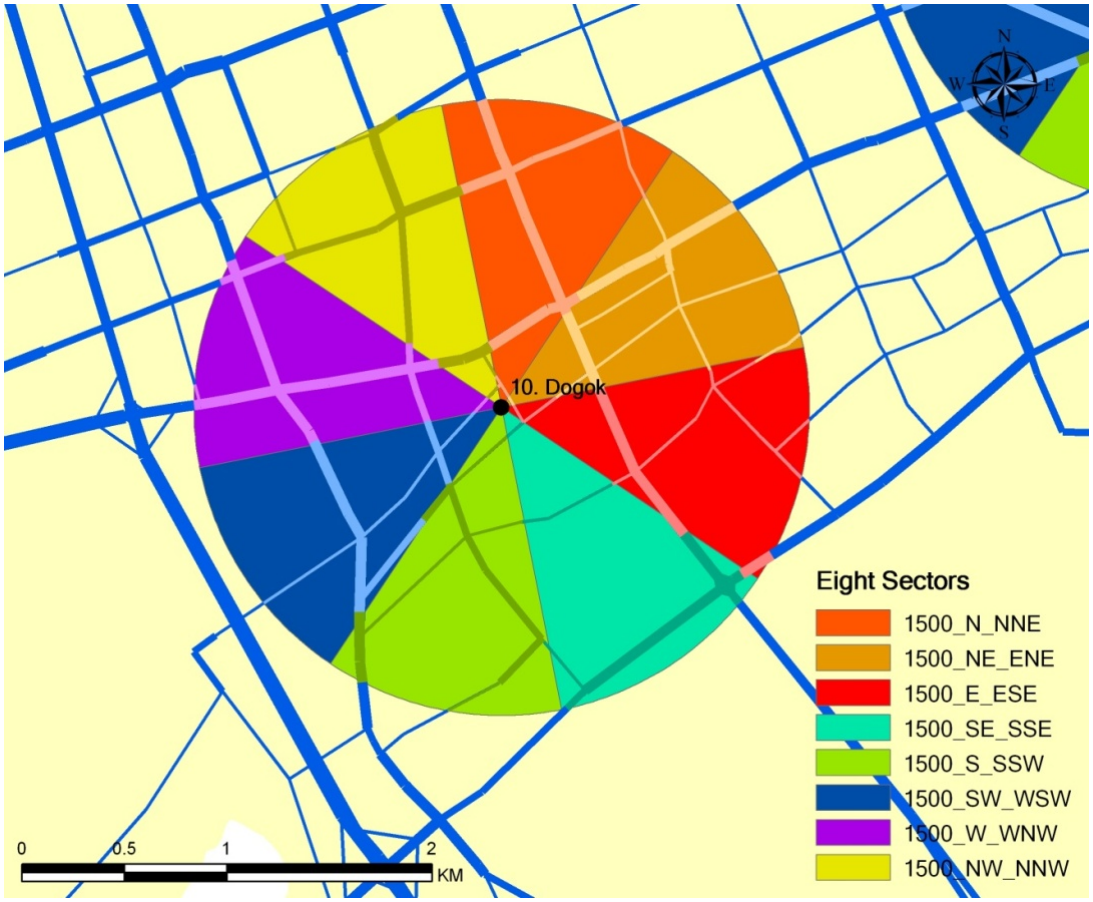

Figure 4.11 Eight-Sector buffer

[8] http://minwon.kma.go.kr/index.jsp

Since meteorological factors are measured on an hourly basis, WD data include 8,760 observations (365 days × 24 hours) in 2003. To account for WD impacts on pollution concentrations, WVKT is calculated as follows:

$$WVKT_{iR}^{h} = \sum_{d=1}^{8} \left(WD_{d}^{h} \times VKT_{diR}^{h} \right) + \left(CALM^{h} \times VKT_{iR}^{h} \right) \tag{4.13}$$

where,

h: Hour ($365 \times 24 = 8{,}760$),

i: AQM ($1 \rightarrow 34$),

R: Buffer radius ($500 \rightarrow 5500$).

WD_{d}^{h} and $CALM^{h}$ are binary numbers: if wind blows in direction d, WD_{d}^{h} = 1, otherwise = 0. Similarly, if calm conditions are observed (wind speed less than 0.2 meters/sec), $CALM^{h}$ = 1, otherwise = 0. Wind direction is measured every five minutes and the dominant direction is recorded as the hourly wind direction. Therefore the recorded wind direction is not necessarily the only wind direction. The hourly WVKT, calculated according to Eq. (4.13), is averaged out along different time dimensions, such as monthly, seasonal, and annual, and will be used as a possible explanatory variable in the air quality models presented in Chapter 7. Since VKTs are calculated for 11 buffers of different radii R ranging from 500 meters to 5,500 meters, WVKTs are also calculated for the same buffers. The VKTs and WVKTs values are presented in Appendix D.

4.4.4 Traffic Counts

The traffic assignment process estimates the traffic flow on each link of a network. The estimated flow is a daily traffic volume for the link, because the OD table is derived from daily activities. Monitored traffic counts are then used to subdivide the assigned daily flows into hourly traffic volumes. Traffic counts data have been collected at 4 different road classifications, including the CBD (26 locations), Han River bridges (19 locations), arterial roads (36 locations), and cordon line (38 locations). The count data can be downloaded from the Seoul city government website[9] (Seoul City Government, 2008), and are also reported in the 2003 Seoul Traffic Survey Report prepared by Seoul Metropolitan Police Agency (SMPA, 2004).

As illustrated in Figure 4.12 and Appendix E, the hourly traffic counts and shares during weekdays display a typical urban traffic flow pattern characterized by two peaks, in the morning and the evening. Saturday flows have patterns similar to those of weekdays, except in the CBD.[10] On the other hand, the counts during Sunday are different in terms of both the daily peak and the overall pattern. As expected, the volumes of traffic on Sunday are smaller than those on weekdays, with a few exceptions on Han River bridges and cordon lines during the afternoon. According to the Seoul Metropolitan Police Agency, the average daily traffic (ADT) on Sunday is 0.8 times the ADT on weekdays. The morning traffic flow on Sunday increases slowly as compared to weekdays, and peaks occur in the late afternoon. During nighttime, the traffic flows display a reverse pattern, smaller on weekdays and larger on weekend, with the exception of Sunday night in the CBD.

The difference in traffic flows between weekdays and weekends should have an influence on the concentrations of both directly emitted pollutants and secondary pollutants. Detailed comparisons between traffic flows and pollution concentrations during weekdays and weekend are presented in Chapter 5.

---

[9] http://www.seoul.go.kr/info/organ/subhomepage/transport/traffic_data/statisitcs/traffic/traffic1/11166_index.html

[10] In 2005 and 2006, the average daily traffic (ADT) of Saturday and Sunday are 1.00 and 0.80, 0.98 and 0.79, respectively. The ADT of weekdays vary from 0.96 to 1.03 (Seoul Metropolitan Police Agency, 2005, 2006). Since 2003, a five-day workweek system is introduced in Korea, but the traffic flows on Saturday do not have significantly decrease compared to those of weekdays.

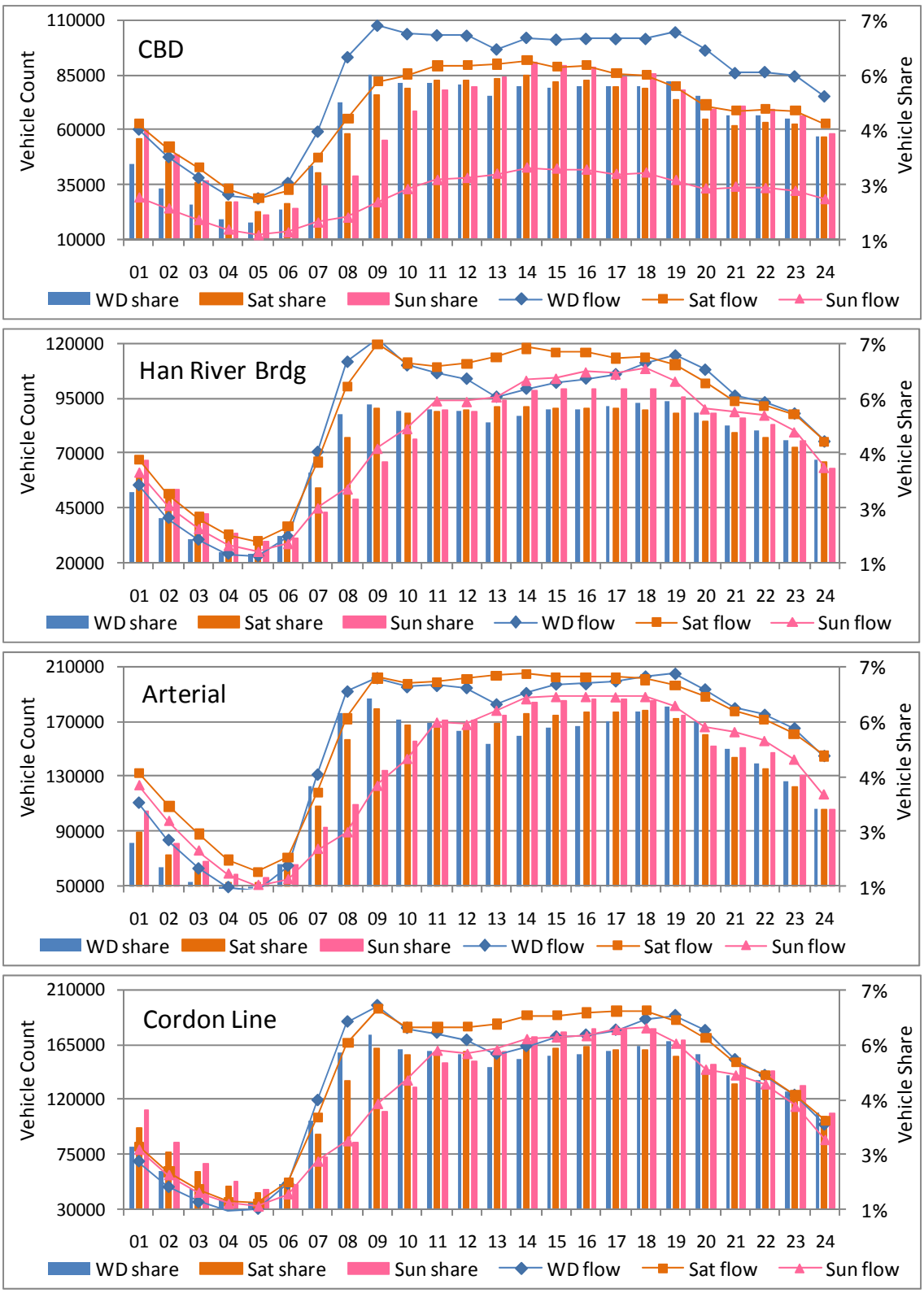

Figure 4.12 Hourly traffic counts and shares of CBD, Han River bridge, arterial roads, and cordon lines during weekday, Saturday, and Sunday

The traffic counts used in the aggregate temporal air quality models estimated in Chapter 6 have been developed by using publicly-released and non-publicly available data. Traffic counts measure the number of cars traveling in both directions on a monitored road. Traffic counts have been measured over a 1-week period at each station in 2003, and were expanded into a 1-year period by using the monthly traffic factors[11] presented in Table 4.2. Since traffic counts were collected at four different road classifications, the monthly traffic factors are also applied for the corresponding classifications. As seen in Table 4.2, the monthly factors display higher values in Spring and Autumn, while those corresponding to the Winter (January and February) and Summer (June and July) vacations display lower values. As the frequency of individual trips varies seasonally, these patterns are reasonable. After expanding traffic counts into 1-year period, all hourly observations are added over any given month.

	2005				2006			
	CBD	Han Bridge	Arterial	Cordon	CBD	Han Bridge	Arterial	Cordon
Jan	1.00	0.99	0.99	0.97	0.98	0.95	0.97	0.96
Feb	0.97	0.98	0.97	0.97	0.98	0.96	0.97	0.96
Mar	1.03	1.02	1.01	1.01	1.02	1.00	1.01	1.01
Apr	1.03	1.04	1.03	1.03	1.03	1.02	1.03	1.03
May	1.02	1.02	1.02	1.03	1.01	1.02	1.02	1.03
Jun	0.98	0.98	0.98	0.99	0.99	0.99	1.00	1.01
Jul	0.97	0.98	0.98	0.98	0.96	0.97	0.97	0.97
Aug	0.98	1.00	1.00	1.00	0.97	0.99	1.00	1.00
Sep	0.98	0.99	0.99	1.00	1.03	1.03	1.03	1.03
Oct	1.02	1.01	1.02	1.02	0.99	1.00	0.99	0.99
Nov	1.03	1.01	1.03	1.02	1.02	1.05	1.02	1.01
Dec	0.99	0.97	1.00	0.98	1.02	1.02	1.01	0.99

Table 4.2 Monthly traffic factors

The patterns of average hourly traffic counts for weekdays and Sunday and for each month are displayed in Figure 4.13. The higher traffic counts during weekdays are also characterized by the typical two peaks, in the morning and the evening. The traffic counts on

11 Monthly traffic factor = MAWT / AAWT, MAWT (Monthly Average Weekday Traffic), AAWT (Annual Average Weekday Traffic)

Sunday are different in terms of daily peak, traffic volume, and pattern of flows. As expected, traffic volumes on Sunday are smaller than on weekdays, with a few exceptions during nighttime. In addition, the traffic flow on Sunday increases slowly in the morning, as compared to weekdays, and peaks in the late afternoon. As Table 4.2 shows, the monthly variations of traffic flows are limited (0.97 ~ 1.03), which is also observed in Figure 4.13. In contrast, hourly traffic flows vary significantly during the day, and these variations are observed across the whole year, weekdays, and weekends. These differences in traffic flows should have an influence on pollution concentrations for both directly emitted and secondary pollutants.

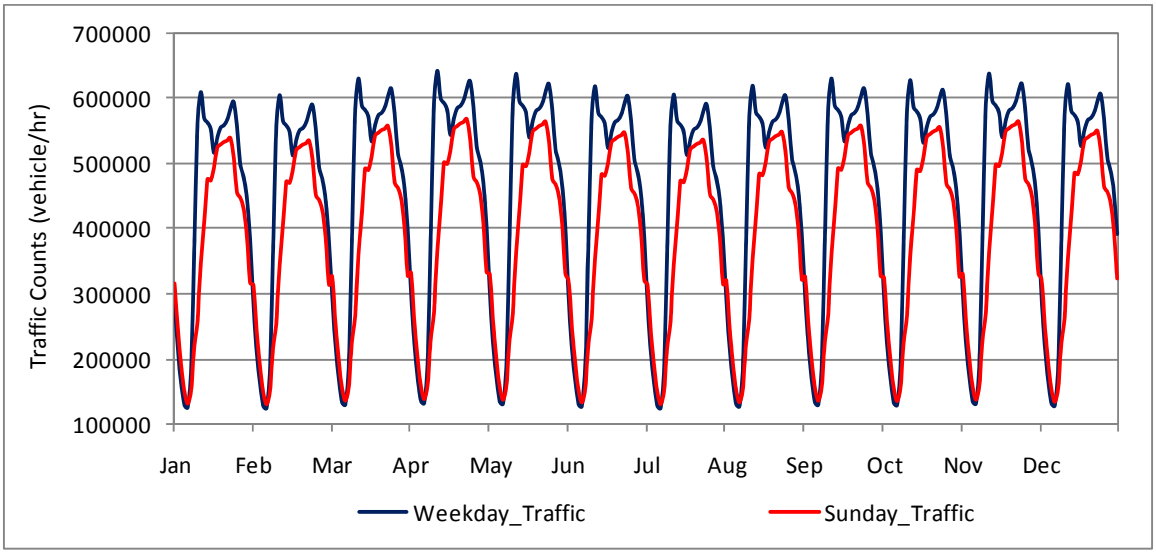

Figure 4.13 Comparing hourly traffic counts on weekdays and Sunday

4.5 LAND USES

4.5.1 Vegetative and Non-vegetative Classification using Satellite Imagery

Urban vegetation is known to assimilate air pollutants and mitigate pollution concentrations. Trees absorb gaseous pollutants from the air and metabolize them through leaf stomata or dissolve water soluble pollutants with moist leaf surfaces (Takahashi et al., 2005). In addition to their air pollution assimilation capability, trees may also play a role in capturing fine particles and reducing air temperature, decreasing occurrences of urban heat island in the summer (Sailor, 1995). Direct deposition of nitrogen dioxide and decreasing temperature may reduce O_3 concentrations. On the other hand, biogenic VOC emissions from vegetation can increase the rate of O_3 formation in either urban or rural areas (Chameides, Lindsay, Richardson, & Kiang, 1988; Trainer et al., 1987).

To quantify the relationship between air pollution concentration and urban vegetation, it is necessary to acquire the satellite image of the study region in order to calculate green areas around AQMs. The Landsat-7 satellite has scanned the earth surface with multispectral images and two of these bands, near-infrared and red, are used to calculate the Normalized Difference Vegetation Index (NDVI). NDVI is a useful tool to classify land surfaces into vegetative and non-vegetative areas (Tucker, 1979). Using a Landsat-7 satellite image taken on September, 2001, the vegetative areas of the Seoul can be delineated, and the results are illustrated in Figure 4.14.

The chlorophyll in plant leaves absorbs visible light for photosynthesis, but the leaves, on the other hand, reflects near-infrared radiations. The images of Landsat-7 satellite (30m × 30m resolution) include these two spectral bands, thus the NDVI can be calculated using the red reflected radiant flux (Red) and the near-infrared radiant flux (NIR), with:

$$\mathrm{NDVI} = \frac{\mathrm{NIR} - \mathrm{Red}}{\mathrm{NIR} + \mathrm{Red}} \tag{4.14}$$

Based on the above equation, the surface of the study region is classified into vegetative and non-vegetative areas. The theoretical range of NDVI values is [-1 ~ 1]. Generally, low values near 0 (less than 0.1) represent barren areas, such as soil, rock, and snow. As the value of each pixel increases, the corresponding cell represents a thicker and healthier green area (Jackson, Slater, & Pinter, 1983; NASA, 2009).

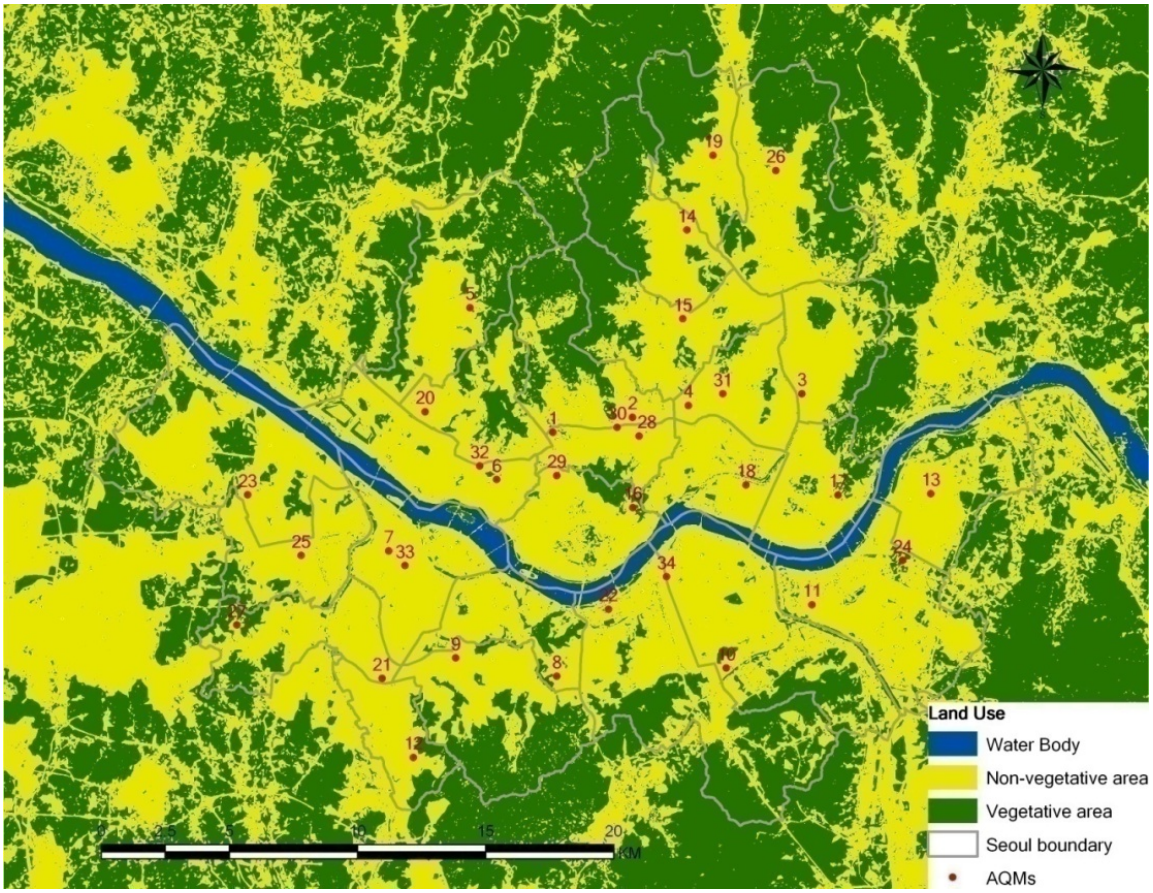

Figure 4.14 Classification of land surface into vegetative and non-vegetative area

4.5.2 Biotope Map (Land Uses)

The Seoul Development Institute (SDI) has released the first biotope map of Seoul, Korea, in 2000 and an updated map was published five years later, including 24,847 land parcels.[12] Each land parcel has been classified into urban or non-urban land uses, with 9 middle classes and 64 detailed classes. The middle-class land-uses classification is illustrated in Figure 4.15. The non-urban land uses include forest, open space, river, stream, and wetland. The urban land uses are sub-classified as residential, commercial, transportation, industrial, urban infrastructure, public facilities, industrial, denuded, and inaccessible areas.

In 2005, non-urban land uses made around 40% and built-up areas 60% of Seoul. Among the built-up land uses, residential and commercial areas made up the largest share, 18.9%. The

[12] http://www.seoul.go.kr/info/organ/subhomepage/urban_new/library/mode_8_04.html

share of transportation areas is 10.5%, and that of public facilities 5.1%. Because of strict restrictions on the expansion and relocation of industrial facilities in the capital region, industrial land uses display a decreasing trend. Meanwhile the largest change occurred in forests and wetlands, which decreased by 1,622 ha and increased by 1,562 ha, respectively. The main reason for these changes originates from the modification of the classification system, including areas at water's edge, which are reclassified as wetland in the 2nd version of biotope map (Cho & Song, 2005). Table 4.3 presents areas and shares for all land uses and changes in land uses between 2000 and 2005.

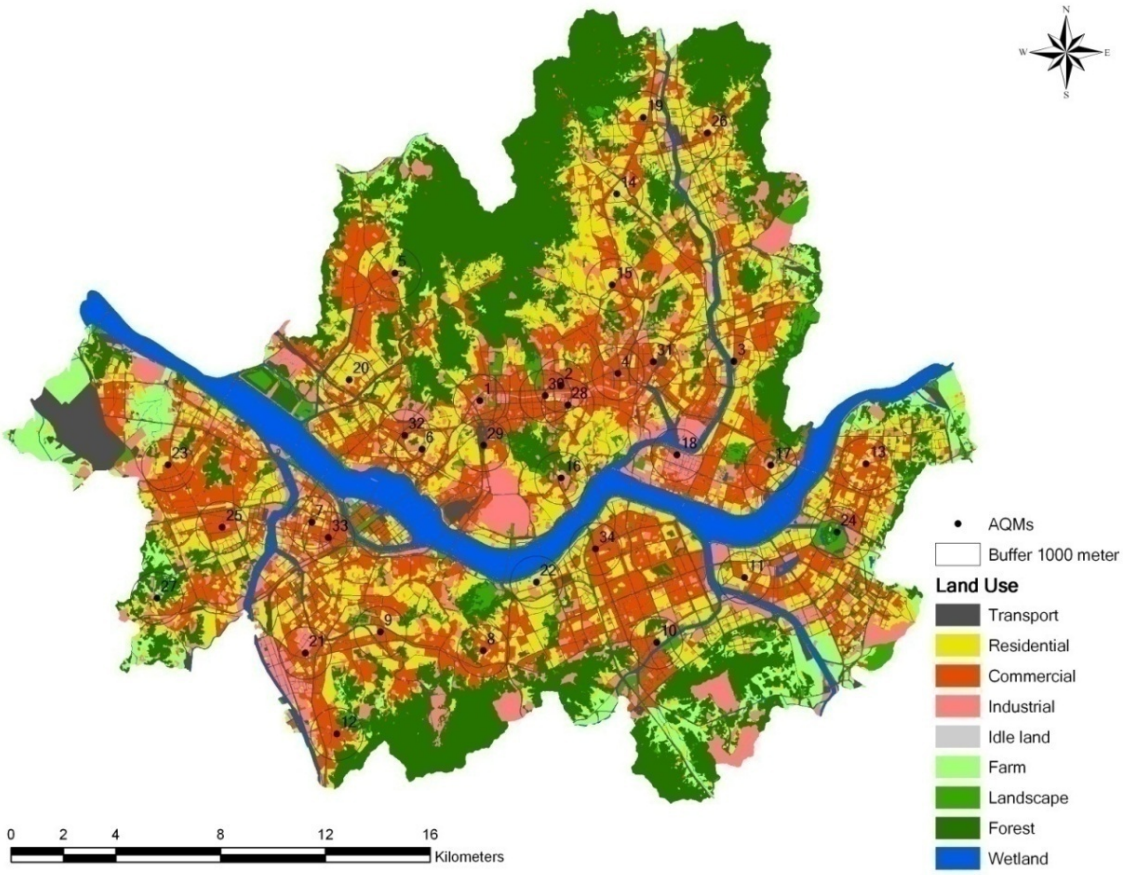

Figure 4.15 Land use classification in Seoul, Korea, 2005

Category	Land Uses	2000		2005		Change of Area
		Area (ha)	**Ratio**	**Area** (ha)	**Ratio**	
Non-urban	Forest	21,041.7	34.6%	19,419.9	31.9%	-1,621.8
	Water Body	3,359.4	5.5%	4,921.1	8.1%	1,561.7
Urban	Residential	10,930.9	18.0%	11,480.3	18.9%	549.4
	Commercial	11,750.1	19.3%	11,473.2	18.9%	-276.9
	Transport	6,344.7	10.4%	6,409.1	10.5%	64.4
	Public Facilities	3,175.8	5.2%	3,128.5	5.1%	-47.3
	Inaccessible area	1,169.8	1.9%	1,495.7	2.5%	325.9
	Denuded area	1,417.4	2.3%	1,113.9	1.8%	-303.5
	Industrial	823.7	1.4%	699.2	1.1%	-124.5
	Urban Infrastructure	800.4	1.3%	690.9	1.1%	-109.5
Sum		60,813.9	100.0%	60,831.8	100.0%	

Table 4.3 Comparisons of land use change in Seoul (2000 ~ 2005)[13]

[13] Rearranged based on the page 204 of Biotope Mapping and Application in Seoul (Cho & Song, 2005). Commercial land use includes mixed residential and business area. Detail classifications for residential, commercial, industrial, urban infrastructure, and transportation are provided in Appendix F.

4.6 METEOROLOGY

Meteorological factors play a major role in determining not only air pollution concentrations but also the removal of pollutants from the atmosphere. Air pollutants in the ambient atmosphere are consistently moving and reacting with other factors, creating secondary pollutants or photolytic processes. As presented in Figure 4.16, the average weekday pollutant concentration varies by a factor of 5 ~ 17 from day to day (for SO_2, the minimum is 2.8 ppb and the maximum 13.8 ppb; for PM10, the minimum is 14.5 μg/m^3 and the maximum 245.9 μg/m^3). Assuming that the anthropogenic emissions of pollutants in the urban region are relatively constant[14], the variability of concentrations can be explained by meteorological factors, such as solar radiation, temperature, wind speed and direction, and humidity changes.

Meteorological factors are used to regression analysis, because these factors are known theoretically to increase or decrease the air pollutants concentrations (Bloomfield, Royle, Steinberg, & Qing, 1996; Jo & Park, 2005; Krupa, Nosal, Ferdinand, Stevenson, & Skelly, 2003; Tsai, Wang, Wang, & Chan, 2008; US EPA, 2006; Tsai et al., 2008). As discussed in the review of the chemical reaction of NO_2 and O_3, ultraviolet (UV) radiations from the sun play a key role in initiating the photochemical dissociation of NO_2, hence in leading to the formation of O_3. Major episodes of high concentrations occur in conditions of slow moving wind. High pressure during warmer seasons is associated with high O_3 episodes, because the inhibition of vertical and horizontal mixing of precursors and the buildup of O_3 occur under these meteorological circumstances. Notable occurrences of elevated O_3 episodes and high temperature have been reported, and there are possible reasons for this relation: (1) high temperatures induce increased photolysis rates of NO_2, (2) biogenic VOC emissions from plants (isoprene and monoterpene) and anthropogenic hydrocarbon emissions (evaporative losses) are increasing with temperature (Cardelino & Chameides, 1990), (3) peroxyacetylnitrate (PAN) is a major sink for NO_x and odd hydrogen (radicals) at low temperatures, but the decomposition of PAN is accelerated at high temperatures, leading to the generation of O_3 (Sillman & Samson, 1995), and (4) high O_3 episodes are observed in the US during summer, with combinations of high temperature and stagnant weather conditions (Jacob et al., 1993). According to measurements of O_3 and temperature in Cleveland, OH, O_3 concentrations have little impacts under 20 ˚C, but, after this threshold point, concentrations increase log-linearly (Camalier, Cox, & Dolwick, 2007). Since humidity is usually

[14]According to the calculation of traffic counts based on 2005 data (Seoul Metropolitan Police Agency, 2005), the ratio of average daily traffic (ADT) shows limited changes. The monthly as well as week day ADT varies between 0.97 and 1.03 (Jan. 0.99, Feb. 0.97, Mar. 1.02, Apr. 1.03, May 1.02, Jun. 0.98, Jul. 0.98, Aug. 0.99, Sep. 0.99, Oct. 1.02, Nov. 1.02, Dec. 0.98; Mon. 0.99, Tues. 1.00, Wed. 1.00, Thur. 1.01, Fri. 1.00, Sat. 1.00, Sun. 0.80).

correlated with cloud cover and atmospheric instability, higher humidity generates unfavorable condition for O_3 formation. Empirical studies have reported the relationship between low humidity and high concentration of O_3, in Taiwan (Tsai et al., 2008), the U.S. (Camalier et al., 2007; Krupa et al., 2003), Korea (Jo & Park, 2005), and Mexico (Gold et al., 1996).

Hourly meteorological data have been downloaded from the website of the Korea Meteorological Administration (2008). Since the measurements are based on hourly average values, the total numbers of observations are 8,760 (365 days × 24 hours). Descriptive analyses of meteorological data are presented at the following section.

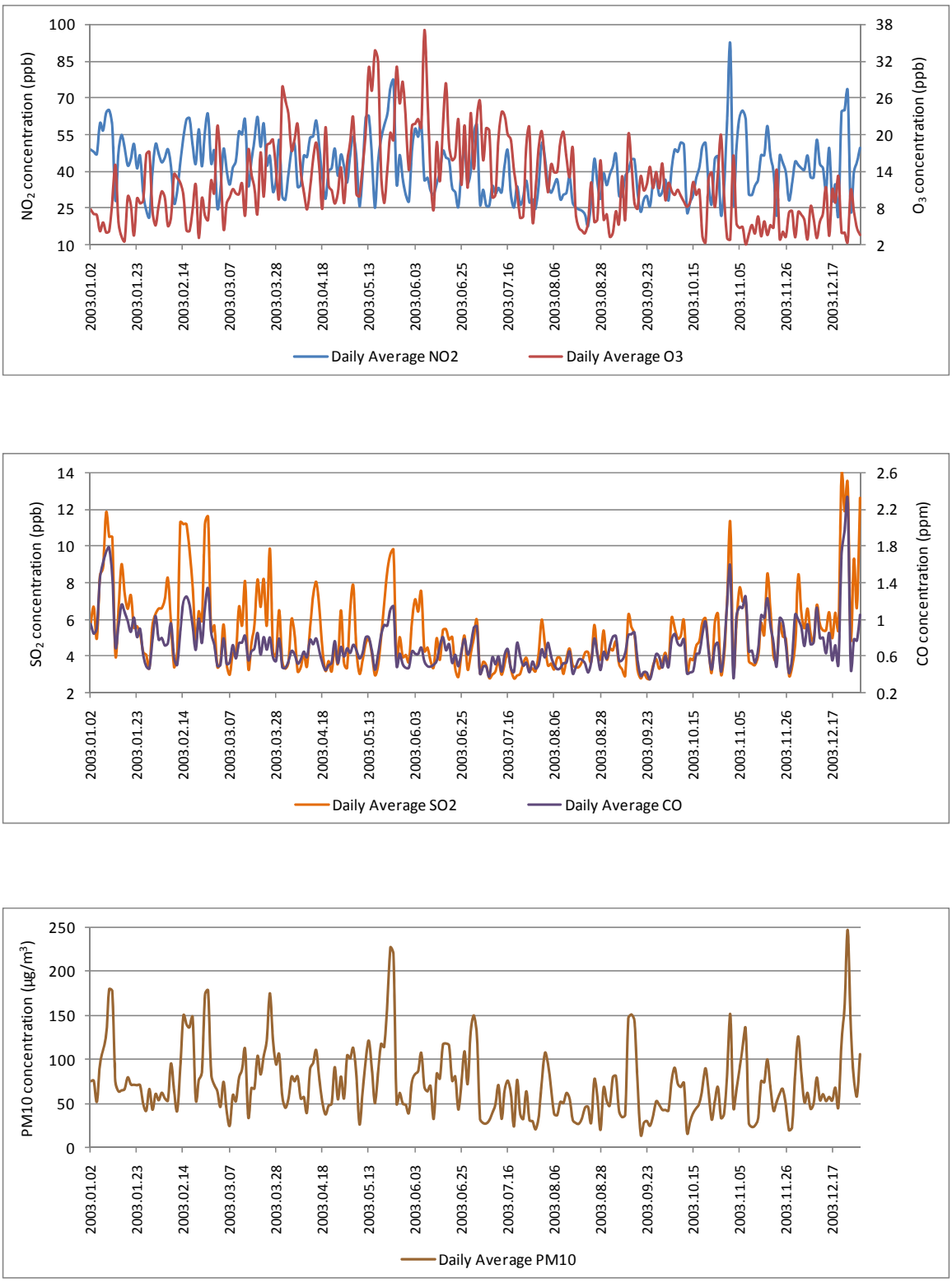

Figure 4.16 Variations of average daily concentrations of pollution during weekday[15]

[15] Figure 4.16 includes daily concentrations during weekdays, thus the values of holidays and weekends are excluded on this graph.

Since the Seoul Metropolitan Area is located in the northern hemisphere, at latitude of 37.3, there are four seasons characterized by different meteorological traits. Figure 4.17 illustrates the daily pattern of solar radiation over the four seasons. As expected, the radiations begin at 6 ~ 9 AM, depending on the season, reach a daily peak around 1 PM, and then decrease in intensity until 6 ~ 8 PM. Radiation intensity during spring is highest, and it is lowest in winter. The high intensity of solar radiation during spring is one of the reasons of high O_3 concentrations.

The hourly variations in humidity represent a pattern reverse to that of solar radiations. The peak of humidity occurs before sunrise, and humidity decreases with sunrise. The minimum is observed around 2 ~ 3 PM, and then humidity gradually increases. This pattern is similar across the seasons. The intra-daily and seasonal variations of humidity are presented at Figure 4.18. Due to the rainy season, humidity in summer is higher than in the other seasons. Spring is the least humid, and this is coincident with high solar radiation.

Because the Korean peninsula is located at mid-latitudes in the northern hemisphere, the prevailing wind direction is westerly. As seen in Figure 4.19, 40% of the wind blows from the west. The frequencies of wind directions change with the season. During winter, wind frequencies from the west increase. On the other hand, in summer, wind frequencies from the west decrease and wind frequencies from the east increase. There are less calm days in winter. The speed of westerly wind is greater than that of easterly wind. Based on the observations of wind directions, it is possible to identify prevailing wind directions in the region. This empirical evidence may be used as decision support data for the location of industrial complexes, the development of residential areas, and the construction of major highways. Figure 4.20 illustrates the daily pattern of wind speed over the four seasons. Generally, wind speed during daytime is greater than during nighttime, and the same pattern occurs across the four seasons. The wind speed in winter and spring is greater than in summer and autumn.

The variations of temperature during the four seasons and its daily fluctuations are illustrated in Figure 4.21 and 4.22. The two graphs display typical temperature pattern of mid-latitudes, high in summer and low in winter. Comparing hourly average temperatures between spring and autumn, the temperature in spring is slightly less than in autumn. The difference between daily maximum and minimum temperatures is around 7.5˚C. The hourly temperature varies with the intensity of solar radiation. Daily low temperatures occur before sunrise and the peak is observed at 3 PM. Since these meteorological factors display different values depending on hours and seasons, they may have different impacts on pollution concentrations.

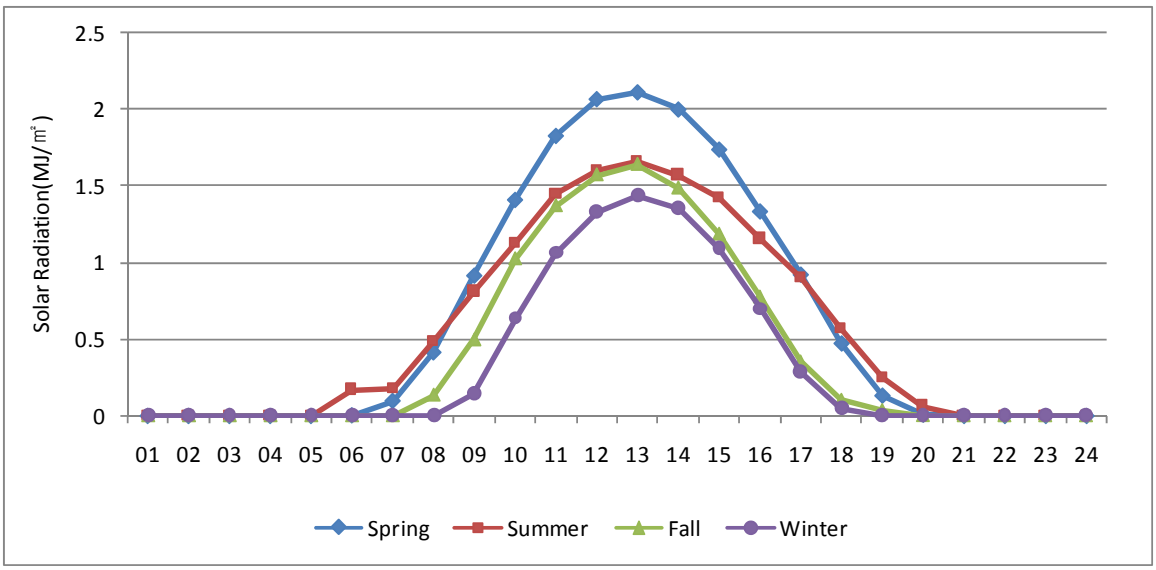

Figure 4.17 Intra-daily and seasonal variations of solar radiations

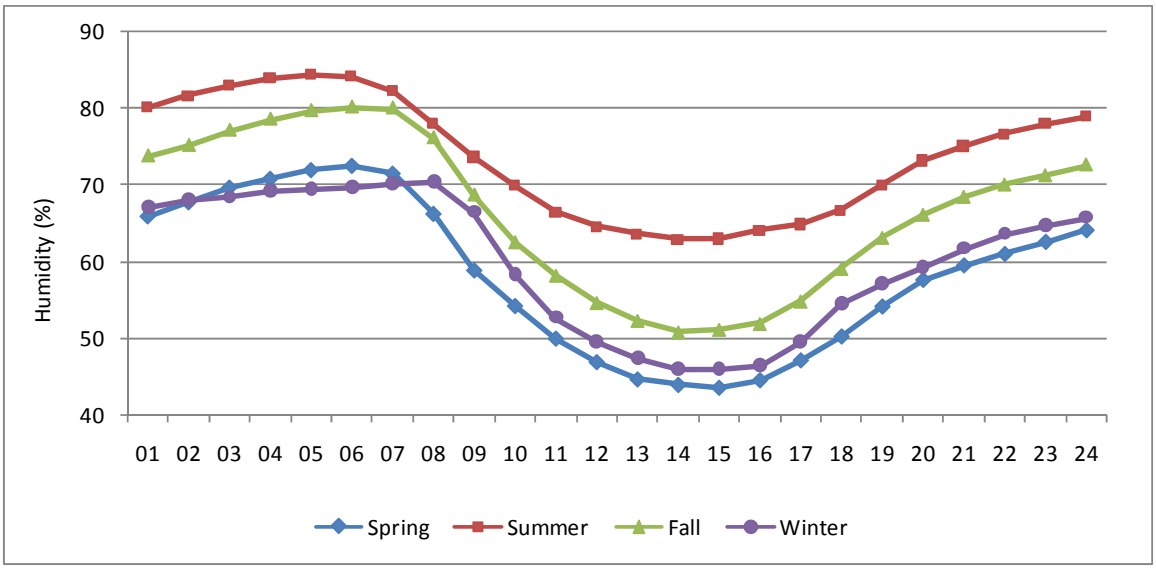

Figure 4.18 Intra-daily and seasonal variations of humidity

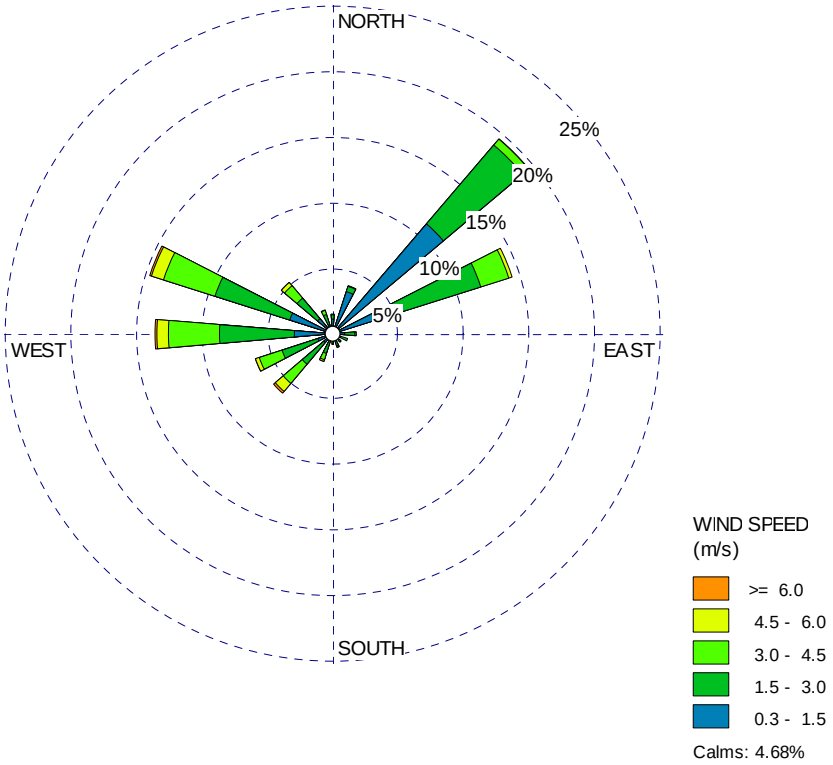

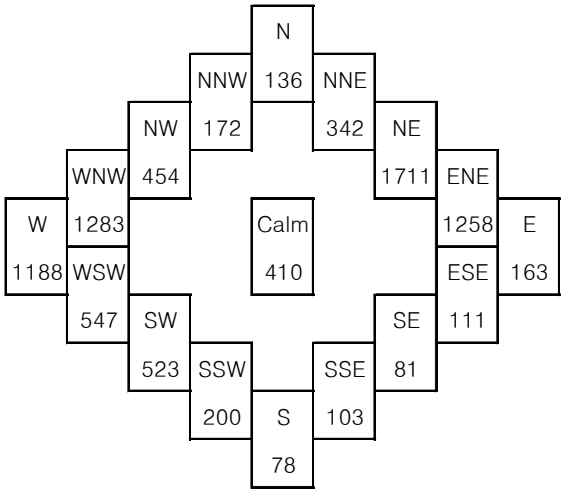

	North	East	South	West	Calm
Year	19.8%	27.7%	7.8%	40.0%	4.68%
Summer[1]	18.8%	31.2%	11.7%	33.9%	4.53%
Winter[2)]	19.5%	17.0%	5.2%	54.6%	3.70%

1) Summer includes June, July, and August
2) Winter includes January, February, and December

Figure 4.19 Wind rose and wind direction frequency

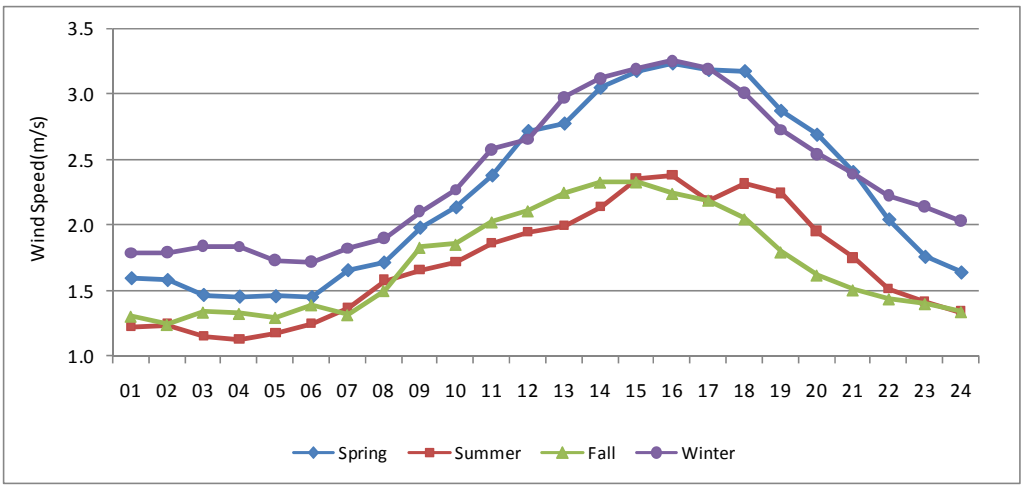

Figure 4.20 Intra-daily and seasonal variations of wind speed

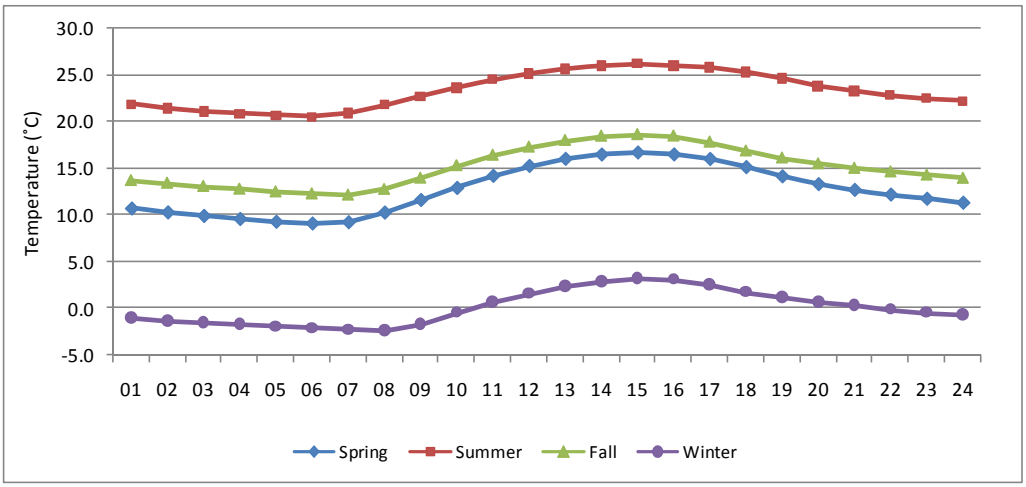

Figure 4.21 Intra-daily and seasonal variations of temperatures

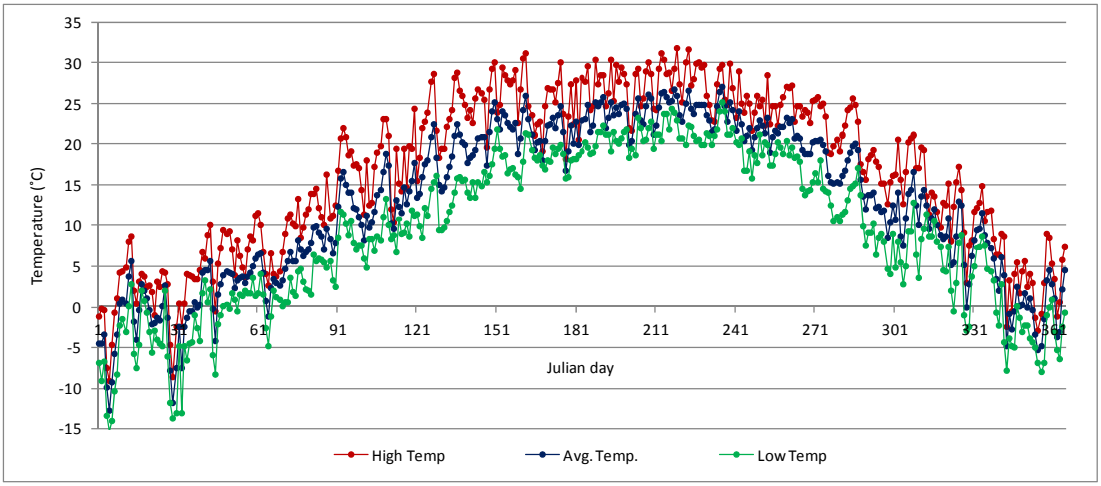

Figure 4.22 Variations of daily high, average, and low temperatures

CHAPTER 5

EXPLORATORY ANALYSIS

Pollution concentration data from 7 roadside and 27 background AQMs in the Seoul Metropolitan Area are analyzed in an exploratory fashion. This chapter discusses the patterns of pollution concentrations along different time dimensions: annual, seasonal, monthly, and hourly. Since transportation is known to be responsible for a substantial share of urban air pollution, traffic counts data collected at 4 different road classifications, including the CBD (26 locations), Han River bridges (19 locations), arterial roads (36 locations), and cordon line (38 locations), are used to compare hourly concentrations and traffic flows across the four seasons. Traffic flows during weekends are considerably lower than those during weekdays, leading to a comparison of concentrations and traffic flows during weekdays, Saturday, and Sunday.

5.1 TRAFFIC VOLUMES AND NO_2 CONCENTRATIONS

In this section, the overall NO_2 concentrations for both roadside and background AQMs are analyzed. The temporal variations of NO_2 concentrations are first described, accounting for seasonal, monthly, and hourly patterns. All data, including NO_2 concentrations and traffic volumes, are hourly and for 2003. The hourly variations of NO_2 concentrations are compared with traffic count data in each season. Comparisons between weekdays and weekend are also performed. Exceedances of NO_2 standard are identified with regard to traffic changes and chemical reactions (creation and removal of NO_2).

5.1.1 Temporal Variations of NO_2 Concentrations

Concentrations of NO_2 are mainly affected by its chemical creation and removal processes. Understanding these reactions is helpful to analyze the temporal variations of NO_2 concentrations. As seen in Table 5.1, the concentrations are varying seasonally, monthly, and hourly. Yearly, seasonal, and monthly values are based on daily-average concentrations, whereas

hourly variations are based on hourly-average concentrations. Spring and Winter have higher NO_2 concentrations than Summer and Fall. The highest monthly average takes place in February, one of the Winter months (Dec, Jan, and Feb). Since the monthly variations of average daily traffic (ADT) are limited (0.96 ~ 1.03)[1] (Seoul Metropolitan Police Agency, 2006), variations in transportation emissions may not be the reason for the seasonal and monthly variations in NO_2 concentrations. One possible factor is residential heating, which starts in late Fall (Nov), and lasts until Spring in the densely developed Seoul Metropolitan Area (16,567 person km^{-1} in 2003[2]). On the other hand, the hourly variations of NO_2 concentrations display a pattern similar to other metropolitan cities in Korea (Daegu), and Azusa in California (Jo & Park, 2005; Fujita et al. 2003). The typical pattern of hourly NO_2 concentrations involves peaks in the morning and the evening, and a trough during daytime. These patterns can be explained as follows. Traffic volumes display significant diurnal and nocturnal changes, with morning and evening peaks. The reason for the diurnal trough may be the photolysis of NO_2 with UV, as explained by Eq. (2.8). Active photodissociations of NO_2 in daytime hinder the accumulation of NO_2, thus the diurnal trough. The daily climax of NO_2 concentration (21:00) has a slight time lag with the traffic peak. There are two possible reasons. One is that the ozone concentration accumulated during daytime is abundant enough so that emitted NO can be easily converted into NO_2 (Eq. 2.1). The other reason is that, after sunset, the NO_2 photolysis no longer happens, and therefore NO_2 can accumulate up to the daily highest level.

Frequencies for exceedances of the Korean Ambient Air Quality Standards (KAAQS) are also provided in Table 5.1, where the KAAQS for NO_2 are 150 ppb per hour, 80 ppb per day, and 50 ppb per year. In 2003, the annual average (38 ppb) did not exceed the standard, but exceedances of daily and hourly standards were common. The numbers of exceedances for both the daily and hourly standards were 76 and 52, respectively. The exceedances of the daily standard were frequently observed in May (23), Oct (17), and Nov (15). The violations of the hourly standard coincide with the afternoon traffic peak, and these exceedances are commonly detected over the period 17:00 to 23:00 pm.

---

[1] Variations of ADT by month: Jan. 0.96, Feb. 0.96, Mar. 1.01, Apr. 1.03, May 1.03, Jun. 1.01, Jul. 0.97, Aug. 1.00, Sep. 1.03, Oct. 0.99, Nov. 1.01, Dec. 0.99

[2] http://www.index.go.kr/egams/stts/jsp/potal/stts/PO_STTS_IdxMain.jsp?idx_cd=1007&bbs=INDX_001

(Unit: ppb)

Time dimension[1)]		Background AQMs			Roadside AQMs			Exceedances[2)]		
		Average	Min	Max	Average	Min	Max	N Obs.	N. Exceed	Percent
Year		38.0	3.7	120	48.7	5.8	124	9855	76	0.77%
Season	Spring	42.6	10.2	120	54.3	10.7	102	2484	26	1.05%
	Summer	31.6	3.7	101	45.0	5.8	98	2484	7	0.28%
	Fall	35.9	4.4	116	45.5	16.5	124	2457	32	1.30%
	Winter	42.5	8.6	97	50.6	17.5	103	2430	11	0.45%
Month	Jan	42.7	10.7	89	50.4	17.5	88	837	1	0.12%
	Feb	45.2	10.8	84	51.8	27.8	80	756	1	0.13%
	Mar	44.3	15.5	93	53.6	24.0	100	837	1	0.12%
	Apr	39.6	12.5	85	50.3	29.2	91	810	2	0.25%
	May	43.9	10.2	120	57.5	10.7	102	837	23	2.75%
	Jun	37.6	7.8	92	48.9	5.8	98	810	4	0.49%
	Jul	30.7	9.5	101	45.7	22.4	91	837	3	0.36%
	Aug	26.5	3.7	61	40.6	16.6	69	837	0	0.00%
	Sep	30.3	4.4	73	41.0	16.5	86	810	0	0.00%
	Oct	38.0	7.0	116	48.6	23.2	124	837	17	2.03%
	Nov	39.7	11.4	108	47.6	17.1	118	810	15	1.85%
	Dec	40.1	8.6	97	49.5	19.0	103	837	9	1.08%
Hour	1	40.1	1.0	150	43.5	1.0	147	9855	1	0.01%
	2	36.8	1.0	148	38.7	1.0	140	9855	.	N/A
	3	34.1	1.0	148	35.6	1.0	134	9855	.	N/A
	4	32.2	1.0	120	33.3	1.0	125	9855	.	N/A
	5	31.4	1.0	118	33.1	3.0	113	9855	.	N/A
	6	32.7	1.0	123	38.7	1.0	110	9855	.	N/A
	7	35.6	1.0	123	44.8	8.0	119	9855	.	N/A
	8	38.7	1.0	144	49.0	6.0	156	9855	.	N/A
	9	40.5	1.0	166	51.1	6.0	151	9855	1	0.01%
	10	40.2	1.0	154	51.8	5.0	176	9855	1	0.01%
	11	39.1	1.0	160	52.2	6.0	146	9855	1	0.01%
	12	37.3	1.0	152	52.0	8.0	146	9855	1	0.01%
	13	34.8	1.0	147	51.7	1.0	140	9855	.	N/A
	14	33.6	1.0	152	52.2	1.0	139	9855	1	0.01%
	15	33.5	1.0	151	53.2	1.0	141	9855	1	0.01%
	16	34.3	3.0	169	54.8	1.0	159	9855	3	0.03%
	17	36.0	3.0	180	56.0	1.0	188	9855	8	0.08%
	18	38.9	2.0	190	55.9	1.0	190	9855	7	0.07%
	19	42.1	1.0	189	56.4	3.0	166	9855	6	0.06%
	20	44.6	1.0	168	56.4	2.0	159	9855	3	0.03%
	21	45.3	2.0	169	55.6	1.0	159	9855	7	0.07%
	22	44.9	1.0	170	54.4	1.0	160	9855	5	0.05%
	23	44.2	0.0	160	53.2	1.0	162	9855	4	0.04%
	24	42.8	1.0	160	49.7	1.0	157	9855	2	0.02%

1) The yearly average is calculated with 27 AQMs × 365 days (9855cases). Other averages are calculated in the same way.

: Min : Max

2) Standards for NO_2: 150 ppb/hour, 80 ppb/day, 50 ppb/year

Table 5. 1 Temporal variations and exceedances of NO_2 standards at background AQMs in 2003

5.1.2 NO_2 Concentration Differences between Roadside and Background AQMs

Seasonal, monthly, and hourly comparisons of NO_2 concentrations between roadside and background AQMs are depicted in Figures 5.1, 5.2, and 5.3, respectively. Concentration trends are evaluated using daily average NO_2 concentrations during the four seasons and 12 months. For hourly variations comparisons, hourly average values are used. Box plots of daily and hourly average concentrations contain the maximum, 95th percentile, higher quartile (3/4), mean, lower quartile (1/4), 5th percentile, and minimum concentrations.

As expected, the concentrations at roadside AQMs are higher than those at background AQMs in all three comparisons. Although roadside AQMs data are not included in the calculations of publicly-announced concentrations, special attention should be given to NO_2 exposure of residents and millions of pedestrians near roadways. The pattern of concentrations at roadside AQMs is also presented in Table 5.1, and is similar to the pattern of background AQMs in terms of seasonal, monthly, and hourly variations. In particular, the average concentrations in Spring (May) frequently exceed the standard. As discussed in Chapter 2, NO_2 concentrations are highly correlated with O_3 concentrations. High accumulations of O_3 occur frequently during Spring, especially in May, and have the potential to be converted into NO_2. Thus, the exceedance of the NO_2 standard in May can be explained by the high O_3 concentrations in that month.

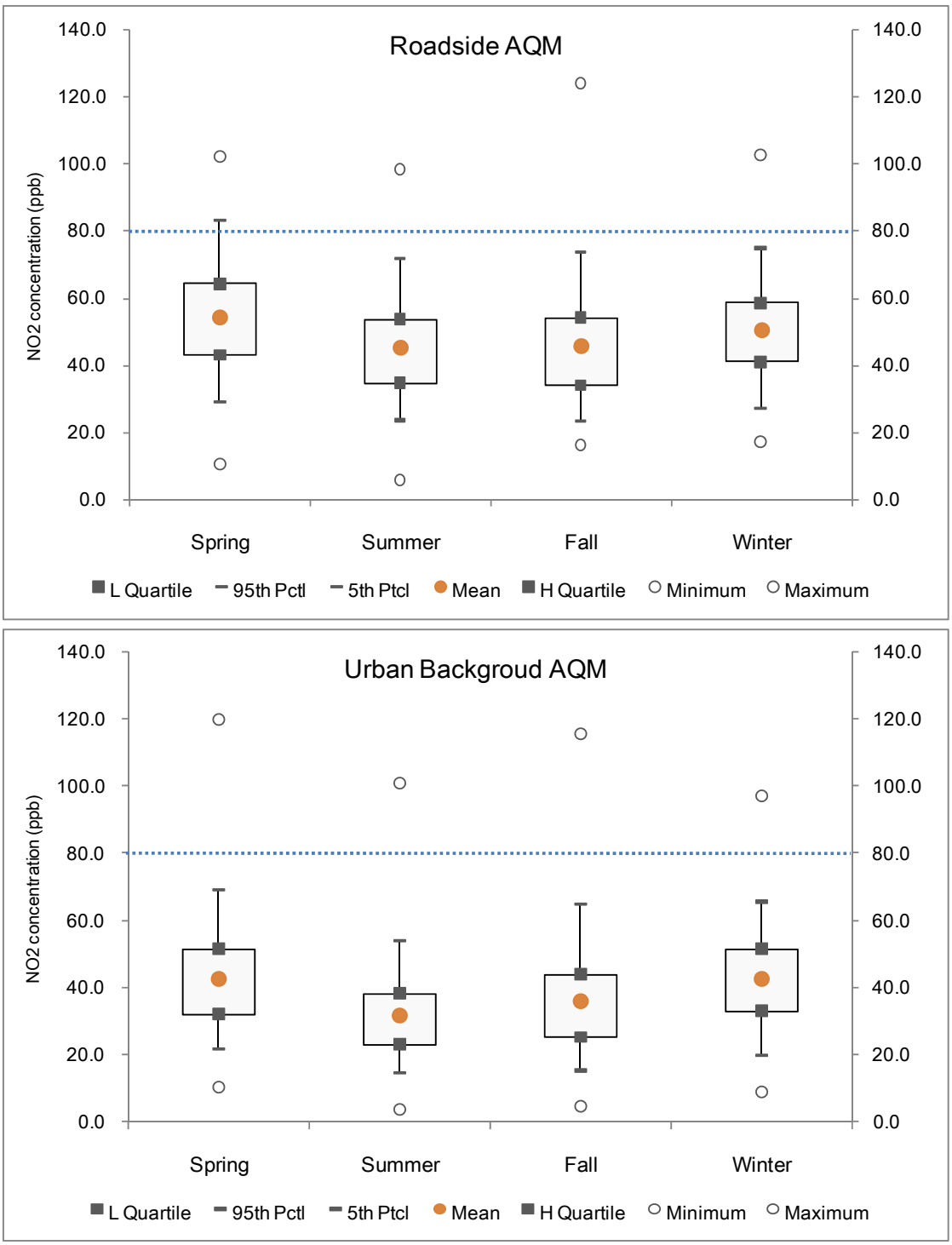

Figure 5.1 Seasonal variations of NO_2 concentrations[3]

[3] Maximum, 95th percentile, higher quartile (3/4), mean, lower quartile (1/4), 5th percentile, and minimum for roadside and urban background AQMs (based on daily NO_2 average concentrations). The dotted line indicates the daily standard for NO_2 concentration: 80 ppb/day.

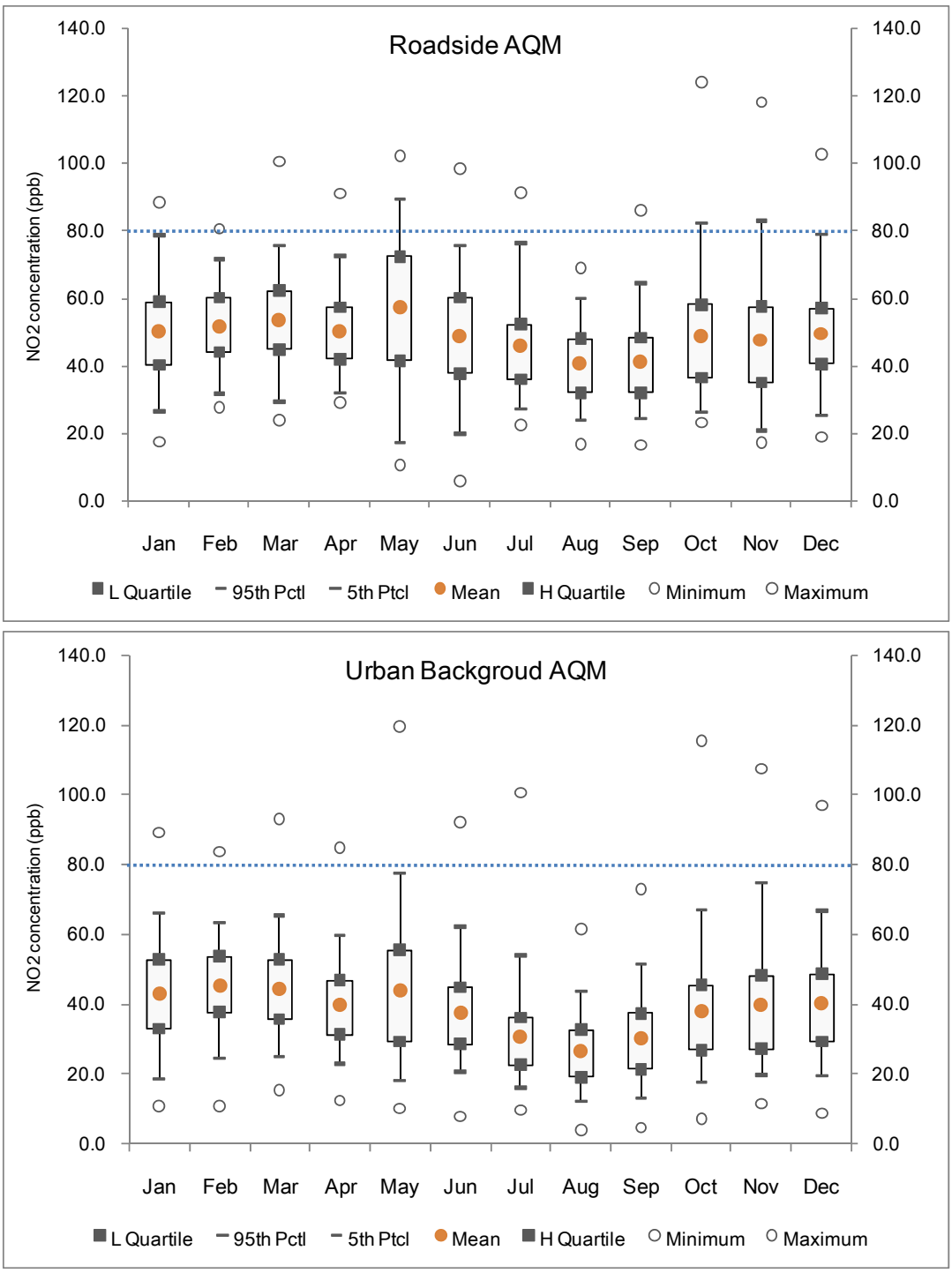

Figure 5.2 Monthly variations of NO_2 concentrations[4]

[4] Maximum, 95th percentile, higher quartile (3/4), mean, lower quartile (1/4), 5th percentile, and minimum for roadside and urban background AQMs (based on daily NO_2 average concentrations). The dotted line indicates the daily standard for NO_2 concentration: 80 ppb/day.

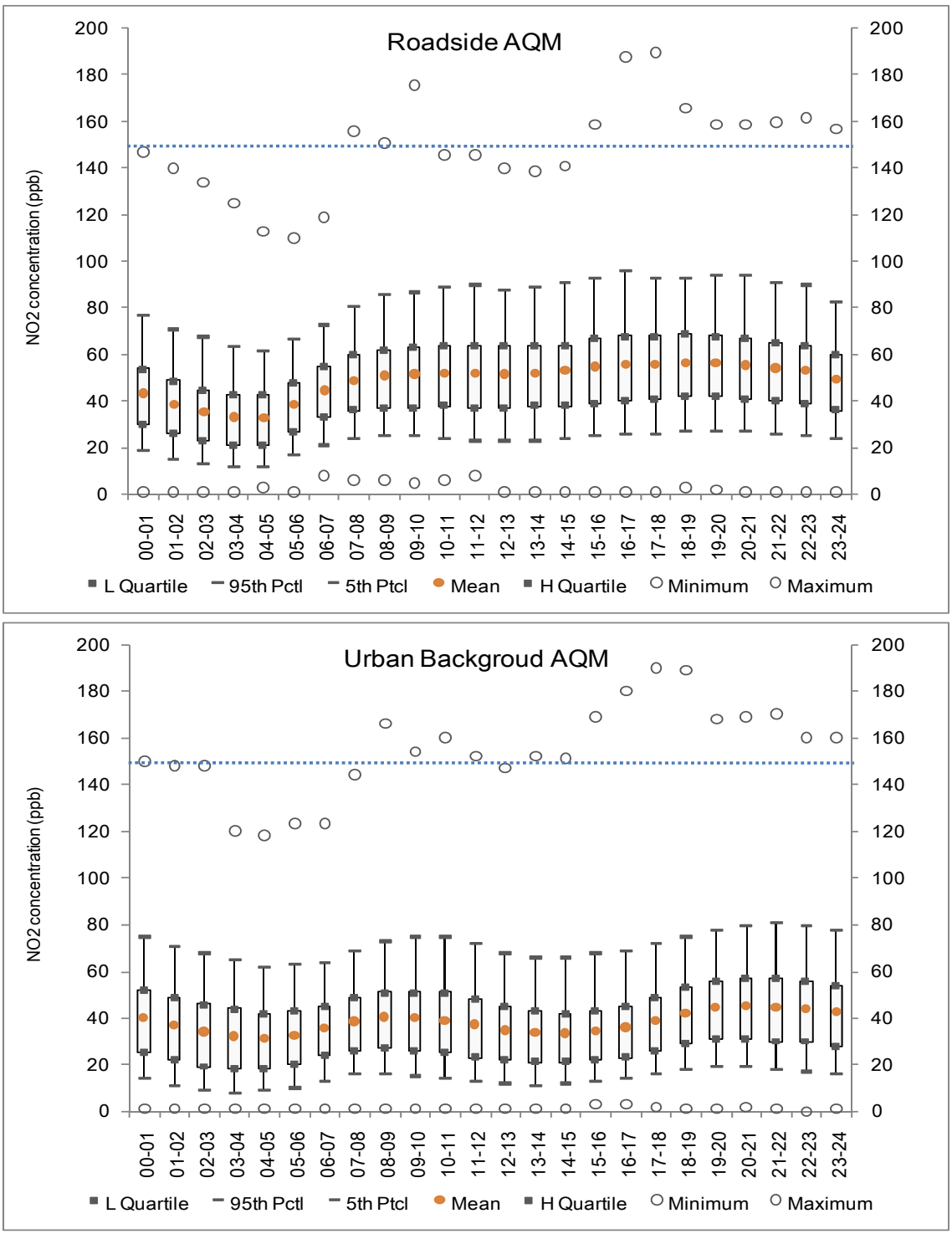

Figure 5.3 Hourly variations of NO_2 concentrations[5]

[5] Maximum, 95th percentile, higher quartile (3/4), mean, lower quartile (1/4), 5th percentile, and minimum for roadside and urban background AQMs (based on hourly NO_2 average concentrations). The dotted line indicates the hourly standard for NO_2 concentration: 150 ppb/hour.

5.1.3 Hourly Traffic and NO_2 Concentrations

It is widely accepted that traffic emissions are the major source of NO_2 concentrations in urban regions (Jo & Park, 2005; Carslaw & Beevers, 2004a; Fujita et al. 2003). Observed traffic counts and diurnal variations of NO_2 concentrations are reviewed for the four seasons. As shown in Figure 5.4, the hourly patterns of NO_2 concentrations for both roadside and background AQMs are similar in all four seasons. Roadside AQMs display a steep increase in the morning, commencing around 6 AM when morning traffic increases, then make a plateau at midday in Spring and Fall, continually increase in Summer, and slightly decline in Winter. In the case of background AQMs, the concentration patterns are similar across the four seasons; double peaks during the day, the highest after the evening traffic peak, and a deep trough during daytime are observed.

There are two notable phenomena in this seasonal comparison. One is that the depth of the trough is shallow in the roadside pattern, as compared to the background one. The reason may be that, during daytime, UV rays stimulate the photolysis of NO_2, but near the roadside freshly emitted NO from the tail pipe is abundant, so that the effects of photolysis are alleviated. The other interesting phenomenon is that the hour of daily peak concentration at background AQMs is changing along with the season. With plenty of daylight, as in Summer and Fall, the peak occurs at 22:00; however, in Winter and Spring, the peak hour starts earlier, at 19:00 and 20:00 PM, respectively. The occurrence of the time lag for the NO_2 peak concentration at background AQMs can also be explained by the photolysis of NO_2. The evening highest NO_2 concentration can be explained by the reaction between the accumulated ozone in daytime and the NO emission in evening traffic peak.

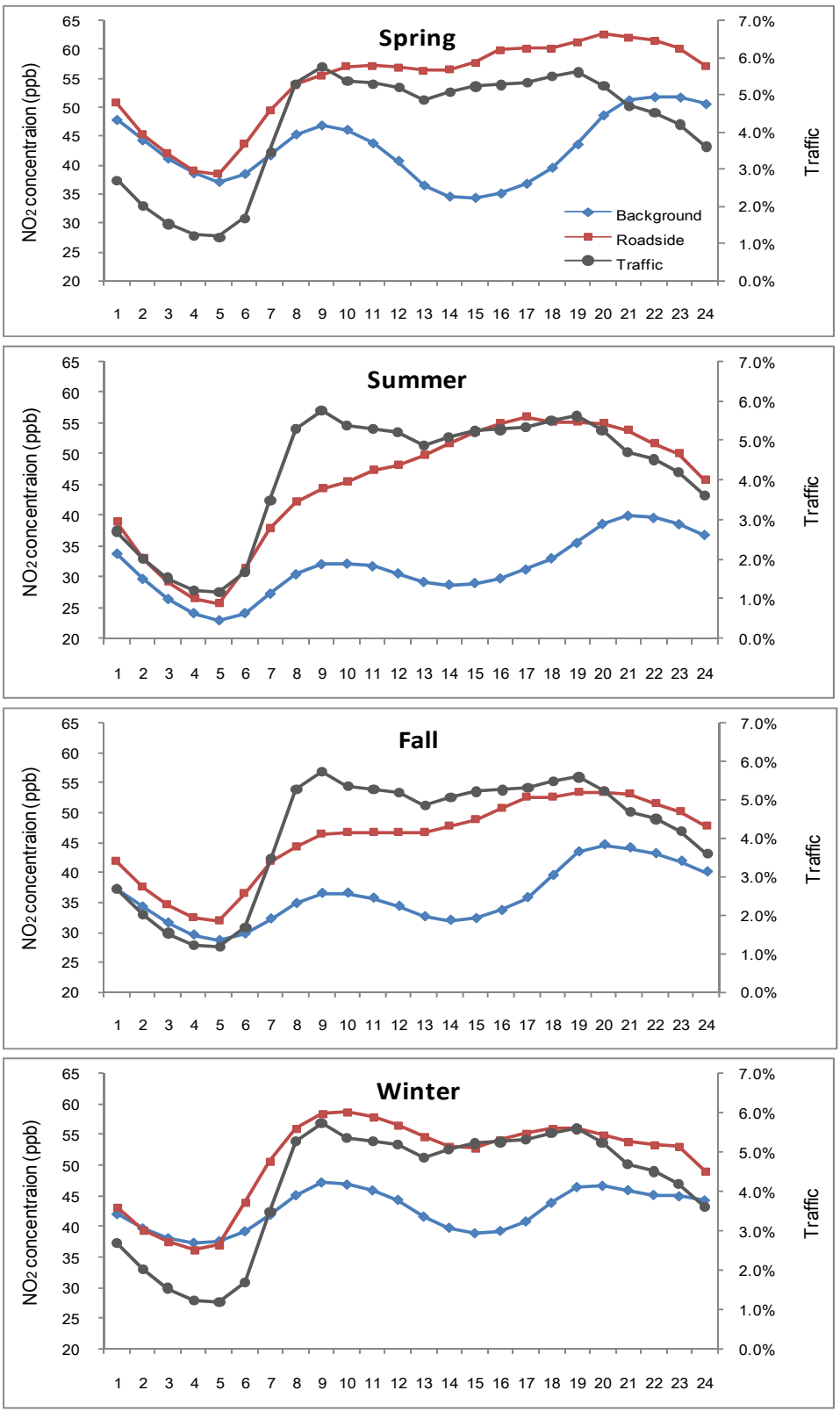

Figure 5.4 Variations of hourly traffic volumes and hourly NO_2 average concentrations at roadside and background AQMs in the four seasons

5.1.4 Comparison Between Weekdays and Weekend

The differences in NO_2 concentrations between roadside and background AQMs are expected to apply to the weekday and weekend patterns. The weekday and weekend concentrations of NO_2 have been analyzed in several studies of California's South Coast Air Basin (Blanchard & Tanenbaum, 2003; Chinkin et al., 2003; Yarwood, Grant, Koo, & Dunker, 2008). In this analysis, two weekend days are included, because traffic counts as well as NO_2 concentrations on Sunday are significantly lower than those of Saturday. As seen in Figure 5.5, the weekday hourly concentrations display consistent and distinctively higher values than the weekend ones. A different pattern occurs at night time (24:00 ~ 05:00). During those five hours, the Saturday traffic exceeds weekday traffic, but the weekday NO_2 concentrations are slightly higher to those of Saturday. Presumably, NO_x ($NO + NO_2$) may be higher on Saturday for those five hours, but because of the lack of available NO data, validation of this assertion is not possible. Better understanding of the nighttime chemistry of NO_x may hepl explain this phenomenon.

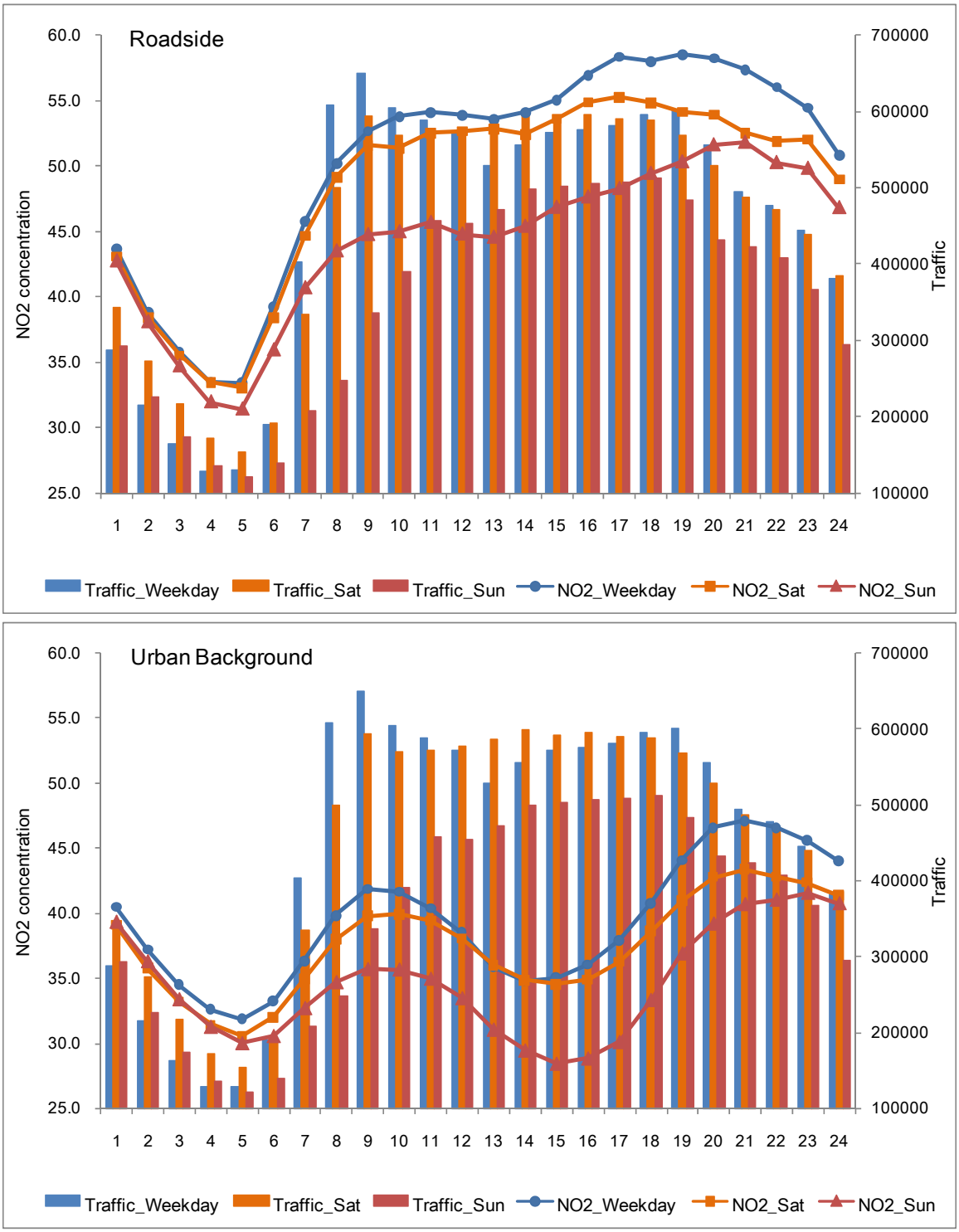

Figure 5.5 Weekday, Saturday, and Sunday hourly NO_2 concentrations and traffic flows at roadside and background AQMs in 2003

5.2 TRAFFIC VOLUMES AND CO CONCENTRATIONS

In this section, the overall CO concentrations for both roadside and background AQMs are analyzed. The temporal variations of CO concentrations at both roadside and background AQMs are first analyzed, accounting for seasonal, monthly, and hourly patterns. All data, including CO concentrations and traffic volumes, are hourly and for 2003. The hourly variations of CO concentrations are compared with traffic count data for each season. In addition, comparisons between weekdays and weekend are also performed.

5.2.1 Temporal Variations of CO Concentrations

Generally, concentrations of ambient air pollutants are closely related to distances to emission sources and chemical reactions among other trace species. As proposed by Tobler (1970), in 'the first law of geography'[6], the distance between emission source and receptor has been primarily accounted for in pollutant dispersion models by considering meteorological impacts. By reviewing the temporal variations of CO concentrations at background and roadside AQMs, one can derive a better understanding of the role of distance between traffic emissions and ambient concentrations.

Table 5.2 presents 2003 monitored CO concentrations statistics along different time dimensions: annual, seasonal, monthly, and hourly averages. All these values satisfy the CO standards[7]. Comparing background and roadside AQMs concentrations along different time scales suggest that roadside AQMs have significantly higher concentrations than those of background AQMs, except for a few cases of maximum concentrations. The low temperatures of winter months (Dec, Jan, and Feb) are the cause of residential heating, cold start, and long idling of vehicles (Mensink, De Vlieger, & Nys, 2000), which results in higher CO concentrations in winter than in the other seasons.

The hourly variations of CO concentrations display patterns similar to Daegu city in Korea (Jo and Park, 2005), with a peak concentration in the morning and a trough during day time. The difference between the peak and the bottom trough is around 0.3 ~ 0.4 ppm for roadside and background AQMs. Because of the relatively stable traffic volumes after the morning peak, the trough in CO concentration in the afternoon can be explained by the chemical reaction between CO and OH· (Eq. 2.10). As discussed in Chapter 2, under typical urban atmospheric

---

[6] "Everything is related to everything else, but near things are more related than distant things." (Tobler, 1970, p.236)

[7] Standards for CO: 25 ppm/1-hour, 9 ppm/8-hour

conditions, a simulation indicates 0.16 ppm/hr of OH· generation (Seinfeld & Pandis, 1998). Since OH· is highly reactive with trace gases as diverse as VOC species, NO_2, SO_2, and CO, it is expected that a significant amount of OH· has interactions with CO, and the recycled OH· (Eqs. 2.10 and 2.7) expedites the chain reactions. In addition, two notable features of the hourly CO variations can be observed: (1) the minimum concentration takes place at 5:00 AM at roadside AQMs, but at 3:00~4:00 PM at background AQMs; (2) the peak concentration at background AQMs takes place one hour earlier (9:00 AM) than roadside AQMs (10:00 AM). The reasons for this time difference is unclear at this point, calling for a better understanding of nighttime chemistry, emission inventory for residential heating, and chemical reaction rate differences between roadside and background locations. Since the concentrations at the roadside AQMs of trace species, such as VOCs, NO_x, SO_2 and CO, are higher than at background AQMs, it is expected that the rates of chemical reactions are different at roadside and background locations.

(Unit: ppm)

Time dimension[1)]		Background AQMs			Roadside AQMs		
		Average	Min	Max	Average	Min	Max
Year		0.64	0.10	4.23	0.97	0.22	4.83
Season	Spring	0.60	0.10	1.89	0.93	0.26	2.30
	Summer	0.49	0.10	1.35	0.88	0.22	2.03
	Fall	0.62	0.10	2.36	0.92	0.25	3.54
	Winter	0.89	0.11	4.23	1.12	0.23	4.83
Month	Jan	0.94	0.11	2.62	1.14	0.23	2.53
	Feb	0.85	0.15	2.22	1.06	0.34	2.25
	Mar	0.63	0.15	1.57	0.90	0.33	1.78
	Apr	0.57	0.14	1.89	0.87	0.27	2.30
	May	0.61	0.10	1.63	1.01	0.26	2.27
	Jun	0.52	0.12	1.10	0.95	0.22	1.82
	Jul	0.49	0.11	1.22	0.92	0.31	2.03
	Aug	0.45	0.10	1.35	0.78	0.25	1.77
	Sep	0.51	0.10	1.39	0.81	0.25	1.87
	Oct	0.64	0.13	2.36	0.83	0.33	2.89
	Nov	0.72	0.11	2.20	1.18	0.38	3.54
	Dec	0.86	0.14	4.23	1.15	0.35	4.83
Hour	1	0.71	0.10	5.00	0.93	0.10	7.20
	2	0.68	0.10	5.00	0.89	0.10	4.70
	3	0.65	0.10	4.60	0.86	0.10	4.60
	4	0.63	0.00	4.40	0.82	0.10	4.30
	5	0.62	0.10	4.00	0.77	0.10	4.80
	6	0.63	0.10	4.00	0.78	0.10	5.60
	7	0.67	0.10	4.00	0.85	0.10	4.40
	8	0.74	0.10	4.10	0.98	0.10	4.80
	9	0.80	0.10	4.50	1.12	0.10	5.60
	10	0.76	0.10	4.80	1.18	0.10	5.50
	11	0.68	0.10	4.90	1.18	0.10	6.40
	12	0.60	0.10	5.20	1.11	0.10	5.40
	13	0.55	0.10	4.90	0.96	0.10	5.40
	14	0.52	0.00	4.60	0.91	0.10	4.80
	15	0.50	0.00	4.10	0.92	0.10	5.10
	16	0.50	0.00	4.20	0.95	0.10	4.70
	17	0.51	0.00	4.70	0.98	0.10	7.50
	18	0.55	0.10	5.20	1.02	0.10	5.70
	19	0.61	0.10	6.50	1.05	0.10	6.50
	20	0.67	0.10	7.70	1.04	0.10	10.00
	21	0.71	0.10	7.30	1.02	0.10	10.00
	22	0.72	0.10	7.10	1.01	0.10	9.40
	23	0.73	0.10	6.40	1.01	0.10	6.90
	24	0.73	0.10	5.20	0.97	0.10	6.60

1) The annual average concentrations in backgroud AQMs are calculated with 9,855 observations (27 AQMs × 365 days) and, for roadside AQMs, the annual average concentrations are calculated with 2,555 observations (7 × 365). Seasonal and monthly averages are calculated in the same way.

Table 5.2 Temporal variations of CO concentrations at both background and roadside AQMs in 2003

5.2.2 CO Concentration Differences between Roadside and Background AQMs

Seasonal, monthly, and hourly comparisons of CO concentrations between roadside and background AQMs are illustrated in Figures 5.6, 5.7, and 5.8, respectively. Daily average CO concentrations are used to analyze seasonal and monthly variations. In the case of hourly variations comparison, hourly average values are used. Each figure uses standard box plots.

The roadside AQMs display higher values and wider distributions of CO concentrations than the background AQMs in all cases. Roadside AQMs are directly affected by traffic emissions, which implies that their concentrations track the fluctuations of nearby traffic flows. The summer season is characterized by lower CO concentration than the other seasons, because, in the summer, CO emissions are limited to vehicle exhaust. Another reason is that the concentrations of hydroxyl radical are significantly higher in summer (Seinfeld and Pandis, 1998, p.250), leading to a reduction of CO concentrations. Although the seasonal pattern of CO concentrations is explainable, unexplainable monthly patterns are also observed at both roadside and background AQMs. The reasons for the relatively high concentrations during May ~July at roadside AQMs and May at background AQMs are unclear at this point.

After the evening traffic peak, traffic flows gradually decrease, but CO concentrations at roadside AQMs do not, remaining flat from 6 PM to 12 PM. Since the concentration of OH· in the atmosphere decreases after sunset, the reaction rate between CO and OH· also decreases, leading to the flat concentration pattern. On the other hand, it is reasonable to expect that diverse human activities, such as cooking and heating, increase during the early evening in residential areas, hence the accumulation of CO at background AQMs occurs until 9 PM, with concentrations leveling off thereafter.

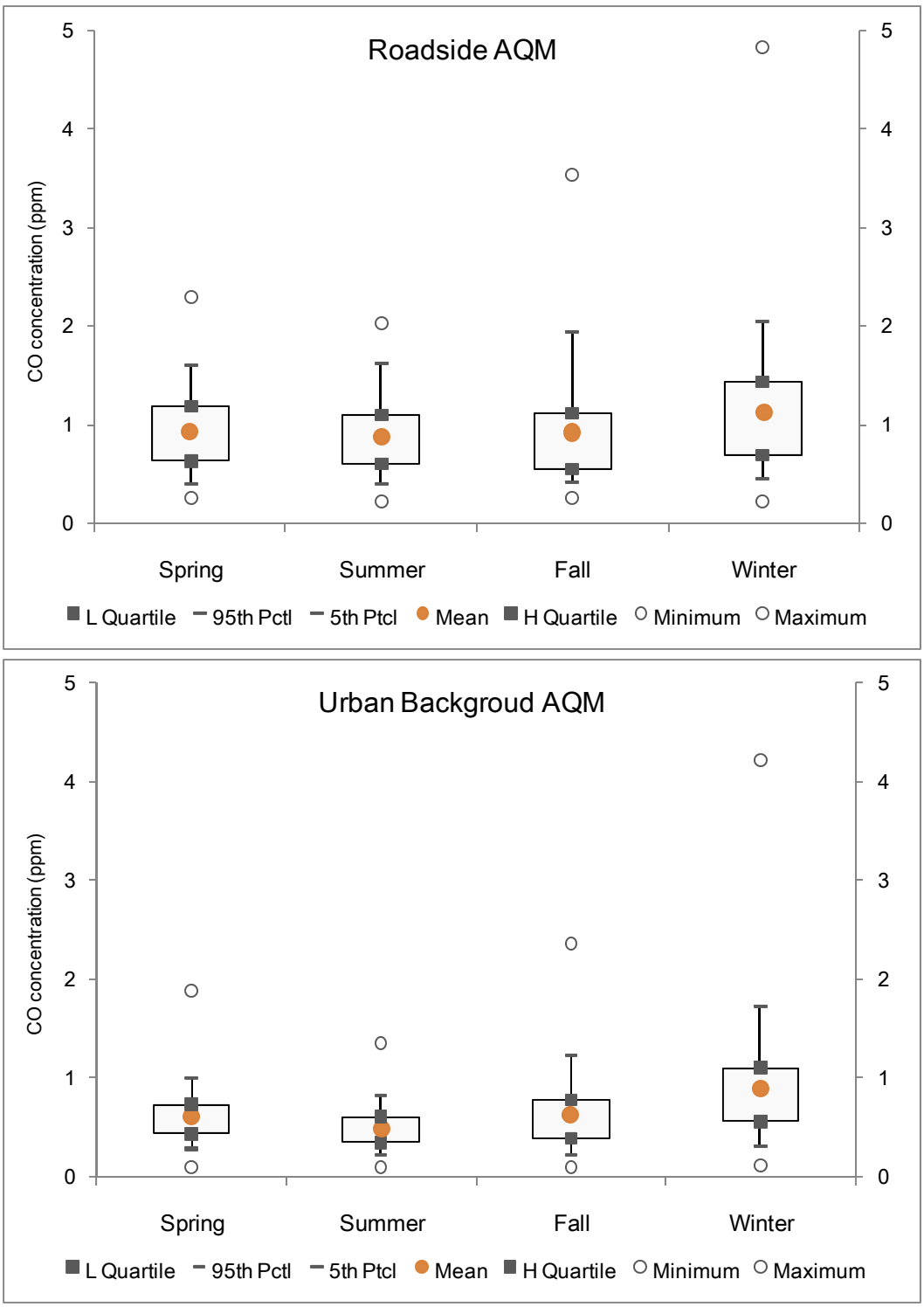

Figure 5.6 Seasonal variations of CO concentrations[8]

[8] Maximum, 95th percentile, higher quartile (3/4), mean, lower quartile (1/4), 5th percentile, and minimum for roadside and urban background AQMs (Standards of CO concentration: 9ppm/8hr, 25ppm/hr)

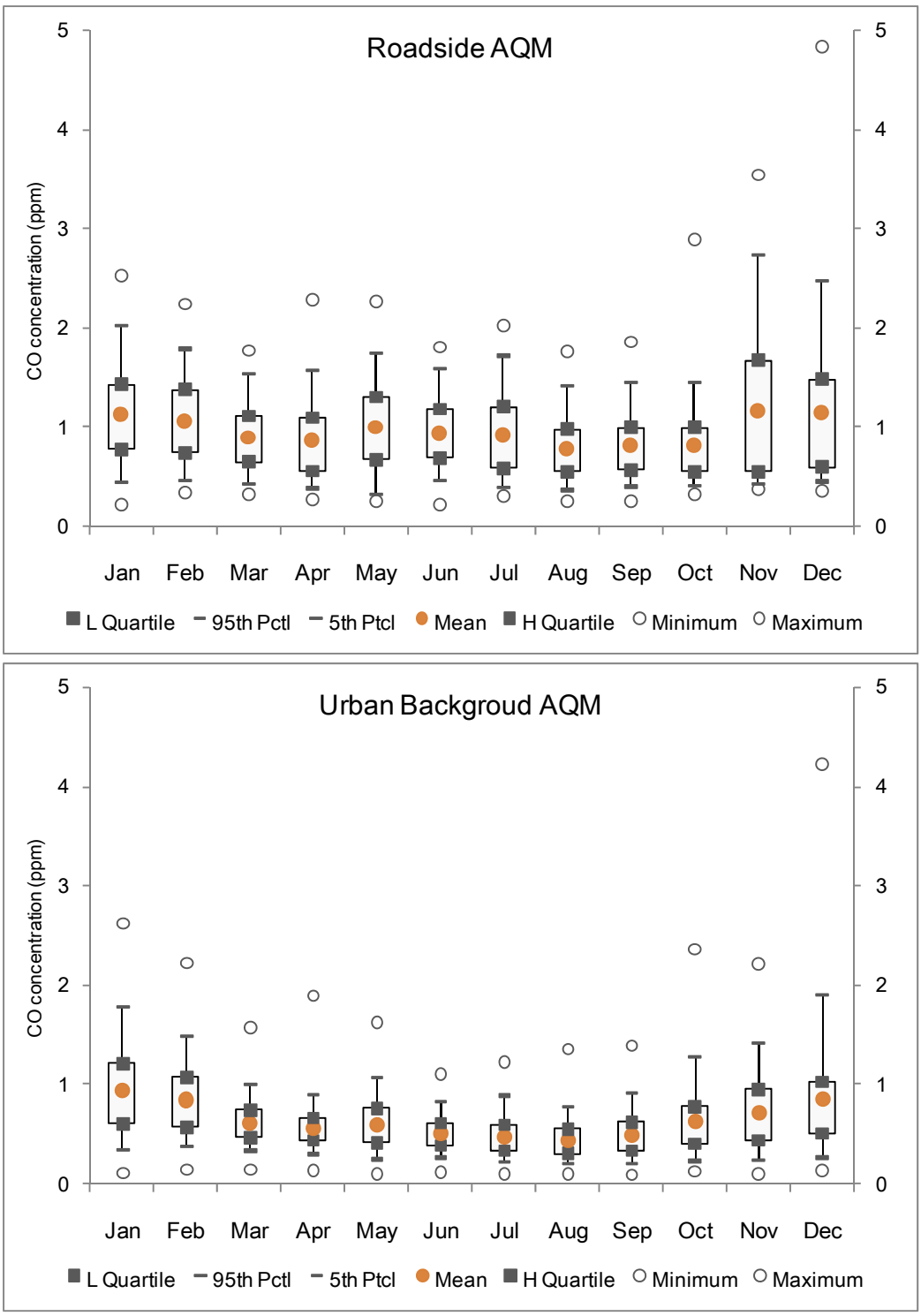

Figure 5.7 Monthly variations of CO concentrations[9]

[9] Maximum, 95th percentile, higher quartile (3/4), mean, lower quartile (1/4), 5th percentile, and minimum for roadside and urban background AQMs (Standards of CO concentration: 9ppm/8hr, 25ppm/hr)

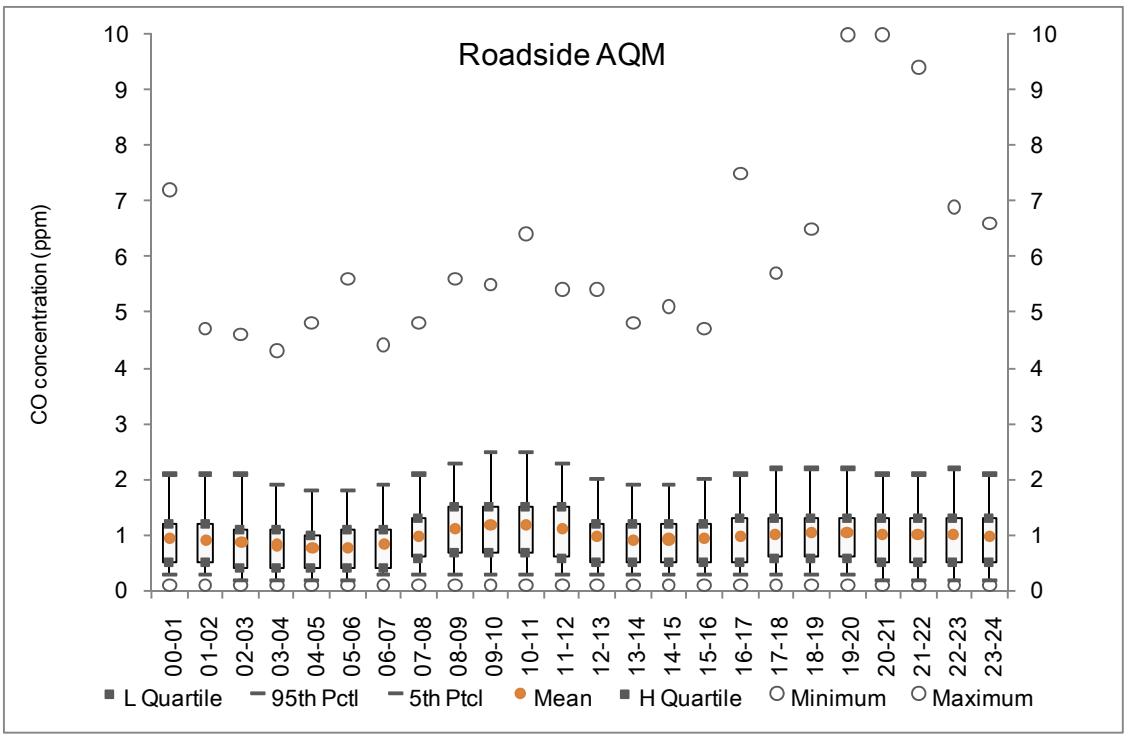

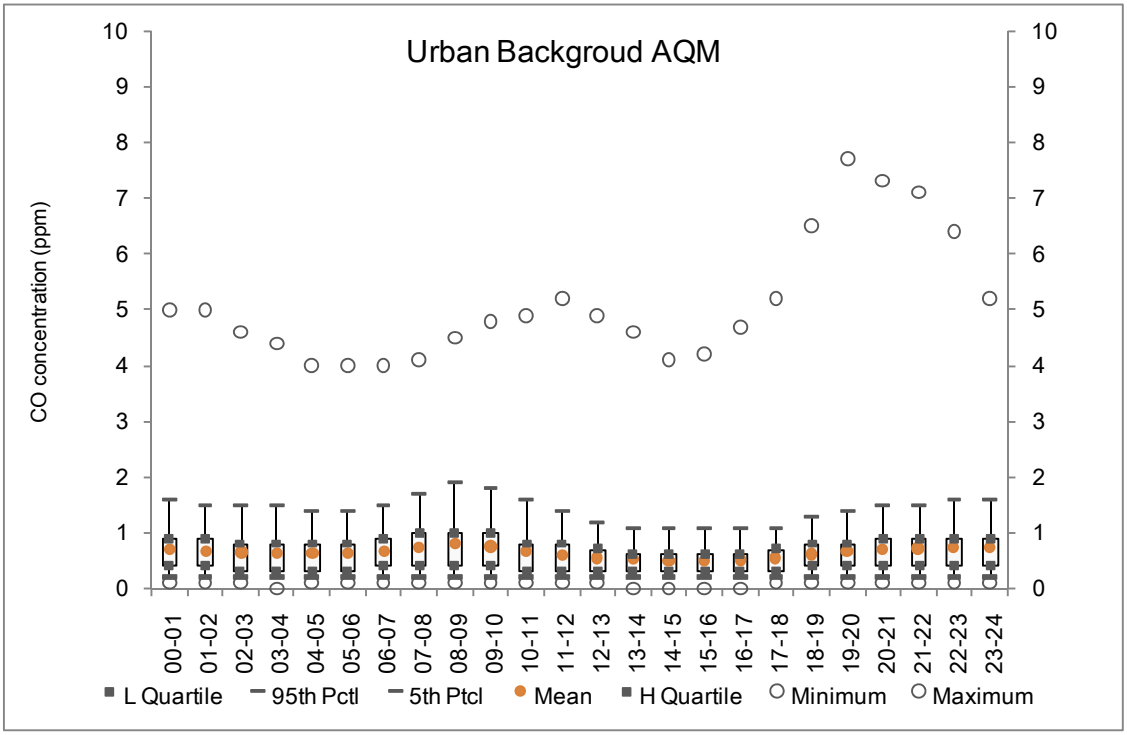

Figure 5.8 Hourly variations of CO concentrations[10]

[10] Maximum, 95th percentile, higher quartile (3/4), mean, lower quartile (1/4), 5th percentile, and minimum for roadside and urban background AQMs (Standards of CO concentration: 9ppm/8hr, 25ppm/hr)

5.2.3 Hourly Traffic and CO Concentrations

Observed hourly traffic counts and CO concentrations are analyzed over the four seasons. As shown in Figure 5.9, the patterns of CO concentrations at both roadside and background AQMs are similar in all four seasons. Since motor vehicles are the major source of CO emissions, roadside AQMs display higher concentrations than background AQMs any hour and any season. Diurnal CO concentrations peak in the morning, after the morning traffic peark hour. The morning peaks at roadside AQMs occur one or two hours later than those at background AQMs. The roadside AQMs, located near major roadways, are directly impacted by vehicle emissions, thus it is unclear why the roadside peak has a lag, as compared to background AQMs. Around 3 ~ 4 PM, concentrations reach a bottom trough in all seasons, and background AQMs display shallower troughs than roadside AQMs. In particular, CO concentrations at background AQMs display limited variations in the summer. Given the relatively stable traffic volumes in the afternoon, these troughs are caused by the reaction between CO and OH· to convert to CO_2 and HO_2· (Eq. 2.10). After sunset, OH· concentration is declining, which provides an opportunity for CO accumulation at both roadside and background AQMs. Although traffic volumes are gradually decreasing after the evening peak, CO concentrations level off. During the winter season, cold temperatures and diverse CO emission sources are added to the condition of low OH· concentrations, which produces favorable circumstances for accumulating CO in the ambient air.

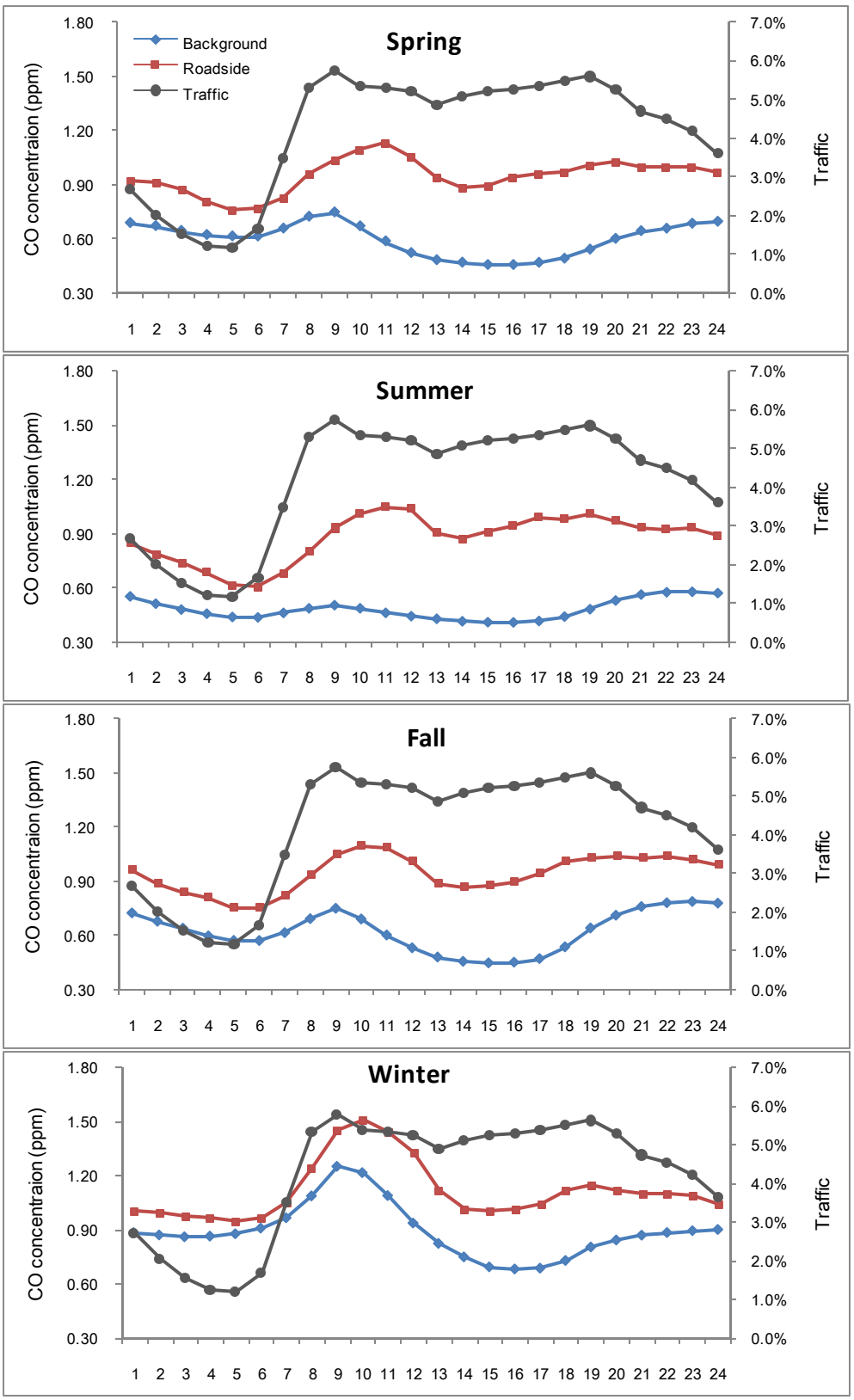

Figure 5.9 Variations of traffic volumes and hourly CO averages at roadside and background AQMs in the four seasons

5.2.4 Comparison between Weekdays and Weekend

Significant differences in CO concentrations between roadside and background AQMs have been observed, resulting from geographical distance between emission sources and receptors. Similarly, traffic volume differences between weekdays and weekend also contribute to differences in concentrations of pollutants. As seen in Figure 5.10, weekend CO concentrations are lower than those of weekdays, both at roadside and background AQMs.

A notable pattern occurs for Sunday roadside concentrations. In comparing traffic patterns across weekdays, Saturday, and Sunday, one can notice that there is no morning peak flow on Sunday (traffic regularly increases from 5:00 AM to 6:00 PM), but CO concentration has a peak at 10:00 AM at roadside AQMs and 9:00 AM at background AQMs, followed by a trough, although traffic continues to increase after these peaks. This phenomenon may be explained by a trade-off between the accumulation of CO from traffic emissions and the chemical reaction of converting CO into CO_2. At midday, the conditions generating OH· are well established and the chemical reactions between CO and OH· counteract the accumulation of CO. The rates of chemical reaction exceed the accumulation of CO due to traffic emissions during midday, inducing the trough at both roadside and background AQMs. In the evening, traffic flows decrease with time, but the concentrations of CO level off on weekdays and, on Saturday and Sunday, CO concentrations are even increasing. Reviewing concentration patterns at background AQMs, one can find that the concentrations of weekdays, Saturday, and Sunday display similar dynamic patterns, with concentrations accumulating along with traffic flows in the early morning to 9 AM. After the morning peaks, troughs follow and concentrations bottom around 3 and 4 PM at their lowest daily values. In the evening, although traffic flow decreases, concentrations increase. Based on these observations, we may infer that, at midday, the chemical reaction effects are dominant in determining CO concentrations at both roadside and backgroud AQMs.

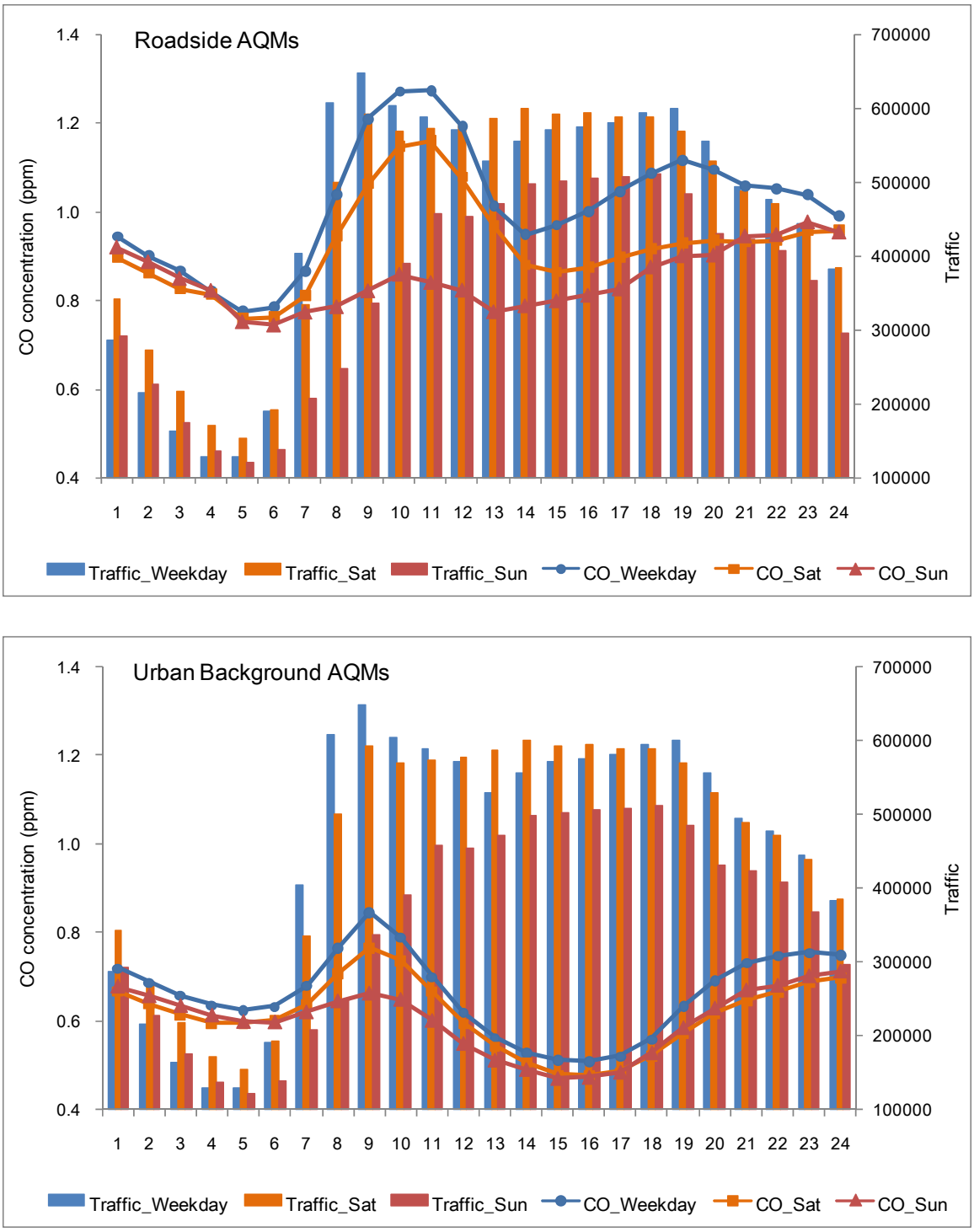

Figure 5.10 Weekday, Saturday, and Sunday hourly CO concentrations and traffic flows at roadside and background AQMs in 2003

5.3 TRAFFIC VOLUMES AND O_3 CONCENTRATIONS

In this section, O_3 concentrations at roadside and background AQMs are analyzed. First, the temporal variations of O_3 concentrations are described, explaining seasonal, monthly, and hourly patterns. Then, the hourly variations of O_3 concentrations are compared with traffic count data for the four seasons. Finally, O_3 concentrations during weekends and weekdays are compared with data for May, 2003.

5.3.1 Temporal Variations of O_3 Concentrations

Because O_3 in the troposphere is a secondary product, generated by photochemical reactions among precursors, such as VOCs and NO_x, the temporal pattern of O_3 concentrations is different from those of directly emitted pollutants, such as CO, NO_x, and SO_2. As discussed in Sections 5.1 and 5.2, the temporal variations of the concentrations of NO_2 and CO are closely related to those of the traffic flows during daytime. The exhaust from tail pipes includes abundant fresh NO gases, which react with ambient O_3 to produce NO_2 (Eq. 2.1) immediately after emission. This process leads to the removal of O_3 and the accumulation of NO_2 near roadside area. As discussed in Section 5.1, there are clear relationships between traffic flows and NO_2 concentrations during daytime. As indicated in Table 5.3, roadside O_3 concentrations are lower than those at background AQMs at any time. As discussed in Section 2.1.3 on O_3 in Chapter 2, empirical research based on observational data reports consistent patterns of O_3 concentrations, higher in rural areas and lower in urban areas.

Table 5.3 presents statistics for the annual, seasonal, monthly, and hourly observed O_3 concentrations at background and roadside AQMs. The violations of the O_3 standards occur during the afternoon (13:00 ~ 19:00) in Spring and Summer, because favorable conditions of O_3 formation exist during these periods, including UV rays under clear sky, low humidity, and high temperature. It is likely that these meteorological conditions occur particularly in the afternoon hours of May and June. The average daily traffic (ADT) in May is higher than that in other months[11], and a high ADT is expected to induce more O_3 titration, leading to lower O_3 concentrations. The monitoring data, however, produce opposite results. Thus, it can be concluded that the leading factors for higher O_3 concentrations are meteorological conditions.

The patterns of hourly average O_3 concentrations at both background and roadside AQMs are similar, starting with an increase in concentration around 9 AM, culminating at 3 ~ 4 PM,

[11] Monthly ADT: Jan. 0.96, Feb. 0.96, Mar. 1.01, Apr. 1.03, May 1.03, Jun. 1.01, Jul. 0.97, Aug. 1.00, Sep. 1.03, Oct. 0.99, Nov. 1.01, Dec. 0.99

decreasing gradually until 22 PM, and then remaining almost steady during the night and early morning. The diurnal variations of O_3 concentrations in Seoul display a pattern similar to those of Azusa, CA (Fujita, Stockwell, Campbell, Keislar, & Lawson, 2003), Daegu, Korea (Jo & Park, 2005), Atlanta, GA, Chicago, IL, and Philadelphia, PA (Pun, Seigneur, & White, 2003). Since the photolysis of NO_2 is required for the formation of O_3, the pattern of O_3 concentrations is closely correlated with the intensity of hourly UV, but with a time lag.

(Unit: ppb)

Time dimension[1)]		Background AQMs			Roadside AQMs		
		Average	Min	Max	Average	Min	Max
Year		13.6	0.0	63.1	8.5	0.1	28.8
Season	Spring	18.0	1.5	63.1	10.5	1.8	28.8
	Summer	17.3	0.8	60.5	11.1	0.1	27.3
	Fall	10.2	0.0	43.0	6.5	0.6	27.5
	Winter	8.6	0.0	42.4	6.4	0.6	22.1
Month	Jan	9.1	0.0	29.2	7.1	1.4	21.3
	Feb	9.4	0.2	42.4	7.9	1.4	22.1
	Mar	13.2	1.5	39.5	8.1	1.8	18.8
	Apr	16.0	1.7	57.6	8.7	3.5	16.2
	May	24.1	3.0	63.1	13.6	4.3	28.8
	Jun	21.3	2.0	60.5	13.4	3.4	27.0
	Jul	17.6	1.4	37.8	11.2	1.6	26.0
	Aug	13.1	0.8	34.7	8.3	0.1	27.3
	Sep	13.2	0.2	43.0	7.7	1.5	27.5
	Oct	10.5	0.1	26.0	7.1	1.5	17.6
	Nov	6.8	0.0	27.5	4.3	0.6	15.3
	Dec	7.4	0.0	35.5	4.5	0.6	13.7
Hour	1	11.5	0.0	61.0	8.7	0.0	38.0
	2	12.6	0.0	70.0	10.0	0.0	43.0
	3	13.2	0.0	74.0	10.5	0.0	45.0
	4	13.4	0.0	73.0	10.8	0.0	44.0
	5	13.2	0.0	72.0	10.8	0.0	41.0
	6	11.2	0.0	62.0	8.9	0.0	39.0
	7	9.5	0.0	68.0	7.4	1.0	25.0
	8	9.9	0.0	71.0	7.9	1.0	24.0
	9	12.5	0.0	68.0	9.2	1.0	31.0
	10	16.7	0.0	62.0	10.9	1.0	28.0
	11	23.7	0.0	71.0	13.4	1.0	36.0
	12	31.8	0.0	86.0	17.1	1.0	55.0
	13	39.8	0.0	100.0	19.9	1.0	68.0
	14	45.5	0.0	112.0	22.3	0.0	72.0
	15	49.2	0.0	110.0	23.4	2.0	69.0
	16	50.2	1.0	116.0	23.6	2.0	76.0
	17	47.8	2.0	122.0	22.5	3.0	83.0
	18	43.0	0.0	106.0	20.1	3.0	84.0
	19	35.8	0.0	101.0	16.7	2.0	59.0
	20	26.0	0.0	90.0	12.7	0.0	37.0
	21	18.8	0.0	75.0	10.6	0.0	29.0
	22	14.6	0.0	76.0	9.3	0.0	29.0
	23	11.8	0.0	66.0	8.1	0.0	31.0
	24	10.9	0.0	66.0	8.0	0.0	36.0

1) The annual average concentrations at backgroud AQMs are calculated with 9,855 observations (27 AQMs × 365 days) and, for roadside AQMs, the annual average concentrations are calculated based on 2,555 observations (7 × 365). Seasonal and monthly averages are calculated in the same way. Hourly averages are based on the values during May 2003.

2) Standards for O_3: 100 ppb/1-hour, 60 ppb/8-hour

: Exceedance of standards

Table 5.3 Temporal variations of O_3 at both background and roadside AQMs in 2003

5.3.2 O_3 Concentration Differences Between Roadside and Background AQMs

Seasonal, monthly, and hourly comparisons of O_3 concentrations at roadside and background AQMs are illustrated in Figures 5.11, 5.12, and 5.13, respectively. Daily average O_3 concentrations are used to analyze seasonal and monthly variations. In the case of hourly variations, average hourly values are used. The three figures use standard box plots.

As discussed in the Section on O_3 chemistry, the areas near traffic flows are abundant in NO gas due to tail pipe emissions, and the concentration of O_3 is very much affected by the ozone titration process (Eq. 2.1; $NO + O_3 \rightarrow NO_2 + O_2$). As seen in Figures 5.11 ~ 5.13, O_3 concentrations at background AQMs are higher than those at roadside AQMs. Some daily and hourly concentrations at background AQMs violate O_3 standards, while all the concentrations monitored at roadside AQMs are within the standards. The favorable meteorological conditions for O_3 formation occur during the afternoon, when higher O_3 concentrations are observed, particularly in May and June. In addition to meteorological factors, biogenic VOCs (BVOCs) are also a factor for higher O_3 concentrations in the growing seasons. Since BVOCs are known as highly reactive hydrocarbons, and the emissions of BVOCs are dependent on sunlight and temperatures, it is a reasonable expectation that BVOCs from plants provide O_3 precursors and, as a result, lead to high O_3 concentrations in the growing seasons (Steiner, Tonse, Cohen, Goldstein, & Harley, 2006).

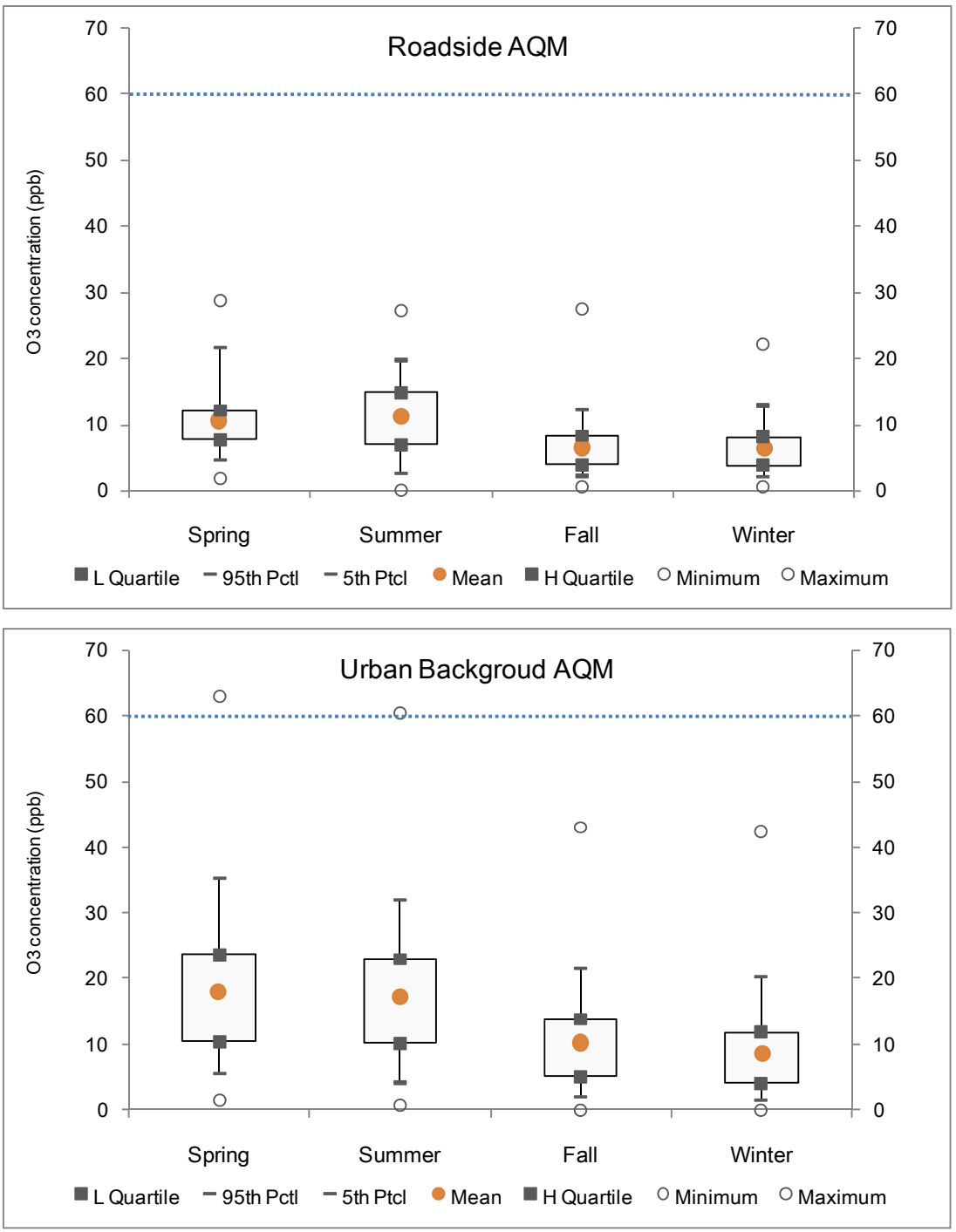

Figure 5.11 Seasonal variations of O_3 concentrations[12]

[12] Maximum, 95th percentile, higher quartile (3/4), mean, lower quartile (1/4), 5th percentile, and minimum for roadside and urban background AQMs (based on daily O_3 average concentrations). The dotted line indicates the 8-hr standard for O_3 concentration: 60 ppb/8hr.

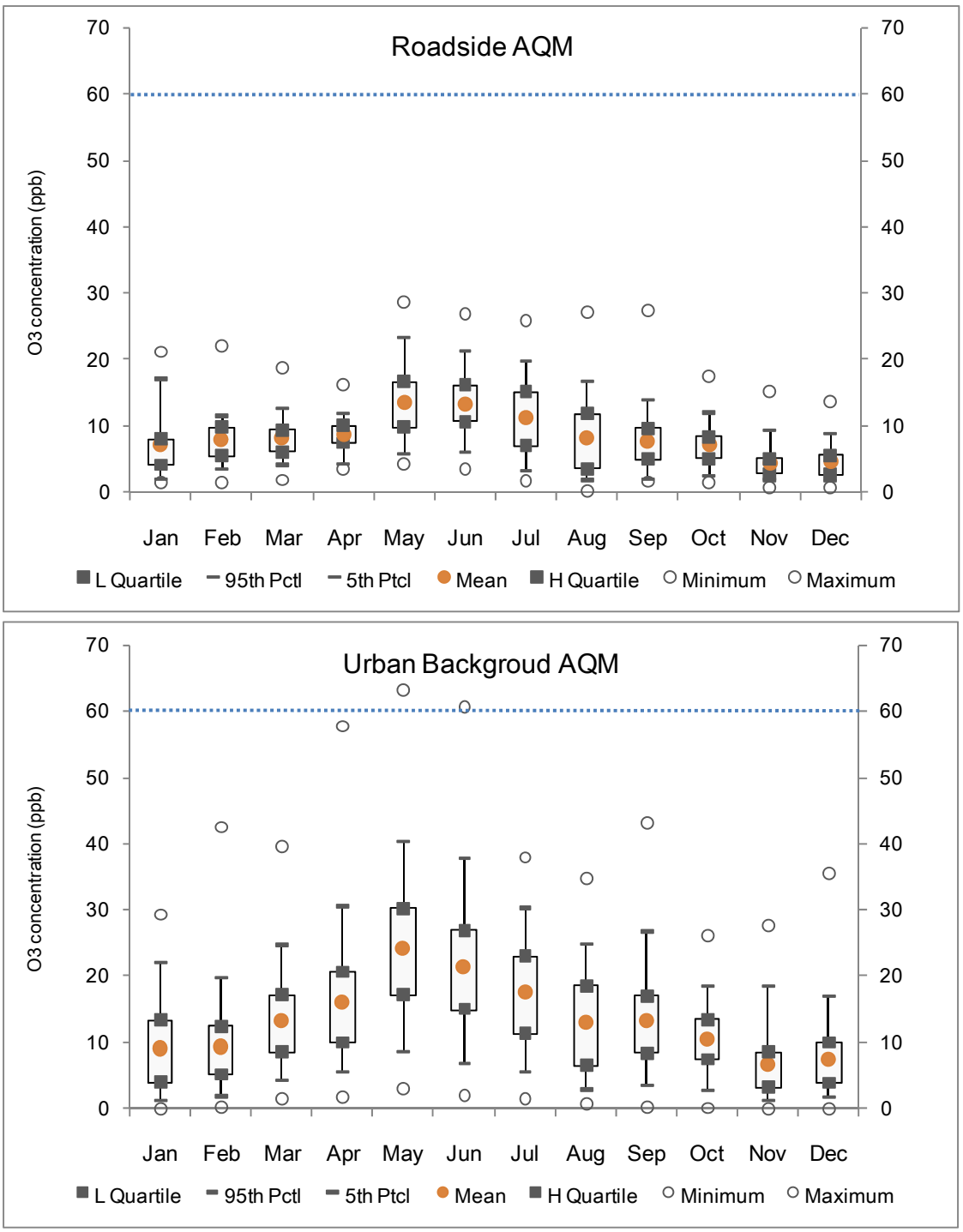

Figure 5.12 Monthly variations of O_3 concentrations[13]

[13] Maximum, 95th percentile, higher quartile (3/4), mean, lower quartile (1/4), 5th percentile, and minimum for roadside and urban background AQMs (based on daily O_3 average concentrations). The dotted line indicates the 8-hr standard for O_3 concentration: 60 ppb/8hr.

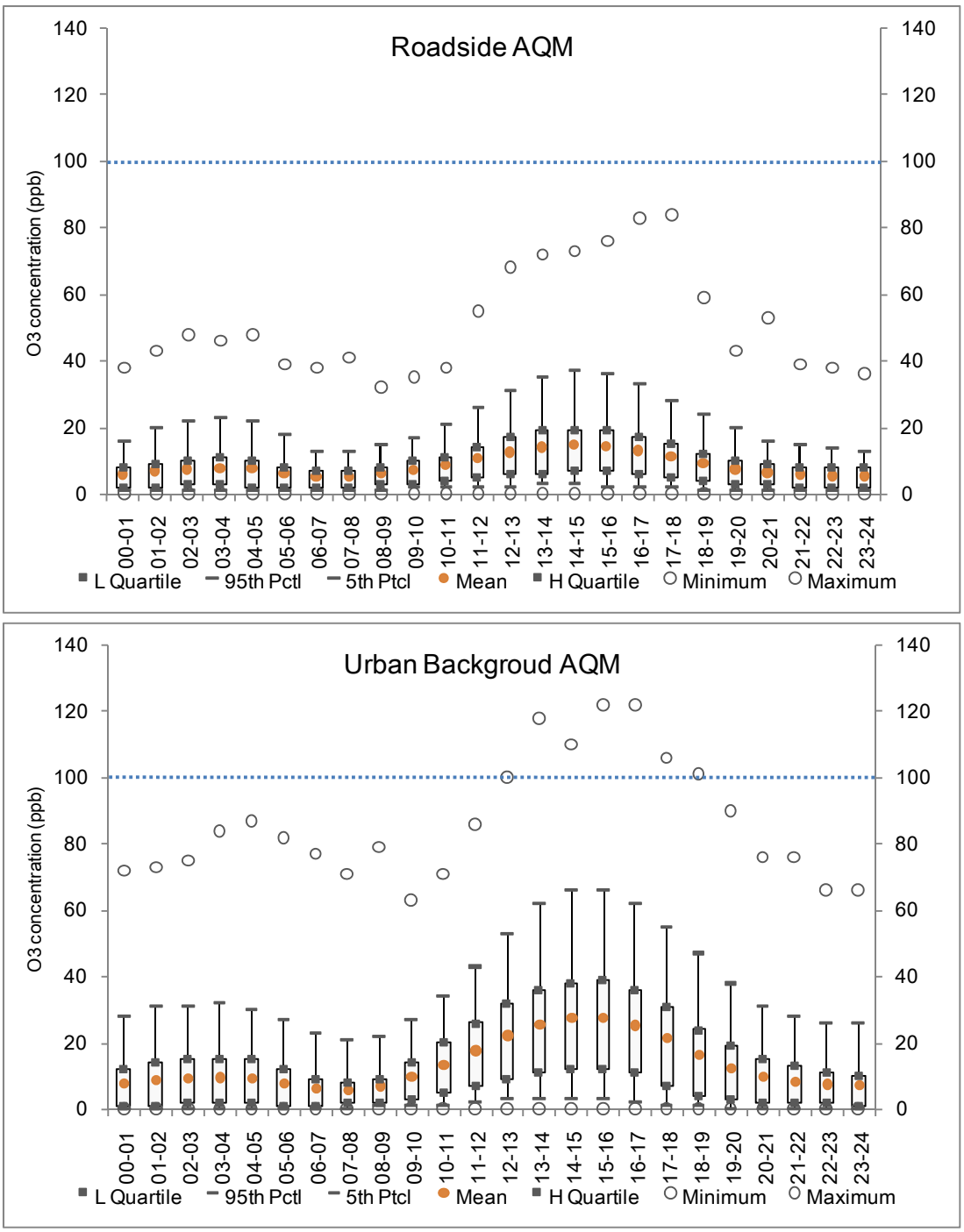

Figure 5.13 Hourly variations of O_3 concentrations[14]

[14] Maximum, 95th percentile, higher quartile (3/4), mean, lower quartile (1/4), 5th percentile, and minimum for roadside and urban background AQMs (based on hourly O_3 average concentrations). The dotted line indicates the 1-hr standard for O_3 concentration: 100 ppb/hr.

5.3.3 Hourly Traffic and O_3 Concentrations

It is known that the formation rates of O_3 are determined by both the ratio and amount of precursor chemicals and specific meteorological conditions. The presence of UV radiation is an essential factor, because the photolysis of NO_2 is initiated by UV. High temperature can directly and indirectly enhance O_3 concentrations by facilitating photochemistry as well as increasing the emission rates of precursors. During the growing seasons (late Spring and Summer), plants emit highly reactive hydrocarbons, which include isoprene, primarily from deciduous trees, and α-pinene, from coniferous trees. Since these biogenic VOCs are sensitive to sunlight and temperature, it is expected that high O_3 formation rates occur during the growing seasons in daylight (Sanderson, Jones, Collins, Johnson, & Derwent, 2003). As illustrated in Figure 5.14, the hourly patterns of O_3 concentrations at both roadside and background AQMs do well match these theoretical considerations. As discussed in chapter 2, O_3 titration dominates roadside areas, leading to the rapid removal of O_3 (Jo & Park, 2005; Marr & Harley, 2002; Yarwood, Stoeckenius, Heiken, & Dunker, 2003). This phenomenon is clearly observed across the four seasons in Seoul.

The diurnal variations of O_3 concentrations display a steep increase with the start of solar radiation, and this time varies across seasons. Usually the peak of UV radiation takes place around 1 PM, but the highest O_3 concentrations occur around 3 ~ 4 PM. Since O_3 is a secondary product generated by a series of chemical reactions among precursors and destroyed by ozone titration, the accumuluation of O_3 depends on the rates of creation and destruction. As long as the rate of creation is higher than that of destruction, O_3 concentration increases. This may a possible reason for the time lag between peak UV and peak O_3 concentration. After this peak, O_3 concentration decreases, because the creation of O_3 is constrained by decreased UV radiation in the late afternoon. In the evening, O_3 is no longer being formed and thus remains at steady levels during the night. Freshly emitted NO increases with morning traffic, scavenging the ambient O_3 and, as a result, the lowest concentration occurs around 7 ~ 8 AM.

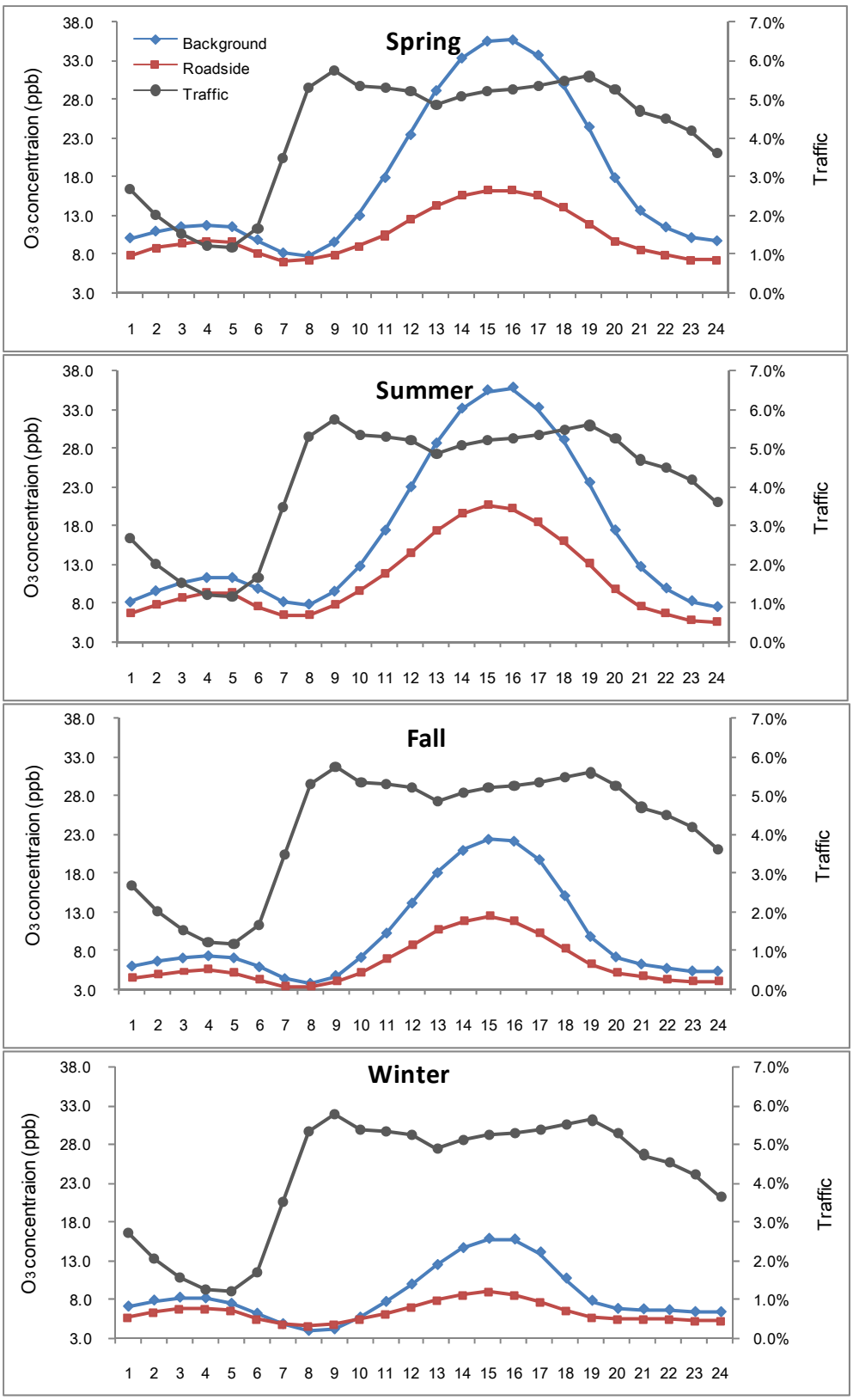

Figure 5.14 Variations of traffic volumes and hourly O_3 averages at roadside and background AQMs in the four seasons

5.3.4 Comparison Between Weekdays and Weekend

In the case of NO_2 and CO, reduced direct emissions lead to lower concentrations during weekends. Since O_3 is a secondary product, however, the reduced weekend traffic decreases NO_x emissions, leading to less O_3 titration and less NO_2+OH· inhibition of O_3 formation. Therefore, the decreased traffic flows result in increased O_3 concentrations during the weekend. As seen in Figure 5.15, the hourly O_3 concentrations during the weekend are higher than those during weekdays, both at roadside and background AQMs. Recent research presents similar patterns of O_3 concentrations in metropolitan areas, including Chicago, IL, and Philadelphia, PA (Pun et al., 2003), Azusa, CA (Fujita et al., 2003), and Daegu, Korea (Jo & Park, 2005). In Phonix, AZ, traffic flows were found negatively correlated with ambient O_3 concentrations, and therefore the average daily O_3 concentrations on Sunday and Saturday are higher than those on weekdays (Shutters & Balling, 2006).

In general, O_3 concentrations on Sunday are higher than those on Saturday and weekdays for both roadside and background AQMs. An interesting pattern, however, occurs after midnight (12 ~ 4 AM). The concentration of O_3 displays a reverse pattern in these hours, with higher concentrations on weekdays. When traffic patterns are compared across weekdays, Saturday, and Sunday, the traffic flows between daytime and midnight have different patterns. During daytime, the flows on weekdays are higher than those on weekend, with a few exceptions on Saturday. On the other hand, at midnight, the flows on Saturday and Sunday are higher than those on weekdays. Thus, O_3 titration occurs more during weekend nights than during weekday nights, resulting in lower O_3 concentrations on weekend nights. Another interesting pattern occurs in the early morning, 3 to 5 AM. As there is no UV radiation at midnight, the creation of O_3 should be impossible at night. However, there is a slight increase in O_3 concentration early in the morning, around 3 AM during weekdays and 5 AM on Sunday and Saturday, which calls for further research regarding the nighttime chemistry of O_3.

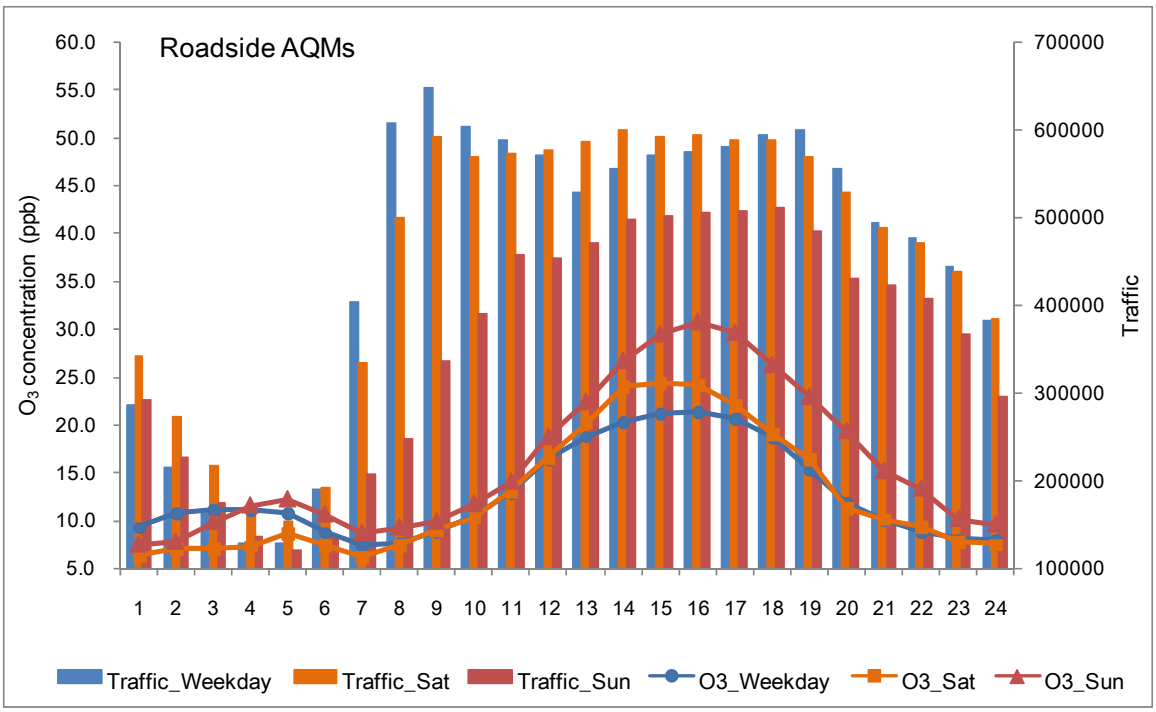

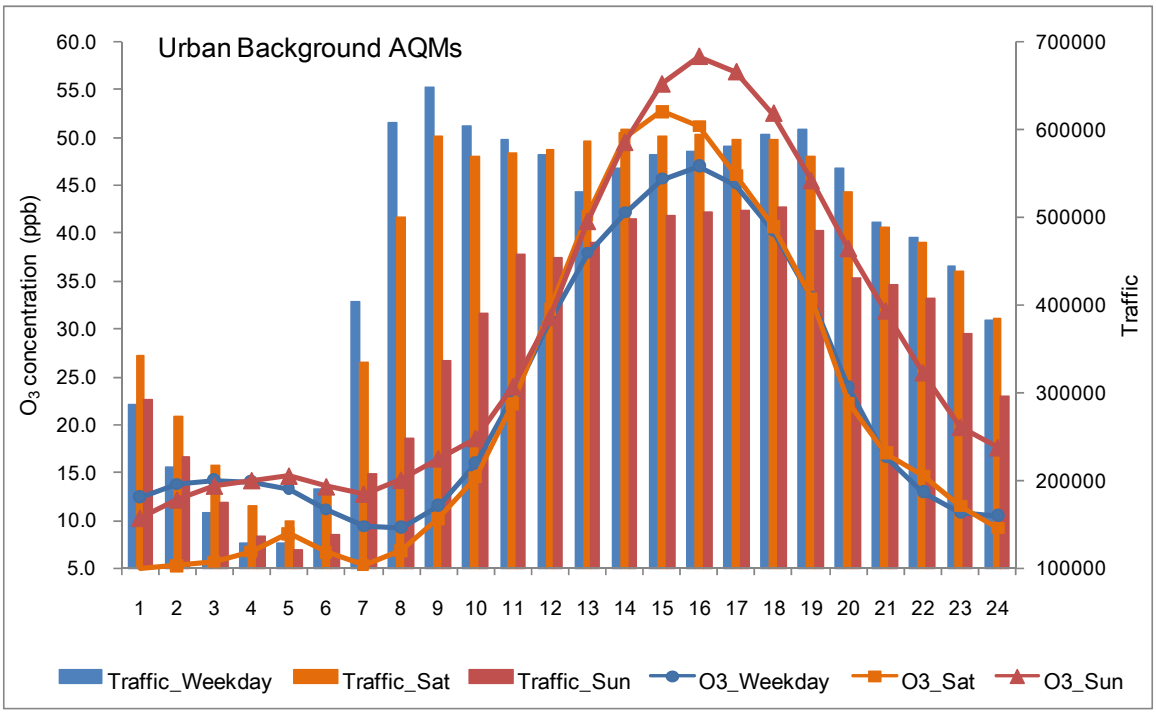

Figure 5.15 Weekday, Saturday, and Sunday hourly O_3 concentrations and traffic flows at roadside and background AQMs during May, 2003[15]

[15] O_3 concentrations on weekends are higher in May than in other months, thus the average concentrations measured during May, 2003, are used in this section.

5.4 TRAFFIC VOLUMES AND SO_2 CONCENTRATIONS

In this section, SO_2 concentrations at both roadside and background AQMs are analyzed. The temporal variations of SO_2 concentrations are reviewed first, accounting for seasonal, monthly, and hourly patterns. Then, the hourly variations of SO_2 concentrations are compared with traffic counts in each season. Finally, traffic flows and SO_2 concentrations during weekdays and weekend are compared.

5.4.1 Temporal Variations of SO_2 Concentrations

Sulfur-containing fossil fuels are the only sources of anthropogenic SO_2 emissions. As for other directly emitted pollutants, such as CO and NO_x, SO_2 concentrations are higher at roadside AQMs than at background AQMs, suggesting that the emissions of diesel vehicles are a major source of SO_2 concentrations in the Seoul Metropolitan area. As seen in Table 5.4, roadside AQMs have significantly higher concentrations across all time dimensions, except in a few cases of maximum concentrations. Since coal and diesel are sources of SO_2 emissions in urban regions, and these fuels are used for heating of residential and commercial buildings in the cold seasons, higher SO_2 concentrations take place in Winter at both background and roadside AQMs.

The hourly variations of SO_2 concentrations display patterns similar to Daegu city, Korea (Jo and Park, 2005), with a peak concentration in the morning around 10 AM for both roadside and background AQMs, and then a gradual decrease until around 4 AM when the lowest concentrations occur, coincident with the lowest traffic flows in the day. Given relatively stable traffic flows during daytime, one would expect an accumulation of SO_2 concentrations, but hourly data display declining concentrations. Given the chemical reaction between SO_2 and OH· (Eq. 2.21), this declining trend may be explained by the OH· reaction. As discussed earlier, OH· is highly reactive and recyclable, causing a significant amount of trace species oxidation, such as VOCs, NO_2, CO, and SO_2. The reaction of SO_2 and OH· decreases SO_2 concentrations. The effects of this reaction are especially well observed at background AQMs.

Peak SO_2 concentrations occur at 10 AM at both roadside and background AQMs, an hour after the traffic peak. The reasons for this time lag is unclear, as there are no data on OH· concentrations that could explain the rate of SO_2 oxidation by OH·. Research on the hourly OH· chemistry of trace species is therefore necessary for better understandings this phenomenon. Since coal is rarely used for the heating of residential buildings in the Seoul Metropolitan region, SO_2 concentrations do not increase during nighttime in cold seasons.

(Unit: ppb)

Time dimension[1)]		Background AQMs			Roadside AQMs		
		Average	Min	Max	Average	Min	Max
Year		4.9	1.0	22.1	6.4	1.0	24.0
Season	Spring	4.9	1.0	20.0	7.0	1.0	24.0
	Summer	3.8	1.0	14.9	5.4	1.0	14.2
	Fall	4.2	1.0	17.0	5.9	1.2	21.5
	Winter	6.8	1.0	22.1	7.4	1.0	18.9
Month	Jan	6.8	1.1	20.8	6.7	1.0	15.9
	Feb	6.9	1.0	21.1	7.6	2.6	14.8
	Mar	5.4	1.0	20.0	8.1	2.8	18.2
	Apr	4.5	1.1	14.5	6.1	1.8	12.8
	May	4.9	1.0	17.1	6.5	1.0	24.0
	Jun	4.3	1.0	14.9	6.7	1.8	14.2
	Jul	3.4	1.0	10.4	4.5	1.7	12.2
	Aug	3.6	1.0	9.2	5.1	1.0	13.3
	Sep	3.6	1.0	9.8	4.1	1.2	12.3
	Oct	4.4	1.1	17.0	6.7	1.3	21.5
	Nov	4.7	1.0	15.5	6.9	2.3	20.4
	Dec	6.7	1.0	22.1	8.0	2.7	18.9
Hour	1	4.5	1.0	29.0	5.7	1.0	27.0
	2	4.4	1.0	29.0	5.4	1.0	28.0
	3	4.3	1.0	31.0	5.2	1.0	31.0
	4	4.2	1.0	27.0	5.1	1.0	35.0
	5	4.2	1.0	33.0	5.2	1.0	34.0
	6	4.3	1.0	33.0	5.8	1.0	37.0
	7	4.5	1.0	29.0	6.4	1.0	33.0
	8	4.9	1.0	29.0	6.7	1.0	28.0
	9	5.4	1.0	43.0	7.0	1.0	37.0
	10	5.7	1.0	34.0	7.1	1.0	28.0
	11	5.7	1.0	37.0	7.1	1.0	28.0
	12	5.6	1.0	33.0	7.0	1.0	25.0
	13	5.4	1.0	36.0	6.8	1.0	27.0
	14	5.2	0.0	34.0	6.7	1.0	31.0
	15	5.2	1.0	36.0	6.8	1.0	32.0
	16	5.1	1.0	35.0	6.9	1.0	31.0
	17	4.9	1.0	40.0	6.9	1.0	44.0
	18	4.8	1.0	28.0	6.8	1.0	33.0
	19	4.8	1.0	34.0	6.8	1.0	41.0
	20	4.8	1.0	38.0	6.8	1.0	40.0
	21	4.8	1.0	34.0	6.7	1.0	32.0
	22	4.8	1.0	30.0	6.6	1.0	32.0
	23	4.8	1.0	29.0	6.7	1.0	29.0
	24	4.7	1.0	28.0	6.4	1.0	31.0

1) The annual average concentrations of backgroud AQMs are calculated with 9,855 observations (27 AQMs × 365 days) and, for roadside AQMs, the annual average is calculated with 2,555 observations (7 × 365). Seasonal and monthly averages are calculated in the same way.

2) Standards for SO_2: 150 ppb/1-hour, 50 ppb/day, 20 ppb/year

: Min : Max

Table 5.4 Temporal variations of SO_2 at both background and roadside AQMs in 2003

5.4.2 SO_2 Concentration Differences between Roadside and Background AQMs

Seasonal, monthly, and hourly comparisons of SO_2 concentrations between roadside and background AQMs are illustrated in Figures 5.16, 5.17, and 5.18, respectively. Daily average SO_2 concentrations are used to analyze seasonal and monthly variations, and hourly average values are used in the case of hourly variations.

Areas near traffic flows are abundant in SO_2 gas due to diesel vehicle emissions. SO_2 concentrations at roadside AQMs are higher than at background AQMs in all cases (seasonal, monthly and hourly). Since strict regulation of sulfur-containing fossil fuels has been introduced in the Seoul Metropolitan Area, SO_2 concentrations have displayed a decreasing annual trend (Korea Ministry of Environment, 2006). All daily and hourly concentrations at both roadside and background AQMs are within the SO_2 standards. Since sulfur-containing fuels are used for heating buildings in the cold seasons, SO_2 concentrations are higher in Winter (December, January, and February), and these patterns are clearly observed at background AQMs. In contrast, the summer season is characterized by lower SO_2 concentrations, because emissions of SO_2 are limited to diesel vehicles. Another possible reason is that the concentrations of OH· radical are significantly higher in Summer (Seinfeld, 1986), leading to chemical reactions with SO_2.

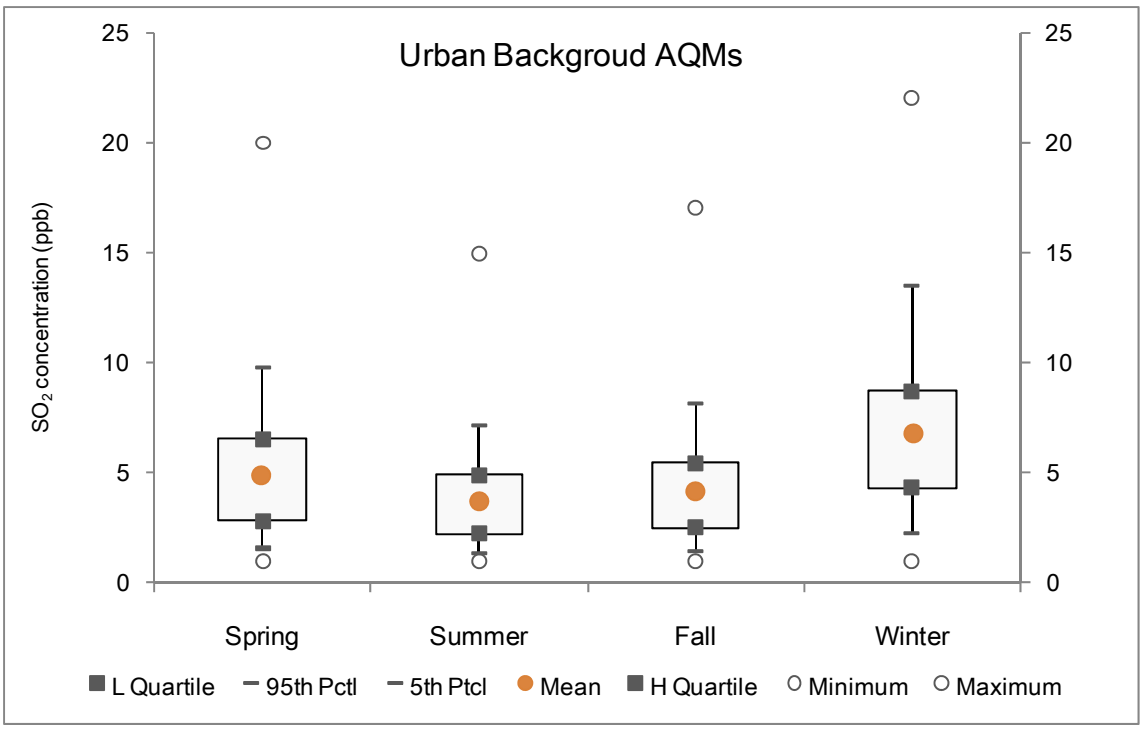

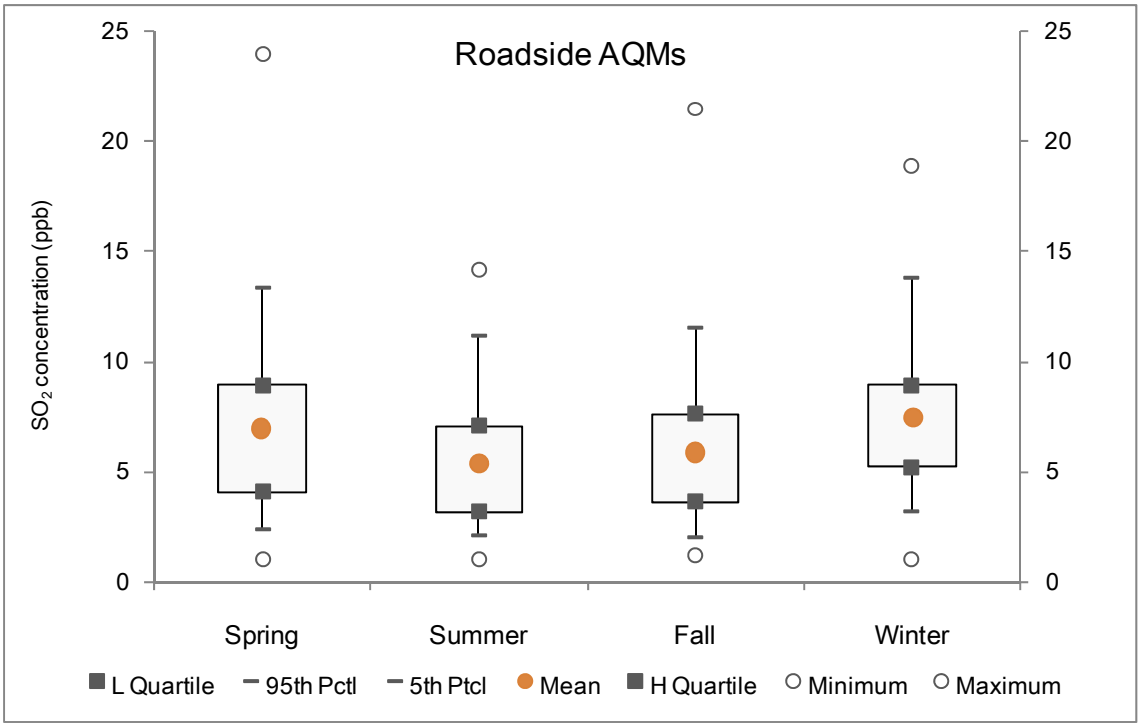

Figure 5.16 Seasonal variations of SO_2 concentrations[16]

[16] Maximum, 95th percentile, higher quartile (3/4), mean, lower quartile (1/4), 5th percentile, and minimum for roadside and urban background AQMs (based on daily SO_2 average concentrations).

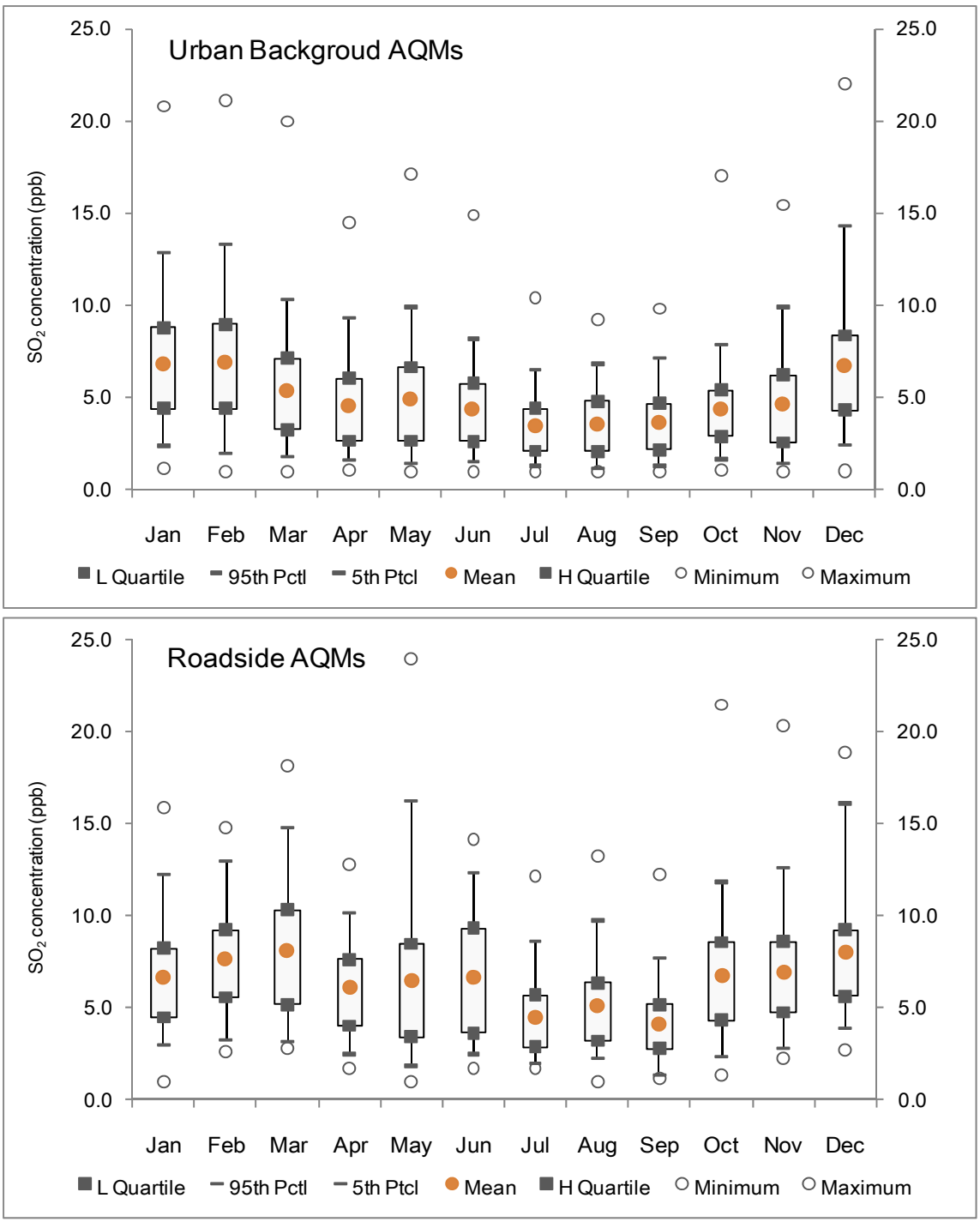

Figure 5.17 Monthly variations of SO_2 concentrations[17]

[17] Maximum, 95th percentile, higher quartile (3/4), mean, lower quartile (1/4), 5th percentile, and minimum for roadside and urban background AQMs (based on daily SO_2 average concentrations).

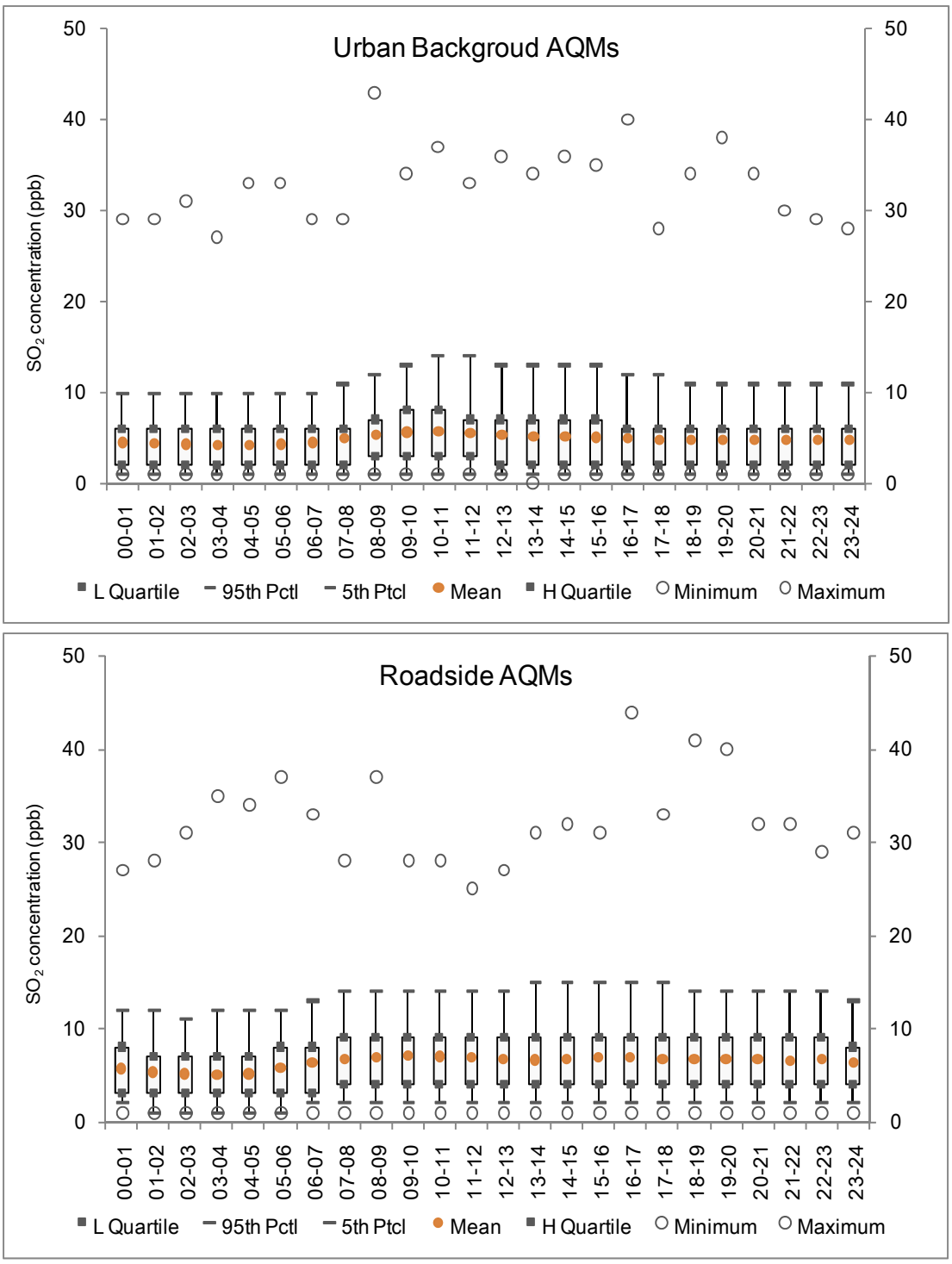

Figure 5.18 Hourly variations of SO_2 concentrations[18]

[18] Maximum, 95th percentile, higher quartile (3/4), mean, lower quartile (1/4), 5th percentile, and minimum for roadside and urban background AQMs (based on daily SO_2 average concentrations).

5.4.3 Hourly Traffic and SO_2 Concentrations

Since diesel vehicles are the major source of SO_2 emission in urban regions, SO_2 concentrations are observed to be higher near roadside areas. The contribution of motor vehicles to SO_2 concentrations is smaller than to other pollutants, such as NO_2 and CO. According to the US EPA (2002), transportation-related emissions contribute around 5% of total SO_2 emission. In the Seoul Metropolitan area, the contribution of transportation to SO_2 concentrations was 11% in 2003 (Korea Ministry of Environment, 2006).

Observed hourly traffic counts and SO_2 concentrations are analyzed over the four seasons. As shown in Figure 5.19, SO_2 concentrations are higher at roadside than at background AQMs, at any hour of day and across the four seasons, primarily because diesel vehicles are the major source of SO_2 emissions. In Winter, an increased use of sulfur-containing fossil fuels for residential and commercial building heating reduces the gap between roadside and background AQMs. Diurnal SO_2 concentrations display peaks in the morning, except in Summer at roadside AQMs, and then gradually decrease. However, in Autumn, there is a second peak in the evening. The morning peaks of SO_2 concentrations occur one hour (Fall) or three hours (Winter) after the traffic peak. As the only chemical reaction of SO_2 is with the OH· radical[19], differences in OH· concentrations across these seasons may be the cause for the time lag between traffic and SO_2 peaks. During nighttime, SO_2 concentrations are influenced only by SO_2 emission. Therefore, smaller traffic flows during nighttime are directly related to lower concentrations of SO_2, and the daily lowest concentration occurs around 5 AM, which is coincident with the lowest traffic flow.

[19] SO_2 also undergo physical removal by dry and wet deposition (Derwent & Hertel, 1998; Seinfeld & Pandis, 2006).

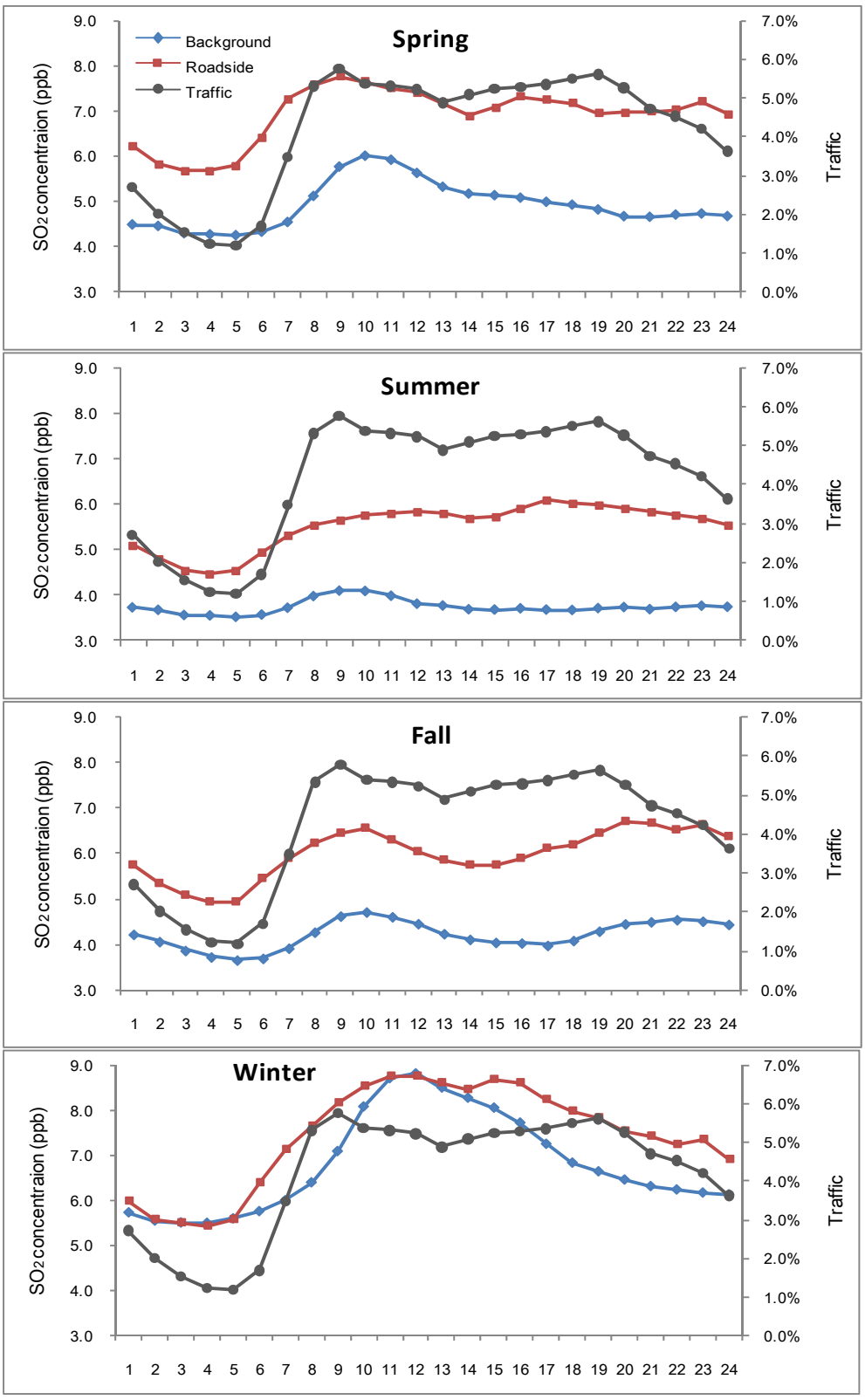

Figure 5.19 Variations of hourly traffic volumes and SO_2 concentrations at roadside and background AQMs in the four seasons

5.4.4 Comparison between Weekdays and Weekend

Traffic flow differences between weekdays and weekend produce differences in SO_2 concentrations between these periods. As seen in Figure 5.20, SO_2 concentrations at roadside AQMs during the weekend are significantly lower than those during weekdays. In contrast, at background AQMs, there are much smaller differences between weekdays, Saturday, and Sunday. This is further evidence that diesel vehicle emissions are the major source for roadside SO_2 concentrations. An interesting phenomenon occurs on Saturday at roadside AQMs when comparing traffic flows and concentrations, as one can notice that Saturday traffic during daytime is as large as and, sometimes, larger than traffic on weekdays, but SO_2 concentations during weekdays are significantly higher than on Saturday. Given this traffic pattern, there is no reason why SO_2 concentrations should be lower on Saturday. As diesel vehicles are the exclusive contributors of SO_2 emissions, it is possible that the vehicle fleet on Saturday includes less diesel vehicles. To confirm the hypothesis, it would be necessary to collect data regarding fleet composition during weekdays and weekend.

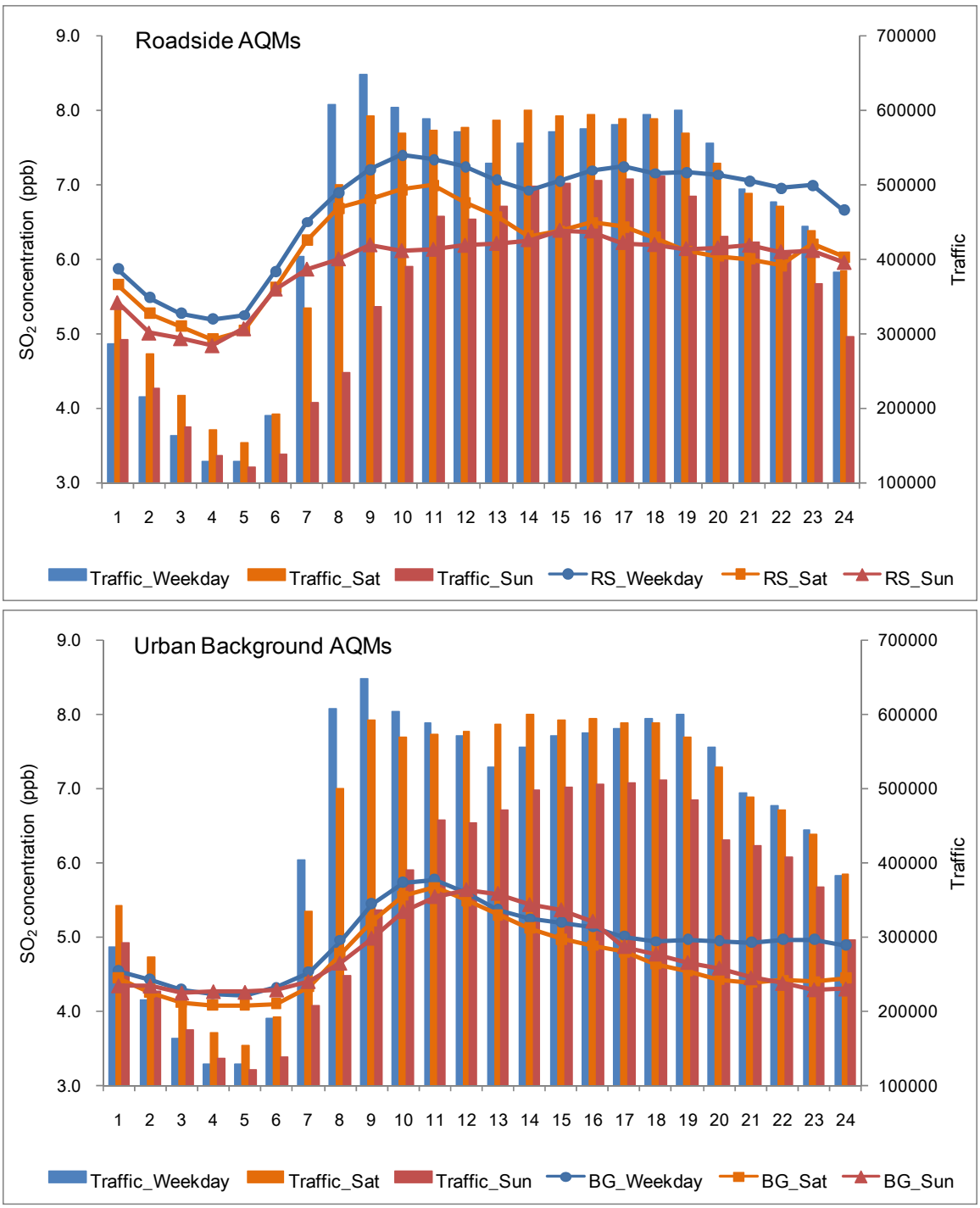

Figure 5.20 Weekday, Saturday, and Sunday hourly SO_2 concentrations and traffic flows at roadside and background AQMs in 2003

5.5 TRAFFIC VOLUMES AND PM10 CONCENTRATIONS

In this section, PM10 concentrations at both roadside and background AQMs are examined. First, the temporal variations of PM10 concentrations are analyzed, accounting for seasonal, monthly, and hourly patterns. Then, the hourly variations of PM10 concentrations are compared with traffic count data in the four seasons. Finally, PM10 concentrations during weekends and weekdays are compared.

5.5.1 Temporal Variations of PM10 Concentrations

As discussed in Chapter 2, there are diverse sources of urban PM10, such as dusts from roads, construction sites, and agricultural land, diesel combustion, wind blowing from China, ammonium sulfate, and ammonium nitrate. Anthropogenic emissions make up a substantial share of PM10 concentrations in urban regions, including a significant role for traffic flows. Vehicle emissions contribute not only direct fine particles, such as soot and elementary carbon, but also secondary fine particles, such as sulfate and nitric acid. In addition, wear of tire and brake pad, asphalt debris, resuspension of paved and unpaved road dust are associated with concentrations of coarse PM (National Center for Environmental Assessment, 2004). As seen in Table 5.5, the Spring and Winter seasons display higher PM10 concentrations. Heating of buildings in winter provides more anthropogenic emissions and creates favorable conditions for generating fine particles. In Spring, natural sources of PM, such as pollen, spores, and plant fragments, increase emissions and, additionally, wind blowing from China (yellow sand phenomenon) occurs frequently. These natural factors may increase the concentrations of PM10 in Spring.

According to the KAAQS, the standards for PM10 are 150 $\mu g/m^3$ for a daily average and 70 $\mu g/m^3$ for an annual average. The measurements at background AQMs are used to assess whether the standards are met. Average annual PM10 concentrations across background AQMs barely satisfy the annual standard[20]. In the case of the daily average, however, exceedance of the standard occurs every month, and frequent daily standard violations are observed in May. As expected, the maximum concentrations of PM10 in Spring and Winter are higher than those of other seasons, and this is also true for the average.

Hourly PM10 concentrations display similar patterns across background and roadside AQMs. Two peaks and two troughs are observed, but the highest and the lowest concentrations occur differently. The highest concentration at background AQMs is observed at 22:00 PM and

[20] Since there are 27 background AQMs,

the lowest at 15:00 PM. In contrast, the highest and lowest concentrations at roadside AQMs take place at 9:00 AM and 5:00 AM.

(Unit: μg/m^3)

Time dimension[1)]		Background AQMs			Roadside AQMs			Exceedances[2)]		
		Avg.	Min	Max	Avg.	Min	Max	N Obs.	N. Exceed	Percent
Year		70	8	299	74	8	293	9855	357	3.6%
Season	Spring	83	11	263	85	20	250	2484	117	4.7%
	Summer	61	10	212	66	13	184	2484	19	0.8%
	Fall	56	9	201	61	8	182	2457	50	2.0%
	Winter	80	8	299	84	18	293	2430	171	7.0%
Month	Jan	79	23	214	82	21	216	837	47	5.6%
	Feb	85	8	245	85	18	207	756	65	8.6%
	Mar	85	16	232	85	25	191	837	28	3.3%
	Apr	70	11	167	70	20	159	810	9	1.1%
	May	93	14	263	93	22	250	837	80	9.6%
	Jun	82	16	212	81	24	163	810	8	1.0%
	Jul	53	11	209	61	20	184	837	10	1.2%
	Aug	46	10	155	55	13	140	837	1	0.1%
	Sep	55	9	187	62	8	179	810	27	3.3%
	Oct	54	10	174	60	19	182	837	11	1.3%
	Nov	59	10	201	63	23	169	810	12	1.5%
	Dec	76	15	299	86	25	293	837	59	7.0%
Hour	1	72	1	393	71	2	334	N/A	N/A	N/A
	2	71	1	397	68	3	425	N/A	N/A	N/A
	3	70	1	402	66	3	564	N/A	N/A	N/A
	4	68	1	406	63	3	416	N/A	N/A	N/A
	5	68	1	400	62	3	293	N/A	N/A	N/A
	6	67	1	385	66	1	343	N/A	N/A	N/A
	7	69	1	357	72	5	424	N/A	N/A	N/A
	8	70	1	335	77	5	310	N/A	N/A	N/A
	9	72	1	308	81	6	334	N/A	N/A	N/A
	10	73	1	354	81	9	326	N/A	N/A	N/A
	11	71	1	455	80	2	327	N/A	N/A	N/A
	12	68	1	390	78	6	357	N/A	N/A	N/A
	13	65	1	393	74	3	348	N/A	N/A	N/A
	14	64	1	390	71	1	362	N/A	N/A	N/A
	15	63	1	399	71	5	371	N/A	N/A	N/A
	16	64	0	377	72	6	365	N/A	N/A	N/A
	17	65	1	390	73	4	376	N/A	N/A	N/A
	18	68	1	392	74	4	370	N/A	N/A	N/A
	19	70	1	397	74	1	373	N/A	N/A	N/A
	20	72	1	393	75	2	370	N/A	N/A	N/A
	21	74	1	390	76	8	375	N/A	N/A	N/A
	22	73	1	395	75	5	380	N/A	N/A	N/A
	23	73	1	406	75	4	358	N/A	N/A	N/A
	24	73	1	401	73	3	326	N/A	N/A	N/A

1) The annual average concentrations in backgroud AQMs are calculated with 9,855 observations (27 AQMs × 365 days) and, for roadside AQMs, the annual average concentrations are calculated with 2,555 observations (7 × 365). Seasonal and monthly averages are calculated in the same way.

2) Standards for PM10: 150 μg/day, 70 μg/year; Exceedances are calculated with background observations

: Exceedance of standards

Table 5.5 Temporal variations of PM10 at both background and roadside AQMs in 2003

5.5.2 PM10 Concentration Differences between Roadside and Background AQMs

Seasonal, monthly, and hourly comparisons of PM concentrations between roadside and background AQMs are illustrated in Figures 5.21, 5.22, and 5.23, respectively. Daily average PM concentrations are used to analyze seasonal and monthly variations, and hourly average values are used in the case of hourly variations.

As discussed earlier, roadside areas tend to be more polluted by fine and coarse particles because of traffic flows. Since there are many more PM sources than traffic-related ones, PM concentrations at roadside AQMs are only slightly higher than those at background AQMs. As seen in Figure 5.21 and 5.22, the 95th percentile PM10 concentrations in Spring and Winter are well above the daily standard, and violations of the daily standard are observed across entire months in 2003. In Spring, higher concentrations are observed in May, which suggests that biogenic sources may start to be active, with increased temperatures and solar radiations stimulating the formation of secondary fine particles.

Considering WHO guidelines for daily and annual average concentration of PM10 and PM2.5[21], around 70 μg/m^3 for the mean concentration and 150 μg/m^3 for the 95th percentile concentration throughout the entire day may be thresholds for adverse health effects in terms of both short-term and long-term exposures.

[21] PM10: 20 μg/m^3 for annual mean and 50 μg/m^3 for 24-h average
PM2.5: 10 μg/m^3 for annual mean and 25 μg/m^3 for 24-h average

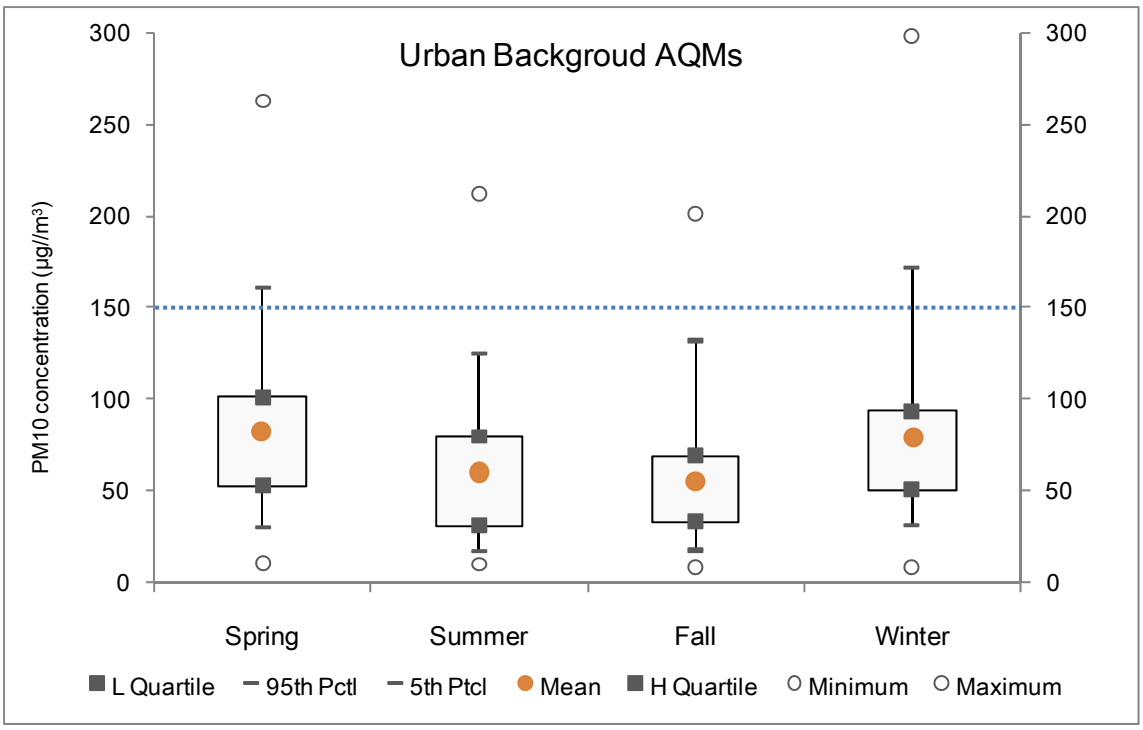

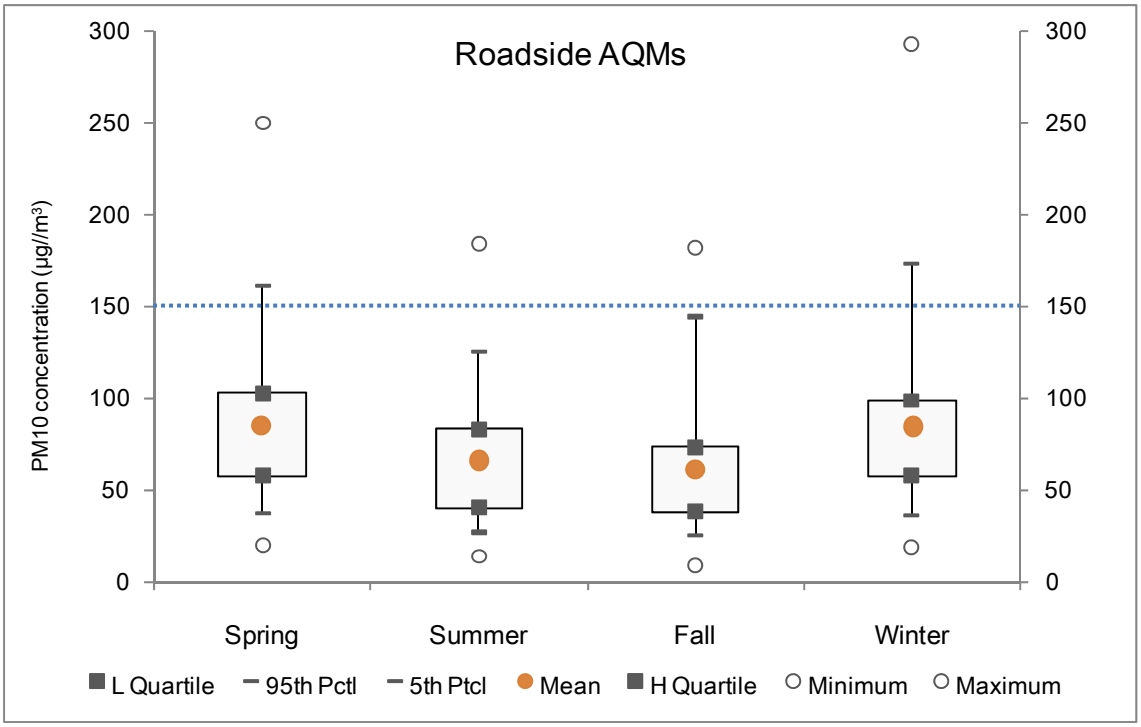

Figure 5.21 Seasonal variations of PM10 concentrations[22]

[22] Maximum, 95th percentile, higher quartile (3/4), mean, lower quartile (1/4), 5th percentile, and minimum for roadside and urban background AQMs (based on daily PM10 average concentrations). The dotted line indicates the daily standard for PM10 concentration: 150 µg/m^3.

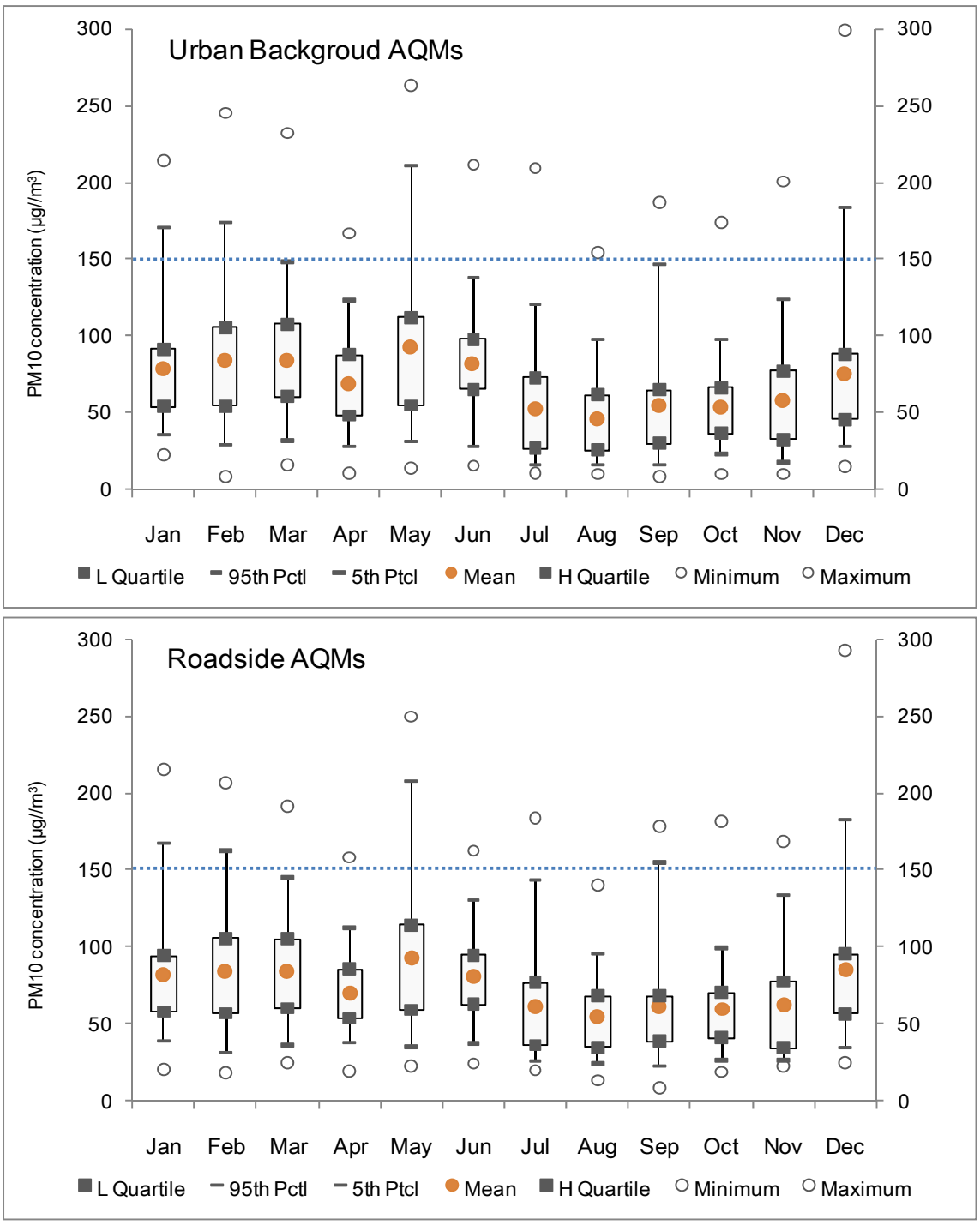

Figure 5.22 Monthly variations of PM10 concentrations[23]

[23] Maximum, 95th percentile, higher quartile (3/4), mean, lower quartile (1/4), 5th percentile, and minimum for roadside and urban background AQMs (based on daily PM10 average concentrations). The dotted line indicates the daily standard for PM10 concentration: 150 µg/m^3.

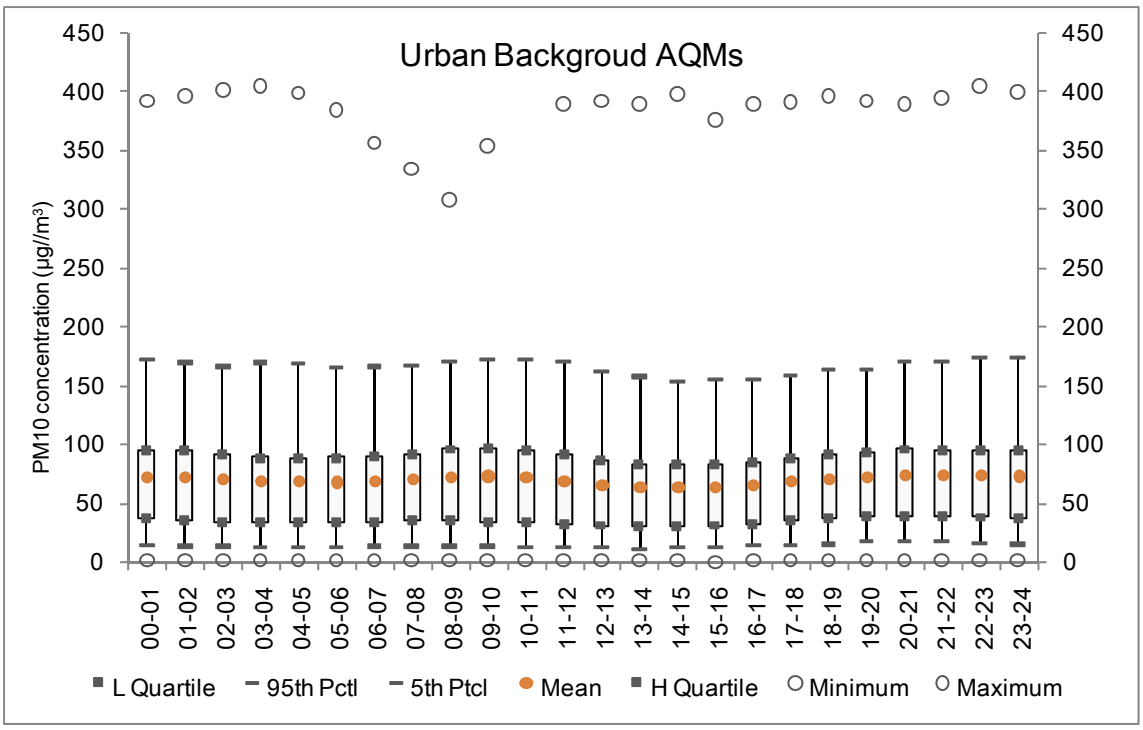

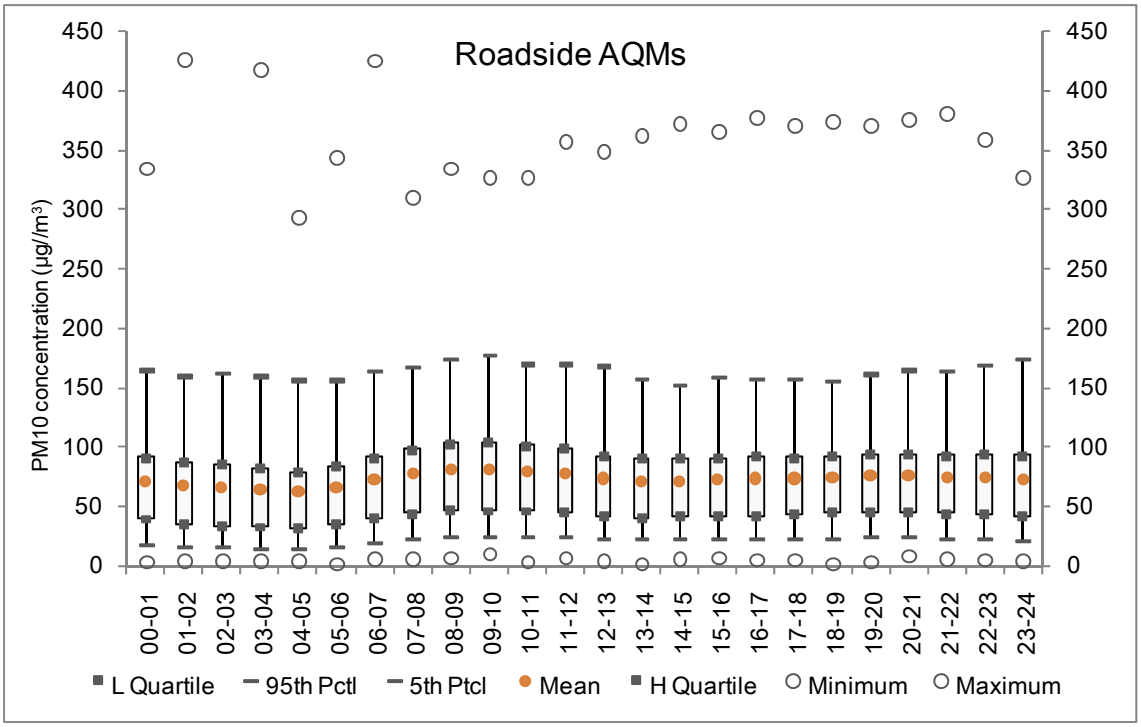

Figure 5.23 Hourly variations of PM10 concentrations[24]

[24] Maximum, 95th percentile, higher quartile (3/4), mean, lower quartile (1/4), 5th percentile, and minimum for roadside and urban background AQMs based on hourly PM10 average concentrations.

5.5.3 Hourly Traffic and PM10 Concentrations

Observed hourly traffic counts and PM10 concentrations are analyzed across the four seasons. Although traffic flows in urban regions contribute a substantial share of PM10 concentrations, the origins of particulate matters vary extensively. As displayed in Figure 5.24, PM10 concentrations at roadside AQMs are higher than those at background AQMs, but the differences are relatively small compared to other pollutants, such as NO_2 and CO, and at nighttime background concentrations exceed roadside ones. It is possible that residential activities, such as heating and cooking, are the sources of this reverse phenomenon. Diurnal PM concentrations display a peak in the morning, coinciding with the morning traffic peak, and then make a slight trough in all seasons, except Winter. The reason for the daytime trough is not clear at this point, and calls for further research in terms of the chemistry of PM10 generation and of the profiles of anthropogenic and biogenic emissions.

As discussed earlier and observed in Figure 5.24, Winter and Spring display higher concentrations than Summer and Autumn. The use of fossil fuels for residential and commercial building heating causes higher PM10 concentrations in Winter, and natural emissions during the growing seasons are possible reasons for higher concentrations in Spring.

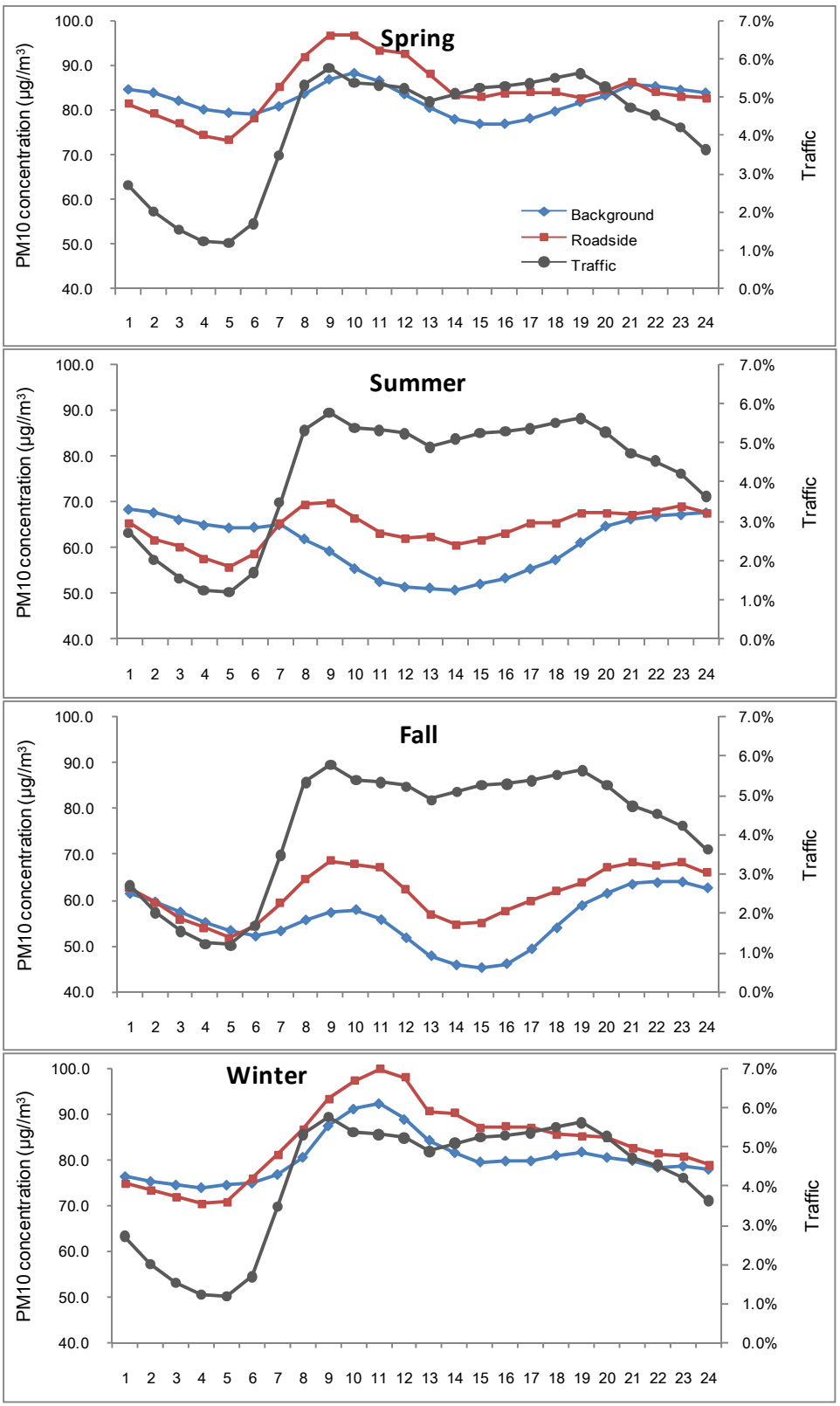

Figure 5.24 Variations of traffic volumes and hourly PM10 averages in roadside and background AQMs in the four seasons

5.5.4 Comparison Between Weekdays and Weekend

Traffic flow differences between weekdays and weekend may cause the differences in PM concentrations between these time periods. As seen in Figure 5.25, PM concentrations during weekdays are higher than those on weekend, at both roadside and background AQMs. Concentrations on Saturday are generally higher than those on Sunday, except during nighttime. The reasons for higher concentrations on Sunday during nighttime are not known. Natural emissions are presumably equal on both days, and therefore an explanation could require collecting human activity profile data in both periods. The peaks of morning concentrations occur one or two hours later than the traffic peaks on both weekdays and Saturday. On Sunday, in contrast, there is no morning traffic peak, but a peak of PM concentration is observed. Althoug troughs take place after the morning peak concentrations at both roadside and background AQMs across all weekdays and weekend, no clear reasons are identified yet, calling for further research.

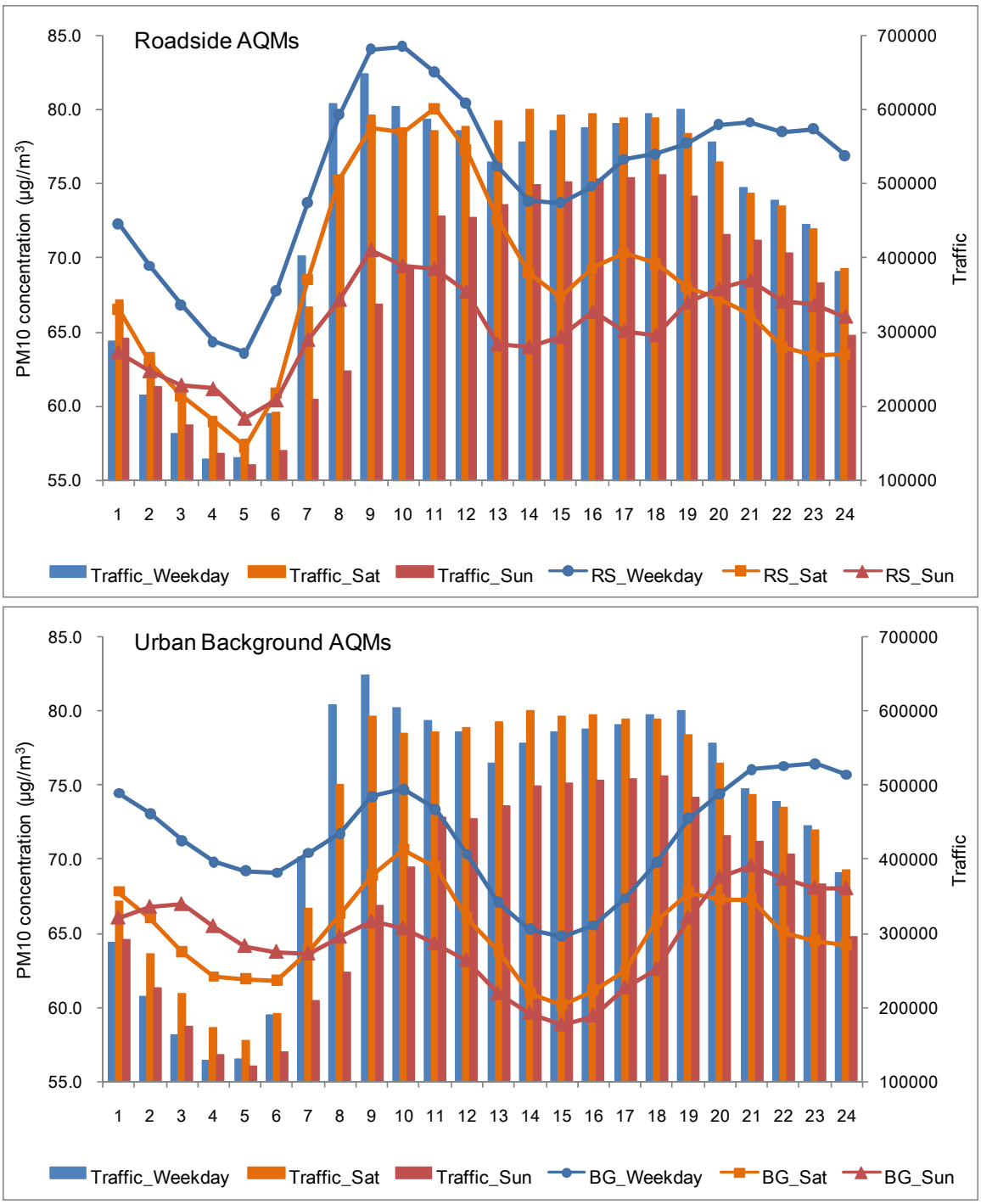

Figure 5.25 Weekday, Saturday, and Sunday hourly PM10 concentrations and traffic flows at roadside and background AQMs in 2003

5.6 SUMMARY ANALYSIS

5.6.1 Descriptive Statistics

Descriptive statistics for the dependent and independent variables are presented. Dependent variables include annual and seasonal concentrations of the five air pollutants discussed in the previous sections, and the explanatory variables include VKT, five land uses, and four meteorological factors. As discussed earlier in the weekday and weekend comparisons, significant concentration differences have been observed. It is, therefore, reasonable to exclude weekend data in the estimation of general air quality models. The descriptive analysis for the dependent variables thus only includes weekday observations. Table 5.6 presents the number of observations, mean, standard deviation, minimum, and maximum for the five pollutants concentrations over the year, and for each season. As expected, there are significant variations across seasons, suggesting that air quality models need to be constructed separately for each season. If all annual data are included in a model, it might be necessary to introduce seasonal dummy variables to account for seasonal effects.

Descriptive statistics for the explanatory variables are presented in Table 5.7 and 5.8. VKT and land-use data have been measured for 11 circular buffers, hence the large number of potential explanatory variables presented in Table 5.7. VKTs, residential areas, commercial areas, industrial areas, transportation areas, and green areas are measured for buffers with radii ranging from 500 to 5500 meters.

Meteorological factors and pollution concentrations are monitored hourly. Daily average values have been calculated and Table 5.8 presents descriptive statistics for these factors across the year and the four seasons.

	Variable[1)]	N	Mean	Std Dev	Minimum	Maximum
Annual	NO_2 (ppb)	6635	41.5	15.9	3.7	124.0
	CO (ppb)	6485	7.3	4.1	1.0	48.3
	O_3 (ppb)	6643	12.2	8.3	0.0	63.1
	SO_2 (ppb)	6382	5.3	3.1	1.0	24.0
	PM10 (μg/m^3)	6168	72.7	40.7	8.5	298.9
Spring	NO_2(ppb)	1611	45.1	15.9	10.7	119.8
	CO (ppb)	1565	6.6	3.0	1.0	23.0
	O_3 (ppb)	1622	16.4	9.1	1.5	63.1
	SO_2 (ppb)	1559	5.1	2.9	1.0	24.0
	PM10 (μg/m^3)	1525	81.4	41.1	14.1	263.2
Summer	NO_2(ppb)	1724	35.9	14.5	3.7	100.7
	CO (ppb)	1678	5.9	2.9	1.0	20.3
	O_3 (ppb)	1705	16.0	8.5	0.1	60.5
	SO_2 (ppb)	1637	4.2	2.2	1.0	14.2
	PM10 (μg/m^3)	1475	63.2	33.6	10.2	211.8
Autumn	NO_2(ppb)	1671	40.0	16.5	7.9	124.0
	CO (ppb)	1651	7.2	4.1	1.1	35.4
	O_3 (ppb)	1691	8.8	5.5	0.0	29.0
	SO_2 (ppb)	1622	4.7	2.6	1.0	21.5
	PM10 (μg/m^3)	1614	60.6	35.7	8.5	187.0
Winter	NO_2(ppb)	1629	45.6	14.5	8.6	102.7
	CO (ppb)	1591	9.7	5.1	1.4	48.3
	O_3 (ppb)	1625	7.6	4.8	0.0	28.5
	SO_2 (ppb)	1564	7.3	3.5	1.0	22.1
	PM10 (μg/m^3)	1554	85.8	45.2	23.1	298.9

1) Weekday monitored values are used

Table 5.6 Descriptive statistics for the dependent variables

	Radius (meter)	N	Mean	Std Dev	Minimum	Maximum
VKT (10^6 veh · km)	500	34	0.10	0.06	0.01	0.24
	1000	34	0.43	0.17	0.14	0.79
	1500	34	0.89	0.32	0.41	1.56
	2000	34	1.49	0.51	0.70	2.69
	2500	34	2.20	0.74	0.98	3.84
	3000	34	3.09	1.00	1.51	5.25
	3500	34	4.15	1.32	1.86	6.72
	4000	34	5.36	1.69	2.25	8.38
	4500	34	6.72	2.10	2.61	10.30
	5000	34	8.14	2.50	3.03	12.45
	5500	34	9.71	2.96	3.37	14.80
Residential Area (km^2)	500	34	0.18	0.15	0.00	0.55
	1000	34	0.78	0.43	0.14	1.61
	1500	34	1.72	0.77	0.53	3.46
	2000	34	2.91	1.13	1.30	5.33
	2500	34	4.46	1.42	2.04	7.86
	3000	34	6.16	1.63	2.67	10.32
	3500	34	8.11	1.98	3.22	13.29
	4000	34	10.30	2.50	3.86	16.77
	4500	34	12.59	3.04	5.02	19.71
	5000	34	15.03	3.64	6.54	21.96
	5500	34	17.81	4.51	7.65	25.75
Commercial Area (km^2)	500	34	0.31	0.17	0.02	0.63
	1000	34	1.11	0.47	0.13	1.92
	1500	34	2.22	0.85	0.48	4.08
	2000	34	3.49	1.31	1.19	6.41
	2500	34	5.01	1.80	1.91	8.71
	3000	34	6.86	2.25	2.82	11.04
	3500	34	8.91	2.71	3.51	13.52
	4000	34	11.11	3.21	4.76	15.72
	4500	34	13.46	3.80	5.68	19.61
	5000	34	16.04	4.67	6.43	23.11
	5500	34	18.83	5.56	7.44	26.20

Table 5.7 Descriptive statistics for VKT and land use variables

Table 5.7 continued

	Radius (meter)	N	Mean	Std Dev	Minimum	Maximum
Industrial Area (km^2)	500	34	0.02	0.07	0.00	0.36
	1000	34	0.06	0.18	0.00	0.92
	1500	34	0.13	0.32	0.00	1.50
	2000	34	0.17	0.40	0.00	1.87
	2500	34	0.21	0.43	0.00	1.88
	3000	34	0.28	0.48	0.00	2.06
	3500	34	0.38	0.58	0.00	2.46
	4000	34	0.51	0.67	0.00	2.79
	4500	34	0.69	0.79	0.00	3.07
	5000	34	0.88	0.90	0.01	3.28
	5500	34	1.08	1.03	0.02	3.58
Transportation Area (km^2)	500	34	0.10	0.05	0.02	0.27
	1000	34	0.41	0.14	0.14	0.67
	1500	34	0.85	0.27	0.36	1.32
	2000	34	1.42	0.45	0.59	2.21
	2500	34	2.08	0.65	0.82	3.30
	3000	34	2.91	0.90	1.08	4.49
	3500	34	3.88	1.20	1.46	5.93
	4000	34	5.00	1.53	1.78	7.45
	4500	34	6.19	1.88	2.09	9.18
	5000	34	7.43	2.24	2.99	11.08
	5500	34	8.79	2.67	3.68	13.01
Green Area (km^2)	500	34	0.06	0.10	0.00	0.39
	1000	34	0.26	0.36	0.00	1.65
	1500	34	0.78	0.72	0.07	3.31
	2000	34	1.82	1.34	0.32	5.92
	2500	34	3.30	2.15	0.63	9.13
	3000	34	5.22	3.35	1.07	12.38
	3500	34	7.60	4.76	1.46	18.91
	4000	34	10.45	6.44	2.04	26.30
	4500	34	13.92	8.31	2.77	34.54
	5000	34	18.03	10.34	4.04	43.08
	5500	34	22.70	12.39	5.66	55.09

	Variable	N	Mean	Std Dev	Minimum	Maximum
Annual	Radiation (MJ/m^3)	365	0.49	0.28	0.00	1.13
	Wind Speed (m/s)	365	2.00	0.76	0.55	4.47
	Temperature (˚C)	365	12.83	9.52	-12.76	26.98
	Humidity (%)	365	64.60	14.87	26.63	95.79
Spring	Radiation (MJ/m^3)	92	0.64	0.30	0.06	1.13
	Wind Speed (m/s)	92	2.23	0.60	1.07	4.31
	Temperature (˚C)	92	12.68	6.04	-1.15	25.15
	Humidity (%)	92	58.23	15.09	26.63	92.46
Summer	Radiation (MJ/m^3)	92	0.56	0.31	0.06	1.13
	Wind Speed (m/s)	92	1.70	0.59	0.66	4.25
	Temperature (˚C)	92	23.22	2.11	16.74	26.98
	Humidity (%)	92	73.65	12.83	37.21	95.17
Autumn	Radiation (MJ/m^3)	91	0.42	0.23	0.00	0.86
	Wind Speed (m/s)	91	1.71	0.77	0.55	4.38
	Temperature (˚C)	91	15.05	5.48	-0.09	23.22
	Humidity (%)	91	66.43	13.98	36.88	95.79
Winter	Radiation (MJ/m^3)	90	0.34	0.16	0.02	0.68
	Wind Speed (m/s)	90	2.37	0.80	1.22	4.47
	Temperature (˚C)	90	0.11	4.30	-12.76	8.78
	Humidity (%)	90	60.01	12.39	35.46	91.58

Table 5.8 Descriptive statistics for of meteorological factors

5.6.2 Correlation Analysis

Correlation tables including all variables are presented in Tables G.1 to G.6 in Appendix G. Tables 5.9 and 5.10 display the most significant correlation coefficients. As discussed in the Sections 5.1 ~ 5.5, higher pollution concentrations are observed during Spring, thus average daily concentrations monitored during Spring weekdays are used to calculate the correlation coefficients. Since VKT and land-use variables have been assessed for the 34 AQMs, the coefficients in Table 5.9 represent cross-sectional relationships between air pollution concentrations, VKT, and land-use data. Since anthropogenic emissions are generally related to the combustion of fossil fuels, directly emitted pollutants, such as NO_2[25], CO, and SO_2, are closely correlated with each other. On the other hand, in the case of O_3, a secondary product, the photochemical decomposition of NO_2 is a necessary condition for the formation of O_3, (Eqs. 2.8 and 2.17), and the reaction of CO and OH· radicals stimulates the generation of NO_2 (Eqs. 2.10 and 2.7), leading to favorable condition for the formation of O_3. Thus, NO_2 and CO are negatively correlated with O_3. As expected, VKT is positively correlated with the concentrations of directly emitted pollutants. In contrast, freshly emitted NO gas from tail pipes reacts with ambient O_3 just after its emissions, and therefore O_3 concentrations are negatively correlated with VKT. This pattern is also observed between O_3 and transportation areas near AQM stations. Since areas of commercial and transportation activities generate anthropogenic emissions, these variables are positively correlated with NO_2, CO, and SO_2 concentrations. Green areas, however, display opposite correlations. If green areas around AQMs increase, other land uses decrease, resulting in lower pollution concentrations. In addition, the assimilative capacity of vegetation may reduce concentrations.[26]

Table 5.10 displays correlations between pollution concentrations and meteorological factors. The meteorological factors are measured on an hourly basis. The signs of the correlation coefficients among pollutant concentrations are the same as those in the cross-sectional case. Notable correlations are observed between PM10 and other pollutants. As discussed in the review

---

[25]According to Derwent and Hertel (1998), over 90% of nitrogen compounds are emitted in the form of nitric oxide (NO). Only less than 10% of nitrogen is directly emitted in NO_2 form. NO produced in the combustion process, however, mainly reacts with ambient O_3 within a few seconds after its emission, and is transformed into NO_2. Thus, strictly, NO_2 can be classified as a secondary product, but, because of its quick and complete reaction, NO_2 can be regarded as a direct emission from vehicles.

[26]In the case of O_3, plants emit highly reactive VOCs, such as isoprene (C_5H_8), primarily from deciduous trees, and α-pinene ($C_{10}H_{16}$), primarily from coniferous trees, during the growing seasons. These biogenic VOCs play a significant role in forming urban O_3 levels (Chameides, Lindsay, Richardson, & Kiang, 1988; Chameides et al., 1992). Since the correlation between VKT and green areas are highly negative (-0.82), it is difficult to separate whether increased biogenic VOCs or decreased VKTs as the major factors for increased O_3 concentrations.

of PM10 chemistry, NO_2 and SO_2 have the potential of being converted into fine particles, leading to increased PM10 concentrations. Solar radiation is indispensable to generate O_3, thus a significant positive correlation between O_3 concentration and solar radiation. Wind is known to expedite the dispersion of pollutants, but light wind contributes to scattering effects that facilitate photochemical reactions. During Spring in the Seoul Metropolitan area, wind speed is positively correlated with O_3 concentration, but negatively so with the other pollutants. Since temperature enhances O_3 photochemical activities, temperature is positively correlated with O_3 concentration. Lower temperatures during the cold seasons lead to more consumption of fossil fuels, thus increased emissions and higher concentrations. Negative correlations are observed between humidity and all pollutant concentrations, because water vapor wipes out ambient pollutants, and humidity is negatively correlated with solar radiation.

	NO2	CO	O3	SO2	PM10	VKT R4000	Residential R0500	Commercial R1000	Transport R0500	Green R3500
NO2	1.00	0.58 0.0003	-0.55 0.0008	0.72 <.0001	-0.02 0.9045	0.57 0.0004	-0.23 0.1817	0.30 0.0846	0.39 0.0211	-0.46 0.0058
CO		1.00	-0.52 0.0015	0.57 0.0005	0.25 0.1566	0.29 0.0903	-0.17 0.3429	0.45 0.0077	0.58 0.0003	-0.30 0.0886
O3			1.00	-0.41 0.0163	-0.24 0.1667	-0.58 0.0003	0.31 0.0723	-0.25 0.155	-0.57 0.0004	0.55 0.0008
SO2				1.00	0.01 0.9743	0.41 0.0153	-0.20 0.2566	0.22 0.2068	0.43 0.0102	-0.34 0.048
PM10					1.00	0.01 0.9758	0.00 0.9987	-0.13 0.4666	0.01 0.9648	-0.04 0.8006
VKT R4000						1.00	-0.30 0.0813	0.10 0.5605	0.34 0.0458	-0.82 <.0001
Residential R0500							1.00	-0.46 0.0057	-0.15 0.3852	0.29 0.0912
Commercial R1000								1.00	0.17 0.3506	-0.12 0.4921
Transport R0500									1.00	-0.43 0.0108
Green Area R3500										1.00

: Possitive correlation
: Negative correlation

Table 5.9 Pearson correlation coefficients between pollutant concentrations, VKT, and land use variables[27]

	NO2	CO	O3	SO2	PM10	Solar Radiation	Wind Speed	Temp.	Humidity
NO2	1.00	0.60 <.0001	-0.32 <.0001	0.55 <.0001	0.52 <.0001	0.10 0.0003	-0.36 <.0001	0.00 0.9151	-0.14 <.0001
CO		1.00	-0.29 <.0001	0.49 <.0001	0.45 <.0001	0.08 0.01	-0.24 <.0001	0.03 0.3751	-0.06 0.038
O3			1.00	-0.22 <.0001	0.03 0.3352	0.44 <.0001	0.08 0.0043	0.42 <.0001	-0.31 <.0001
SO2				1.00	0.50 <.0001	0.09 0.0034	-0.17 <.0001	-0.04 0.2161	-0.14 <.0001
PM10					1.00	0.25 <.0001	-0.15 <.0001	0.12 <.0001	-0.13 <.0001
Solar Rad.						1.00	0.03 0.2855	0.27 <.0001	-0.70 <.0001
Wind Speed							1.00	-0.29 <.0001	-0.09 0.0012
Temp.								1.00	0.02 0.4433
Humidity									1.00

: Possitive correlation
: Negative correlation

Table 5.10 Pearson correlation coefficients between pollutant concentrations and meteorological variables[28]

[27]Weekday average during spring seasons for 34 AQMs are used for calculation.

[28]Panel data (34 AQMs × 63 days of spring weekday) is used for calculation.

5.6.3 Solar Radiation vs. O_3 Concentrations

As reviewed in Section 2.1.3 on O_3 chemical reactions, meteorological factors play important roles in determining O_3 concentrations. In particular, solar radiation is indispensible for generating O_3, and it is necessary to focus on the relationship between intensity of solar radiation and O_3 concentration. It is common scientific knowledge that the intensity of UV radiation plays an important role in the formation of O_3, because solar radiation initiates the photodissociation of NO_2 (Eq. 2.8), followed by the reaction of ground-state atomic oxygen ($O(^3P)$) and O_2 to generate O_3 (Eq. 2.17). As illustrated in Figure 5.26, hourly-averaged O_3 concentrations during May 2003 have a pattern similar to UV radiation, but with a time lag. As expected, the peak of solar radiation occurs around 1:00 PM, but O_3 concentration peaks at 4:00 PM. The three-hour time lag between the two peaks may be explained by the accumulation of O_3. Since ambient O_3 concentrations are determined by rates of creation and decomposition, the rate of creation is greater than the decomposition one, leading to the accumulation of O_3. The time lag suggests that the creation rate exceeds the decomposition rate until 4:00 PM. To consider this accumulation effect, a moving average method may be considered for introducing a new radiation-related variable.

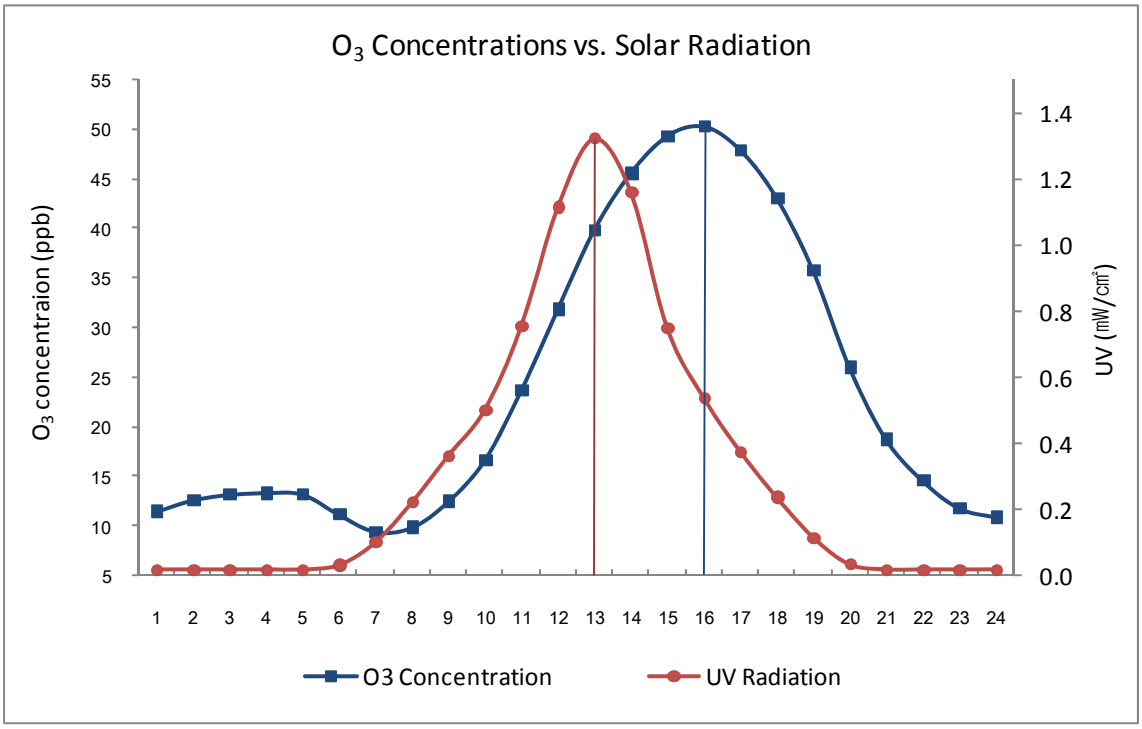

Figure 5.26 Comparison between O_3 concentrations and UV radiation during May 2003

CHAPTER 6

TIME-SERIES ANALYSES OF AIR QUALITY

This chapter presents the estimation of the time-series air quality models outlined in Section 3.3.2. Models explaining the variations of the concentrations of five pollutants (O_3, NO_2, CO, SO_2, and PM10) are estimated. Elasticity analyses are performed to assess the varying impacts of traffic flows and meteorological factors on concentrations on weekdays vs. Sunday and at roadside vs. background air quality monitoring stations (AQMs).

6.1 OVERVIEW

Pollutants emitted by motor vehicles influence ambient concentrations over both time and space. Vehicles are a key source of directly emitted pollutants, such as NO_x, CO, SO_2, and particulate matter. Transportation is responsible for a substantial share of emissions in urban regions, and it is logical to infer that decreased vehicle flows lead to decreased direct emissions. However, in the case of ozone (O_3), a secondary product, chemical reactions are the major determinant of this pollutant, and, as discussed in the analysis of the ozone isopleth plot in Chapter 2, decreased vehicle flows in NO_x-saturated regions increase O_3 concentrations. Specifically, reduced traffic flows during the weekend induce change in the VOC/NO_x concentration ratio and, consequently, less O_3 titration (NO + O_3 reaction) and less HNO_3 formation (NO_2 + OH· reaction). A decrease in these two reactions leads to favorable conditions for O_3 generation (Fujita et al., 2003; Heuss, Kahlbaum, & Wolff, 2003; Seinfeld, 1989). A similar differentiation phenomenon is observed for roadside areas and urban background regions. Roadside areas are abundant in NO emissions and are dominated by O_3 titration, hence roadside areas have frequently lower O_3 concentrations than background regions (or suburban regions).

In addition to traffic flows, meteorological factors also influence O_3 concentrations. Tropospheric O_3 is produced by photochemical reactions involving UV rays and forerunner chemicals, such as VOCs and NO_x. The formation of O_3 is known to be a complicated and nonlinear process, depending on the concentrations of precursors, their mixing ratio, and the

intensity of UV rays (Derwent & Hertel, 1998; Seinfeld & Pandis, 2006). Episodes of high O_3 concentrations occur in late Spring and Summer, under such meteorological conditions as high pressure, warm temperature, low cloud cover, and light wind. Temperature has direct and indirect impacts on O_3 creation. A high temperature enhances O_3 concentrations directly by facilitating the photochemistry of O_3, and indirectly by increasing the emission rates of biogenic VOCs. Wind is known to expedite the dispersion of pollutants, but light wind contributes to scattering effects, facilitating photochemical reactions. Humidity has a negative correlation with O_3 concentrations, because water vapor in the ambient atmosphere wipes out pollutants and high humidity is also correlated with cloud cover. While O_3 formation is solely dependent on a photochemical process, these meteorological factors interact with the sources of O_3 precursors (e.g. traffic emissions), leading to different impacts on O_3 concentrations.

Hourly pollution concentrations have been measured at 34 AQMs across the Seoul Metropolitan Area in 2003: 27 are classified as urban background AQMs, and the other 7 AQMs are located near heavily traveled roads to measure roadside air quality. To capture the temporal and spatial differences in pollution concentrations between weekdays and Sundays, and between roadside AQMs and background AQMs, these hourly-measured concentrations are averaged over the two sets of AQMs.

For the directly emitted pollutants (NO_2, CO, SO_2, and PM10), the average hourly concentrations averaged over the whole year 2003 are distinctively higher during weekdays than during Sundays, which is consistent with the results from several studies of California's South Coast Air Basin (Blanchard & Tanenbaum, 2003; Chinkin et al., 2003; Yarwood et al., 2008). In contrast, the average hourly O_3 concentrations are higher on Sunday than on Saturday and weekdays. Recent research has pointed to similar patterns for O_3 concentrations in different metropolitan areas: Chicago, IL, and Philadelphia, PA (Pun, Seigneur, & White, 2003), Azusa, CA (Fujita, Stockwell, Campbell, Keislar, & Lawson, 2003), and Daegu, Korea (Jo & Park, 2005). The patterns of hourly concentrations are presented in Figures 6.1 ~ 6.5. Note that the Saturday concentration patterns are generally closer to the weekday patterns than to the Sunday ones, particularly in the case of O_3 and NO_2.

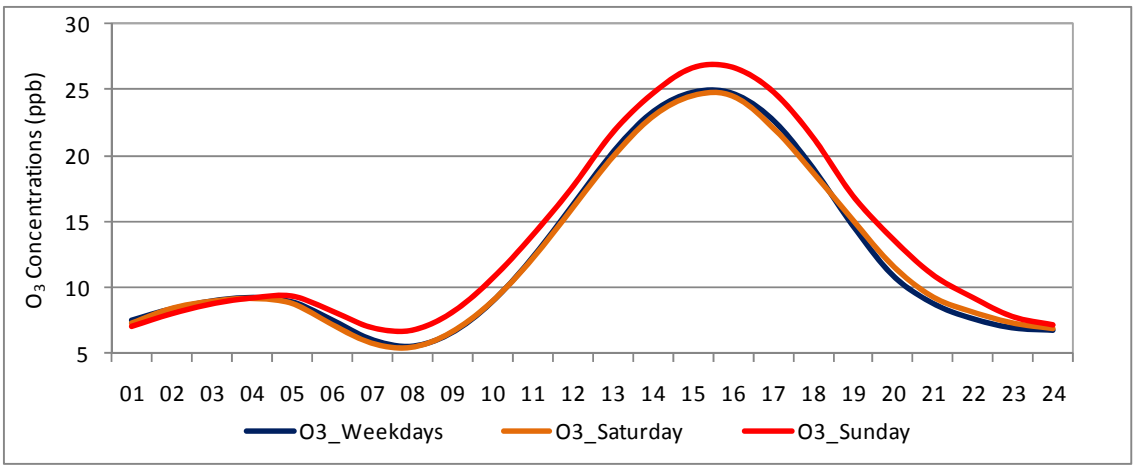

Figure 6.1 Hourly O_3 concentrations for weekdays, Saturday, and Sunday

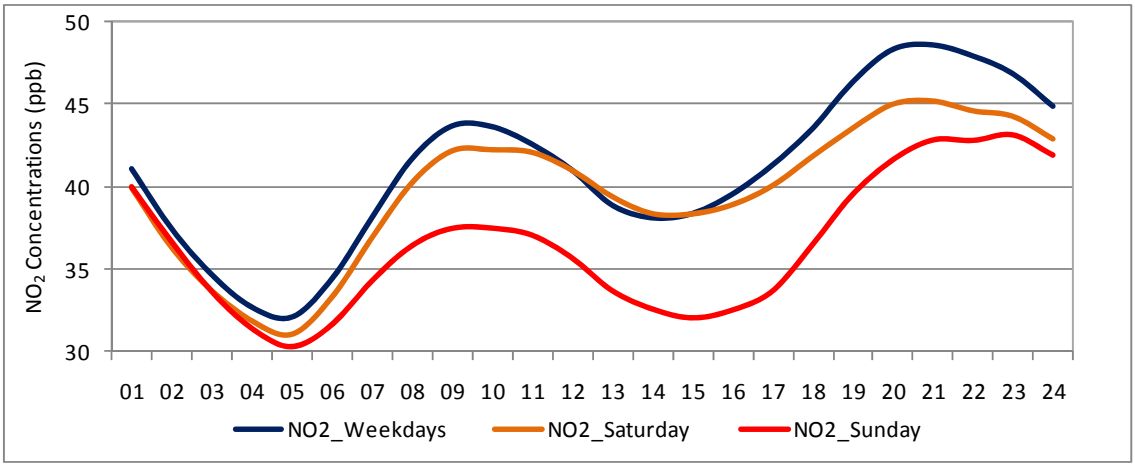

Figure 6.2 Hourly NO_2 concentrations for weekdays, Saturday, and Sunday

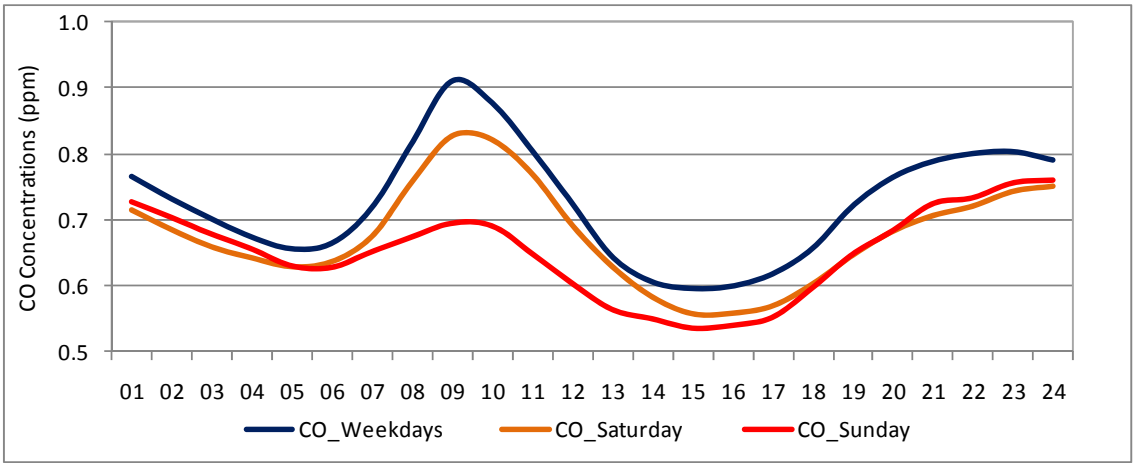

Figure 6.3 Hourly CO concentrations for weekdays, Saturday, and Sunday

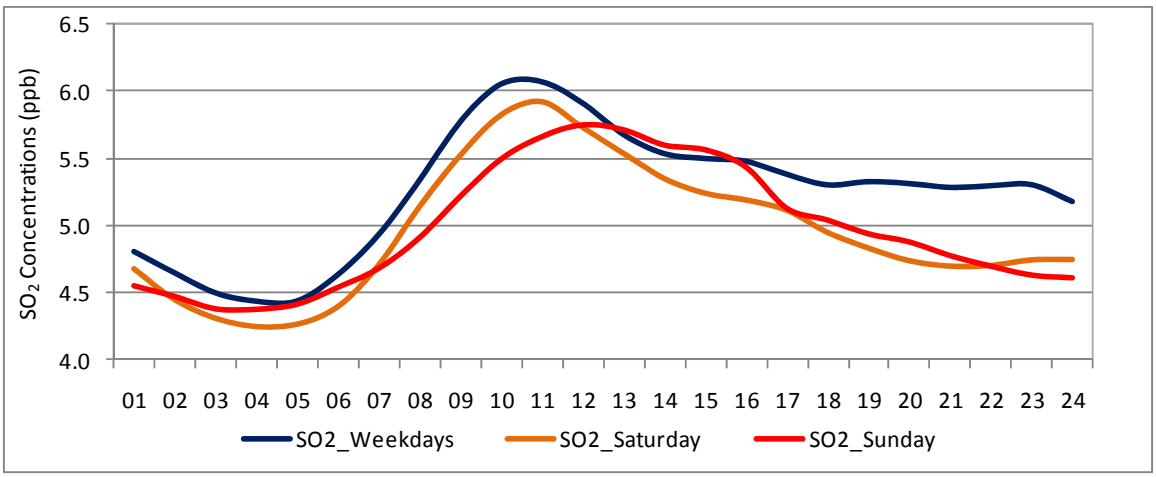

Figure 6.4 Hourly SO_2 concentrations for weekdays, Saturday, and Sunday

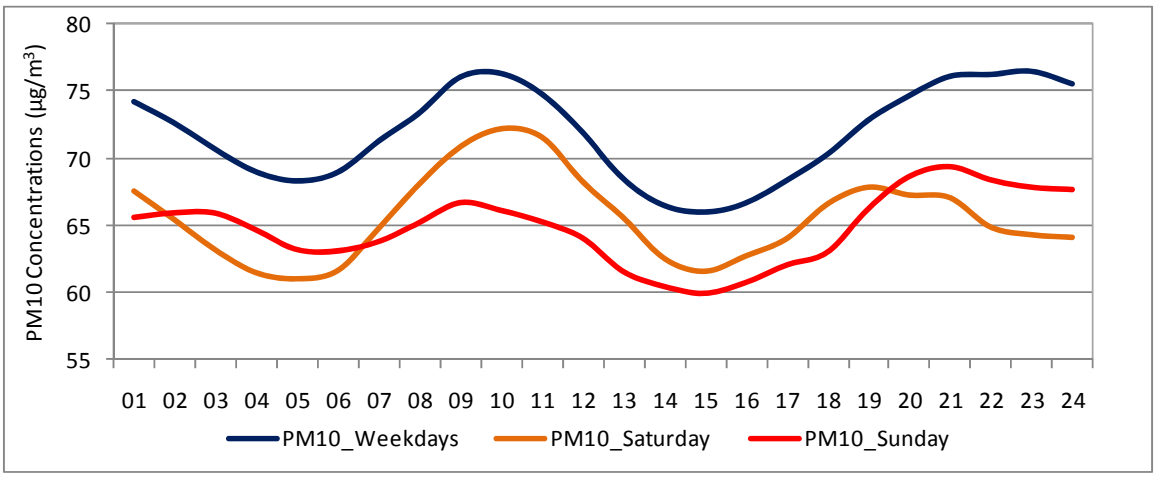

Figure 6.5 Hourly PM10 concentrations for weekdays, Saturday, and Sunday

To analyze the different patterns of pollution concentrations along the temporal (weekdays vs. Sunday) and spatial (roadside AQMs vs. background AQMs) dimensions, diverse statistics, such as the minimum, 10th percentile, lower quartile, mean, higher quartile, 90th percentile, and maximum, are calculated. Using these statistics, box plots for the five pollutants are illustrated in Figures 6.6 ~ 6.10. In view of the influence of traffic flows on O_3 concentrations, background areas on Sunday have the most favorable conditions for generating O_3, while roadside areas during weekdays have the least favorable ones. Figure 6.6 presents box plots of O_3

concentrations along the temporal (weekdays vs. Sunday) and spatial (roadside AQMs vs. background AQMs) dimensions. As expected, O_3 concentrations at roadside AQMs during weekdays are the lowest. In contrast, those at background AQMs during Sundays are the highest. The average annual O_3 concentration at background AQMs on Sunday is 14.6 ppb, and on weekdays 13.0 ppb. The same measure at roadside AQMs during Sunday is 9.4 ppb, and during weekdays 8.2 ppb. These patterns, observed in the Seoul Metropolitan Area, are consistent with the theoretical framework represented by the ozone isopleth diagram (Chapter 2). As there are presumably no significant differences in meteorological conditions between weekdays and Sunday, it is necessary to investigate what are the factors that have major influences on the differences observed in Figure 6.6.

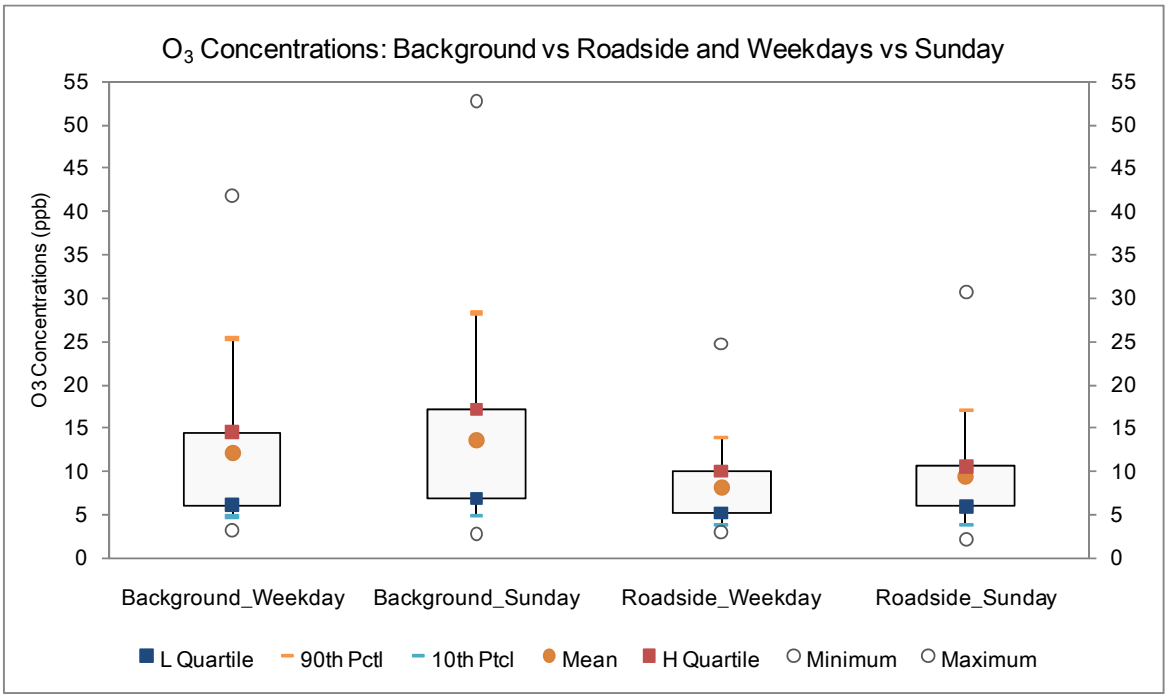

Figure 6.6 Box plots of O_3 concentrations among the four data sets

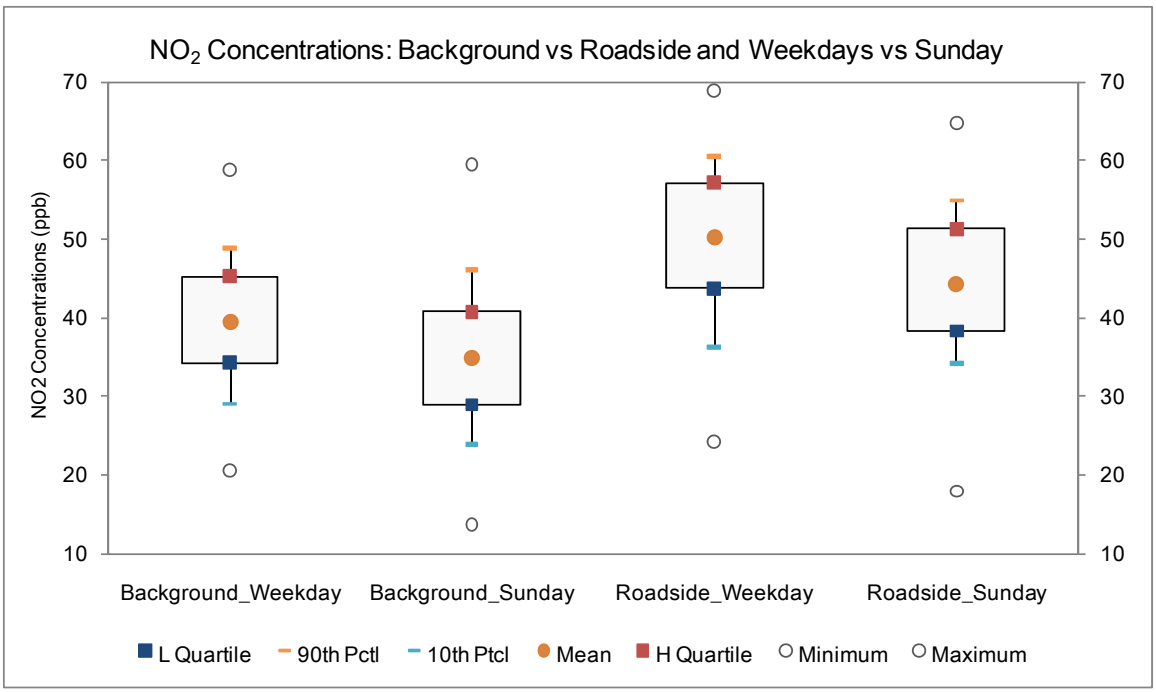

Figure 6.7 Box plots of NO_2 concentrations among the four data sets

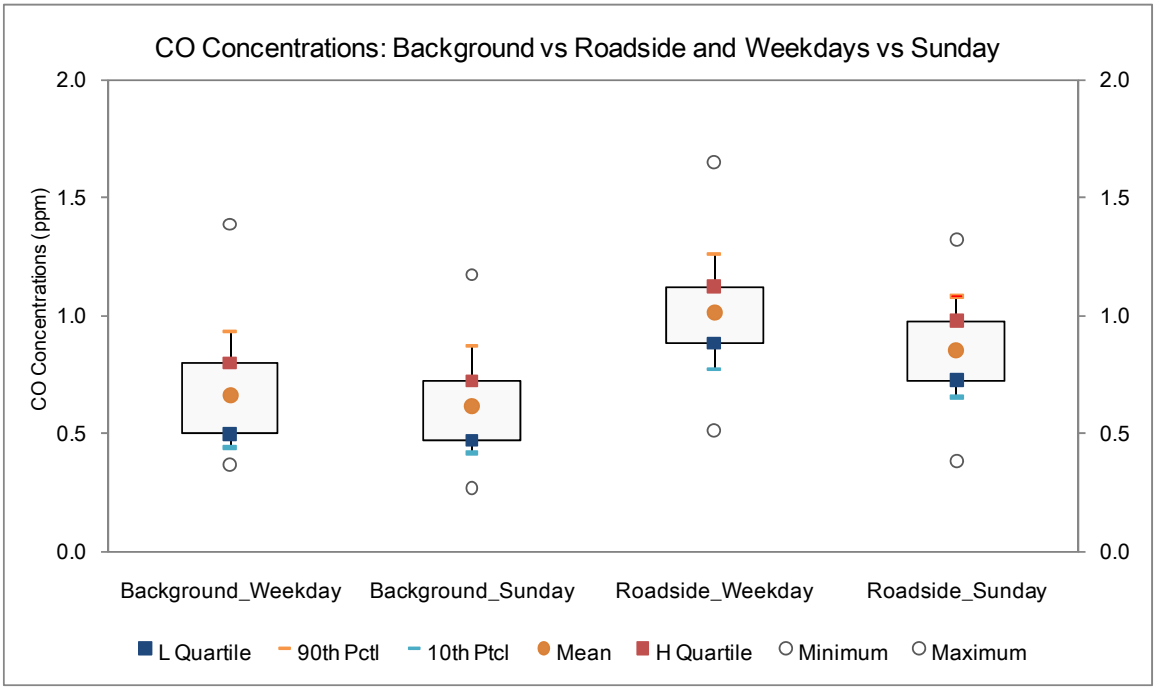

Figure 6.8 Box plots of CO concentrations among the four data sets

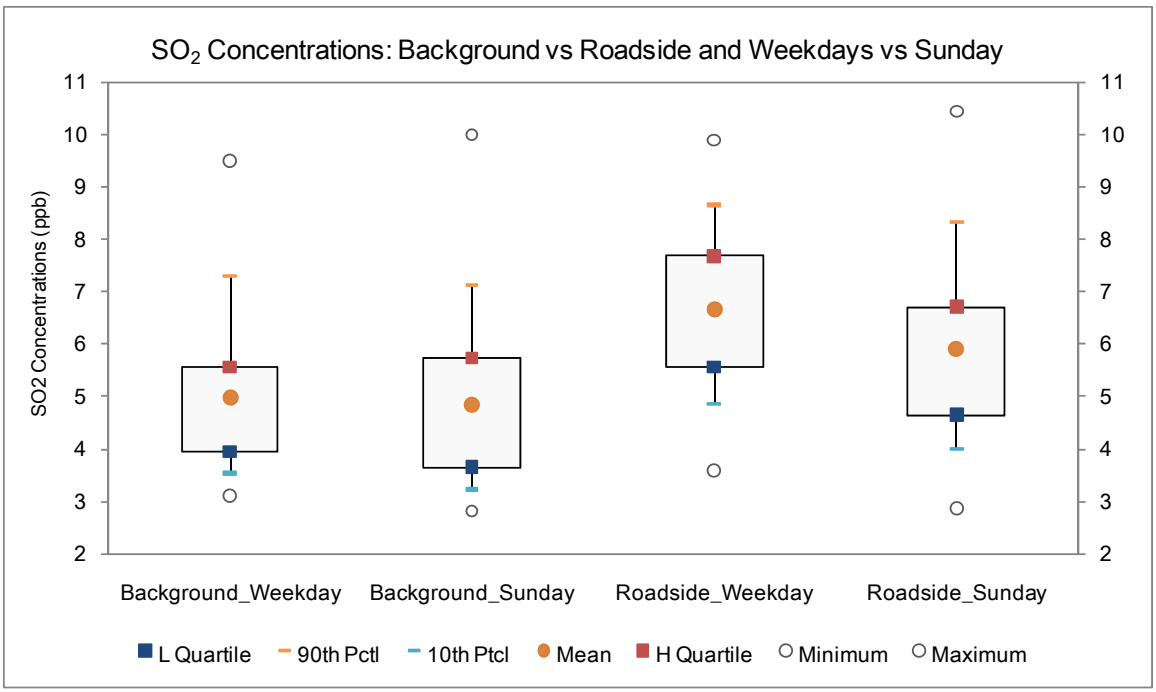

Figure 6.9 Box plots of SO_2 concentrations among the four data sets

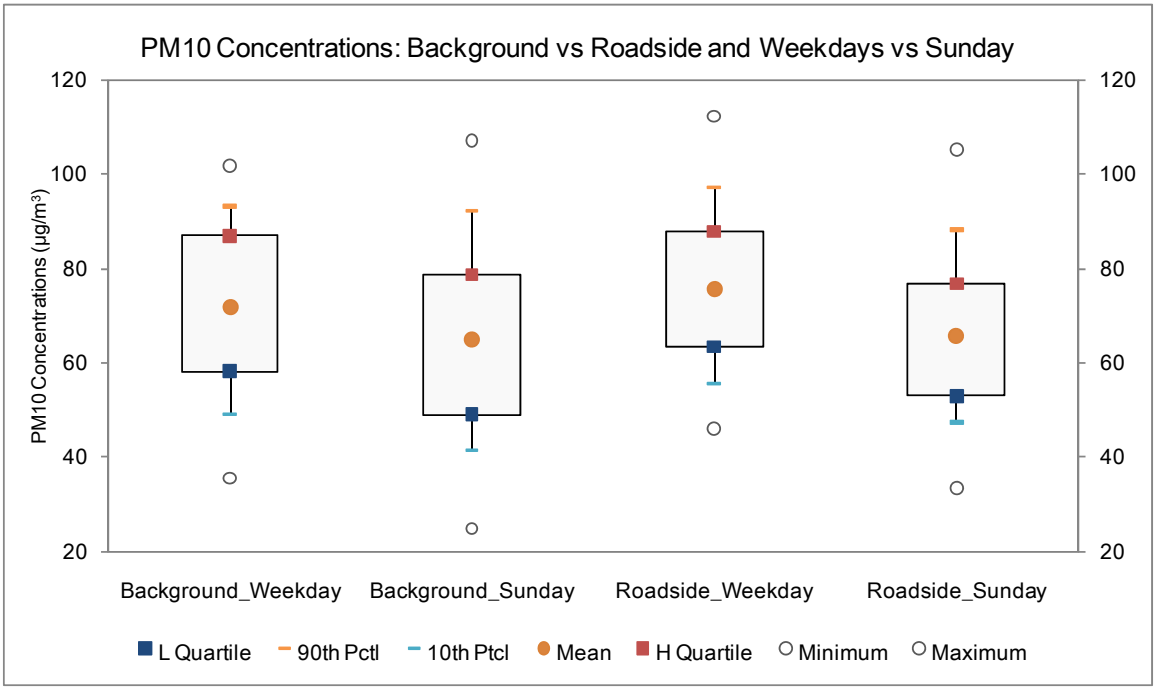

Figure 6.10 Box plots of PM10 concentrations among the four data sets

Figures 6.7 ~ 6.10 show that the box plots of directly emitted pollutants display higher values during weekdays than on Sunday. In view of the decreased traffic flows and production activities on Sunday, these results are very reasonable. Since roadside areas tend to be significantly affected by traffic emissions, the concentrations measured at roadside AQMs are higher than at background AQMs. Thus, for the four directly emitted pollutants, the concentrations measured at roadside AQMs during weekdays are the highest and those at background AQMs during Sunday are the lowest.

6.2 TIME SERIES MODELING

6.2.1 Data

Descriptive statistics for the dependent variables (concentrations) are presented in Table 6.1. The background statistics are based on the average values across the 27 background AQMs. Similarly, the roadside statistics use the average values across the 7 roadside AQMs. In 2003, the number of weekdays was 250, thus 6,000 observations for weekdays (250 days × 24 hours). There was 52 Saturdays, 52 Sundays, and 11 national holidays in 2003. The number of observations for Saturday is 1,248. Since traffic flows on holidays are expected to be similar to those on Sunday, it is reasonable to include holidays in the Sunday classification. 1,512 observations are used for Sunday. There are no missing data for background AQMs, but, in the case of roadside AQMs, 9 missing values for weekdays and 24 missing ones for Sunday. In total, 8,760 and 8,727 serial observations are used for the background and roadside models, respectively[1]. The descriptive statistics of pollution concentrations in Table 6.1 are consistent with the discussions in Section 6.1. O_3 concentrations at background AQMs are higher than those at roadside AQMs. In the cases of directly emitted pollutants, the roadside concentrations are higher than the background ones. In addition, concentrations can be compared across the days of week (weekdays, Saturday, and Sunday). There is little difference between weekdays and Saturday. In contrast, O_3 concentrations on Sunday are clearly higher than those on weekdays and Saturday. In the case of directly emitted pollutants, the concentrations on Sunday are lower than those on weekdays and Saturday.

Descriptive statistics for the explanatory variables are presented in Table 6.2. Traffic counts have been collected at 4 different road classifications, including the CBD (26 locations), Han River bridges (19 locations), arterial roads (36 locations), and cordon line (38 locations). As discussed in Chapter 4, these data have been expanded into series of 8,760 hourly observations by using monthly adjustment factors. Since the 5-day working week was not yet completely implemented in 2003, the traffic counts are not significantly different between weekdays and Saturday. However, the traffic counts on Sunday are considerably smaller than those on weekdays and Saturday. As for the meteorological factors, there are no significant differences among weekdays, Saturday and Sunday.

[1] There are no averaged values during the period 11/16 01:00 ~ 11/17 09:00 (33 hours) for all five pollutants at roadside AQMs. Since 11/16 is a Sunday and 11/17 is a Monday, the missing values are replaced by the corresponding average hourly values of Sundays and Mondays in November.

Classification		Variable	N	Mean	Std.	Minimum	Maximum
Weekday	Background	O_3 (ppb)	6000	13.0	13.0	1.2	85.4
		NO_2 (ppb)	6000	39.5	15.4	7.3	130.5
		CO (ppm)	6000	0.7	0.4	0.2	3.1
		SO_2 (ppb)	6000	5.0	2.6	2.0	21.0
		PM10 (μg/m^3)	6000	71.7	45.8	7.0	319.6
	Roadside	O_3 (ppb)	5991	8.2	6.0	1.0	48.4
		NO_2 (ppb)	5991	50.4	15.7	9.3	142.2
		CO (ppm)	5991	1.0	0.4	0.2	3.6
		SO_2 (ppb)	5991	6.7	2.9	1.9	23.0
		PM10 (μg/m^3)	5991	75.4	43.1	8.1	319.3
Saturday	Background	O_3 (ppb)	1248	13.2	12.1	1.3	70.2
		NO_2 (ppb)	1248	37.7	15.6	6.5	98.5
		CO (ppm)	1248	0.6	0.3	0.2	2.8
		SO_2 (ppb)	1248	4.7	2.2	2.2	17.8
		PM10 (μg/m^3)	1248	65.2	42.4	8.0	280.8
	Roadside	O_3 (ppb)	1248	8.4	5.7	0.0	36.9
		NO_2 (ppb)	1248	48.5	15.8	11.0	115.7
		CO (ppm)	1248	0.9	0.3	0.3	3.6
		SO_2 (ppb)	1248	6.3	2.6	1.3	20.0
		PM10 (μg/m^3)	1248	68.9	40.1	7.7	266.8
Sunday	Background	O_3 (ppb)	1512	15.2	14.4	1.3	85.3
		NO_2 (ppb)	1512	34.0	13.5	8.2	78.8
		CO (ppm)	1512	0.6	0.3	0.2	2.5
		SO_2 (ppb)	1512	4.8	2.5	1.9	25.3
		PM10 (μg/m^3)	1512	65.0	39.4	6.9	283.1
	Roadside	O_3 (ppb)	1488	9.7	7.3	0.9	44.9
		NO_2 (ppb)	1488	43.7	13.5	10.2	119.3
		CO (ppm)	1488	0.8	0.3	0.3	2.6
		SO_2 (ppb)	1488	5.7	2.6	1.6	22.5
		PM10 (μg/m^3)	1488	65.9	36.2	6.3	290.9

Table 6.1 Descriptive statistics for the dependent variables on weekdays, Saturday, and Sunday

Day of week	Variable	N	Mean	Std.	Minimum	Maximum
Weekday	Traffic (10^5 vehicle)	6000	4.6	1.7	1.3	6.5
	Solar radiation (MJ/㎡)	6000	0.5	0.7	0.0	3.1
	Wind Speed (m/s)	6000	2.0	1.3	0.0	8.8
	Temperature (˚C)	6000	12.7	9.9	-14.1	31.8
	Humidity (%)	6000	64.3	19.8	13.0	99.0
Saturday	Traffic (10^5 vehicle)	1248	4.6	1.5	1.5	6.2
	Solar radiation (MJ/㎡)	1248	0.5	0.7	0.0	3.0
	Wind Speed (m/s)	1248	2.1	1.2	0.0	7.5
	Temperature (˚C)	1248	13.0	10.0	-13.4	30.3
	Humidity (%)	1248	64.7	19.9	18.0	98.0
Sunday	Traffic (10^5 vehicle)	1512	3.6	1.3	1.2	5.3
	Solar radiation (MJ/㎡)	1512	0.5	0.7	0.0	3.1
	Wind Speed (m/s)	1512	1.9	1.2	0.0	6.2
	Temperature (˚C)	1512	13.2	9.9	-15.4	30.4
	Humidity (%)	1512	65.7	19.4	20.0	99.0

Table 6.2 Descriptive statistics for the explanatory variables on weekdays, Saturday and Sunday

Solar radiation is averaged over 6-hour periods. As seen in Figure 6.11, the 6-hour averaged UV radiation curve exactly overlaps the hourly O_3 concentrations curve, with only a few exceptions during nighttime. Therefore, 6-hour averaged solar radiation are expected to explain O_3 concentrations better than 1-hour to 5-hour averages. The rates of O_3 creation and O_3 destruction are major factors in determining O_3 concentrations. As O_3 creation is positively correlated with solar radiation and ambient O_3 concentration is negatively correlated with NO emissions, one can expect that solar radiation and traffic flows are the major determinants in the O_3 models. The statistics of solar radiation in Table 6.2 are very similar on weekdays, Saturday, and Sunday, suggesting that the decreased traffic flows on Sunday induce more favorable conditions for photochemical reactions generating O_3.

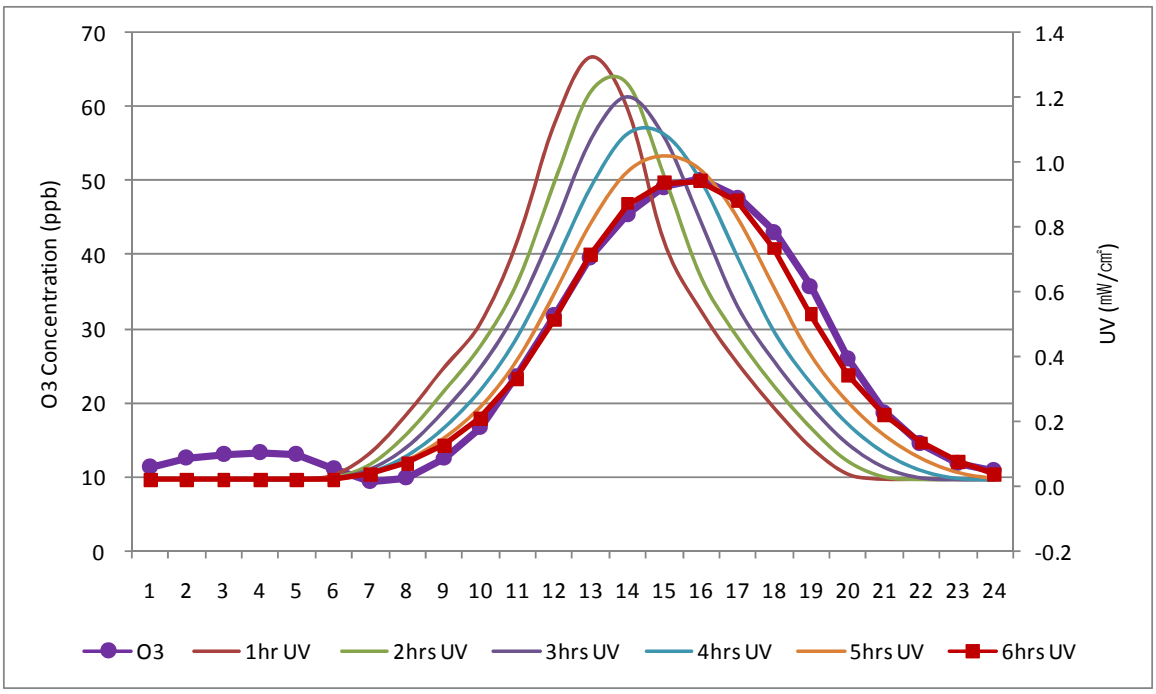

Figure 6.11 Comparison between hourly O_3 concentration and 6 hour-averaged UV radiation

6.2.2 Model Specification

A time-series data set is a set of evenly spaced sequential observations over time. In this research, the interval between observations is an hour, and therefore 8,760 observations are used to measure the impacts of traffic flows and meteorological factors on pollution concentrations. When time-series data are used in a regression model, the error term may be serially correlated, affecting the efficiency of the estimates of ordinary least squares (OLS), though not their unbiasedness and consistency. The existence of serial correlation (or autocorrelation) can be checked with the Durbin-Watson (DW) test. If there is autocorrelation, then an autoregressive error model must be estimated together with the original regression model. The proposed concentration model then takes the following form:

$$C_t^p = \alpha + \sum_{i=1}^{I} \beta_i X_{t,i} + \sum_{i=1}^{I} \gamma_i X_{t,i}^2 + \sum_{j=1}^{J} \delta_j CX_{t,j} + \sum_{i=1}^{I} \sum_{l=1}^{L} \mu_{i,l} \left(X_{t,i} \times D_{t,l}\right)$$
$$+ \sum_{i=1}^{I} \sum_{l=1}^{L} \sigma_{i,l} \left(X_{t,i}^2 \times D_{t,l}\right) + \sum_{j=1}^{J} \sum_{l=1}^{L} \tau_{j,l} \left(CX_{t,j} \times D_{t,l}\right) + v_t \qquad (6.1)$$

$$v_t = -\rho_1 v_{t-1} - \rho_2 v_{t-2} - \cdots - \rho_m v_{t-m} + \varepsilon_t \tag{6.2}$$

where the indices and variables are defined as follows:

p: Pollutant (O_3, NO_2, SO_2, CO, and PM10),

t: Hourly observation (1 → 8,760),

C: Pollution concentration

X: Explanatory variables (traffic, solar radiation, wind speed, temperature, and humidity; $I = 5$),

X^2: Square of explanatory variable,

CX: Cross-product terms between explanatory variables (traffic counts × solar radiation, traffic counts × wind speed, traffic counts × temperature, traffic counts × humidity, solar radiation × wind speed, solar radiation × temperature, solar radiation × humidity, wind speed × temperature, wind speed × humidity, temperature × humidity; $J = 10$),

D: Dummy variables: Sunday dummy variable and eleven monthly dummy variables ($L = 12$).

Since the values of the concentrations and of the explanatory variables on Saturday are similar to those on weekdays, Saturday is included in weekdays.[2] If the tth observation is measured on Sunday then $D_{t,1} = 1$, otherwise $D_{t,1} = 0$. Therefore, the observations during weekdays are the benchmark. Non-linear relationships between emission factors and concentrations are considered for both direct and secondary pollutants. Therefore, quadratic terms (squares and cross products) for the original independent variables are considered. Interactions terms between the original variables and their quadratic forms, and the two types of dummy variables (Sunday and monthly) are also included to account for Sunday and monthly effects. The inclusion of these interaction variables allows for different slopes for the regressors under different time conditions. This model specification generates several potentially different regressions relating pollution concentrations to the explanatory variables, depending on the values of dummy variables. By simultaneously estimating the regression coefficients in Eq. (6.1) and the autoregressive parameters in Eq. (6.2),

[2] As discussed in the previous section, the descriptive statistics of the explanatory variables for weekdays and Saturday are very similar. The main reason for the variations in concentrations for both directly emitted and secondary pollutants is the change in traffic flows.

the autocorrelation can be corrected for and the parameters are efficiently estimated. The error term in Eq (6.2), ε_t, is normally and independently distributed with mean 0 and variance σ^2.

To test the presence of autocorrelations, the DW statistics are calculated. The significance levels of the DW tests are reported in the following result sections. From one to three orders autoregressive models are considered to eliminate the autocorrelation. The autoregressive parameters are also reported.

Since the number of explanatory variables used in each pollutant model is numerous (five original regressors, five square terms, ten cross products, twenty interaction variables between the Sunday dummy and the regressors, eleven interactions variables between the monthly dummy variables and traffic counts, etc.), the significant explanatory variables are selected in an incremental way. The following steps are implemented: 1) Consider first the five original regressors and the fifteen quadratic terms, estimate the model, then eliminate insignificant variables[3]; 2) Include Sunday interaction variables, estimate the new model, and delete insignificant variables; 3) Include monthly interaction variables, estimate the new model, and delete insignificant variables. Some theoretically significant variables may have been deleted in the earlier three steps because of multicollinearity, and are re-considered when generating the final set of explanatory variables.

[3] This deletion accounts for both theoretical considerations and possible multicollinearity effects.

6.3 ESTIMATION RESULTS

6.3.1 Results for O_3

The estimation results for the O_3 models, based on Eqs. (6.1) and (6.2), are presented in Table 6.3. The parameters have been estimated by the maximum likelihood method. The autoregressive parameters, labeled AR1, AR2, and AR3, are estimated simultaneously with the original parameters. The DW statistics is close to 2 for both background and roadside models, indicating that serial correlation has been corrected. The total R^2 generated by the autoregressive model is 0.98 for background data, and is greater than the regress R^2=0.37, suggesting that the goodness-of-fit is improved by the autoregressive terms.[4] A similar R^2 improvement is observed in the roadside case.

As discussed in Section 6.1, conditions of lower traffic flows with more solar radiation are expected to generate more O_3, as compared to more traffic and less solar radiation. The coefficient of traffic is negative and that of solar radiation is positive, supporting the theory. However, both background and roadside models include quadratic terms with the traffic and solar radiation variables, indicating that the impacts of these two variables are not linear. In the case of traffic, the estimates of the square of traffic are positive in both models, suggesting that traffic has generally a negative impact on O_3 concentrations because of O_3 titration, but that under specific conditions this impact may turn out to be positive. To discover when and how this change occurs, it is necessary to analyze the derivative of the O_3 concentration function with regard to (w.r.t.) traffic. UV radiation is the only necessary condition to generate O_3, and the estimates for the original solar radiation variable and its square are both positive. Therefore, O_3 concentration has a second-order relationship with solar radiation. As for traffic, the derivative of the O_3 function w.r.t. solar radiation is also calculated to understand the impact of solar radiation on O_3 concentrations. The derivative functions w.r.t. each explanatory variable is presented in Table 6.4.

---

[4] $R^2_{\text{total}} = 1 - \frac{\text{SSE}}{\text{SST}}$ $\quad R^2_{\text{regress}} = 1 - \frac{\text{TSSE}}{\text{TSST}}$

where,

SST: the sum of squares for the original variable corrected for the mean,

SSE: the final error sum of squares,

TSST: the total sum of squares of the transformed variable corrected for the transformed intercept,

TSSE: the error sum of squares for this transformed regression problem (Detailed explanation are presented in Appendix L).

Location	Explanatory variables					Regress R^2	DW
	Regressors		Parameter	t Value	Pr > | t |	Total R^2	p-value
Background	Intercept	α1	12.136	19.90	<.0001	0.37	1.99
	Traffic	β1	-1.110	-7.95	<.0001		
	Traffic Square	β2	0.047	2.91	0.004		Pr < DW
	Solar Radiation	β3	1.759	1.58	0.114		0.32
	Solar Radiation Square	β4	0.784	3.92	<.0001	0.98	
	Wind Speed	β5	-0.091	-3.66	0.000		Pr > DW
	Humidity	β6	-0.019	-3.61	0.000		0.68
	Traffic × Solar	β7	0.617	4.02	<.0001		
	Solar × Temperature	β8	0.054	1.71	0.087		
	Solar × Wind Speed	β9	0.084	2.95	0.003		
	Traffic × Sun Dummy	β10	-0.707	-4.50	<.0001		
	Traffic square × Sun Dummy	β11	0.164	3.57	0.000		
	Solar × Sun Dummy	β12	5.169	4.46	<.0001		
	Solar square × Sun Dummy	β13	-1.659	-3.75	0.000		
	Solar × Feb Dummy	β14	2.765	2.77	0.006		
	Solar × Mar Dummy	β15	2.631	2.99	0.003		
	Solar × Apr Dummy	β16	4.228	4.69	<.0001		
	Solar × May Dummy	β17	10.083	10.75	<.0001		
	Solar × Jun Dummy	β18	12.821	12.10	<.0001		
	Solar × Jul Dummy	β19	7.857	7.32	<.0001		
	Solar × Aug Dummy	β20	3.395	3.12	0.002		
	Solar × Sep Dummy	β21	6.094	5.74	<.0001		
	Solar × Oct Dummy	β22	3.756	3.99	<.0001		
	AR1	β23	-1.595	-150.95	<.0001		
	AR2	β24	0.870	48.86	<.0001		
	AR3	β25	-0.209	-19.86	<.0001		
Roadside	Intercept	α1	9.474	22.60	<.0001	0.29	1.99
	Traffic	β1	-1.324	-12.90	<.0001		
	Traffic Square	β2	0.119	9.71	<.0001		Pr < DW
	Solar Radiation Square	β3	0.890	10.77	<.0001		0.21
	Temperature	β4	0.054	3.66	0.000	0.94	
	Humidity	β5	-0.015	-3.58	0.000		Pr > DW
	Traffic × Sun Dummy	β6	-0.473	-3.56	0.000		0.79
	Traffic Square × Sun Dummy	β7	0.109	2.90	0.004		
	Solar × Sun Dummy	β8	3.140	4.61	<.0001		
	Solar square × Sun Dummy	β9	-0.793	-3.14	0.002		
	Traffic × Feb Dummy	β10	0.169	1.79	0.073		
	Traffic × Sep Dummy	β11	-0.370	-4.06	<.0001		
	Solar × Jan Dummy	β12	0.977	1.84	0.066		
	Solar × Feb Dummy	β13	1.467	2.91	0.004		
	Solar × Mar Dummy	β14	0.838	2.07	0.038		
	Solar × May Dummy	β15	5.007	14.07	<.0001		
	Solar × Jun Dummy	β16	8.576	20.74	<.0001		
	Solar × Jul Dummy	β17	7.072	16.91	<.0001		
	Solar × Aug Dummy	β18	3.838	8.93	<.0001		
	Solar × Sep Dummy	β19	5.543	12.16	<.0001		
	Solar × Oct Dummy	β20	3.643	9.12	<.0001		
	AR1	β21	-1.185	-114.94	<.0001		
	AR2	β22	0.302	29.33	<.0001		

Table 6.3 Results of time series regression for O_3 models

As expected, wind speed and humidity have negative impacts on O_3 concentrations, whereas temperature has a positive and significant effect, as a high temperature facilitates O_3 generation. There are several significant interaction effects between independent variables. The product of solar radiation and temperature variables has a positive effect, indicating that O_3 generation is enhanced during hot summer afternoons (with high UV and temperature). The products of solar radiation with traffic and wind speed have positive effects on O_3 concentrations, suggesting that intense UV radiation counteracts the negative impacts of traffic and wind speed.

Solar radiation interactions with the monthly dummy variables are included in both the background and roadside models. Solar radiation are more intense during late Spring and early Summer, and the estimated coefficients for the months of May, June, and July reflect this effect and are higher than those of the other months, in both the roadside and background models. The rainy season starts late July and lasts until the end of August, which explains why the coefficient for August is smaller than that for September.

As discussed in Section 6.1, O_3 concentrations on Sundays are consistently higher than those on weekdays. Reduced traffic flows on Sunday change the ratio between NO_x and VOCs concentrations, leading to favorable conditions for the generation on O_3. As seen in the Table 6.3, the original regressors, their quadratic forms, and diverse interaction terms have been selected as significant explanatory variables in both the background and roadside models. It is difficult, however, to directly interpret the impacts of these variables on O_3 concentrations, and therefore derivatives of the estimated O_3 model w.r.t. these variables must be considered. The derivative functions of the O_3 models w.r.t. each explanatory variable are presented in Table 6.4. For example, the derivative function w.r.t. traffic measures the change in O_3 concentration as a result of a unit change in traffic. Since the derivative functions w.r.t. traffic and solar radiation include Sunday dummy variables and interaction terms related to the Sunday dummy variable, the changes in O_3 concentrations necessarily vary between weekdays and Sunday. In addition, different coefficient estimates are obtained in the background and roadside models. Therefore, it is possible to compare the derivatives w.r.t. traffic and solar radiation across the four cases.

Model	Variable	Derivative functions
Background	Traffic	β1 + 2*β2*Traffic + β7*Solar + β10*Sun Dummy + 2*β11*Traffic_Sun Dummy
	Solar Radiation	β3 + 2*β4*Solar + β7*Traffic + β8*Temp + β9*WS + β12* Sun Dummy + 2*β13*Solar_Sun Dummy + β14*Feb + β15*Mar + β16*Apr + β17*May + β18*Jun + β19*Jul + β20*Aug + β21*Sep + β22*Oct
	Wind Speed	β5 + β9*Solar
	Temperature	β8*Solar
	Humidity	β6
Roadside	Traffic	β1 + 2*β2*Traffic + β6*Sun Dummy + 2*β7*Traffic_Sun Dummy + β10*Feb + β11*Sep
	Solar Radiation	2*β3*Solar + β8*Sun Dummy + 2*β9* Solar_Sun Dummy + β12*Jan + β13*Feb + β14*Mar + β15*May + β16*Jun + β17*Jul + β18*Aug + β19*Sep + β20*Oct
	Wind Speed	N/A
	Temperature	β4
	Humidity	β5

Table 6.4 Derivative functions of O_3 models with regard to each explanatory variable[5]

The original data (8,760 observations) are used to calculate the change in O_3 concentrations resulting from a unit change in traffic. Summary statistics for the calculated derivatives are presented in Table 6.5. The impacts of traffic on O_3 concentrations vary from negative to positive. A similar pattern is observed for wind speed. As expected, the derivatives with regard to solar radiation are always positive.

[5] The indices of parameters are corresponding to the order of explanatory variables in Table 6.3 except for intercept.

Model	Variable	Minimum	10th Pctl	Lower Quartile	Median	Upper Quartile	90th Pctl	Maximum
Background	Traffic	-1.32	-0.95	-0.79	-0.47	0.05	0.59	2.25
	Solar Radiation	1.86	5.42	7.40	10.68	14.44	18.34	24.51
	Wind Speed	-0.09	-0.09	-0.09	-0.08	-0.03	0.04	0.17
	Temperature	0.00	0.00	0.00	0.01	0.04	0.09	0.17
	Humidity	-0.02	-0.02	-0.02	-0.02	-0.02	-0.02	-0.02
Roadside	Traffic	-1.61	-0.94	-0.60	-0.07	0.08	0.18	0.65
	Solar Radiation	0.00	0.05	1.32	3.98	7.07	8.85	13.71
	Wind Speed	N/A	N/A	N/A	N/A	N/A	N/A	N/A
	Temperature	0.05	0.05	0.05	0.05	0.05	0.05	0.05
	Humidity	-0.01	-0.01	-0.01	-0.01	-0.01	-0.01	-0.01

Table 6.5 Summary statistics for the derivatives with regard to the explanatory variables in the O_3 models

The derivatives are calculated for the four groups – background-weekdays, background-Sunday, roadside-weekdays, and roadside-Sunday – and then are averaged out over the year for each hour of the day. The results are illustrated in Figures 6.12 and 6.13 for traffic and solar radiation, respectively. The derivatives w.r.t. traffic are negative during nighttime and positive during daytime, suggesting that traffic flows induce O_3 titration as the dominant reaction during the night and early morning, leading to a decrease in O_3 concentration. However, when the intensity of solar radiation exceeds a certain level, the rate of O_3 generation exceeds the rate of O_3 destruction, providing a shift from negative to positive impacts. As discussed in Section 6.1, the best condition for O_3 generation is background-Sunday, and indeed the highest positive derivative is observed during daytime in the background-Sunday case. Since O_3 titration is the dominant reaction in roadside areas, the hourly pattern of the derivatives is similar to the pattern of hourly traffic flows presented in Figure 4.12. As seen in Table 6.4, the derivative function w.r.t. traffic in the background case contains a solar radiation term (β7*Solar), but does not in the roadside case. Since this term is positive and varies with hourly solar radiation, the patterns of the hourly derivatives in background cases in Figure 6.12 are similar to the hourly pattern of UV radiation presented in Figure 6.11.

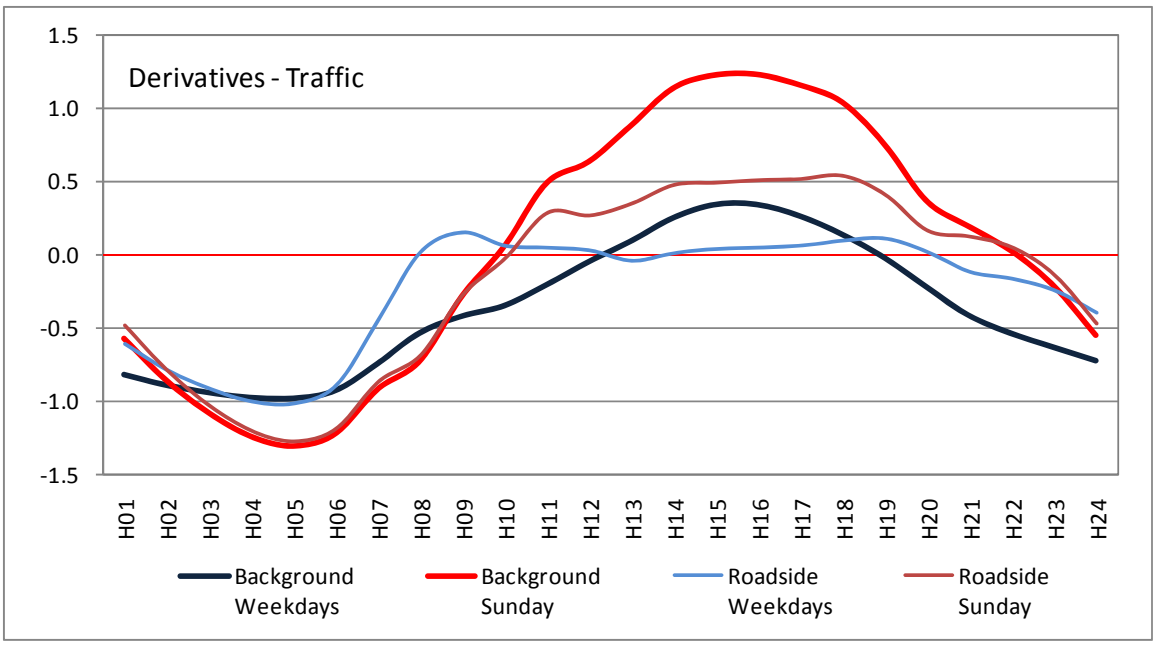

Figure 6.12 Average hourly derivatives w.r.t. traffic in the O_3 models

Average hourly derivatives w.r.t. solar radiation are presented in the Figure 6.13. Solar radiation is an indispensible condition for generating O_3, and thus, as expected, the derivatives w.r.t. solar radiation are positive in all four cases. As seen in Figure 6.13, the strongest conditions for O_3 generation take place in the background-Sunday case with the highest derivatives. In contrast, the weekdays-roadside case corresponds to the least favorable conditions, with the lowest derivatives. Figure 6.13 clearly shows that the changes in O_3 concentrations are different in the four cases. Since solar radiation is equal to zero at night, the real impacts of solar radiation during nighttime are zero.

The other derivatives w.r.t. wind speed, temperature, and humidity are almost constant and near zero, suggesting that changes in these variables have limited impacts on O_3 concentrations.

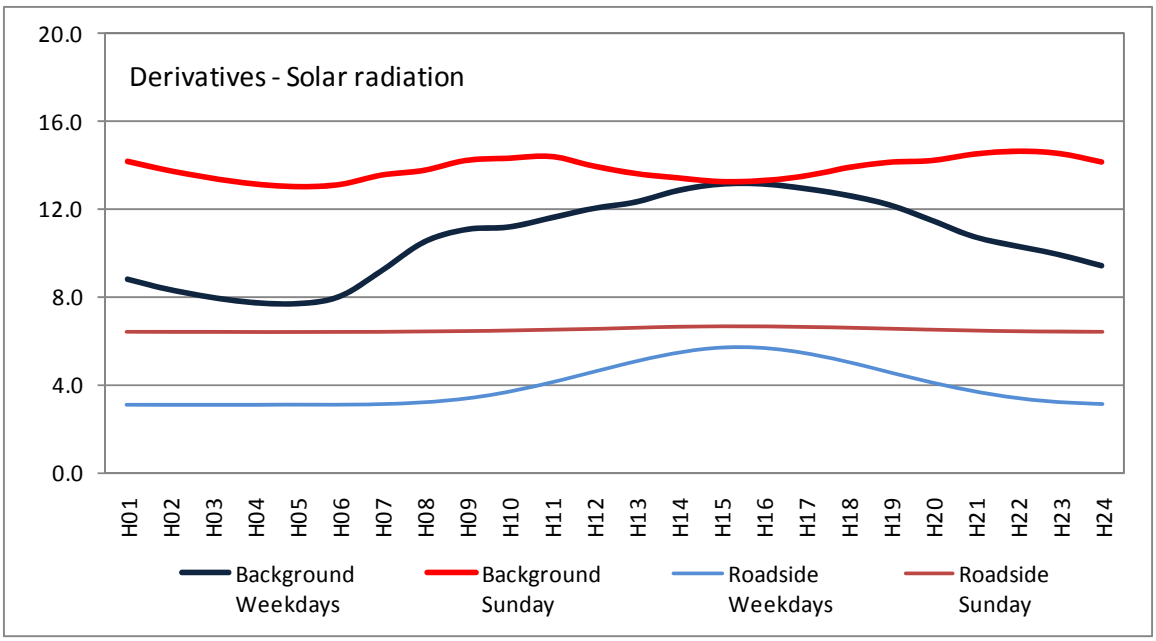

Figure 6.13 Average hourly derivatives w.r.t. solar radiation in the O_3 models

Using the parameters in Table 6.3 and the estimated derivative functions in Table 6.4, the elasticities w.r.t. the explanatory variables are computed across all input data. Descriptive statistics for these elasticities are presented in Table 6.6. As discussed above, traffic flows are generally negatively correlated with O_3 concentrations. However, these negative impacts turn out to be positive in certain situations, such as high solar radiation intensity. The shift from negative to positive impacts is also observed for wind speed and temperature. As in the case of traffic flows, the impacts of these two variables on O_3 concentrations vary. Since the derivative functions w.r.t. wind speed and temperature in the background case presented in Table 6.4 include a solar radiation term, the elasticities w.r.t. these variables also change depending on solar radiation. As expected, solar radiation has a positive impact on O_3 concentrations. However, 25% of the observations produce zero impacts on O_3 concentrations because solar radiation has no impact during nighttime. A 1% change in solar radiation induces a maximum 4.52% increase in O_3 concentrations in the background case, but only a maximum 2.72% in the roadside case, suggesting that the theory reviewed in Section 6.1 is supported by empirical observations. Humidity is always associated with negative impacts on O_3 concentrations. The hourly patterns of elasticities would help understand when and how these changes occur across the four groups.

Model	Variable	Minimum	10th Pctl	Lower Quartile	Median	Upper Quartile	90th Pctl	Maximum
Background	Traffic	-2.41	-1.11	-0.58	-0.18	0.02	0.13	1.55
	Solar Radiation	0.00	0.00	0.00	0.23	0.68	1.07	4.52
	Wind Speed	-0.19	-0.06	-0.03	-0.01	0.00	0.00	0.02
	Temperature	-0.09	0.00	0.00	0.01	0.04	0.07	0.51
	Humidity	-1.49	-0.65	-0.37	-0.14	-0.06	-0.03	-0.01
Roadside	Traffic	-2.14	-0.48	-0.25	-0.04	0.06	0.15	1.39
	Solar Radiation	0.00	0.00	0.00	0.07	0.42	0.79	2.72
	Wind Speed	N/A	N/A	N/A	N/A	N/A	N/A	N/A
	Temperature	-0.37	-0.01	0.04	0.08	0.16	0.27	1.30
	Humidity	-1.33	-0.38	-0.23	-0.14	-0.07	-0.04	-0.01

Table 6.6 Summary statistics for the elasticities w.r.t. explanatory variables in the O_3 models[6]

The patterns of average hourly elasticities of the five explanatory variables are illustrated in Figures 6.14 ~ 6.18. The hourly patterns of the four groups – background-weekdays, background-Sunday, roadside-weekdays, and roadside-Sunday – can be compared on each graph. Figure 6.14 presents the elasticities w.r.t. traffic flows. Since O_3 titration dominates across all hours of the day in the background-weekdays case, most elasticities are negative but the negative elasticities decrease during daytime and approach zero and slightly exceed zero when cumulative UV radiation reach peak hours (around 3 to 4 P.M.). Similar patterns are observed in the other three cases, but with more positive elasticities. The elasticities on Sunday for both background and roadside areas are higher than those on weekdays, especially during daytime, supporting the theory discussed in Section 6.1.

The elasticities of solar radiation across the hours of the day are illustrated in Figure 6.15. As background regions have better conditions than roadside areas for generating O_3, the elasticities for background areas are higher than those for roadside areas. The elasticities on Sunday are lower than those on weekdays in the background case, which does not mean that O_3 concentrations on Sunday are lower than those on weekdays. Since O_3 concentrations are determined by the aggregation of impacts of all explanatory variables, the elasticities of traffic, solar radiation, and the other meteorological factors need all to be considered. As seen in Figure 6.16 ~ 6.18, the elasticities w.r.t. wind speed, temperature, and humidity are small, and therefore traffic and solar radiation are the major determinants. Traffic emissions include O_3 precursors and

[6] Detailed statistics on the hourly elasticities for each explanatory variable in the O_3 models are presented in Appendix H.

the decreased traffic flows on Sunday changes the ratio of NO_x and VOCs, leading to better conditions for O_3 formation on Sunday. As seen in Figure 6.14, in the background case the elasticities w.r.t. traffic on Sunday are greater than those on weekdays from early morning (6:00 a.m.) to 2:00 a.m. past midnight and the differences of these elasticities between Sunday and weekdays are larger than those related to solar radiation, leading to higher O_3 concentrations on Sunday than on weekdays.

The patterns of elasticities for each explanatory variable are determined by the derivative function in Table 6.4. The derivative functions w.r.t. traffic and solar radiation include the Sunday dummy variable and interaction terms related to the Sunday dummy, suggesting that the impacts of these two variables on O_3 concentrations are different between weekdays and Sunday. In the case of the other meteorological variables, however, terms related to the Sunday dummy variable are not included in the derivative functions, indicating that the Sunday dummy has no significant impacts on O_3 concentrations for these variables. The derivative functions for wind speed and temperature in the background case include the solar radiation variable. Therefore, the elasticities w.r.t. these two variables are determined by the intensity of solar radiation. As seen in Table H.3 and H.4 in Appendix H, the elasticity patterns are similar to those of UV radiation, characterized by an afternoon peak, but the differences are very limited, as shown on Figures 6.16 and 6.17. The elasticity patterns w.r.t. temperature in the roadside case are difficult to interpret. Since temperature is known to facilitate O_3 formation, higher temperature is expected to induce higher O_3 concentrations. However, the roadside curves in Figure 6.16 defy this expectation. Since humidity is lower during daytime, the effects of humidity on O_3 concentrations are also lower during daytime. Since the derivative functions w.r.t. humidity include only one parameter, $\beta 6$ and $\beta 5$, for background and roadside respectively (see Table 6.4), the elasticities w.r.t. humidity are determined by this parameter and the ratio between humidity and O_3 concentration. Since O_3 concentrations are higher in background areas, the elasticities for roadside areas are higher than those for background areas.

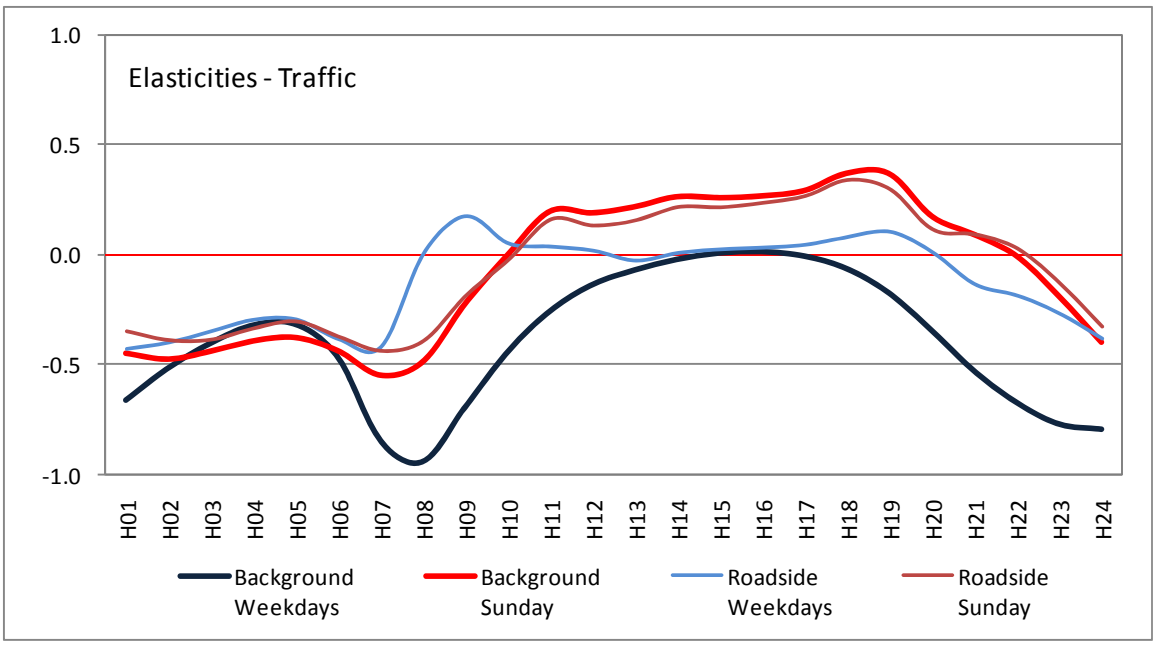

Figure 6.14 Average hourly elasticities w.r.t. traffic in the O_3 models

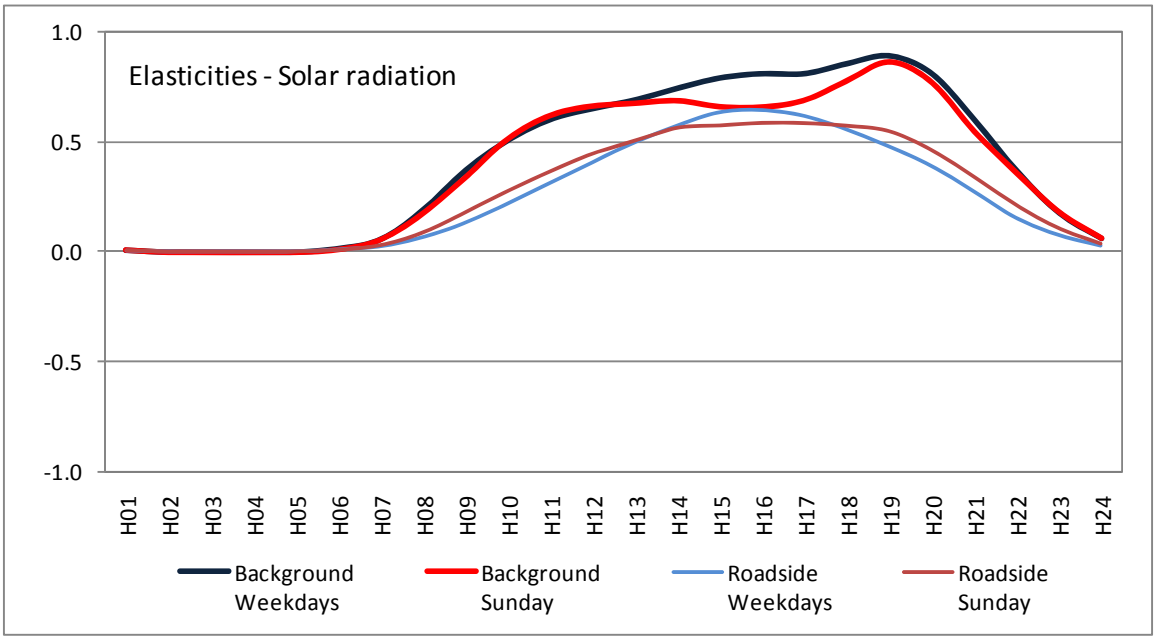

Figure 6.15 Average hourly elasticities w.r.t. solar radiation in the O_3 models

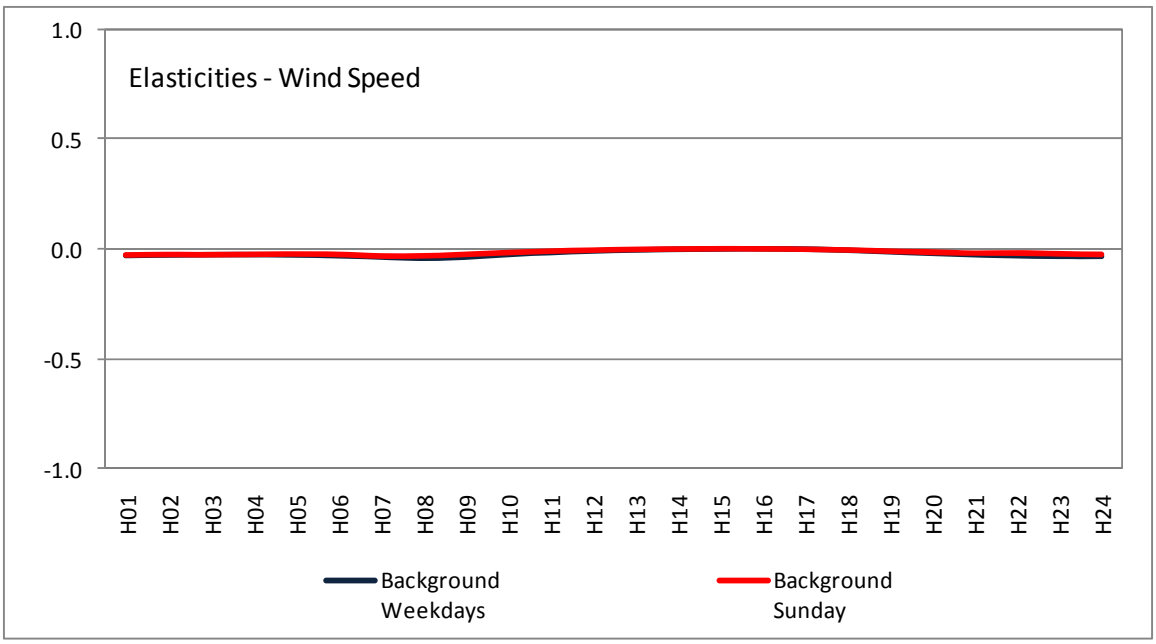

Figure 6.16 Average hourly elasticities w.r.t. wind speed in the O_3 models

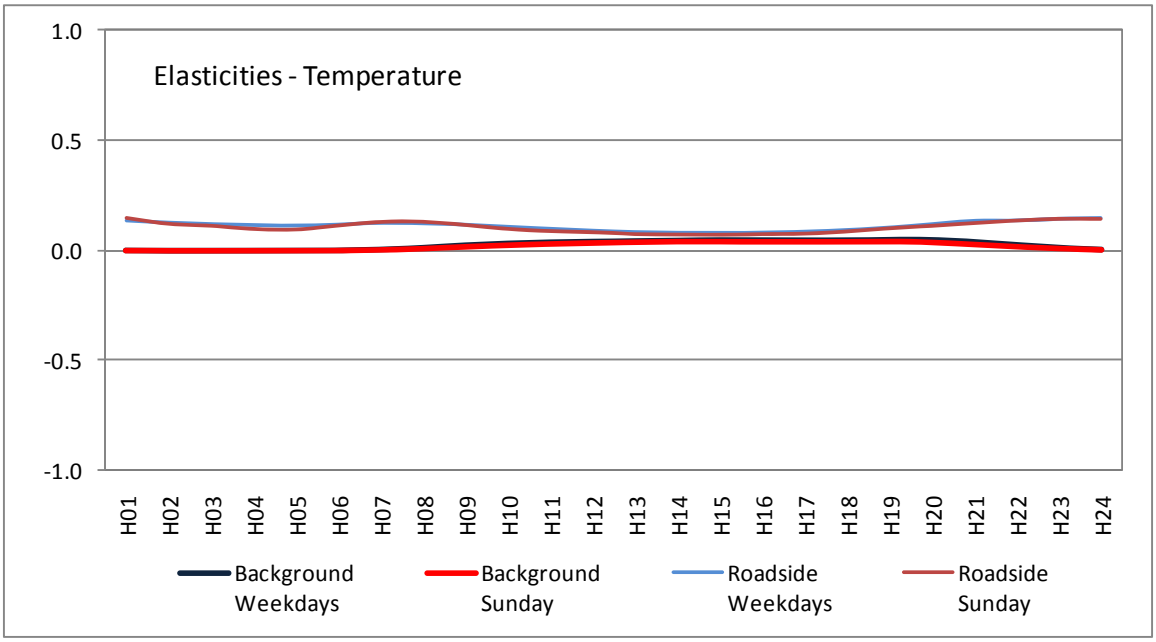

Figure 6.17 Average hourly elasticities w.r.t. temperature in the O_3 models

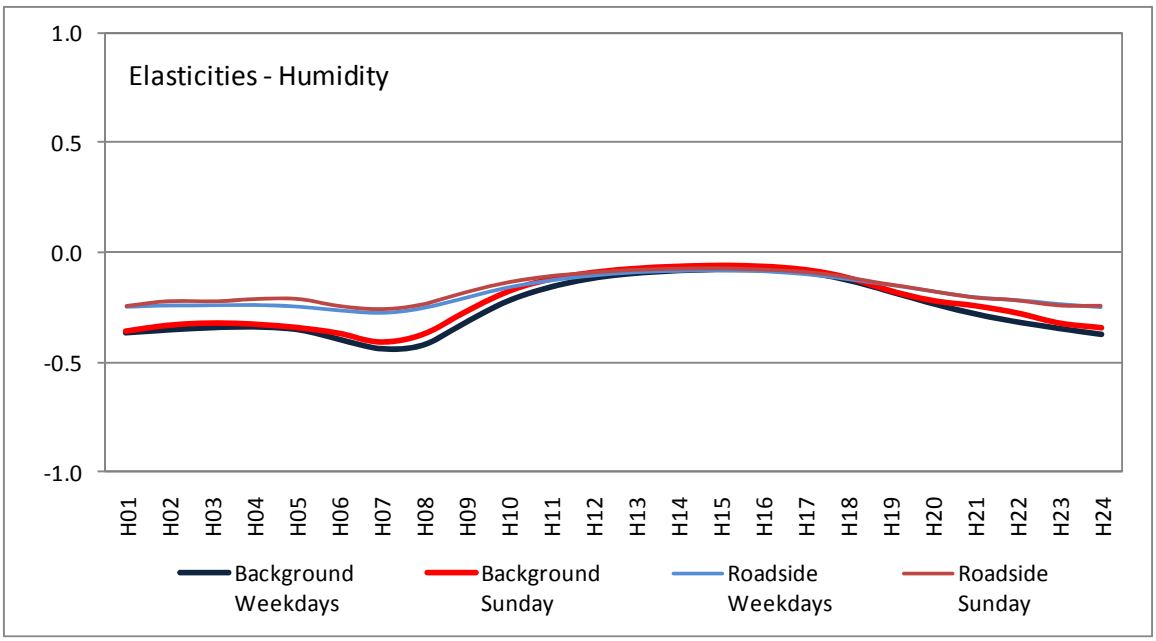

Figure 6.18 Average hourly elasticities w.r.t. humidity in the O_3 models

6.3.2 Results for NO_2

Vehicle emissions are direct sources of NO_x (NO and NO_2). Ambient NO_2 is decomposed by UV radiation, and therefore larger traffic flows with less solar radiation represent the best conditions for high NO_2 concentrations. The estimation results for NO_2 models are presented in Table 6.7, and are as expected: a positive coefficient estimate for traffic counts and a negative one for solar radiation. Both background and roadside NO_2 models include the quadratic terms for the traffic and solar radiation variables. Since the coefficients of the traffic square variables are negative, the positive impacts of traffic on NO_2 concentrations decrease with an increase in traffic flows. The coefficients of the solar radiation square variable are also negative, indicating that the negative impacts of solar radiation are magnified by an increase in solar radiation. As discussed in Chapter 2, the photolysis of NO_2 is directly related to the generation of O_3: solar radiation has a negative impact on NO_2 but a positive one on O_3. The estimation results support the theory. The cross-product terms between traffic and other regressors (traffic × solar and traffic × humidity) have significant and negative effects, suggesting that the positive impacts of traffic may become negative, depending on changes in solar radiation and humidity.

As discussed in Section 6.1, NO_2 concentrations on Sundays are consistently lower than those on weekdays. Reduced traffic flows on Sunday directly decrease the NO_2 concentrations. In addition, Sunday conditions are more favorable for generating O_3, and therefore the

decomposition of NO_2 is facilitated, resulting in lower NO_2 concentrations on Sunday. As seen in Table 6.7, the NO_2 models include diverse estimates of the interaction variables related to the Sunday dummy variables, with both positive and negative coefficients, and therefore it is difficult to clearly determine the Sunday dummy impacts. The derivative functions of the NO_2 models w.r.t. the explanatory variables are presented in Table 6.8, and the hourly derivatives are calculated for the four groups – background-weekdays, background- Sunday, roadside-weekdays, and roadside-Sunday. By comparing the derivatives across the four groups, it is possible to identify and compare the impacts of the differences between weekdays and Sunday, and background and roadside locations.

Traffic emissions are a major NO_x source during the warm seasons, and therefore the effects of the interaction between the monthly dummy variables and traffic are expected to be positive. However, the only three significant interactions appear in the roadside model for September, October, and November, and are all negative. All the excluded months represent the benchmark. There is no clear explanation for this result, calling for further research. Intense solar radiation during the Summer induce the active decomposition of NO_2, leading to a negative impact on NO_2 concentrations. However, the retained solar interaction terms are positive during the Summer months, a result also calling for further research.

Location	Explanatory variables					Regress R^2	DW
	Regressors		Parameter	t Value	Pr > | t |	Total R^2	p-value
Background	Intercept	α1	30.5470	23.85	<.0001		2.01
	Traffic	β1	2.8874	13.61	<.0001	0.16	
	Traffic Square	β2	-0.0754	-3.75	0.000		Pr < DW
	Solar Radiation	β3	-3.8769	-3.08	0.002		0.59
	Solar Radiation Square	β4	-0.7759	-3.39	0.001	0.97	
	Wind Speed	β5	0.1306	5.21	<.0001		Pr > DW
	Temperature	β6	0.1226	2.66	0.008		0.41
	Traffic × Solar	β7	-0.8362	-4.42	<.0001		
	Traffic × Humidity	β8	-0.0066	-4.18	<.0001		
	Solar × Humidity	β9	0.0672	7.28	<.0001		
	Traffic square × Sun Dummy	β10	-0.1708	-4.26	<.0001		
	Traffic_Humidity × Sun Dummy	β11	0.0119	6.32	<.0001		
	Solar_Temp × Sun Dummy	β12	0.0727	1.78	0.075		
	Solar_Humidity × Sun Dummy	β13	-0.0839	-5.67	<.0001		
	Solar × Feb Dummy	β14	-1.8060	-1.70	0.088		
	Solar × Apr Dummy	β15	-1.7122	-2.10	0.036		
	Solar × Aug Dummy	β16	2.4492	2.69	0.007		
	Solar × Sep Dummy	β17	2.5507	2.78	0.006		
	AR1	β18	-1.5996	-151.26	<.0001		
	AR2	β19	0.8311	45.82	<.0001		
	AR3	β20	-0.2064	-19.63	<.0001		
Roadside	Intercept	α1	26.4782	27.03	<.0001		2.00
	Traffic	β1	8.9386	28.97	<.0001	0.25	
	Traffic Square	β2	-0.5635	-17.45	<.0001		Pr < DW
	Traffic × Solar Radiation	β3	-1.3694	-11.68	<.0001		0.51
	Traffic × Humidity	β4	-0.0135	-6.15	<.0001	0.92	
	Solar × Humidity	β5	0.1139	9.45	<.0001		Pr > DW
	Traffic Square × Sun Dummy	β6	-0.4066	-6.08	<.0001		0.49
	Traffic_Humidity × Sun Dummy	β7	0.0325	7.71	<.0001		
	Solar_Humidity × Sun Dummy	β8	-0.0771	-4.29	<.0001		
	Temp_Humidity × Sun Dummy	β9	-0.0022	-4.10	<.0001		
	Traffic × Sep Dummy	β10	-0.9239	-3.64	0.000		
	Traffic × Oct Dummy	β11	-0.5338	-2.21	0.027		
	Traffic × Nov Dummy	β12	-0.4474	-1.81	0.070		
	Solar × Mar Dummy	β13	2.5242	2.70	0.007		
	Solar × Apr Dummy	β14	3.0094	3.43	0.001		
	Solar × May Dummy	β15	4.5559	5.68	<.0001		
	Solar × Jun Dummy	β16	4.9896	5.23	<.0001		
	Solar × Jul Dummy	β17	6.1832	6.20	<.0001		
	Solar × Aug Dummy	β18	3.7635	3.75	0.000		
	Solar × Sep Dummy	β19	5.4248	5.38	<.0001		
	AR1	β20	-0.9775	-89.59	<.0001		
	AR2	β21	0.0325	2.99	0.003		

Table 6.7 Results of time series regression for NO_2 models

Model	Variable	Derivative function
Background	Traffic	β1 + 2*β2*Traffic + β7*Solar + β8*Humidity + 2*β10*Traffic_Sun Dummy + β11*Humidity_Sun Dummy
	Solar Radiation	β3 + 2*β4*Solar + β7*Traffic + β9*Humidity + β12*Temp_Sun Dummy + β13*Humidity_Sun Dummy + β14*Feb + β15*Apr + β16*Aug + β17*Sep
	Wind Speed	β5
	Temperature	β6 + β12*Solar_Sun Dummy
	Humidity	β8*Traffic + β9*Solar + β11*Traffic_Sun Dummy + β13*Solar_Sun Dummy
Roadside	Traffic	β1 + 2*β2*Traffic + β3*Solar + β4*Humidity + 2*β6*Traffic_Sun Dummy + β7*Humidity_Sun Dummy + β10* Sep + β11*Oct + β11*Nov
	Solar Radiation	β3*Traffic + β5*Humidity + β8*Humidity_SunDummy + β13*Mar + β14*Apr + β15*May + β16*Jun + β17*Jul + β18*Aug + β19*Sep
	Wind Speed	N/A
	Temperature	β9* Humidity_Sun Dummy
	Humidity	β4*Traffic + β5*Solar + β7*Traffic_Sun Dummy + β8*Solar_Sun Dummy + β9*Temp_Sun Dummy

Table 6.8 Derivative functions of NO_2 models w.r.t. each explanatory variable

As for the O_3 models, the original data are used to calculate the changes in NO_2 concentrations resulting from unit changes in the explanatory variables. Summary statistics for the calculated derivatives are presented in Table 6.9. The impact of traffic on NO_2 concentrations is generally positive, but, under certain situations, this impact turns out to be negative. Similar shifts from negative to positive values are observed in the cases of solar radiation and humidity. 90% of the derivatives w.r.t. solar radiation are negative in the background case, but less than 50% are negative in the roadside case, suggesting that background areas have better conditions for NO_2 photodissociation, leading to lower NO_2 and higher O_3 concentrations. In order to further investigate the conditions for shifts from negative to positive derivatives, the hourly derivatives across the four groups are calculated and averaged out over the year for each hour of the day, as presented in Figures 6.19 and 6.20.

Model	Variable	Minimum	10th Pctl	Lower Quartile	Median	Upper Quartile	90th Pctl	Maximum
Background	Traffic	-2.07	0.20	0.88	1.41	1.93	2.16	2.81
	Solar Radiation	-13.68	-9.23	-7.23	-4.69	-2.08	-0.02	3.96
	Wind Speed	0.13	0.13	0.13	0.13	0.13	0.13	0.13
	Temperature	0.12	0.12	0.12	0.12	0.12	0.13	0.35
	Humidity	-0.20	-0.03	-0.02	-0.01	0.04	0.13	0.32
Roadside	Traffic	-4.82	-0.85	0.29	1.41	4.35	6.04	8.46
	Solar Radiation	-6.30	-3.01	-0.56	2.78	6.19	9.29	15.61
	Wind Speed	N/A	N/A	N/A	N/A	N/A	N/A	N/A
	Temperature	-0.22	-0.14	0.00	0.00	0.00	0.00	0.00
	Humidity	-0.09	-0.06	-0.05	-0.02	0.04	0.11	0.28

Table 6.9 Summary statistics for the derivatives w.r.t. the explanatory variable in the NO_2 models

Interesting patterns emerge when comparing Figures 6.12 and 6.19. O_3 titration ($NO + O_3 \rightarrow NO_2 + O_2$) is the dominant reaction during nighttime, leading to an increase in NO_2 concentration and a decrease in O_3 concentration. When NO_2 is decomposed by solar radiation ($NO_2 + hv \rightarrow NO + O$), the impacts of O_3 titration decrease and the photolysis effects increase and culminate around 3 ~ 4 P.M., when accumulated solar radiation reaches its peak. Since these two factors act in opposite directions on NO_2 and O_3 concentrations, the hourly derivatives for these two pollutants display reverse patterns.

Average hourly derivatives w.r.t. solar radiation are presented in Figure 6.20. The derivative patterns are clearly differentiated across the four cases. Since there is no solar radiation at night, the nighttime differences between derivatives are not informative. Solar radiation decomposes NO_2, and therefore the derivatives w.r.t. solar radiation are expected to be negative. In the background case, the impacts of direct vehicle emissions are smaller than in roadside areas, and, consequently, NO_2 concentrations in background areas are more sensitive to solar radiation than those in roadside areas, and the derivatives are always negative. In the roadside-weekdays case, the impact of traffic emissions is the greatest among the four cases and offsets the negative impacts of solar radiation, leading to derivatives w.r.t. solar radiation close to zero during daytime. The mean background derivatives w.r.t. wind speed, temperature, and humidity are 0.13, 0.13, and 0.02, respectively. These derivatives are much smaller than those of traffic and solar radiation (1.31 and -4.63), suggesting that changes in these variables have limited impacts on NO_2 concentrations.

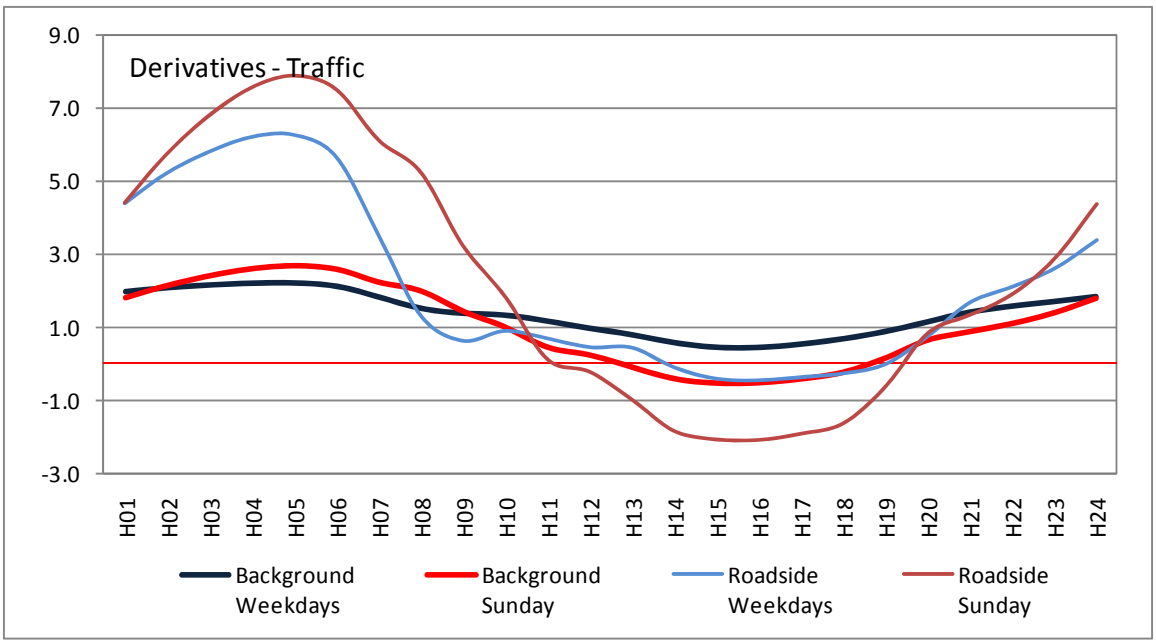

Figure 6.19 Average hourly derivatives w.r.t. traffic in the NO_2 models

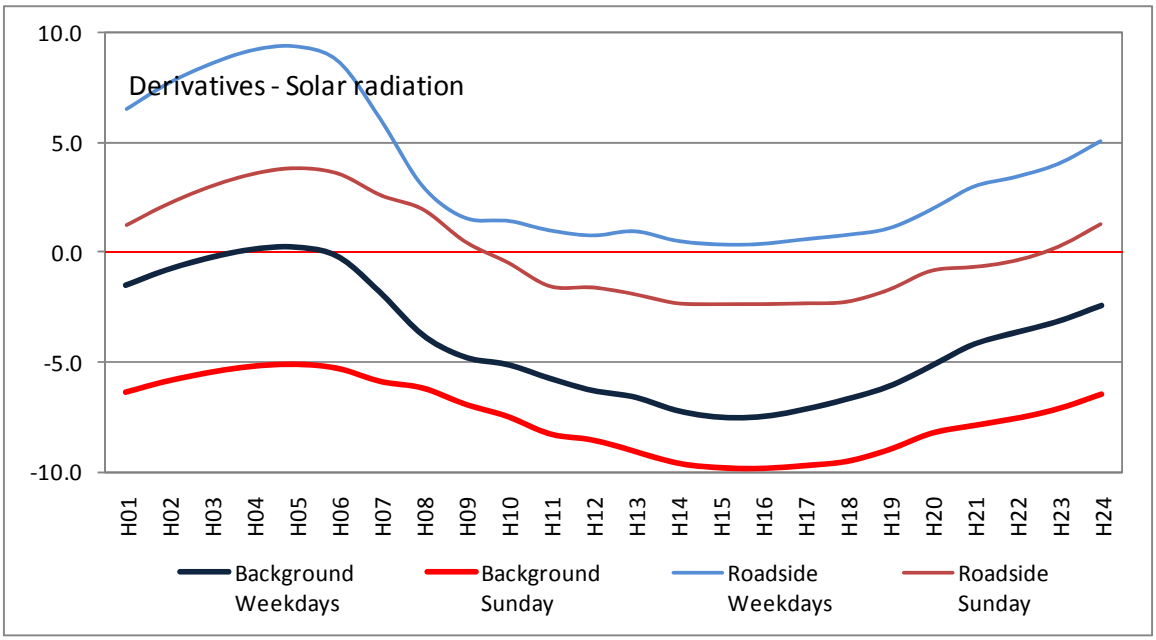

Figure 6.20 Average hourly derivatives w.r.t. solar radiation in the NO_2 models

The elasticities w.r.t. the explanatory variables are computed using the estimated coefficients in Table 6.7 and the derivative functions in Table 6.8. Descriptive statistics for these elasticities are presented in Table 6.10. Generally, traffic flows positively impact NO_2 concentrations, but these impacts turn out to be negative when the intensity of solar radiation reaches a certain level. The shift from negative to positive impacts is also observed for solar radiation and temperature. The derivative functions w.r.t. traffic flows in both the background and roadside cases include a solar radiation term and Sunday interaction terms, and therefore the elasticities w.r.t. traffic change depend on the solar radiation and Sunday dummy effects. More than 50% of the elasticities w.r.t. solar radiation in the background case are negative, but less than 25% are negative in the roadside case, suggesting that NO_2 photolysis occur more frequently in background areas than in roadside areas. Humidity has always a negative impact on NO_2 concentrations.

Model	Variable	Minimum	10th Pctl	Lower Quartile	Median	Upper Quartile	90th Pctl	Maximum
Background	Traffic	-0.85	0.03	0.09	0.14	0.20	0.13	1.55
	Solar Radiation	-2.92	-0.41	-0.12	-0.01	0.00	1.07	4.52
	Wind Speed	0.00	0.00	0.00	0.01	0.01	0.00	0.02
	Temperature	-0.17	0.00	0.01	0.04	0.09	0.07	0.51
	Humidity	-0.78	-0.07	-0.04	-0.02	0.06	-0.03	-0.01
Roadside	Traffic	-0.82	-0.09	0.03	0.14	0.26	0.15	1.39
	Solar Radiation	-0.46	-0.05	0.00	0.00	0.01	0.79	2.72
	Wind Speed	N/A	N/A	N/A	N/A	N/A	N/A	N/A
	Temperature	-0.41	-0.03	0.00	0.00	0.00	0.27	1.30
	Humidity	-0.30	-0.11	-0.07	-0.03	0.05	-0.04	-0.01

Table 6.10 Summary statistics for the elasticities w.r.t. the explanatory variables in the NO_2 models[7]

The patterns of average hourly elasticities for the five explanatory variables are illustrated in Figures 6.21 ~ 6.25. Figure 6.21 presents the elasticities w.r.t. traffic flows. Since O_3 titration dominates during nighttime, elasticities during this period are higher than during the other hours of the day. These patterns are clearly observed in the roadside case. Background areas are less

[7] Detailed statistics on the hourly elasticities for each explanatory variable in the NO_2 models are presented in Appendix H.

influenced by O_3 titration because these areas are away from direct NO emissions. In addition, weekdays have more traffic flows than Sunday, resulting in weekdays having a higher chance to accumulate NO_2 concentrations than Sunday. For these two reasons, the elasticities w.r.t. traffic in the background-weekdays case are all positive across the hours of the day. As discussed in the case of O_3, Sunday provides better conditions for generating O_3 (or for decomposing NO_2), and therefore the elasticities w.r.t. traffic on Sunday during daytime are lower than those on weekdays, supporting the theory.

The elasticities w.r.t. solar radiation across the hours of the day are illustrated in Figure 6.22. Background areas have lower ratios of NO_x to VOCs concentrations than roadside areas, leading to worse conditions for O_3 titration and better conditions for NO_2 photolysis. In other words, in background areas, NO_2 creation through O_3 titration is limited but the rate of NO_2 decomposition can be large. In roadside areas, however, these two reactions take place in reverse patterns. As seen in Table 6.8, the derivative functions w.r.t. solar radiation in the background and roadside models have different terms. The derivative function of the background model includes solar radiation and traffic terms (2*β4*Solar and β7*Traffic, β4 and β7 negative), but that of the roadside model includes only a traffic term (β3*Traffic, β3 negative). These terms play major roles in determining the elasticities of background and roadside models. As seen in Figure 6.22, the elasticities w.r.t. solar radiation in the background case are lower than those in the roadside case, supporting the theories regarding O_3 titration and NO_2 photolysis. Traffic flows on Sunday are lower than those on weekdays, leading to worse conditions for O_3 titration and better conditions for NO_2 photolysis. These two conditions are similar in the background and roadside cases. As expected, the elasticities w.r.t. solar radiation on Sunday are lower than those on weekdays in both the background and roadside cases.

The derivative functions w.r.t. traffic and solar radiation variables include interaction terms related to the Sunday dummy variable, suggesting that the impacts of these two variables on NO_2 concentrations are different between weekdays and Sunday. In the case of wind speed, however, Sunday related variables are not included. Although the derivative functions w.r.t. temperature include Sunday interaction terms, the differences between weekdays and Sunday are small because the estimated coefficients of these interaction terms are close to zero. The elasticity pattern w.r.t. humidity in the background-Sunday case is difficult to interpret. Generally, humidity is known to be negatively correlated with pollutant concentrations, but the elasticities in the background-Sunday case are significantly positive, calling for further research.

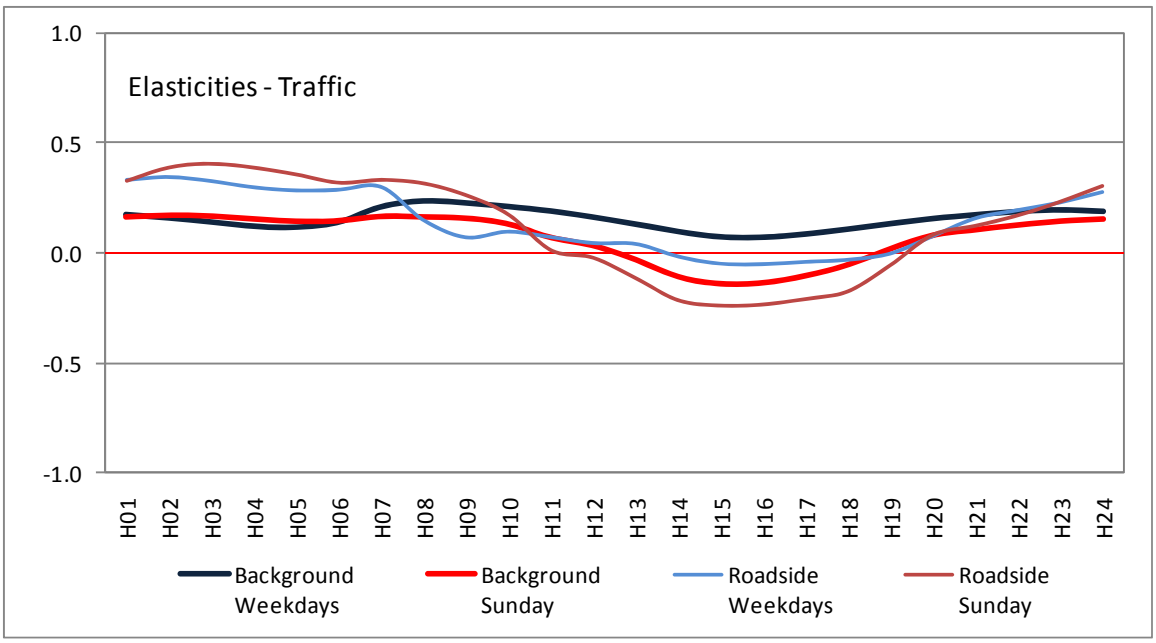

Figure 6.21 Average hourly elasticities w.r.t. traffic in the NO_2 models

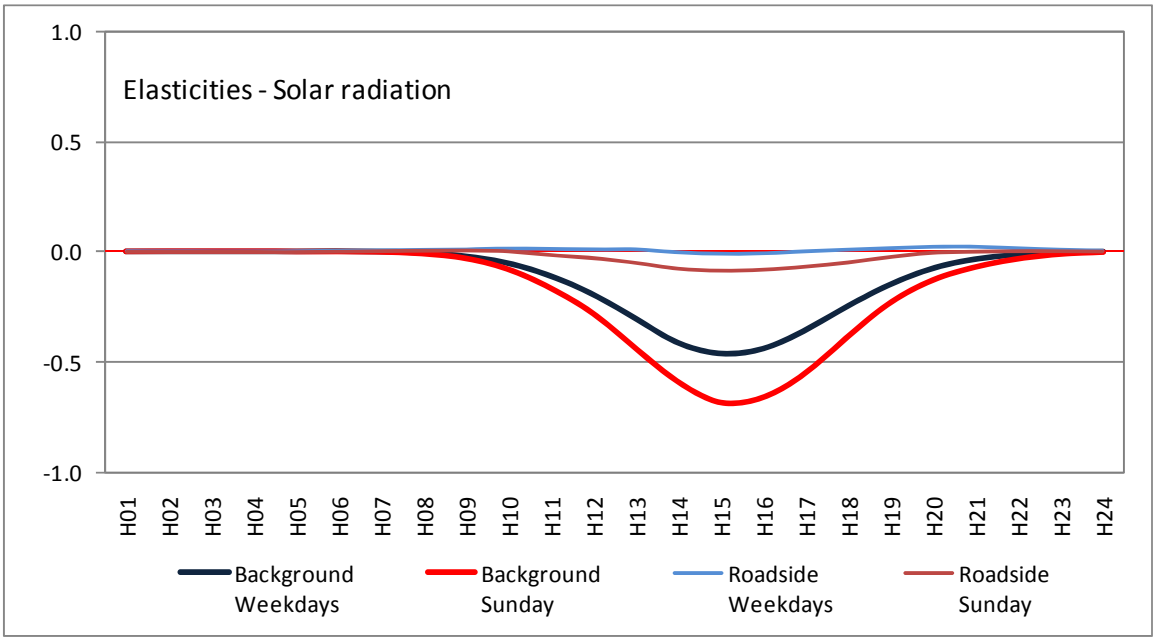

Figure 6.22 Average hourly elasticities w.r.t. solar radiation in the NO_2 models

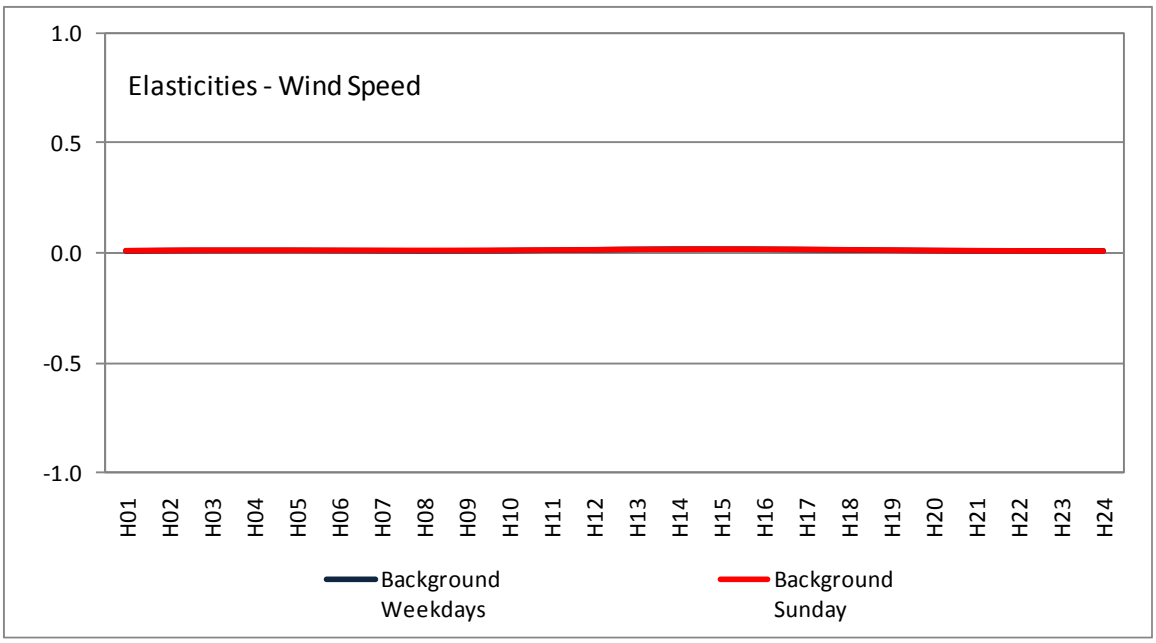

Figure 6.23 Average hourly elasticities w.r.t. wind speed in the NO_2 models

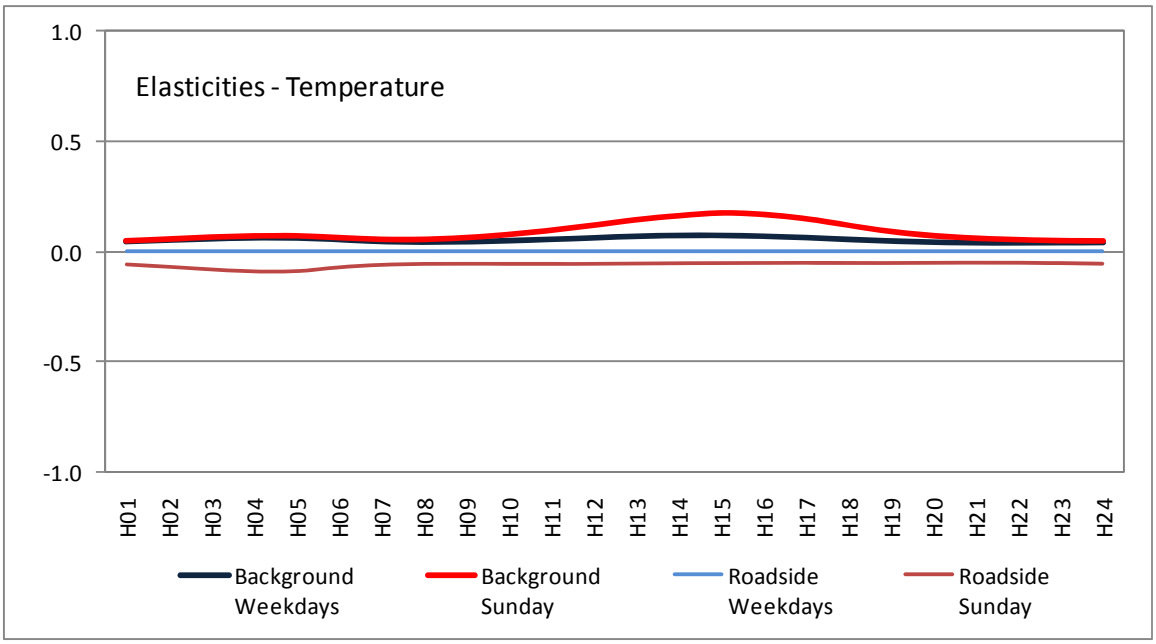

Figure 6.24 Average hourly elasticities w.r.t. temperature in the NO_2 models

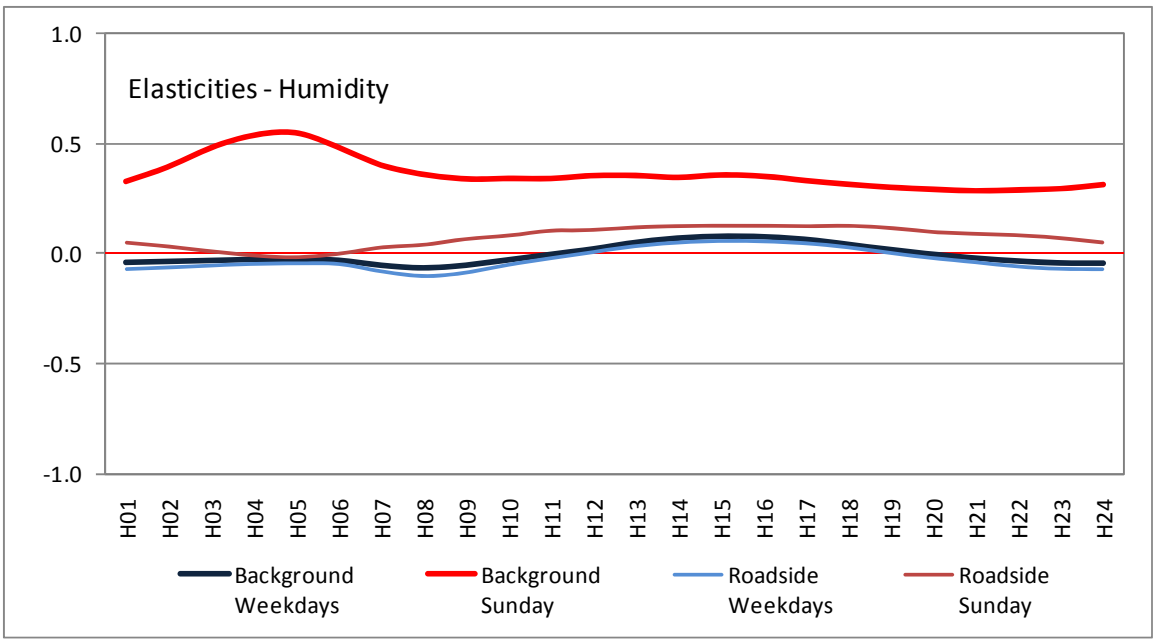

Figure 6.25 Average hourly elasticities w.r.t. humidity in the NO_2 models

6.3.3 Results for CO

The estimation results for the CO models are presented in Table 6.11, and are as expected: a positive coefficient for traffic and a negative one for solar radiation. Since CO is a directly emitted pollutant, traffic has a positive impact on CO concentrations. As discussed in Chapter 2, CO reacts with the hydroxyl radical (OH·) and is converted into CO_2 (Eq. 2.10) and hydroperoxyl radical (HO_2·) (Eq. 2.11). Generally, OH· radicals in the troposphere are generated in the presence of UV radiation, suggesting that solar radiation is negatively correlated with CO concentrations. In addition, the process of CO oxidation is interwoven in the reaction of O_3 creation: favorable conditions for O_3 creation can induce active CO oxidation, leading to lower CO concentrations. Wind is expected to expedite the dispersion of pollutant, and thus higher wind speed is correlated with lower CO concentrations. Higher temperatures reduce the consumption of fossil fuels and result in decreased CO concentrations. The results in Table 6.11 indicate that the coefficient estimates for the original regressors are significant and have the expected signs. The cross-product of traffic and solar radiation is significant in both the background and roadside models, but with a negative sign in the background case and a positive one in the roadside case, pointing to opposite effects depending on the local conditions. These effects will be analyzed in more detail through the analyses of derivatives and elasticities w.r.t. traffic and solar radiation.

Table 6.1 showed earlier that the concentrations of directly emitted pollutants are lower on Sundays than on weekdays. Reduced traffic flows on Sunday are expected to decrease CO concentrations. In addition, the conditions for generating O_3 are better on Sunday, and therefore CO oxidation, interwoven in the O_3 creation process, is expedited, resulting in lower CO concentrations on Sunday. However, as seen in Table 6.11, the CO models include diverse estimates of interaction variables related to the Sunday dummy variables, and the coefficients display both positive and negative signs. To interpret the impacts of these Sunday interaction variables, it is necessary to use the derivative functions and elasticities w.r.t. the explanatory variables.

CO is generated by the incomplete combustion of carbon-containing materials. Heating of buildings is limited during the warm season, and incomplete combustion occurs more often during the cold season, leading to higher CO concentrations in the cold season. Traffic during the warm seasons is expected to emit smaller amounts of CO than during the cold seasons, and therefore the monthly dummy interaction with traffic is expected to be negative during the warm season. These negative effects do indeed take place from April to October in both models. CO oxidation is related to solar radiation, and intense solar radiation during the Summer are expected to increase the generation of O_3, leading to more active CO oxidation and a decrease in CO concentrations. However, the retained monthly solar interaction terms are positive during Spring and Summer months, an expected result calling for further research.

The derivative functions of the CO models w.r.t. each explanatory variable are presented in Table 6.12. Since the derivative functions w.r.t. traffic and solar radiation include the Sunday dummy variable and interaction terms related to the Sunday dummy, the impacts of these variables on CO concentrations will necessarily be different for these two time periods. The derivative functions w.r.t. wind speed and humidity in the background model also include a Sunday-related interaction term (β16*Humidity_WS*Sun Dummy), but β16 is close to zero, thus generating very small differences between weekdays and Sunday.

Location	Explanatory variables					Regress R^2	DW
	Regressors		Parameter	t Value	Pr > | t |	Total R^2	p-value
Background	Intercept	α1	6.9892	23.97	<.0001	0.17	2.00
	Traffic Square	β1	0.0495	19.73	<.0001		
	Solar Radiation	β2	-2.1690	-7.96	<.0001	0.97	Pr < DW
	Solar Radiation Square	β3	0.4956	9.98	<.0001		0.55
	Wind Speed	β4	-0.0480	-1.79	0.074		
	Temperature Square	β5	-0.0016	-3.76	0.000		Pr > DW
	Humidity	β6	0.0107	1.84	0.067		0.45
	Humidity Square	β7	-0.0001	-3.14	0.002		
	Traffic × Solar	β8	-0.3502	-8.44	<.0001		
	Traffic × Temp	β9	0.0053	2.38	0.017		
	Solar × Temp	β10	0.0343	3.50	0.001		
	Solar × Wind Speed	β11	0.0364	3.09	0.002		
	Temp × Wind Speed	β12	-0.0023	-3.38	0.001		
	Humidity × Wind Speed	β13	0.0013	3.48	0.001		
	Traffic × Sun Dummy	β14	0.1618	3.67	0.000		
	Traffic square × Sun Dummy	β15	-0.0427	-3.52	0.000		
	Humidity_WS × Sun Dummy	β16	0.0004	1.69	0.092		
	Traffic × Feb Dummy	β17	0.1071	2.26	0.024		
	Traffic × Apr Dummy	β18	-0.1775	-3.66	0.000		
	Traffic × May Dummy	β19	-0.1527	-2.74	0.006		
	Traffic × Jun Dummy	β20	-0.2722	-4.47	<.0001		
	Traffic × Jul Dummy	β21	-0.2692	-4.28	<.0001		
	Traffic × Aug Dummy	β22	-0.2743	-4.25	<.0001		
	Traffic × Sep Dummy	β23	-0.2235	-3.80	0.000		
	Traffic × Oct Dummy	β24	-0.1039	-2.10	0.035		
	Solar × Mar Dummy	β25	0.8156	3.72	0.000		
	Solar × Apr Dummy	β26	0.8184	3.73	0.000		
	Solar × May Dummy	β27	0.8342	3.69	0.000		
	Solar × Jun Dummy	β28	1.1124	4.15	<.0001		
	Solar × Jul Dummy	β29	1.1651	4.27	<.0001		
	Solar × Aug Dummy	β30	0.9695	3.51	0.001		
	Solar × Sep Dummy	β31	1.0016	3.76	0.000		
	Solar × Nov Dummy	β32	-0.7446	-2.42	0.015		
	AR1	β33	-1.5418	-143.73	<.0001		
	AR2	β34	0.6986	38.15	<.0001		
	AR3	β35	-0.1232	-11.51	<.0001		

Table 6.11 Results of time series regression for CO models

Table 6.11 continued

Location	Explanatory variables					Regress R^2	DW
	Regressors		Parameter	t Value	Pr > | t |	Total R^2	p-value
Roadside	Intercept	α1	8.8277	43.05	<.0001	0.10	2.00
	Traffic Square	β1	0.0908	19.06	<.0001		
	Solar Radiation	β2	-5.4647	-7.94	<.0001		Pr < DW
	Wind Speed	β3	-0.0649	-3.06	0.002		0.44
	Traffic × Solar	β4	0.3801	3.35	0.001	0.81	
	Solar × Humidity	β5	0.0197	4.59	<.0001		Pr > DW
	Temp × Humidity	β6	-0.0006	-3.77	0.000		0.56
	Traffic × Sun Dummy	β7	0.4776	3.95	<.0001		
	Traffic square × Sun Dummy	β8	-0.1192	-3.86	0.000		
	Solar square × Sun Dummy	β9	0.1709	1.69	0.091		
	Traffic × Jan Dummy	β10	0.2695	3.54	0.000		
	Traffic × Feb Dummy	β11	0.3289	4.26	<.0001		
	Traffic × Apr Dummy	β12	-0.2487	-3.34	0.001		
	Traffic × Aug Dummy	β13	-0.1858	-2.31	0.021		
	Traffic × Sep Dummy	β14	-0.2094	-2.66	0.008		
	Traffic × Oct Dummy	β15	-0.2356	-3.18	0.002		
	Traffic × Nov Dummy	β16	0.2642	3.66	0.000		
	Solar × Mar Dummy	β17	1.1805	3.43	0.001		
	Solar × Apr Dummy	β18	1.8139	5.38	<.0001		
	Solar × May Dummy	β19	1.9069	6.38	<.0001		
	Solar × Jun Dummy	β20	1.6900	4.93	<.0001		
	Solar × Jul Dummy	β21	1.8533	5.17	<.0001		
	Solar × Aug Dummy	β22	1.6717	4.34	<.0001		
	Solar × Sep Dummy	β23	1.5908	4.18	<.0001		
	Solar × Oct Dummy	β24	1.2399	3.53	0.000		
	AR1	β25	-0.9213	-85.89	<.0001		
	AR2	β26	0.0635	5.91	<.0001		

Model	Variable	Derivative function
Background	Traffic	2*β1*Traffic + β8*Solar + β9*Temp + β14*Sun Dummy + 2*β15*Traffic_SunDummy + β17*Feb + β18*Apr + β19*May + β20*Jun + β21*Jul + β22*Aug + β23*Sep + β24*Oct
	Solar Radiation	β2 + 2*β3*Solar + β8*Traffic + β10*Temp + β11*Wind Speed + β25*Mar + β26*Apr + β27*May + β28*Jun + β29*Jul + β30*Aug + β31*Sep + β31*Nov
	Wind Speed	β4 + β11*Solar + β12*Temp + β13*Humidity + β16*Humidity_Sun Dummy
	Temperature	2*β5*Temp + β9*Traffic + β10*Solar
	Humidity	β6 + 2* β7*Humidity + β13*WS + β16*WS_Sun Dummy
Roadside	Traffic	2*β1*Traffic + β4*Solar + β7*Sun Dummy + 2*β8*Traffic_Sun Dummy + β10*Jan + β11*Feb + β12*Apr + β13*Aug + β14* Sep + β15*Oct + β16*Nov
	Solar Radiation	β2 + β4*Traffic + β5*Humidity + 2*β9*Solar_Sun Dummy + β17*Mar + β18*Apr + β19*May + β20*Jun + β21*Jul + β22*Aug + β23*Sep + β24*Oct
	Wind Speed	β3
	Temperature	β6* Humidity
	Humidity	β5* Solar + β6*Temp

Table 6.12 Derivative functions of the CO models w.r.t. each explanatory variable

Summary statistics for the calculated derivatives are presented in Table 6.13. The impacts of traffic on CO concentrations are generally positive. In a certain situation, however, these impacts turn out to be negative: about 10% of the observations in the background case and only a very few observations in the roadside case. Roadside areas are directly under the positive influence of traffic emissions, whereas conditions for positive to negative shifts frequently occur in background regions. Negative to positive shifts are also observed for solar radiation, wind speed, temperature, and humidity. More than 90% of the derivatives w.r.t. solar radiation are negative in both the background and roadside models, indicating that solar radiation is a major factor for decreasing CO concentrations. To further investigate these shifts, the hourly average values of these derivatives are calculated across the four groups, and presented in Figures 6.26 and 6.27.

Model	Variable	Minimum	10th Pctl	Lower Quartile	Median	Upper Quartile	90th Pctl	Maximum
Background	Traffic	-0.96	-0.11	0.05	0.20	0.37	0.50	0.72
	Solar Radiation	-5.17	-3.75	-3.10	-2.13	-1.39	-0.83	1.31
	Wind Speed	-0.05	0.00	0.01	0.03	0.05	0.06	0.13
	Temperature	-0.08	-0.05	-0.03	0.00	0.03	0.05	0.12
	Humidity	-0.01	-0.01	0.00	0.00	0.00	0.01	0.01
Roadside	Traffic	-0.01	0.23	0.48	0.94	1.33	1.61	2.18
	Solar Radiation	-4.23	-2.85	-2.19	-1.31	-0.52	-0.12	0.72
	Wind Speed	-0.06	-0.06	-0.06	-0.06	-0.06	-0.06	-0.06
	Temperature	-0.06	-0.05	-0.05	-0.04	-0.03	-0.02	-0.01
	Humidity	-0.02	-0.01	-0.01	0.00	0.01	0.02	0.05

Table 6.13 Summary statistics for the derivatives w.r.t. each explanatory variable in the CO models

CO oxidation (Eqs. 2.10 ~ 2.12) involves the hydroxyl radical (OH·) and hydroperoxyl radical (HO_2·). The HO_2· generated in the reaction between CO and OH· (Eq. 2.12) plays a key role in the accumulation of O_3. Under relatively abundant NO concentrations, HO_2· radicals typically react with NO to generate NO_2 and OH· (Eq. 2.7). Since this reaction replaces O_3 titration, O_3 has a chance to accumulate. In addition, the created NO_2 plays a role in generating O_3. OH· is consumed in the reaction with CO and then regenerated in the reaction between HO_2· and NO, resulting in the reactions between CO and OH· to occur repeatedly. Therefore, it is reasonable to expect that if conditions are favorable for O_3 accumulation, CO concentrations will tend to be low. As seen in Figure 6.26, the hourly derivatives w.r.t. traffic display opposite patterns in the roadside and background cases during daytime. Since background regions are favorable to O_3 accumulation, OH· can be used to oxidize CO over and over again. Therefore the derivatives w.r.t traffic in background areas are lower than those in roadside areas. These patterns are clearly observed during daytime and the greatest difference occur around 3 ~ 4 P.M., when O_3 accumulation reaches its peak. Since CO oxidation effects are lesser in roadside areas and direct traffic emissions are more influential than in background areas, the derivatives w.r.t traffic for roadside-weekdays are higher than those for roadside-Sundays.

Average hourly derivatives w.r.t. solar radiation are presented in Figure 6.27. Since solar radiation generally decrease CO concentrations, the derivatives are all negative across the four cases. During nighttime, solar radiation have no impacts on CO concentrations, and therefore the derivatives at night do not provide information. In the background case, the impacts of direct vehicle emissions are smaller than those in roadside areas, and, consequently, CO concentrations in background areas are more sensitive to solar radiation than those in roadside areas.

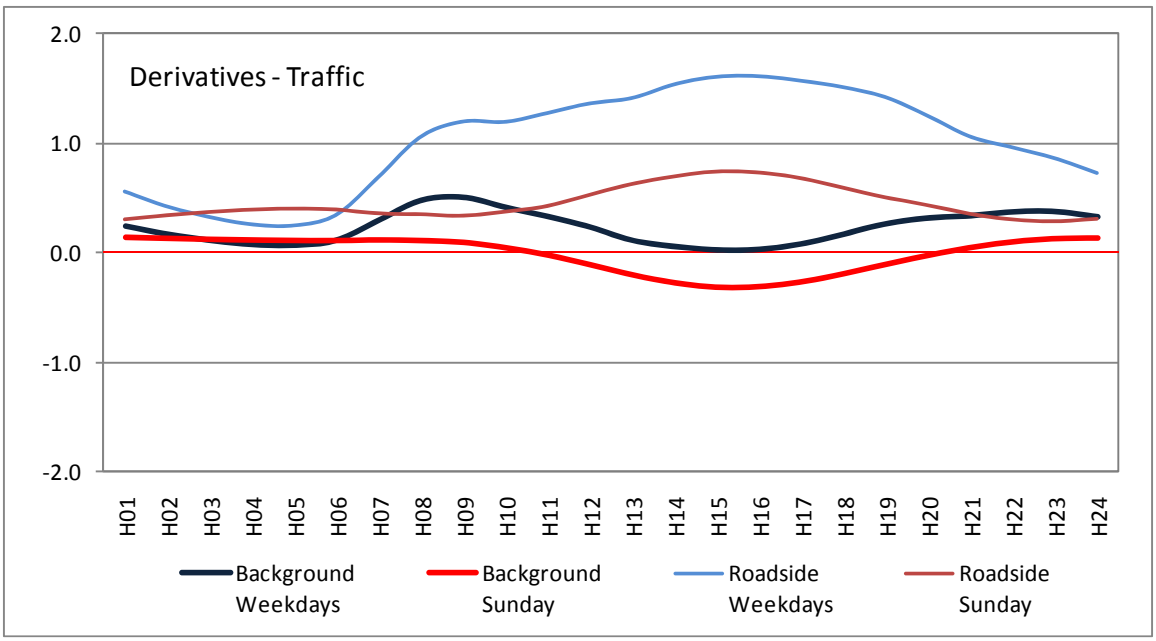

Figure 6.26 Average hourly derivatives w.r.t. traffic in the CO models

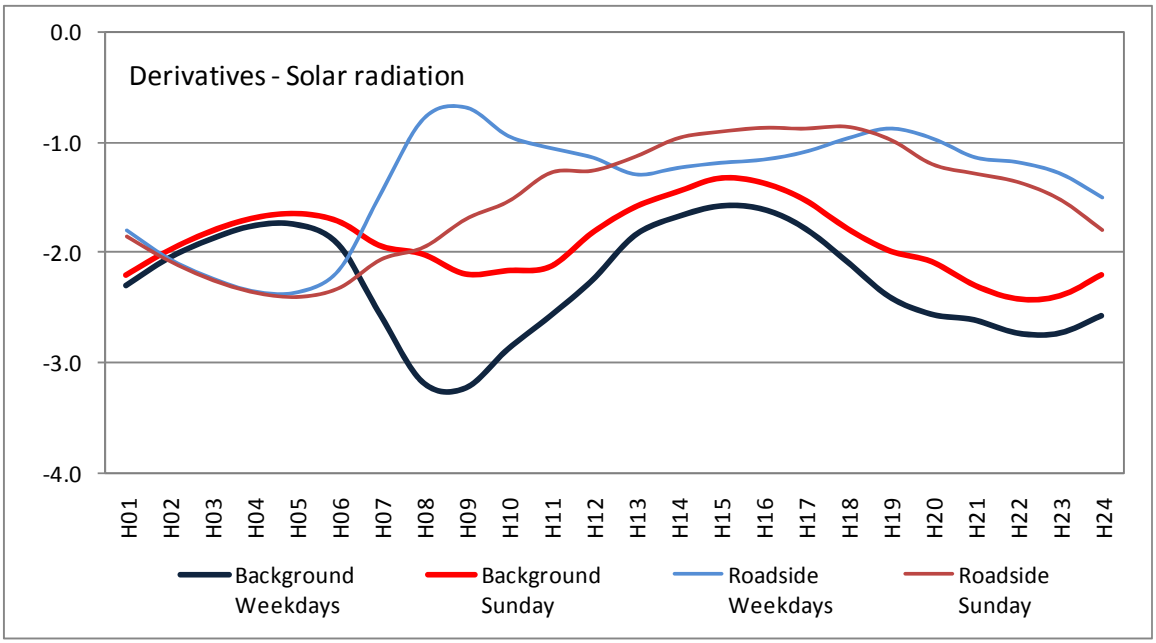

Figure 6.27 Average hourly derivatives w.r.t. solar radiation in the CO models

The elasticities w.r.t. the explanatory variables are computed using the estimated coefficients in Table 6.11 and the derivative functions in Table 6.12. Descriptive statistics of these elasticities are presented in Table 6.14. Generally, traffic flows are positively related to CO concentrations. These positive impacts turn out to be negative when conditions for O_3 generation become favorable. The shift from positive elasticities w.r.t. traffic to negative ones is observed only in the background case, supporting the theory that background areas provide more favorable conditions for O_3 generation than roadside areas. These shifts are also observed for the other variables. As in the case of traffic flows, the impacts of solar radiation, wind speed, temperature, and humidity on CO concentrations vary. Since the derivative functions w.r.t. traffic flows and solar radiation in both the background and roadside cases include Sunday interaction terms, the elasticities w.r.t. traffic change depend on solar radiation and Sunday dummy effects. More than 50% of the elasticities w.r.t. solar radiation in both the background and roadside cases are negative, but the values of elasticities in the background case are lower than those in the roadside case, suggesting that the negative solar radiation impacts on CO concentrations are greater in background areas than in roadside areas. The elasticities w.r.t. wind speed, temperature, and humidity are relatively low, except for a few extreme observations.

Model	Variable	Minimum	10th Pctl	Lower Quartile	Median	Upper Quartile	90th Pctl	Maximum
Background	Traffic	-1.83	-0.13	0.02	0.12	0.28	0.45	1.27
	Solar Radiation	-1.72	-0.40	-0.21	-0.04	0.00	0.00	1.41
	Wind Speed	-0.04	0.00	0.00	0.01	0.02	0.03	0.13
	Temperature	-1.07	-0.25	-0.12	-0.01	0.01	0.08	0.53
	Humidity	-0.36	-0.09	-0.04	0.00	0.03	0.06	0.16
Roadside	Traffic	0.00	0.05	0.14	0.45	0.75	1.04	3.22
	Solar Radiation	-1.16	-0.19	-0.06	-0.01	0.00	0.00	0.15
	Wind Speed	-0.10	-0.03	-0.02	-0.01	-0.01	0.00	0.00
	Temperature	-0.44	-0.15	-0.10	-0.05	-0.01	0.00	0.12
	Humidity	-0.44	-0.13	-0.06	-0.01	0.04	0.10	0.50

Table 6.14 Summary statistics for the elasticities w.r.t. each explanatory variable in the CO models[8]

[8] Detailed statistics on the hourly elasticities for each explanatory variable in the CO models are presented in Appendix H.

The patterns of the average hourly elasticities for the five explanatory variables are illustrated in Figures 6.28 ~ 6.32. Figure 6.28 presents the elasticities w.r.t. traffic flows. As discussed in the analysis of the derivatives, the impacts of traffic emissions on CO concentrations vary, depending on the conditions for O_3 generation. Urban background areas have more favorable conditions for generating O_3 than roadside areas, and therefore the elasticities w.r.t. traffic display different patterns in the background and roadside cases. O_3 generation depends on the intensity of solar radiation, and therefore, during daytime, the differences between the four cases are clearly observable. O_3 generation is active in background areas, and thus CO oxidation is also active in these areas, leading to lower elasticities in the background case than in the roadside case. Since background-Sunday is better for O_3 generation than background-weekdays, the elasticities for background-Sunday are lower than those for background-weekdays. In the case of roadside areas, direct emissions from tail pipes dominate CO concentrations. Weekdays have more traffic flows than Sunday, resulting in higher CO concentrations.

The elasticities w.r.t. solar radiation across the hours of the day are illustrated in Figure 6.29. CO oxidation is caused by OH· radicals in the troposphere, generated by UV radiation. In addition, CO oxidation is interwoven in the process of O_3 creation, and repeatedly occurs with recycled OH·, indicating that solar radiation has negative impacts on CO concentrations. The hourly elasticities w.r.t. solar radiation are negative, supporting this theory. Background areas are favorable conditions for O_3 generation, and therefore the elasticities for background areas are lower than those for roadside areas.

In the case of wind speed and humidity in the background case, Sunday related variables are included, but, as seen in Figures 6.30 and 6.32, the differences between weekdays and Sunday are very small because the coefficients of the interaction variables in the derivative functions are close to zero. The elasticity w.r.t. wind speed is close to zero across all hours of the day, suggesting that wind speed is not a major factor determining CO concentrations. Since temperature is related to the consumption of fossil fuels, the impacts of temperature may vary depending on the season. These impacts will be more precisely discussed in Chapter 7. Humidity is known to be negatively correlated with pollutant concentrations. The elasticities are generally negative, but with some positive values during the afternoon (low humidity hours).

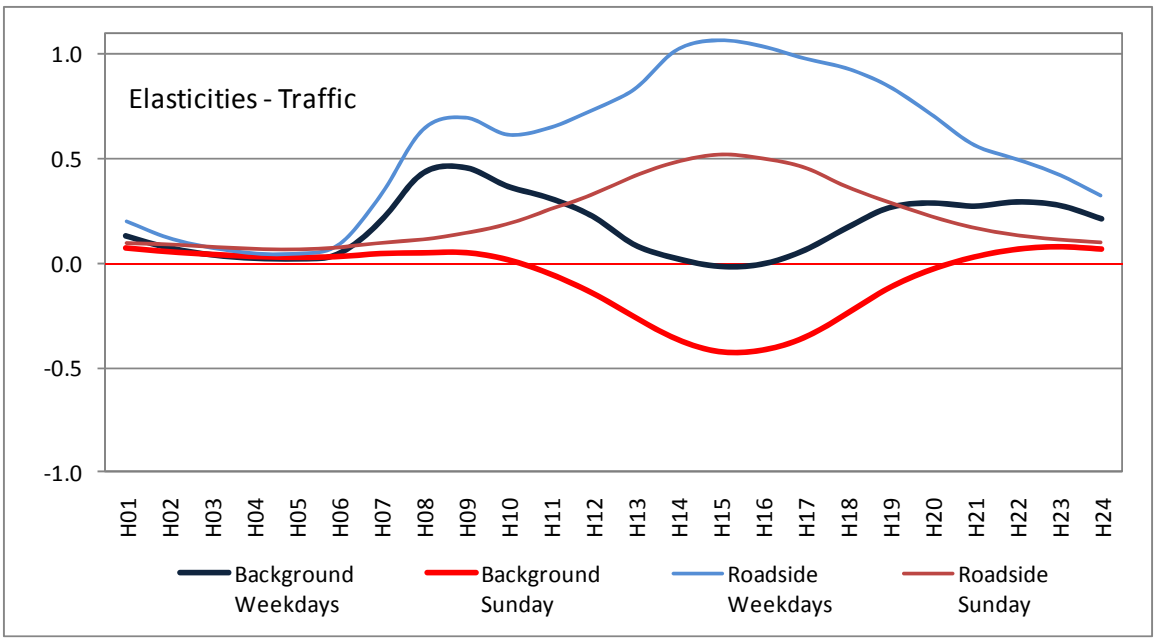

Figure 6.28 Average hourly elasticities w.r.t. traffic in the CO models

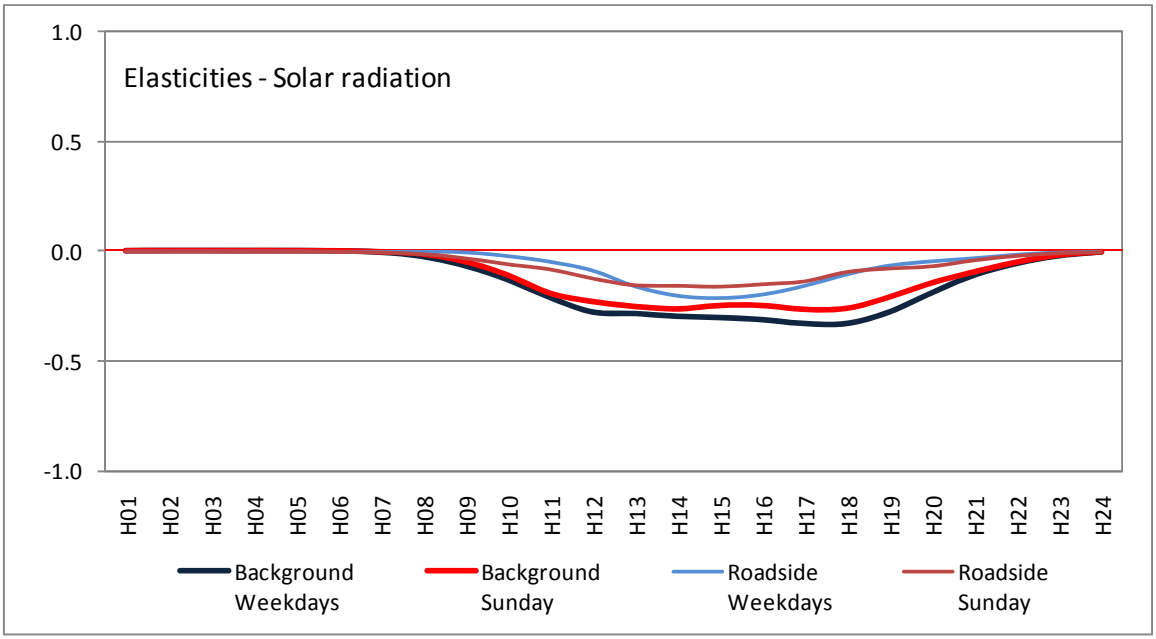

Figure 6.29 Average hourly elasticities w.r.t. solar radiation in the CO models

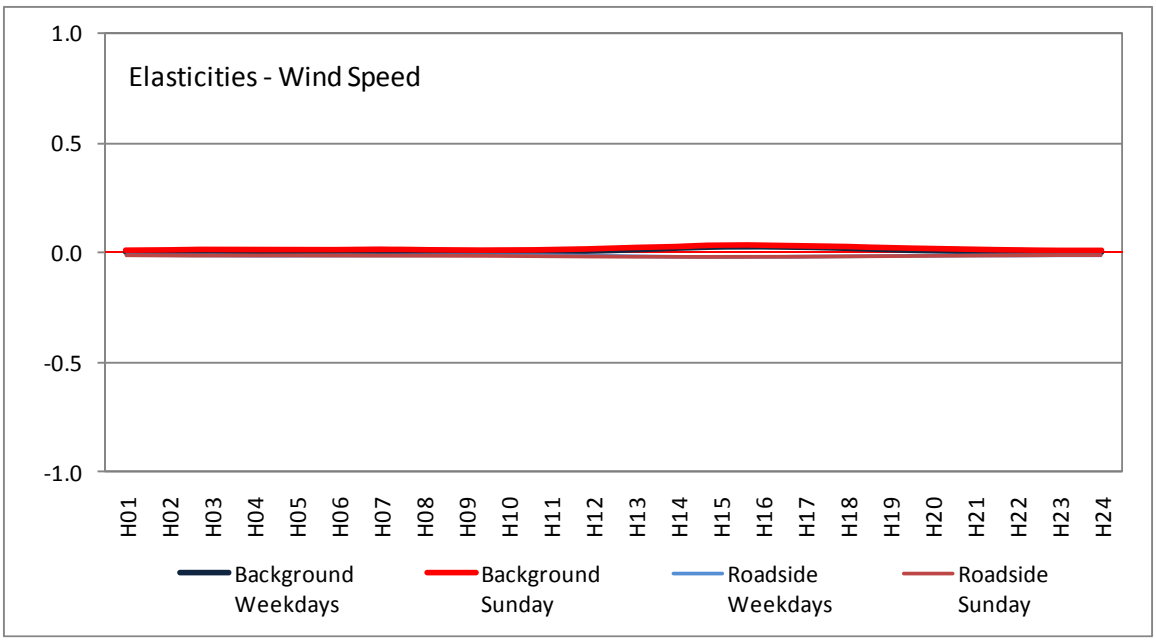

Figure 6.30 Average hourly elasticities w.r.t. wind speed in the CO models

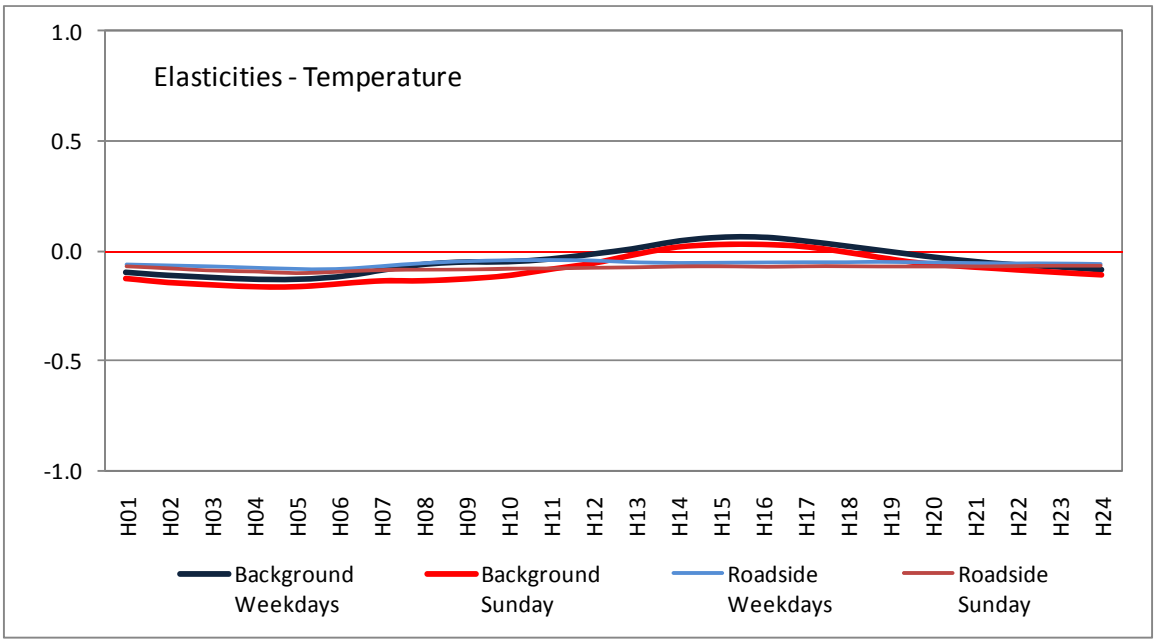

Figure 6.31 Average hourly elasticities w.r.t. temperature in the CO models

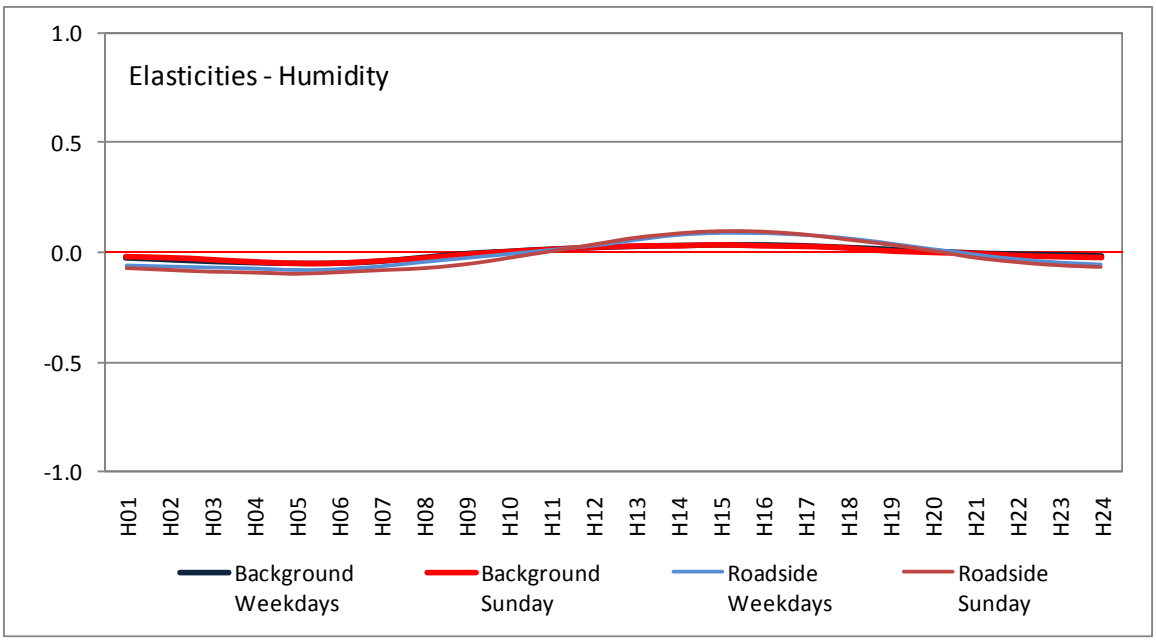

Figure 6.32 Average hourly elasticities w.r.t. humidity in the CO models

6.3.4 Results for SO_2

SO_2 is a directly emitted pollutant from diesel vehicles, and thus traffic flows are expected to have a positive impact on SO_2 concentrations. As discussed in Chapter 2, SO_2 reacts with OH· and water vapor, and is then converted into sulfuric acid (H_2SO_4) (Eqs. 2.24 ~ 2.26). As OH· radicals in the troposphere are generated under UV radiation, solar radiation is expected to be negatively correlated with SO_2 concentrations, as in the NO_2 and CO cases. The estimation results are presented in Table 6.15. The coefficient estimates for the traffic and solar radiation variables have the expected signs and are significant. Both background and roadside models include quadratic terms of the explanatory variables, indicating that the impacts of these variables are not linear. In the case of traffic in the roadside case, the estimate of the square of traffic is negative, indicating that traffic has generally a positive impact on SO_2 concentrations because of the direct impacts of diesel emissions, but that under specific conditions this impact may turn out to be negative. In the background case, a similar shift from negative to positive impact may take place for solar radiation. To discover when and how this shift occurs, it is necessary to analyze the derivative of the SO_2 concentration function w.r.t. traffic and solar radiation. As expected, humidity is negatively related to SO_2 concentrations because water vapor enhances the conversion of SO_2 into sulfuric acid.

There are several significant interaction effects between the independent variables. The product of the traffic and humidity variables has negative effects in both models, indicating that the positive impact of traffic may shift to negative under high humidity. Since SO_2 has strong hygroscopic (water-soluble) characteristics, high humidity may offset the positive impact of traffic flows.

SO_2 is generated by the combustion of sulfur-containing fossil fuels. Diesel vehicles are a major source of SO_2 emissions in urban regions. The monthly traffic interaction terms are negative in the roadside model during the Spring and Summer. There are well-known seasonal variations in combustion conditions, which may be reflected by these results. Also, SO_2 conversion to sulfuric acid is related to the OH· radical, and intense solar radiation during the Summer provide better conditions for generating OH·, leading to more active conversions. This is reflected by the estimated coefficients of the monthly solar interaction terms, which are negative and particularly large in the Summer and early Autumn months. These effects are much smaller in the background case.

As seen in the Table 6.15, the original regressors, their quadratic forms, and diverse interaction terms have been selected as significant explanatory variables. Since it is difficult to directly interpret the impacts of these variables on SO_2 concentrations, the derivatives of SO_2 models w.r.t. the explanatory variables are considered. These derivative functions are presented in Table 6.16. Since the derivative functions w.r.t. traffic and meteorological factors include Sunday interaction terms, changes in SO_2 concentrations necessarily vary between weekdays and Sunday.

Location	Explanatory variables					Regress R^2	DW
	Regressors		Parameter	t Value	Pr > | t |	Total R^2	p-value
Background	Intercept	α1	4.1028	16.02	<.0001		2.00
	Traffic	β1	0.3792	9.65	<.0001	0.08	
	Solar Radiation	β2	-1.5389	-9.17	<.0001		Pr < DW
	Solar Radiation Square	β3	0.1489	3.81	0.000		0.43
	Temperature	β4	0.1036	5.41	<.0001	0.96	
	Temperature Square	β5	-0.0035	-7.99	<.0001		Pr > DW
	Wind speed Square	β6	-0.0043	-1.97	0.049		0.57
	Humidity Square	β7	-0.0001	-5.43	<.0001		
	Traffic × Humidity	β8	-0.0039	-7.76	<.0001		
	Solar × Wind Speed	β9	0.0309	3.12	0.002		
	Solar × Humidity	β10	0.0186	9.62	<.0001		
	Temp × Humidity	β11	0.0006	4.13	<.0001		
	Temp × Wind Speed	β12	-0.0016	-2.52	0.012		
	Humidity × Wind Speed	β13	0.0008	4.35	<.0001		
	Solar × Sun Dummy	β14	1.9806	3.93	<.0001		
	Traffic_Solar × Sun Dummy	β15	-0.3181	-3.39	0.001		
	Traffic × Feb Dummy	β16	0.1422	3.73	0.000		
	Solar × Aug Dummy	β17	-0.3302	-2.02	0.043		
	Solar × Oct Dummy	β18	-0.4286	-2.96	0.003		
	Solar × Nov Dummy	β19	-0.8112	-3.68	0.000		
	AR1	β20	-1.3538	-135.70	<.0001		
	AR2	β21	0.3826	38.29	<.0001		

Table 6.15 Results of time series regression for SO_2 models

Table 6.11 continued

Location	Explanatory variables					Regress R^2	DW
	Regressors		Parameter	t Value	Pr > | t |	Total R^2	p-value
Roadside	Intercept	α1	2.5652	4.83	<.0001		2.00
	Traffic	β1	1.1906	14.26	<.0001	0.11	
	Traffic Square	β2	-0.0615	-10.82	<.0001		Pr < DW
	Solar Radiation	β3	-0.5255	-2.49	0.013		0.36
	Wind speed	β4	0.1050	3.57	0.000	0.93	
	Temperature Square	β5	-0.0032	-6.15	<.0001		Pr > DW
	Humidity	β6	0.0496	4.47	<.0001		0.64
	Humidity Square	β7	-0.0003	-4.35	<.0001		
	Traffic × Temp	β8	0.0128	5.25	<.0001		
	Traffic × Wind Speed	β9	-0.0261	-4.03	<.0001		
	Traffic × Humidity	β10	-0.0048	-5.93	<.0001		
	Solar × Temp	β11	0.0520	4.70	<.0001		
	Solar × Wind Speed	β12	0.0378	2.50	0.013		
	Solar × Humidity	β13	0.0089	3.24	0.001		
	Temp × Humidity	β14	0.0005	3.33	0.001		
	Wind Speed × Sun Dummy	β15	-0.1205	-2.17	0.030		
	Humidity × Sun Dummy	β16	0.0236	4.22	<.0001		
	Traffic Square × Sun Dummy	β17	-0.0389	-4.97	<.0001		
	WS Square × Sun Dummy	β18	0.0248	2.16	0.031		
	Humidity Square × Sun Dummy	β19	-0.0002	-3.37	0.001		
	Traffic × Jan Dummy	β20	0.1202	2.21	0.027		
	Traffic × Feb Dummy	β21	0.1917	3.71	0.000		
	Traffic × Apr Dummy	β22	-0.1018	-2.09	0.037		
	Traffic × May Dummy	β23	-0.3092	-5.59	<.0001		
	Traffic × Jun Dummy	β24	-0.3135	-5.18	<.0001		
	Traffic × Jul Dummy	β25	-0.3732	-5.97	<.0001		
	Traffic × Aug Dummy	β26	-0.3478	-5.41	<.0001		
	Traffic × Sep Dummy	β27	-0.3596	-6.20	<.0001		
	Traffic × Nov Dummy	β28	-0.1495	-3.11	0.002		
	Solar × Feb Dummy	β29	-0.4755	-1.98	0.048		
	Solar × Mar Dummy	β30	-0.6553	-2.87	0.004		
	Solar × Apr Dummy	β31	-1.3197	-5.12	<.0001		
	Solar × May Dummy	β32	-1.0095	-3.48	0.001		
	Solar × Jun Dummy	β33	-0.9515	-2.90	0.004		
	Solar × Jul Dummy	β34	-1.1054	-3.21	0.001		
	Solar × Aug Dummy	β35	-1.4249	-4.06	<.0001		
	Solar × Sep Dummy	β36	-1.3222	-4.06	<.0001		
	Solar × Oct Dummy	β37	-1.9098	-7.17	<.0001		
	Solar × Nov Dummy	β38	-1.7887	-5.75	<.0001		
	AR1	β39	-1.0512	-97.57	<.0001		
	AR2	β40	0.0988	9.16	<.0001		

Model	Variable	Derivative function
Background	Traffic	β1 + β8*Humidity + β15*Solar_Sun Dummy + β16*Feb
	Solar Radiation	β2 + 2*β3*Solar + β9*Wind Speed + β10*Humidity + β14*Sun Dummy + β15*Traffic_Sun Dummy + β17*Aug + β18*Oct + β19*Nov
	Wind Speed	2*β6*Wind Speed + β9*Solar + β12*Temp + β13*Humidity
	Temperature	β4 + 2*β5*Temp + β11*Humidity + β12*WS
	Humidity	2*β7*Humidity + β8*Traffic + β10*Solar + β11*Temp + β13*WS
Roadside	Traffic	β1 + 2*β2*Traffic + β8*Temp + β9*WS + β10*Humidity + 2*β17*Traffic_SunDummy + β20*Jan + β21*Feb + β22*Apr + β23*May + β24*Jun + β25*Jul + β26*Aug + β27* Sep + β28*Nov
	Solar Radiation	β3 + β11*Temp + β12*WS + β13*Humidity + β29*Feb + β30*Mar + β31*Apr + β32*May + β33*Jun + β34*Jul + β35*Aug + β36*Sep + β37*Oct + β38*Nov
	Wind Speed	β4 + β9*Traffic + β12*Solar + β15*Sun Dummy + 2*β18*WS_Sun Dummy
	Temperature	2*β5*Temp + β8*Traffic + β11*Solar + β14*Humidity
	Humidity	β6 + 2*β7*Humidity + β10*Traffic + β13* Solar + β14*Temp + β16*SunDummy + 2*β19*Humidity_Sun Dummy

Table 6.16 Derivative functions of SO_2 models w.r.t. each explanatory variable

The original data are used to calculate the changes in SO_2 concentrations resulting from unit changes in the explanatory variables. Summary statistics for the calculated derivatives are presented in Table 6.17. The impacts of traffic on SO_2 concentrations are generally positive, but, in certain situations, turn out to be negative. A shift from negative to positive impacts is observed for all meteorological factors. 75% of the derivatives w.r.t. humidity are negative in the background case, but less than 50% are negative in the roadside case, indicating that abundant roadside traffic emissions more often compensate for the negative humidity impacts. To investigate when these shifts occur, the average hourly derivatives across the four groups are presented in Figures 6.33 and 6.34.

Model	Variable	Minimum	10th Pctl	Lower Quartile	Median	Upper Quartile	90th Pctl	Maximum
Background	Traffic	-0.74	0.01	0.05	0.11	0.19	0.25	0.45
	Solar Radiation	-1.73	-0.71	-0.44	-0.14	0.15	0.46	1.91
	Wind Speed	-0.04	0.01	0.02	0.03	0.04	0.05	0.09
	Temperature	-0.10	-0.03	-0.01	0.04	0.10	0.14	0.24
	Humidity	-0.05	-0.03	-0.02	-0.01	-0.01	0.01	0.05
Roadside	Traffic	-0.46	-0.02	0.09	0.25	0.43	0.58	0.94
	Solar Radiation	-2.04	-1.02	-0.50	-0.10	0.17	0.38	1.08
	Wind Speed	-0.15	-0.06	-0.05	-0.04	0.00	0.06	0.07
	Temperature	-0.10	-0.05	-0.02	0.03	0.08	0.12	0.25
	Humidity	-0.04	-0.02	-0.01	0.00	0.01	0.02	0.06

Table 6.17 Summary statistics for the derivatives w.r.t. each explanatory variables in the SO_2 models

SO_2 is directly emitted from vehicles and reacts with OH· and water vapor. OH· radicals in the atmosphere are generated by solar radiation. Therefore, the impacts of traffic, solar radiation, and humidity are interrelated in determining SO_2 concentrations. Since roadside areas are directly affected by traffic emissions, the derivatives w.r.t. traffic are generally positive, except for a few hours on Sunday. Since OH· radicals are abundant during the afternoon, SO_2 conversion is active at that time. In addition, it is expected that diesel vehicles, such as freight trucks and buses, travel less on Sunday than on weekdays. Therefore, less diesel vehicles emissions combined with high solar radiation explain the negative derivatives in the background-Sunday and roadside-Sunday cases.

Average hourly derivatives w.r.t. humidity are presented in the Figure 6.34. Since humidity decreases SO_2 concentrations, the derivatives are generally negative across the four cases, except during the afternoon hours. As shown in Figure 4.18, the average hourly humidity displays a typical pattern: higher during nighttime, lower during daytime, and lowest when UV radiation reaches peak hours (around 3 to 4 P.M.). The hourly pattern of humidity matches the hourly derivatives of the SO_2 function, lower during nighttime and higher during daytime, culminating around 3 to 4 P.M. As expected, humidity has less impact in the roadside case than in the background one.

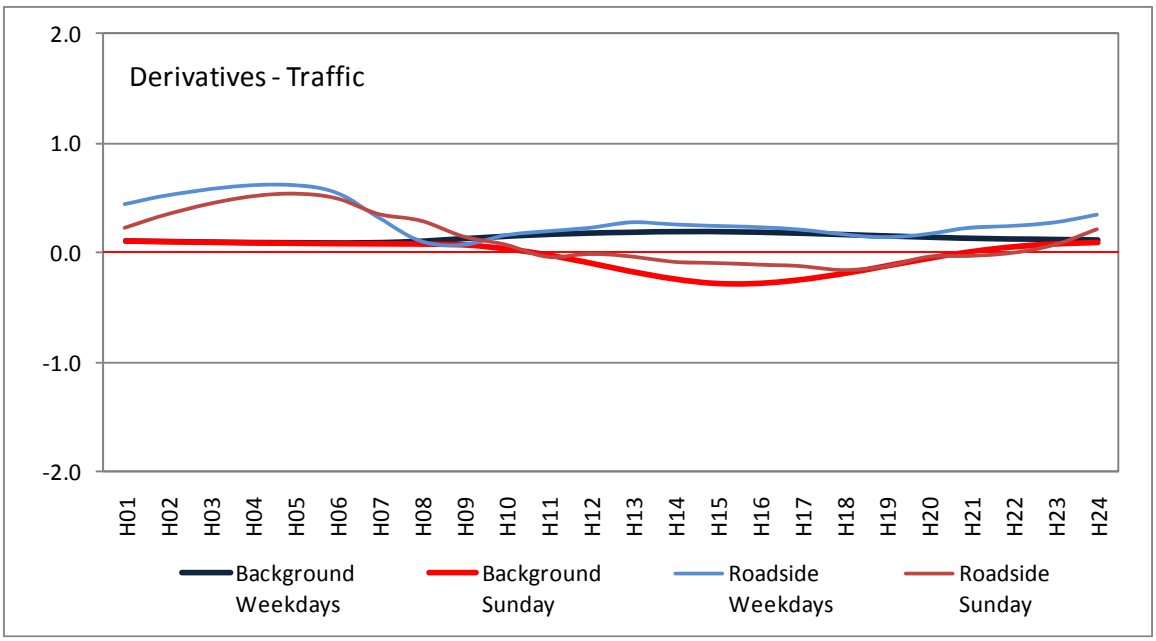

Figure 6.33 Average hourly derivatives w.r.t. traffic in the SO_2 models

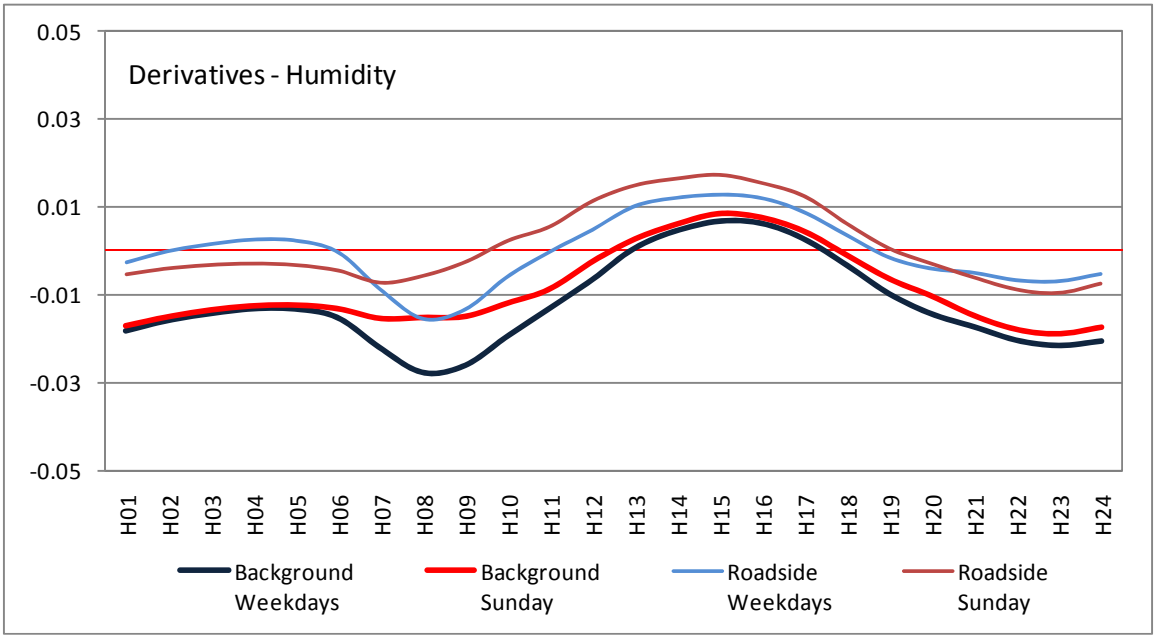

Figure 6.34 Average hourly derivatives w.r.t. humidity in the SO_2 models

Using the estimated parameters in Table 6.15 and the derivative functions in Table 6.16, the elasticities w.r.t. the explanatory variables are computed. Descriptive statistics for these elasticities are presented in Table 6.18. As discussed above, traffic flows are generally positively correlated with SO_2 concentrations. However, these positive impacts turn out to be negative in certain situations, such as high solar radiation intensity. Shifts from negative to positive impacts are also observed for meteorological factors. Since the derivative functions w.r.t. wind speed, temperature, and humidity (Table 6.16) include a solar radiation term, the elasticities w.r.t. these variables also depend on solar radiation. As expected, solar radiation has generally a negative impact on SO_2 concentrations. During nighttime, the impact of solar radiation is zero. Around 10% of the observations produce positive impacts on SO_2 concentrations. Humidity is negatively correlated with SO_2 concentrations because of the water-solubility of SO_2. A 1% change in humidity induces a maximum 1.50% decrease in SO_2 concentrations in the background case, and a maximum 1.45% decrease in the roadside case. Humidity is the strongest impact factor for decreasing SO_2 concentrations in both locations.

Model	Variable	Minimum	10th Pctl	Lower Quartile	Median	Upper Quartile	90th Pctl	Maximum
Background	Traffic	-1.39	0.01	0.03	0.09	0.19	0.31	1.01
	Solar Radiation	-0.94	-0.09	-0.02	0.00	0.00	0.03	0.76
	Wind Speed	-0.09	0.00	0.00	0.01	0.02	0.03	0.10
	Temperature	-1.41	-0.27	-0.08	0.03	0.10	0.18	0.39
	Humidity	-1.50	-0.57	-0.36	-0.21	-0.06	0.10	0.68
Roadside	Traffic	-1.24	-0.02	0.07	0.15	0.23	0.33	1.01
	Solar Radiation	-1.03	-0.07	-0.01	0.00	0.00	0.03	0.32
	Wind Speed	-0.14	-0.03	-0.02	-0.01	0.00	0.01	0.18
	Temperature	-1.09	-0.27	-0.10	0.01	0.06	0.14	0.89
	Humidity	-1.45	-0.33	-0.14	-0.01	0.07	0.15	0.63

Table 6.18 Summary statistics for elasticities for each explanatory variable in the SO_2 models[9]

The patterns of average hourly elasticities for the five explanatory variables are illustrated in Figures 6.35 ~ 6.39. Figure 6.35 presents the elasticities w.r.t. traffic flows. Since there is more traffic on weekdays than on Sunday, the elasticities on weekdays are positive. However, some

[9] Detailed statistics on the hourly elasticities for each explanatory variable in the SO_2 models are presented in Appendix H.

negative elasticities are observed for the Sunday cases during daytime. As discussed in Chapter 2, cumulative UV radiation peak around 3 to 4 P.M., and the generated OH· radicals have negative impacts on SO_2 concentrations. For this reason, the shift from positive to negative elasticities w.r.t. traffic occurs on the Sunday cases, when this effect overwhelms traffic effects. The patterns of elasticities for each explanatory variable are determined by the derivative functions (Table 6.16). The derivative functions w.r.t. traffic include interaction terms related to the Sunday dummy variable, indicating that the impacts of traffic on SO_2 concentrations are different on weekdays and Sunday.

The elasticities w.r.t. solar radiation across the hours of the day are illustrated in Figure 6.36. SO_2 is converted into sulfuric acid by OH· radicals, and therefore solar radiation is expected to have negative impact on SO_2 concentrations. The hourly elasticities are negative in the two roadside cases and in the background-weekdays case, but are positive in the background-Sunday case. There are no clear theoretical reasons for this unexpected result, calling for further research.

The derivative functions w.r.t. wind speed include diverse terms such as wind speed, solar radiation, temperature, humidity, traffic, and therefore so do the corresponding elasticity functions. Since there is a mix of positive and negative coefficients, with some close to zero, the effects of these variables cancel out and the impacts of wind speed on SO_2 concentrations are very small across the four cases, as shown in Figure 6.37. The derivative function w.r.t. temperature has a solar radiation term in the roadside case, but not in the background case. There is no theoretical interpretation for the observed pattern.

Since humidity is lower during daytime, the negative effects of humidity on SO_2 concentrations decrease during daytime, and are close to zero around 3 to 4 P.M. when cumulative UV radiation reach their peak. Roadside areas are heavily affected by traffic emissions, and the negative impact of humidity is smaller in roadside areas than in background areas.

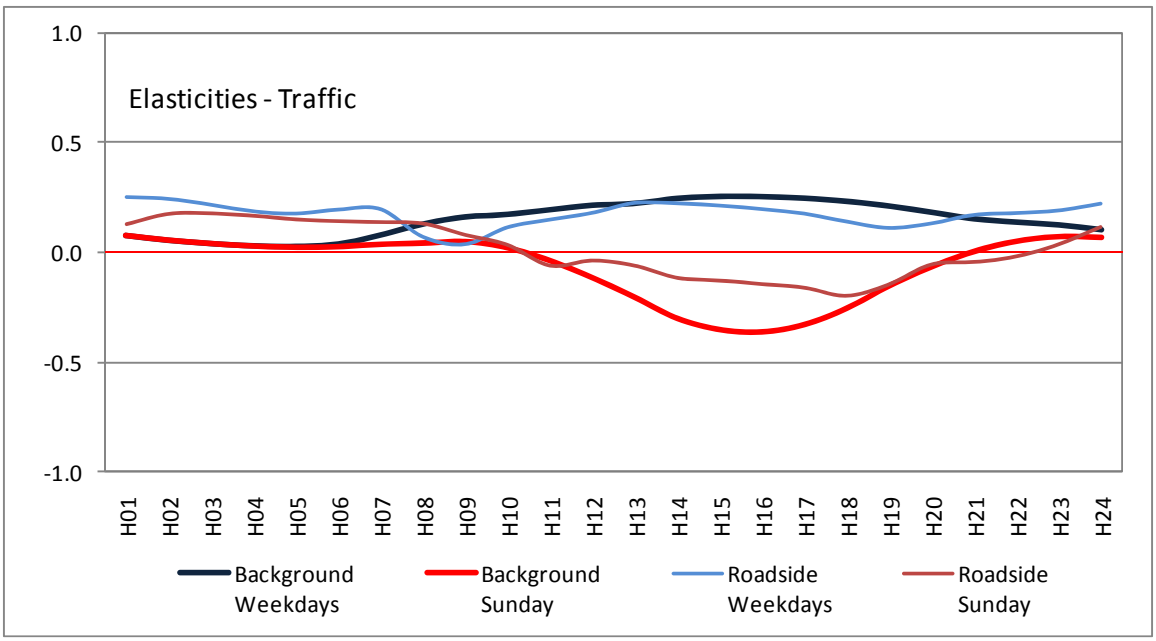

Figure 6.35 Average hourly elasticities w.r.t. traffic in the SO_2 models

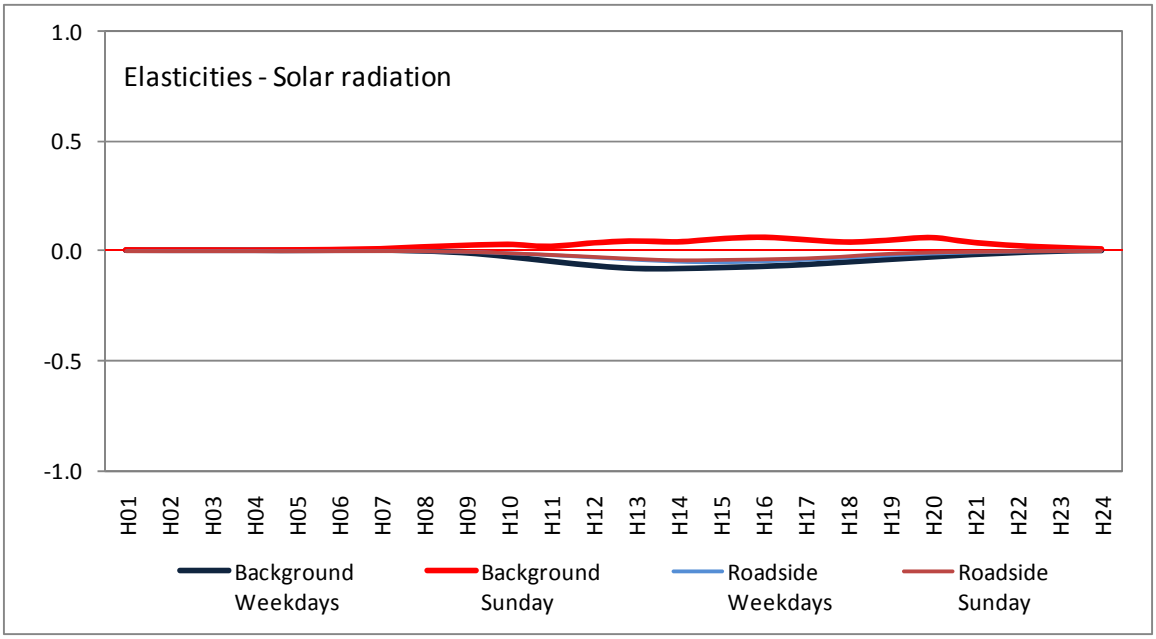

Figure 6.36 Average hourly elasticities w.r.t. solar radiation in the SO_2 models

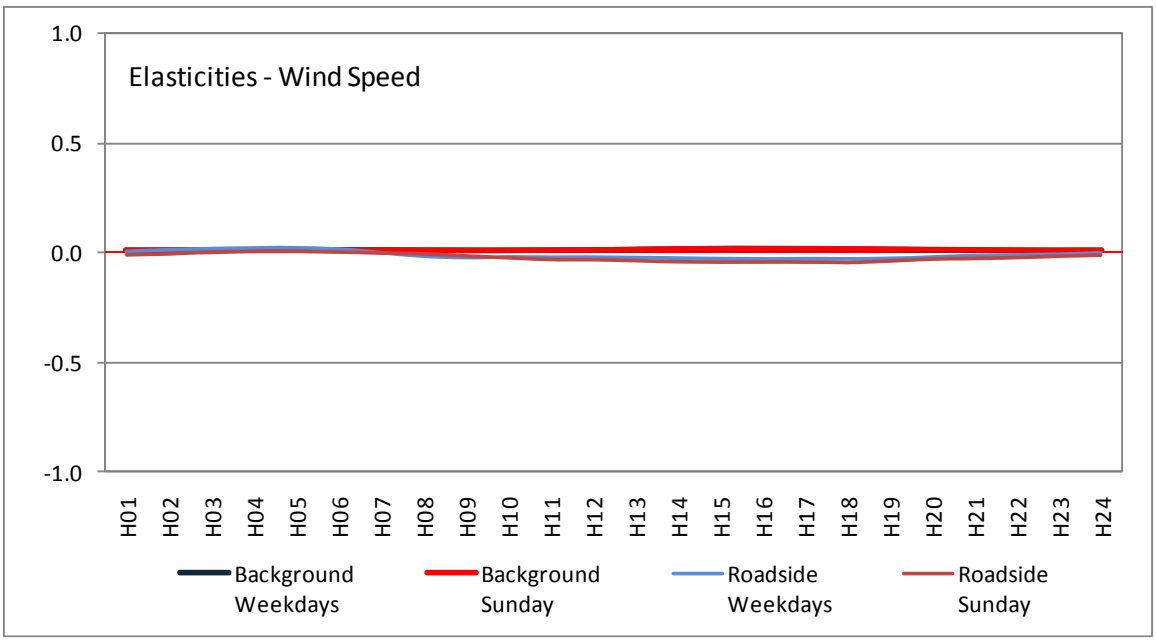

Figure 6.37 Average hourly elasticities w.r.t. wind speed in the SO_2 models

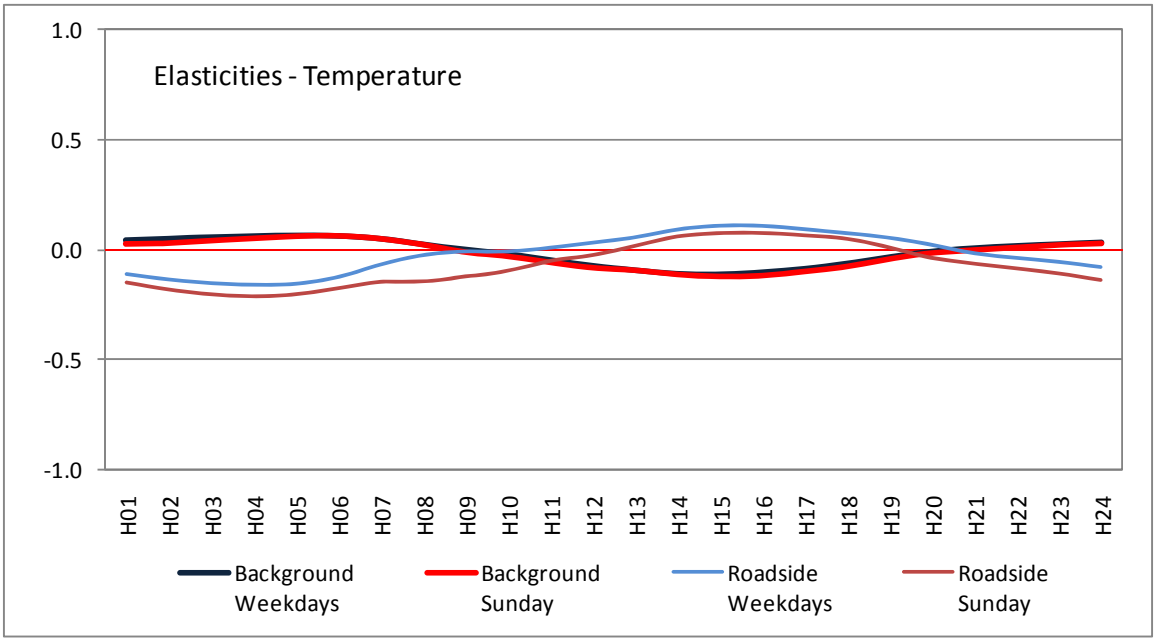

Figure 6.38 Average hourly elasticities w.r.t. temperature in the SO_2 models

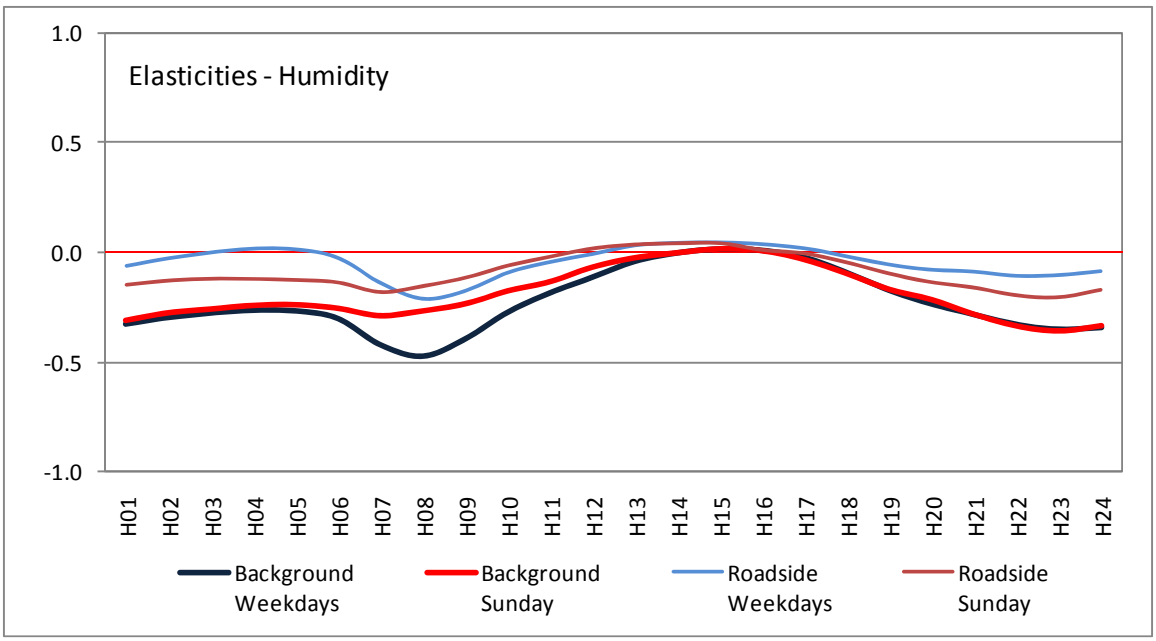

Figure 6.39 Average hourly elasticities w.r.t. humidity in the SO_2 models

6.3.5 Results for PM10

As discussed in Chapter 2, the sources of PM10 vary from man-made to natural, including dusts from roads, construction sites, and agricultural land, particles produced by electric generation and internal combustion engines, ammonia from agriculture, marine aerosols, pollen, biomass burning, yellow sand blown from China, and secondary particles, such as ammonium sulfate and ammonium nitrate. Thus, traffic and meteorological factors are not, by far, the only variables explaining PM10 concentrations. As the estimation results presented in Table 6.19 indicate, the regress R^2s of both the background (0.04) and roadside models (0.06) are lower than those of the other pollution models. However, the selected explanatory variables are significant, and it is assumed that they are not correlated with the error term. Under such circumstances, an impact analysis focused on these variables is still relevant.

Vehicles generate emissions of fine particles directly and indirectly as coagulated particles. In addition, wear of tire and brake pad, asphalt debris, and re-suspension of paved and unpaved road dust, are also associated with traffic flows. Table 6.19 shows that traffic has positive impacts on PM10 concentrations in both the background and roadside models. Although solar radiation is known to increase the generation of fine particles (PM2.5) through the formation of sulfuric acid and ammonium compounds, the coefficient estimate for solar radiation is negative. Since clear days are positively correlated with high pressure and low wind, these

meteorological combinations may reduce PM10 concentrations. Increasing temperatures reduce the consumption of fossil fuels, but biogenic emissions increase with higher temperatures, and hence the impacts of high temperature on PM10 concentrations may cancel out. Water vapor in the atmosphere plays a role in coagulating fine particles, but rain drops scavenge ambient particles, and therefore the impacts of humidity vary, depending on other meteorological conditions.

As Table 6.19 indicates, the coefficient estimates for traffic have the expected signs and are significant. The coefficient in the roadside model is greater (6.668) than that in the background model (0.840), because the roadside model includes the square of traffic with a negative sign, indicating that traffic impact on PM10 concentrations decreases with increased traffic. Since it is difficult to directly interpret the impacts of the basic explanatory variables on PM10 concentrations, the derivatives functions of the PM10 models w.r.t. the explanatory variables are formulated and presented in Table 6.20. Since the derivative function w.r.t. traffic for the roadside model include interaction terms related to the Sunday dummy variable, changes in PM10 concentrations differ on weekdays and Sunday.

Solar radiation has a negative effect on PM10 concentrations. The monthly solar interaction terms are negative in July, August, October, and November in the roadside model. Since plants no longer actively emit biogenic VOCs during Autumn, October and November are likely the lowest biogenic-emissions months. This is reflected in the estimated coefficients for the monthly solar interaction terms with the coefficients for October and November much lower than those of the other months.

Location	Explanatory variables					Regress R^2	DW
	Regressors		Parameter	t Value	Pr > | t |	Total R^2	p-value
Background	Intercept	α1	77.672	17.11	<.0001		2.00
	Traffic	β1	0.840	3.70	0.000	0.04	
	Solar Radiation	β2	-12.614	-7.30	<.0001		Pr < DW
	Temperature Square	β3	-0.016	-3.42	0.001		0.50
	Humidity	β4	-0.325	-4.46	<.0001	0.98	
	Humidity Square	β5	0.002	3.62	0.000		Pr > DW
	Traffic × Temp	β6	-0.025	-1.61	0.108		0.50
	Solar × Temp	β7	0.201	2.79	0.005		
	Solar × Humidity	β8	0.064	2.79	0.005		
	Temp × Humidity	β9	0.011	7.56	<.0001		
	Temp × Wind Speed	β10	0.013	3.45	0.001		
	Traffic × Feb Dummy	β11	1.392	2.72	0.007		
	Traffic × Jul Dummy	β12	-1.097	-2.24	0.025		
	Solar × Nov Dummy	β13	-9.612	-3.07	0.002		
	AR1	β14	-1.617	-152.21	<.0001		
	AR2	β15	0.773	41.63	<.0001		
	AR3	β16	-0.138	-12.97	<.0001		
Roadside	Intercept	α1	51.321	13.63	<.0001		1.97
	Traffic	β1	6.668	8.47	<.0001	0.06	
	Traffic Square	β2	-0.225	-3.29	0.001		Pr < DW
	Solar Radiation	β3	-15.472	-7.47	<.0001		0.10
	Wind speed Square	β4	0.132	3.07	0.002	0.95	
	Temperature	β5	0.649	2.07	0.039		Pr > DW
	Temperature Square	β6	-0.041	-4.81	<.0001		0.90
	Traffic × Wind Speed	β7	-0.148	-2.65	0.008		
	Traffic × Humidity	β8	-0.021	-3.30	0.001		
	Solar × Temp	β9	0.391	4.21	<.0001		
	Solar × Humidity	β10	0.124	4.40	<.0001		
	Temp × Humidity	β11	0.009	3.79	0.000		
	Humidity × Wind Speed	β12	0.009	2.74	0.006		
	Traffic × Sun Dummy	β13	3.056	4.46	<.0001		
	Traffic Square × Sun Dummy	β14	-0.764	-4.14	<.0001		
	Traffic × Feb Dummy	β15	1.127	1.77	0.077		
	Solar × Jul Dummy	β16	-4.571	-1.75	0.080		
	Solar × Aug Dummy	β17	-5.971	-2.25	0.024		
	Solar × Oct Dummy	β18	-6.757	-3.04	0.002		
	Solar × Nov Dummy	β19	-11.630	-3.29	0.001		
	AR1	β20	-1.209	-115.67	<.0001		
	AR2	β21	0.240	22.98	<.0001		

Table 6.19 Results of time series regression for PM10 models

Model	Variable	Derivative function
Background	Traffic	β1 + β6*Temp + β11*Feb + β12*Jul
	Solar Radiation	β2 + β7*Temp + β8*Humidity + β13*Nov
	Wind Speed	β10*Temp
	Temperature	2*β3*Temp + β6*Traffic + β7*Solar + β9*Humidity + β10*WS
	Humidity	β4 + 2*β5*Humidity + β8*Solar + β9*Temp
Roadside	Traffic	β1 + 2*β2*Traffic + β7*WS + β8*Humidity + β13*Sun Dummy + 2*β14*Traffic_Sun Dummy + β15*Feb
	Solar Radiation	β3 + β9*Temp + β10*Humidity + β16*Jul + β17*Aug + β18*Oct + β19*Nov
	Wind Speed	2*β4*WS + β7*Traffic + β12*Humidity
	Temperature	β5 + 2*β6*Temp + β9*Solar + β11*Humidity
	Humidity	β8*Traffic + β10* Solar + β11*Temp + β12*WS

Table 6.20 Derivative functions of PM10 models w.r.t. each explanatory variable

The original data are used to calculate the changes in PM10 concentrations resulting from unit changes in the explanatory variables. Summary statistics for the calculated derivatives are presented in Table 6.21. The impacts of traffic on PM concentrations are in most cases positive. However, in certain situations, the impacts may turn out to be negative. To investigate under what conditions the shift from positive to negative values occurs, summary statistics for the hourly derivatives w.r.t. traffic across the background and roadside models are presented in Table 6.21. A shift from negative to positive impacts is observed for the meteorological factors. Solar radiation effects in the background model are always negative, but more than 10% of the derivatives are positive in the roadside model.

Model	Variable	Minimum	10th Pctl	Lower Quartile	Median	Upper Quartile	90th Pctl	Maximum
Background	Traffic	-1.01	0.14	0.29	0.49	0.74	0.99	2.56
	Solar Radiation	-20.24	-11.01	-8.47	-6.08	-3.83	-2.62	-0.52
	Wind Speed	-0.20	-0.01	0.06	0.18	0.28	0.33	0.42
	Temperature	-0.46	-0.06	0.07	0.25	0.50	0.70	1.20
	Humidity	-0.30	-0.10	-0.01	0.10	0.22	0.28	0.39
Roadside	Traffic	-3.29	1.08	2.24	2.81	3.62	4.25	7.17
	Solar Radiation	-23.27	-12.13	-8.60	-4.27	-0.91	1.85	7.36
	Wind Speed	-0.64	-0.02	0.17	0.44	0.70	0.94	2.12
	Temperature	-1.19	-0.53	-0.28	0.24	0.93	1.38	2.45
	Humidity	-0.23	-0.06	0.00	0.09	0.16	0.27	0.55

Table 6.21 Summary statistics for the derivatives w.r.t. each explanatory variable in the PM10 models

Vehicle flows are positively related to PM10 concentrations. Therefore, the derivatives in the background cases are generally lower than those in the roadside cases, and quite close to zero. Since roadside areas are directly affected by traffic emissions, tire debris, and re-suspended particles, the corresponding derivatives w.r.t. traffic are positive except a few hours on Sunday. The derivative function w.r.t. the traffic variable in the roadside PM10 model, as displayed in Table 6.20, includes seven terms. Four terms in this function have negative impacts on PM10 concentrations: 2*β2*Traffic, β7*WS, β8*Humidity, and 2*β14*Traffic_Sun Dummy. As seen in Table 6.19, the coefficient β2 of the traffic squared is negative, indicating that the positive impact of traffic diminishes with increasing traffic. Since the product of the traffic squared and the Sunday dummy variable has also a negative coefficient, this negative impact is further increased on Sunday. These factors explain the counterintuitive result that the elasticity is negative at roadside locations on Sunday. However, this pattern clearly calls for further research.

The average hourly derivatives w.r.t. solar radiation are presented in the Figure 6.41. Since solar radiation decrease PM10 concentrations, the derivatives are all negative across the four cases. Since there is no solar radiation during nighttime, the impact of solar radiation is zero. However, the derivative functions w.r.t. solar radiation includes other meteorological factors in both the background and roadside models, and therefore the calculated derivatives are not zero. In the background case, the impacts of direct vehicle emissions are smaller than those in the roadside case, and therefore PM10 concentrations in background areas are more sensitive to solar radiation than those in roadside areas.

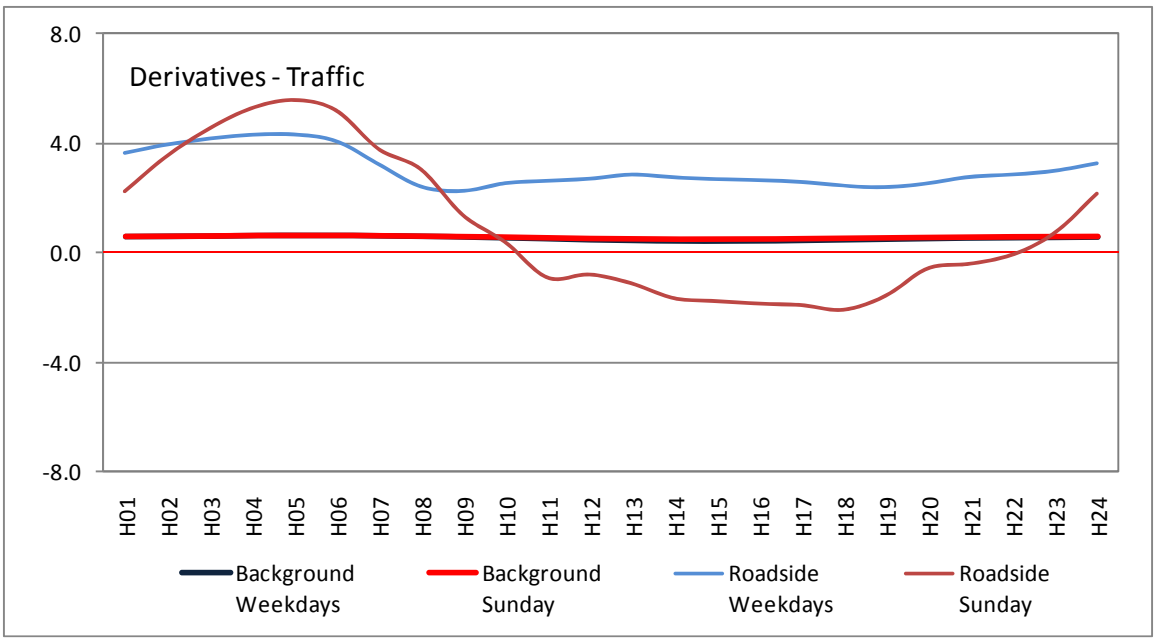

Figure 6.40 Average hourly derivatives w.r.t. traffic in the PM10 models

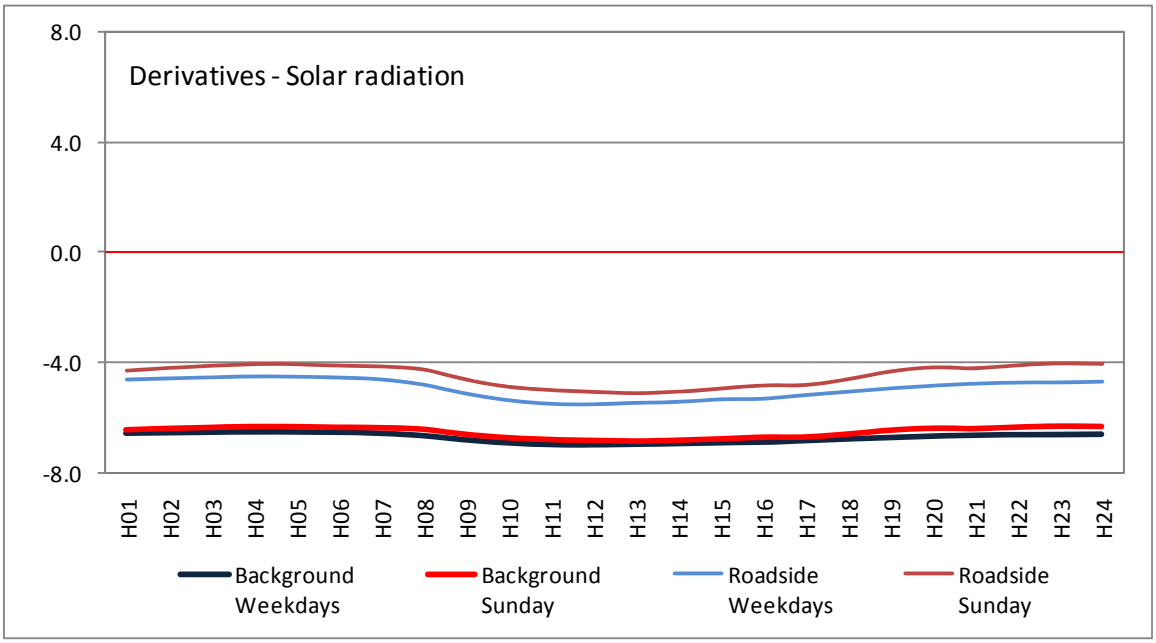

Figure 6.41 Average hourly derivatives w.r.t. solar radiation in the PM10 models

The elasticities w.r.t. the explanatory variables are computed using the estimated coefficients in Table 6.19 and the derivative functions in Table 6.20. Descriptive statistics for these elasticities are presented in Table 6.22. Generally, traffic flows are positively related to PM10 concentrations. These positive impacts turn out to be negative when the negative impacts of solar radiation on PM10 concentrations exceed a certain level. More than 50% of the elasticities w.r.t. solar radiation in the background model is negative, while the others are equal to zero. Therefore, the impact of solar radiation in background areas is purely negative. In the roadside case, less than 50% of elasticities are negative, and a shift from negative to positive values is observed for a few extreme observations. Based on these results, the negative solar radiation impacts on PM10 concentrations are greater in background areas than in roadside areas. The elasticities w.r.t. wind speed is significantly lower than those for the other variables, indicating a limited impact of wind speed on PM10 concentrations. The shifts from positive to negative elasticities are also observed for the temperature and humidity variables. As for traffic flows, the impacts of solar radiation, temperature, and humidity on PM10 concentrations vary. The derivative functions w.r.t. traffic flows in the roadside case include the Sunday dummy variable and interaction term related to the Sunday dummy variable, and therefore the elasticities w.r.t. traffic vary, depending on the Sunday effect.

Model	Variable	Minimum	10th Pctl	Lower Quartile	Median	Upper Quartile	90th Pctl	Maximum
Background	Traffic	-0.49	0.01	0.02	0.03	0.06	0.11	1.21
	Solar Radiation	-1.46	-0.20	-0.07	-0.01	0.00	0.00	0.00
	Wind Speed	-0.03	0.00	0.00	0.00	0.01	0.02	0.16
	Temperature	-0.52	-0.06	0.00	0.02	0.06	0.12	0.92
	Humidity	-0.50	-0.08	-0.01	0.09	0.29	0.70	3.86
Roadside	Traffic	-1.22	0.04	0.10	0.17	0.27	0.38	1.01
	Solar Radiation	-1.32	-0.15	-0.04	0.00	0.00	0.00	0.20
	Wind Speed	-0.01	0.00	0.00	0.01	0.03	0.06	0.72
	Temperature	-1.38	-0.31	-0.13	-0.01	0.05	0.09	0.58
	Humidity	-0.43	-0.05	0.00	0.08	0.19	0.36	2.18

Table 6.22 Summary statistics for elasticities for each explanatory variable in the PM10 models[10]

[10] Detailed statistics on the hourly elasticities for each explanatory variable in the PM10 models are presented in Appendix H.

The patterns of the average hourly elasticities of the five explanatory variables in the PM10 models are illustrated in Figures 6.42 ~ 6.46. The hourly patterns of the four cases can be compared on each graph. Figure 6.42 presents the elasticities w.r.t. traffic. As the impact of traffic flows on PM10 concentrations are greater at roadside areas, elasticities are generally higher in the roadside cases than in the background cases. However, there are negative elasticities in the roadside-Sunday case during daytime, because solar radiation has a negative impact on PM10 concentrations and traffic flows on Sunday are smaller than on weekdays. The roadside model is the only one to include Sunday interaction terms, leading to significantly different impacts of traffic on PM10 concentrations on weekdays and Sunday.

The elasticities of solar radiation across the hours of the day are illustrated in Figure 6.43. When cumulative UV radiation reaches their peak around 3 to 4 P.M., they lead to the highest decrease in PM10 concentrations. The hourly elasticities w.r.t. solar radiation is negative for both the roadside and background models, but there are no significant differences between them. Since the derivative functions w.r.t. solar radiation does not contain Sunday related variables, this is as expected.

The derivative function w.r.t. wind speed for the background model includes only one term and the coefficient of this term is close to zero ($\beta 10=0.013$), leading to very limited impacts of wind speed on PM10 concentrations. In the case of roadside model, the derivative function includes three terms, with both positive and negative effects, and the impacts of these variables cancel out, with the resulting elasticities close to zero. The derivative functions w.r.t. temperature for both the background and roadside models have terms with positive and negative effects, resulting in limited impacts on PM10 concentrations.

Since the interaction between humidity and solar radiation produces a positive impact on PM10 concentrations in both the background and roadside cases, the elasticities w.r.t. humidity are higher during daytime. Similar positive effects are observed for the interaction between humidity and temperature, because higher temperatures take place during the afternoon.

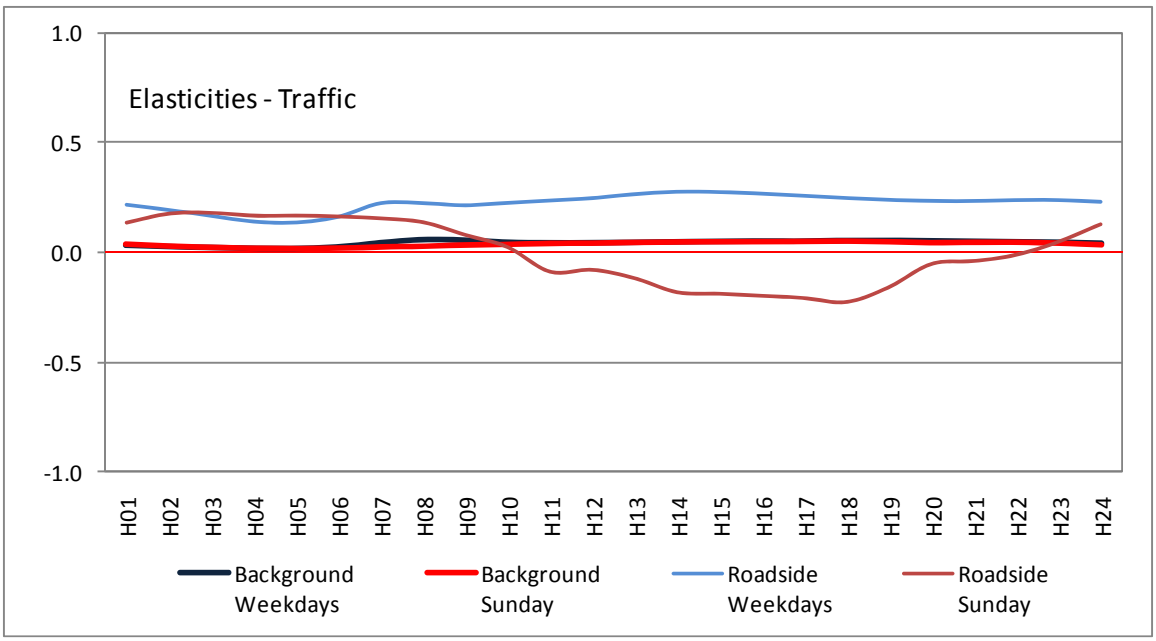

Figure 6.42 Average hourly elasticities w.r.t. traffic in the PM10 models

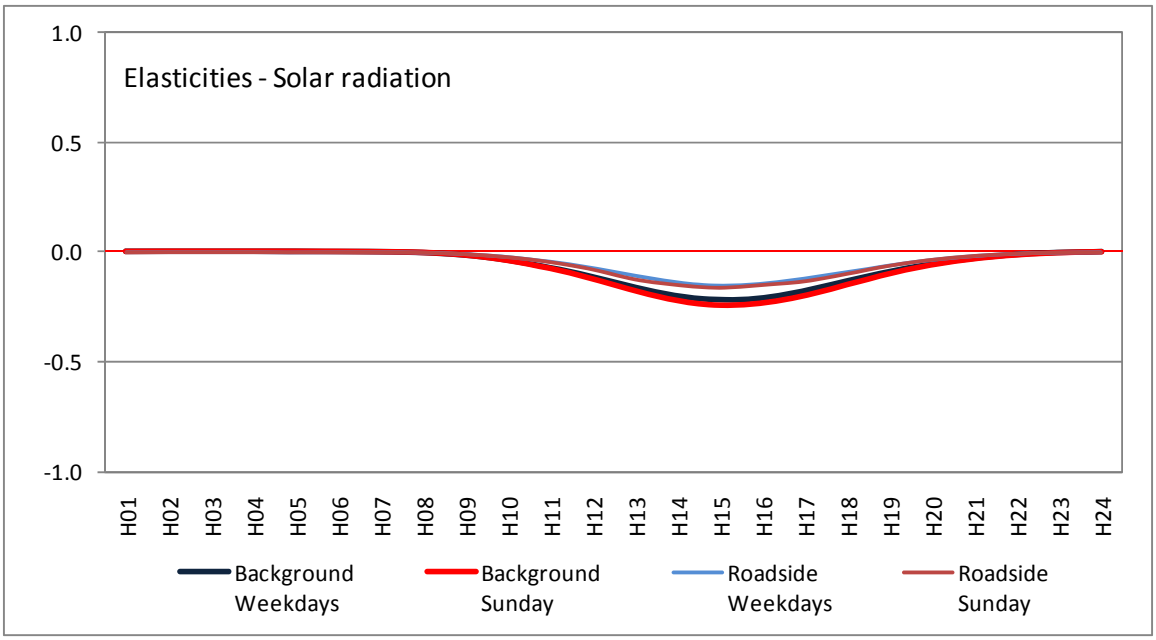

Figure 6.43 Average hourly elasticities w.r.t. solar radiation in the PM10 models

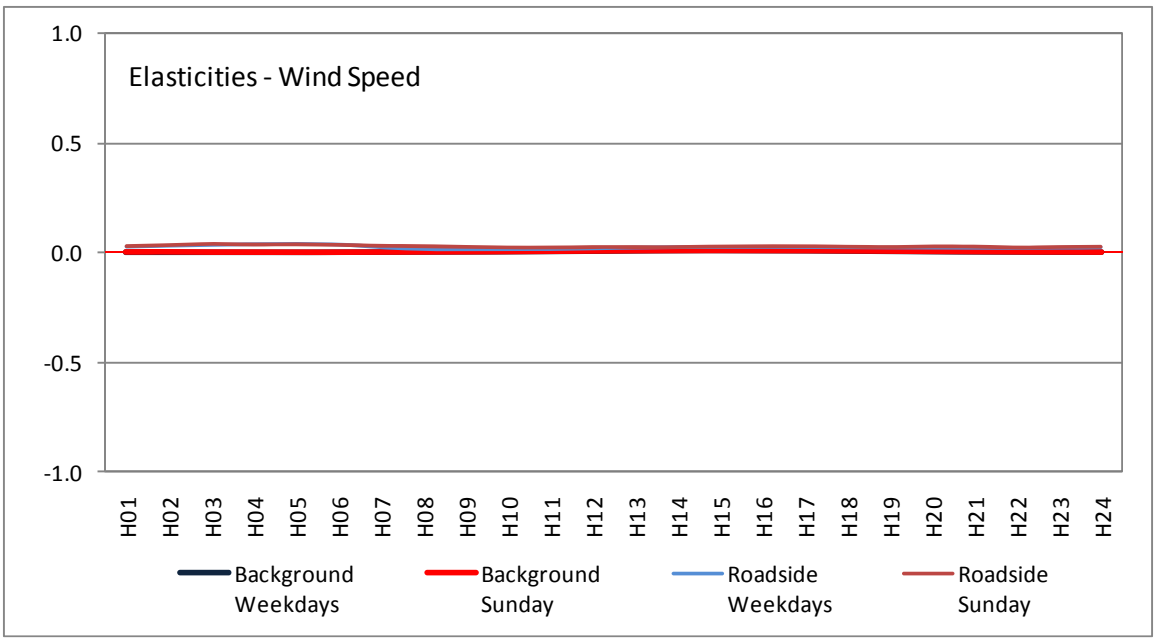

Figure 6.44 Average hourly elasticities w.r.t. wind speed in the PM10 models

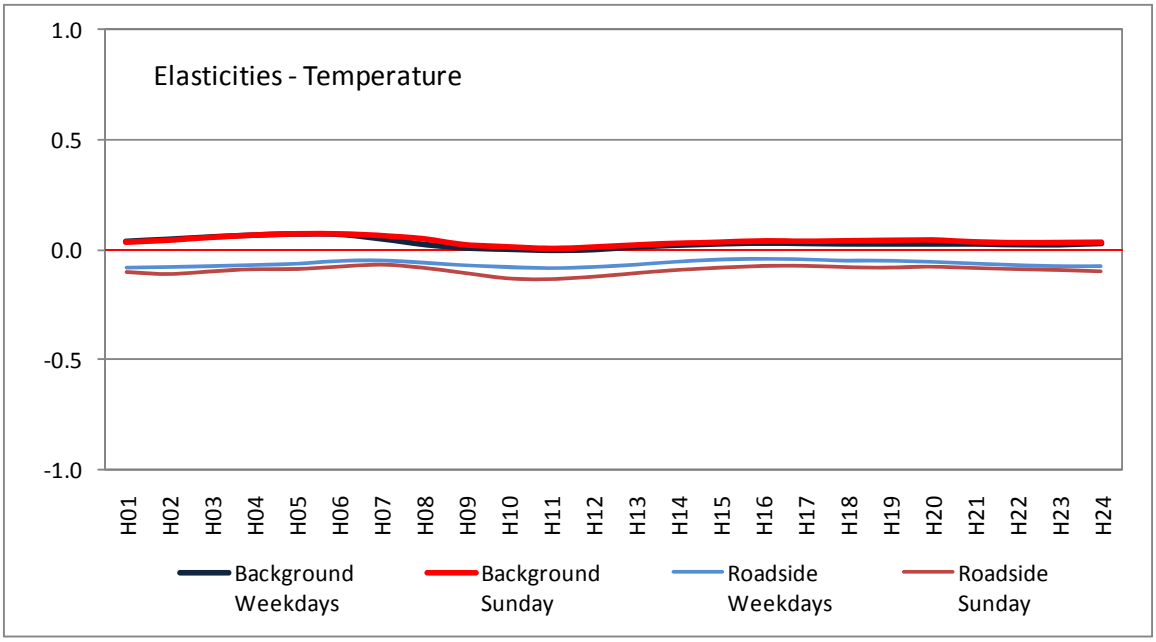

Figure 6.45 Average hourly elasticities w.r.t. temperature in the PM10 models

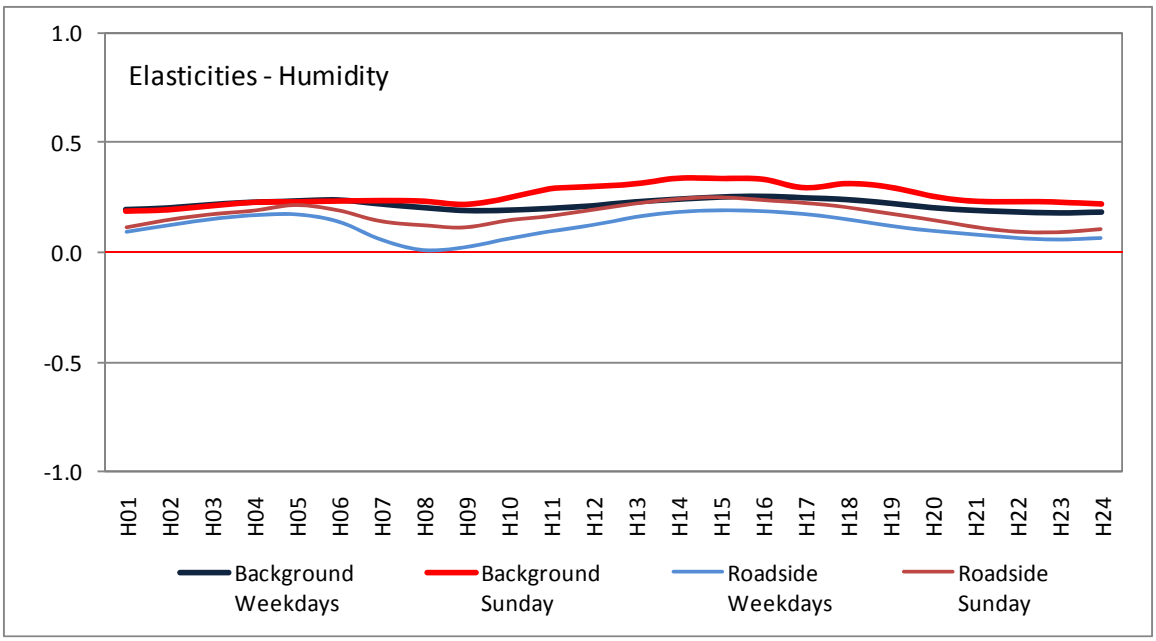

Figure 6.46 Average hourly elasticities w.r.t. humidity in the PM10 models

6.4 SUMMARY

In this chapter, the determinants of hourly pollution concentrations have been analyzed while accounting for temporal and spatial differences. The results for the O_3 models suggest that the impacts of vehicle flows are negative and those of solar radiation are positive. Specifically, the emissions from tail pipes contain abundant NO gas, leading to O_3 titration, and therefore traffic flows have a negative impact on O_3 concentrations. In contrast, tropospheric O_3 is generated by the photodissociation of NO_2 under the presence of UV radiation, and therefore solar radiation has strong positive impacts. The derivatives and elasticities analyses for traffic flows and solar radiation exactly reflect these theoretical assumptions. O_3 concentrations are determined by rates of chemical creation and destruction. These rates depend on the following two factors: (1) the level of precursor concentrations and their mixing ratio and (2) the impacts of solar radiation on O_3 generation, depending upon changes in precursors' mixing ratio. Taken together, the changes in precursors (reduced traffic on Sunday) induce better conditions for solar radiation impacts on O_3 generation, resulting in higher O_3 concentrations on Sunday. The elasticities w.r.t. traffic on Sunday are higher than those on weekdays. In addition, the elasticities w.r.t. solar radiation in the background model are higher than those in the roadside model. The theory that reduced traffic flows in NO_x-saturated regions provide favorable conditions for generating O_3 is supported by the empirical models.

In the case of directly emitted pollutants, such as NO_2, CO, SO_2, and PM10, traffic flows have generally positive impacts on pollution concentrations, with some non-linear effects. UV radiation decompose NO_2. OH· radicals produced under UV radiation react chemically with CO and SO_2. Because of these reactions, solar radiation have negative impacts on the concentrations of NO_2, CO, and SO_2. As for the traffic variable, the impacts of solar radiation on these direct pollutants also involve non-linear effects. Since diverse interaction terms have been selected as significant variables, it is necessary to introduce the derivative functions w.r.t. these variables to investigate the exact impacts on pollution concentrations. As discussed in the hourly elasticities graphs, a shift from negative to positive impacts are frequently observed, suggesting that the impacts of the explanatory variables are not constant. These phenomena occur for both secondary and directly emitted pollutants. Including cross-product terms and interactions variables related to the temporal dummy variables generally enhances goodness-of-fit. Since the concentrations of directly emitted pollutants at the roadside areas and on weekdays are generally higher than those at background areas and on Sunday, traffic impacts on these pollutants are clear. In contrast, the impacts of the meteorological factors vary, depending on the characteristics of the pollutants.

CHAPTER 7

AIR QUALITY PANEL MODELS

This chapter presents the estimation results for the air quality models outlined in Section 3.3.3, using seasonally-summarized panel data. Panel regression models are formulated to analyze the impacts of vehicle-kilometers-traveled (VKT), land uses, and meteorological factors on the concentrations of five pollutants: O_3, NO_2, CO, SO_2, and PM10. Locational and temporal dummy variables are introduced, and interaction terms related to these dummy variables are included in the models to measure different impacts on concentrations.

7.1 GENERAL PROCESS

The intensity and timing of emissions influence the spatial and temporal variations of pollution concentrations. In addition, several other factors, such as the formation and destruction of pollutants through chemical and physical reactions, the impacts of meteorological factors, and the assimilative effects of vegetative areas, also impact concentrations. Since transportation is responsible for a substantial share of urban air pollution emissions, VKT is considered as a better regressor to explain pollution concentrations than other transportation-related variables, such as the surface area of roads, distances to major roads, etc. (Briggs, 2007; Jerrett et al., 2007; Kahyaoğlu-Koračin, Bassett, Mouat, & Gertler, 2009; Kim, 2007; Kim & Guldmann, 2008).

Land-use areas around AQMs have been measured with GIS techniques and used as input variables in land-use regression (LUR) models to explain pollution concentrations over space and time. In this chapter, VKTs and land use shares around AQMs are calculated and used as explanatory variables. As presented in Figure 7.1, pollution concentrations monitored at each AQM are used as the dependent variables. Link VKT in the Seoul transportation network is estimated based on the results of a traffic assignment model. The areas of five land uses - residential, commercial, industrial, transportation, and vegetative - are calculated using a biotope map and satellite imagery. These explanatory variables are measured over 11 buffers and 8 sectors, and wind-direction (WD) frequencies are used to calculate WD weighted VKT (WVKT) and land

uses (WLU). Since emission sources located closer to the AQMs are expected to have greater impacts on concentrations than those located farther away, distance decay effects are expected to occur. Therefore, distance decay parameters must be estimated, that maximize the explanatory power of WVKT and WLU. As discussed in Chapter 2, meteorological factors induce chemical and physical reactions, leading to the creation, destruction, and dispersion of pollutants. Hourly measured solar radiation, temperature, humidity, and wind speed are seasonally summarized and included in the panel regression models to investigate these impacts.

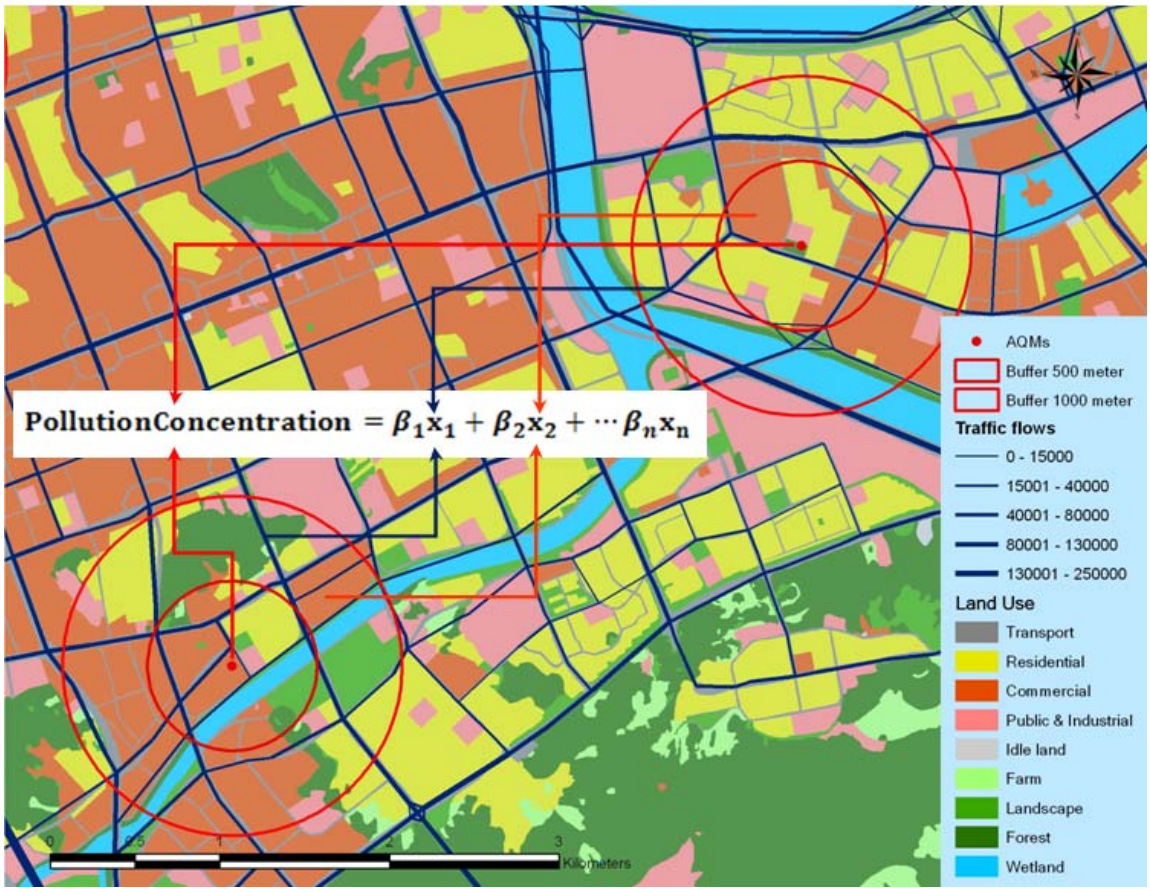

Figure 7.1 Components of a LUR model: AQMs, buffers, traffic flows, and land uses

The overall research process for the estimation of panel models based on the LUR approach is illustrated in Figure 7.2. Pollution concentrations have been measured hourly at 34 AQMs in the Seoul Metropolitan Area in 2003. As discussed in Chapter 5, pollution

concentrations vary significantly across the four seasons, and the hourly concentrations are averaged over each season and used to estimate seasonal air quality models. In addition, the concentrations of directly emitted and secondary pollutants at roadside and background AQMs present significant differences, and therefore, building on the modeling insights presented in Chapter 6, a dummy variable representing this spatial difference is included in the models. As discussed in Chapter 2, the rates of chemical creation and destruction vary depending on meteorological conditions, the concentrations of precursors, and the mixing ratio of the precursors. While buffer systems can capture distance effects to some extent, the spatial dummy variable can help to explain the differences in chemical reactions between these two AQM locations.

Since the dataset used in the seasonal air quality model is both cross-sectional (34 AQMs) and temporal (24 hours), this set includes 816 observations. The pooled cross-sectional and time-series data is referred to as panel data. As discussed in Chapter 6, if the error term in a time-series model is serially correlated, then OLS estimates are not efficiently estimated, although they are unbiased. The estimation methods for panel data are grouped into several categories, depending on the specification of the error term. The PANEL procedure in SAS/ETS® version 9.2[1] is used to estimate the parameters of the panel data.

[1] http://support.sas.com/documentation/cdl/en/etsug/60372/HTML/default/panel_toc.htm

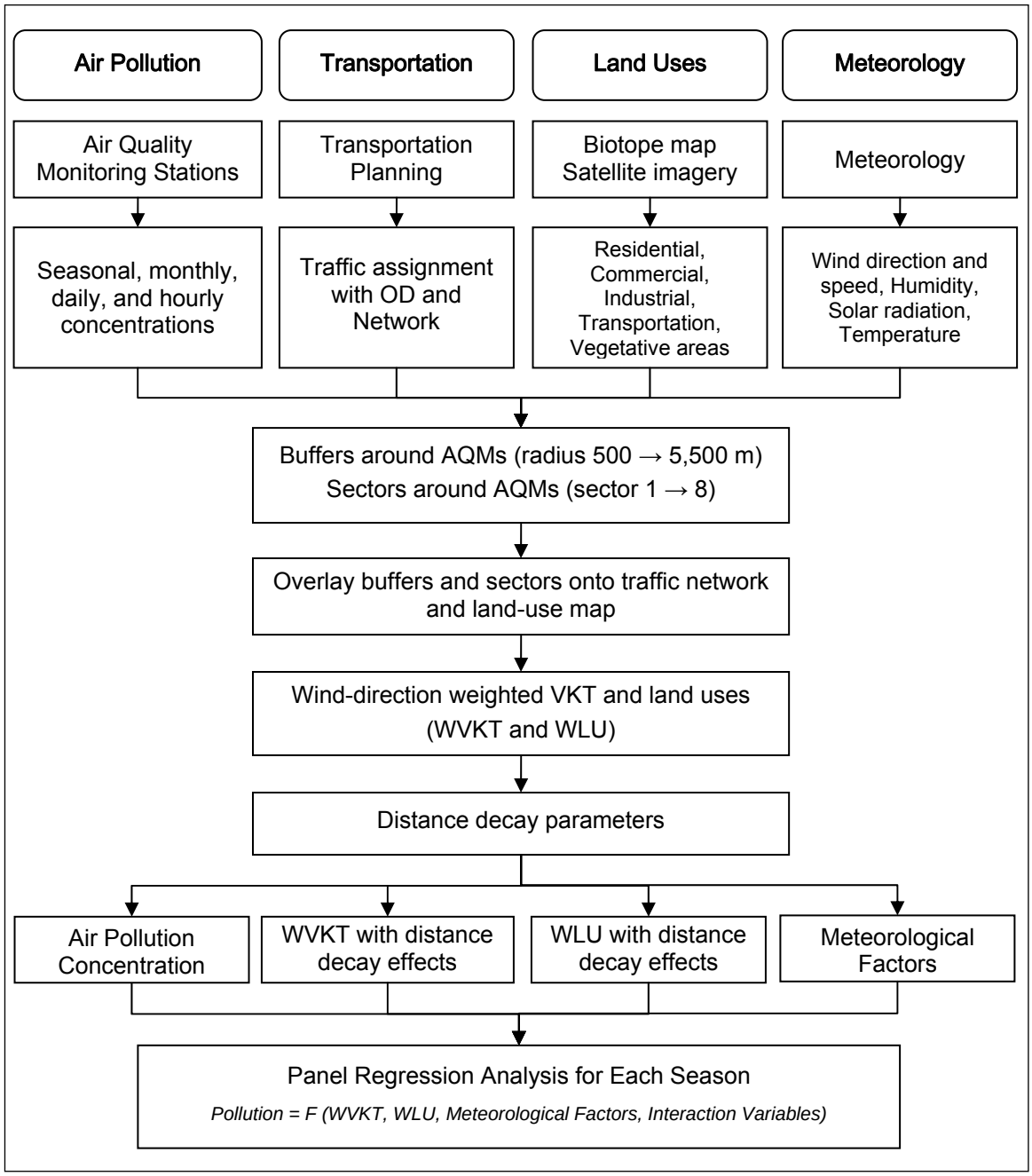

Figure 7.2 Research process for air quality panel models

7.2 AIR QUALITY MODELING METHOD

7.2.1 Data

Eleven circular buffers, with radii varying from 500 to 5,500 meters, and eight sectors are delineated around each AQM. VKTs for entire transportation links are calculated and then apportioned to each buffer and sector. WD frequencies are used to calculate WD-weighted VKT (WVKT). The same process is applied to the five land uses (WLU). Generally, concentrations at receptors are closely related to the distances between emission sources and receptors, and thus it is logical to expect that closer sources have more impacts on receptors than farther ones. VKT and land uses calculated based on the buffer system generate several variables, depending on their radii (e.g. VKT_R0500 → VKT_R5500). As expected, high correlations are observed among these variables with different radii. Additive functional forms (e.g. $\sum_r \alpha_r WVKT_r$) induce multicollinearity in regression models, making this additive form unsuitable for measuring distance decay effects. In addition, if the number of observations is limited, estimation may not be possible because of the number of degrees of freedom. Since pollution concentrations decrease exponentially with the distance from emission sources (Roorda-Knape et al., 1998) and dispersion modeling generally assumes that the dispersion of pollutant follows a Gaussian distribution (Karppinen et al., 2000; Lin & Lin, 2002), an appropriate mathematical function for measuring the distance decay effects is likely to be an exponential form. To investigate the optimal distance decay function, an exponentially decreasing form is proposed, depending on the radius, with:

$$X^p_DD = \sum_{r=1}^{11} X_r^p \times R_r^{-\alpha_X^p} \tag{7.1}$$

where:

p: Pollutant (p = 1 → 5),

r: Eleven radii (r = 1 → 11),

X^p_DD: Summary explanatory variable accounting for distance decay for pollutant p,

X_r^p: Measures of WVKT and WLU for each ring r and pollutant p,

R: Radius for each ring (500 to 5,500 meters with intervals of 500),

$-\alpha_X^p$: Parameter of the exponential decay function for pollutant p and explanatory variable X (α is always positive),

$R_r^{-\alpha_X^p}$: Distance decay factor for radius R_r .

An optimal solution means maximizing the explanatory power of explanatory variable. To find the optimal solution, an objective function is formulated as correlation between pollution concentrations and explanatory variable (e.g. *WVKT_DD*). The parameter of the exponential function, α, is a decision variable. The optimization problem is solved by Solver program®[2] implemented in Microsoft Office Excel®. The distance decay factors for each pollutant p and explanatory variable X are presented in the following results sections. If the distance decay factor does not improve explanatory power, the best radius among the 11 buffers[3] is chosen and included in the air quality model.

Descriptive statistics of the dependent variables and meteorological factors used in the panel models are presented in Tables 7.1 and 7.2. As seen in Table 7.1, the hourly concentrations of the five pollutants vary across the four seasons, as well as between background and roadside AQMs. The spatial differences suggest that including a dummy locational variable and related interaction terms in models may enhance their explanatory power. Wind speed, solar radiation, temperature, and humidity are measured hourly and are assumed to be invariant across the 34 AQMs. These hourly measurements are averaged over each season and used as explanatory variables. Since 6-hour averaged solar radiation has been proved to be appropriate to explain concentrations in the time-series models presented in Chapter 6, this average is used as the explanatory variable.

---

[2] http://www.solver.com

[3] A buffer is different from a ring in this research. For example, the buffer for VKT over a 1000-m radius (VKT_R1000) includes the sum of all VKTs within the circle with a 1000 meter radius. The 1000-m ring represents the difference between VKT_R1000 and VKT_R0500.

AQMs	Season	Variable	Mean	Minimum	Maximum	Std
Background AQMs	Spring	O_3 (ppb)	17.60	4.27	44.89	9.82
		NO_2 (ppb)	42.98	22.4	79.64	8.95
		CO (ppm)	0.61	0.29	1.06	0.16
		SO_2 (ppb)	4.76	2.63	8.12	1.29
		PM10 (μg/m^3)	81.23	53.72	131.80	12.98
	Summer	O_3 (ppb)	17.11	3.90	45.28	10.70
		NO_2 (ppb)	32.83	14.9	59.66	7.9
		CO (ppm)	0.61	0.29	1.06	0.16
		SO_2 (ppb)	4.76	2.63	8.12	1.29
		PM10 (μg/m^3)	61.95	37.46	95.98	11.82
	Autumn	O_3 (ppb)	9.47	1.36	29.72	6.29
		NO_2 (ppb)	38.04	20.93	62.82	8.89
		CO (ppm)	0.50	0.23	0.88	0.12
		SO_2 (ppb)	4.34	1.98	8.17	1.11
		PM10 (μg/m^3)	58.43	35.07	90.73	9.97
	Winter	O_3 (ppb)	7.88	0.80	20.78	3.88
		NO_2 (ppb)	43.29	21.29	63.92	6.97
		CO (ppm)	0.91	0.29	1.73	0.25
		SO_2 (ppb)	6.98	3.16	11.20	1.75
		PM10 (μg/m^3)	85.18	58.60	133.46	12.87
Roadside AQMs	Spring	O_3 (ppb)	10.65	4.44	25.11	4.78
		NO_2 (ppb)	55.99	28.26	81.22	11.89
		CO (ppm)	1.02	0.38	1.69	0.31
		SO_2 (ppb)	7.56	3.02	14.38	2.42
		PM10 (μg/m^3)	87.01	49.42	122.94	14.60
	Summer	O_3 (ppb)	10.88	3.23	23.34	5.17
		NO_2 (ppb)	47.29	19.92	70.59	12.18
		CO (ppm)	0.93	0.33	1.72	0.33
		SO_2 (ppb)	5.72	2.06	9.08	1.93
		PM10 (μg/m^3)	66.16	33.80	90.29	10.79
	Autumn	O_3 (ppb)	6.11	1.92	13.15	2.85
		NO_2 (ppb)	47.24	23.05	78.45	12.87
		CO (ppm)	0.99	0.37	1.67	0.37
		SO_2 (ppb)	6.34	2.82	10.75	1.57
		PM10 (μg/m^3)	64.89	41.79	86.07	9.06
	Winter	O_3 (ppb)	5.75	1.95	10.33	1.68
		NO_2 (ppb)	52.42	27.05	79.81	11.66
		CO (ppm)	1.16	0.37	2.24	0.44
		SO_2 (ppb)	7.89	3.95	11.65	1.66
		PM10 (μg/m^3)	89.31	60.32	118.35	13.90

Table 7.1 Descriptive statistics for seasonally-summarized hourly concentrations

Season	Variable	Mean	Minimum	Maximum	Std
Spring	Solar radiation (MJ/㎡)	0.64	0.00	1.86	0.68
	Wind Speed (m/s)	2.27	1.50	3.24	0.62
	Temperature (˚C)	12.50	8.93	16.61	2.60
	Humidity (%)	57.10	42.75	71.38	9.72
Summer	Solar radiation (MJ/㎡)	0.56	0.00	1.49	0.55
	Wind Speed (m/s)	1.68	1.12	2.35	0.41
	Temperature (˚C)	23.24	20.63	25.93	1.81
	Humidity (%)	73.68	62.56	84.65	7.92
Autumn	Solar radiation (MJ/㎡)	0.42	0.00	1.37	0.49
	Wind Speed (m/s)	1.74	1.23	2.38	0.40
	Temperature (˚C)	14.73	11.65	18.40	2.20
	Humidity (%)	66.57	50.80	80.30	10.14
Winter	Solar radiation (MJ/㎡)	0.34	0.00	1.17	0.42
	Wind Speed (m/s)	2.32	1.68	3.20	0.53
	Temperature (˚C)	0.33	-2.17	3.49	1.83
	Humidity (%)	59.88	45.62	70.30	8.86

Table 7.2 Descriptive statistics of seasonally-summarized hourly meteorological factors

With the growing use of GIS techniques and related geocoded data, there is an increasing concern regarding spatial autocorrelation in regression models. Spatial dependence[4] was initially defined by Tobler's (1970) first law of geography, in which "everything is related to everything else, but the near things are more related than distant things." The existence of spatial autocorrelation can be expressed by the following equation (Anselin and Bera, 1998):

$$Cov(y_i, y_j) = E(y_i y_j) - E(y_i) \cdot E(y_j) \neq 0 \qquad for\ i \neq j \tag{7.2}$$

where y_i and y_j are observations on a random variable y at locations i and j.

Moran's I (Moran, 1950) is a classic statistics measuring the degree of spatial dependency among observations located over a Cartesian space. Moran's I values are computed with three spatial weight matrices, including the inverse distance, the inverse distance squared, and the 4 nearest neighbors. Moran's I values range from -1 to 1, and 0 indicates no spatial correlation. Z-scores are derived from Moran's I values. If the absolute value of the Z-score is greater than 1.96,

[4] The terms of spatial dependence and spatial autocorrelation are used interchangeably by Anselin (1988).

then spatial autocorrelations exists at the 5% significance level. Table 7.3 shows that there is no spatial autocorrelation in the annual averaged concentrations of the five pollutants.

Weight Matrix	Pollutants	Moran's I	Z-score	p-value
Inverse distance	NO_2	0.07	0.74	0.46
	CO	-0.01	0.16	0.87
	O_3	0.20	1.65	0.10
	SO_2	-0.07	-0.27	0.79
	PM10	-0.03	-0.02	0.98
Inverse distance squared	NO_2	-0.20	-0.70	0.48
	CO	-0.03	-0.02	0.99
	O_3	0.32	1.45	0.15
	SO_2	-0.31	-1.14	0.25
	PM10	0.01	0.16	0.87
K-Nearest neighbors (4 neighbors)	NO_2	0.05	0.78	0.44
	CO	-0.15	-1.19	0.23
	O_3	0.00	0.31	0.76
	SO_2	-0.03	0.00	1.00
	PM10	-0.02	0.08	0.93

Table 7.3 Moran's I for the annual average pollution concentrations

7.2.2 Model Specification

A panel data set is created by the pooling of time-series and cross-sectional observations. It is also called as pooled dataset, time-series cross-sectional dataset, or longitudinal dataset. Regression models based on such data are called panel data regression models. As demonstrated in Chapter 6, traffic flows are a key determinant of the concentrations of both directly emitted and secondary pollutants. Since concentrations and traffic flows vary over space and time, it is proposed here to measure the spatiotemporal variations of the dependent and independent variables across geographical locations (AQMs) and hours of the day in a given region and period (e.g. season). As a reasonable proxy for traffic emissions, daily VKT is calculated for each link and apportioned to each buffer (ring and sector), as discussed in Chapter 4. Ordinary weekday activities are the basis of constructing the OD table, and hence the estimated VKT can be used to explain the pollution concentrations measured during weekdays. Since transportation activities are

expected to display significant differences between weekdays and weekend, VKTs calculated using weekday OD cannot be converted into weekend VKTs. The total daily weekday VKT is divided into hourly VKTs by using hourly traffic counts, as discussed in Chapter 4. These hourly estimated VKTs are next adjusted for each of the 12 months by using the monthly adjustment factors presented in Table 4.2. Since weekend VKTs are missing, a complete hourly panel data set for a whole year is not possible. As shown in Chapter 5, pollution concentrations display significant differences among the four seasons. In order to compare the differential impacts of the explanatory variables on pollution concentrations across the four seasons, weekday hourly concentrations are averaged over each season, generating four seasonal hourly panel data sets, each with 816 observations (34 AQMs × 24 hours).

The basic explanatory variables in the panel regression model are VKTs, four land uses[5], four meteorological factors, and two dummy variables (a roadside vs. background AQM dummy variable as discussed in Chapter 6, and a daytime dummy variable). Interaction terms between the dummy variables and the other regressors are included in the models. VKTs vary over space (AQMs) and time (24 hours). In contrast, land uses are time-invariant and meteorological variables, such as solar radiation, temperature, wind speed, and humidity, are space-invariant. Hourly meteorological variables are averaged over each season. Four regression models are formulated and their estimates are compared. Wind-direction-weighted VKTs and land-use variables are recomputed for each season, and optimal distance decay parameters are determined. If a distance decay function does not improve the explanatory power of the model, then the best-radius-buffer for a variable is used instead. The proposed panel regression model is expressed as:

$$C_{it}^{p} = \alpha + \sum_{j=1}^{J} \beta_j X_{itj} + \sum_{j=1}^{J} \gamma_{jl} \left(X_{itj} \times D_R \right) + \sum_{j=1}^{J} \delta_{jl} \left(X_{itj} \times D_D \right) + u_{it} \tag{7.3}$$

where the indices and variables are defined as follows:

p: Pollutant (O_3, NO_2, SO_2, CO, and PM10),

i: Cross-sectional observation (1 → 34 AQMs),

t: Time-series observation (1 → 24 hours),

C: Pollution concentration

[5] Since there is a strong collinearity between VKT and transportation land-use, the latter is not retained in this analysis.

X: Explanatory variables (VKT, four land uses, and four meteorological factors; $J = 9$),

D_R: AQM dummy variable (if the observation is measured at a roadside AQM, then $D_R = 1$, otherwise $D_R = 0$),

D_D: Daytime dummy variable (if the observation is measured during daytime, then $D_D = 1$, otherwise $D_D = 0$),

u_{it}: Error term for AQM i and hour t.

As demonstrated in Chapter 6, the impacts of VKT and solar radiation on concentrations vary spatially (roadside vs. background) and temporally (weekdays vs. Sunday). These differentiated impacts are also likely in the panel models. Since roadside AQMs tend to be more impacted by vehicle emissions than background AQMs, the concentrations at roadside AQMs are generally higher for directly emitted pollutants. In contrast, in the case of O_3, the concentrations at roadside AQMs are lower, because O_3 titration is a dominant reaction in roadside areas, resulting in less O_3 accumulation. The introduction of interaction terms between the basic explanatory variables and the locational dummy variable will allow for testing the effects of the original regressors under different locational conditions. In addition, the chemical reaction rates are different in daytime and nighttime. Including a temporal dummy variable and related interaction terms may help assess these temporal differences.

Seasonal conditions generate different direct and indirect impacts on pollution concentrations. For example, the cold season requires more fossil fuel consumption for space heating, and also induces incomplete combustion, which further increases concentrations. In contrast, there is less consumption of fossil fuels during the warm season, but biogenic VOCs (BVOCs) are actively emitted by vegetation, leading to favorable conditions for generating O_3. The differential impacts of the explanatory variables across the four seasons can be analyzed by comparing the estimate coefficients of the four seasonal panel models.

If the error term in Eq. (7.3), u_{it}, is uncorrelated with the regressors, the estimates of the pooled data regression model are unbiased and efficient. However, such a model would not differentiate the impacts of the explanatory variables across AQMs or their hourly impacts along the temporal dimension. If time-invariant and space-invariant variables contribute to explaining concentrations, it is necessary to include these variables into the panel regression models. Since land uses are constant over time and meteorological factors are constant over space, the former

variables are classified as time-invariant, and the latter as space-invariant. The unobserved time-invariant and space-invariant factors must be represented in the error term, with:

$$u_{it} = \mu_i + \lambda_t + \varepsilon_{it} \tag{7.4}$$

where μ_i denotes the unobservable cross-sectional effect, λ_t the unobservable time-series effect, and ε_{it} the remaining disturbance[6]. The general assumptions of the random effects model are:

$$\mu_i \sim \mathrm{N}\,(0,\ \sigma_\mu^2),$$
$$\lambda_t \sim \mathrm{N}\,(0,\ \sigma_\lambda^2),$$
$$\varepsilon_{it} \sim \mathrm{N}\,(0,\ \sigma_\varepsilon^2),$$
$$E(\mu_i\, \varepsilon_{it}) = 0,\ \ E(\mu_i\, \mu_j) = 0\ \ (i \neq j),$$
$$E(\lambda_t\, \varepsilon_{it}) = 0,\ \ E(\lambda_t\, \lambda_s) = 0\ \ (t \neq s),$$
$$E(\varepsilon_{it}\, \varepsilon_{jt}) = E(\varepsilon_{it}\, \varepsilon_{is}) = E(\varepsilon_{it}\, \varepsilon_{js}) = 0\ \ (i \neq j;\ t \neq s).$$

The unobservable AQM-specific effects are explained by μ_i, possibly including unobserved emissions from biogenic and other anthropogenic sources. λ_t is space-invariant, and thus accounts for specific time-series effects not included in the regression equation. Model (7.4) is referred to as a two-way random model. If the error specification (7.4) includes only one of these effects, it is called one-way random model.

If the intercept in Eq. (7.3), α, is replaced by α_i (different intercept for each cross-sectional unit), the model is called as a one-way fixed-effects regression model with respect to space. If the intercept varies across time but not across AQMs, then the intercept is expressed as α_t. If the intercept varies over both time and space, it is noted α_{it}, and the model is a two-way fixed model. As seen in Appendix I, in the case of O_3 and the spring season, the intercept coefficients of the one-way fixed effects regression model with respect to (w.r.t.) space are statistically significant, except for a few AQMs, and the F-test for the null hypothesis of no fixed effects is rejected, suggesting that the 34 AQMs are heterogeneous. Similarly, the intercept coefficients of the one-way fixed effects regression model w.r.t. time are significant, and the F-test indicates that the

[6] It is assumed that the error term is $\varepsilon_{it} \sim IID\ (0,\sigma_\varepsilon^2)$, independently and identically distributed with zero mean and constant variance.

hourly observations across AQMs are also heterogeneous. Land uses are not included in the one-way fixed-effects model w.r.t. space and meteorological factors are not included in the one-way fixed-effects model w.r.t. time, because land uses are time-invariant and meteorological factors are space-invariant. These two sets of variables could cause perfect multicollinearity with α_i and α_t, respectively. Although the results of the F-tests for both models suggest that fixed effects models are better than random effects models, they are not sufficient to conclude that the fixed effects model is appropriate to estimate the air quality panel models.

If serial correlation is present in panel data, estimation without correcting for auto-correlation is inefficient. If the error structure is assumed to be first-order autoregressive, the Parks method (Parks, 1967) can be considered for estimating the regression model. The specification of the first-order autoregressive error term is as follows:

$$u_{it} = \rho_i u_{i,t-1} + \varepsilon_{it} \tag{7.5}$$

where ρ_i is the first order autoregressive parameter, which is estimated for each cross-section. Since there are fixed effects w.r.t. space (AQMs) and time (hours), this error specification has limitations in differentiating these effects. According to Kmenta (1986)[7], the use of dummy variables is a cover-up of the incomplete knowledge regarding the true model. However, the theoretical reviews in Chapter 2 suggest that the traffic emissions and solar radiation variables create different impacts between roadside and background areas. In addition, the impacts of the original regressors vary, depending on the intensity of solar radiation. The inclusion of the locational dummy variable in the time-series models in Chapter 6 has provided reasonable and significant results. Therefore, it is reasonable to assume that the two proposed dummy variables and their interactions with the regressors will help capture these locational and temporal differences. Panel data including hourly measured pollution concentrations can be expected to have strong positive autocorrelation, and therefore the estimation method should correct for autocorrelation. The error specification in Eq. (7.5) and the introduction of both cross-sectional

[7] Jan Kmenta (1986), Elements of Econometrics, 2nd ed., Macmillan, New York, p. 633. "*An obvious question in connection with the covariance model (e.g. fixed effects model) is whether the inclusion of the dummy variables – and the consequent loss of the number of degree of freedom – is really necessary. The reasoning underlying the covariance model is that in specifying the regression model we have failed to include relevant explanatory variables that do not change over time (and possibly others that do change over time but have the same value for all cross-sectional units), and that the inclusion of dummy variables is a cover-up of our ignorance*."

and time-series dummy variables should produce a realistic model. Parks method is used to estimate the parameters of the panel regression models (See the SAS® PANEL procedure[8]).

The input panel data set must be sorted by cross-section and by time-series. Inappropriately sorted panel data generates irrelevant results. The debates between Ailawadi, Farris, & Parry (1994) and Balasubramanian & Kumar (1990) indicate the importance of sorting panel data appropriately before estimating the parameters.

[8] http://support.sas.com/documentation/cdl/en/etsug/60372/HTML/default/etsug_panel_sect033.htm
If the number of time-series units is less than the number of cross-section units, then the Parks method produces an error message that the phi matrix is singular. To fix this problem, the number of cross-sectional observations is reduced to the number of time-series observations. In order to compare the different impacts of background AQMs and roadside AQMs, 17 out of the 27 background AQMs are randomly selected. In the case of roadside AQMs, all 7 AQMs are selected. Therefore, the number of observations for the estimation of the panel models in Chapter 7 is 576 (24 AQMs × 24 hours).

7.3 ESTIMATION RESULTS

Four seasonal panel models are estimated for each pollutant. The explanatory variables related to emission sources are recalculated with distance decay factors depending on ring radii. The parameters of the distance decay functions presented in Eq. (7.1) are calculated and the results are presented in Table 7.4. The estimated parameters for the distance decay functions vary across emission sources and pollutants. Some pollutants and emission sources have no distance decay effect. If there is an optimal solution, then the parameters for the closer rings are greater than those for the farther ones, suggesting that the distance decay approach can improve the results of the panel models. If there are no distance decay effects, then the best radius buffer is used instead.

Pollutant	Variables	Ring Radius										
		500	1000	1500	2000	2500	3000	3500	4000	4500	5000	5500
O_3	WVKT	-	-	-	-	-	-	-	-	-	-	-
	Commercial	4.5	3.2	2.6	2.2	2.0	1.8	1.7	1.6	1.5	1.4	1.3
	Residential	-	-	-	-	-	-	-	-	-	-	-
	Industrial	-	-	-	-	-	-	-	-	-	-	-
	Vegetative	-	-	-	-	-	-	-	-	-	-	-
NO_2	WVKT	1.4	0.7	0.4	0.3	0.3	0.2	0.2	0.2	0.1	0.1	0.1
	Commercial	1.8	1.5	1.3	1.2	1.1	1.1	1.0	1.0	1.0	0.9	0.9
	Residential	-	-	-	-	-	-	-	-	-	-	-
	Industrial	-	-	-	-	-	-	-	-	-	-	-
	Vegetative	-	-	-	-	-	-	-	-	-	-	-
SO_2	WVKT	1.8	0.4	0.2	0.1	0.1	0.0	0.0	0.0	0.0	0.0	0.0
	Commercial	-	-	-	-	-	-	-	-	-	-	-
	Residential	-	-	-	-	-	-	-	-	-	-	-
	Industrial	-	-	-	-	-	-	-	-	-	-	-
	Vegetative	-	-	-	-	-	-	-	-	-	-	-
CO	WVKT	1.0	0.2	0.1	0.0	0.0	0.0	0.0	0.0	0.0	0.0	0.0
	Commercial	3.6	1.5	0.9	0.6	0.5	0.4	0.3	0.3	0.2	0.2	0.2
	Residential	-	-	-	-	-	-	-	-	-	-	-
	Industrial	-	-	-	-	-	-	-	-	-	-	-
	Vegetative	-	-	-	-	-	-	-	-	-	-	-
PM10	WVKT	-	-	-	-	-	-	-	-	-	-	-
	Commercial	-	-	-	-	-	-	-	-	-	-	-
	Residential	6.4	1.3	0.5	0.3	0.2	0.1	0.1	0.1	0.0	0.0	0.0
	Industrial	1.0	0.3	0.2	0.1	0.1	0.1	0.1	0.0	0.0	0.0	0.0
	Vegetative	-	-	-	-	-	-	-	-	-	-	-

Table 7.4 Parameters of distance decay functions

7.3.1 Results for O_3 panel models

The estimation results for the O_3 panel regression model, based on Eqs. (7.3) and (7.5), are presented in Table 7.5. The first-order autoregressive parameters are obtained before estimating the regressor coefficients. The autocorrelation in the panel dataset is removed, and then the generalized least squares (GLS) method is applied to calculate consistent estimators. The estimated first-order autoregressive parameters (Rho) are presented in Appendix J.

As discussed in Chapter 6, traffic and solar radiation generate opposite effects on O_3 concentrations. NO emissions from traffic flows are generally related to O_3 titration, leading to a decrease in O_3 concentrations. In contrast, UV radiation decomposes NO_2 and provides ground-state oxygen for the generation of O_3. As expected, the signs of the WVKT coefficients are negative and those of the solar radiation coefficients are positive across the four seasons. The coefficients of WVKT are relatively stable (-0.69 ~ -0.81) across the four models, but those of solar radiation vary significantly (5.35 ~ 27.43), higher during Spring and Summer, and lower during Autumn and Winter. Since intense UV radiation in Summer create very favorable conditions for O_3 generation, the magnitude of the corresponding coefficient (27.43) is not surprising. Interestingly, the coefficients for Spring and Autumn are close, reflecting the intermediate solar radiation conditions in these two seasons. Figure 4.17 in Chapter 4 displays the seasonal variations of solar radiation, and these are consistent with the variations of the coefficients of solar radiation. The theory regarding the impacts of UV radiation on O_3 generation is further confirmed here.

The hourly time-series O_3 models presented in Chapter 6 include quadratic terms for traffic counts and solar radiation. However, inclusion of similar terms in the panel models was not possible, due to multicollinearity. Interaction terms between the locational and temporal dummy variables and the regressors have been retained, allowing for different slopes for the regressors under different locational (roadside AQMs vs. background AQMs) and temporal (daytime vs. nighttime) conditions. There are two significant interaction terms between WVKT and these dummy variables, both with positive coefficients. Thus, the negative effect of WVKT on O_3 concentrations is reduced at roadside locations and during daytime. The interaction term between solar radiation and the roadside dummy variable is retained across the four models, and its coefficient of is always significant and negative, suggesting that conditions for O_3 generation are less favorable in roadside areas. In Winter, the resulting effect of solar radiation is close to zero at roadside areas. Since there is no solar radiation during nighttime, the interaction between solar radiation and the daytime dummy variable is not retained in the final model.

Three land uses – commercial, residential, and vegetative area – are included in the O_3 models. The estimate coefficients for these three variables are consistent across the four seasons, except for the commercial variable. Since NO gases are emitted from commercial and residential areas, the estimates of these two variables are expected to be negative. For the commercial variable, the Spring and Summer models display negative signs, but the Autumn and Winter models display positive signs. A possible explanation for this unexpected result is that commercial activities also emit anthropogenic VOCs during Autumn and Winter, which may act towards increasing O_3 concentrations, overcoming the negative NO effects, particularly in seasons of reduced solar radiation. Vegetative areas have two types of impacts on O_3 concentrations. Plants have an O_3 assimilation capacity, but also emit biogenic VOCs (BVOC) during the growing seasons, generating simultaneous negative and positive impacts. In addition, green areas near AQMs may crowd out other land uses that would generate NO and reduce O_3 concentrations. The coefficient estimates for the vegetation variable are all positive, suggesting that overall green areas increase O_3 concentrations.

There are both negative and positive impacts of wind on O_3 concentrations. Strong wind expedites the dispersion of pollutants. Light wind, however, contributes to scattering effects that enhance photochemical reactions. Figure 4.20 in Chapter 4 displays the seasonal variations of wind speed. Wind speed during Spring and Winter is higher than during Summer and Autumn, which is not consistent with the magnitude and sign of the coefficients across the four seasons, calling for further research. Temperature is known to facilitate O_3 generation, and thus hot Summer days are generally related to high O_3 episodes. Therefore, the coefficient estimates for temperature are expected to be positive during the warm season and negative during the cold season. The results are unexpected. Since there is a close correlation between solar radiation and temperature, multicollinearity may be the reason. Water vapor in the atmosphere scavenges pollutants and humidity is also correlated with cloud cover. Therefore, humidity is expected to have a negative impact on O_3 concentrations. Overall, humidity has negative effects, except in Winter. However, the negative effect in Summer is not significant. As seen in Figure 4.18 in Chapter 4, the seasonal patterns of hourly humidity are opposite to the hourly O_3 concentrations. The differences of humidity between nighttime and daytime during Summer are relatively smaller than in the other seasons, possible producing the insignificant Summer coefficient.

Season	Spring			Summer			Autumn			Winter		
Regressors	Parameter	t Value	Pr > | t |	Parameter	t Value	Pr > | t |	Parameter	t Value	Pr > | t |	Parameter	t Value	Pr > | t |
Intercept	68.53	14.65	<.0001	52.96	4.26	<.0001	15.53	4.87	<.0001	3.00	3.61	0.000
WVKT_R5500	-0.81	-14.13	<.0001	-0.71	-7.39	<.0001	-0.71	-44.72	<.0001	-0.69	-26.69	<.0001
Commercial_DD	-2.48	-2.64	0.009	-1.53	-1.85	0.065	2.39	9.79	<.0001	3.40	9.56	<.0001
Residential_R5000	-2.47	-9.92	<.0001	-2.22	-18.37	<.0001	-1.37	-12.29	<.0001	-0.67	-10.30	<.0001
Vegetative_R1000	2.33	6.14	<.0001	0.87	2.85	0.005	0.02	0.14	0.888	0.70	3.46	0.001
Solar Radiation	17.53	28.76	<.0001	27.43	39.80	<.0001	12.90	53.80	<.0001	5.35	22.46	<.0001
Wind Speed	-1.12	-2.35	0.019	-3.26	-6.06	<.0001	-0.47	-2.83	0.005	0.45	2.89	0.004
Temperature	-1.99	-8.94	<.0001	-1.43	-4.21	<.0001	0.01	0.13	0.898	1.11	14.30	<.0001
Humidity	-0.44	-11.88	<.0001	-0.04	-0.65	0.517	-0.08	-3.45	0.001	0.07	6.41	<.0001
WVKT × Roadside Dummy	0.36	9.20	<.0001	0.44	8.03	<.0001	0.44	31.70	<.0001	0.47	27.57	<.0001
Solar × Roadside Dummy	-8.74	-64.00	<.0001	-11.77	-127.06	<.0001	-7.97	-64.77	<.0001	-5.62	-67.50	<.0001
WVKT × Daytime Dummy	0.06	4.87	<.0001	0.37	27.76	<.0001	0.09	6.13	<.0001	0.05	5.53	<.0001
Roadside AQM Dummy	-1.88	-4.61	<.0001	-1.80	-8.61	<.0001	-2.63	-21.88	<.0001	-2.36	-22.88	<.0001
Daytime Dummy	-0.85	-5.09	<.0001	-3.88	-13.42	<.0001	-0.97	-7.21	<.0001	-0.53	-6.12	<.0001
R^2		0.993			0.992			0.989			0.979	

Table 7.5 Results of O_3 panel regression models estimation

The two interaction variables related to the roadside dummy variable indicate that both the negative effect of WVKT and the positive effect of solar radiation are reduced at roadside locations. In addition, there is a negative intercept shift at roadside areas in all seasons, suggesting that there are additional unfavorable factors for O_3 generation at roadside areas. During daytime, O_3 the creation and destruction reactions occur simultaneously. Since the estimate of the WVKT interaction variable related to the daytime dummy variable is positive, the destruction impact is reduced during daytime. However, there may be other factors reducing O_3 concentrations during daytime, as reflected by the negative and significant coefficients of the daytime dummy variable in all seasons.

To interpret the impacts of traffic emissions and solar radiation on O_3 concentrations, the elasticities of the O_3 model w.r.t. these two variables are computed, using the derivative functions of the O_3 models and the original observations for each season. Summary statistics for the calculated elasticities are presented in Table 7.6. Since the derivative functions calculated across the four models include the roadside and daytime dummy variables, the elasticities w.r.t. WVKT and solar radiation necessarily vary between roadside AQMs and background AQMs, and daytime and nighttime.

As discussed in Chapter 2, traffic flows are generally negatively correlated with O_3 concentrations, because NO emissions from tail pipes react with ambient O_3, and generate NO_2 and O_2. The generated NO_2 is then converted into NO again under the presence of UV radiation. If radicals, such as $RO_2\cdot$ and $HO_2\cdot$, are abundant in the atmosphere, NO reacts with these radicals instead of O_3, providing a chance to accumulate O_3. The radicals are generally correlated with VOCs and their oxidation processes. Therefore, O_3 concentrations are determined by diverse factors, including the amount of NO_x and VOCs emissions, the intensity of solar radiation, the ratio of VOCs/NO_x, and the interactions between these factors. As expected, the elasticities w.r.t. WVKT are mostly negative. However, they turn out to be positive in specific situations, such as intense solar radiation. When solar radiation exceeds a certain level, the rate of O_3 generation exceeds the rate of O_3 destruction, leading to a shift from negative to positive impacts. This shift is observed only in Summer in the roadside case. Significantly lower elasticities are observed in the background case in the Autumn and Winter models. These low elasticities cannot be explained with this summary table, calling for further analysis of the timing of these extreme elasticities.

The elasticities of the O_3 functions w.r.t. solar radiation are generally positive. Since nighttime is longer in the cold season, zero impacts are more frequently observed in Autumn and Winter in both the background and roadside cases. In addition, background areas have more

favorable conditions for generating O_3 than roadside areas, and the background elasticities w.r.t. solar radiation are higher than the roadside elasticities. A 1% change in solar radiation in Summer induces an average 0.73% and 0.68% increase in O_3 concentrations in background and roadside areas, respectively. When average elasticities are compared across the four seasons, the Summer elasticities are the highest, supporting the theory that intense UV radiation induce high O_3 concentrations. A shift from positive to negative impacts is observed in the Winter roadside case, since Winter solar radiation is very weak, leading to lower O_3 generation than in the other seasons. In addition, as discussed in Chapter 6, O_3 titration is active in roadside areas. The combination of these two effects leads to a shift from positive to negative impacts in the Winter roadside case.

Variable	AQM	Season	Min	10th Pctl	Lower Quartile	Median	Mean	Upper Quartile	90th Pctl	Max
WVKT	Background	Spring	-1.16	-0.60	-0.39	-0.21	-0.29	-0.14	-0.08	-0.01
		Summer	-1.07	-0.47	-0.24	-0.12	-0.19	-0.07	-0.04	-0.01
		Autumn	-3.77	-1.07	-0.65	-0.33	-0.50	-0.21	-0.11	-0.02
		Winter	-6.09	-1.04	-0.70	-0.37	-0.54	-0.23	-0.12	-0.02
	Roadside	Spring	-0.85	-0.51	-0.37	-0.29	-0.29	-0.16	-0.11	-0.06
		Summer	-0.60	-0.25	-0.10	0.04	-0.03	0.08	0.11	0.22
		Autumn	-1.10	-0.55	-0.35	-0.23	-0.28	-0.15	-0.12	-0.09
		Winter	-0.77	-0.36	-0.28	-0.21	-0.23	-0.16	-0.09	-0.06
Solar Radiation	Background	Spring	0.00	0.00	0.01	0.51	0.49	0.88	1.00	1.29
		Summer	0.00	0.00	0.11	0.92	0.73	1.14	1.33	1.77
		Autumn	0.00	0.00	0.00	0.37	0.41	0.77	0.93	1.31
		Winter	0.00	0.00	0.00	0.08	0.18	0.35	0.48	0.95
	Roadside	Spring	0.00	0.00	0.01	0.39	0.46	0.71	1.21	1.74
		Summer	0.00	0.00	0.10	0.83	0.68	1.18	1.30	1.55
		Autumn	0.00	0.00	0.00	0.17	0.26	0.51	0.60	0.77
		Winter	-0.07	-0.04	-0.03	-0.01	-0.01	0.00	0.00	0.00

Table 7.6 Summary statistics for the elasticities w.r.t. WVKT and solar radiation in the O_3 models[9]

The patterns of average hourly elasticities w.r.t. the WVKT and solar radiation variables are illustrated in Figures 7.3 and 7.4. As discussed in Chapter 6, traffic emissions and solar radiation are key factors in determining O_3 concentrations, and therefore analyses of hourly elasticities are conducted for these two variables. The hourly elasticities are classified into eight groups (background and roadside by four seasons), and these groups are compared on each graph.

[9] Detailed statistics on the hourly elasticities in the O_3 models are presented in Appendix K.

Since background areas provide better conditions for O_3 generation than roadside areas, background elasticities are generally lower than those of roadside. The negative WVKT elasticities decrease during daytime and reach zero around 3 to 4 P.M., when cumulative UV radiation reach their peak. During nighttime, O_3 generation is not possible because there is no solar radiation. The concentrations of ambient O_3 during nighttime are lower than during daytime, and therefore O_3 titration is less active at night. Consequently, the negative elasticities decrease and approach zero again. The lowest elasticities occur in the morning traffic peak hours around 8 to 9 A.M., when solar radiation is not yet intense enough to generate O_3, particularly in Autumn and Winter. The increased emissions from morning traffic flows induce active O_3 titration and ambient O_3 scavenging. As seen in Chapter 5, the hourly O_3 concentrations are the lowest during the morning traffic peak hours. A shift from negative to positive elasticities is observed during daytime in the Summer roadside case. For this time period, solar radiation exceeds a certain level, and its effect overwhelms traffic effects.

The hourly elasticities w.r.t. solar radiation are illustrated in Figure 7.4. As background regions have better conditions for generating O_3, the elasticities for background areas are positive and higher than those for roadside areas across the four seasons, except for a few cases during daytime in the Summer and Spring. Since the intensity of solar radiation in Summer is the highest among the four seasons, the Summer elasticities are the highest in both the background and roadside cases, supporting the positive relationship between UV radiation and O_3 generation. Negative elasticities are observed in the Winter roadside case. Weak solar radiation in Winter lead to lower O_3 generation. In addition, O_3 titration is active in roadside areas. These two factors induce the lowest O_3 concentrations in Winter roadside areas. The rate of Winter O_3 generation induced by solar radiation turns out to be negated by the increased O_3 titration effect at roadside areas, with, consequently, negative elasticities.

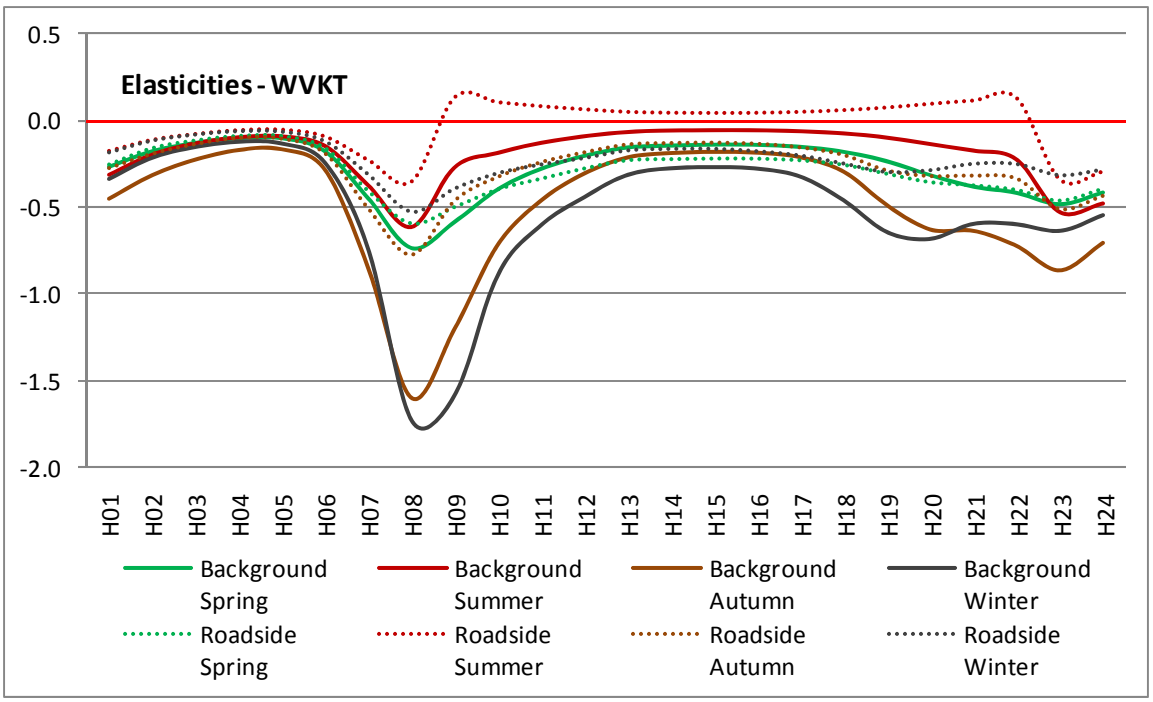

Figure 7.3 Average hourly-seasonal elasticities w.r.t. WVKT in the O_3 models

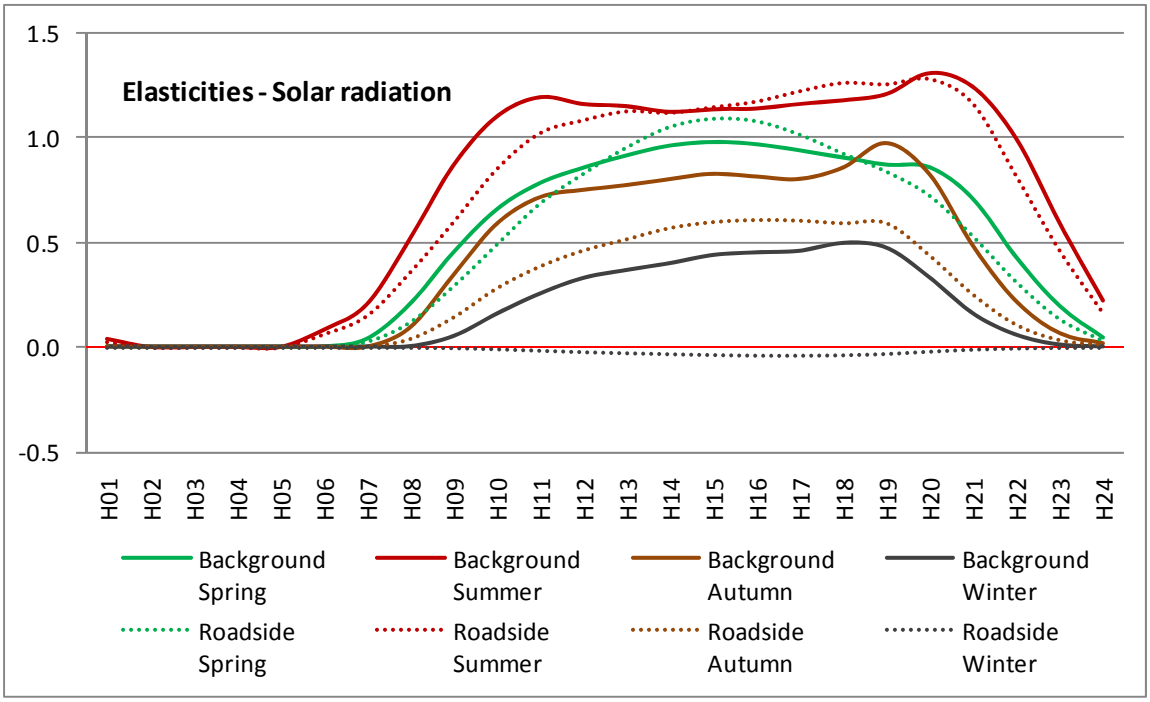

Figure 7.4 Average hourly-seasonal elasticities w.r.t. solar radiation in the O_3 models

7.3.2 Results for NO_2 panel models

The estimation results for the NO_2 panel models are presented in Table 7.7. The results point to positive and very significant coefficient estimates for WVKT across the four seasons. Emissions from traffic flows are the direct sources of NO_x, and most of the NO_x are emitted in the form of NO, which is quickly transformed into NO_2 by reaction with O_3 (Eq. 2.1), organic peroxy radicals (Eq. 2.2), and hydroperoxy radicals (Eq. 2.7). In the urban atmosphere, these two radicals are generated in the process of anthropogenic and biogenic VOCs oxidation.

As discussed in Chapter 2, solar radiation has a negative impact on NO_2 concentrations, because NO_2 is decomposed by UV radiation (Eq. 2.8) during daytime. The coefficient estimates for solar radiation are negative and significant in all models. Since the intensity of UV radiation is lower during the cold season, the coefficient estimate for Winter solar radiation is, as expected, the smallest in absolute term among the four models.

Since NO gases emitted from vehicles are more likely to be converted into NO_2 at roadside locations, higher NO_2 concentrations are generally observed there. The NO_2 models include two significant interaction variables related to the roadside dummy variable. The coefficient estimates for the WVKT interaction term are positive, supporting the theory that roadside areas represent favorable conditions for high NO_2 concentrations. In addition, a significant interaction variable related to the daytime dummy variable is also included in the NO_2 models. During daytime, negative and positive impacts on NO_2 concentrations occur simultaneously. The negative effects include NO_2 photodissociation and decreased space heating during the warm season. In contrast, anthropogenic activities generally take place during daytime, leading to more NO_x emissions. The coefficient estimates for the daytime interaction variable with WVKT are negative in Spring and Winter, and positive in Summer and Autumn, indicating that the negative effects are dominant in Spring and Winter, and the positive effects in Summer and Autumn. However, the effect in Winter is insignificant. The coefficient estimates for the solar radiation interaction variables are also positive, indicating that the negative impact of solar radiation on NO_2 concentrations is reduced at roadside areas. As background areas are more favorable for generating O_3, the rate of NO_2 photodissociation is greater in background areas than in roadside areas.

Since NO_x gases are expected to be emitted from commercial, residential, and industrial land uses, the estimate coefficients of these three variables are positive, except in the Summer for residential areas. Residential fossil fuel consumption is small in Summer, with much reduced NO_x

emissions. However, instead of being equal to zero (i.e. insignificant), the residential Summer coefficient is negative and significant, an unexpected result calling for further research.

Generally, higher temperatures reduce the consumption of fossil fuels, leading to decreased NO_x emissions, thus explaining the negative coefficient of temperature in Winter. However, the coefficient estimates for temperature are positive for the Spring, Summer, and Autumn models, possibly because of the coincidences of high traffic flows and high temperatures during daytime, and low traffic flows and low temperatures during nighttime. The effects of temperature on NO_2 are essentially opposite those on O_3 (see Table 7.5). As discussed Section 7.3.1, wind may have both positive and negative impacts on pollution concentrations. As wind speed during Spring and Winter is higher than in the other seasons, dispersion effects are expected to be dominant. However, the coefficient estimates for these seasons are positive. The Autumn coefficient is negative, and the Winter one positive. Explaining these unexpected patterns calls for further research. Finally, humidity has generally negative impact on pollution concentrations. This is only true in Winter, and these unexpected results also call for further research. The two dummy variables for roadside AQMs and daytime are not included in the final NO_2 panel models, because the estimate coefficients are insignificant.

Season	Spring			Summer			Autumn			Winter		
Regressors	Parameter	t Value	Pr > | t |	Parameter	t Value	Pr > | t |	Parameter	t Value	Pr > | t |	Parameter	t Value	Pr > | t |
Intercept	-159.67	-16.08	<.0001	-339.61	-20.25	<.0001	-111.57	-13.63	<.0001	45.27	15.46	<.0001
WVKT_DD	5.85	30.92	<.0001	6.08	33.29	<.0001	8.53	35.77	<.0001	7.87	27.78	<.0001
Commercial_DD	4.55	18.68	<.0001	1.30	13.31	<.0001	1.22	4.38	<.0001	0.86	5.27	<.0001
Residential_R1000	1.82	5.87	<.0001	-0.45	-8.67	<.0001	2.20	4.68	<.0001	0.02	0.10	0.923
Industrial_R4500	3.15	18.12	<.0001	1.01	11.65	<.0001	1.90	5.28	<.0001	1.50	16.45	<.0001
Solar Radiation	-29.82	-32.50	<.0001	-18.47	-29.42	<.0001	-12.03	-26.80	<.0001	-7.25	-10.86	<.0001
Wind Speed	7.29	12.24	<.0001	5.42	10.87	<.0001	-2.51	-5.64	<.0001	1.74	3.25	0.001
Temperature	9.13	20.45	<.0001	10.57	23.79	<.0001	5.81	21.14	<.0001	-0.58	-2.23	0.026
Humidity	1.25	15.43	<.0001	1.61	17.81	<.0001	0.86	15.06	<.0001	-0.23	-5.71	<.0001
WVKT × Roadside Dummy	1.34	3.05	0.002	2.26	12.60	<.0001	0.34	1.13	0.257	2.90	35.92	<.0001
Solar × Roadside Dummy	8.46	24.57	<.0001	10.26	48.85	<.0001	5.87	15.26	<.0001	2.19	12.08	<.0001
WVKT × Daytime Dummy	-0.26	-3.97	<.0001	0.82	16.71	<.0001	0.77	9.13	<.0001	-0.12	-0.80	0.422
R^2	0.976			0.984			0.956			0.948		

Table 7.7 Results of NO_2 panel regression models estimation

Summary statistics for the calculated elasticities w.r.t. the WVKT and solar radiation variables are presented in Table 7.8. The hourly elasticities for these two variables are compared across roadside AQMs and background AQMs, and across the four seasons. Traffic flows have positive impacts on NO_2 concentrations at both locations and in all seasons. Higher elasticities are observed at roadside AQMs. A 1% increase in WVKT at background AQMs induces an average 0.14% to 0.26% increase in NO_2 concentrations. In contrast, for roadside AQMs, a 1% increase in WVKT leads to an average 0.18% to 0.29% increase. Two reasons explain these differences in the elasticities w.r.t. WVKT: (1) roadside areas are directly influenced by traffic emissions, and (2) NO emissions from tail pipes immediately react with ambient O_3, generating NO_2. In addition, if radicals, such as $RO_2\cdot$ and $HO_2\cdot$, are present in the atmosphere, NO reacts with these radicals instead of O_3. Generally, these radicals are associated with VOCs oxidation, and anthropogenic and biogenic VOCs are abundant in the urban atmosphere. Therefore, NO emissions can be easily converted into NO_2.

Variable	AQM	Season	Min	10th Pctl	Lower Quartile	Median	Mean	Upper Quartile	90th Pctl	Max
WVKT	Background	Spring	0.02	0.05	0.08	0.13	0.14	0.19	0.23	0.30
		Summer	0.04	0.08	0.11	0.19	0.20	0.29	0.33	0.43
		Autumn	0.04	0.10	0.14	0.25	0.26	0.37	0.44	0.62
		Winter	0.03	0.07	0.11	0.17	0.18	0.24	0.28	0.42
	Roadside	Spring	0.06	0.09	0.13	0.20	0.18	0.24	0.26	0.29
		Summer	0.09	0.14	0.19	0.26	0.26	0.32	0.37	0.53
		Autumn	0.08	0.14	0.21	0.27	0.29	0.39	0.46	0.60
		Winter	0.09	0.14	0.21	0.29	0.28	0.37	0.41	0.48
Solar Radiation	Background	Spring	-2.00	-1.43	-0.89	-0.21	-0.49	0.00	0.00	0.00
		Summer	-1.37	-0.85	-0.58	-0.18	-0.32	-0.02	0.00	0.00
		Autumn	-0.61	-0.43	-0.27	-0.04	-0.14	0.00	0.00	0.00
		Winter	-0.27	-0.18	-0.11	-0.02	-0.06	0.00	0.00	0.00
	Roadside	Spring	-0.92	-0.64	-0.44	-0.12	-0.23	0.00	0.00	0.00
		Summer	-0.26	-0.21	-0.16	-0.06	-0.09	-0.01	0.00	0.00
		Autumn	-0.23	-0.16	-0.09	-0.02	-0.05	0.00	0.00	0.00
		Winter	-0.16	-0.10	-0.06	-0.01	-0.03	0.00	0.00	0.00

Table 7.8 Summary statistics for the elasticities w.r.t. WVKT and solar radiation in the NO_2 models

Since ambient NO_2 is decomposed by UV radiation, the elasticities of the NO_2 functions w.r.t. solar radiation are negative. During nighttime, the photodissociation of NO_2 does not occur,

providing a zero elasticity. Since the Summer season has the shortest nighttime, zero impacts are less frequently observed in the Summer than in the other seasons. As discussed in Chapter 2, background areas are more favorable conditions for generating O_3, suggesting that UV impacts on NO_2 decomposition are greater in background areas. In addition, the impacts of direct NO_x emissions are smaller in background areas, leading to NO_2 concentrations that are more sensitive to solar radiation in background areas. Therefore, stronger negative elasticities are observed at background AQMs than at roadside AQMs. For example, a 1% change in solar radiation in Spring induces an average 0.49% decrease at background AQMs, but the same change at roadside AQMs leads to only an average 0.23% decrease.

The patterns of average hourly elasticities w.r.t. the WVKT and solar radiation on NO_2 concentrations are illustrated in Figures 7.5 and 7.6. Since roadside areas are directly impacted by traffic emissions, the hourly elasticities w.r.t. WVKT are higher at roadside AQMs across the four seasons. The patterns of hourly elasticities match the hourly traffic flow patterns (see Chapter 5). Traffic flow patterns are characterized by two peaks, in the morning and the evening, and sustaining volumes during daytime. The elasticities display similar patterns, except for the evening traffic peak.

The hourly elasticities w.r.t. solar radiation at background AQMs are lower than those at roadside AQMs across the four seasons. Since the intensity of solar radiation in Spring and Summer is higher than in the other seasons, the elasticities during these seasons are the lowest in both the background and roadside cases. During Spring, emissions from space heating are added to traffic emissions, leading to higher NO_2 concentrations in Spring than in Summer. Higher NO_2 concentrations in Spring provide more opportunities for solar radiation to actively decompose NO_2, which may explain the more sensitive elasticities w.r.t. solar radiation during Spring. Weak solar radiation in Winter lead to lower NO_2 decomposition both for roadside and background AQMs.

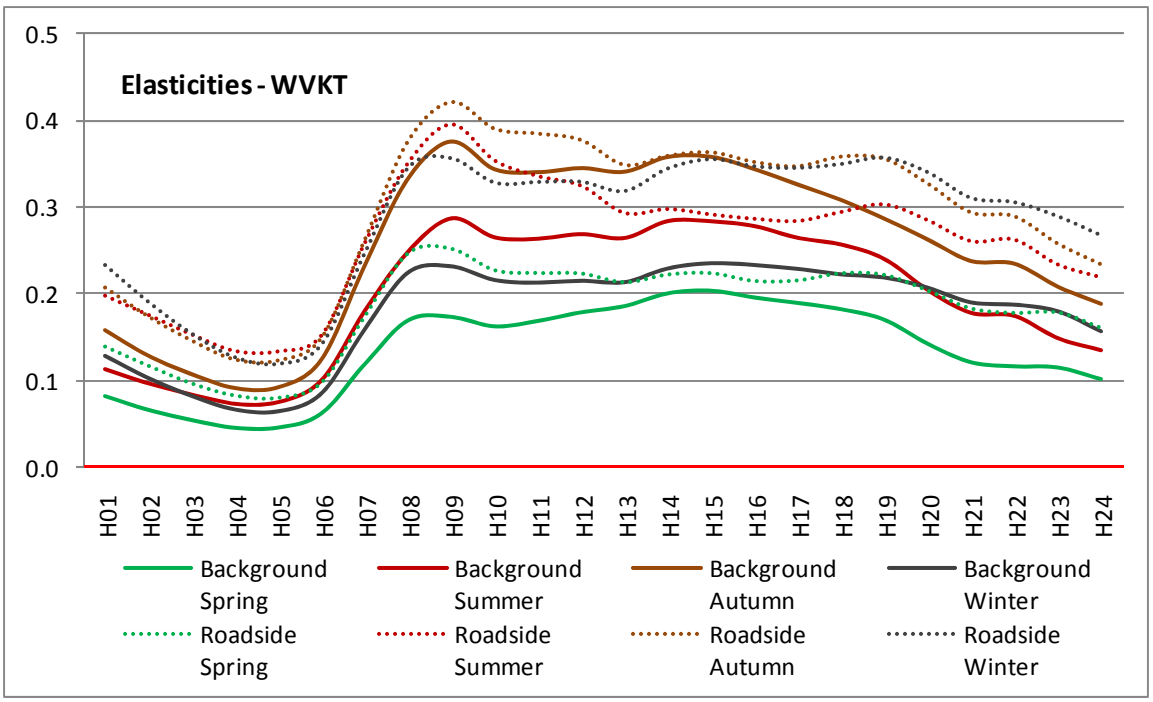

Figure 7.5 Average hourly-seasonal elasticities w.r.t. VKT in the NO_2 models

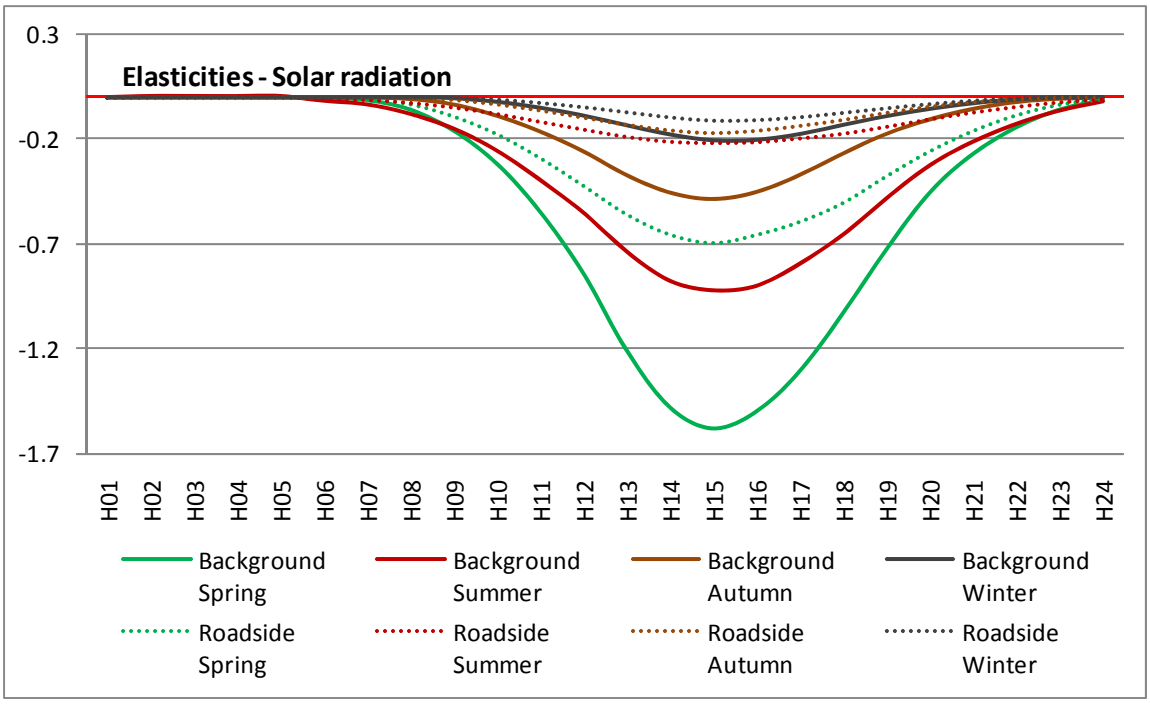

Figure 7.6 Average hourly-seasonal elasticities w.r.t. solar radiation in the NO_2 models

7.3.3 Results for CO panel models

The estimation results for the CO panel models are presented in Table 7.9. Since CO is a directly emitted pollutant, traffic flows are expected to have a positive impact on CO concentrations. The coefficient estimates for WVKT in the CO models are positive across the four seasons, but the Summer estimate is insignificant. The interaction term between WVKT and the roadside dummy variable is positive and significant in all cases. As the benchmark case is background AQMs, the result suggest that traffic flows in roadside areas have more impact on CO concentrations across the all seasons. In addition, the coefficient estimates for the interaction variable between WVKT and the daytime dummy variable are all positive and significant, indicating that, during daytime, positive effects on CO concentrations (traffic and other anthropogenic emissions) overwhelm negative effects (CO oxidation) in all cases. The combination of roadside dummy and daytime dummy effects suggests that roadside areas during daytime provide the best conditions to accumulate CO concentrations.

CO reacts with the OH· and is converted into CO_2 and HO_2·. OH· is generated under the presence of UV radiation, suggesting that solar radiation has a negative impact on CO concentrations. The coefficient estimates of solar radiation are negative for all models. Since the intensity of UV radiation is higher during the warm season, the coefficient estimates for Summer and Autumn are higher in absolute term than for the other seasons. CO oxidation is interwoven with the reaction generating O_3, and thus favorable conditions for O_3 creation induce active CO oxidation, resulting in lower CO concentrations. As discussed in the analysis of the O_3 panel models results, background regions are better places for O_3 generation, and therefore CO oxidation occurs more frequently in background regions. In addition, CO gases are directly emitted from vehicles. For these two reasons, the estimates of the interaction terms between the roadside dummy variable and WVKT are positive across the four models: WVKT impacts on CO concentrations increase at roadside locations. In contrast, the estimates for the roadside dummy and solar radiation interaction term are positive, indicating that the generally negative solar impacts are reduced at roadside areas, supporting the theory that CO oxidation is closely related to O_3 creation.

Residential areas are a source of CO emissions and vegetative areas have pollutant assimilative capacity, and therefore residential areas are expected to have a positive impact on CO concentrations, and vegetative areas to have a negative one. The coefficient estimates of residential land use are positive and significant across the four models, as expected. In contrast, the estimates for the vegetative variables are negative during Spring and Summer, but positive during Autumn and Winter. The negative effects reflect the assimilative capacity of full-grown vegetation

in Spring and Summer. However, the positive impacts during Autumn and Winter are unexpected, calling for further research

In the previous O_3 and NO_2 models, wind speed had both positive and negative effects on pollution concentrations. Although CO is related to O_3 creation, there is no theoretical support for the idea that the scattering effects of wind speed, that favor O_3 creation, also expedite the CO oxidation process. Therefore, it is reasonable to expect that higher wind speed leads to dispersion effects, and thus negative effects on CO concentrations. However, all estimates are positive, except in Autumn.

Since CO is generated by the combustion of fossil fuels for space heating, higher temperatures are expected to produce lower CO emissions. However, as discussed in the analysis of the NO_2 models, lower temperatures do not always increase fossil fuel combustion. Space heating is required only when the temperature crosses a specific threshold during the cold season. The negative estimate for temperature observed in the Winter model supports this rationale. In contrast, the coefficient estimates for the other seasons are positive, though insignificant in Spring. The effects in summer and Autumn call for further research. Finally, a negative relationship would be expected between humidity and CO concentrations, which is the case in all seasons, except Summer.

Season	Spring			Summer			Autumn			Winter		
Regressors	Parameter	t Value	Pr > | t |	Parameter	t Value	Pr > | t |	Parameter	t Value	Pr > | t |	Parameter	t Value	Pr > | t |
Intercept	10.05	12.16	<.0001	-28.75	-6.27	<.0001	4.75	1.13	0.258	21.52	14.21	<.0001
WVKT_DD	2.77	40.95	<.0001	0.06	0.38	0.702	4.90	9.35	<.0001	8.38	15.36	<.0001
Residential_R5000	0.40	7.01	<.0001	1.17	14.78	<.0001	0.93	24.31	<.0001	0.90	12.43	<.0001
Vegetative_R5500	-5.05	-16.09	<.0001	-5.05	-7.57	<.0001	1.34	5.06	<.0001	5.66	28.20	<.0001
Solar Radiation	-2.46	-35.04	<.0001	-4.15	-25.77	<.0001	-4.43	-17.33	<.0001	-2.84	-8.15	<.0001
Wind Speed	0.21	3.25	0.001	0.65	4.97	<.0001	-0.46	-1.88	0.061	0.86	2.95	0.003
Temperature	0.04	1.07	0.284	1.21	10.36	<.0001	0.32	2.37	0.018	-1.67	-12.32	<.0001
Humidity	-0.05	-7.29	<.0001	0.08	3.34	0.001	-0.04	-1.42	0.156	-0.29	-13.52	<.0001
WVKT × Roadside Dummy	5.20	10.31	<.0001	6.36	22.01	<.0001	4.49	15.98	<.0001	3.84	7.47	<.0001
Solar × Roadside Dummy	0.92	15.08	<.0001	1.12	10.25	<.0001	1.44	20.96	<.0001	0.79	3.66	0.000
WVKT × Daytime Dummy	0.24	7.57	<.0001	1.36	23.11	<.0001	1.12	7.56	<.0001	2.91	10.19	<.0001
R^2		0.989			0.933			0.948			0.904	

Table 7.9 Results of CO panel regression models estimation

Table 7.10 present summary statistics for the calculated elasticities w.r.t. the WVKT and solar radiation variables across all seasons and locations. Since traffic flows are a major source of CO emissions, positive elasticities are observed across all cases. Elasticities w.r.t. WVKT are higher at roadside AQMs than at background AQMs. A 1% increase in WVKT leads to an average 0.25% to 0.38% increase in CO concentrations at roadside AQMs, but only 0.09% to 0.22% at background AQMs, as roadside areas are directly influenced by traffic emissions.

Variable	AQM	Season	Min	10th Pctl	Lower Quartile	Median	Mean	Upper Quartile	90th Pctl	Max
WVKT	Background	Spring	0.01	0.03	0.05	0.09	0.09	0.13	0.17	0.24
		Summer	0.00	0.00	0.00	0.04	0.04	0.07	0.08	0.13
		Autumn	0.02	0.05	0.08	0.15	0.17	0.25	0.32	0.48
		Winter	0.03	0.06	0.11	0.19	0.22	0.30	0.42	0.68
	Roadside	Spring	0.05	0.09	0.15	0.24	0.25	0.32	0.42	0.49
		Summer	0.04	0.09	0.15	0.21	0.24	0.35	0.40	0.64
		Autumn	0.05	0.10	0.18	0.30	0.33	0.46	0.62	0.84
		Winter	0.05	0.12	0.19	0.36	0.38	0.49	0.72	0.96
Solar Radiation	Background	Spring	-1.27	-0.89	-0.58	-0.11	-0.30	0.00	0.00	0.00
		Summer	-2.52	-1.34	-0.93	-0.27	-0.50	-0.03	0.00	0.00
		Autumn	-1.68	-1.15	-0.63	-0.08	-0.35	0.00	0.00	0.00
		Winter	-0.77	-0.39	-0.21	-0.02	-0.12	0.00	0.00	0.00
	Roadside	Spring	-0.48	-0.27	-0.19	-0.05	-0.10	0.00	0.00	0.00
		Summer	-0.83	-0.48	-0.32	-0.11	-0.19	-0.02	0.00	0.00
		Autumn	-0.77	-0.41	-0.24	-0.04	-0.14	0.00	0.00	0.00
		Winter	-0.41	-0.22	-0.11	-0.01	-0.07	0.00	0.00	0.00

Table 7.10 Summary statistics for the elasticities w.r.t. WVKT and solar radiation in the CO models

OH· radicals are abundant during daytime, because they are generated in the presence of UV radiation. CO reacts with OH·, and is then converted into CO_2, resulting in elasticities w.r.t. solar radiation that are all negative, except for some zero elasticities, which are more frequently observed during the cold season. Since higher UV radiation cause active CO oxidation, the elasticities during Summer are higher than in other seasons in absolute term. Background regions present favorable conditions for O_3 generation and CO oxidation, and therefore more active CO oxidation is expected in background regions, hence the higher elasticities. CO oxidation is accompanied by OH· radicals, and these radicals are recycled in the O_3 creation process, suggesting that the same amounts of UV radiation in both background and roadside areas lead to

different rates of CO oxidation. As seen in the Table 7.10, the elasticities w.r.t. solar radiation are higher at background AQMs in absolute term, supporting this theory. For example, a 1% increase in solar radiation in Summer leads to an average 0.50% decrease at background AQMs, but only 0.19% decrease at roadside AQMs.

The patterns of average hourly elasticities w.r.t. WVKT and solar radiation are illustrated in Figures 7.7 and 7.8. Since roadside areas are directly influenced by traffic emissions, the hourly elasticities w.r.t. WVKT are higher at roadside AQMs across the four seasons. During daytime, CO gases are actively emitted from traffic flows and other anthropogenic sources, and thus the hourly elasticities are higher during this time period. Since higher temperature reduces incomplete fossil fuel combustion, CO emissions are smaller during the warm season. For these two reasons, the elasticities during Spring and Summer are lower than those during Autumn and Winter at both background and roadside locations.

The hourly elasticities w.r.t. solar radiation are illustrated in Figure 7.8. UV radiation produces OH· radicals, which lead to CO oxidation, resulting in lower CO concentrations. High UV radiation during the Summer produces the lowest elasticities among the four seasons. Background regions have better conditions for O_3 creation and CO is frequently converted into CO_2 in these regions, hence the hourly elasticities for background AQMs are lower than those for roadside AQMs. The negative elasticities w.r.t. solar radiation reach peak around 3 to 4 P.M., when the cumulative UV radiation reach their peak and the generated OH· radicals also reach their maximum.

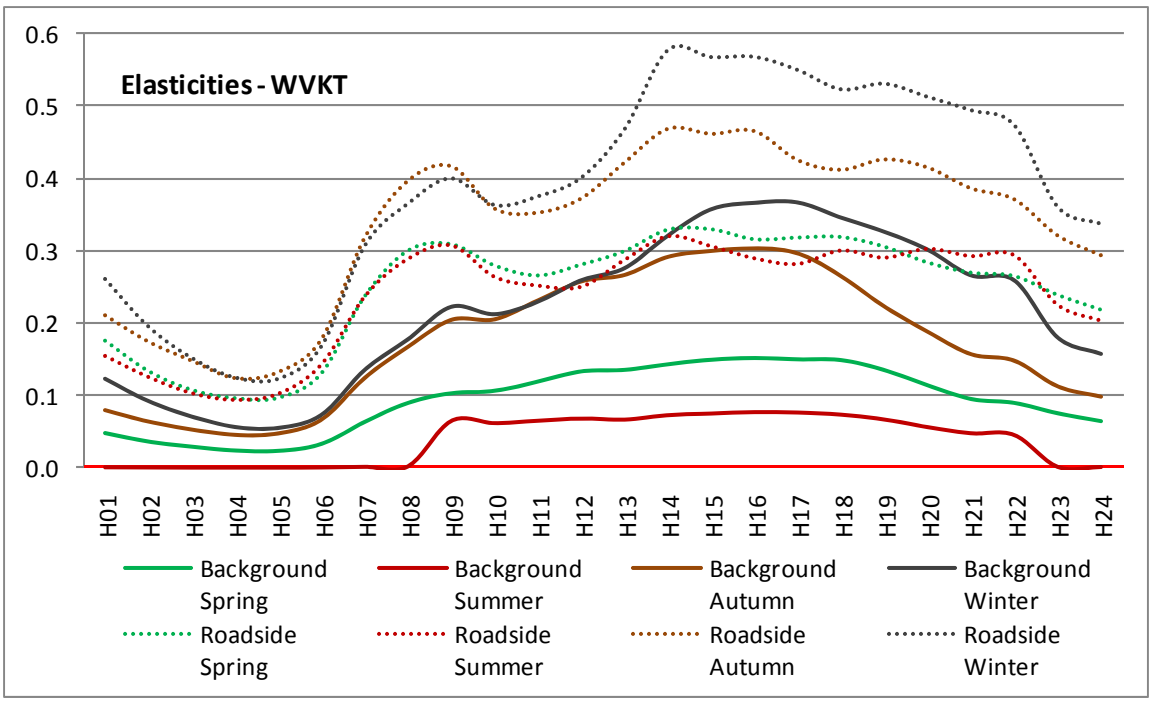

Figure 7.7 Average hourly-seasonal elasticities w.r.t. VKT in the CO models

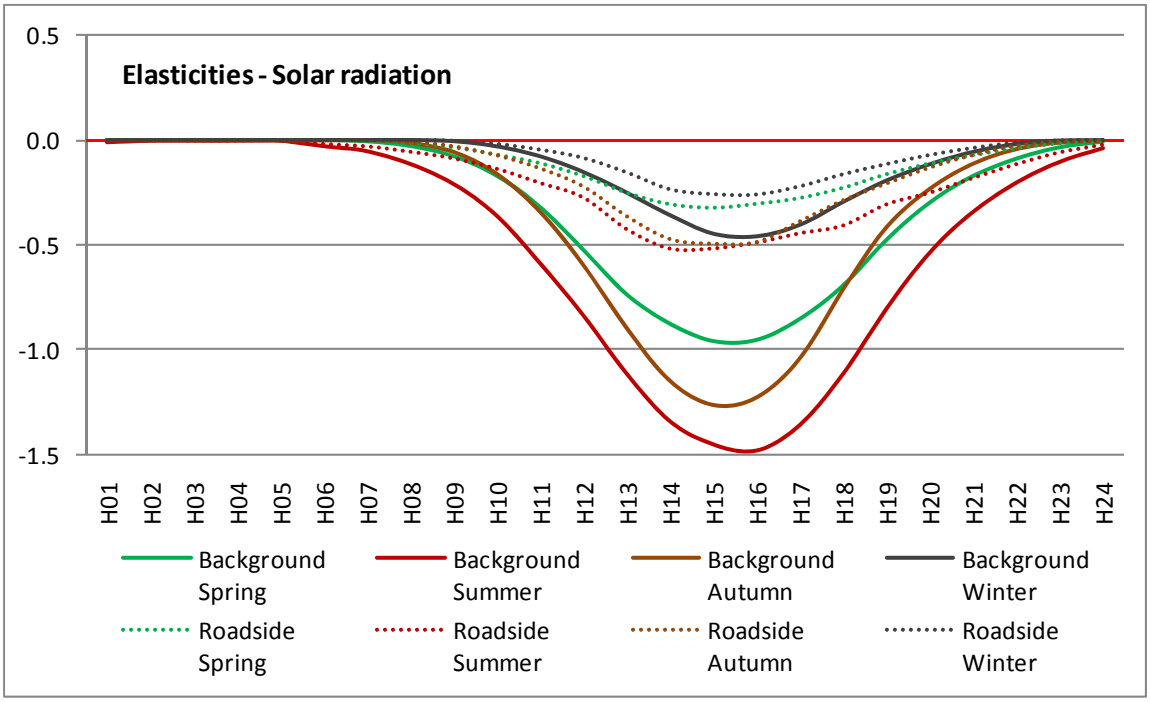

Figure 7.8 Average hourly-seasonal elasticities w.r.t. solar radiation in the CO models

7.3.4 Results for SO_2 panel models

The estimation results for the SO_2 panel models are presented in Table 7.11. Since SO_2 is a directly emitted from diesel vehicles, traffic flows are expected to have a positive impact on SO_2 concentrations. The results point to positive and highly significant coefficient estimates for WVKT across the four seasons. The interaction terms between WVKT and the roadside dummy variable are also positive and significant, suggesting that emissions from diesel vehicles have more impacts on SO_2 concentrations at roadside areas.

Since SO_2 has strong hygroscopic characteristics, OH· and water vapor convert SO_2 into sulfuric acid (H_2SO_4). UV radiation generate OH· radicals. Therefore, solar radiation and humidity are expected to be negatively correlated with SO_2 concentrations. The coefficient estimate of solar radiation and humidity are all negative and highly significant across the four seasons, supporting this theory. The roadside interaction terms related to solar radiation and humidity have been retained in the models, because of their significance across the four models, except for the humidity interaction variable in Winter. The signs of these interaction terms vary, depending on the season. The negative impact of solar radiation is reduced during Spring, Summer, and Autumn at roadside areas, but is increased during Winter. Humidity increases concentrations in Spring and Autumn at roadside areas, but decreases them in Summer.

SO_2 is generated by the combustion of sulfur-containing fossil fuels, and hence a positive relationship is expected between commercial areas and SO_2 concentrations. The estimated coefficients for commercial areas are positive in Spring and Summer, but negative in Autumn and Winter. Since SO_2 emissions are assumed to be higher during the cold season, the negative sign in the Winter model is unexpected. Urban vegetation absorbs gaseous pollutants and metabolize them through leaves, or dissolve water soluble pollutants with moist leaf surfaces (Takahashi et al., 2005). The water-soluble characteristics of SO_2 explain the negative impact of green areas, which are significant in all models.

Wind induces a dispersion of pollutants. Therefore, the effects of wind speed are expected to be negative. The coefficient estimates are negative and significant, except in Spring. Sulfur-containing fossil fuels are generally used for heating buildings. Temperatures below a specific threshold increase the consumption these fuels, leading to increased SO_2 emissions. These effects are observed in Spring and Winter. However, the coefficient estimates for temperature are positive for Summer and Autumn. The consumption of space-heating fossil fuels is reduced during these seasons, and therefore this unexpected result may be linked to other factors, calling for further research.

Season	Spring			Summer			Autumn			Winter		
Regressors	Parameter	t Value	Pr > | t |	Parameter	t Value	Pr > | t |	Parameter	t Value	Pr > | t |	Parameter	t Value	Pr > | t |
Intercept	13.22	35.11	<.0001	4.16	28.45	<.0001	3.28	21.21	<.0001	18.93	46.43	<.0001
WVKT_DD	11.35	23.91	<.0001	11.02	46.18	<.0001	16.39	78.27	<.0001	25.97	14.24	<.0001
Commercial_R1000	8.25	26.71	<.0001	4.37	10.62	<.0001	-0.98	-2.75	0.006	-2.13	-2.37	0.018
Vegetative_R1000	-0.36	-10.22	<.0001	-0.67	-8.82	<.0001	-0.65	-10.68	<.0001	-0.85	-8.42	<.0001
Solar Radiation	-0.52	-14.55	<.0001	-0.41	-44.70	<.0001	-1.49	-90.40	<.0001	-0.29	-3.68	0.000
Wind Speed	0.12	5.00	<.0001	-0.01	-4.15	<.0001	-0.26	-39.71	<.0001	-0.25	-5.27	<.0001
Temperature	-0.27	-16.04	<.0001	0.02	6.02	<.0001	0.23	42.98	<.0001	-0.43	-15.31	<.0001
Humidity	-0.11	-37.12	<.0001	-0.01	-15.72	<.0001	-0.02	-17.81	<.0001	-0.19	-38.06	<.0001
WVKT × Roadside Dummy	10.95	18.83	<.0001	3.99	4.11	<.0001	1.43	7.37	<.0001	7.72	4.89	<.0001
Solar × Roadside Dummy	0.12	5.11	<.0001	0.35	10.74	<.0001	0.20	5.39	<.0001	-0.29	-5.92	<.0001
Humidity × Roadside Dummy	0.01	17.16	<.0001	-0.005	-3.94	<.0001	0.01	8.81	<.0001	-0.002	-0.89	0.373
R^2	0.979			0.996			0.999			0.980		

Table 7.11 Results of SO_2 panel regression models estimation

Summary statistics for the calculated elasticities w.r.t. the WVKT, solar radiation, and humidity variables are presented in Table 7.12. Traffic flows have positive impacts on SO_2 concentrations in all cases. Higher elasticities are observed at roadside AQMs. A 1% increase in WVKT induces an average 0.08% to 0.13% increase in SO_2 concentrations at background AQMs, but an average 0.16% to 0.22% increase at roadside areas, which are directly impacted by diesel vehicles.

Variable	AQM	Season	Min	10th Pctl	Lower Quartile	Median	Mean	Upper Quartile	90th Pctl	Max
WVKT	Background	Spring	0.01	0.03	0.05	0.08	0.08	0.10	0.13	0.20
		Summer	0.02	0.04	0.06	0.09	0.10	0.13	0.16	0.30
		Autumn	0.02	0.05	0.08	0.13	0.13	0.17	0.20	0.37
		Winter	0.02	0.05	0.08	0.12	0.12	0.15	0.20	0.34
	Roadside	Spring	0.06	0.08	0.14	0.20	0.18	0.23	0.25	0.31
		Summer	0.04	0.06	0.11	0.14	0.16	0.21	0.25	0.36
		Autumn	0.04	0.07	0.12	0.17	0.16	0.20	0.25	0.36
		Winter	0.07	0.11	0.19	0.24	0.22	0.27	0.31	0.38
Solar Radiation	Background	Spring	-0.33	-0.20	-0.13	-0.03	-0.07	0.00	0.00	0.00
		Summer	-0.38	-0.17	-0.11	-0.04	-0.07	0.00	0.00	0.00
		Autumn	-0.80	-0.45	-0.28	-0.05	-0.15	0.00	0.00	0.00
		Winter	-0.07	-0.04	-0.02	0.00	-0.01	0.00	0.00	0.00
	Roadside	Spring	-0.15	-0.10	-0.07	-0.02	-0.04	0.00	0.00	0.00
		Summer	-0.02	-0.02	-0.01	0.00	-0.01	0.00	0.00	0.00
		Autumn	-0.41	-0.28	-0.16	-0.03	-0.09	0.00	0.00	0.00
		Winter	-0.09	-0.07	-0.04	-0.01	-0.02	0.00	0.00	0.00
Humidity	Background	Spring	-2.68	-2.03	-1.66	-1.33	-1.39	-1.06	-0.81	-0.60
		Summer	-0.55	-0.40	-0.32	-0.25	-0.27	-0.20	-0.16	-0.12
		Autumn	-0.70	-0.48	-0.39	-0.31	-0.33	-0.26	-0.22	-0.14
		Winter	-3.44	-2.64	-2.14	-1.74	-1.76	-1.23	-1.00	-0.82
	Roadside	Spring	-2.27	-1.24	-1.00	-0.81	-0.88	-0.64	-0.54	-0.49
		Summer	-0.72	-0.46	-0.32	-0.25	-0.28	-0.19	-0.14	-0.12
		Autumn	-0.26	-0.14	-0.12	-0.10	-0.11	-0.08	-0.07	-0.05
		Winter	-3.37	-2.49	-1.95	-1.48	-1.62	-1.15	-1.00	-0.77

Table 7.12 Summary statistics for the elasticities w.r.t. WVKT, solar radiation, and humidity in the SO_2 models

Since SO_2 is converted into H_2SO_4 in the presence of OH· and water vapor, the elasticities of the SO_2 functions w.r.t. solar radiation and humidity are negative across all cases. The elasticities w.r.t. solar radiation are zero during nighttime, in all four models. Background areas generally present favorable conditions for O_3 generation, and therefore the OH· radicals are

recycled more easily in these areas, suggesting that solar radiation impacts on SO_2 decomposition are greater in background areas. Indeed, stronger negative elasticities are observed at background AQMs. For example, a 1% increase in solar radiation in Autumn decreases SO_2 concentrations by an average 0.15% at background AQMs, but only an average 0.09% at roadside AQMs. The impacts of humidity are greater during Spring and Winter than during Summer and Autumn at both locations. The reasons for these seasonal differences are not clear, calling for further research.

The patterns of the average hourly elasticities w.r.t. WVKT, solar radiation, and humidity are illustrated in Figures 7.9 ~ 7.11. The hourly elasticities w.r.t. WVKT are higher at roadside AQMs across the four seasons. The patterns of the hourly elasticities match the hourly traffic flow patterns, as analyzed in Chapter 5, with morning and evening peaks, and sustained volumes during daytime.

The hourly elasticities w.r.t. solar radiation are illustrated in Figure 7.10. Since OH· radicals are abundant at background regions, the hourly solar elasticities are lower in background AQMs, except in Winter. Although the intensity of solar radiation is higher in Summer, the elasticities for Autumn are the lowest, an unexpected result calling for further research.

The hourly elasticities w.r.t. humidity are illustrated in Figure 7.11. As discussed in Chapter 5, SO_2 concentrations are higher during Winter and Spring than in the other seasons, because of fossil fuel combustion for space heating in the colder seasons. Higher SO_2 concentrations in the cold seasons provide more opportunities for humidity to convert SO_2 into H_2SO_4, which may explain the lower elasticities w.r.t. humidity during Winter and Spring. Since background areas are more favorable for SO_2 conversion, the elasticities for background AQMs are generally lower than for roadside AQMs.

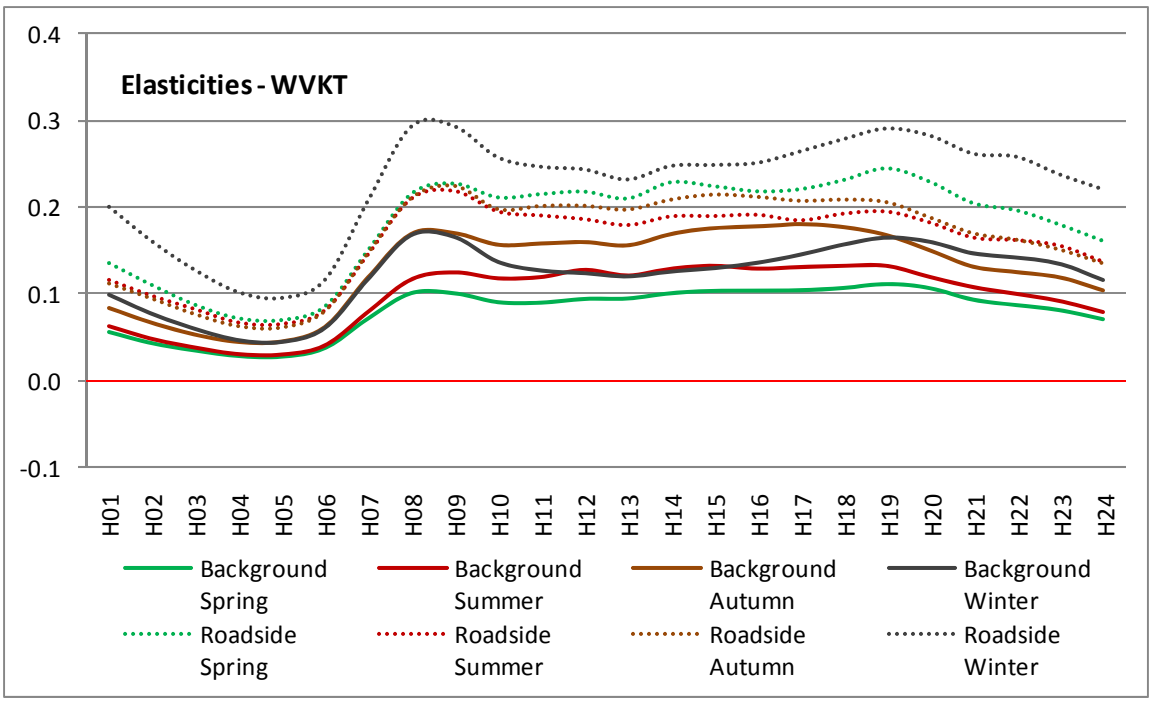

Figure 7.9 Average hourly-seasonal elasticities w.r.t. VKT in the SO_2 models

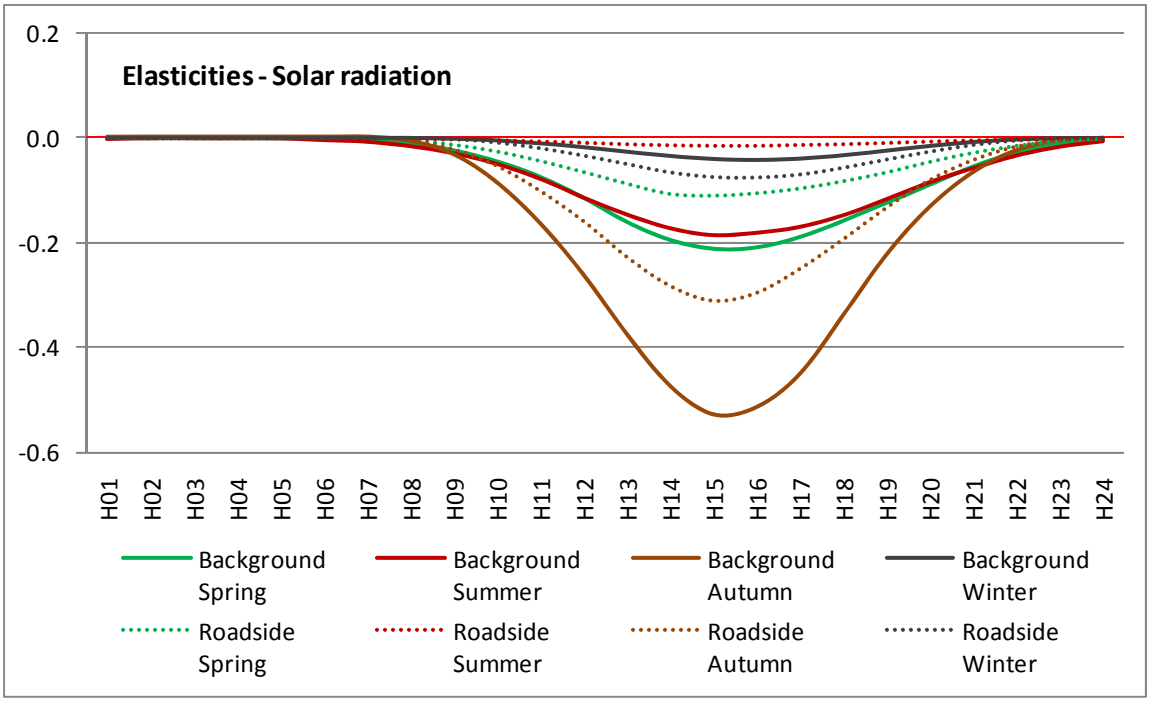

Figure 7.10 Average hourly-seasonal elasticities w.r.t. solar radiation in the SO_2 models

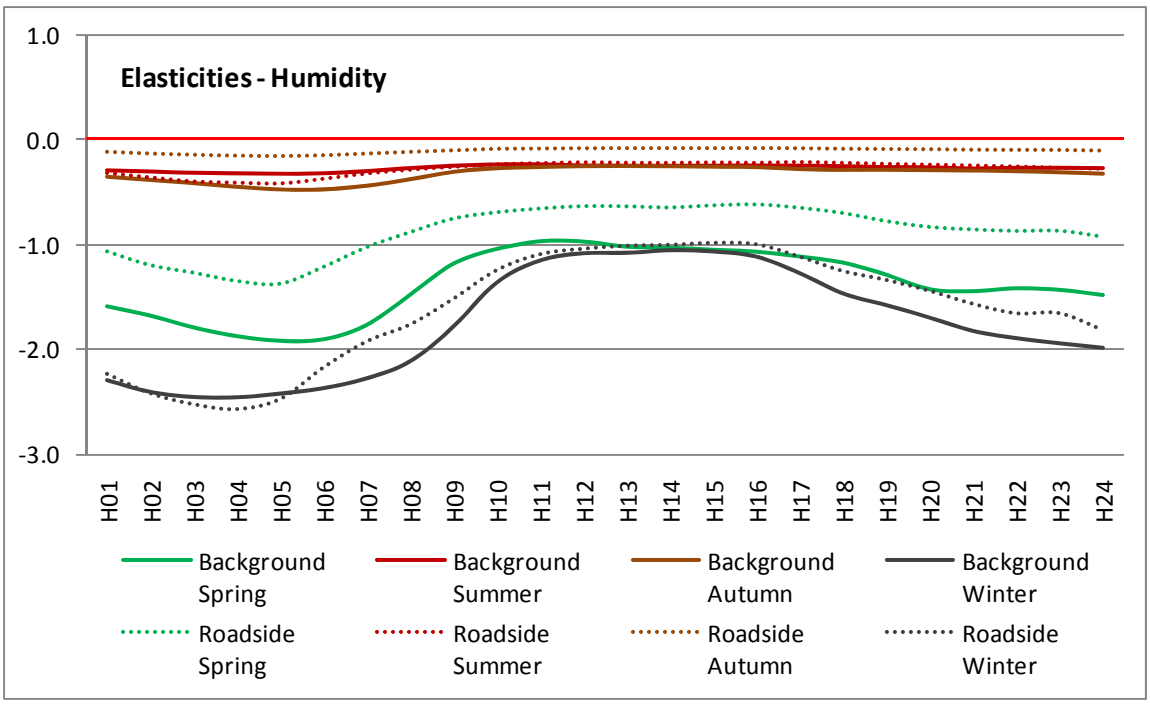

Figure 7.11 Average hourly-seasonal elasticities w.r.t. humidity in the SO_2 models

7.3.5 Results for PM10 panel models

The estimation results for the PM10 panel models are presented in Table 7.13. Traffic flows generate direct emissions related to fine particles, and indirect particles, such as wear of tire and brake pad, asphalt debris, and re-suspension of paved and unpaved road dust. The emitted fine particles are easily coagulated into secondary particles. Therefore, traffic flows are expected to have a positive impact on PM10 concentrations. The results of the PM10 models provide positive coefficient estimates for WVKT across the four seasons. The interaction terms between the WVKT and roadside dummy variable are positive and significant, suggesting that traffic flows have more impacts on PM10 concentrations at roadside areas.

In Chapter 6, results of the time-series models indicated that solar radiation have a negative effect on PM10 concentrations. The estimated coefficients for solar radiation are here also all negative. The roadside interaction term with solar radiation is also positive and significant in all cases, suggesting that the negative impacts of solar radiation are reduced at roadside AQMs.

PM10 is generated by anthropogenic activities, such as space heating, electric generation, and building construction, and a positive relationship would be expected between commercial areas and PM10 concentrations. The estimated coefficients for commercial areas are positive in Autumn and Winter, and negative in Spring and Summer, though insignificant in Spring and

Autumn. The negative and highly significant coefficient for Summer calls for further research. Vegetative areas have two types of impacts on PM10 concentrations: plants capture drifting particles, but also emit BVOC during the growing seasons, generating simultaneous negative and positive impacts. The coefficient estimates for the vegetation variable are all negative across the four seasons, suggesting that overall the filtering effects of green areas are dominant.

Wind encourages the movement of suspended particles, and hence the effect of wind speed could be expected to be positive. The coefficient estimates for Spring and Winter are positive, in support of this hypothesis. The Summer wind effect is insignificant, while the Autumn one is negative, possibly indicating the dominance of pure dispersion effects. Space heating generally occurs in Winter, and hence lower temperatures in Winter increase fossil fuel consumption, leading to increased PM10 concentrations, and indeed the coefficient in Winter is negative, as expected. However, the coefficient estimates for the other seasons are positive, an unexpected result calling for further research.

Stand-alone roadside and daytime dummy variables have been retained in the PM10 models. Except for the daytime dummy variable in the Autumn model, all these dummy variables are significant, indicating intercept shifts across the four seasons. Since anthropogenic activities occur more frequently during daytime, the estimated coefficients for the daytime dummy variable are positive, as expected. In contrast, those for the roadside dummy variable are negative. Since the WVKT interaction term with the roadside dummy variable has always a positive coefficient, the effects of WVKT are stronger at roadside AQMs. As seen in Figure 5.24, the PM10 concentrations at roadside AQMs are lower than those at background AQMs during nighttime, and higher during daytime. The positive estimates for the roadside WVKT interaction variable and the negative estimates for the stand-alone roadside dummy variable support these patterns of PM10 concentrations at roadside and background AQMs across the four models.

Season	Spring			Summer			Autumn			Winter		
Regressors	Parameter	t Value	Pr > | t |	Parameter	t Value	Pr > | t |	Parameter	t Value	Pr > | t |	Parameter	t Value	Pr > | t |
Intercept	37.93	13.90	<.0001	-210.75	-6.36	<.0001	-30.51	-3.46	0.001	156.20	34.31	<.0001
WVKT_R0500	5.65	11.82	<.0001	2.51	3.62	0.000	3.75	9.51	<.0001	7.56	21.97	<.0001
Commercial_R1000	-0.32	-0.99	0.324	-10.98	-12.43	<.0001	0.76	1.29	0.198	1.79	3.00	0.003
Vegetative_R1000	-2.76	-2.49	0.013	-8.19	-2.15	0.032	-4.90	-1.91	0.057	-5.32	-2.63	0.009
Solar Radiation	-13.67	-24.56	<.0001	-7.97	-6.00	<.0001	-22.31	-48.35	<.0001	-4.84	-4.20	<.0001
Wind Speed	1.85	6.90	<.0001	0.15	0.16	0.869	-3.50	-8.28	<.0001	3.52	3.74	0.000
Temperature	3.11	22.44	<.0001	6.55	7.36	<.0001	5.08	16.93	<.0001	-5.68	-13.69	<.0001
Humidity	0.18	7.84	<.0001	1.88	10.55	<.0001	0.39	6.44	<.0001	-1.39	-20.86	<.0001
WVKT × Roadside Dummy	4.66	39.21	<.0001	11.36	30.32	<.0001	7.14	9.75	<.0001	6.85	19.80	<.0001
Solar × Roadside Dummy	0.69	2.59	0.010	1.69	5.24	<.0001	1.40	2.54	0.011	0.56	1.26	0.207
Roadside Dummy	-5.14	-5.30	<.0001	-5.94	-7.56	<.0001	-5.40	-6.12	<.0001	-9.43	-9.62	<.0001
Daytime Dummy	0.70	9.00	<.0001	0.89	2.63	0.009	0.07	0.61	0.543	1.65	5.18	<.0001
R^2		0.998			0.916			0.959			0.955	

Table 7.13 Results of PM10 panel regression models estimation

Summary statistics for the calculated elasticities w.r.t. the WVKT and solar radiation variables are presented in Table 7.14. Traffic flows have positive impacts on PM10 concentrations in all cases. Higher elasticities are observed at roadside AQMs. A 1% increase in WVKT induces an average 0.03% to 0.06% increase in PM10 concentrations at background AQMs, and an average 0.13% to 0.23% increase at roadside AQMs.

Variable	AQM	Season	Min	10th Pctl	Lower Quartile	Median	Mean	Upper Quartile	90th Pctl	Max
WVKT	Background	Spring	0.01	0.02	0.02	0.04	0.05	0.07	0.10	0.16
		Summer	0.00	0.01	0.01	0.02	0.03	0.04	0.06	0.10
		Autumn	0.00	0.01	0.02	0.04	0.05	0.07	0.09	0.17
		Winter	0.01	0.02	0.03	0.05	0.06	0.08	0.11	0.21
	Roadside	Spring	0.03	0.05	0.09	0.13	0.13	0.18	0.22	0.32
		Summer	0.05	0.08	0.14	0.21	0.23	0.32	0.39	0.57
		Autumn	0.04	0.07	0.12	0.17	0.19	0.26	0.31	0.42
		Winter	0.04	0.07	0.12	0.17	0.17	0.23	0.27	0.34
Solar Radiation	Background	Spring	-0.42	-0.31	-0.22	-0.06	-0.11	0.00	0.00	0.00
		Summer	-0.29	-0.22	-0.15	-0.05	-0.08	0.00	0.00	0.00
		Autumn	-0.87	-0.58	-0.36	-0.05	-0.19	0.00	0.00	0.00
		Winter	-0.08	-0.06	-0.04	0.00	-0.02	0.00	0.00	0.00
	Roadside	Spring	-0.43	-0.26	-0.19	-0.05	-0.10	0.00	0.00	0.00
		Summer	-0.20	-0.14	-0.11	-0.04	-0.06	0.00	0.00	0.00
		Autumn	-0.58	-0.45	-0.27	-0.04	-0.14	0.00	0.00	0.00
		Winter	-0.06	-0.05	-0.03	0.00	-0.02	0.00	0.00	0.00

Table 7.14 Summary statistics for the elasticities w.r.t. WVKT and solar radiation in the PM10 models

Solar radiation decrease PM10 concentrations, and the elasticities w.r.t. solar radiation are all negative, except during nighttime when there is no solar radiation. Stronger negative elasticities are observed at background AQMs. A 1% increase in solar radiation in Autumn leads to an average 0.19% decrease at background AQMs, and an average 0.14% decrease at roadside AQMs.

The patterns of average hourly elasticities w.r.t. WVKT and solar radiation are illustrated in Figures 7.12 and 7.13. Since roadside areas are directly impacted by traffic flows, the hourly elasticities w.r.t. WVKT are higher for roadside AQMs across the four seasons. The patterns of hourly elasticities are similar to the traffic flow patterns. The seasonal elasticities for background AQMs do not vary significantly. The patterns of elasticities for roadside AQMs display distinctive

shifts across seasons. The Summer elasticities are the highest and the Spring ones the lowest, but the reasons for these differences are not clear, calling for further research.

The hourly elasticities w.r.t. solar radiation are illustrated in Figure 7.13. Since the signs of the solar radiation interaction with the roadside dummy variable are positive across all four models, the negative solar impacts are greater at background AQMs. Although the intensity of solar radiation in Summer is the higher than in the other seasons, the elasticities during Autumn are the lowest, an unexpected result calling for further research.

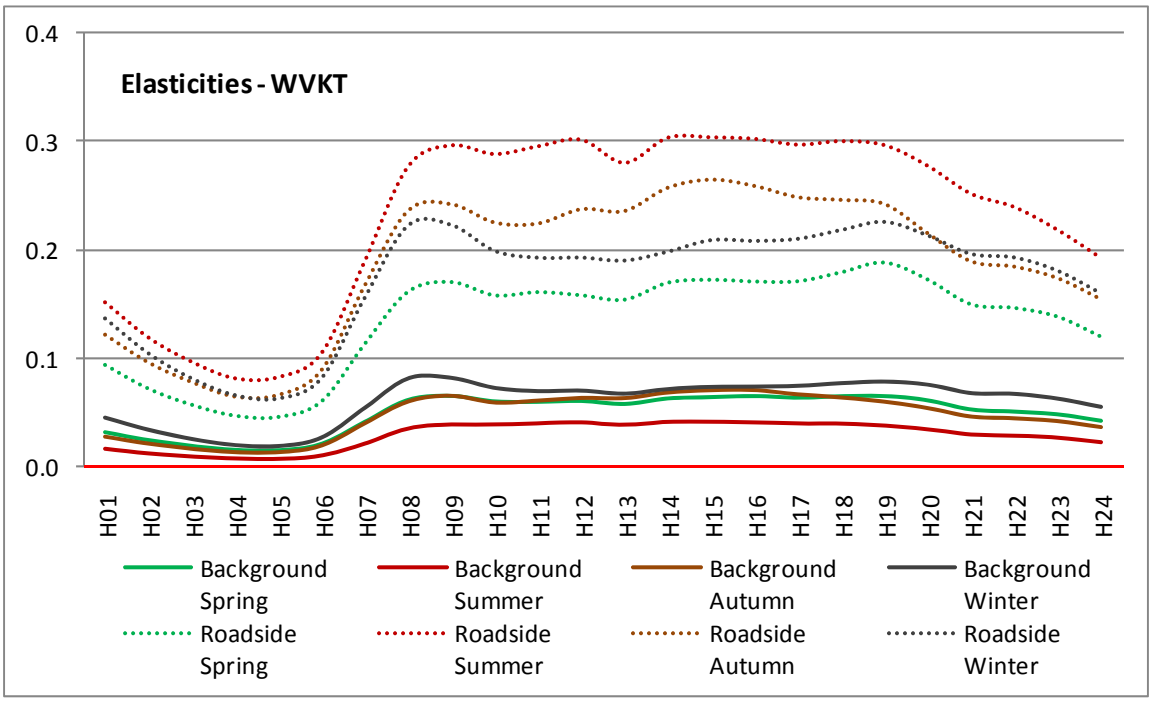

Figure 7.12 Average hourly-seasonal elasticities w.r.t. VKT in the PM10 models

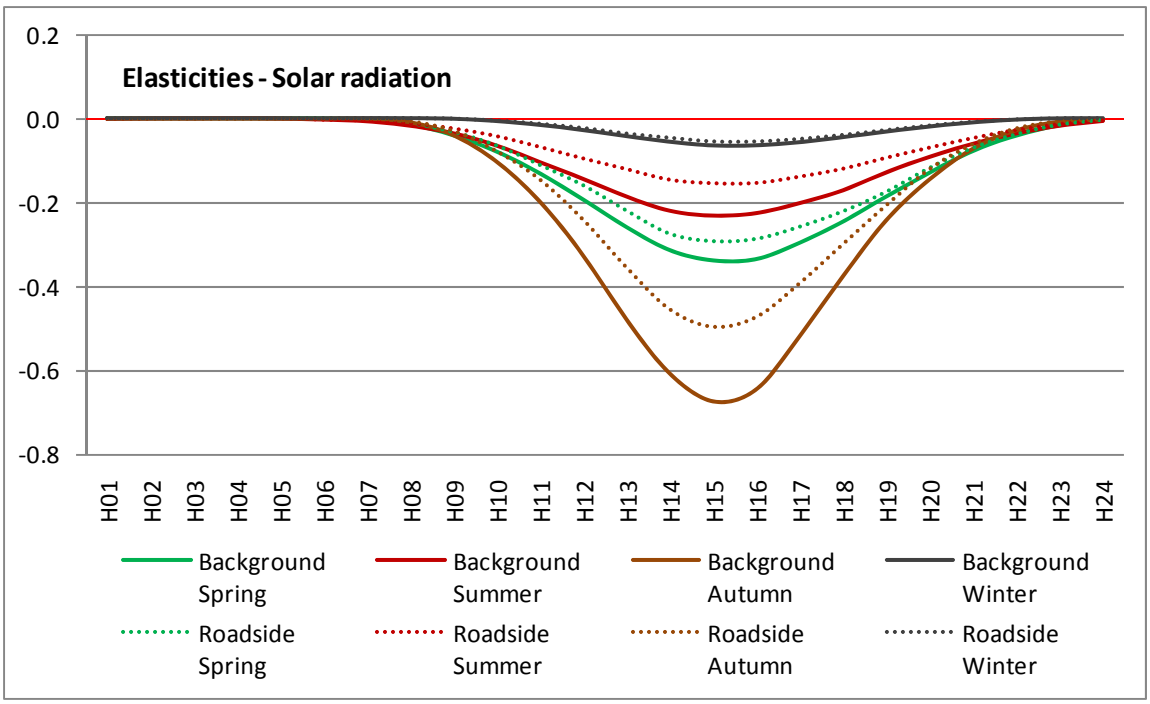

Figure 7.13 Average hourly-seasonal elasticities w.r.t. solar radiation in the PM10 models

7.4 SUMMARY

In this chapter, air quality panel models have been formulated and estimated, accounting for the impacts of WVKT, land uses, and meteorological factors on hourly-averaged concentrations across the four seasons. Locational and daytime dummy variables are included in the panel models to assess the impacts of AQM general location and daytime variations on pollution concentrations. Traffic emissions, proxied by WVKT, have negative impacts in the O_3 panel models. The analyses of hourly-seasonal elasticities show that the impacts of WVKT vary along the hours of the day, depending on the locations of the AQMs. Solar radiation has positive impacts on O_3 concentrations. These two effects are consistent to the estimation results of the time-series O_3 models in Chapter 6. The emissions from tail pipes contain abundant NO gas, leading to O_3 titration, and thus WVKT display negative effects on O_3 concentrations. However, tropospheric O_3 is also generated by the photodissociation of NO_2 under the presence of UV radiation, and therefore solar radiation have strong positive impacts on O_3 concentrations. Relatively intense solar radiation during Spring and Summer lead to favorable conditions for O_3 generation, and, consequently, the rates of O_3 creation during Spring and Summer are significantly higher than those during Autumn and Winter. The coefficient estimates and elasticities analysis w.r.t. WVKT and solar radiation support these theoretical assumptions.

For directly emitted pollutants, such as NO_2, CO, SO_2, and PM10, WVKT has a positive impact on their concentrations. As these pollutants are generated by vehicle flows, concentrations are higher at roadside AQMs than at background AQMs across the four seasonal models. The OH· radicals produced under UV radiation react chemically with NO_2, CO, and SO_2, leading to a decrease in the concentrations of these pollutants. Since background regions provide more favorable conditions for the regenerations of OH· radicals, solar radiation have greater negative impacts on the concentrations of NO_2, CO, and SO_2 in background regions. The hourly elasticities w.r.t. solar radiation indicate that these negative impacts peak when the solar radiation also peak.

It is reasonable to expect that the emission rates of urban land uses are different, depending on the intensity of anthropogenic activities across the hours of the day and the seasons. In the O_3 models, three land uses (commercial, residential, and vegetative areas) are retained as significant variables. NO emitted from commercial and residential areas have generally a negative impact on O_3 concentrations. Vegetative areas have both positive and negative impacts. The overall vegetative areas impact on O_3 concentrations is positive. However, for directly emitted pollutants, vegetative areas have a negative impact. Since residential, commercial, and industrial

areas generate anthropogenic emissions, the effects for these land uses for directly emitted pollutants are generally positive. However, these effects vary, depending on the seasons.

As discussed above, solar radiation is the most important factor in determining pollutant concentrations, but the other meteorological factors are also significant. Wind has both negative and positive impacts of pollution concentrations. However, the threshold of these two effects has not been clearly investigated, and it is difficult to interpret the estimated coefficients for wind speed across the four seasons. Temperatures are closely related to the consumption of fossil fuels for space heating, and therefore lower temperatures lead to an increase in directly emitted pollutants. However, this is expected to occur when temperatures are below a specific threshold, and therefore the negative relationships between temperature and the concentrations of directly emitted pollutants generally hold in the Winter models. Humidity has an overall negative impact on pollution concentrations. In particular, SO_2 has hygroscopic characteristics, and therefore humidity has a strong negative impact on SO_2 concentrations.

CHAPTER 8

CONCLUSIONS

The objectives of this research were to (1) develop and estimate metropolitan-wide air quality time-series models and location-specific air quality panel models based on the land-use regression (LUR) framework, and (2) use these models to investigate the impacts of transportation, land uses, and meteorological factors on pollution concentrations. The research has involved a detailed review of air pollutants chemistry, and an exploration of pollutants concentrations in the Seoul Metropolitan Area from both spatial and temporal perspectives. The understanding of pollutants chemistry has provided the rationale for the inclusion of such explanatory variable as vehicle-kilometers-traveled (VKT), land uses, and meteorological factors – solar radiation, temperature, humidity, and wind speed – in the statistical models. Descriptive analyses and comparisons of pollution concentrations at roadside and background air quality monitoring stations (AQMs) have pointed to significant differences, which are measured using a locational dummy variable. In addition, since concentrations vary across seasons, the inclusion of monthly dummy variables has enhanced the accuracy of the estimated time-series models.

Diverse land-use variables have been identified as proxies of emission sources and pollution uptakes in LUR models. Traffic flows are known to account for a substantial share of urban air pollution, and to be responsible for temporal and geographical hotspots. Among these land-use variables, transportation-related variables play an essential role in explaining pollution concentrations. Traffic counts and WVKT have been used as significant independent variables to explain the concentrations of both directly emitted (NO_X, CO, SO_2, and PM10) and secondary pollutants (O_3). The concentrations of directly emitted pollutants are positively correlated with the traffic counts and WVKT. In the case of O_3, however, WVKT has a negative impact on O_3 concentrations. O_3 is destructed by its reaction with NO (O_3 titration), and this reaction occurs anytime fresh emissions from tail pipes are provided. In urban regions, such as the Seoul Metropolitan Area, vehicle emissions are plentiful, leading to a negative impact of traffic on O_3 concentrations. Decreased traffic flows in NO_x-saturated regions increase O_3 concentrations. As

discussed in the results on time-series O_3 models, reduced traffic flows on Sunday increase the ratio of VOC to NO_x and, consequently, lead to favorable conditions for O_3 generation. Therefore less O_3 titration and less HNO_3 formation occur on Sunday than on weekdays, resulting in higher O_3 concentrations on Sunday. For directly emitted pollutants, reduced traffic flows on Sunday induce a decrease in concentrations.

The locations of AQMs influence WVKT impacts on pollution concentrations. Traffic emissions closer to AQMs have larger impacts on pollution concentrations. The interaction terms between WVKT and roadside dummy variable present the expected results: for directly emitted pollutants, the interaction variables have significant and positive coefficients, suggesting that the impacts of roadside WVKT are greater than those of background WVKT. In the case of O_3, the estimated coefficients for the interaction variable w.r.t. WVKT are negative, indicating that O_3 titration effects are greater at roadside AQMs than at background AQMs.

Meteorological factors - solar radiation, temperature, humidity, and wind speed - are closely correlated with pollution concentrations. These factors induce chemical interactions and physical dispersions. Among these factors, solar radiation is indispensible for creating O_3 in the troposphere. UV radiation is the cause of the photodissociation of NO_2. OH· radicals produced under UV radiation react chemically with CO and SO_2. Therefore, solar radiation is negatively correlated with NO_2, CO, and SO_2 concentrations. The 6-hour averaged solar radiation is used in the models, and the estimated coefficients for solar radiation are all significant. Higher temperatures reduce the consumption of fossil fuels, leading to a decrease in directly emitted pollutants. Space heating is required only when the temperature decreases below a specific threshold. Therefore, a negative relation is likely to occur during the cold season. The coefficient estimates for temperature are negative in all Winter models, supporting this argument. Humidity slows down the photodissociation of NO_2 and, as a result, increases NO_2 concentrations and decreases O_3 concentrations. The results are consistent with these expectations, except in the Winter models. Water vapor in the ambient air interacts with gaseous pollutants, converting them into fine particles. Therefore, an increase in humidity positively impacts PM10 concentrations. Since SO_2 is easily converted into H_2SO_4 with the OH· radicals and water vapor, the humidity coefficient estimates are negative. Wind speed is characterized by more complicated interactions, as compared to the other meteorological factors, because a strong wind expedites the dispersion of pollutants, but a light wind expedites pollutants photochemistry. The wind speed threshold between these two situations, however, has not been clearly identified. The coefficient estimates

for the hourly wind speed are both positive and negative, and there are no discernable seasonal patterns, calling for further research.

The time-series air quality models include quadratic terms for the traffic and solar radiation variables, indicating that the impacts of these two variables are non-linear. In the case of traffic counts, the effects of the original regressor and quadratic term present opposite directions, suggesting that the original impact of traffic emissions on pollution concentrations may change under specific conditions. Different additional interaction terms between regressors have been selected as significant explanatory variables, and therefore the interpretation of the original regressors impacts on pollution concentrations are complex. In order to clarify these quadratic and interaction effects, the derivatives of the concentration functions w.r.t. traffic variable are introduced. Using the estimated parameters and the derivative functions, elasticities w.r.t. the explanatory variables are computed across all input data. Analyses of these elasticities help interpret when and how the negative and positive effects occur. In the O_3 models, hourly elasticities w.r.t. traffic are negative but they decrease during daytime, and even exceed zero when the cumulative UV radiation reaches their peak. Since traffic volumes decrease on Sunday, the concentrations of directly emitted pollutants are lower on Sunday than on weekdays. The elasticities w.r.t. traffic for the directly emitted pollutants are generally positive across the hours of the day. However, the reduced traffic on Sunday provides better conditions for decomposing NO_2, leading to better conditions for O_3 generation, and therefore the Sunday elasticities w.r.t. traffic are higher for O_3 and lower for NO_2.

The coefficient estimates of the explanatory variables in the air quality panel models are significant and consistent with the results of the time-series air quality models. WVKT has negative and solar radiation has positive impacts on O_3 concentrations and vice versa for the other directly emitted pollutants. Since intense solar radiation during Spring and Summer leads to favorable conditions for O_3 generation, the hourly elasticities w.r.t. solar radiation in these seasons are higher than in the other seasons. For the directly emitted pollutants, WVKT has positive impacts, and the coefficient estimates for the roadside interaction variables are also positive, indicating that roadside concentrations are higher than the background one. The elasticities w.r.t. solar radiation are negative across all seasons, because OH· radicals produced by UV radiation react chemically with the directly emitted pollutants. Background elasticities are lower than roadside ones, indicating that background regions are more favorable conditions for the regenerations of OH· radicals. This result is consistent with the O_3 panel models.

Future research can be summarized as follows. The air quality models based on emission inventories and dispersion processes have limitations for developing pollution maps for urban regions, because of large data and computational requirements. In contrast, since improvements in GIS techniques allow for the easy collection of land-use and transportation data needed for urban-scale air quality analysis, LUR approaches present the potential to develop high-resolution air quality maps, which can then be used for the assessment of epidemiological impacts, the location/allocation of public facilities, and the evaluation of pollution mitigation policies.

The empirical results obtained with the time-series and panel models can be used for the evaluation of pollution mitigation plans and policies. Some counterintuitive results, such as the negative effect of traffic on ozone concentrations, call into question the validity of public policies intended to reduce traffic in the case of critical ozone episodes. Diverse energy and urban planning related policies, such as low or zero emission vehicles, ultra-low sulfur diesel, transit-oriented development, mixed land uses, etc., could influence the intensity of anthropogenic emissions, resulting in the change of spatial and temporal pollution concentrations.

High-resolution geographical maps can be expanded into high-resolution temporal maps. VKT, as used in this research, is hourly measured, and thus delineating dynamic hourly air quality maps is also possible. Land-use variables are time-invariant, and thus only spatial differences have been accounted for in the models. To investigate the temporal impacts of land uses, it is necessary to include the temporal profiles of human activities across land uses. Diverse proxy variables, such as hourly demand for electricity, LNG, and water, would be used to measure these temporal profiles.

The use of wind fields has significantly improved the NO_2 exposure assessment in Hamilton, Canada (Arain et al., 2007). Meteorological factors, such as temperature and wind direction, may vary significantly depending on local conditions (adjacent land use and topography), and therefore the assumption of homogeneity across the study region may be unrealistic. The introduction of temperature and wind direction fields would enhance the accuracy of the air quality models.

Since transportation planning programs, such as TransCAD® and Emme 3®, are widely used and include diverse GIS interfaces, results from transportation planning can be easily introduced into air quality models. In this research, the calculated VKT, based on traffic flows assigned on transportation network, has been used as a significant explanatory variable. In addition, a biotope map (GIS vector data) and a satellite image (GIS raster data) have been used to measure land-use areas surrounding the AQMs. These land-use variables are also used in the

air quality models. According to Briggs (2007), simple traffic-related variables, such as areas of road and distances to major highways, need to be replaced by estimated traffic flows in LUR models.

It is increasingly hard to discuss planning issues without the concepts of sustainability and smart growth. There is growing consensus that sustainable models must include relevant systems, such as the physical environment (air, water, land, noise, odor, and aesthetics), the economic system (energy, resources, employment, housing, and land uses), and the social system (health, safety, mobility, welfare, education, and equity). Since the sustainability paradigm includes those diverse factors, sustainable models are inevitably complex. Diverse indicators have been proposed as tools for implementing sustainable policies. Quantifiable city models (May, Mitchell, & Kupiszewska, 1997), energy and environmental prediction models (Tweed & Jones, 2000), ecological footprint and sustainable development indices (O'Regan, Morrissey, Foley, & Moles, 2009), and the Energy Efficient Cities initiative in England[1] are good examples of such models. The air quality modeling systems based on the LUR approach and presented in this research can be used as one of the tools of sustainable models.

[1] http://www.eeci.cam.ac.uk/index.shtml

REFERENCES

Aguilera, I., Sunyer, J., Fernández-Patier, R., Hoek, G., Aguirre-Alfaro, A., Meliefste, K., et al. (2008). Estimation of outdoor NO_x, NO_2, and BTEX exposure in a cohort of pregnant women using land use regression modeling. *Environmental Science & Technology, 42*(3), 815-821.

Air Quality Expert Group. (2004). *Nitrogen dioxide in the united kingdom-summary*. London: UK.

American Thoracic Society. (2000). What constitutes and adverse health effect of air pollution? *American Journal of Respiratory and Critical Care Medicine, 161*(2), 665-673.

Arain, M. A., Blair, R., Finkelstein, N., Brook, J. R., Sahsuvaroglu, T., Beckerman, B., et al. (2007). The use of wind fields in a land use regression model to predict air pollution concentrations for health exposure studies. *Atmospheric Environment, 41*(16), 3453-3464.

Bachman, W., Sarasua, W., Hallmark, S., & Guensler, R. (2000). Modeling regional mobile source emissions in a geographic information system framework. *Transportation Research Part C: Emerging Technologies, 8*(1-6), 205-229.

Beelen, R., Hoek, G., Fischer, P., Brandt, P. A. v. d., & Brunekreef, B. (2007). Estimated long-term outdoor air pollution concentrations in a cohort study. *Atmospheric Environment, 41*(7), 1343-1358.

Beelen, R., Hoek, G., Pebesma, E., Vienneau, D., de Hoogh, K., & Briggs, D. J. (2009). Mapping of background air pollution at a fine spatial scale across the European Union. *Science of the Total Environment, 407*(6), 1852-1867.

Bell, M. L., & Dominici, F. (2008). Effect modification by community characteristics on the short-term effects of ozone exposure and mortality in 98 US communities. *American Journal of Epidemiology, 167*(8), 986-997.

Bell, M. L., McDermott, A., Zeger, S. L., Samet, J. M., & Dominici, F. (2004). Ozone and short-term mortality in 95 US urban communities, 1987-2000. *JAMA: The Journal of the American Medical Association, 292*(19), 2372-2378.

Berkowicz, R. (1998). Street scale models. In J. Fenger, O. Hertel & F. Palmgren (Eds.), *Urban air pollution-European aspects*. Netherlands: Kluwer Academic Publishers.

Berkowicz, R. (2000). OSPM - A parameterised street pollution model. *Environmental Monitoring and Assessment, 65*(1), 323-331.

Berkowicz, R., Winther, M., & Ketzel, M. (2006). Traffic pollution modelling and emission data. *Environmental Modelling and Software, 21*(4), 454-460.

Blanchard, C. L., & Tanenbaum, S. J. (2003). Differences between weekday and weekend air pollutant levels in southern California. *Journal of the Air & Waste Management Association, 53*(7), 816-828.

Bloomfield, P., Royle, J. A., Steinberg, L. J., & Qing, Y. (1996). Accounting for meteorological effects in measuring urban ozone levels and trends. *Atmospheric Environment*, 30(17), 3067-3077.

Bøhler, T., Karatzas, K., Peinel, G., Rose, T., & San Jose, R. (2002). Providing multi-modal access to environmental data—customizable information services for disseminating urban air quality information in APNEE. *Computers, Environment and Urban Systems, 26*(1), 39-61.

Briggs, D. (2005). The role of GIS: Coping with space (and time) in air pollution exposure assessment. *Journal of Toxicology & Environmental Health: Part A, 68*(13), 1243-1261.

Briggs, D. J. (2007). The use of GIS to evaluate traffic-related pollution. *Occup Environ Med, 64*(1), 1-2.

Briggs, D. J., Collins, S., Elliott, P., Fischer, P., Kingham, S., Lebret, E., et al. (1997). Mapping urban air pollution using GIS: A regression-based approach. *International Journal of Geographical Information Science, 11*(7), 699-718.

Briggs, D. J., de Hoogh, C., Gulliver, J., Wills, J., Elliott, P., Kingham, S., et al. (2000). A regression-based method for mapping traffic-related air pollution: Application and testing in four contrasting urban environments. *The Science of the Total Environment, 253*(1-3), 151-167.

Camalier, L., Cox, W., & Dolwick, P. (2007). The effects of meteorology on ozone in urban areas and their use in assessing ozone trends. *Atmospheric Environment, 41*(33), 7127-7137.

Cameron, E., & Environmental Systems Research Institute. (2005). *ArcGIS 9*. Redlands, CA: ESRI.

Cardelino, C. A., & Chameides, W. L. (1990). Natural hydrocarbons, urbanization, and urban ozone. *Journal of Geophysical Research, 95*, 13971-13979.

Carslaw, D. C., & Beevers, S. D. (2004). Investigating the potential importance of primary NO_2 emissions in a street canyon. *Atmospheric Environment, 38*(22), 3585-3594.

Carr, D., von Ehrenstein, O., Weiland, S., Wagner, C., Wellie, O., Nicolai, T., et al. (2002). Modeling annual benzene, toluene, NO_2, and soot concentrations on the basis of road traffic characteristics. *Environmental Research, 90*(2), 111-118.

Chameides, W. L., Fehsenfeld, F., Rodgers, M. O., Cardelino, C., Martinez, J., Parrish, D., et al. (1992). Ozone precursor relationships in the ambient atmosphere. *Journal of Geophysical Research [Atmospheres], 97*(D5), 6037-6055.

Chameides, W. L., Lindsay, R. W., Richardson, J., & Kiang, C. S. (1988). The role of biogenic hydrocarbons in urban photochemical smog: Atlanta as a case study. *Science, 241*(4872), 1473-1475.

Chinkin, L. R., Coe, D. L., Funk, T. H., Hafner, H. R., Roberts, P. T., Ryan, P. A., et al. (2003). Weekday versus weekend activity patterns for ozone precursor emissions in California's south coast air basin. *Journal of the Air & Waste Management Association, 53*(7), 829-843.

Cho, Y., & Song, I. (2005). Biotope mapping and application in Seoul. *International Symposium on Mapping Biotope Map and its Application in Metropolitan Area,* Seoul, Korea. 195-209.

Chock, D. P., Terrell, T. R., & Levitt, S. B. (1975). Time-series analysis of riverside, California air quality data. *Atmospheric Environment, 9*, 978-989.

Connell, D. P., Withum, J. A., Winter, S. E., Statnick, R. M., & Bilonick, R. A. (2005). The Steubenville comprehensive air monitoring program (SCAMP): Associations among fine particulate matter, co-pollutants, and meteorological conditions. *Journal of the Air & Waste Management Association, 55*(4), 1064-1074.

Cook, R. D. (1979). Influential observations in linear regression. *Journal of the American Statistical Association, 74*(365), 169-174.

CORINAIR. (2003). *Atmospheric emission inventory guidebook* (3rd ed.) Co-operative Programme for Monitoring and Evaluation of the Long Range Transmission of Air Pollutants in Europe.

Coyle, M., Smith, R. I., Stedman, J. R., Weston, K. J., & Fowler, D. (2002). Quantifying the spatial distribution of surface ozone concentration in the UK. *Atmospheric Environment, 36*(6), 1013-1024.

Derwent, R. G., & Hertel, O. (1998). Transformation of air pollutants. In J. Fenger, O. Hertel & F. Palmgren (Eds.), *Urban air pollution: European aspects*. Dordrecht; Boston: Kluwer Academic Publishers.

Dockery, Pope CA, Xu, Spengler, Ware, Fay, et al. (1993). An association between air pollution and mortality in six U.S. cities. *The New England Journal of Medicine, 329*(24), 1753-1759.

Dominici, & Burnett. (2003). Risk models for particulate air pollution. *Journal of Toxicology and Environmental Health.Part A, 66*(16-19), 1883-1889.

Elbir, T. (2004). A GIS based decision support system for estimation, visualization and analysis of air pollution for large Turkish cities. *Atmospheric Environment, 38*(27), 4509-4517.

Elbir, T., & Muezzinoglu, A. (2004). Estimation of emission strengths of primary air pollutants in the city of Izmir, Turkey. *Atmospheric Environment, 38*(13), 1851-1857.

Environmental Systems Research Institute. (2006). *ArcGIS 9-using ArcGIS desktop*. Redlands, CA: ESRI.

Ezzati, M., & World Health Organization. (2004). *Comparative quantification of health risks: Global and regional burden of disease attributable to selected major risk factors*. Geneva: World Health Organization.

Franklin, , Zeka, , & Schwartz, . (2007). Association between $PM_{2.5}$ and all-cause and specific-cause mortality in 27 US communities. *Journal of Exposure Science & Environmental Epidemiology, 17*(3), 279-287.

Fujita, E. M., Stockwell, W. R., Campbell, D. E., Keislar, R. E., & Lawson, D. R. (2003). Evolution of the magnitude and spatial extent of the weekend ozone effect in California's south coast air basin, 1981-2000. *Journal of the Air & Waste Management Association, 53*, 802-815.

Gilbert, N. L., Goldberg, M. S., Beckerman, B., Brook, J. R., & Jerrett, M. (2005). Assessing spatial variability of ambient nitrogen dioxide in Montreal, Canada, with a land-use regression model. *Journal of the Air & Waste Management Association, 55*(8), 1059-1063.

Gregg, J. W., Jones, C. G., & Dawson, T. E. (2003). Urbanization effects on tree growth in the vicinity of New York City. *Nature, 424*(6945), 183-187.

Gryparis, A., Forsberg, B., Katsouyanni, K., Analitis, A., Touloumi, G., Schwartz, J., et al. (2004). Acute effects of ozone on mortality from the "air pollution and health: A European approach" project. *Am.J.Respir.Crit.Care Med., 170*(10), 1080-1087.

Gualtieri, G., & Tartaglia, M. (1998). Predicting urban traffic air pollution: A GIS framework. *Transportation Research Part D: Transport and Environment, 3*(5), 329-336.

Guldmann, J., & Kim, H. (2001). Modeling air quality in urban areas: A cell-based statistical approach. *Geographical Analysis, 33*(2), 156-180.

Guenther, A., Geron, C., Pierce, T., Lamb, B., Harley, P., & Fall, R. (2000). Natural emissions of non-methane volatile organic compounds, carbon monoxide, and oxides of nitrogen from North America. *Atmospheric Environment, 34*(12-14), 2205-2230.

Hall, J. V., Winer, A. M., Kelinman, M. T., Lurmann, F. W., Brajer, V., & Colome, S. D. (1992). Valuing the health benefits of clean air. *Science, 255*(5046), 812-817.

Harrison, R. M. (2001). *Pollution: Causes, effects and control* (4th ed.). Cambridge: Royal Society of Chemistry.

Hawley, G. G., & Lewis, R. J. (2002). *Hawley's condensed chemical dictionary* (14th ed.). New York: Wiley.

Henderson, S. B., Beckerman, B., Jerrett, M., & Brauer, M. (2007). Application of land use regression to estimate long-term concentrations of traffic-related nitrogen oxides and fine particulate matter. *Environmental Science & Technology, 41*(7), 2422-2428.

Heuss, J. M., Kahlbaum, D. F., & Wolff, G. T. (2003). Weekday/weekend ozone differences: What can we learn from them? *Journal of the Air & Waste Management Association, 53*(7), 772-788.

Hochadel, M., Heinrich, J., Gehring, U., Morgenstern, V., Kuhlbusch, T., Link, E., et al. (2006). Predicting long-term average concentrations of traffic-related air pollutants using GIS-based information. *Atmospheric Environment, 40*(3), 542-553.

Hoek, G., Beelen, R., de Hoogh, K., Vienneau, D., Gulliver, J., Fischer, P., et al. (2008). A review of land-use regression models to assess spatial variation of outdoor air pollution. *Atmospheric Environment, 42*(33), 7561-7578.

Horowitz, A. J. (1991). *Delay-volume relations for travel forecasting: Based on the 1985 highway capacity manual*, Federal Highway Administration, FHWA-PD-92-015.

Intergovernmental Panel on Climate Change. (2007). *Climate change 2007: The physical science basis: Contribution of working group I to the fourth assessment report of the intergovernmental panel on climate change*. Cambridge; New York: Cambridge University Press.

Jackson, R. D., Slater, P. N., & Pinter, P. J. (1983). Discrimination of growth and water stress in wheat by various vegetation indices through clear and turbid atmospheres. *Remote Sensing of Environment, 13*, 187-208.

Jacob, D. J., Logan, J. A., Gardner, G. M., Yevich, R. M., Spivakovsky, C. M., Wofsy, S. C., et al. (1993). Factors regulating ozone over the United States and its export to the global atmosphere. *Journal of Geophysical Research [Atmospheres], 98*(D8), 14,817-14,826.

Jensen, S. S., Berkowicz, R., Sten Hansen, H., & Hertel, O. (2001). A Danish decision-support GIS tool for management of urban air quality and human exposures. *Transportation Research Part D: Transport and Environment, 6*(4), 229-241.

Jerrett, M., Arain, M. A., Kanaroglou, P., Beckerman, B., Crouse, D., Gilbert, N. L., et al. (2007). Modeling the intraurban variability of ambient traffic pollution in Toronto, Canada. *Journal of Toxicology & Environmental Health: Part A, 70*(3), 200-212.

Jo, W., & Park, J. (2005). Characteristics of roadside air pollution in Korean metropolitan city (Daegu) over last 5 to 6 years: Temporal variations, standard exceedances, and dependence on meteorological conditions. *Chemosphere, 59*(11), 1557-1573.

Kahyaoğlu-Koračin, J., Bassett, S. D., Mouat, D. A., & Gertler, A. W. (2009). Application of a scenario-based modeling system to evaluate the air quality impacts of future growth. *Atmospheric Environment, 43*(5), 1021-1028.

Kanaroglou, P. S., Jerrett, M., Morrison, J., Beckerman, B., Arain, M. A., Gilbert, N. L., et al. (2005). Establishing an air pollution monitoring network for intra-urban population exposure assessment: A location-allocation approach. *Atmospheric Environment, 39*(13), 2399-2409.

Karppinen, A., Kukkonen, J., Elolähde, T., Konttinen, M., & Koskentalo, T. (2000). A modelling system for predicting urban air pollution: Comparison of model predictions with the data of an urban measurement network in Helsinki. *Atmospheric Environment, 34*(22), 3735-3743.

Karppinen, A., Kukkonen, J., Elolähde, T., Konttinen, M., Koskentalo, T., & Rantakrans, E. (2000). A modelling system for predicting urban air pollution: Model description and applications in the Helsinki metropolitan area. *Atmospheric Environment, 34*(22), 3723-3733.

Katsouyanni, K., Touloumi, G., Samoli, E., Gryparis, A., Le Tertre, A., Monopolis, Y., et al. (2001). Confounding and effect modification in the short-term effects of ambient particles on total mortality: Results from 29 European cities within the APHEA2 project. *Epidemiology, 12*(5), 521-531.

Kim, C. W., Phipps, T. T., & Anselin, L. (2003). Measuring the benefits of air quality improvement: A spatial hedonic approach. *Journal of Environmental Economics and Management, 45*(1), 24-39.

Kim, Y. (2007). Air pollution concentration, urban traffic flow and vegetation area: Focus on cities in Gyeonggi province. *Gyeonggi Research Institute Paper Competition,* Gyeonggi-do, South Korea. 2-33. (Korean version)

Kim, Y., & Guldmann, J. (2008). Traffic volumes and wind directions impacts on air pollution concentrations in Seoul, Korea. Paper presented at the *7Th Annual Community Modeling and Analysis System Conference,* Chapel Hill, North Carolina.

Kmenta, Jan (1987). *Elements of Econometrics* (2nd ed.). New York: Macmillan.

Korea Development Institute. (2004). *The standard guideline of pre-feasibility study for road and railroad sectors*. Seoul, Korea:

Korea Ministry of Environment. (2003). *2003 Environment White Paper*. South Korea:

Korea Ministry of Environment. (2006). 2006 *Environment White Paper*. South Korea:

Kraft, M., Eikmann, T., Kappos, A., Künzli, N., Rapp, R., Schneider, K., et al. (2005). The German view: Effects of nitrogen dioxide on human health – derivation of health-related short-term and long-term values. *International Journal of Hygiene and Environmental Health, 208*(4), 305-318.

Krupa, S., Nosal, M., Ferdinand, J. A., Stevenson, R. E., & Skelly, J. M. (2003). A multi-variate statistical model integrating passive sampler and meteorology data to predict the frequency distributions of hourly ambient ozone (O_3) concentrations. *Environmental Pollution, 124*(1), 173-178.

Krupnick, A. J., & Portney, P. R. (1991). Controlling urban air pollution: A benefit-cost assessment. *Science, 252*(5005), 522-528.

Kukkonen, J., Härkönen, J., Walden, J., Karppinen, A., & Lusa, K. (2001). Evaluation of the CAR-FMI model against measurements near a major road. *Atmospheric Environment, 35*(5), 949-960.

Lamb, B., Guenther, A., Gay, D., & Westberg, H. (1987). A national inventory of biogenic hydrocarbon emissions. *Atmospheric Environment, 21*(8), 1695-1705.

Lau, J., Hung, W. T., Cheung, C. S., & Yuen, D. (2008). Contributions of roadside vehicle emissions to general air quality in Hong Kong. *Transportation Research Part D, 13*(1), 19-26.

Lewné, M., Cyrys, J., Meliefste, K., Hoek, G., Brauer, M., Fischer, P., et al. (2004). Spatial variation in nitrogen dioxide in three European areas. *Science of the Total Environment, 332*(1-3), 217-230.

Lin, M., & Lin, Y. (2002). The application of GIS to air quality analysis in Taichung city, Taiwan, ROC. *Environmental Modelling and Software, 17*(1), 11-19.

Liu, P. G., & Johnson, R. (2002). Forecasting peak daily ozone levels--I. A regression with time series errors model having a principal component trigger to fit 1991 ozone levels. *Journal of the Air & Waste Management Association, 52*(9), 1064-1074.

Madsen, C., Carlsen, K. C. L., Hoek, G., Oftedal, B., Nafstad, P., et al. (2007). Modeling the intra-urban variability of outdoor traffic pollution in Oslo, Norway—A GA^2LEN project. *Atmospheric Environment, 41*(35), 7500-7511.

Marr, L. C., & Harley, R. A. (2002). Modeling the effect of weekday-weekend differences in motor vehicle emissions on photochemical air pollution in central California. *Environmental Science & Technology, 36*(19), 4099-4106.

Mass, C. F., Ovens, D., Westrick, K., & Colle, B. A. (2002). Does increasing horizontal resolution produce more skillful forecasts? *Bulletin of the American Meteorological Society, 83*(3), 407.

May, A. D., Mitchell, G., & Kupiszewska, D. (1997). The development of the Leeds quantifiable city model. In P. S. Brandon, P. L. Lombardi & V. Bentivegna (Eds.), *Evaluation of the built environment for sustainability* (1st ed., pp. 568). London; New York: E. & F.N. Spon.

Mensink, C., De Vlieger, I., & Nys, J. (2000). An urban transport emission model for the Antwerp area. *Atmospheric Environment, 34*(27), 4595-4602.

Millionis, A. E., & Davies, T. D. (1994). Regression and stochastic models for air pollution - I. Review, comments and suggestions. *Atmospheric Environment, 28*(17), 2801-2810.

Moran, P. A. P. (1950). Notes on continuous stochastic phenomena. *Biometrika, 37*(1/2), 17-23.

Morgenstern, V., Zutavern, A., Cyrys, J., Brockow, I., Gehring, U., Koletzko, S., et al. (2007). Respiratory health and individual estimated exposure to traffic-related air pollutants in a cohort of young children. *Occup Environ Med, 64*(1), 8-16.

Namdeo, A., & Colls, J. J. (1996). Development and evaluation of SBLINE, a suite of models for the prediction of pollution concentrations from vehicles in urban areas. *Science of the Total Environment, 189-190*, 311-320.

Namdeo, A., Mitchell, G., & Dixon, R. (2002). TEMMS: An integrated package for modelling and mapping urban traffic emissions and air quality. *Environmental Modelling and Software, 17*(2), 177-188.

National Aeronautics and Space Administration, Earth Observatory. (2009). Measuring vegetation (NDVI & EVI), Web site: http://earthobservatory.nasa.gov/Features/MeasuringVegetation/

National Ambient Air Quality Standards for Carbon monoxide—final Decision, F. R. (August 1), 59, 38,906-38,917. (1994).

National Ambient Air Quality Standards for Particulate Matter; Final Rule, 62, 38,652-38,752Cong. (1997).

National Center for Environmental Assessment. (2004). *Air quality criteria for particulate matter*. Research Triangle Park, NC: National Center for Environmental Assessment-RTP Office, Office of Research and Development, U.S. Environmental Protection Agency.

National Institute of Environmental Research. (2004). *Annual report of air quality in Korea 2003*. Seoul, Korea: Ministry of Environment.

National Research Council. (1991). *Rethinking the ozone problem in urban and regional air pollution*. Washington, D.C.: National Academy Press.

Nguyen, H. T., & Kim, K. (2006). Comparison of spatiotemporal distribution patterns of NO_2 between four different types of air quality monitoring stations. *Chemosphere, 65*(2), 201-212.

Pandey, S. K., Kim, K., Chung, S., Cho, S. -., Kim, M. -., & Shon, Z. (2008). Long-term study of NO_x behavior at urban roadside and background locations in Seoul, Korea. *Atmospheric Environment, 42*(4), 607-622.

Parks, R. W. (1967), "Efficient Estimation of a System of Regression Equations When Disturbances Are Both Serially and Contemporaneously Correlated," *Journal of the American Statistical Association*, 62, 500-509.

Potoglou, D., & Kanaroglou, P. S. (2005). Carbon monoxide emissions from passenger vehicles: Predictive mapping with an application to Hamilton, Canada. *Transportation Research Part D, 10*(2), 97-109.

Proposed Revisions to the nation's Ambient Air Quality Standards for Particulate Matter, 49, 10408–10435Cong. (1987).

Pun, B. K., Seigneur, C., & White, W. (2003). Day-of-week behavior of atmospheric ozone in three U.S. cities. *Journal of the Air & Waste Management Association, 53*(7), 789-801.

Raub, J. A., Mathieu-Nolf, M., Hampson, N. B., & Thom, S. R. (2000). Carbon monoxide poisoning - a public health perspective. *Toxicology, 145*(1), 1-14.

Raub, J., United Nations Environment Programme, International Labour Organisation, World Health Organization, Inter-Organization Programme for the Sound Management of Chemicals, & International Program on Chemical Safety. (1999). *Carbon monoxide* (2nd ed.). Geneva: World Health Organization.

Rinne, H. J. I., Guenther, A. B., Greenberg, J. P., & Harley, P. C. (2002). Isoprene and monoterpene fluxes measured above Amazonian rainforest and their dependence on light and temperature. *Atmospheric Environment, 36*(14), 2421-2426.

Roorda-Knape, M. C., Janssen, N. A. H., De Hartog, J. J., Van Vliet, Patricia H. N., Harssema, H., & Brunekreef, B. (1998). Air pollution from traffic in city districts near major motorways. *Atmospheric Environment, 32*(11), 1921-1930.

Roorda-Knape, M. C., Janssen, N. A. H., de Hartog, J., Van Vliet, P. H. N., Harssema, H., & Brunekreef, B. (1999). Traffic related air pollution in city districts near motorways. *The Science of the Total Environment, 235*(1-3), 339-341.

Ross, Z., English, P.,B., Scalf, R., Gunier, R., Smorodinsky, S., Wall, S., et al. (2006). Nitrogen dioxide prediction in southern California using land use regression modeling: Potential for environmental health analyses. *Journal of Exposure Science and Environmental Epidemiology, 16*(2), 106-114.

Ross, Z., Jerrett, M., Ito, K., Tempalski, B., & Thurston, G. D. (2007). A land use regression for predicting fine particulate matter concentrations in the New York City region. *Atmospheric Environment, 41*(11), 2255-2269.

Sahsuvaroglu, T., Arain, A., Kanaroglou, P., Finkelstein, N., Newbold, B., Jerrett, M., et al. (2006). A land use regression model for predicting ambient concentrations of nitrogen dioxide in Hamilton, Ontario, Canada. *Journal of the Air & Waste Management Association, 56*(8), 1059-1069.

Sailor, D. J. (1995). Simulated urban climate response to modifications in surface albedo and vegetative cover. *Journal of Applied Meteorology, 34*, 1694-1704.

Samet, J., Zeger, S., Dominici, F., Curriero, F., Coursac, I., Dockery, D., et al. (2000). National morbidity, mortality, and air pollution study. part II: Morbidity and mortality from air pollution in the united states. Research Reports of the Health Effects Institute (94-II):

Sanderson, M. G., Jones, C. D., Collins, W. J., Johnson, C. E., & Derwent, R. G. (2003). Effect of climate change on isoprene emissions and surface ozone levels. *Geophysical Research Letters, 30*

Schatzmann, M., Rafailidis, S., & Duum, N. I. (1998). Wind tunnel experiments. In J. Fenger, O. Hertel & F. Palmgren (Eds.), *Urban air pollution-European aspects*. Netherlands: Kluwer Academic Publishers.

Schwartz, J., & Zanobetti, A. (2000). Using meta-smoothing to estimate dose-response trends across multiple studies, with application to air pollution and daily death. *Epidemiology, 11*(6), 666-672.

Seaman, N. L. (2000). Meteorological modeling for air-quality assessments. *Atmospheric Environment, 34*(12-14), 2231-2259.

Seinfeld, J. H. (1986). *Atmospheric chemistry and physics of air pollution*. New York: Wiley.

Seinfeld, J. H. (1989). Urban air pollution: State of the science. *Science, 243*(4892), 745-752.

Seinfeld, J. H., & Pandis, S. N. (2006). *Atmospheric chemistry and physics: From air pollution to climate change, 2nd ed.* New York: John Wiley & Sons, Inc.

Seoul Metropolitan Police Agency. (2003). *2003 Seoul traffic monitoring data*. Seoul, Korea: Seoul Metropolitan Police Agency.

Seoul Metropolitan Police Agency. (2006). *2006 Seoul traffic monitoring data*. Seoul, Korea: Seoul Metropolitan Police Agency.

Setton, E., Hystad, P., & Keller, C. P. (2005). Opportunities for using spatial property assessment data in air pollution exposure assessments. *International Journal of Health Geographics, 4*(1), 26.

Sheffi, Y. (1984; 1985). *Urban transportation networks :Equilibrium analysis with mathematical programming methods*. Englewood Cliffs, N.J.: Prentice-Hall.

Shutters, S. T., & Balling, R. C. (2006). Weekly periodicity of environmental variables in Phoenix, Arizona. *Atmospheric Environment, 40*(2), 304-310.

Sillman, S., & Samson, P. J. (1995). Impact of temperature on oxidant photochemistry in urban, polluted rural and remote environments. *Journal of Geophysical Research [Atmospheres], 100*(D6), 11,497-11,508.

Sivacoumar, R., Bhanarkar, A. D., Goyal, S. K., Gadkari, S. K., & Aggarwal, A. L. (2001). Air pollution modeling for an industrial complex and model performance evaluation. *Environmental Pollution, 111*(3), 471-477.

Shen, K. (2004). *Airshed-based statistical modeling of the spatial distribution of air pollution: The case of sulfur dioxide*. Ph.D. Dissertation, Ohio State University, Columbus, Ohio.

Shi, J. P., & Harrison, R. M. (1997). Regression modelling of hourly NO_x and NO_2 concentrations in urban air in London. *Atmospheric Environment, 31*(24), 4081-4094.

Smith, L., Mukerjee, S., Gonzales, M., Stallings, C., Neas, L., Norris, G., et al. (2006). Use of GIS and ancillary variables to predict volatile organic compound and nitrogen dioxide levels at unmonitored locations. *Atmospheric Environment, 40*(20), 3773-3787.

Steiner, A. L., Tonse, S., Cohen, R. C., Goldstein, A. H., & Harley, R. A. (2006). Influence of future climate and emissions on regional air quality in California. *Journal of Geophysical Research, 111,* D18303.

Sullivan, D. C., Reid, S., Stiefer, P., Penfold, B., Chinkin, L., & Funk, T. (2004). *Collection and analysis of weekend/weekday emissions activity data in the south coast air basin* No. STI-901140/901150-2477-FR). Petaluma, CA: California Air Resources Board.

Takahashi, M., Higaki, A., Nohno, M., Kamada, M., Okamura, Y., Matsui, K., et al. (2005). Differential assimilation of nitrogen dioxide by 70 taxa of roadside trees at an urban pollution level. *Chemosphere, 61*(5), 633-639.

Tobler, W. R. (1970). A computer movie simulating urban growth in the Detroit region. *Economic Geography, 46* (Supplement: Proceedings. International Geographical Union. Commission on Quantitative Methods), 234-240.

Trainer, M., Williams, E. J., Parrish, D. D., Buhr, M. P., Allwine, E. J., Westberg, H. H., et al. (1987). Models and observations of the impact of natural hydrocarbons on rural ozone. *Nature, 329*(6141), 705-707.

Tsai, D., Wang, J., Wang, C., & Chan, C. (2008). A study of ground-level ozone pollution, ozone precursors and subtropical meteorological conditions in central Taiwan. *Journal of Environmental Monitoring, 10*(1), 109-118.

Tucker, C. J. (1979). Red and photographic infrared linear combinations for monitoring vegetation. *Remote Sensing of Environment, 8*, 127-150.

US EPA. (2000). *National air pollutant emission trends, 1900-1998* (EPA-454/R-00-002 ed.). Research Triangle Park, NC: Office of Air Quality Planning and Standards.

US EPA. (2006). *Air quality criteria for ozone and related photochemical oxidants, volume I of III*. Research Triangle Park, NC: EPA 600/R-05/004aF: National Center for Environmental Assessment. doi:http://cfpub.epa.gov.proxy.lib.ohio-state.edu/ncea/cfm/recordisplay.cfm?deid=149923

US EPA. (2008). *Integrated science assessment (ISA) for sulfur oxides – health criteria (final report).* Washington, DC, EPA/600/R-08/047F: U.S. Environmental Protection Agency.

WHO Regional Office for Europe. (2006). *Air quality guidelines global updates 2005*. Copenhagen, Denmark: WHO Regional Office for Europe.

WHO. (2006). *WHO air quality guidelines for particulate matter, ozone, nitrogen dioxide and sulfur dioxide, global update 2005,summary of risk assessment*. Geneva, Switzerland: WHO Press.

World Health Organization. (2000). *Air quality guidelines for Europe, 2nd ed.* Copenhagen: World Health Organization, Regional Office for Europe.

Xia, L., & Shao, Y. (2005). Modelling of traffic flow and air pollution emission with application to Hong Kong island. *Environmental Modelling and Software, 20*(9), 1175-1188.

Yang, J., & Miller, D. R. (2002). Trends and variability of ground-level O_3 in Connecticut over the period 1981-1997. *Journal of the Air & Waste Management Association, 52*, 1354-1361.

Yarwood, G., Grant, J., Koo, B., & Dunker, A. M. (2008). Modeling weekday to weekend changes in emissions and ozone in the Los Angeles basin for 1997 and 2010. *Atmospheric Environment, 42*(16), 3765-3779.

Yarwood, G., Stoeckenius, T. E., Heiken, J. G., & Dunker, A. M. (2003). Modeling weekday/weekend ozone differences in the Los Angeles region for 1997. *Journal of the Air & Waste Management Association, 53*(7), 864-875.

Zanobetti, A., & Schwartz, J. (2008). Mortality displacement in the association of ozone with mortality: An analysis of 48 cities in the united states. *Am.J.Respir.Crit.Care Med., 177*(2), 184-189.

Zmirou, D., Gauvin, S., Pin, I., Momas, I., Just, J., Sahraoui, F., et al. (2002). Five epidemiological studies on transport and asthma: Objectives, design and descriptive results. *Journal of Exposure Analysis & Environmental Epidemiology, 12*(3), 186-196.

Appendix A. Matrix of Distances between AQMs

Table A.1 Distance matrix between AQMs

(Unit: km)

	1	2	3	4	5	6	7	8	9	10	11	12	13	14	15	16	17	18	19	20	21	22	23	24	25	26	27	28	29	30	31	32	33	34	Min
1. Jung		3.2	9.8	5.4	5.9	2.9	7.9	9.5	9.6	11.4	12.1	13.8	14.9	9.5	6.7	4.3	11.4	7.8	12.5	5.1	11.7	7.2	12.2	14.5	11.0	13.4	14.4	3.4	1.7	2.5	6.8	3.2	7.8	7.2	1.7
2. Hyoje	3.2		6.7	2.2	7.7	5.8	10.8	10.5	11.7	10.5	10.1	15.8	12.0	7.6	4.3	3.5	8.6	5.2	10.7	8.1	14.1	7.5	15.3	11.9	14.0	11.1	17.4	0.8	3.7	0.7	3.6	6.3	10.6	6.4	0.7
3. Myeonmok	9.8	6.7		4.5	13.4	12.4	17.3	14.6	17.0	11.1	8.3	20.8	6.4	7.8	5.5	8.0	4.2	4.2	9.9	14.7	19.8	11.3	22.0	7.6	20.5	8.8	23.8	6.6	10.1	7.3	3.1	12.9	16.9	8.9	3.1
4. Yongdu	5.4	2.2	4.5		9.3	8.0	13.0	11.7	13.4	10.4	9.2	17.4	10.1	6.9	3.4	4.5	6.8	3.8	9.8	10.3	16.0	8.5	17.5	10.3	16.2	9.8	19.6	2.3	5.8	2.9	1.4	8.5	12.7	6.7	1.4
5. Bulgwang	5.9	7.7	13.4	9.3		6.8	10.0	14.8	13.7	17.3	17.7	17.7	19.4	9.0	8.3	10.1	16.1	12.8	11.2	4.4	14.9	13.0	11.3	19.6	11.7	13.1	15.4	8.3	7.4	7.4	10.4	6.2	10.4	13.0	4.4
6. Mapo	2.9	5.8	12.4	8.0	6.8		5.1	8.0	7.1	11.6	13.2	11.3	17.0	12.2	9.6	5.4	13.3	9.7	15.2	3.8	9.0	6.7	9.7	16.2	8.2	16.3	11.6	5.8	2.3	5.1	9.4	0.9	4.9	7.6	0.9
7. Dangsan	7.9	10.8	17.3	13.0	10.0	5.1		8.2	4.9	13.9	16.7	8.1	21.3	17.1	14.6	9.7	17.7	14.2	20.0	5.6	5.0	8.9	5.9	20.1	3.4	21.2	6.6	10.8	7.2	10.1	14.4	4.9	0.9	10.9	0.9
8. Sadang	9.5	10.5	14.6	11.7	14.8	8.0	8.2		4.0	6.6	10.4	6.4	16.2	18.1	14.8	7.2	13.1	10.5	21.2	11.5	6.8	3.3	14.0	14.2	11.0	21.5	12.6	9.9	7.8	10.0	12.8	8.7	7.3	5.8	3.3
9. Sillim	9.6	11.7	17.0	13.4	13.7	7.1	4.9	4.0		10.6	14.1	4.2	19.6	19.0	15.9	9.1	16.2	13.2	22.0	9.7	3.0	6.3	10.3	17.8	7.2	22.8	8.6	11.2	8.1	11.0	14.7	7.6	4.1	8.8	3.0
10. Dogok	11.4	10.5	11.1	10.4	17.3	11.6	13.9	6.6	10.6		4.2	12.7	10.5	17.2	13.7	7.3	8.0	7.2	20.0	15.4	13.4	5.1	19.9	8.1	17.2	19.5	19.2	9.7	10.0	10.3	10.7	12.4	13.2	4.3	4.2
11. Jamsil	12.1	10.1	8.3	9.2	17.7	13.2	16.7	10.4	14.1	4.2		16.7	6.3	15.4	12.2	8.0	4.4	5.3	18.0	16.9	17.0	7.9	22.4	3.9	20.0	17.0	22.5	9.4	11.2	10.3	8.9	14.1	16.0	5.8	3.9
12. Siheung	13.8	15.8	20.8	17.4	17.7	11.3	8.1	6.4	4.2	12.7	16.7		22.7	23.2	20.1	13.0	19.5	16.8	26.3	13.5	3.3	9.6	12.1	20.6	9.0	26.9	8.6	15.3	12.3	15.1	18.6	11.7	7.5	12.1	3.3
13. Cheonho	14.9	12.0	6.4	10.1	19.4	17.0	21.3	16.2	19.6	10.5	6.3	22.7		14.0	11.8	11.6	3.6	7.2	15.7	20.0	22.6	13.4	26.7	2.8	24.7	14.0	27.6	11.6	14.6	12.5	9.0	17.6	20.7	10.8	2.8
14. Beon	9.5	7.6	7.8	6.9	9.0	12.2	17.1	18.1	19.0	17.2	15.4	23.2	14.0		3.5	11.0	11.9	10.2	3.1	12.4	21.2	15.1	20.0	15.4	19.7	4.2	23.4	8.3	10.8	8.2	6.5	12.3	17.1	13.6	3.1
15. Gireum	6.7	4.3	5.5	3.4	8.3	9.6	14.6	14.8	15.9	13.7	12.2	20.1	11.8	3.5		7.6	9.2	6.9	6.5	10.7	18.3	11.7	18.3	12.8	17.5	6.8	21.1	4.9	7.8	4.9	3.3	9.8	14.5	10.1	3.3
16. Hannam	4.3	3.5	8.0	4.5	10.1	5.4	9.7	7.2	9.1	7.3	8.0	13.0	11.6	11.0	7.6		8.0	4.5	14.1	8.9	11.8	4.1	15.0	10.7	13.1	14.3	16.1	2.8	3.2	3.2	5.7	6.2	9.2	3.0	2.8
17. Guui	11.4	8.6	4.2	6.8	16.1	13.3	17.7	13.1	16.2	8.0	4.4	19.5	3.6	11.9	9.2	8.0		3.6	14.1	16.4	19.2	10.0	23.0	3.6	21.1	12.9	24.0	8.1	11.0	9.0	6.0	14.0	17.1	7.4	3.6
18. Seongsu	7.8	5.2	4.2	3.8	12.8	9.7	14.2	10.5	13.2	7.2	5.3	16.8	7.2	10.2	6.9	4.5	3.6		12.9	12.8	16.1	7.2	19.5	6.8	17.6	12.3	20.6	4.6	7.4	5.5	3.7	10.4	13.7	4.7	3.6
19. Banghak	12.5	10.7	9.9	9.8	11.2	15.2	20.0	21.2	22.0	20.0	18.0	26.3	15.7	3.1	6.5	14.1	14.1	12.9		15.0	24.2	18.2	22.5	17.5	22.4	2.5	26.1	11.3	13.9	11.3	9.3	15.2	20.0	16.6	2.5
20. Namgaja	5.1	8.1	14.7	10.3	4.4	3.8	5.6	11.5	9.7	15.4	16.9	13.5	20.0	12.4	10.7	8.9	16.4	12.8	15.0		10.5	10.5	7.6	19.5	7.4	16.6	11.1	8.4	5.7	7.5	11.6	3.0	6.1	11.4	3.0
21. Guro	11.7	14.1	19.8	16.0	14.9	9.0	5.0	6.8	3.0	13.4	17.0	3.3	22.6	21.2	18.3	11.8	19.2	16.1	24.2	10.5		9.2	8.9	20.8	5.7	25.1	6.0	13.8	10.4	13.4	17.3	9.1	4.5	11.8	3.0
22. Banpo	7.2	7.5	11.3	8.5	13.0	6.7	8.9	3.3	6.3	5.1	7.9	9.6	13.4	15.1	11.7	4.1	10.0	7.2	18.2	10.5	9.2		14.8	11.6	12.2	18.3	14.5	6.9	5.6	7.1	9.5	7.5	8.1	2.6	2.6
23. Hwagok	12.2	15.3	22.0	17.5	11.3	9.7	5.9	14.0	10.3	19.9	22.4	12.1	26.7	20.0	18.3	15.0	23.0	19.5	22.5	7.6	8.9	14.8		25.7	3.2	24.2	5.1	15.4	12.1	14.7	18.9	9.1	6.7	16.6	3.2
24. Bangi	14.5	11.9	7.6	10.3	19.6	16.2	20.1	14.2	17.8	8.1	3.9	20.6	2.8	15.4	12.8	10.7	3.6	6.8	17.5	19.5	20.8	11.6	25.7		23.5	16.0	26.1	11.4	13.9	12.3	9.6	16.9	19.4	9.2	2.8
25. Sinjeong	11.0	14.0	20.5	16.2	11.7	8.2	3.4	11.0	7.2	17.2	20.0	9.0	24.7	19.7	17.5	13.1	21.1	17.6	22.4	7.4	5.7	12.2	3.2	23.5		23.9	3.7	14.0	10.5	13.3	17.6	7.8	4.1	14.3	3.2
26. Sanggye	13.4	11.1	8.8	9.8	13.1	16.3	21.2	21.5	22.8	19.5	17.0	26.9	14.0	4.2	6.8	14.3	12.9	12.3	2.5	16.6	25.1	18.3	24.2	16.0	23.9		27.5	11.7	14.7	11.8	9.0	16.3	21.2	16.4	2.5
27. Gung	14.4	17.4	23.8	19.6	15.4	11.6	6.6	12.6	8.6	19.2	22.5	8.6	27.6	23.4	21.1	16.1	24.0	20.6	26.1	11.1	6.0	14.5	5.1	26.1	3.7	27.5		17.3	13.8	16.7	21.0	11.3	6.9	16.9	3.7
28. Dongdaemun_st	3.4	0.8	6.6	2.3	8.3	5.8	10.8	9.9	11.2	9.7	9.4	15.3	11.6	8.3	4.9	2.8	8.1	4.6	11.3	8.4	13.8	6.9	15.4	11.4	14.0	11.7	17.3		3.6	0.9	3.7	6.3	10.4	5.6	0.8
29. SeoulStation_st	1.7	3.7	10.1	5.8	7.4	2.3	7.2	7.8	8.1	10.0	11.2	12.3	14.6	10.8	7.8	3.2	11.0	7.4	13.9	5.7	10.4	5.6	12.1	13.9	10.5	14.7	13.8	3.6		3.0	7.2	3.0	6.9	5.8	1.7
30. Cheongge_st	2.5	0.7	7.3	2.9	7.4	5.1	10.1	10.0	11.0	10.3	10.3	15.1	12.5	8.2	4.9	3.2	9.0	5.5	11.3	7.5	13.4	7.1	14.7	12.3	13.3	11.8	16.7	0.9	3.0		4.3	5.6	9.9	6.1	0.7
31. Cheongyangni_st	6.8	3.6	3.1	1.4	10.4	9.4	14.4	12.8	14.7	10.7	8.9	18.6	9.0	6.5	3.3	5.7	6.0	3.7	9.3	11.6	17.3	9.5	18.9	9.6	17.6	9.0	21.0	3.7	7.2	4.3		9.9	14.1	7.5	1.4
32. Shinchon_st	3.2	6.3	12.9	8.5	6.2	0.9	4.9	8.7	7.6	12.4	14.1	11.7	17.6	12.3	9.8	6.2	14.0	10.4	15.2	3.0	9.1	7.5	9.1	16.9	7.8	16.3	11.3	6.3	3.0	5.6	9.9		4.9	8.5	0.9
33. Yeongdeungpo_st	7.8	10.6	16.9	12.7	10.4	4.9	0.9	7.3	4.1	13.2	16.0	7.5	20.7	17.1	14.5	9.2	17.1	13.7	20.0	6.1	4.5	8.1	6.7	19.4	4.1	21.2	6.9	10.4	6.9	9.9	14.1	4.9			0.9
34. Sinsa_st	7.2	6.4	8.9	6.7	13.0	7.6	10.9	5.8	8.8	4.3	5.8	12.1	10.8	13.6	10.1	3.0	7.4	4.7	16.6	11.4	11.8	2.6	16.6	9.2	14.3	16.4	16.9	5.6	5.8	6.1	7.5	8.5	10.2		2.6
Min	1.7	0.7	3.1	1.4	4.4	0.9	0.9	3.3	3.0	4.2	3.9	3.3	2.8	3.1	3.3	2.8	3.6	3.6	2.5	3.0	3.0	2.6	3.2	2.8	3.2	2.5	3.7	0.8	1.7	0.7	1.4	0.9	0.9	2.6	

Appendix B. Annual, Seasonal, and Hourly Average Concentrations

Table B.1 Annual and Seasonal Variations of NO_2 Concentrations at each AQM[1]

(Unit: ppb)

AQM No. and Name	Annual				Spring				Summer				Fall				Winter			
	Mean	N	Min	Max	Mean	N	Min	Max	Mean	N	Min	Max	Mean	N	Min	Max	Mean	N	Min	Max
1. Jung	39.0	220	11.1	78.6	43.4	57	24.6	77.5	35.5	55	11.1	68.0	30.6	52	12.9	74.4	45.9	56	20.0	78.6
2. Hyoje	33.2	146	7.9	78.9	40.6	20	18.9	78.2	35.6	55	18.2	60.3	29.1	53	7.9	78.9	29.5	18	11.9	55.5
3. Myeonmok	42.5	215	18.8	92.2	46.1	53	20.8	79.1	36.8	56	18.8	75.5	40.4	54	20.0	92.2	47.1	52	19.4	74.3
4. Yongdu	40.4	196	14.3	108.1	44.2	42	22.5	79.2	33.8	58	14.3	57.2	39.5	47	16.8	108.1	45.9	49	17.1	76.8
5. Bulgwang	33.7	222	13.5	92.4	34.7	59	13.5	68.7	29.2	54	15.3	57.2	33.0	55	14.5	92.4	38.0	54	16.9	69.5
6. Mapo	46.1	164	18.0	90.6	52.0	52	20.6	90.6	40.1	48	18.0	70.6	45.1	34	22.3	79.9	46.7	30	20.1	73.6
7. Dangsan	49.1	193	3.7	119.8	63.3	48	32.9	119.8	46.7	51	3.7	100.7	42.4	49	22.0	77.0	43.9	45	18.3	72.1
8. Sadang	39.3	196	14.8	95.3	37.3	50	19.7	56.6	30.5	48	14.8	47.2	41.2	49	18.4	95.3	48.2	49	20.8	73.4
9. Sillim	47.0	193	14.5	107.5	50.9	52	18.6	92.9	38.7	48	14.5	68.5	49.3	49	19.8	107.5	49.2	44	16.0	83.7
10. Dogok	41.1	195	14.0	95.2	43.1	45	20.2	70.1	34.3	58	14.0	57.7	41.3	49	21.4	95.2	48.1	43	25.2	82.1
11. Jamsil	40.0	184	13.1	96.9	44.7	40	17.6	77.1	31.9	51	13.1	67.4	38.6	45	18.4	92.2	45.9	48	17.5	96.9
12. Siheung	44.6	190	18.9	107.8	44.8	51	22.8	70.6	40.0	44	18.9	72.7	47.9	49	25.7	107.8	45.1	46	26.0	79.3
13. Cheonho	37.0	193	13.0	86.3	39.8	48	13.2	68.0	32.4	45	13.0	69.8	30.7	52	16.0	53.8	45.5	48	20.4	86.3
14. Beon	32.8	226	16.1	71.6	36.1	55	18.8	60.7	27.8	57	16.1	46.5	32.7	58	17.6	71.6	34.8	56	18.7	54.2
15. Gireum	29.5	149	7.6	74.2	37.2	38	22.5	58.9	23.1	47	7.6	47.8	29.5	48	8.0	74.2	29.8	16	8.6	50.1
16. Hannam	44.4	209	14.2	93.2	53.1	53	26.8	93.2	38.7	52	14.2	76.8	32.4	54	17.7	67.1	54.1	50	20.9	93.2
17. Guui	33.4	183	10.0	89.2	36.6	43	18.8	68.3	22.7	46	10.0	49.7	30.7	42	11.0	75.1	42.5	52	16.6	89.2
18. Seongsu	36.8	211	11.6	88.9	42.3	58	17.3	79.1	27.6	53	11.6	51.1	39.3	47	23.3	88.9	37.7	53	19.2	62.1
19. Banghak	32.5	215	8.2	77.3	33.4	59	15.5	56.0	26.7	52	9.1	58.2	29.3	54	8.2	77.3	40.9	50	12.7	71.2
20. Namgaja	42.5	198	15.4	115.5	44.8	52	15.4	79.1	31.2	43	17.8	56.3	44.6	49	18.3	115.5	47.6	54	20.8	80.1
21. Guro	41.6	190	14.9	112.6	41.0	47	16.7	82.5	36.0	44	14.9	64.0	45.6	48	19.6	112.6	43.1	51	17.0	72.6
22. Banpo	45.8	211	16.8	107.9	44.3	53	19.8	100.3	41.0	51	16.8	66.0	49.6	52	27.3	107.9	48.3	55	23.5	71.3
23. Hwagok	42.3	206	16.5	105.7	46.6	53	18.5	76.8	36.2	53	16.5	63.4	44.6	48	18.0	105.7	42.1	52	17.0	73.8
24. Bangi	35.6	188	12.6	71.7	34.0	38	12.6	59.6	31.1	56	14.8	66.5	34.6	43	21.2	56.8	42.7	51	16.0	71.7
25. Sinjeong	36.8	207	11.3	64.3	43.8	57	21.4	64.3	29.7	49	11.3	53.2	32.3	46	20.2	64.3	39.5	55	19.4	62.5
26. Sanggye	34.0	199	10.4	86.2	40.0	48	12.5	86.2	26.6	52	11.3	50.1	28.7	47	10.4	71.0	40.8	52	13.0	70.0
27. Gung	39.9	207	14.0	92.5	39.8	46	14.4	85.3	29.5	55	15.9	43.8	46.1	53	16.5	92.5	44.7	53	14.0	73.4
28. Dongdaemun_st	54.4	177	23.5	124.0	65.7	30	32.5	97.0	49.5	50	23.5	81.7	55.3	47	33.0	124.0	51.8	50	26.3	88.3
29. SeoulStation_st	45.2	187	19.6	91.1	55.0	48	33.0	91.1	38.5	47	19.6	67.1	36.1	47	20.5	69.7	51.2	45	29.7	74.0
30. Cheongge_st	57.6	203	25.9	120.5	58.3	54	30.1	91.0	52.2	46	29.8	85.5	64.8	53	39.9	120.5	54.1	50	25.9	72.9
31. Cheongyangni_st	56.5	175	29.0	102.2	68.6	26	47.9	102.2	54.4	44	29.0	98.4	51.5	53	35.2	101.3	57.4	52	31.9	80.3
32. Shinchon_st	40.3	208	19.0	83.5	43.1	51	25.4	71.2	42.6	53	25.6	65.4	36.8	52	19.0	81.9	38.8	52	22.1	83.5
33. Yeongdeungpo_st	49.1	200	5.8	102.7	46.2	56	10.7	72.3	45.2	52	5.8	91.3	38.9	42	23.5	57.8	64.9	50	34.7	102.7
34. Sinsa_st	50.1	179	23.2	98.6	56.0	29	24.0	98.6	50.9	51	23.8	78.3	46.6	51	23.2	75.8	49.4	48	24.4	82.3
Average*	39.3	197	13.2	92.6	42.9	49	19.1	77.0	33.1	51	13.9	61.7	38.1	49	17.5	86.5	43.2	47	18.0	74.0
Min*	29.5	146	3.7	64.3	33.4	20	12.5	56.0	22.7	43	3.7	43.8	28.7	34	7.9	53.8	29.5	16	8.6	50.1
Max*	49.1	226	18.9	119.8	63.3	59	32.9	119.8	46.7	58	18.9	100.7	49.6	58	27.3	115.5	54.1	56	26.0	96.9

* Values are based on urban background AQMs (No 1. ~ No. 27)

[1] Values are based on daily average in 2003. Exclude weekend and national holiday.

Table B.2 Hourly Variations of NO_2 Concentrations at each AQM[1]

(Unit: ppb)

AQM No. and Name	01	02	03	04	05	06	07	08	09	10	11	12	13	14	15	16	17	18	19	20	21	22	23	24	Avg.
1. Jung	48.9	44.5	40.6	37.1	36.6	36.9	40.9	46.3	48.7	48.6	51.3	48.4	40.8	43.1	44.3	46.7	48.6	47.9	50.1	54.0	56.2	58.0	60.8	57.7	47.4
2. Hyoje	50.1	45.4	40.6	38.5	37.8	37.3	35.7	36.4	36.3	41.9	41.5	41.2	40.4	39.5	36.7	38.6	37.0	39.4	41.4	49.5	54.8	56.6	59.5	58.3	43.1
3. Myeonmok	52.5	44.4	38.7	35.3	34.8	38.3	40.3	42.6	44.2	43.3	39.1	36.5	39.9	38.3	37.8	40.1	44.4	49.8	52.6	62.7	66.2	68.8	65.5	57.7	46.4
4. Yongdu	54.3	49.0	43.7	40.4	38.7	40.8	44.1	46.0	47.9	47.3	43.9	40.1	38.2	38.7	35.2	38.0	39.5	40.8	42.0	50.4	56.8	61.2	63.1	62.3	45.9
5. Bulgwang	33.5	30.0	27.4	24.7	21.6	23.6	28.1	38.2	44.4	42.5	41.4	43.1	38.2	35.4	32.9	33.9	32.7	30.7	33.1	39.1	41.4	41.0	39.5	40.2	34.8
6. Mapo	60.5	56.8	52.5	51.2	51.8	51.8	55.3	59.0	60.1	59.9	57.1	54.8	44.0	41.8	43.8	43.3	46.1	49.9	56.5	60.4	70.1	75.4	78.3	72.3	56.3
7. Dangsan	76.2	68.2	58.4	58.4	57.4	61.5	69.3	73.0	74.4	75.9	75.8	71.7	59.7	59.6	62.5	59.3	58.7	63.4	72.7	85.1	97.0	96.1	91.7	86.5	71.3
8. Sadang	32.2	28.4	29.4	28.7	27.7	29.4	33.4	36.2	41.3	42.1	39.0	37.5	32.9	29.5	28.9	29.4	28.7	31.1	31.1	34.2	36.2	37.6	37.9	38.6	33.4
9. Sillim	71.4	67.4	59.9	57.2	56.0	61.8	68.3	71.3	72.3	74.3	68.6	58.3	48.4	44.5	44.7	42.3	46.0	48.9	56.1	69.7	81.3	86.1	86.5	81.4	63.4
10. Dogok	47.1	42.8	39.2	38.1	37.8	40.1	41.2	44.8	46.1	44.6	42.4	37.7	33.8	31.5	31.4	38.4	38.6	40.7	45.4	55.6	64.6	63.3	59.6	56.5	44.2
11. Jamsil	55.4	51.3	48.3	42.6	39.8	40.1	42.8	46.9	48.9	44.7	42.7	38.0	32.0	34.8	32.8	38.3	43.1	43.8	50.3	58.7	64.3	64.5	63.4	62.5	47.1
12. Siheung	45.3	42.3	38.5	37.7	36.0	37.8	42.6	48.1	50.2	50.6	50.1	47.5	40.0	38.3	39.3	39.1	38.1	40.7	43.2	45.7	47.7	49.4	49.8	47.9	43.6
13. Cheonho	48.7	43.8	39.5	35.4	33.5	32.4	35.1	37.9	39.4	39.6	36.8	33.0	28.6	31.3	33.0	31.6	39.6	40.6	45.6	52.0	60.3	60.2	59.6	56.2	41.4
14. Beon	43.4	37.7	32.7	32.1	32.8	34.5	34.5	34.7	35.4	37.4	34.7	34.3	32.1	30.8	29.0	29.7	32.8	32.4	34.4	39.5	43.9	49.2	49.1	47.9	36.5
15. Gireum	43.7	39.9	36.5	34.6	32.9	35.7	38.0	39.1	40.6	41.0	38.8	37.6	37.2	34.6	34.4	34.7	33.2	33.9	36.0	41.5	44.3	47.2	50.8	48.2	38.9
16. Hannam	60.3	57.5	55.2	50.4	48.2	48.8	48.5	51.4	58.1	61.0	56.9	53.6	50.6	48.1	49.7	53.1	54.7	56.8	58.8	66.8	72.1	68.5	68.0	68.5	56.9
17. Guui	36.1	32.4	29.8	27.6	26.1	25.5	27.6	30.9	32.7	36.1	36.0	32.7	31.8	32.6	31.1	31.8	32.9	33.9	36.2	37.6	40.7	40.8	39.3	38.3	33.4
18. Seongsu	48.3	42.8	40.1	37.4	35.7	35.6	38.4	41.2	44.6	47.0	42.7	43.2	38.2	38.4	37.3	36.3	38.7	41.7	42.3	46.4	49.7	52.7	54.4	53.2	42.7
19. Banghak	39.8	36.3	33.3	30.8	29.9	30.9	35.2	36.2	38.9	40.4	35.8	29.3	28.8	26.4	25.4	23.8	24.3	24.3	26.7	31.1	36.1	42.3	44.3	45.2	33.1
20. Namgaja	55.3	51.0	46.0	38.9	35.9	38.6	42.7	47.3	50.1	49.6	47.7	45.1	42.5	40.3	37.8	38.4	38.8	38.5	42.6	49.9	54.5	60.2	64.7	61.8	46.6
21. Guro	48.9	44.9	39.5	37.9	38.6	41.8	46.5	50.0	52.1	51.7	49.0	41.6	35.2	32.7	38.9	36.9	38.5	43.9	47.4	55.5	62.3	61.3	58.7	55.0	46.2
22. Banpo	48.3	44.8	41.8	38.2	37.7	37.9	43.2	47.6	49.4	50.2	47.5	49.2	45.3	41.8	43.0	45.1	42.6	47.2	50.6	55.5	59.3	61.0	60.0	56.1	47.6
23. Hwagok	56.4	50.0	43.8	39.3	39.4	43.9	48.3	55.0	57.7	57.5	55.3	48.8	40.7	40.4	40.8	40.3	43.6	45.0	47.2	57.1	63.6	66.1	64.7	60.7	50.2
24. Bangi	42.2	37.2	36.7	34.3	28.2	27.9	28.8	38.2	40.7	41.0	39.5	35.6	26.1	28.2	27.4	26.3	30.3	32.6	38.3	40.8	47.1	50.3	50.9	48.9	36.6
25. Sinjeong	48.7	45.7	40.9	38.4	37.5	39.2	44.6	48.9	51.6	52.5	51.5	46.7	34.2	36.4	39.2	34.1	35.1	39.7	43.1	51.0	56.5	56.6	55.4	53.8	45.0
26. Sanggye	52.7	47.8	46.6	41.8	41.0	43.7	49.8	52.9	59.0	53.5	45.4	39.8	36.4	38.8	35.9	35.3	36.6	36.5	40.2	49.7	57.8	62.6	57.2	55.6	46.5
27. Gung	42.6	38.6	34.8	32.4	31.2	35.7	38.5	45.1	42.5	41.5	37.8	31.4	31.1	28.2	32.1	30.9	31.1	33.3	36.9	42.6	47.1	49.5	47.1	47.2	37.9
28. Dongdaemun_st	62.8	57.2	53.6	49.5	47.8	51.4	55.1	57.6	61.1	63.9	65.9	62.3	65.1	65.8	70.0	73.6	72.0	69.5	71.7	75.5	78.5	81.4	79.2	74.2	65.2
29. SeoulStation_st	62.4	51.7	46.3	41.6	37.9	38.6	43.6	48.0	53.1	54.7	59.4	61.6	62.2	64.9	66.8	72.4	78.8	75.4	72.3	73.4	68.6	70.2	68.3	68.2	60.0
30. Cheongge_st	57.4	52.0	50.1	45.5	43.7	47.2	50.8	53.3	54.9	61.3	65.4	69.4	68.9	68.8	72.2	75.0	73.9	72.2	72.6	73.3	70.4	73.4	68.9	64.0	62.7
31. Cheongyangni_st	62.9	55.3	50.3	46.3	45.6	53.9	60.9	65.8	74.3	73.3	69.5	72.1	73.3	77.8	76.6	80.7	83.3	82.1	78.9	84.3	85.2	84.3	80.9	74.6	70.5
32. Shinchon_st	44.1	38.6	35.2	32.2	33.0	42.6	52.7	59.8	55.8	58.8	59.5	55.9	52.7	54.3	54.9	59.8	58.7	59.3	61.9	60.7	62.3	61.0	61.5	56.2	53.0
33. Yeongdeungpo_st	24.8	19.4	17.6	17.2	17.7	23.4	28.4	29.9	31.4	32.9	30.9	29.1	29.8	28.1	29.4	32.1	30.8	31.9	33.3	35.7	35.9	36.0	32.4	29.8	28.7
34. Sinsa_st	66.6	62.6	60.3	57.2	52.2	55.2	56.0	64.3	69.5	73.9	71.1	73.3	67.7	68.3	65.8	71.1	70.6	69.5	73.1	76.1	78.0	77.5	73.9	76.5	67.9
Average*	49.7	45.2	41.3	38.5	37.2	38.9	42.3	46.1	48.4	48.7	46.2	42.8	38.0	37.2	37.2	37.6	39.0	41.0	44.5	51.2	56.7	58.7	58.5	56.2	45.0
Min*	32.2	28.4	27.4	24.7	21.6	23.6	27.6	30.9	32.7	36.1	34.7	29.3	26.1	26.4	25.4	23.8	24.3	24.3	26.7	31.1	36.1	37.6	37.9	38.3	33.1
Max*	76.2	68.2	59.9	58.4	57.4	61.8	69.3	73.0	74.4	75.9	75.8	71.7	59.7	59.6	62.5	59.3	58.7	63.4	72.7	85.1	97.0	96.1	91.7	86.5	71.3

* Values are based on urban background AQMs (No 1. ~ No. 27)

[1] Values are based on hourly average during May 2003. Exclude weekend and national holiday.

Table B.3 Annual and Seasonal Variations of CO Concentrations at each AQM[1]

(Unit: ppm)

AQM No. and Name	Annual				Spring				Summer				Fall				Winter			
	Mean	N	Min	Max	Mean	N	Min	Max	Mean	N	Min	Max	Mean	N	Min	Max	Mean	N	Min	Max
1. Jung	0.83	208	0.18	2.58	0.74	49	0.24	1.89	0.68	52	0.18	1.27	0.80	52	0.18	1.73	1.09	55	0.40	2.58
2. Hyoje	0.65	147	0.12	1.63	0.79	20	0.46	1.29	0.60	55	0.12	1.10	0.62	54	0.15	1.63	0.68	18	0.28	1.60
3. Myeonmok	0.68	221	0.28	2.36	0.64	54	0.31	1.19	0.56	58	0.30	0.98	0.65	57	0.28	1.51	0.87	52	0.35	2.36
4. Yongdu	0.90	201	0.10	4.23	0.85	41	0.10	1.35	0.67	59	0.31	1.35	0.79	47	0.13	2.36	1.29	54	0.50	4.23
5. Bulgwang	0.62	204	0.17	2.10	0.48	50	0.23	0.83	0.51	49	0.26	0.98	0.58	50	0.17	1.40	0.89	55	0.27	2.10
6. Mapo	0.72	166	0.35	1.77	0.69	51	0.39	1.31	0.63	48	0.38	1.10	0.68	34	0.35	1.36	0.91	33	0.38	1.77
7. Dangsan	0.68	188	0.13	2.29	0.56	41	0.23	1.29	0.52	55	0.20	1.05	0.82	49	0.13	1.88	0.85	43	0.20	2.29
8. Sadang	0.66	183	0.11	2.17	0.50	49	0.18	1.11	0.50	44	0.19	1.11	0.72	46	0.11	2.17	0.93	44	0.46	2.12
9. Sillim	0.76	196	0.18	2.51	0.73	54	0.34	1.10	0.62	48	0.31	1.20	0.64	48	0.22	1.36	1.07	46	0.18	2.51
10. Dogok	0.67	193	0.26	3.37	0.60	48	0.30	1.01	0.47	58	0.27	0.76	0.59	47	0.26	1.30	1.16	40	0.43	3.37
11. Jamsil	0.67	192	0.20	2.68	0.71	46	0.23	1.63	0.45	51	0.20	0.80	0.61	47	0.26	1.39	0.91	48	0.30	2.68
12. Siheung	0.68	173	0.11	2.05	0.58	51	0.18	1.15	0.33	36	0.11	0.60	0.78	43	0.20	2.05	0.98	43	0.49	1.98
13. Cheonho	0.72	192	0.14	3.03	0.70	48	0.27	1.18	0.45	44	0.14	0.83	0.68	53	0.25	1.53	1.01	47	0.42	3.03
14. Beon	0.71	214	0.12	2.29	0.57	52	0.14	1.18	0.47	56	0.12	0.97	0.80	56	0.23	2.20	1.01	50	0.15	2.29
15. Gireum	0.68	157	0.26	2.03	0.70	39	0.40	1.11	0.64	51	0.41	1.00	0.69	48	0.26	1.58	0.75	19	0.30	2.03
16. Hannam	0.57	195	0.22	2.14	0.54	49	0.23	0.89	0.46	47	0.22	0.92	0.61	54	0.25	1.39	0.68	45	0.27	2.14
17. Guui	0.62	216	0.14	2.40	0.60	54	0.28	1.28	0.52	55	0.25	0.99	0.52	51	0.14	1.45	0.83	56	0.24	2.40
18. Seongsu	0.57	205	0.22	2.34	0.51	54	0.26	0.86	0.49	53	0.27	0.73	0.59	45	0.22	1.26	0.68	53	0.28	2.34
19. Banghak	0.36	212	0.20	1.15	0.40	59	0.29	0.58	0.28	51	0.20	0.53	0.29	52	0.20	0.62	0.45	50	0.20	1.15
20. Namgaja	0.65	192	0.11	2.39	0.46	51	0.17	0.89	0.38	43	0.20	0.70	0.79	47	0.11	2.03	0.95	51	0.21	2.39
21. Guro	0.79	172	0.10	2.58	0.66	48	0.32	1.14	0.49	37	0.10	0.96	0.82	47	0.34	1.92	1.17	40	0.33	2.58
22. Banpo	0.56	207	0.20	1.55	0.52	51	0.27	1.07	0.47	52	0.26	0.79	0.55	53	0.20	1.19	0.68	51	0.40	1.55
23. Hwagok	0.68	193	0.19	1.81	0.73	52	0.45	1.40	0.42	49	0.19	0.68	0.62	44	0.24	1.81	0.96	48	0.42	1.69
24. Bangi	0.45	185	0.13	1.45	0.44	38	0.24	0.98	0.31	56	0.13	0.59	0.39	44	0.23	0.82	0.68	47	0.14	1.45
25. Sinjeong	0.75	175	0.21	1.98	0.64	45	0.28	1.17	0.47	43	0.21	0.75	0.84	44	0.33	1.98	1.05	43	0.25	1.90
26. Sanggye	0.75	195	0.12	2.62	0.53	42	0.15	1.14	0.53	46	0.18	1.00	0.71	50	0.12	1.59	1.12	57	0.40	2.62
27. Gung	0.60	220	0.21	1.68	0.57	56	0.28	0.95	0.48	56	0.24	0.78	0.60	53	0.21	1.44	0.76	55	0.22	1.68
28. Dongdaemun_st	1.08	179	0.35	2.68	1.17	28	0.59	2.30	0.81	52	0.48	1.23	1.02	46	0.39	2.68	1.35	53	0.35	2.50
29. SeoulStation_st	1.16	188	0.62	2.74	1.12	45	0.62	1.69	1.08	45	0.77	1.57	1.25	48	0.70	2.31	1.19	50	0.64	2.74
30. Cheongge_st	0.83	204	0.38	1.86	0.90	55	0.40	1.60	0.79	48	0.40	1.34	0.66	52	0.38	1.15	0.99	49	0.38	1.86
31. Cheongyangni_st	1.45	170	0.36	4.83	1.41	27	0.91	2.27	1.20	44	0.52	2.03	1.35	49	0.36	3.54	1.80	50	1.11	4.83
32. Shinchon_st	0.75	191	0.26	1.92	0.74	47	0.26	1.55	0.80	43	0.43	1.18	0.64	50	0.41	1.30	0.83	51	0.41	1.92
33. Yeongdeungpo_st	0.55	181	0.23	1.22	0.55	51	0.27	1.22	0.52	45	0.26	0.87	0.55	41	0.33	0.81	0.58	44	0.23	1.05
34. Sinsa_st	1.34	170	0.50	3.05	1.33	20	0.57	2.03	1.36	49	0.70	1.93	1.27	50	0.56	2.15	1.39	51	0.50	3.05
Average*	0.67	193	0.18	2.26	0.61	48	0.27	1.15	0.50	50	0.22	0.91	0.66	49	0.21	1.59	0.90	46	0.31	2.25
Min*	0.36	147	0.10	1.15	0.40	20	0.10	0.58	0.28	36	0.10	0.53	0.29	34	0.11	0.62	0.45	18	0.14	1.15
Max*	0.90	221	0.35	4.23	0.85	59	0.46	1.89	0.68	59	0.41	1.35	0.84	57	0.35	2.36	1.29	57	0.50	4.23

* Values are based on urban background AQMs (No 1. ~ No. 27)

[1] Values are based on hourly average during May 2003. Exclude weekend and national holiday.

Table B.4 Hourly Variations of CO Concentrations at each AQM[1]

(Unit: ppm)

AQM No. and Name	01	02	03	04	05	06	07	08	09	10	11	12	13	14	15	16	17	18	19	20	21	22	23	24	Avg.
1. Jung	0.98	0.99	1.11	1.20	1.11	1.13	1.22	1.39	1.59	1.51	1.43	1.36	1.15	0.94	0.84	0.78	0.89	0.94	0.96	1.00	1.08	1.15	1.07	1.02	1.12
2. Hyoje	N/A	N/A	N/A	N/A	N/A	N/A	N/A	N/A	N/A	N/A	N/A	N/A	N/A	N/A	N/A	N/A	N/A	N/A	N/A	N/A	N/A	N/A	N/A	N/A	N/A
3. Myeonmok	0.89	0.78	0.79	0.77	0.76	0.82	0.95	1.03	1.20	1.04	0.99	0.96	0.86	0.80	0.76	0.71	0.69	0.83	0.97	1.04	1.11	1.16	1.14	1.08	0.92
4. Yongdu	1.25	1.30	1.22	1.16	1.18	1.26	1.32	1.39	1.62	1.72	1.66	1.45	1.39	1.27	1.17	1.16	1.10	1.13	1.20	1.17	1.23	1.32	1.27	1.31	1.30
5. Bulgwang	0.79	0.75	0.76	0.82	0.84	0.87	0.81	0.93	1.25	1.21	1.07	1.07	0.90	0.93	0.91	0.85	0.85	0.83	0.89	0.94	0.95	0.90	0.88	0.85	0.91
6. Mapo	0.99	1.02	0.98	1.08	1.06	1.05	1.16	1.30	1.48	1.33	1.33	1.20	1.00	0.93	0.83	0.85	0.80	0.87	0.89	0.91	0.93	0.92	0.96	1.02	1.04
7. Dangsan	0.80	0.77	0.74	0.82	0.89	0.91	0.98	1.13	1.34	1.39	1.29	1.10	0.94	0.81	0.75	0.70	0.73	0.86	0.90	0.90	0.98	0.97	0.97	0.92	0.94
8. Sadang	0.76	0.79	0.78	0.84	0.84	0.87	0.94	1.16	1.52	1.41	1.12	0.92	0.79	0.68	0.59	0.64	0.65	0.75	0.84	0.78	0.84	0.86	0.94	0.96	0.89
9. Sillim	1.43	1.44	1.42	1.44	1.50	1.50	1.59	1.73	1.87	1.89	1.84	1.62	1.52	1.43	1.26	1.14	1.18	1.19	1.17	1.22	1.27	1.36	1.45	1.44	1.45
10. Dogok	1.27	1.20	1.12	1.24	1.18	1.17	1.34	1.50	1.70	1.84	1.42	1.16	1.17	1.01	0.91	0.91	0.95	0.91	1.05	1.04	1.04	1.26	1.24	1.26	1.20
11. Jamsil	0.99	0.96	0.91	0.91	0.86	0.87	0.98	1.11	1.30	1.34	1.21	0.94	0.95	0.98	0.82	0.83	0.85	0.84	0.86	0.85	0.92	0.95	1.04	1.08	0.97
12. Siheung	1.13	1.09	1.04	1.01	1.10	1.09	1.18	1.43	1.77	1.50	1.29	1.05	1.05	1.03	0.92	0.79	0.86	1.06	1.20	1.14	1.23	1.28	1.23	1.20	1.15
13. Cheonho	0.90	0.90	0.88	0.85	0.84	0.86	0.89	1.00	1.28	1.18	1.04	0.89	0.83	0.83	0.84	0.83	0.81	0.86	0.93	1.01	1.04	1.05	1.11	1.06	0.95
14. Beon	0.93	0.92	0.89	0.89	0.90	0.90	0.94	1.03	1.18	1.30	1.30	1.20	1.21	1.18	1.16	1.10	0.98	0.90	0.88	0.91	0.95	0.96	1.01	1.01	1.03
15. Gireum	N/A	N/A	N/A	N/A	N/A	N/A	N/A	N/A	N/A	N/A	N/A	N/A	N/A	N/A	N/A	N/A	N/A	N/A	N/A	N/A	N/A	N/A	N/A	N/A	N/A
16. Hannam	0.63	0.70	0.83	0.74	0.73	0.79	0.74	0.93	0.98	1.03	0.90	0.73	0.71	0.62	0.52	0.40	0.50	0.71	0.70	0.69	0.68	0.70	0.83	0.69	0.73
17. Guui	1.03	0.99	0.89	0.86	0.87	0.87	0.90	1.10	1.24	1.16	1.09	0.98	0.89	0.89	0.84	0.76	0.72	0.77	0.85	0.97	1.03	1.13	1.15	1.15	0.96
18. Seongsu	0.61	0.65	0.59	0.59	0.61	0.65	0.62	0.65	0.81	1.10	1.10	0.91	0.77	0.86	0.71	0.70	0.71	0.71	0.68	0.66	0.67	0.66	0.62	0.66	0.72
19. Banghak	0.55	0.51	0.49	0.53	0.57	0.61	0.60	0.72	0.95	0.95	0.64	0.47	0.43	0.38	0.34	0.32	0.38	0.40	0.57	0.75	0.91	0.99	0.94	0.83	0.62
20. Namgaja	0.92	0.89	0.90	0.91	0.98	0.98	1.00	1.21	1.32	1.15	1.04	0.98	0.87	0.77	0.72	0.69	0.71	0.73	0.75	0.80	0.89	0.98	0.99	1.04	0.93
21. Guro	1.26	1.22	1.18	1.25	1.24	1.25	1.32	1.50	1.77	1.64	1.52	1.40	1.24	1.11	1.05	1.02	1.11	1.19	1.21	1.29	1.34	1.30	1.36	1.32	1.30
22. Banpo	0.65	0.64	0.69	0.76	0.87	0.82	0.81	0.99	1.19	1.21	1.09	0.96	0.68	0.46	0.37	0.39	0.41	0.40	0.52	0.64	0.68	0.69	0.72	0.68	0.72
23. Hwagok	1.03	0.96	0.92	0.95	1.04	1.05	1.19	1.53	1.77	1.61	1.40	1.13	1.04	0.95	0.80	0.83	0.86	0.90	0.97	1.00	1.05	1.07	1.08	1.16	1.10
24. Bangi	0.79	0.83	0.78	0.81	0.78	0.76	0.76	0.90	0.98	0.98	0.72	0.61	0.55	0.55	0.58	0.53	0.50	0.50	0.57	0.64	0.69	0.86	0.90	0.94	0.73
25. Sinjeong	0.99	0.95	0.96	0.99	1.09	1.19	1.28	1.42	1.65	1.77	1.68	1.39	1.15	0.86	0.60	0.55	0.47	0.57	0.70	0.83	0.94	1.00	1.05	1.09	1.05
26. Sanggye	1.08	1.10	1.04	1.02	1.07	1.07	1.15	1.28	1.54	1.51	1.46	1.19	1.15	1.12	1.07	1.05	1.02	1.02	1.13	1.26	1.23	1.25	1.20	1.17	1.17
27. Gung	0.72	0.71	0.67	0.68	0.68	0.73	0.82	1.11	1.48	1.38	1.09	0.87	0.73	0.60	0.58	0.55	0.57	0.66	0.81	0.85	0.90	0.89	0.89	0.84	0.83
28. Dongdaemun_st	1.26	1.41	1.39	1.29	1.26	1.30	1.37	1.49	1.66	1.70	1.70	1.59	1.59	1.50	1.46	1.44	1.44	1.50	1.59	1.51	1.43	1.49	1.41	1.36	1.46
29. SeoulStation_st	1.09	0.91	0.97	1.07	0.99	1.04	1.05	1.16	1.32	1.30	1.27	1.30	1.27	1.07	1.06	1.06	1.09	1.09	1.08	1.10	1.12	1.09	1.09	1.01	1.11
30. Cheongge_st	0.82	0.91	0.96	0.96	0.88	0.95	0.99	1.28	1.47	1.75	1.86	1.79	1.28	0.99	0.84	0.96	0.90	1.04	0.97	0.85	0.76	0.82	0.87	0.97	1.08
31. Cheongyangni_st	1.33	1.25	1.20	1.16	1.19	1.35	1.42	1.67	1.97	2.00	2.00	2.15	1.81	1.81	1.73	1.81	1.84	1.90	1.90	1.75	1.63	1.72	1.67	1.52	1.66
32. Shinchon_st	0.77	0.61	0.62	0.56	0.56	0.59	0.82	1.36	1.64	1.48	1.26	1.20	0.67	0.56	0.55	0.59	0.74	0.62	0.77	0.89	1.09	1.11	1.14	1.07	0.89
33. Yeongdeungpo_st	0.57	0.52	0.47	0.52	0.46	0.41	0.44	0.54	0.69	0.77	0.94	0.89	0.60	0.48	0.73	0.65	0.66	0.80	0.75	0.74	0.56	0.53	0.54	0.38	0.61
34. Sinsa_st	1.24	1.24	1.39	1.35	1.29	1.32	1.30	1.48	1.83	1.93	1.90	1.75	1.47	1.38	1.15	1.06	1.11	1.29	1.34	1.29	1.24	1.28	1.30	1.33	1.38
Average*	0.93	0.92	0.90	0.92	0.94	0.96	1.02	1.18	1.39	1.36	1.23	1.06	0.96	0.88	0.80	0.76	0.77	0.82	0.89	0.93	0.98	1.03	1.04	1.03	0.99
Min*	0.55	0.51	0.49	0.53	0.57	0.61	0.60	0.65	0.81	0.95	0.64	0.47	0.43	0.38	0.34	0.32	0.38	0.40	0.52	0.64	0.67	0.66	0.62	0.66	0.62
Max*	1.43	1.44	1.42	1.44	1.50	1.50	1.59	1.73	1.87	1.89	1.84	1.62	1.52	1.43	1.26	1.16	1.18	1.19	1.21	1.29	1.34	1.36	1.45	1.44	1.45

* Values are based on urban background AQMs (No 1. ~ No. 27)

[1] Values are based on hourly average during May 2003. Exclude weekend and national holiday.

Table B.5 Annual and Seasonal Variations of O_3 Concentrations at each AQM[1]

(Unit: ppb)

AQM No. and Name	Annual				Spring				Summer				Fall				Winter			
	Mean	N	Min	Max	Mean	N	Min	Max	Mean	N	Min	Max	Mean	N	Min	Max	Mean	N	Min	Max
1. Jung	15.4	51	4.3	37.8	18.2	13	5.8	32.9	17.4	14	5.3	32.4	11.1	12	4.3	37.8	14.5	12	4.9	28.0
2. Hyoje	12.8	34	0.6	35.7	19.2	5	6.5	27.2	15.1	14	2.3	35.7	8.5	12	0.6	22.2	9.0	3	1.3	19.4
3. Myeonmok	13.9	46	2.8	35.3	17.4	11	4.9	35.3	16.0	13	3.2	27.0	11.5	12	4.8	25.0	10.1	10	2.8	24.0
4. Yongdu	13.8	45	1.1	37.3	17.8	9	5.5	33.5	17.6	14	3.7	34.4	9.9	12	2.4	37.3	9.6	10	1.1	20.9
5. Bulgwang	21.0	52	2.6	56.0	27.1	13	11.7	56.0	25.5	14	5.9	47.3	14.1	13	5.1	36.0	16.6	12	2.6	36.8
6. Mapo	17.2	41	1.3	39.7	21.6	13	3.4	38.7	18.4	13	5.3	39.7	13.3	8	4.3	38.9	11.5	7	1.3	24.3
7. Dangsan	14.4	46	1.4	35.2	20.4	11	6.2	35.2	18.0	12	3.2	30.1	10.0	12	1.4	34.3	9.5	11	1.8	21.5
8. Sadang	14.2	48	2.3	35.5	14.3	12	3.3	26.0	16.0	14	4.9	34.4	13.4	11	5.5	32.2	12.5	11	2.3	35.5
9. Sillim	15.3	49	1.0	40.1	21.0	12	4.3	40.1	18.4	13	5.2	37.8	11.3	13	2.9	26.1	10.2	11	1.0	27.9
10. Dogok	13.1	44	1.1	30.0	19.3	11	8.5	30.0	16.6	13	4.4	29.3	7.0	10	3.1	11.4	7.6	10	1.1	19.3
11. Jamsil	14.4	46	2.4	32.8	18.0	12	5.8	30.2	17.5	13	4.1	31.6	11.2	11	2.8	32.8	9.7	10	2.4	24.1
12. Siheung	14.7	46	1.8	40.9	21.1	12	1.8	40.9	17.2	12	4.6	33.0	9.7	12	2.0	31.8	10.2	10	3.3	27.5
13. Cheonho	17.4	49	2.2	43.0	20.4	13	7.2	35.1	22.2	13	4.5	34.8	14.9	12	5.0	43.0	10.9	11	2.2	30.8
14. Beon	13.8	52	0.3	34.8	18.2	13	4.2	32.3	18.5	14	5.0	30.9	10.0	13	3.9	34.8	7.8	12	0.3	20.6
15. Gireum	13.9	39	1.0	31.7	21.6	9	10.0	29.9	15.7	14	4.5	30.0	8.8	12	2.3	31.7	5.6	4	1.0	16.2
16. Hannam	14.0	50	1.1	35.0	16.2	13	5.6	32.6	19.8	13	2.8	35.0	9.4	13	1.1	33.3	9.9	11	1.4	24.6
17. Guui	13.0	47	2.5	38.4	13.7	12	4.7	21.6	17.5	11	4.6	25.5	12.1	12	3.1	38.4	9.0	12	2.5	22.1
18. Seongsu	13.4	50	1.0	36.3	20.6	13	4.4	36.3	14.8	12	2.5	30.1	9.8	13	2.9	32.9	8.0	12	1.0	28.2
19. Banghak	13.4	50	0.9	37.8	20.6	13	5.2	37.8	16.7	12	2.7	32.5	7.4	13	0.9	33.5	8.7	12	1.0	22.8
20. Namgaja	13.1	50	1.5	40.8	16.1	12	3.7	40.8	16.7	13	2.5	31.8	10.3	13	3.3	31.0	9.1	12	1.5	23.0
21. Guro	12.9	44	1.0	33.3	19.0	11	5.7	32.9	15.7	12	4.2	33.3	7.5	10	1.6	18.6	8.8	11	1.0	19.1
22. Banpo	14.4	51	1.6	40.4	18.6	13	4.0	33.5	18.6	13	3.4	36.9	10.5	13	2.6	40.4	9.5	12	1.6	22.6
23. Hwagok	17.1	49	3.0	38.8	21.8	13	5.4	34.5	20.5	13	4.9	38.2	13.0	12	3.0	38.8	12.2	11	3.7	21.8
24. Bangi	15.0	45	2.0	35.6	16.8	9	6.9	35.6	20.7	13	7.5	33.4	12.4	11	4.1	35.6	9.8	12	2.0	25.2
25. Sinjeong	13.8	51	1.5	38.1	17.2	13	3.5	32.9	16.7	14	3.0	38.1	10.5	12	2.6	29.7	10.0	12	1.5	20.8
26. Sanggye	15.6	50	3.8	43.0	21.2	12	7.9	43.0	19.0	13	7.2	34.7	10.6	13	4.5	24.2	11.8	12	3.8	27.7
27. Gung	12.2	52	0.4	28.1	17.4	13	4.3	27.4	12.3	14	1.4	28.1	9.3	13	2.5	22.4	9.5	12	0.4	26.3
28. Dongdaemun_st	11.0	40	1.7	26.5	16.3	8	6.9	26.5	13.2	11	2.3	22.4	6.9	11	2.8	20.8	8.8	10	1.7	22.1
29. SeoulStation_st	8.4	46	2.5	22.6	7.0	12	4.1	16.2	12.3	13	4.8	22.6	6.9	10	4.0	14.9	6.7	11	2.5	16.3
30. Cheongge_st	9.2	45	2.5	24.7	9.6	12	5.1	14.8	13.2	13	5.1	20.1	5.9	10	2.7	24.7	7.0	10	2.5	17.0
31. Cheongnyangni_st	8.7	30	1.1	23.7	17.7	3	15.8	18.9	11.6	12	3.8	23.7	4.5	11	2.2	8.7	4.4	4	1.1	11.4
32. Shinchon_st	9.1	45	2.0	18.3	10.6	11	7.7	13.2	11.8	10	2.4	18.3	8.0	12	4.0	16.3	6.8	12	2.0	11.7
33. Yeongdeungpo_st	10.2	45	0.8	27.3	10.2	13	8.0	20.8	14.7	10	0.8	27.3	7.6	12	2.4	16.4	8.6	10	3.8	17.5
34. Sinsa_st	9.9	41	2.0	27.5	16.3	6	2.9	23.1	11.0	14	2.0	22.5	7.7	10	2.0	27.5	6.8	11	2.0	18.4
Average	13.5	46	1.7	34.8	17.7	11	5.9	31.3	16.7	13	3.9	31.3	9.9	12	3.0	28.9	9.4	10	1.9	22.8
Min	8.4	30	0.3	18.3	7.0	3	1.8	13.2	11.0	10	0.8	18.3	4.5	8	0.6	8.7	4.4	3	0.3	11.4
Max	21.0	52	4.3	56.0	27.1	13	15.8	56.0	25.5	14	7.5	47.3	14.9	13	5.5	43.0	16.6	12	4.9	36.8

* Values are based on urban background AQMs (No 1. ~ No. 27)

[1] Values are based on hourly average during May 2003. Exclude weekend and national holiday.

Table B.6 Hourly Variations of O_3 Concentrations at each AQM[1]

(Unit: ppb)

AQM No. and Name	01	02	03	04	05	06	07	08	09	10	11	12	13	14	15	16	17	18	19	20	21	22	23	24	Avg.
1. Jung	8.8	9.4	10.8	13.1	15.5	12.1	11.0	11.5	15.2	17.7	22.6	30.0	43.5	49.5	53.3	52.4	45.8	39.6	33.8	28.7	24.0	18.8	13.9	12.1	24.7
2. Hyoje	5.4	5.5	7.0	6.2	9.0	7.2	6.2	7.9	10.0	12.5	17.6	26.3	35.9	44.2	47.6	45.5	42.4	38.5	32.5	28.1	22.7	16.6	9.8	7.4	20.5
3. Myeonmok	11.2	12.0	14.2	13.9	13.9	12.0	13.2	16.5	21.0	27.5	36.1	41.7	48.5	53.4	56.5	54.9	51.8	42.6	33.4	22.0	17.9	14.4	10.2	8.9	27.0
4. Yongdu	7.0	7.0	8.1	10.1	11.7	6.8	6.3	10.5	14.7	19.4	25.4	38.1	47.5	57.0	61.5	62.5	59.6	54.4	44.0	30.3	22.1	19.0	11.3	10.3	26.8
5. Bulgwang	23.8	26.5	24.3	26.6	28.3	25.6	19.8	20.0	25.5	27.3	35.4	49.0	63.5	72.0	75.2	75.1	68.1	65.2	60.4	51.3	43.9	40.0	33.5	27.2	42.0
6. Mapo	12.2	14.8	11.9	14.4	17.9	12.6	11.1	11.8	17.3	22.7	28.2	37.8	50.3	61.4	68.7	68.6	62.5	57.9	48.7	36.8	26.6	18.0	17.3	16.1	31.1
7. Dangsan	6.9	6.1	8.3	8.2	11.5	7.3	6.0	6.8	9.4	13.4	20.6	25.3	39.1	48.8	52.9	51.8	46.8	43.9	36.0	25.2	20.7	14.6	12.3	9.9	22.2
8. Sadang	8.6	9.0	8.5	10.4	10.7	8.7	6.8	7.3	9.2	10.7	14.7	19.2	27.1	36.9	42.5	43.8	39.7	35.2	29.0	22.9	16.4	14.4	12.4	9.8	18.9
9. Sillim	11.4	12.2	12.8	14.6	14.0	12.4	8.9	10.7	14.3	19.2	25.9	32.3	45.5	55.5	61.9	59.5	55.4	52.2	43.5	30.1	19.2	14.8	9.7	11.6	27.0
10. Dogok	6.3	7.5	7.9	8.5	8.3	8.2	8.5	9.9	11.6	13.7	21.2	29.5	39.1	45.2	52.2	53.5	50.5	44.3	33.8	23.5	13.5	10.0	7.7	6.9	21.7
11. Jamsil	7.0	8.5	8.5	8.6	8.5	8.1	8.6	10.3	14.0	15.8	25.2	38.2	45.0	55.5	60.5	63.8	60.0	52.3	41.2	24.2	17.7	13.5	9.3	6.5	25.5
12. Siheung	14.7	15.9	19.1	19.0	19.5	17.3	15.5	13.8	14.6	20.5	23.8	28.6	38.1	46.2	50.6	50.3	48.3	44.1	36.3	27.5	23.1	19.8	17.2	16.9	26.7
13. Cheonho	9.2	9.0	10.2	11.5	9.6	9.4	8.2	11.5	15.6	22.9	30.5	41.5	50.8	56.5	63.1	63.2	63.0	56.3	49.4	35.4	24.9	16.3	11.7	10.3	28.7
14. Beon	7.8	11.1	13.4	12.0	10.9	8.5	8.4	10.2	13.8	19.7	28.0	38.5	47.4	57.9	60.4	59.7	58.7	53.7	45.5	31.4	25.5	23.5	17.8	12.1	28.2
15. Gireum	9.3	11.0	13.6	14.8	11.4	9.1	8.5	11.9	14.6	19.5	27.0	33.4	43.0	50.6	54.5	55.9	53.5	49.8	39.5	32.5	26.5	20.2	11.4	9.1	26.3
16. Hannam	12.2	13.2	13.5	14.4	17.6	16.1	14.1	16.4	17.9	18.9	26.1	32.7	39.5	47.6	50.6	52.2	49.5	42.4	33.9	25.6	21.0	15.7	13.5	13.1	25.7
17. Guui	7.4	7.6	7.6	7.6	7.4	8.1	7.3	8.4	9.8	11.9	16.7	22.6	28.0	33.2	35.8	39.0	38.1	33.4	29.3	20.9	15.1	13.3	9.8	8.1	17.8
18. Seongsu	9.1	9.5	9.5	10.2	13.8	12.0	8.5	10.8	14.5	18.0	26.0	34.0	45.2	51.2	53.6	59.2	55.1	50.5	41.5	28.4	21.3	18.4	10.7	7.3	25.8
19. Banghak	8.9	8.7	10.5	8.5	8.1	9.0	6.2	6.9	11.0	18.0	28.1	41.6	52.2	62.8	67.6	68.5	67.2	65.4	58.2	47.6	37.8	27.7	20.9	16.3	31.6
20. Namgaja	6.6	8.2	10.1	10.1	14.5	10.0	8.6	8.7	12.2	13.0	21.6	25.8	37.5	42.5	46.0	47.8	42.6	42.0	39.3	32.2	24.7	15.8	12.5	10.1	22.6
21. Guro	9.5	8.8	11.2	11.7	10.1	12.1	8.0	9.3	13.5	18.3	21.5	29.9	38.8	47.8	51.0	47.1	44.3	39.0	32.5	23.7	18.5	13.1	13.4	11.2	22.7
22. Banpo	10.0	10.7	11.9	13.8	14.6	13.9	10.8	11.5	14.3	17.0	23.4	32.7	39.3	50.8	55.0	59.3	52.5	43.5	34.4	20.7	13.6	12.2	10.5	10.9	24.5
23. Hwagok	10.9	14.5	14.3	16.2	16.8	13.8	11.5	12.7	15.4	19.6	27.7	38.5	46.5	54.8	59.6	56.5	54.5	52.4	46.2	33.5	26.5	21.3	18.0	17.2	29.1
24. Bangi	11.0	11.2	10.4	12.1	11.9	11.3	10.4	11.2	14.9	21.4	25.8	34.4	41.9	46.2	49.6	52.4	52.0	45.1	36.0	27.4	22.6	16.0	11.9	11.0	24.9
25. Sinjeong	6.5	7.8	8.7	8.5	13.6	10.6	8.1	7.9	8.6	9.8	13.1	18.2	30.8	43.4	46.4	46.0	45.1	43.8	37.6	27.2	20.7	15.5	12.5	10.2	20.9
26. Sanggye	14.4	12.5	13.7	13.0	11.6	11.4	11.0	14.4	15.0	17.9	31.1	42.4	54.0	62.5	66.2	67.6	66.9	65.9	57.9	47.5	34.3	23.9	21.8	18.4	33.1
27. Gung	7.3	8.5	8.5	7.7	9.1	8.6	8.4	10.2	13.4	17.7	25.2	32.9	44.5	52.1	53.5	50.5	47.3	42.5	36.6	22.9	14.5	11.0	9.4	6.9	22.9
28. Dongdaemun_st	6.0	7.3	8.5	8.8	10.7	7.5	6.5	9.1	11.8	15.8	18.3	26.3	32.3	40.9	40.6	41.1	37.8	30.6	25.1	17.4	12.6	10.7	7.6	7.3	18.4
29. SeoulStation_st	5.7	6.8	7.7	8.2	9.4	10.6	6.0	5.1	5.8	7.0	7.6	8.5	10.5	12.2	15.4	16.2	19.3	17.2	16.2	13.2	10.2	8.5	7.5	6.7	10.1
30. Cheongge_st	8.4	7.9	8.3	9.3	10.5	9.2	7.5	8.8	9.7	10.7	11.7	14.3	16.2	17.5	20.9	20.6	19.2	17.9	15.7	14.1	12.4	11.7	9.8	8.8	12.5
31. Cheongnyangni_st	6.2	8.3	9.1	12.5	11.2	5.5	5.1	7.3	10.1	12.6	18.4	25.4	30.2	36.1	36.6	34.9	31.7	26.4	20.4	13.7	10.6	10.6	5.8	5.6	16.4
32. Shinchon_st	9.7	10.4	11.3	11.5	11.7	10.8	10.0	10.2	11.2	11.9	13.1	14.8	16.1	17.5	16.3	17.4	16.5	14.0	13.0	11.5	10.5	10.5	9.9	10.1	12.5
33. Yeongdeungpo_st	10.6	10.6	11.2	11.5	11.9	10.6	9.7	10.3	10.5	10.9	12.2	13.5	15.5	18.6	18.8	18.4	16.6	15.4	12.6	12.2	12.0	11.4	11.3	11.2	12.8
34. Sinsa_st	7.6	8.6	9.9	10.2	10.9	10.0	7.3	8.1	11.0	13.7	18.3	24.7	32.9	37.9	41.1	43.6	39.0	36.0	31.1	18.9	13.6	8.5	6.2	6.5	19.0
Average	9.3	10.2	11.0	11.7	12.5	10.8	9.2	10.5	13.3	16.7	22.6	30.1	38.7	46.1	49.6	50.0	47.1	42.7	36.0	26.7	20.5	16.2	12.6	10.9	23.5
Min	5.4	5.5	7.0	6.2	7.4	5.5	5.1	5.1	5.8	7.0	7.6	8.5	10.5	12.2	15.4	16.2	16.5	14.0	12.6	11.5	10.2	8.5	5.8	5.6	10.1
Max	23.8	26.5	24.3	26.6	28.3	25.6	19.8	20.0	25.5	27.5	36.1	49.0	63.5	72.0	75.2	75.1	68.1	65.9	60.4	51.3	43.9	40.0	33.5	27.2	42.0

* Values are based on urban background AQMs (No 1. ~ No. 27)

[1] Values are based on hourly average during May 2003. Exclude weekend and national holiday.

Table B.7 Annual and Seasonal Variations of SO_2 Concentrations at each AQM[1]

(Unit: ppb)

AQM No. and Name	Annual				Spring				Summer				Fall				Winter			
	Mean	N	Min	Max	Mean	N	Min	Max	Mean	N	Min	Max	Mean	N	Min	Max	Mean	N	Min	Max
1. Jung	5.3	219	1.2	15.8	4.1	56	1.2	9.6	4.9	54	3.1	10.1	5.0	52	1.8	11.5	6.9	57	2.5	15.8
2. Hyoje	3.6	147	1.1	11.1	5.3	19	2.0	11.1	3.5	55	1.1	9.2	2.8	55	1.1	7.6	4.6	18	1.4	10.2
3. Myeonmok	7.0	217	2.9	17.0	7.4	53	5.0	10.8	5.9	55	4.4	9.5	5.9	57	2.9	8.4	9.0	52	3.3	17.0
4. Yongdu	6.3	190	2.5	17.0	6.5	43	3.4	11.7	5.3	52	3.0	8.9	5.3	47	2.5	9.0	8.4	48	3.5	17.0
5. Bulgwang	4.5	213	1.4	12.7	4.0	55	1.8	12.6	3.2	51	1.4	7.9	3.5	53	1.6	7.6	7.3	54	2.7	12.7
6. Mapo	5.5	160	1.4	17.1	6.0	52	1.5	17.1	4.4	44	1.4	9.3	3.9	33	1.5	8.1	8.1	31	2.2	14.8
7. Dangsan	6.9	184	1.8	17.0	6.8	46	1.8	16.4	6.4	52	4.3	11.7	6.5	41	2.0	11.6	7.9	45	2.4	17.0
8. Sadang	4.3	190	1.1	15.7	4.4	49	1.8	7.8	3.2	42	1.1	6.6	3.7	48	1.4	9.7	5.5	51	1.6	15.7
9. Sillim	5.7	192	1.1	17.5	4.4	52	2.1	9.8	5.3	48	2.8	7.8	4.6	46	1.1	13.8	8.6	46	2.4	17.5
10. Dogok	6.3	193	1.0	21.1	7.0	45	4.0	13.3	4.8	58	1.0	8.8	5.6	49	1.3	12.1	8.4	41	2.8	21.1
11. Jamsil	4.9	190	1.2	14.5	4.2	48	1.8	9.2	4.0	51	3.0	5.7	4.4	47	1.8	9.7	7.0	44	1.2	14.5
12. Siheung	4.8	188	1.0	13.9	4.4	52	1.0	12.9	5.2	45	1.6	9.2	3.8	47	1.1	13.5	6.0	44	1.1	13.9
13. Cheonho	4.8	174	1.2	15.7	4.6	41	1.2	11.6	4.0	37	1.2	10.4	3.7	52	1.3	10.7	7.1	44	1.4	15.7
14. Beon	4.8	213	1.1	18.1	4.4	52	1.3	9.1	2.9	55	1.1	11.6	4.8	54	2.1	11.7	7.4	52	3.1	18.1
15. Gireum	3.4	153	1.2	10.5	3.4	35	1.3	6.9	2.3	51	1.2	4.9	3.9	48	1.6	10.5	5.4	19	2.6	8.5
16. Hannam	5.4	192	1.2	14.4	5.6	49	1.7	13.5	3.1	46	1.2	7.1	5.3	49	1.9	11.7	7.7	48	1.3	14.4
17. Guui	3.8	212	1.0	17.6	3.2	54	1.1	12.0	2.2	52	1.4	5.0	3.5	51	1.0	10.7	6.2	55	1.5	17.6
18. Seongsu	4.4	210	1.4	14.3	4.1	56	2.0	8.6	3.2	52	1.8	7.9	4.2	47	1.7	12.8	6.0	55	1.4	14.3
19. Banghak	5.0	215	1.0	19.9	4.7	59	1.2	10.3	2.7	52	1.0	8.5	5.0	54	1.3	13.4	7.5	50	1.9	19.9
20. Namgaja	4.0	190	1.0	14.5	3.6	51	1.2	9.0	2.2	41	1.0	5.8	3.2	47	1.0	7.9	6.5	51	1.7	14.5
21. Guro	5.7	183	1.2	22.1	4.8	44	1.3	10.6	3.5	43	1.2	8.3	5.1	45	1.2	15.4	9.1	51	1.5	22.1
22. Banpo	6.0	201	1.2	19.7	5.0	49	1.7	9.3	4.9	50	2.1	9.8	5.7	52	1.2	17.0	8.2	50	2.5	19.7
23. Hwagok	3.9	197	1.0	14.8	3.9	53	1.2	10.6	2.4	49	1.0	6.0	3.7	49	1.2	10.1	5.9	46	1.5	14.8
24. Bangi	4.4	179	1.9	10.7	3.7	37	2.3	5.5	4.1	53	2.2	6.3	3.6	43	1.9	6.9	6.2	46	1.9	10.7
25. Sinjeong	4.1	168	1.0	12.6	3.8	43	1.0	9.2	2.6	41	1.0	6.9	3.7	38	1.6	6.8	6.0	46	1.8	12.6
26. Sanggye	4.9	180	1.1	20.8	3.6	46	1.4	9.7	3.5	44	1.3	8.0	4.4	42	1.5	11.2	8.0	48	1.1	20.8
27. Gung	4.1	221	1.0	11.5	4.9	55	1.6	8.8	3.2	58	1.1	6.1	2.8	53	1.1	7.2	5.7	55	1.0	11.5
28. Dongdaemun_st	8.1	159	2.1	21.5	8.1	26	2.2	14.3	8.4	35	4.5	14.2	8.5	46	2.3	21.5	7.6	52	2.1	15.8
29. SeoulStation_st	4.9	190	1.9	14.8	4.8	43	2.3	8.9	3.5	50	1.9	9.8	5.0	48	2.4	14.8	6.4	49	3.2	11.3
30. Cheongge_st	6.5	191	1.3	18.8	7.8	49	1.8	16.6	4.3	41	1.8	10.1	4.8	52	1.3	13.3	9.0	49	3.0	18.8
31. Cheongyangni_st	8.2	116	2.5	24.0	13.4	12	6.2	24.0	7.6	35	3.4	12.7	7.4	50	2.5	12.6	8.4	19	3.8	16.1
32. Shinchon_st	7.1	189	1.0	18.0	7.0	52	1.0	13.2	5.8	45	1.0	12.4	7.6	46	1.8	17.8	7.9	46	1.0	18.0
33. Yeongdeungpo_st	5.3	205	1.7	13.7	5.6	55	2.8	12.8	3.7	56	1.7	7.2	4.9	43	2.3	13.4	6.9	51	3.5	13.7
34. Sinsa_st	7.5	161	1.2	18.9	7.1	28	2.0	13.8	7.4	44	2.1	12.8	5.7	38	1.2	10.3	9.1	51	2.9	18.9
Average*	5.0	192	1.3	15.8	4.7	48	1.8	10.6	3.8	49	1.8	8.0	4.4	48	1.5	10.6	7.0	46	2.0	15.6
Min*	3.4	147	1.0	10.5	3.2	19	1.0	5.5	2.2	37	1.0	4.9	2.8	33	1.0	6.8	4.6	18	1.0	8.5
Max*	7.0	221	2.9	22.1	7.4	59	5.0	17.1	6.4	58	4.4	11.7	6.5	57	2.9	17.0	9.1	57	3.5	22.1

* Values are based on urban background AQMs (No 1. ~ No. 27)

[1] Values are based on hourly average during May 2003. Exclude weekend and national holiday.

Table B.8 Hourly Variations of SO_2 Concentrations at each AQM[1]

(Unit: ppb)

AQM No. and Name	01	02	03	04	05	06	07	08	09	10	11	12	13	14	15	16	17	18	19	20	21	22	23	24	Avg.
1. Jung	5.9	5.4	5.4	5.3	5.5	6.0	6.6	7.6	8.7	9.2	9.2	8.9	9.1	8.4	8.2	7.5	7.0	6.7	6.8	6.8	6.7	6.9	6.7	6.6	7.1
2. Hyoje	4.2	3.9	4.0	4.2	4.3	4.2	4.8	5.2	6.0	6.3	6.2	5.6	5.1	5.3	5.2	4.9	4.7	4.7	4.7	4.3	4.0	4.2	3.9	4.2	4.8
3. Myeonmok	7.0	7.0	6.9	7.1	7.2	7.8	7.4	8.0	8.0	7.8	8.8	9.0	8.8	9.5	9.5	9.4	9.6	9.0	9.3	9.3	9.5	9.2	8.8	8.4	8.4
4. Yongdu	6.5	6.5	6.2	6.8	6.6	7.0	7.1	7.0	7.6	8.0	8.6	9.0	9.1	9.2	10.3	10.0	9.6	8.8	9.1	8.9	8.7	8.2	7.9	7.4	8.1
5. Bulgwang	4.8	4.6	4.7	4.5	4.6	4.8	5.0	5.4	6.0	6.4	6.9	7.6	7.6	7.8	8.3	8.3	7.3	6.7	6.3	6.0	5.7	5.8	5.8	5.9	6.1
6. Mapo	N/A	N/A	N/A	N/A	N/A	N/A	N/A	N/A	N/A	N/A	N/A	N/A	N/A	N/A	N/A	N/A	N/A	N/A	N/A	N/A	N/A	N/A	N/A	N/A	N/A
7. Dangsan	8.0	7.7	7.6	7.4	7.7	8.0	8.0	8.3	8.8	9.6	10.4	11.6	12.2	12.2	12.4	11.9	11.4	11.2	11.0	10.3	10.1	9.7	9.5	9.5	9.8
8. Sadang	5.7	5.6	5.9	6.0	6.0	5.8	5.9	6.5	7.0	8.1	8.2	8.4	7.8	7.9	7.6	7.4	6.9	6.5	6.4	6.4	6.5	6.4	6.3	6.2	6.7
9. Sillim	5.9	6.0	6.3	6.1	6.5	5.6	5.4	6.1	6.1	7.1	8.0	7.7	9.5	10.3	10.8	12.4	12.9	10.9	10.9	9.3	8.1	7.9	7.3	7.3	8.1
10. Dogok	7.5	7.5	7.9	7.9	8.2	8.2	8.1	8.7	8.6	9.4	10.5	11.1	12.0	12.4	11.7	11.0	10.0	9.7	10.3	9.7	8.8	8.7	8.8	8.7	9.4
11. Jamsil	6.0	6.3	6.1	6.5	6.7	6.7	6.9	7.3	7.2	8.4	9.0	9.3	9.1	9.2	9.2	9.0	9.0	8.5	7.8	7.6	7.3	7.1	7.4	7.2	7.7
12. Siheung	4.1	4.4	4.3	4.0	4.0	4.1	4.2	4.7	5.7	7.9	9.3	9.9	8.2	7.9	7.8	7.5	7.1	6.3	6.0	5.5	5.0	5.0	4.8	4.9	6.0
13. Cheonho	6.2	5.9	5.5	4.8	4.7	5.2	5.4	5.8	6.8	8.3	8.7	9.5	9.7	10.0	9.5	9.5	8.9	8.2	8.4	8.1	7.3	7.1	6.8	6.5	7.4
14. Beon	4.1	4.3	4.9	5.3	6.1	6.8	7.0	7.2	7.8	8.6	8.5	7.6	6.7	6.0	6.2	6.1	5.2	5.1	5.3	5.1	5.1	5.4	5.2	5.1	6.0
15. Gireum	4.2	4.5	4.8	4.8	4.7	5.1	5.1	5.2	6.1	7.0	6.9	7.3	7.2	6.9	6.1	6.5	5.6	5.4	5.4	5.2	5.1	4.8	4.6	4.6	5.5
16. Hannam	6.8	7.1	7.3	7.0	7.3	7.7	8.3	8.8	9.2	10.1	10.4	11.2	10.6	9.8	9.5	9.0	8.1	7.7	7.5	7.4	7.6	7.2	7.0	7.5	8.3
17. Guui	4.1	3.8	3.9	3.8	4.0	4.4	4.5	4.5	4.6	5.8	6.7	7.1	7.1	7.2	7.2	6.9	6.5	6.4	6.2	6.0	5.6	5.0	5.0	4.6	5.5
18. Seongsu	5.5	5.3	5.5	5.8	5.7	6.5	6.4	6.6	6.6	7.3	8.8	9.8	9.4	10.3	9.4	9.6	8.4	8.3	7.5	7.1	6.9	6.7	6.5	6.0	7.3
19. Banghak	7.3	7.2	7.4	7.4	7.7	7.7	8.0	9.0	11.0	13.4	12.8	11.1	9.7	8.4	8.0	7.6	7.2	7.0	7.8	7.4	7.6	7.9	7.4	7.8	8.5
20. Namgaja	6.1	5.6	5.2	5.5	5.8	5.8	6.4	6.7	7.3	7.5	8.0	8.3	8.7	8.6	8.4	7.7	7.1	6.1	6.8	6.9	6.4	6.1	6.3	6.7	6.8
21. Guro	9.8	9.4	9.4	9.8	9.6	10.0	10.8	11.3	12.0	13.0	14.0	13.8	12.8	12.0	11.6	11.6	11.2	11.1	12.1	11.6	10.8	10.4	10.5	10.3	11.2
22. Banpo	6.6	6.4	6.3	7.0	7.3	7.8	8.8	9.4	10.0	10.6	11.2	11.0	11.0	10.0	9.5	8.7	8.5	8.2	8.3	8.0	7.9	7.7	7.6	7.4	8.6
23. Hwagok	4.5	4.4	4.7	4.8	5.3	5.2	5.7	6.6	7.2	8.1	8.5	8.9	8.5	8.7	7.9	7.0	6.4	6.0	6.2	5.9	5.8	6.1	5.9	5.9	6.4
24. Bangi	3.8	3.5	3.3	2.8	2.7	3.1	3.4	4.0	4.5	5.9	6.6	6.6	6.7	6.7	7.0	6.7	5.9	5.2	4.8	4.4	4.3	4.2	4.0	4.0	4.7
25. Sinjeong	3.9	4.0	4.0	4.1	4.2	4.5	4.9	5.5	6.4	7.2	7.2	6.8	5.6	5.1	4.8	4.1	4.0	3.8	3.9	4.2	4.3	4.4	4.5	4.4	4.8
26. Sanggye	7.6	7.0	7.0	7.2	7.8	7.7	8.1	8.3	9.1	10.4	11.5	9.8	8.9	8.1	7.9	8.2	8.0	7.8	7.7	7.0	7.4	7.4	7.1	7.2	8.1
27. Gung	1.9	1.9	1.7	1.9	1.9	2.0	1.8	2.0	2.1	3.8	5.0	5.9	6.3	6.5	6.3	5.8	5.2	4.3	3.3	3.2	2.6	2.6	2.9	2.1	3.5
28. Dongdaemun_st	6.5	6.1	6.2	6.3	6.8	7.3	8.0	7.7	8.1	8.4	8.8	9.2	9.1	9.7	10.2	10.1	9.7	9.6	9.2	9.4	9.2	8.7	8.9	8.1	8.4
29. SeoulStation_st	4.9	4.3	3.8	3.8	3.8	3.9	4.6	5.6	6.3	7.4	7.9	9.1	9.7	9.5	8.7	8.2	7.5	6.7	6.3	6.3	6.0	6.0	5.5	5.5	6.3
30. Cheongge_st	7.1	6.6	7.3	7.8	8.6	10.5	10.8	10.2	11.0	12.3	12.0	11.6	11.6	11.2	12.0	12.2	11.6	11.2	10.8	9.9	9.8	9.2	9.5	8.4	10.1
31. Cheongyangni_st	6.7	6.1	6.1	6.2	6.5	8.1	8.6	8.9	9.2	9.4	9.4	9.9	9.1	9.2	9.5	9.6	9.3	8.9	9.1	9.3	9.6	9.1	8.4	7.8	8.5
32. Shinchon_st	7.7	8.2	8.1	7.9	8.3	8.3	8.7	8.6	9.1	9.4	10.1	10.5	9.4	8.7	8.5	8.6	8.6	8.8	8.6	8.3	8.0	8.2	8.6	8.1	8.6
33. Yeongdeungpo_st	4.5	4.2	4.0	3.7	4.0	5.4	7.0	8.3	8.0	8.6	8.6	7.8	7.8	7.3	7.3	7.0	7.0	7.3	6.7	6.8	6.7	6.6	6.0	5.9	6.5
34. Sinsa_st	8.8	8.5	8.2	8.0	8.1	8.6	9.3	9.8	10.0	10.2	10.6	11.1	11.7	12.2	12.9	12.9	12.7	12.4	12.0	11.7	11.4	11.0	10.7	10.1	10.5
Average*	5.7	5.6	5.6	5.7	5.9	6.1	6.3	6.7	7.3	8.3	8.8	8.9	8.7	8.6	8.5	8.2	7.7	7.3	7.3	7.0	6.7	6.6	6.5	6.4	7.1
Min*	1.9	1.9	1.7	1.9	1.9	2.0	1.8	2.0	2.1	3.8	5.0	5.6	5.1	5.1	4.8	4.1	4.0	3.8	3.3	3.2	2.6	2.6	2.9	2.1	3.5
Max*	9.8	9.4	9.4	9.8	9.6	10.0	10.8	11.3	12.0	13.4	14.0	13.8	12.8	12.4	12.4	12.4	12.9	11.2	12.1	11.6	10.8	10.4	10.5	10.3	11.2

* Values are based on urban background AQMs (No 1. ~ No. 27)

[1] Values are based on hourly average during May 2003. Exclude weekend and national holiday.

Table B.9 Annual and Seasonal Variations of PM10 Concentrations at each AQM[1]

(Unit: μg/m3)

AQM No. and Name	Annual				Spring				Summer				Fall				Winter			
	Mean	N	Min	Max	Mean	N	Min	Max	Mean	N	Min	Max	Mean	N	Min	Max	Mean	N	Min	Max
1. Jung	81.1	216	19.4	225.0	91.1	57	37.1	225.0	63.7	52	26.9	134.8	66.4	50	19.4	151.3	99.7	57	44.2	224.4
2. Hyoje	67.7	145	9.1	227.0	94.7	20	29.9	227.0	63.6	53	17.0	175.9	60.2	55	9.1	171.6	72.6	17	45.3	168.5
3. Myeonmok	62.2	189	8.7	226.0	67.2	49	19.5	226.0	55.2	48	16.3	155.0	53.1	49	8.7	163.8	74.7	43	32.9	223.9
4. Yongdu	63.2	160	16.3	201.3	58.5	34	22.7	115.4	48.1	50	19.5	129.5	62.6	44	16.3	140.0	92.3	32	39.6	201.3
5. Bulgwang	75.8	205	25.3	218.3	87.9	58	25.3	218.3	65.9	53	27.9	137.3	63.9	47	28.4	156.5	84.1	47	31.8	213.7
6. Mapo	71.2	140	9.9	242.0	82.7	40	25.7	242.0	67.4	42	12.2	211.8	50.7	32	9.9	158.6	84.7	26	38.2	187.8
7. Dangsan	70.9	165	11.1	243.4	89.5	42	34.0	243.4	75.8	34	11.1	140.8	48.7	45	15.5	132.7	72.2	44	27.3	210.5
8. Sadang	61.4	204	12.0	293.1	57.9	49	16.3	204.8	57.7	52	13.6	135.2	55.1	49	12.0	135.5	73.8	54	28.8	293.1
9. Sillim	69.5	188	12.5	253.5	68.3	50	26.7	162.4	64.1	43	21.3	142.0	63.9	47	12.5	148.5	80.9	48	34.5	253.5
10. Dogok	62.6	178	8.5	248.6	96.0	38	51.9	248.6	48.9	53	12.8	130.6	44.8	49	8.5	127.4	71.4	38	35.1	174.2
11. Jamsil	66.6	173	10.8	234.6	70.6	45	23.0	214.5	64.0	32	13.4	165.9	49.4	48	10.8	130.7	81.8	48	34.4	234.6
12. Siheung	67.8	192	15.5	204.3	75.1	53	25.4	204.3	57.4	43	15.5	173.9	60.5	44	18.5	151.5	75.1	52	33.5	191.8
13. Cheonho	68.4	206	9.4	250.3	75.8	54	14.1	203.0	58.1	47	12.8	126.8	52.3	53	9.4	144.3	86.6	52	36.6	250.3
14. Beon	78.5	204	15.8	253.8	89.1	56	21.6	253.8	72.3	48	19.4	209.4	63.0	52	15.8	187.0	89.2	48	39.6	210.6
15. Gireum	81.8	127	8.5	259.2	103.5	28	36.8	259.2	81.5	31	25.9	158.0	65.6	48	8.5	147.3	90.6	20	49.4	257.6
16. Hannam	71.2	198	12.6	283.3	79.6	53	17.3	199.3	51.9	48	15.3	127.4	58.2	49	12.6	153.1	94.4	48	44.5	283.3
17. Guui	83.3	193	13.8	298.9	96.6	50	25.7	263.2	67.9	43	16.4	166.0	58.8	48	13.8	164.0	105.9	52	51.3	298.9
18. Seongsu	80.1	191	16.4	245.9	89.9	50	19.1	245.9	70.1	42	19.2	147.9	68.8	44	16.4	175.5	88.1	55	42.9	224.8
19. Banghak	69.4	214	11.5	267.2	81.3	59	16.5	215.0	46.6	51	14.4	103.1	56.7	54	11.5	137.8	92.5	50	36.3	267.2
20. Namgaja	67.5	151	10.3	246.1	69.5	48	16.3	246.1	66.8	24	12.1	141.5	57.9	37	10.3	167.0	74.3	42	23.1	172.1
21. Guro	74.1	139	10.9	255.0	78.8	39	27.8	193.9	77.5	20	16.1	154.7	64.8	31	10.9	152.9	74.8	49	24.5	255.0
22. Banpo	67.9	204	13.5	281.2	69.9	50	27.3	198.5	59.9	49	18.9	135.3	63.8	52	13.5	156.8	77.5	53	33.0	281.2
23. Hwagok	70.5	192	10.2	198.2	78.5	51	23.7	198.2	55.2	47	10.2	130.1	64.7	44	17.3	174.0	82.0	50	41.1	182.9
24. Bangi	69.7	163	10.5	249.1	63.0	28	24.3	116.4	62.2	39	19.7	145.4	65.2	44	10.5	185.0	82.6	52	33.7	249.1
25. Sinjeong	72.8	204	9.0	220.6	85.6	53	25.7	220.6	67.6	44	14.7	160.2	52.8	52	9.0	158.5	83.5	55	35.8	219.8
26. Sanggye	70.1	202	10.1	217.9	75.3	56	19.3	217.9	54.2	37	12.0	163.8	62.1	56	10.1	174.4	84.2	53	35.6	194.6
27. Gung	91.0	181	17.0	240.5	114.4	43	25.1	232.3	74.2	35	17.0	161.7	67.6	52	17.1	163.0	106.6	51	46.3	240.5
28. Dongdaemun_st	76.0	126	14.3	281.5	100.8	17	27.6	231.3	66.0	47	24.2	161.1	67.9	44	14.3	174.7	98.6	18	47.0	281.5
29. SeoulStation_st	69.9	182	13.3	222.2	72.8	45	29.6	178.3	69.2	46	13.3	184.4	58.2	43	15.7	157.9	78.5	48	31.5	222.2
30. Cheongge_st	80.2	201	27.1	282.2	83.8	55	27.1	207.6	68.7	48	31.8	124.5	69.8	49	29.8	167.3	97.8	49	48.8	282.2
31. Cheongyangni_st	79.2	163	26.2	248.6	96.6	23	43.0	238.1	77.8	37	30.2	158.2	66.7	51	26.2	152.1	84.6	52	46.0	248.6
32. Shinchon_st	81.8	209	24.2	263.6	91.8	50	34.8	221.1	68.2	51	28.2	149.2	67.7	53	24.2	173.8	98.9	55	55.0	263.6
33. Yeongdeungpo_st	61.9	193	17.9	175.0	64.0	55	25.0	141.2	49.7	42	20.8	94.7	52.0	46	17.9	116.2	78.8	50	39.9	175.0
34. Sinsa_st	87.5	170	22.0	293.0	105.6	27	41.3	250.0	81.5	44	23.1	159.0	73.3	53	22.0	182.3	99.1	46	27.9	293.0
Average*	71.7	182	12.5	243.9	81.1	46	25.1	214.6	62.9	43	16.7	150.5	59.3	47	13.2	155.9	84.3	46	37.0	228.3
Min*	61.4	127	8.5	198.2	57.9	20	14.1	115.4	46.6	20	10.2	103.1	44.8	31	8.5	127.4	71.4	17	23.1	168.5
Max*	91.0	216	25.3	298.9	114.4	59	51.9	263.2	81.5	53	27.9	211.8	68.8	56	28.4	187.0	106.6	57	51.3	298.9

* Values are based on urban background AQMs (No 1. ~ No. 27)

[1] Values are based on hourly average during May 2003. Exclude weekend and national holiday.

Table B.10 Hourly Variations of PM10 Concentrations at each AQM[1]

(Unit: μg/m3)

AQM No. and Name	01	02	03	04	05	06	07	08	09	10	11	12	13	14	15	16	17	18	19	20	21	22	23	24	Avg.
1. Jung	95.5	95.0	93.4	93.5	95.7	97.4	99.8	103.8	114.4	111.3	106.5	109.4	106.3	107.1	106.4	107.2	113.2	116.7	110.4	109.7	114.0	110.7	101.8	99.5	104.9
2. Hyoje	85.7	84.8	87.2	87.4	92.7	95.0	97.7	104.2	105.6	103.4	97.8	100.0	97.2	94.5	95.2	91.9	95.6	98.7	87.0	86.6	89.9	90.8	88.4	89.5	93.6
3. Myeonmok	84.1	82.7	93.1	90.7	85.7	95.5	89.3	90.2	94.4	89.1	83.9	79.9	82.2	79.3	79.8	77.4	75.7	88.6	80.2	81.0	86.1	81.6	82.7	90.5	85.1
4. Yongdu	73.3	73.6	74.4	70.4	75.3	74.1	84.6	82.8	84.5	86.4	88.8	87.2	83.7	78.5	78.9	75.5	90.1	82.2	76.2	71.2	72.5	72.7	75.2	75.5	78.6
5. Bulgwang	93.5	90.0	89.4	90.5	90.2	90.1	92.5	95.3	107.6	107.4	105.0	106.8	107.2	110.1	110.8	110.1	115.9	112.6	107.1	106.8	104.0	105.8	101.5	96.6	101.9
6. Mapo	98.3	102.1	102.8	104.8	100.3	107.8	111.3	119.7	106.2	102.3	102.9	95.4	91.9	101.4	96.7	102.4	105.8	100.4	98.4	94.1	104.9	102.3	109.5	103.0	102.7
7. Dangsan	104.4	103.1	102.4	108.3	115.8	103.7	106.1	105.6	104.6	95.9	110.6	102.9	90.4	92.5	93.1	96.3	96.8	90.1	97.9	98.8	105.2	111.6	112.8	107.9	102.4
8. Sadang	66.6	67.0	68.2	70.7	70.7	70.1	73.8	84.2	90.2	96.4	97.9	95.7	90.4	84.9	85.4	75.2	84.6	82.7	78.9	77.4	79.5	80.2	74.7	72.5	79.9
9. Sillim	85.1	84.5	85.7	87.3	83.6	84.2	87.2	94.2	90.6	94.6	96.1	87.2	70.6	77.1	78.3	87.0	89.7	86.4	86.8	85.4	91.9	93.1	90.9	92.1	87.1
10. Dogok	102.7	95.3	102.3	94.7	91.8	105.2	103.9	108.7	116.6	110.3	100.6	94.9	100.7	100.4	91.3	92.4	99.3	100.4	95.9	92.6	103.3	109.9	105.7	112.0	101.3
11. Jamsil	86.4	85.0	87.9	83.7	90.0	86.5	86.1	88.6	88.5	78.7	87.4	79.1	78.6	85.6	84.3	89.8	98.8	97.0	97.0	101.9	96.3	96.6	97.0	93.4	89.3
12. Siheung	88.6	87.2	84.2	91.6	89.7	87.9	83.5	75.2	70.3	68.8	72.9	73.1	66.1	68.1	77.5	83.1	85.8	91.5	101.3	108.1	116.6	106.9	100.4	93.3	86.3
13. Cheonho	90.3	87.8	87.2	87.3	84.2	81.1	79.9	82.4	84.8	85.2	84.8	78.8	75.7	68.4	72.6	71.7	78.5	84.4	81.4	75.7	80.6	87.1	88.0	85.3	81.8
14. Beon	101.7	97.7	97.4	99.8	105.4	102.9	104.7	101.4	104.5	99.5	98.1	102.1	94.8	88.1	88.6	92.0	100.5	107.2	105.5	112.3	103.9	107.9	107.2	105.6	101.2
15. Gireum	105.1	106.4	98.2	104.1	111.6	111.7	118.8	118.8	120.9	121.0	113.3	106.9	105.5	96.9	102.4	103.6	105.0	105.6	103.5	102.2	101.8	102.5	106.5	103.9	107.3
16. Hannam	82.6	89.0	89.9	86.3	81.7	82.1	88.4	92.3	101.3	97.4	93.2	89.3	84.4	83.5	83.7	90.9	98.6	93.3	82.0	76.0	78.0	77.6	84.2	85.1	87.1
17. Guui	121.1	119.9	123.8	119.6	118.3	117.3	120.9	112.0	112.2	112.5	104.6	105.3	99.8	101.2	96.6	111.2	108.2	109.0	111.6	107.0	111.9	113.5	111.3	112.8	111.7
18. Seongsu	111.9	104.3	106.1	107.4	106.2	113.4	119.0	122.2	119.8	120.8	118.3	111.3	112.1	114.2	110.8	106.9	109.5	118.3	111.3	104.0	104.3	112.3	111.5	109.5	111.9
19. Banghak	91.8	93.7	88.1	86.0	85.0	82.7	93.3	105.6	115.5	113.7	102.8	95.9	87.5	84.5	85.4	82.2	82.9	85.0	77.9	75.6	80.3	87.7	93.1	94.2	90.4
20. Namgaja	89.7	99.0	96.2	93.5	103.9	103.6	113.2	123.1	110.6	114.6	114.5	106.6	101.4	92.2	88.0	96.4	98.2	91.6	88.9	90.9	94.7	93.7	100.5	97.4	100.1
21. Guro	81.1	80.6	79.8	77.2	79.3	80.4	87.2	90.6	92.9	93.3	86.2	81.9	77.5	78.3	81.3	70.5	71.2	73.5	68.1	77.1	88.3	93.4	93.0	91.8	82.3
22. Banpo	79.7	81.4	80.5	77.7	73.8	74.0	79.6	84.7	87.6	90.2	89.6	93.2	87.7	78.6	75.9	75.8	86.0	75.7	73.8	71.6	72.1	75.7	83.2	79.1	80.3
23. Hwagok	95.3	91.0	91.7	88.2	88.9	89.2	93.8	100.0	107.1	89.7	83.1	84.7	86.9	84.5	89.7	87.0	82.4	86.2	87.2	93.8	93.7	96.4	92.5	97.1	90.8
24. Bangi	86.8	85.6	87.9	85.9	82.0	75.5	62.1	48.5	60.2	77.5	78.8	68.9	63.4	63.8	58.1	56.3	79.5	80.9	80.7	77.6	84.6	88.8	98.9	93.6	76.1
25. Sinjeong	101.2	98.0	93.7	96.1	96.9	97.1	98.6	89.7	89.7	96.3	99.1	92.7	87.6	86.8	90.9	95.8	91.5	94.2	98.7	108.6	109.4	112.8	111.4	113.8	97.9
26. Sanggye	86.6	86.2	85.4	84.3	83.2	81.9	86.9	87.4	96.5	98.4	87.7	80.7	75.8	75.0	81.8	80.0	83.5	89.3	85.0	90.6	93.2	90.8	90.4	87.3	86.1
27. Gung	143.9	132.6	124.9	123.9	121.0	121.2	129.0	144.3	129.9	111.8	108.4	116.6	113.2	117.5	109.2	121.9	110.2	107.7	115.1	110.3	122.7	139.8	157.2	152.7	124.4
28. Dongdaemun_st	92.6	91.1	92.3	91.2	94.0	101.7	108.6	113.7	112.2	107.1	103.1	100.3	97.9	99.0	98.1	101.9	107.4	102.2	93.7	96.5	98.1	99.7	101.1	101.4	100.2
29. SeoulStation_st	93.3	85.9	88.3	87.2	80.0	94.2	98.9	104.1	108.4	106.9	96.3	95.6	92.5	89.3	87.0	91.1	96.8	93.3	89.8	92.6	95.3	92.3	94.7	98.5	93.8
30. Cheongge_st	91.5	92.7	88.3	82.7	84.1	87.3	90.7	96.5	90.4	97.4	98.7	100.1	105.4	102.5	101.7	105.1	107.9	104.4	101.6	98.6	95.2	95.2	96.8	96.0	96.3
31. Cheongyangni_st	104.1	102.4	105.0	105.3	104.7	114.7	119.2	117.8	123.3	122.4	110.4	111.1	110.3	111.4	114.1	109.3	114.9	108.5	100.7	103.2	110.1	107.9	104.9	102.9	109.9
32. Shinchon_st	96.0	88.7	87.8	79.1	84.6	91.8	104.2	114.8	128.3	120.2	118.7	121.1	104.7	99.8	102.1	116.8	105.4	102.3	102.9	98.9	105.1	101.2	106.0	110.3	103.8
33. Yeongdeungpo_st	61.7	60.0	55.2	51.7	52.3	57.6	79.1	98.1	91.0	90.5	82.8	89.5	76.3	63.3	61.2	61.4	61.9	60.6	61.6	64.1	67.4	69.2	69.4	66.9	68.8
34. Sinsa_st	103.4	105.2	109.8	105.5	102.6	112.3	122.0	129.1	135.8	134.6	126.3	130.1	120.7	114.4	112.6	114.1	114.5	111.3	107.2	102.9	105.8	103.0	108.2	109.0	114.2
Average*	93.8	92.7	92.6	92.2	92.7	93.0	96.0	98.3	100.2	98.8	96.8	93.6	89.6	88.6	88.6	90.0	94.0	94.4	92.1	92.1	95.7	97.8	98.9	97.6	94.2
Min*	66.6	67.0	68.2	70.4	70.7	70.1	62.1	48.5	60.2	68.8	72.9	68.9	63.4	63.8	58.1	56.3	71.2	73.5	68.1	71.2	72.1	72.7	74.7	72.5	76.1
Max*	143.9	132.6	124.9	123.9	121.0	121.2	129.0	144.3	129.9	121.0	118.3	116.6	113.2	117.5	110.8	121.9	115.9	118.3	115.1	112.3	122.7	139.8	157.2	152.7	124.4

* Values are based on urban background AQMs (No 1. ~ No. 27)

[1] Values are based on hourly average during May 2003. Exclude weekend and national holiday.

Appendix C. Hourly Concentrations Across the Four Seasons

Table C.1 Hourly variations of pollution concentrations across the four seasons

	Hour	1	2	3	4	5	6	7	8	9	10	11	12	13	14	15	16	17	18	19	20	21	22	23	24	Avg.	Max	Min
NO_2 (ppb)	Spring	48.0	44.1	41.1	38.5	37.4	39.7	43.6	47.7	49.3	48.7	46.3	43.3	39.5	38.4	38.9	40.2	42.1	44.2	47.8	52.2	54.1	54.2	53.3	51.6	45.2	54.2	37.4
	Summer	35.8	31.3	27.8	25.3	24.2	26.2	30.1	33.9	36.1	36.7	36.8	35.9	35.0	34.7	35.4	36.4	38.0	39.6	41.9	44.5	45.2	44.3	42.7	40.2	35.7	45.2	24.2
	Autumn	39.1	35.9	33.1	31.0	30.0	31.9	35.2	38.0	40.2	40.5	39.9	39.0	37.7	37.5	38.2	40.0	42.1	44.9	48.3	49.2	48.6	47.6	45.9	43.8	39.9	49.2	30.0
	Winter	42.2	39.4	37.6	37.0	37.6	40.6	44.6	48.8	51.3	51.2	50.2	48.7	46.1	44.6	44.1	44.9	46.3	48.6	50.6	50.4	49.4	48.5	48.1	46.5	45.7	51.3	37.0
	Annual	41.3	37.7	34.9	32.9	32.3	34.6	38.4	42.1	44.2	44.3	43.3	41.7	39.6	38.8	39.2	40.4	42.1	44.3	47.1	49.1	49.3	48.6	47.5	45.5	41.6	49.3	32.3
CO (ppm)	Spring	7.6	7.4	7.1	6.8	6.6	6.7	7.2	8.1	8.5	7.9	7.2	6.5	5.9	5.7	5.7	5.7	5.9	6.1	6.6	7.1	7.4	7.5	7.6	7.6	6.9	8.5	5.7
	Summer	6.4	5.9	5.5	5.2	4.9	4.8	5.2	5.8	6.4	6.4	6.3	6.0	5.4	5.2	5.2	5.2	5.4	5.6	6.1	6.4	6.6	6.7	6.7	6.5	5.8	6.7	4.8
	Autumn	8.2	7.6	7.1	6.7	6.3	6.2	6.8	7.8	8.7	8.2	7.4	6.6	5.9	5.6	5.6	5.7	6.0	6.6	7.6	8.2	8.7	8.9	8.9	8.7	7.3	8.9	5.6
	Winter	8.8	8.6	8.6	8.6	8.7	9.1	9.8	11.5	13.6	13.3	12.1	10.7	9.2	8.4	7.9	7.9	8.1	8.6	9.2	9.4	9.5	9.6	9.6	9.4	9.6	13.6	7.9
	Annual	7.7	7.4	7.1	6.8	6.6	6.7	7.3	8.3	9.3	9.0	8.3	7.5	6.6	6.2	6.1	6.2	6.3	6.7	7.4	7.8	8.0	8.2	8.2	8.1	7.4	9.3	6.1
O_3 (ppb)	Spring	10.1	11.2	11.6	11.7	11.3	9.6	7.9	7.5	9.2	12.3	16.7	21.7	26.2	29.1	30.8	30.9	29.2	25.7	20.9	15.0	11.6	10.1	9.2	9.1	16.2	30.9	7.5
	Summer	7.7	8.9	9.9	10.8	10.9	9.6	7.9	7.5	8.8	11.4	15.5	20.9	26.3	31.0	33.0	33.2	30.6	26.4	20.8	14.9	10.8	8.6	7.4	6.9	15.8	33.2	6.9
	Autumn	5.3	5.8	6.1	6.3	6.1	5.2	3.8	3.4	4.1	6.0	8.7	12.1	15.8	18.4	19.6	19.2	17.1	13.0	8.5	6.3	5.5	5.0	4.7	4.7	8.8	19.6	3.4
	Winter	6.6	7.4	7.8	7.6	6.8	5.5	4.1	3.4	3.6	4.9	6.6	8.5	10.7	12.5	13.4	13.1	11.8	9.0	6.7	5.8	5.9	5.8	5.6	5.6	7.4	13.4	3.4
	Annual	7.4	8.3	8.8	9.1	8.8	7.4	6.0	5.4	6.4	8.6	11.9	15.8	19.7	22.8	24.2	24.1	22.2	18.5	14.2	10.5	8.5	7.4	6.7	6.6	12.1	24.2	5.4
SO_2 (ppb)	Spring	5.0	4.8	4.6	4.6	4.6	4.8	5.2	5.7	6.2	6.3	6.1	5.8	5.5	5.4	5.5	5.5	5.5	5.4	5.3	5.2	5.3	5.4	5.4	5.3	5.3	6.3	4.6
	Summer	4.1	4.0	3.8	3.8	3.7	3.9	4.1	4.3	4.5	4.5	4.4	4.3	4.2	4.2	4.2	4.3	4.3	4.3	4.3	4.4	4.3	4.4	4.4	4.3	4.2	4.5	3.7
	Autumn	4.7	4.5	4.3	4.1	4.0	4.2	4.4	4.8	5.2	5.3	5.1	4.9	4.7	4.6	4.5	4.5	4.6	4.7	5.0	5.2	5.2	5.2	5.2	5.1	4.8	5.3	4.0
	Winter	5.7	5.5	5.5	5.5	5.6	6.0	6.3	6.8	7.6	8.5	9.0	9.0	8.7	8.6	8.5	8.3	7.8	7.5	7.3	7.1	6.9	6.8	6.8	6.6	7.2	9.0	5.5
	Annual	4.9	4.7	4.6	4.5	4.5	4.7	5.0	5.4	5.9	6.1	6.2	6.0	5.8	5.7	5.7	5.6	5.5	5.5	5.5	5.5	5.4	5.4	5.4	5.3	5.4	6.2	4.5
PM10 ($\mu g/m^3$)	Spring	84.1	82.2	80.3	78.1	77.6	78.2	81.0	84.9	88.1	89.0	87.1	84.8	81.5	78.6	78.5	78.6	80.2	81.0	81.4	82.7	85.4	85.7	85.1	84.1	82.4	89.0	77.6
	Summer	70.8	69.4	66.9	65.1	64.7	66.3	68.6	66.3	64.3	60.6	57.2	55.0	54.2	52.7	53.5	54.7	56.9	58.8	62.7	65.3	66.6	68.1	69.3	69.6	62.8	70.8	52.7
	Autumn	65.4	63.0	60.6	58.4	56.0	55.3	56.8	59.7	62.0	62.6	60.8	56.7	52.6	50.3	49.8	50.7	53.9	58.2	62.8	66.3	68.5	68.5	68.4	66.7	59.8	68.5	49.8
	Winter	76.9	75.8	75.3	75.1	76.3	78.0	80.8	85.3	93.2	97.2	98.1	95.3	90.6	89.4	87.9	88.7	88.7	89.4	89.8	88.6	87.6	86.0	86.2	84.6	86.0	98.1	75.1
	Annual	74.3	72.6	70.8	69.2	68.7	69.5	71.8	74.0	76.9	77.3	75.8	72.9	69.7	67.7	67.5	68.2	69.9	71.8	74.2	75.7	77.0	77.1	77.2	76.3	72.8	77.3	67.5

Appendix D. Vehicle-Kilometers-Traveled (VKT) and Wind-Direction Weighted VKT

Table D.1 Daily Vehicle-Kilometers-Traveled for each Air Quality Monitoring Station

(Unit: vehicle*km)

AQM	Radius (meter)										
	500	1000	1500	2000	2500	3000	3500	4000	4500	5000	5500
1	150,362	759,705	1,479,650	2,120,119	2,744,487	3,460,054	4,742,050	6,075,412	7,509,069	8,918,889	10,755,593
2	168,609	662,362	1,200,413	1,919,645	2,734,852	3,707,902	4,857,919	6,282,212	7,812,848	9,264,042	10,737,505
3	107,151	322,014	602,166	1,008,552	1,544,025	2,146,009	2,612,500	3,734,475	5,167,033	6,423,371	7,875,936
4	110,220	517,131	1,055,965	1,656,146	2,508,602	3,585,800	4,553,626	5,641,114	7,116,599	8,963,662	10,838,592
5	106,375	222,422	532,447	793,930	1,203,438	1,577,757	1,916,257	2,327,129	2,694,506	3,427,078	4,171,639
6	48,285	419,617	1,124,969	1,746,552	2,759,560	3,834,870	5,276,087	7,360,164	9,441,139	11,371,013	13,594,201
7	122,354	554,326	1,503,304	2,596,501	3,543,773	5,073,620	6,492,456	7,949,460	9,594,785	11,220,926	13,783,473
8	36,726	372,400	701,034	1,082,002	1,602,609	2,360,183	3,243,440	4,266,422	5,741,458	7,463,963	9,207,656
9	129,510	350,604	682,441	1,210,327	1,863,529	2,777,082	3,956,848	5,425,281	6,992,787	8,826,087	10,748,820
10	132,623	473,754	981,866	1,886,583	2,882,107	3,899,676	4,968,800	6,048,792	7,296,987	8,553,233	10,166,558
11	58,526	412,704	887,735	1,749,738	2,526,246	3,444,803	4,453,506	5,777,318	7,063,003	8,590,876	10,666,307
12	48,586	271,760	559,164	895,329	1,275,553	1,713,255	2,567,304	3,389,576	4,145,304	4,923,469	5,949,194
13	28,270	161,148	576,621	978,098	1,358,651	1,974,808	2,524,433	3,306,388	4,074,978	5,063,276	6,029,888
14	100,222	344,283	609,536	869,944	1,246,548	1,695,459	2,320,435	3,153,793	4,142,649	4,831,263	5,435,233
15	218,680	540,924	942,178	1,406,843	1,934,692	2,558,907	3,477,580	4,323,156	5,536,491	6,931,017	8,216,235
16	95,602	286,198	806,161	1,505,948	2,310,673	3,749,806	5,596,609	7,679,354	9,706,183	12,029,555	14,299,300
17	87,080	380,468	685,368	1,180,594	1,845,430	2,655,627	3,486,266	4,608,838	5,834,564	7,112,213	8,677,756
18	69,528	205,035	598,837	1,372,455	2,345,109	3,362,869	4,585,465	5,900,452	7,604,441	9,532,721	11,245,931
19	99,534	285,144	504,531	938,285	1,246,304	1,598,339	2,008,341	2,391,146	2,797,577	3,123,332	3,481,721
20	39,277	300,785	642,647	1,095,218	1,595,071	2,526,338	3,694,299	4,987,285	6,319,801	7,985,742	9,860,193
21	168,988	517,645	943,750	1,749,067	2,362,619	3,187,732	4,113,678	5,136,883	6,110,930	7,360,567	8,935,524
22	127,639	658,877	1,318,125	2,192,101	3,130,188	4,346,175	5,993,350	7,678,363	9,262,599	10,863,621	12,491,303
23	36,733	180,747	463,415	927,523	1,700,491	2,457,232	3,379,687	4,103,927	5,290,148	6,611,289	8,135,751
24	47,079	363,001	651,551	1,249,509	1,948,726	2,854,699	3,680,484	4,542,936	5,497,077	6,248,837	7,359,865
25	52,532	499,414	925,537	1,499,049	2,269,486	3,417,443	4,706,514	6,094,942	7,370,795	9,006,437	10,580,436
26	66,002	257,450	497,141	771,556	1,133,576	1,554,294	1,919,419	2,347,593	2,813,345	3,472,661	4,075,611
27	10,448	149,278	419,847	724,987	1,016,126	1,595,860	2,507,841	3,690,816	4,858,123	6,041,486	7,329,708
28	197,836	710,775	1,189,459	1,813,747	2,623,375	3,843,318	5,112,125	6,514,587	8,027,470	9,700,599	11,350,535
29	127,542	495,845	1,140,472	1,877,700	2,773,072	3,937,681	5,406,188	6,787,004	8,737,922	10,607,828	13,227,975
30	234,984	729,109	1,333,720	2,078,705	2,887,198	3,847,198	4,855,881	6,053,480	7,730,169	9,470,522	11,154,654
31	86,078	426,785	940,802	1,393,734	2,083,630	2,986,810	4,293,707	5,614,560	7,020,168	8,208,985	9,704,828
32	143,349	468,083	919,146	1,710,782	2,459,598	3,617,109	4,982,811	6,940,032	9,248,570	11,376,767	13,050,614
33	118,421	624,142	1,295,200	2,411,854	3,638,853	4,970,286	6,400,005	8,000,637	9,952,188	11,917,060	13,828,977
34	171,406	652,681	1,383,007	2,339,081	3,713,139	4,814,331	6,344,269	8,099,638	9,798,592	11,386,315	13,273,655

Table D.2 Daily Wind-Direction Weighted VKT for each Air Quality Monitoring Station

(Unit: vehicle*km)

AQM	Radius (meter)										
	500	1000	1500	2000	2500	3000	3500	4000	4500	5000	5500
1	31,537	108,496	202,606	275,550	335,118	411,101	570,912	716,056	869,536	1,043,804	1,246,182
2	23,496	67,620	126,230	243,552	385,339	514,004	689,732	871,479	1,049,170	1,198,447	1,348,391
3	18,197	37,711	71,161	111,187	174,007	257,852	320,987	445,103	615,492	795,030	989,333
4	21,646	79,220	141,194	203,934	317,865	477,623	571,162	704,370	878,700	1,112,430	1,336,706
5	17,448	26,515	67,423	102,360	129,185	155,319	178,223	202,423	225,904	273,797	316,747
6	6,666	39,284	128,032	209,312	331,844	521,790	751,156	1,028,353	1,306,761	1,592,885	1,893,989
7	19,864	60,041	165,284	256,919	341,957	480,404	649,868	837,610	1,048,262	1,248,231	1,531,389
8	8,379	40,620	102,538	172,347	244,973	328,241	454,460	631,089	817,578	1,066,417	1,350,204
9	15,474	35,035	63,972	128,910	205,275	332,694	458,182	651,455	908,817	1,195,435	1,524,165
10	27,436	75,570	143,894	271,367	404,171	546,508	709,384	861,545	1,046,409	1,245,376	1,453,511
11	9,872	51,501	126,146	271,465	385,168	503,156	642,767	823,883	1,030,497	1,270,713	1,586,048
12	8,241	44,039	83,747	126,976	162,926	210,588	286,329	370,141	451,581	552,755	707,577
13	6,956	28,180	76,767	120,965	166,890	256,910	324,735	435,368	528,015	637,816	766,443
14	15,282	40,953	72,193	102,603	137,253	178,264	252,645	333,115	403,988	454,761	485,229
15	45,996	79,259	117,241	168,547	222,913	316,187	397,468	479,427	616,379	769,036	919,413
16	16,964	35,484	91,871	163,342	215,231	363,569	594,121	874,338	1,095,646	1,363,184	1,642,827
17	17,475	49,390	88,347	147,856	231,671	330,251	415,914	542,573	681,146	842,367	1,033,233
18	11,655	32,690	77,984	184,979	309,325	419,672	570,083	716,306	879,253	1,106,067	1,293,231
19	16,510	33,025	49,319	99,862	118,485	134,955	150,096	165,074	180,301	192,157	204,706
20	5,538	31,148	71,872	121,286	176,367	261,019	425,420	547,618	657,699	797,142	999,341
21	21,873	71,947	125,807	233,929	309,051	407,637	529,014	641,796	752,037	920,719	1,131,635
22	18,586	88,869	192,354	303,975	436,714	615,370	802,099	1,052,978	1,275,329	1,487,322	1,725,032
23	3,842	10,994	45,129	101,324	164,582	239,977	349,652	417,669	551,502	675,050	816,500
24	13,604	57,326	106,018	192,757	281,445	387,690	492,034	609,146	735,034	842,015	1,042,690
25	6,090	53,172	121,732	211,984	310,790	432,900	611,688	831,329	994,370	1,207,623	1,387,083
26	12,511	41,591	64,963	90,070	143,043	196,117	230,513	275,444	306,989	347,201	385,036
27	1,024	5,870	38,288	82,670	107,320	160,731	253,757	370,377	535,933	700,399	902,401
28	32,727	114,794	213,241	332,441	479,736	708,741	891,929	1,096,134	1,271,805	1,432,740	1,601,523
29	19,710	71,592	173,002	270,910	396,613	582,642	837,355	1,045,341	1,272,412	1,500,350	1,791,996
30	44,415	114,578	200,445	331,112	457,694	607,818	737,339	885,423	1,057,833	1,255,214	1,437,342
31	17,286	69,113	131,636	191,386	281,409	396,922	554,106	739,158	916,678	1,040,131	1,202,534
32	33,984	77,122	126,850	182,318	261,644	446,706	590,847	872,423	1,145,717	1,402,170	1,604,244
33	13,587	76,509	144,708	266,459	386,764	513,643	667,780	912,244	1,154,076	1,382,371	1,604,047
34	29,710	80,229	154,570	262,424	443,997	574,491	779,206	974,848	1,166,830	1,411,242	1,694,948

Appendix E. Traffic Counts

Table E.1 Hourly Traffic Counts during Weekdays (Average of 5 days)

(Unit: vehicle)

Time	CBD			Han River Bridges			Arterial			Cordon Line			**Sum**		
	Sum	Inflow	Outflow	Sum	Inflow	Outflow	Sum	Inflow	Outflow	Sum	Inflow	Outflow	Sum	Inflow	Outflow
00-01	60,287	28,667	31,620	55,808	28,055	27,754	111,460	51,015	60,445	69,308	31,651	37,657	296,864	139,387	157,477
01-02	47,662	22,615	25,048	40,939	20,688	20,251	84,283	39,475	44,808	48,260	22,302	25,957	221,143	105,079	116,064
02-03	38,206	17,919	20,287	31,000	15,986	15,014	63,592	29,506	34,087	35,874	16,563	19,310	168,672	79,974	88,698
03-04	30,560	14,104	16,457	24,575	12,837	11,738	50,042	22,935	27,107	28,452	13,261	15,192	133,629	63,135	70,494
04-05	28,759	13,749	15,010	23,611	12,266	11,345	47,477	23,516	23,961	30,403	15,068	15,334	130,249	64,599	65,650
05-06	35,800	18,380	17,420	32,312	15,677	16,635	65,651	35,483	30,169	50,890	25,971	24,918	184,653	95,511	89,143
06-07	59,282	33,535	25,747	70,903	34,539	36,364	131,870	77,106	54,764	119,505	62,241	57,264	381,561	207,421	174,140
07-08	93,296	53,768	39,529	111,923	56,507	55,416	192,346	109,704	82,642	183,897	95,873	88,025	581,463	315,852	265,611
08-09	107,726	60,883	46,843	122,441	61,878	60,563	202,100	110,310	91,790	197,241	101,361	95,880	629,508	334,432	295,076
09-10	103,894	56,138	47,756	110,321	56,377	53,944	195,558	106,002	89,555	178,732	92,428	86,304	588,505	310,946	277,559
10-11	103,324	53,800	49,523	106,758	54,654	52,104	196,480	101,649	94,831	174,740	87,539	87,201	581,301	297,643	283,658
11-12	103,138	52,457	50,681	104,212	53,066	51,146	194,932	97,687	97,244	168,876	82,338	86,538	571,157	285,549	285,608
12-13	96,884	48,307	48,577	96,000	47,723	48,277	182,976	89,534	93,443	157,424	75,417	82,006	533,284	260,981	272,303
13-14	102,177	50,611	51,565	99,667	50,022	49,645	191,144	95,257	95,887	163,762	81,138	82,624	556,750	277,028	279,721
14-15	101,329	50,357	50,972	102,379	52,248	50,131	197,519	98,372	99,147	171,556	86,618	84,939	572,783	287,595	285,188
15-16	101,689	50,032	51,656	104,292	52,944	51,348	197,741	98,174	99,567	173,060	87,647	85,413	576,782	288,797	287,985
16-17	101,613	49,397	52,217	106,270	53,949	52,322	199,840	97,992	101,848	177,146	89,887	87,260	584,870	291,224	293,646
17-18	101,674	48,442	53,232	111,428	56,561	54,867	203,267	98,088	105,179	185,884	94,700	91,184	602,252	297,790	304,462
18-19	104,662	47,642	57,020	114,782	58,916	55,865	205,243	95,995	109,248	189,068	92,728	96,340	613,754	295,281	318,473
19-20	96,390	42,881	53,510	108,292	55,278	53,014	193,873	87,078	106,795	176,775	84,572	92,203	575,330	269,809	305,521
20-21	86,037	38,892	47,145	96,477	49,424	47,052	180,090	79,512	100,578	152,856	71,757	81,099	515,460	239,585	275,875
21-22	86,536	40,691	45,845	93,469	47,914	45,556	175,377	78,826	96,551	139,935	65,072	74,862	495,317	232,503	262,814
22-23	84,563	40,297	44,266	88,357	45,210	43,147	165,537	74,363	91,175	123,692	56,045	67,647	462,149	215,915	246,235
23-24	75,435	36,199	39,236	75,634	38,666	36,968	145,484	65,781	79,703	99,430	44,249	55,181	395,984	184,896	211,089
Sum	1,950,924	969,761	981,162	2,031,849	1,031,385	1,000,464	3,773,883	1,863,358	1,910,525	3,196,764	1,576,426	1,620,338	10,953,420	5,440,930	5,512,489

Table E.2 Hourly Shares of Traffic Counts during Weekdays

Time	CBD			Han River Bridges			Arterial			Cordon Line			**Average**		
	Sum	Inflow	Outflow	Sum	Inflow	Outflow	Sum	Inflow	Outflow	Sum	Inflow	Outflow	Sum	Inflow	Outflow
00-01	3.09%	2.96%	3.22%	2.75%	2.72%	2.77%	2.95%	2.74%	3.16%	2.17%	2.01%	2.32%	2.74%	2.61%	2.87%
01-02	2.44%	2.33%	2.55%	2.01%	2.01%	2.02%	2.23%	2.12%	2.35%	1.51%	1.41%	1.60%	2.05%	1.97%	2.13%
02-03	1.96%	1.85%	2.07%	1.53%	1.55%	1.50%	1.69%	1.58%	1.78%	1.12%	1.05%	1.19%	1.57%	1.51%	1.64%
03-04	1.57%	1.45%	1.68%	1.21%	1.24%	1.17%	1.33%	1.23%	1.42%	0.89%	0.84%	0.94%	1.25%	1.19%	1.30%
04-05	1.47%	1.42%	1.53%	1.16%	1.19%	1.13%	1.26%	1.26%	1.25%	0.95%	0.96%	0.95%	1.21%	1.21%	1.22%
05-06	1.84%	1.90%	1.78%	1.59%	1.52%	1.66%	1.74%	1.90%	1.58%	1.59%	1.65%	1.54%	1.69%	1.74%	1.64%
06-07	3.04%	3.46%	2.62%	3.49%	3.35%	3.63%	3.49%	4.14%	2.87%	3.74%	3.95%	3.53%	3.44%	3.72%	3.16%
07-08	4.78%	5.54%	4.03%	5.51%	5.48%	5.54%	5.10%	5.89%	4.33%	5.75%	6.08%	5.43%	5.28%	5.75%	4.83%
08-09	5.52%	6.28%	4.77%	6.03%	6.00%	6.05%	5.36%	5.92%	4.80%	6.17%	6.43%	5.92%	5.77%	6.16%	5.39%
09-10	5.33%	5.79%	4.87%	5.43%	5.47%	5.39%	5.18%	5.69%	4.69%	5.59%	5.86%	5.33%	5.38%	5.70%	5.07%
10-11	5.30%	5.55%	5.05%	5.25%	5.30%	5.21%	5.21%	5.46%	4.96%	5.47%	5.55%	5.38%	5.31%	5.46%	5.15%
11-12	5.29%	5.41%	5.17%	5.13%	5.15%	5.11%	5.17%	5.24%	5.09%	5.28%	5.22%	5.34%	5.22%	5.26%	5.18%
12-13	4.97%	4.98%	4.95%	4.72%	4.63%	4.83%	4.85%	4.80%	4.89%	4.92%	4.78%	5.06%	4.87%	4.80%	4.93%
13-14	5.24%	5.22%	5.26%	4.91%	4.85%	4.96%	5.06%	5.11%	5.02%	5.12%	5.15%	5.10%	5.08%	5.08%	5.08%
14-15	5.19%	5.19%	5.20%	5.04%	5.07%	5.01%	5.23%	5.28%	5.19%	5.37%	5.49%	5.24%	5.21%	5.26%	5.16%
15-16	5.21%	5.16%	5.26%	5.13%	5.13%	5.13%	5.24%	5.27%	5.21%	5.41%	5.56%	5.27%	5.25%	5.28%	5.22%
16-17	5.21%	5.09%	5.32%	5.23%	5.23%	5.23%	5.30%	5.26%	5.33%	5.54%	5.70%	5.39%	5.32%	5.32%	5.32%
17-18	5.21%	5.00%	5.43%	5.48%	5.48%	5.48%	5.39%	5.26%	5.51%	5.81%	6.01%	5.63%	5.47%	5.44%	5.51%
18-19	5.36%	4.91%	5.81%	5.65%	5.71%	5.58%	5.44%	5.15%	5.72%	5.91%	5.88%	5.95%	5.59%	5.41%	5.76%
19-20	4.94%	4.42%	5.45%	5.33%	5.36%	5.30%	5.14%	4.67%	5.59%	5.53%	5.36%	5.69%	5.23%	4.95%	5.51%
20-21	4.41%	4.01%	4.81%	4.75%	4.79%	4.70%	4.77%	4.27%	5.26%	4.78%	4.55%	5.01%	4.68%	4.41%	4.94%
21-22	4.44%	4.20%	4.67%	4.60%	4.65%	4.55%	4.65%	4.23%	5.05%	4.38%	4.13%	4.62%	4.52%	4.30%	4.72%
22-23	4.33%	4.16%	4.51%	4.35%	4.38%	4.31%	4.39%	3.99%	4.77%	3.87%	3.56%	4.17%	4.23%	4.02%	4.44%
23-24	3.87%	3.73%	4.00%	3.72%	3.75%	3.70%	3.86%	3.53%	4.17%	3.11%	2.81%	3.41%	3.64%	3.45%	3.82%

Table E.3 Hourly Traffic Counts during Saturday

(Unit: vehicle)

Time	CBD			Han River Bridges			Arterial			Cordon Line			**Sum**		
	Sum	Inflow	Outflow	Sum	Inflow	Outflow	Sum	Inflow	Outflow	Sum	Inflow	Outflow	Sum	Inflow	Outflow
00-01	62,704	33,208	36,455	67,526	34,372	33,154	132,604	59,480	73,125	81,708	36,283	45,425	344,542	163,343	188,159
01-02	52,053	27,523	29,657	51,579	25,873	25,706	108,596	50,838	57,758	61,477	27,975	33,503	273,705	132,209	146,623
02-03	42,858	23,597	25,637	40,908	20,977	19,932	88,161	41,860	46,301	46,812	21,379	25,433	218,738	107,812	117,302
03-04	33,489	18,555	21,351	33,032	17,509	15,523	69,379	32,227	37,153	36,786	16,957	19,830	172,686	85,247	93,857
04-05	28,945	16,576	18,483	30,272	15,990	14,281	60,677	29,193	31,484	35,659	17,201	18,458	155,553	78,961	82,706
05-06	32,933	19,297	19,187	36,618	17,985	18,633	71,368	37,315	34,053	52,637	25,983	26,653	193,556	100,580	98,527
06-07	47,098	29,003	24,536	66,223	32,041	34,183	118,814	65,428	53,386	105,865	51,543	54,322	338,000	178,015	166,427
07-08	64,898	44,547	34,572	100,870	49,978	50,893	172,404	96,763	75,641	166,344	83,091	83,253	504,517	274,379	244,360
08-09	82,290	54,930	43,101	119,868	59,858	60,011	201,945	112,492	89,453	194,315	100,437	93,878	598,419	327,716	286,444
09-10	85,376	52,048	46,191	111,389	56,503	54,885	197,916	106,327	91,589	179,314	90,956	88,358	573,995	305,835	281,023
10-11	89,179	51,641	47,772	109,379	56,247	53,132	199,251	102,831	96,420	179,491	89,517	89,974	577,299	300,236	287,298
11-12	89,444	51,058	49,088	111,018	56,380	54,637	201,059	101,288	99,772	180,081	89,475	90,606	581,602	298,201	294,103
12-13	89,945	49,591	50,776	114,028	57,765	56,263	204,095	100,857	103,238	182,095	89,806	92,289	590,163	298,019	302,566
13-14	91,659	48,529	51,618	118,230	59,961	58,269	204,805	98,256	106,549	189,603	91,044	98,559	604,298	297,791	314,995
14-15	88,658	45,978	51,539	116,150	59,971	56,179	202,912	96,470	106,441	189,045	90,031	99,015	596,765	292,450	313,174
15-16	89,361	47,148	50,466	116,123	58,976	57,148	202,640	96,422	106,218	191,395	91,009	100,386	599,519	293,554	314,218
16-17	85,892	45,652	48,039	113,618	56,551	57,067	202,181	97,606	104,575	192,505	93,194	99,312	594,197	293,003	308,993
17-18	85,296	44,423	47,852	113,947	56,735	57,212	201,006	95,895	105,111	193,209	94,522	98,688	593,459	291,574	308,863
18-19	80,106	42,613	47,542	110,610	54,994	55,616	196,734	94,147	102,587	185,327	89,986	95,341	572,778	281,740	301,087
19-20	71,309	37,670	43,082	102,305	52,300	50,006	188,789	89,573	99,216	170,957	83,951	87,006	533,359	263,493	279,309
20-21	68,617	34,187	39,046	93,797	48,345	45,452	177,655	83,223	94,432	150,860	72,529	78,330	490,928	238,284	257,260
21-22	69,646	35,859	38,797	91,943	46,783	45,160	171,437	81,230	90,207	140,509	66,968	73,542	473,535	230,841	247,706
22-23	68,902	36,379	37,608	87,891	44,630	43,260	161,386	75,730	85,656	123,449	57,850	65,599	441,628	214,589	232,123
23-24	62,963	34,206	35,491	75,631	37,283	38,348	145,149	67,503	77,646	103,395	47,957	55,438	387,137	186,949	206,923
Sum	1,663,619	924,219	937,888	2,132,956	1,078,006	1,054,949	3,880,965	1,912,954	1,968,010	3,332,840	1,619,641	1,713,199	11,010,380	5,534,820	5,674,046

Table E.4 Hourly Shares of Traffic Counts during Saturday

Time	CBD			Han River Bridges			Arterial			Cordon Line			**Average**		
	Sum	Inflow	Outflow	Sum	Inflow	Outflow	Sum	Inflow	Outflow	Sum	Inflow	Outflow	Sum	Inflow	Outflow
00-01	3.77%	3.59%	3.89%	3.17%	3.19%	3.14%	3.42%	3.11%	3.72%	2.45%	2.24%	2.65%	3.20%	3.03%	3.35%
01-02	3.13%	2.98%	3.16%	2.42%	2.40%	2.44%	2.80%	2.66%	2.93%	1.84%	1.73%	1.96%	2.55%	2.44%	2.62%
02-03	2.58%	2.55%	2.73%	1.92%	1.95%	1.89%	2.27%	2.19%	2.35%	1.40%	1.32%	1.48%	2.04%	2.00%	2.12%
03-04	2.01%	2.01%	2.28%	1.55%	1.62%	1.47%	1.79%	1.68%	1.89%	1.10%	1.05%	1.16%	1.61%	1.59%	1.70%
04-05	1.74%	1.79%	1.97%	1.42%	1.48%	1.35%	1.56%	1.53%	1.60%	1.07%	1.06%	1.08%	1.45%	1.47%	1.50%
05-06	1.98%	2.09%	2.05%	1.72%	1.67%	1.77%	1.84%	1.95%	1.73%	1.58%	1.60%	1.56%	1.78%	1.83%	1.77%
06-07	2.83%	3.14%	2.62%	3.10%	2.97%	3.24%	3.06%	3.42%	2.71%	3.18%	3.18%	3.17%	3.04%	3.18%	2.93%
07-08	3.90%	4.82%	3.69%	4.73%	4.64%	4.82%	4.44%	5.06%	3.84%	4.99%	5.13%	4.86%	4.52%	4.91%	4.30%
08-09	4.95%	5.94%	4.60%	5.62%	5.55%	5.69%	5.20%	5.88%	4.55%	5.83%	6.20%	5.48%	5.40%	5.89%	5.08%
09-10	5.13%	5.63%	4.93%	5.22%	5.24%	5.20%	5.10%	5.56%	4.65%	5.38%	5.62%	5.16%	5.21%	5.51%	4.98%
10-11	5.36%	5.59%	5.09%	5.13%	5.22%	5.04%	5.13%	5.38%	4.90%	5.39%	5.53%	5.25%	5.25%	5.43%	5.07%
11-12	5.38%	5.52%	5.23%	5.20%	5.23%	5.18%	5.18%	5.29%	5.07%	5.40%	5.52%	5.29%	5.29%	5.39%	5.19%
12-13	5.41%	5.37%	5.41%	5.35%	5.36%	5.33%	5.26%	5.27%	5.25%	5.46%	5.54%	5.39%	5.37%	5.39%	5.34%
13-14	5.51%	5.25%	5.50%	5.54%	5.56%	5.52%	5.28%	5.14%	5.41%	5.69%	5.62%	5.75%	5.50%	5.39%	5.55%
14-15	5.33%	4.97%	5.50%	5.45%	5.56%	5.33%	5.23%	5.04%	5.41%	5.67%	5.56%	5.78%	5.42%	5.28%	5.50%
15-16	5.37%	5.10%	5.38%	5.44%	5.47%	5.42%	5.22%	5.04%	5.40%	5.74%	5.62%	5.86%	5.44%	5.31%	5.51%
16-17	5.16%	4.94%	5.12%	5.33%	5.25%	5.41%	5.21%	5.10%	5.31%	5.78%	5.75%	5.80%	5.37%	5.26%	5.41%
17-18	5.13%	4.81%	5.10%	5.34%	5.26%	5.42%	5.18%	5.01%	5.34%	5.80%	5.84%	5.76%	5.36%	5.23%	5.41%
18-19	4.82%	4.61%	5.07%	5.19%	5.10%	5.27%	5.07%	4.92%	5.21%	5.56%	5.56%	5.57%	5.16%	5.05%	5.28%
19-20	4.29%	4.08%	4.59%	4.80%	4.85%	4.74%	4.86%	4.68%	5.04%	5.13%	5.18%	5.08%	4.77%	4.70%	4.86%
20-21	4.12%	3.70%	4.16%	4.40%	4.48%	4.31%	4.58%	4.35%	4.80%	4.53%	4.48%	4.57%	4.41%	4.25%	4.46%
21-22	4.19%	3.88%	4.14%	4.31%	4.34%	4.28%	4.42%	4.25%	4.58%	4.22%	4.13%	4.29%	4.28%	4.15%	4.32%
22-23	4.14%	3.94%	4.01%	4.12%	4.14%	4.10%	4.16%	3.96%	4.35%	3.70%	3.57%	3.83%	4.03%	3.90%	4.07%
23-24	3.78%	3.70%	3.78%	3.55%	3.46%	3.64%	3.74%	3.53%	3.95%	3.10%	2.96%	3.24%	3.54%	3.41%	3.65%

Table E.5 Hourly Traffic Counts during Sunday

(Unit: vehicle)

Time	CBD			Han River Bridges			Arterial			Cordon Line			**Sum**		
	Sum	Inflow	Outflow	Sum	Inflow	Outflow	Sum	Inflow	Outflow	Sum	Inflow	Outflow	Sum	Inflow	Outflow
00-01	29,496	29,496	31,744	61,518	30,524	30,994	123,899	56,394	67,505	79,283	36,318	42,965	294,196	152,732	173,208
01-02	24,530	24,530	26,109	46,462	23,820	22,642	97,835	46,095	51,740	58,455	27,550	30,904	227,282	121,995	131,395
02-03	19,261	19,261	21,199	35,881	18,150	17,731	76,229	36,149	40,079	44,005	20,532	23,474	175,376	94,092	102,483
03-04	14,934	14,934	16,653	28,234	14,314	13,920	59,404	27,267	32,137	34,840	16,294	18,546	137,412	72,809	81,256
04-05	12,369	12,369	13,710	25,528	12,904	12,625	51,105	24,075	27,030	32,748	15,505	17,243	121,751	64,853	70,608
05-06	13,636	13,636	13,513	29,104	14,306	14,798	55,283	27,794	27,490	42,688	20,387	22,302	140,712	76,122	78,102
06-07	18,094	18,094	16,133	45,295	21,532	23,763	77,447	40,624	36,823	69,556	32,818	36,738	210,392	113,068	113,457
07-08	20,351	20,351	18,320	53,855	26,054	27,800	89,513	46,822	42,691	86,240	40,470	45,770	249,959	133,697	134,581
08-09	27,361	27,361	23,217	72,336	35,982	36,353	123,446	66,992	56,454	116,873	58,029	58,844	340,016	188,365	174,868
09-10	33,328	33,328	28,781	81,282	40,786	40,496	143,062	75,312	67,750	136,081	66,008	70,074	393,753	215,433	207,101
10-11	37,538	37,538	33,357	93,932	48,023	45,909	169,619	90,225	79,394	160,421	81,656	78,765	461,509	257,441	237,425
11-12	38,386	38,386	34,474	93,569	47,738	45,832	167,874	86,736	81,139	157,785	79,023	78,762	457,615	251,883	240,206
12-13	40,354	40,354	37,525	95,740	48,384	47,356	178,267	90,372	87,895	161,014	80,694	80,320	475,375	259,804	253,096
13-14	43,129	43,129	41,602	103,258	52,153	51,105	186,666	93,878	92,789	169,966	84,591	85,375	503,020	273,751	270,871
14-15	42,680	42,680	42,976	104,204	52,519	51,684	188,227	93,656	94,571	171,304	85,381	85,923	506,414	274,236	275,154
15-16	42,213	42,213	43,339	107,058	54,085	52,972	188,264	92,364	95,900	172,467	85,494	86,974	510,002	274,156	279,185
16-17	40,240	40,240	43,389	106,123	52,644	53,480	188,038	92,538	95,500	177,485	90,602	86,883	511,886	276,024	279,251
17-18	40,873	40,873	43,117	108,641	55,253	53,387	188,252	91,557	96,696	178,778	92,692	86,085	516,544	280,376	279,285
18-19	37,493	37,493	41,469	102,846	52,970	49,876	181,811	87,551	94,260	166,197	85,786	80,412	488,347	263,800	266,016
19-20	33,639	33,639	37,757	90,267	46,751	43,516	166,306	81,540	84,766	144,898	76,453	68,444	435,110	238,384	234,483
20-21	34,430	34,430	37,881	89,064	45,677	43,387	162,604	79,455	83,149	140,173	72,100	68,073	426,271	231,662	232,490
21-22	33,786	33,786	36,370	87,449	44,633	42,816	156,135	75,303	80,832	132,837	66,857	65,980	410,207	220,579	225,998
22-23	32,523	32,523	34,034	79,801	40,492	39,310	142,552	67,816	74,737	114,515	57,464	57,050	369,392	198,295	205,131
23-24	28,756	28,756	30,577	63,691	31,352	32,339	117,210	55,344	61,867	87,301	43,771	43,530	296,959	159,223	168,313
Sum	739,401	739,401	747,245	1,805,138	911,047	894,091	3,279,050	1,625,858	1,653,192	2,835,910	1,416,474	1,419,436	8,659,498	4,692,779	4,713,964

Table E.6 Hourly Shares of Traffic Counts during Sunday

Time	CBD			Han River Bridges			Arterial			Cordon Line			**Average**		
	Sum	Inflow	Outflow	Sum	Inflow	Outflow	Sum	Inflow	Outflow	Sum	Inflow	Outflow	Sum	Inflow	Outflow
00-01	3.99%	3.99%	4.25%	3.41%	3.35%	3.47%	3.78%	3.47%	4.08%	2.80%	2.56%	3.03%	3.49%	3.34%	3.71%
01-02	3.32%	3.32%	3.49%	2.57%	2.61%	2.53%	2.98%	2.84%	3.13%	2.06%	1.94%	2.18%	2.73%	2.68%	2.83%
02-03	2.60%	2.60%	2.84%	1.99%	1.99%	1.98%	2.32%	2.22%	2.42%	1.55%	1.45%	1.65%	2.12%	2.07%	2.22%
03-04	2.02%	2.02%	2.23%	1.56%	1.57%	1.56%	1.81%	1.68%	1.94%	1.23%	1.15%	1.31%	1.66%	1.60%	1.76%
04-05	1.67%	1.67%	1.83%	1.41%	1.42%	1.41%	1.56%	1.48%	1.64%	1.15%	1.09%	1.21%	1.45%	1.42%	1.52%
05-06	1.84%	1.84%	1.81%	1.61%	1.57%	1.66%	1.69%	1.71%	1.66%	1.51%	1.44%	1.57%	1.66%	1.64%	1.67%
06-07	2.45%	2.45%	2.16%	2.51%	2.36%	2.66%	2.36%	2.50%	2.23%	2.45%	2.32%	2.59%	2.44%	2.41%	2.41%
07-08	2.75%	2.75%	2.45%	2.98%	2.86%	3.11%	2.73%	2.88%	2.58%	3.04%	2.86%	3.22%	2.88%	2.84%	2.84%
08-09	3.70%	3.70%	3.11%	4.01%	3.95%	4.07%	3.76%	4.12%	3.41%	4.12%	4.10%	4.15%	3.90%	3.97%	3.68%
09-10	4.51%	4.51%	3.85%	4.50%	4.48%	4.53%	4.36%	4.63%	4.10%	4.80%	4.66%	4.94%	4.54%	4.57%	4.35%
10-11	5.08%	5.08%	4.46%	5.20%	5.27%	5.13%	5.17%	5.55%	4.80%	5.66%	5.76%	5.55%	5.28%	5.42%	4.99%
11-12	5.19%	5.19%	4.61%	5.18%	5.24%	5.13%	5.12%	5.33%	4.91%	5.56%	5.58%	5.55%	5.26%	5.34%	5.05%
12-13	5.46%	5.46%	5.02%	5.30%	5.31%	5.30%	5.44%	5.56%	5.32%	5.68%	5.70%	5.66%	5.47%	5.51%	5.32%
13-14	5.83%	5.83%	5.57%	5.72%	5.72%	5.72%	5.69%	5.77%	5.61%	5.99%	5.97%	6.01%	5.81%	5.83%	5.73%
14-15	5.77%	5.77%	5.75%	5.77%	5.76%	5.78%	5.74%	5.76%	5.72%	6.04%	6.03%	6.05%	5.83%	5.83%	5.83%
15-16	5.71%	5.71%	5.80%	5.93%	5.94%	5.92%	5.74%	5.68%	5.80%	6.08%	6.04%	6.13%	5.87%	5.84%	5.91%
16-17	5.44%	5.44%	5.81%	5.88%	5.78%	5.98%	5.73%	5.69%	5.78%	6.26%	6.40%	6.12%	5.83%	5.83%	5.92%
17-18	5.53%	5.53%	5.77%	6.02%	6.06%	5.97%	5.74%	5.63%	5.85%	6.30%	6.54%	6.06%	5.90%	5.94%	5.91%
18-19	5.07%	5.07%	5.55%	5.70%	5.81%	5.58%	5.54%	5.38%	5.70%	5.86%	6.06%	5.67%	5.54%	5.58%	5.62%
19-20	4.55%	4.55%	5.05%	5.00%	5.13%	4.87%	5.07%	5.02%	5.13%	5.11%	5.40%	4.82%	4.93%	5.02%	4.97%
20-21	4.66%	4.66%	5.07%	4.93%	5.01%	4.85%	4.96%	4.89%	5.03%	4.94%	5.09%	4.80%	4.87%	4.91%	4.94%
21-22	4.57%	4.57%	4.87%	4.84%	4.90%	4.79%	4.76%	4.63%	4.89%	4.68%	4.72%	4.65%	4.71%	4.71%	4.80%
22-23	4.40%	4.40%	4.55%	4.42%	4.44%	4.40%	4.35%	4.17%	4.52%	4.04%	4.06%	4.02%	4.30%	4.27%	4.37%
23-24	3.89%	3.89%	4.09%	3.53%	3.44%	3.62%	3.57%	3.40%	3.74%	3.08%	3.09%	3.07%	3.52%	3.46%	3.63%

Appendix F. Sub-Classification of Land Uses in the Seoul Metropolitan Area

Table F.1 Sub-classification of residential land use

Land Uses	Code	Sub-classification	Area (Sq. meter)	Ratio
Residential	A1	detached houses with high impermeable pavement ratio (over 70%)	53,126,318	46.3%
	A2	detached houses with low impermeable pavement ratio (under 70%)	2,060,059	1.8%
	A3	1 ~ 4 story apartment houses with high impermeable pavement ratio (over 70%)	9,669,319	8.4%
	A4	1 ~ 4 story apartment houses with low impermeable pavement ratio (under 70%)	299,835	0.3%
	A5	5 ~ 10 story apartment houses with high impermeable pavement ratio (over 70%)	8,004,994	7.0%
	A6	5 ~ 10 story apartment houses with low impermeable pavement ratio (under 70%)	3,003,652	2.6%
	A7	over 10 story apartment houses with high impermeable pavement ratio (over 70%)	34,951,222	30.4%
	A8	over 10 story apartment houses with low impermeable pavement ratio (under 70%)	3,701,073	3.2%
Sum			114,816,472	100.0%

Table F.2 Sub-classification of commercial land use

Land Uses	Code	Sub-classification	Area (Sq. meter)	Ratio
Commercial	B1	1 ~ 5 story high commercial or business area	28,417,848	24.8%
	B2	6 ~ 10 story high commercial or business area	4,268,272	3.7%
	B3	over 10 story high commercial or business area	2,980,038	2.6%
	B4	mixed landuse area with high impermeable pavement ratio (over 70%)	78,730,254	68.7%
	B5	mixed landuse area with low impermeable pavement ratio (under 70%)	218,972	0.2%
Sum			114,615,383	100.0%

Table F.3 Sub-classification of industrial land use

Land Uses	Code	Sub-classification	Area (Sq. meter)	Ratio
Industrial & Urban infrastructure	C1	industrial area with high impermeable pavement ratio (over 70%)	6,289,759	9.0%
	C2	industrial area with low impermeable pavement ratio (under 70%)	701,997	1.0%
	C3	sewage treatment facilities	2,001,679	2.8%
	C4	storm water retention pond	1,267,053	1.8%
	C5	water supply reservoir	228,623	0.3%
	C6	waste landfill area	149,027	0.2%
	C7	water purification plant	862,801	1.2%
	C8	power plant and transformer substation	416,264	0.6%
	C9	trash incineration	323,330	0.5%
	C10	agricultural and fishery products market	1,058,869	1.5%
	C11	trash related facilities	619,442	0.9%
	C12	public facilities larger than 1 ha	26,990,813	38.4%
	C13	public facilities smaller than 1 ha	3,766,991	5.4%
	C14	construction site	9,968,339	14.2%
	C15	loading area	616,301	0.9%
	C16	inaccessible area (militaray land uses)	15,010,050	21.4%
Sum			70,271,338	100.0%

Table F.4 Sub-classification of transportation land use

Land Uses	Code	Sub-classification	Area (Sq. meter)	Ratio
Transport	D1	railroad and related facilities area with high impermeable pavement ratio (over 70%)	1,505,147	2.3%
	D2	railroad and related facilities area with low impermeable pavement ratio (under 70%)	4,835,848	7.5%
	D3	road	48,370,120	75.4%
	D4	large parking area	3,320,103	5.2%
	D5	airport area	6,127,768	9.6%
Sum			64,158,985	100.0%

Appendix G. Correlation Analysis

Table G.1 Pearson correlation coefficients between pollutant concentrations and VKT

	NO2	CO	O3	SO2	PM10	VKT R0500	VKT R1000	VKT R1500	VKT R2000	VKT R2500	VKT R3000	VKT R3500	VKT R4000	VKT R4500	VKT R5000	VKT R5500
NO2	1.00	0.58	-0.55	0.72	-0.02	0.27	0.40	0.51	0.50	0.52	0.55	0.57	0.57	0.58	0.57	0.57
		0.00	0.00	<.0001	0.90	0.12	0.02	0.00	0.00	0.00	0.00	0.00	0.00	0.00	0.00	0.00
CO		1.00	-0.52	0.57	0.25	0.31	0.36	0.39	0.29	0.31	0.29	0.30	0.29	0.29	0.28	0.29
			0.00	0.00	0.16	0.08	0.04	0.02	0.10	0.08	0.10	0.08	0.09	0.09	0.11	0.10
O3			1.00	-0.41	-0.24	-0.46	-0.57	-0.52	-0.54	-0.55	-0.56	-0.58	-0.58	-0.60	-0.59	-0.57
				0.02	0.17	0.01	0.00	0.00	0.00	0.00	0.00	0.00	0.00	0.00	0.00	0.00
SO2				1.00	0.01	0.39	0.38	0.45	0.44	0.43	0.43	0.41	0.41	0.41	0.38	0.36
					0.97	0.02	0.02	0.01	0.01	0.01	0.01	0.02	0.02	0.02	0.03	0.03
PM10					1.00	0.19	0.04	0.03	-0.03	-0.04	-0.07	-0.03	0.01	0.02	0.01	-0.01
						0.29	0.82	0.85	0.87	0.81	0.71	0.87	0.98	0.93	0.97	0.97
VKT R0500						1.00	0.77	0.64	0.58	0.52	0.46	0.41	0.37	0.36	0.34	0.32
							<.0001	<.0001	0.00	0.00	0.01	0.01	0.03	0.04	0.05	0.07
VKT R1000							1.00	0.92	0.85	0.79	0.73	0.70	0.66	0.63	0.60	0.58
								<.0001	<.0001	<.0001	<.0001	<.0001	<.0001	<.0001	0.00	0.00
VKT R1500								1.00	0.96	0.91	0.88	0.85	0.82	0.79	0.75	0.74
									<.0001	<.0001	<.0001	<.0001	<.0001	<.0001	<.0001	<.0001
VKT R2000									1.00	0.98	0.96	0.93	0.89	0.86	0.82	0.81
										<.0001	<.0001	<.0001	<.0001	<.0001	<.0001	<.0001
VKT R2500										1.00	0.99	0.96	0.92	0.89	0.87	0.85
											<.0001	<.0001	<.0001	<.0001	<.0001	<.0001
VKT R3000											1.00	0.99	0.96	0.94	0.92	0.91
												<.0001	<.0001	<.0001	<.0001	<.0001
VKT R3500												1.00	0.99	0.97	0.96	0.95
													<.0001	<.0001	<.0001	<.0001
VKT R4000													1.00	0.99	0.98	0.97
														<.0001	<.0001	<.0001
VKT R4500														1.00	1.00	0.99
															<.0001	<.0001
VKT R5000															1.00	1.00
																<.0001
VKT R5500																1.00

Table G.2 Pearson correlation coefficients between pollutant concentrations and residential areas

	NO2	CO	O3	SO2	PM10	Residential R0500	Residential R1000	Residential R1500	Residential R2000	Residential R2500	Residential R3000	Residential R3500	Residential R4000	Residential R4500	Residential R5000	Residential R5500
NO2	1.00	0.58	-0.55	0.72	-0.02	-0.23	-0.22	-0.26	-0.19	-0.20	-0.21	-0.09	0.02	0.09	0.14	0.18
		0.00	0.00	<.0001	0.90	0.18	0.20	0.14	0.28	0.25	0.24	0.62	0.91	0.62	0.43	0.32
CO		1.00	-0.52	0.57	0.25	-0.17	-0.14	-0.13	-0.09	-0.05	-0.02	0.10	0.25	0.31	0.34	0.36
			0.00	0.00	0.16	0.34	0.44	0.46	0.61	0.80	0.91	0.57	0.16	0.07	0.05	0.04
O3			1.00	-0.41	-0.24	0.31	0.30	0.23	0.14	0.07	-0.02	-0.18	-0.31	-0.39	-0.46	-0.49
				0.02	0.17	0.07	0.08	0.20	0.43	0.70	0.93	0.32	0.08	0.02	0.01	0.00
SO2				1.00	0.01	-0.20	-0.11	-0.09	0.00	0.05	0.09	0.19	0.26	0.28	0.30	0.31
					0.97	0.26	0.54	0.62	0.98	0.77	0.60	0.28	0.14	0.11	0.09	0.08
PM10					1.00	0.00	-0.14	-0.07	-0.09	-0.03	0.01	0.09	0.11	0.12	0.14	0.13
						1.00	0.44	0.71	0.63	0.87	0.94	0.62	0.55	0.50	0.41	0.45
Residential R0500						1.00	0.83	0.68	0.61	0.58	0.52	0.42	0.28	0.17	0.10	0.05
							<.0001	<.0001	0.00	0.00	0.00	0.01	0.10	0.33	0.59	0.79
Residential R1000							1.00	0.91	0.85	0.82	0.70	0.54	0.36	0.22	0.13	0.06
								<.0001	<.0001	<.0001	<.0001	0.00	0.04	0.21	0.47	0.74
Residential R1500								1.00	0.97	0.92	0.80	0.65	0.48	0.34	0.24	0.16
									<.0001	<.0001	<.0001	<.0001	0.00	0.05	0.17	0.38
Residential R2000									1.00	0.96	0.85	0.72	0.57	0.43	0.33	0.25
										<.0001	<.0001	<.0001	0.00	0.01	0.05	0.15
Residential R2500										1.00	0.95	0.84	0.70	0.58	0.48	0.40
											<.0001	<.0001	<.0001	0.00	0.00	0.02
Residential R3000											1.00	0.95	0.84	0.73	0.64	0.56
												<.0001	<.0001	<.0001	<.0001	0.00
Residential R3500												1.00	0.96	0.87	0.79	0.72
													<.0001	<.0001	<.0001	<.0001
Residential R4000													1.00	0.97	0.91	0.85
														<.0001	<.0001	<.0001
Residential R4500														1.00	0.98	0.94
															<.0001	<.0001
Residential R5000															1.00	0.99
																<.0001
Residential R5500																1.00

Table G.3 Pearson correlation coefficients between pollutant concentrations and commercial areas

	NO2	CO	O3	SO2	PM10	Commercial R0500	Commercial R1000	Commercial R1500	Commercial R2000	Commercial R2500	Commercial R3000	Commercial R3500	Commercial R4000	Commercial R4500	Commercial R5000	Commercial R5500
NO2	1.00	0.58	-0.55	0.72	-0.02	0.24	0.30	0.30	0.27	0.36	0.43	0.46	0.50	0.52	0.51	0.50
		0.00	0.00	<.0001	0.90	0.16	0.08	0.08	0.13	0.04	0.01	0.01	0.00	0.00	0.00	0.00
CO		1.00	-0.52	0.57	0.25	0.33	0.45	0.43	0.43	0.49	0.49	0.46	0.42	0.38	0.36	0.35
			0.00	0.00	0.16	0.06	0.01	0.01	0.01	0.00	0.00	0.01	0.01	0.03	0.04	0.04
O3			1.00	-0.41	-0.24	-0.22	-0.25	-0.28	-0.29	-0.34	-0.41	-0.46	-0.50	-0.53	-0.53	-0.54
				0.02	0.17	0.21	0.16	0.11	0.09	0.05	0.02	0.01	0.00	0.00	0.00	0.00
SO2				1.00	0.01	0.16	0.22	0.22	0.21	0.29	0.33	0.35	0.40	0.43	0.43	0.43
					0.97	0.38	0.21	0.21	0.24	0.09	0.05	0.04	0.02	0.01	0.01	0.01
PM10					1.00	-0.30	-0.13	-0.16	-0.11	-0.11	-0.08	-0.06	-0.03	-0.02	0.00	0.01
						0.09	0.47	0.38	0.54	0.55	0.65	0.73	0.86	0.90	0.99	0.97
Commercial R0500						1.00	0.81	0.69	0.60	0.50	0.40	0.31	0.24	0.17	0.11	0.09
							<.0001	<.0001	0.00	0.00	0.02	0.07	0.16	0.33	0.53	0.60
Commercial R1000							1.00	0.93	0.84	0.74	0.60	0.48	0.38	0.28	0.21	0.18
								<.0001	<.0001	<.0001	0.00	0.00	0.03	0.11	0.23	0.30
Commercial R1500								1.00	0.96	0.89	0.79	0.69	0.57	0.45	0.36	0.31
									<.0001	<.0001	<.0001	<.0001	0.00	0.01	0.04	0.07
Commercial R2000									1.00	0.97	0.88	0.78	0.66	0.52	0.43	0.37
										<.0001	<.0001	<.0001	<.0001	0.00	0.01	0.03
Commercial R2500										1.00	0.96	0.87	0.74	0.61	0.51	0.44
											<.0001	<.0001	<.0001	0.00	0.00	0.01
Commercial R3000											1.00	0.96	0.86	0.74	0.65	0.58
												<.0001	<.0001	<.0001	<.0001	0.00
Commercial R3500												1.00	0.96	0.88	0.80	0.74
													<.0001	<.0001	<.0001	<.0001
Commercial R4000													1.00	0.97	0.92	0.87
														<.0001	<.0001	<.0001
Commercial R4500														1.00	0.98	0.96
															<.0001	<.0001
Commercial R5000															1.00	0.99
																<.0001
Commercial R5500																1.00

Table G.4 Pearson correlation coefficients between pollutant concentrations and industrial areas

	NO2	CO	O3	SO2	PM10	Industrial R0500	Industrial R1000	Industrial R1500	Industrial R2000	Industrial R2500	Industrial R3000	Industrial R3500	Industrial R4000	Industrial R4500	Industrial R5000	Industrial R5500
NO2	1.00	0.58	-0.55	0.72	-0.02	-0.10	-0.06	0.02	0.05	0.06	0.07	0.08	0.12	0.23	0.27	0.29
		0.00	0.00	<.0001	0.90	0.58	0.74	0.89	0.80	0.73	0.69	0.65	0.50	0.20	0.12	0.09
CO		1.00	-0.52	0.57	0.25	-0.14	-0.14	-0.11	-0.12	-0.13	-0.14	-0.11	-0.04	0.06	0.07	0.06
			0.00	0.00	0.16	0.42	0.42	0.54	0.51	0.45	0.44	0.55	0.80	0.76	0.69	0.76
O3			1.00	-0.41	-0.24	-0.08	-0.08	-0.08	-0.08	-0.09	-0.06	-0.08	-0.08	-0.11	-0.14	-0.18
				0.02	0.17	0.66	0.67	0.64	0.64	0.61	0.72	0.67	0.65	0.53	0.41	0.31
SO2				1.00	0.01	-0.12	-0.09	-0.01	-0.01	-0.05	-0.09	-0.09	-0.06	0.08	0.13	0.11
					0.97	0.50	0.62	0.94	0.94	0.80	0.60	0.63	0.75	0.66	0.47	0.55
PM10					1.00	0.14	0.16	0.08	0.04	0.01	-0.02	-0.02	-0.03	-0.05	-0.05	-0.04
						0.42	0.36	0.65	0.84	0.95	0.89	0.91	0.87	0.80	0.79	0.83
Industrial R0500						1.00	0.98	0.80	0.76	0.71	0.64	0.56	0.48	0.39	0.32	0.27
							<.0001	<.0001	<.0001	<.0001	<.0001	0.00	0.00	0.02	0.07	0.13
Industrial R1000							1.00	0.88	0.85	0.80	0.73	0.65	0.56	0.47	0.40	0.35
								<.0001	<.0001	<.0001	<.0001	<.0001	0.00	0.01	0.02	0.04
Industrial R1500								1.00	0.99	0.96	0.90	0.84	0.75	0.65	0.58	0.54
									<.0001	<.0001	<.0001	<.0001	<.0001	<.0001	0.00	0.00
Industrial R2000									1.00	0.98	0.93	0.87	0.79	0.69	0.62	0.58
										<.0001	<.0001	<.0001	<.0001	<.0001	<.0001	0.00
Industrial R2500										1.00	0.98	0.93	0.86	0.76	0.70	0.67
											<.0001	<.0001	<.0001	<.0001	<.0001	<.0001
Industrial R3000											1.00	0.99	0.94	0.84	0.79	0.76
												<.0001	<.0001	<.0001	<.0001	<.0001
Industrial R3500												1.00	0.97	0.89	0.84	0.81
													<.0001	<.0001	<.0001	<.0001
Industrial R4000													1.00	0.96	0.92	0.88
														<.0001	<.0001	<.0001
Industrial R4500														1.00	0.98	0.94
															<.0001	<.0001
Industrial R5000															1.00	0.99
																<.0001
Industrial R5500																1.00

Table G.5 Pearson correlation coefficients between pollutant concentrations and transportation areas

	NO2	CO	O3	SO2	PM10	Transport R0500	Transport R1000	Transport R1500	Transport R2000	Transport R2500	Transport R3000	Transport R3500	Transport R4000	Transport R4500	Transport R5000	Transport R5500
NO2	1.00	0.58	-0.55	0.72	-0.02	0.39	0.42	0.36	0.33	0.38	0.45	0.45	0.45	0.46	0.46	0.48
		0.00	0.00	<.0001	0.90	0.02	0.01	0.04	0.06	0.03	0.01	0.01	0.01	0.01	0.01	0.00
CO		1.00	-0.52	0.57	0.25	0.58	0.43	0.31	0.21	0.24	0.27	0.27	0.25	0.24	0.23	0.26
			0.00	0.00	0.16	0.00	0.01	0.07	0.22	0.17	0.12	0.12	0.15	0.17	0.18	0.14
O3			1.00	-0.41	-0.24	-0.57	-0.64	-0.42	-0.43	-0.44	-0.48	-0.52	-0.53	-0.54	-0.54	-0.55
				0.02	0.17	0.00	<.0001	0.01	0.01	0.01	0.00	0.00	0.00	0.00	0.00	0.00
SO2				1.00	0.01	0.43	0.36	0.39	0.38	0.40	0.44	0.44	0.44	0.44	0.43	0.41
					0.97	0.01	0.04	0.02	0.03	0.02	0.01	0.01	0.01	0.01	0.01	0.02
PM10					1.00	0.01	0.04	-0.09	-0.15	-0.17	-0.14	-0.07	-0.04	-0.02	-0.01	0.00
						0.96	0.83	0.63	0.40	0.33	0.44	0.68	0.83	0.90	0.94	0.99
Transport R0500						1.00	0.73	0.56	0.50	0.51	0.54	0.53	0.50	0.49	0.47	0.46
							<.0001	0.00	0.00	0.00	0.00	0.00	0.00	0.00	0.01	0.01
Transport R1000							1.00	0.91	0.88	0.87	0.86	0.83	0.77	0.73	0.70	0.69
								<.0001	<.0001	<.0001	<.0001	<.0001	<.0001	<.0001	<.0001	<.0001
Transport R1500								1.00	0.97	0.96	0.91	0.85	0.78	0.72	0.69	0.67
									<.0001	<.0001	<.0001	<.0001	<.0001	<.0001	<.0001	<.0001
Transport R2000									1.00	0.98	0.92	0.87	0.80	0.74	0.71	0.70
										<.0001	<.0001	<.0001	<.0001	<.0001	<.0001	<.0001
Transport R2500										1.00	0.97	0.93	0.86	0.81	0.78	0.77
											<.0001	<.0001	<.0001	<.0001	<.0001	<.0001
Transport R3000											1.00	0.98	0.93	0.90	0.87	0.86
												<.0001	<.0001	<.0001	<.0001	<.0001
Transport R3500												1.00	0.98	0.96	0.94	0.93
													<.0001	<.0001	<.0001	<.0001
Transport R4000													1.00	0.99	0.98	0.96
														<.0001	<.0001	<.0001
Transport R4500														1.00	0.99	0.98
															<.0001	<.0001
Transport R5000															1.00	0.99
																<.0001
Transport R5500																1.00

Table G.6 Pearson correlation coefficients between pollutant concentrations and green areas

	NO2	CO	O3	SO2	PM10	Green Area R0500	Green Area R1000	Green Area R1500	Green Area R2000	Green Area R2500	Green Area R3000	Green Area R3500	Green Area R4000	Green Area R4500	Green Area R5000	Green Area R5500
NO2	1.00	0.58	-0.55	0.72	-0.02	-0.13	-0.15	-0.26	-0.29	-0.36	-0.42	-0.46	-0.48	-0.49	-0.49	-0.50
		0.00	0.00	<.0001	0.90	0.47	0.40	0.14	0.10	0.04	0.01	0.01	0.00	0.00	0.00	0.00
CO		1.00	-0.52	0.57	0.25	-0.35	-0.34	-0.34	-0.30	-0.29	-0.29	-0.30	-0.31	-0.31	-0.31	-0.31
			0.00	0.00	0.16	0.04	0.05	0.05	0.08	0.09	0.10	0.09	0.08	0.08	0.08	0.07
O3			1.00	-0.41	-0.24	0.12	0.23	0.37	0.41	0.43	0.50	0.55	0.56	0.57	0.56	0.55
				0.02	0.17	0.51	0.20	0.03	0.02	0.01	0.00	0.00	0.00	0.00	0.00	0.00
SO2				1.00	0.01	-0.22	-0.29	-0.34	-0.33	-0.34	-0.35	-0.34	-0.33	-0.32	-0.32	-0.31
					0.97	0.20	0.10	0.05	0.05	0.05	0.04	0.05	0.06	0.06	0.07	0.07
PM10					1.00	0.23	0.23	0.18	0.13	0.12	0.04	-0.04	-0.09	-0.10	-0.10	-0.09
						0.19	0.18	0.31	0.45	0.50	0.80	0.80	0.60	0.58	0.58	0.62
Green Area R0500						1.00	0.85	0.65	0.52	0.40	0.26	0.15	0.08	0.04	0.03	0.03
							<.0001	<.0001	0.00	0.02	0.14	0.41	0.66	0.80	0.85	0.85
Green Area R1000							1.00	0.92	0.81	0.68	0.54	0.44	0.37	0.33	0.31	0.29
								<.0001	<.0001	<.0001	0.00	0.01	0.03	0.06	0.08	0.10
Green Area R1500								1.00	0.95	0.88	0.79	0.71	0.65	0.61	0.58	0.56
									<.0001	<.0001	<.0001	<.0001	<.0001	0.00	0.00	0.00
Green Area R2000									1.00	0.97	0.91	0.84	0.78	0.75	0.73	0.71
										<.0001	<.0001	<.0001	<.0001	<.0001	<.0001	<.0001
Green Area R2500										1.00	0.98	0.93	0.88	0.85	0.83	0.81
											<.0001	<.0001	<.0001	<.0001	<.0001	<.0001
Green Area R3000											1.00	0.98	0.95	0.93	0.91	0.88
												<.0001	<.0001	<.0001	<.0001	<.0001
Green Area R3500												1.00	0.99	0.98	0.96	0.93
													<.0001	<.0001	<.0001	<.0001
Green Area R4000													1.00	0.99	0.98	0.96
														<.0001	<.0001	<.0001
Green Area R4500														1.00	0.99	0.98
															<.0001	<.0001
Green Area R5000															1.00	0.99
																<.0001
Green Area R5500																1.00

Appendix H. Descriptive Statistics of Elasticities: Time-Series Air Quality Models

Table H.1 Hourly elasticities w.r.t. the traffic variable in the O_3 models

Variable	Hour	Weekdays					Sunday				
		N	Mean	Std.	Min	Max	N	Mean	Std.	Min	Max
Background Traffic Elasticities	H01	302	-0.66	0.46	-1.98	-0.06	63	-0.45	0.33	-1.27	-0.05
	H02	302	-0.52	0.39	-1.76	-0.05	63	-0.48	0.39	-1.44	-0.05
	H03	302	-0.40	0.32	-1.41	-0.04	63	-0.44	0.38	-1.45	-0.05
	H04	302	-0.32	0.26	-1.08	-0.03	63	-0.39	0.35	-1.35	-0.04
	H05	302	-0.32	0.25	-1.06	-0.03	63	-0.38	0.33	-1.20	-0.04
	H06	302	-0.47	0.35	-1.51	-0.04	63	-0.44	0.35	-1.31	-0.05
	H07	302	-0.85	0.54	-2.41	-0.08	63	-0.55	0.41	-1.45	-0.06
	H08	302	-0.94	0.57	-2.37	-0.08	63	-0.49	0.36	-1.31	-0.06
	H09	302	-0.69	0.49	-2.24	-0.04	63	-0.22	0.21	-0.74	-0.01
	H10	302	-0.44	0.42	-2.37	0.02	63	0.00	0.07	-0.20	0.15
	H11	302	-0.26	0.36	-1.93	0.12	63	0.19	0.12	0.03	0.59
	H12	302	-0.14	0.30	-1.63	0.18	63	0.19	0.11	0.03	0.60
	H13	302	-0.07	0.27	-1.65	0.22	63	0.22	0.12	0.05	0.73
	H14	302	-0.02	0.26	-1.73	0.25	63	0.26	0.14	0.09	0.91
	H15	302	0.01	0.25	-1.83	0.32	63	0.26	0.13	0.09	0.66
	H16	302	0.01	0.25	-1.69	0.37	63	0.26	0.14	0.09	0.80
	H17	302	-0.01	0.26	-1.76	0.39	63	0.29	0.18	0.09	0.92
	H18	302	-0.07	0.31	-1.80	0.35	63	0.37	0.32	0.09	1.55
	H19	302	-0.18	0.39	-1.88	0.33	63	0.36	0.34	0.07	1.35
	H20	302	-0.35	0.46	-2.13	0.13	63	0.17	0.14	0.00	0.58
	H21	302	-0.53	0.52	-2.23	-0.01	63	0.09	0.09	-0.02	0.45
	H22	302	-0.67	0.55	-2.26	-0.05	63	-0.01	0.07	-0.20	0.13
	H23	302	-0.77	0.55	-2.41	-0.08	63	-0.19	0.17	-0.60	-0.01
	H24	302	-0.79	0.53	-2.33	-0.08	63	-0.40	0.30	-1.16	-0.04
Roadside Traffic Elasticities	H01	301	-0.43	0.29	-1.84	-0.06	62	-0.35	0.23	-1.05	-0.05
	H02	301	-0.40	0.27	-1.65	-0.05	62	-0.39	0.26	-1.35	-0.06
	H03	301	-0.35	0.25	-1.32	-0.04	62	-0.38	0.28	-1.53	-0.06
	H04	301	-0.30	0.22	-1.34	-0.03	62	-0.33	0.28	-1.87	-0.05
	H05	301	-0.30	0.23	-1.21	-0.03	62	-0.30	0.22	-1.06	-0.05
	H06	301	-0.39	0.26	-1.43	-0.05	62	-0.37	0.26	-1.42	-0.07
	H07	301	-0.42	0.30	-2.14	-0.07	62	-0.43	0.28	-1.12	-0.09
	H08	301	0.00	0.21	-0.94	0.29	62	-0.39	0.23	-1.06	-0.09
	H09	301	0.17	0.18	-0.45	0.66	62	-0.18	0.16	-0.80	-0.03
	H10	302	0.05	0.13	-0.54	0.25	62	-0.02	0.09	-0.35	0.07
	H11	302	0.03	0.11	-0.75	0.24	62	0.16	0.12	-0.04	0.56
	H12	301	0.01	0.10	-0.75	0.19	62	0.13	0.10	-0.05	0.38
	H13	301	-0.03	0.10	-0.98	0.20	62	0.16	0.11	0.00	0.50
	H14	302	0.00	0.09	-0.70	0.44	62	0.22	0.15	0.02	0.72
	H15	302	0.02	0.08	-0.59	0.26	62	0.22	0.16	0.02	0.84
	H16	302	0.03	0.08	-0.60	0.27	62	0.24	0.18	0.03	1.10
	H17	302	0.04	0.09	-0.50	0.34	62	0.27	0.21	0.04	1.09
	H18	302	0.08	0.10	-0.48	0.34	62	0.34	0.28	0.05	1.39
	H19	302	0.10	0.13	-0.64	0.43	62	0.30	0.24	0.02	1.02
	H20	302	0.01	0.13	-0.67	0.20	62	0.12	0.13	-0.23	0.55
	H21	302	-0.14	0.16	-1.02	0.04	62	0.09	0.14	-0.38	0.52
	H22	302	-0.19	0.17	-1.01	-0.01	62	0.03	0.12	-0.40	0.22
	H23	302	-0.27	0.21	-1.64	-0.04	62	-0.13	0.16	-0.71	0.00
	H24	302	-0.39	0.24	-1.62	-0.07	62	-0.32	0.24	-1.05	-0.07

Table H.2 Hourly elasticities w.r.t. the solar radiation variable in the O_3 models

Variable	Hour	Weekdays					Sunday				
		N	Mean	Std.	Min	Max	N	Mean	Std.	Min	Max
Background Solar Radiation Elasticities	H01	302	0.01	0.02	0.00	0.13	63	0.01	0.02	0.00	0.12
	H02	302	0.00	0.00	0.00	0.00	63	0.00	0.00	0.00	0.00
	H03	302	0.00	0.00	0.00	0.00	63	0.00	0.00	0.00	0.00
	H04	302	0.00	0.00	0.00	0.00	63	0.00	0.00	0.00	0.00
	H05	302	0.00	0.00	0.00	0.00	63	0.00	0.00	0.00	0.00
	H06	302	0.02	0.05	0.00	0.45	63	0.01	0.03	0.00	0.14
	H07	302	0.06	0.11	0.00	0.72	63	0.06	0.11	0.00	0.56
	H08	302	0.19	0.27	0.00	1.26	63	0.18	0.26	0.00	1.19
	H09	302	0.37	0.40	0.00	1.80	63	0.34	0.33	0.00	1.39
	H10	302	0.50	0.42	0.00	2.12	63	0.51	0.36	0.01	1.52
	H11	302	0.60	0.41	0.00	2.21	63	0.62	0.38	0.06	2.02
	H12	302	0.65	0.38	0.00	2.03	63	0.66	0.38	0.10	2.24
	H13	302	0.69	0.37	0.00	2.07	63	0.67	0.36	0.13	2.35
	H14	302	0.74	0.37	0.02	2.13	63	0.69	0.35	0.17	2.48
	H15	302	0.79	0.39	0.03	2.64	63	0.66	0.28	0.19	1.81
	H16	302	0.81	0.44	0.03	3.10	63	0.66	0.31	0.19	2.11
	H17	302	0.81	0.46	0.02	2.88	63	0.69	0.37	0.17	2.36
	H18	302	0.85	0.55	0.01	3.59	63	0.78	0.54	0.14	3.51
	H19	302	0.89	0.64	0.00	4.52	63	0.86	0.67	0.12	3.75
	H20	302	0.81	0.66	0.00	4.22	63	0.77	0.62	0.09	2.55
	H21	302	0.60	0.60	0.00	4.38	63	0.55	0.49	0.00	2.06
	H22	302	0.37	0.44	0.00	3.20	63	0.36	0.38	0.00	1.44
	H23	302	0.18	0.25	0.00	1.60	63	0.18	0.22	0.00	0.94
	H24	302	0.06	0.11	0.00	0.77	63	0.06	0.09	0.00	0.32
Roadside Solar Radiation Elasticities	H01	301	0.00	0.01	0.00	0.10	62	0.01	0.01	0.00	0.05
	H02	301	0.00	0.00	0.00	0.00	62	0.00	0.00	0.00	0.00
	H03	301	0.00	0.00	0.00	0.00	62	0.00	0.00	0.00	0.00
	H04	301	0.00	0.00	0.00	0.00	62	0.00	0.00	0.00	0.00
	H05	301	0.00	0.00	0.00	0.00	62	0.00	0.00	0.00	0.00
	H06	301	0.01	0.03	0.00	0.24	62	0.01	0.02	0.00	0.10
	H07	301	0.02	0.05	0.00	0.33	62	0.03	0.05	0.00	0.19
	H08	301	0.07	0.10	0.00	0.58	62	0.09	0.11	0.00	0.52
	H09	301	0.13	0.17	0.00	1.00	62	0.18	0.18	0.00	0.61
	H10	302	0.22	0.25	0.00	1.39	62	0.28	0.22	0.00	0.82
	H11	302	0.31	0.31	0.00	1.77	62	0.37	0.24	0.03	0.98
	H12	301	0.41	0.35	0.00	1.83	62	0.45	0.26	0.05	1.22
	H13	301	0.50	0.38	0.00	2.08	62	0.51	0.26	0.09	1.19
	H14	302	0.57	0.40	0.00	2.65	62	0.57	0.27	0.11	1.34
	H15	302	0.63	0.41	0.00	2.18	62	0.58	0.26	0.10	1.28
	H16	302	0.64	0.41	0.00	2.72	62	0.59	0.26	0.12	1.26
	H17	302	0.62	0.41	0.00	2.45	62	0.59	0.27	0.10	1.23
	H18	302	0.55	0.40	0.00	2.33	62	0.58	0.28	0.07	1.33
	H19	302	0.48	0.41	0.00	2.20	62	0.55	0.35	0.05	1.72
	H20	302	0.39	0.42	0.00	2.24	62	0.47	0.36	0.03	1.61
	H21	302	0.27	0.35	0.00	2.06	62	0.34	0.32	0.00	1.27
	H22	302	0.15	0.21	0.00	1.00	62	0.21	0.24	0.00	1.04
	H23	302	0.08	0.12	0.00	0.81	62	0.11	0.14	0.00	0.66
	H24	302	0.03	0.05	0.00	0.43	62	0.04	0.06	0.00	0.24

Table H.3 Hourly elasticities w.r.t. the wind speed variable in the O_3 models

Variable	Hour	Weekdays					Sunday				
		N	Mean	Std.	Min	Max	N	Mean	Std.	Min	Max
Background Wind Speed Elasticities	H01	302	-0.03	0.03	-0.14	0.00	63	-0.03	0.03	-0.11	0.00
	H02	302	-0.03	0.03	-0.16	0.00	63	-0.03	0.03	-0.11	0.00
	H03	302	-0.03	0.03	-0.15	0.00	63	-0.03	0.03	-0.13	0.00
	H04	302	-0.03	0.03	-0.18	0.00	63	-0.03	0.03	-0.13	0.00
	H05	302	-0.03	0.03	-0.19	0.00	63	-0.02	0.03	-0.14	0.00
	H06	302	-0.03	0.03	-0.15	0.00	63	-0.03	0.03	-0.12	0.00
	H07	302	-0.04	0.03	-0.14	0.00	63	-0.03	0.03	-0.18	0.00
	H08	302	-0.04	0.03	-0.18	0.00	63	-0.03	0.03	-0.14	0.00
	H09	302	-0.04	0.03	-0.14	0.00	63	-0.03	0.03	-0.11	0.00
	H10	302	-0.02	0.02	-0.13	0.00	63	-0.02	0.02	-0.08	0.00
	H11	302	-0.02	0.02	-0.13	0.00	63	-0.01	0.01	-0.05	0.00
	H12	302	-0.01	0.02	-0.09	0.01	63	-0.01	0.01	-0.06	0.01
	H13	302	-0.01	0.02	-0.11	0.02	63	0.00	0.01	-0.03	0.01
	H14	302	0.00	0.02	-0.11	0.02	63	0.00	0.01	-0.03	0.01
	H15	302	0.00	0.02	-0.16	0.02	63	0.00	0.01	-0.03	0.01
	H16	302	0.00	0.01	-0.08	0.02	63	0.00	0.01	-0.03	0.01
	H17	302	0.00	0.01	-0.06	0.02	63	0.00	0.01	-0.05	0.01
	H18	302	-0.01	0.02	-0.11	0.02	63	0.00	0.01	-0.05	0.01
	H19	302	-0.01	0.02	-0.15	0.01	63	-0.01	0.02	-0.10	0.01
	H20	302	-0.02	0.03	-0.12	0.01	63	-0.02	0.02	-0.08	0.00
	H21	302	-0.03	0.03	-0.15	0.00	63	-0.02	0.03	-0.10	0.00
	H22	302	-0.03	0.03	-0.16	0.00	63	-0.02	0.02	-0.10	0.00
	H23	302	-0.03	0.03	-0.14	0.00	63	-0.02	0.03	-0.12	0.00
	H24	302	-0.03	0.03	-0.17	0.00	63	-0.03	0.03	-0.12	0.00
Roadside Wind Speed Elasticities	H01	N/A	N/A	N/A	N/A	N/A	N/A	N/A	N/A	N/A	N/A
	H02	N/A	N/A	N/A	N/A	N/A	N/A	N/A	N/A	N/A	N/A
	H03	N/A	N/A	N/A	N/A	N/A	N/A	N/A	N/A	N/A	N/A
	H04	N/A	N/A	N/A	N/A	N/A	N/A	N/A	N/A	N/A	N/A
	H05	N/A	N/A	N/A	N/A	N/A	N/A	N/A	N/A	N/A	N/A
	H06	N/A	N/A	N/A	N/A	N/A	N/A	N/A	N/A	N/A	N/A
	H07	N/A	N/A	N/A	N/A	N/A	N/A	N/A	N/A	N/A	N/A
	H08	N/A	N/A	N/A	N/A	N/A	N/A	N/A	N/A	N/A	N/A
	H09	N/A	N/A	N/A	N/A	N/A	N/A	N/A	N/A	N/A	N/A
	H10	N/A	N/A	N/A	N/A	N/A	N/A	N/A	N/A	N/A	N/A
	H11	N/A	N/A	N/A	N/A	N/A	N/A	N/A	N/A	N/A	N/A
	H12	N/A	N/A	N/A	N/A	N/A	N/A	N/A	N/A	N/A	N/A
	H13	N/A	N/A	N/A	N/A	N/A	N/A	N/A	N/A	N/A	N/A
	H14	N/A	N/A	N/A	N/A	N/A	N/A	N/A	N/A	N/A	N/A
	H15	N/A	N/A	N/A	N/A	N/A	N/A	N/A	N/A	N/A	N/A
	H16	N/A	N/A	N/A	N/A	N/A	N/A	N/A	N/A	N/A	N/A
	H17	N/A	N/A	N/A	N/A	N/A	N/A	N/A	N/A	N/A	N/A
	H18	N/A	N/A	N/A	N/A	N/A	N/A	N/A	N/A	N/A	N/A
	H19	N/A	N/A	N/A	N/A	N/A	N/A	N/A	N/A	N/A	N/A
	H20	N/A	N/A	N/A	N/A	N/A	N/A	N/A	N/A	N/A	N/A
	H21	N/A	N/A	N/A	N/A	N/A	N/A	N/A	N/A	N/A	N/A
	H22	N/A	N/A	N/A	N/A	N/A	N/A	N/A	N/A	N/A	N/A
	H23	N/A	N/A	N/A	N/A	N/A	N/A	N/A	N/A	N/A	N/A
	H24	N/A	N/A	N/A	N/A	N/A	N/A	N/A	N/A	N/A	N/A

Table H.4 Hourly elasticities w.r.t. the temperature variable in the O_3 models

Variable	Hour	Weekdays					Sunday				
		N	Mean	Std.	Min	Max	N	Mean	Std.	Min	Max
Background Temperature Elasticities	H01	302	0.00	0.00	0.00	0.01	63	0.00	0.00	0.00	0.01
	H02	302	0.00	0.00	0.00	0.00	63	0.00	0.00	0.00	0.00
	H03	302	0.00	0.00	0.00	0.00	63	0.00	0.00	0.00	0.00
	H04	302	0.00	0.00	0.00	0.00	63	0.00	0.00	0.00	0.00
	H05	302	0.00	0.00	0.00	0.00	63	0.00	0.00	0.00	0.00
	H06	302	0.00	0.01	0.00	0.04	63	0.00	0.00	0.00	0.01
	H07	302	0.00	0.01	0.00	0.06	63	0.00	0.01	0.00	0.03
	H08	302	0.01	0.02	0.00	0.11	63	0.01	0.01	0.00	0.06
	H09	302	0.02	0.03	-0.01	0.12	63	0.02	0.02	0.00	0.07
	H10	302	0.03	0.04	-0.02	0.16	63	0.03	0.02	-0.01	0.09
	H11	302	0.04	0.04	-0.03	0.21	63	0.03	0.03	-0.02	0.10
	H12	302	0.04	0.03	-0.03	0.22	63	0.04	0.03	-0.02	0.13
	H13	302	0.04	0.03	-0.04	0.21	63	0.04	0.03	-0.02	0.12
	H14	302	0.05	0.03	-0.04	0.17	63	0.04	0.03	-0.03	0.13
	H15	302	0.05	0.03	-0.04	0.17	63	0.04	0.03	-0.03	0.15
	H16	302	0.05	0.04	-0.04	0.21	63	0.04	0.03	-0.03	0.15
	H17	302	0.05	0.04	-0.06	0.23	63	0.04	0.04	-0.03	0.17
	H18	302	0.05	0.05	-0.09	0.35	63	0.04	0.04	-0.06	0.17
	H19	302	0.05	0.06	-0.07	0.41	63	0.04	0.05	-0.06	0.17
	H20	302	0.05	0.06	-0.05	0.51	63	0.04	0.04	-0.03	0.16
	H21	302	0.04	0.05	-0.02	0.36	63	0.03	0.03	-0.01	0.12
	H22	302	0.03	0.04	-0.01	0.28	63	0.02	0.02	0.00	0.09
	H23	302	0.01	0.02	0.00	0.12	63	0.01	0.01	0.00	0.06
	H24	302	0.01	0.01	0.00	0.07	63	0.00	0.01	0.00	0.02
Roadside Temperature Elasticities	H01	301	0.14	0.17	-0.29	1.30	62	0.14	0.14	-0.15	0.51
	H02	301	0.13	0.15	-0.30	0.76	62	0.12	0.12	-0.16	0.39
	H03	301	0.12	0.16	-0.29	0.97	62	0.11	0.12	-0.19	0.41
	H04	301	0.11	0.15	-0.35	0.71	62	0.10	0.11	-0.28	0.38
	H05	301	0.11	0.15	-0.31	0.85	62	0.09	0.10	-0.15	0.37
	H06	301	0.12	0.15	-0.37	0.68	62	0.11	0.12	-0.16	0.39
	H07	301	0.13	0.16	-0.30	1.10	62	0.13	0.14	-0.16	0.45
	H08	301	0.12	0.15	-0.24	0.82	62	0.13	0.13	-0.13	0.42
	H09	301	0.12	0.13	-0.20	0.51	62	0.11	0.12	-0.09	0.51
	H10	302	0.11	0.10	-0.13	0.48	62	0.10	0.10	-0.07	0.47
	H11	302	0.10	0.09	-0.09	0.52	62	0.09	0.09	-0.06	0.46
	H12	301	0.09	0.08	-0.08	0.50	62	0.08	0.09	-0.05	0.46
	H13	301	0.08	0.08	-0.07	0.56	62	0.07	0.08	-0.04	0.46
	H14	302	0.08	0.07	-0.06	0.45	62	0.07	0.08	-0.04	0.47
	H15	302	0.08	0.07	-0.04	0.43	62	0.07	0.09	-0.04	0.53
	H16	302	0.08	0.07	-0.04	0.47	62	0.07	0.10	-0.04	0.64
	H17	302	0.08	0.09	-0.05	0.75	62	0.08	0.09	-0.05	0.51
	H18	302	0.09	0.10	-0.06	1.09	62	0.09	0.11	-0.08	0.68
	H19	302	0.10	0.11	-0.09	1.17	62	0.10	0.13	-0.11	0.73
	H20	302	0.12	0.13	-0.10	1.11	62	0.11	0.14	-0.15	0.80
	H21	302	0.14	0.15	-0.10	1.28	62	0.12	0.16	-0.21	0.79
	H22	302	0.14	0.14	-0.11	0.71	62	0.13	0.17	-0.20	0.79
	H23	302	0.15	0.15	-0.11	0.84	62	0.14	0.19	-0.28	0.99
	H24	302	0.15	0.15	-0.10	0.91	62	0.14	0.18	-0.26	0.86

Table H.5 Hourly elasticities w.r.t. the humidity variable in the O_3 models

Variable	Hour	Weekdays					Sunday				
		N	Mean	Std.	Min	Max	N	Mean	Std.	Min	Max
Background Humidity Elasticities	H01	302	-0.36	0.28	-1.31	-0.02	63	-0.36	0.29	-1.22	-0.04
	H02	302	-0.35	0.28	-1.35	-0.02	63	-0.33	0.29	-1.24	-0.04
	H03	302	-0.34	0.28	-1.22	-0.02	63	-0.32	0.29	-1.24	-0.04
	H04	302	-0.34	0.28	-1.24	-0.01	63	-0.33	0.31	-1.25	-0.03
	H05	302	-0.35	0.29	-1.37	-0.02	63	-0.34	0.32	-1.33	-0.03
	H06	302	-0.39	0.31	-1.49	-0.02	63	-0.36	0.30	-1.35	-0.04
	H07	302	-0.44	0.30	-1.44	-0.03	63	-0.40	0.31	-1.23	-0.04
	H08	302	-0.42	0.27	-1.27	-0.03	63	-0.37	0.28	-1.19	-0.03
	H09	302	-0.32	0.22	-1.23	-0.02	63	-0.27	0.22	-0.92	-0.03
	H10	302	-0.22	0.19	-1.32	-0.02	63	-0.18	0.16	-0.66	-0.02
	H11	302	-0.16	0.17	-1.04	-0.01	63	-0.12	0.11	-0.51	-0.02
	H12	302	-0.12	0.14	-0.87	-0.01	63	-0.09	0.09	-0.39	-0.01
	H13	302	-0.09	0.13	-0.88	-0.01	63	-0.07	0.08	-0.31	-0.01
	H14	302	-0.08	0.13	-0.87	-0.01	63	-0.07	0.08	-0.37	-0.01
	H15	302	-0.08	0.12	-1.02	-0.01	63	-0.06	0.07	-0.42	-0.01
	H16	302	-0.08	0.12	-0.89	-0.01	63	-0.07	0.08	-0.48	-0.01
	H17	302	-0.09	0.13	-0.94	-0.01	63	-0.08	0.10	-0.49	-0.01
	H18	302	-0.12	0.16	-1.00	-0.01	63	-0.12	0.15	-0.56	-0.01
	H19	302	-0.18	0.20	-1.11	-0.01	63	-0.17	0.21	-0.87	-0.01
	H20	302	-0.23	0.23	-1.17	-0.01	63	-0.22	0.24	-1.05	-0.02
	H21	302	-0.28	0.25	-1.25	-0.02	63	-0.24	0.24	-0.87	-0.02
	H22	302	-0.31	0.26	-1.26	-0.02	63	-0.27	0.26	-1.07	-0.03
	H23	302	-0.34	0.26	-1.39	-0.02	63	-0.32	0.28	-1.01	-0.03
	H24	302	-0.37	0.28	-1.43	-0.02	63	-0.34	0.28	-1.12	-0.03
Roadside Humidity Elasticities	H01	301	-0.25	0.18	-1.29	-0.03	62	-0.25	0.17	-0.91	-0.05
	H02	301	-0.24	0.17	-0.99	-0.02	62	-0.23	0.17	-0.91	-0.04
	H03	301	-0.24	0.19	-0.98	-0.02	62	-0.23	0.17	-0.77	-0.04
	H04	301	-0.24	0.19	-1.33	-0.02	62	-0.22	0.17	-0.98	-0.04
	H05	301	-0.24	0.20	-1.17	-0.02	62	-0.22	0.17	-1.00	-0.04
	H06	301	-0.26	0.18	-1.18	-0.03	62	-0.25	0.19	-1.23	-0.05
	H07	301	-0.27	0.17	-1.15	-0.05	62	-0.26	0.17	-0.86	-0.06
	H08	301	-0.25	0.14	-0.85	-0.04	62	-0.24	0.14	-0.67	-0.05
	H09	301	-0.21	0.12	-0.76	-0.03	62	-0.19	0.12	-0.53	-0.03
	H10	302	-0.16	0.10	-0.52	-0.02	62	-0.14	0.10	-0.45	-0.03
	H11	302	-0.13	0.09	-0.53	-0.02	62	-0.11	0.09	-0.43	-0.03
	H12	301	-0.11	0.09	-0.50	-0.01	62	-0.10	0.08	-0.40	-0.02
	H13	301	-0.09	0.08	-0.59	-0.01	62	-0.08	0.08	-0.41	-0.01
	H14	302	-0.09	0.09	-0.61	-0.01	62	-0.08	0.08	-0.40	-0.01
	H15	302	-0.08	0.08	-0.46	-0.01	62	-0.08	0.08	-0.45	-0.01
	H16	302	-0.09	0.08	-0.45	-0.01	62	-0.08	0.09	-0.57	-0.01
	H17	302	-0.10	0.10	-0.66	-0.01	62	-0.09	0.09	-0.45	-0.01
	H18	302	-0.12	0.11	-0.98	-0.01	62	-0.12	0.12	-0.63	-0.01
	H19	302	-0.15	0.12	-1.13	-0.02	62	-0.15	0.13	-0.69	-0.02
	H20	302	-0.18	0.13	-1.14	-0.03	62	-0.18	0.16	-0.77	-0.03
	H21	302	-0.20	0.16	-1.33	-0.03	62	-0.21	0.18	-0.93	-0.04
	H22	302	-0.22	0.14	-0.77	-0.04	62	-0.22	0.18	-0.83	-0.04
	H23	302	-0.23	0.15	-0.86	-0.04	62	-0.25	0.20	-1.06	-0.05
	H24	302	-0.25	0.16	-1.01	-0.04	62	-0.25	0.19	-0.87	-0.05

Table H.6 Hourly elasticities w.r.t. the traffic variable in the NO_2 models

Variable	Hour	Weekdays					Sunday				
		N	Mean	Std.	Min	Max	N	Mean	Std.	Min	Max
Background Traffic Elasticities	H01	302	0.17	0.08	0.07	0.59	63	0.16	0.08	0.07	0.42
	H02	302	0.16	0.09	0.06	0.63	63	0.17	0.10	0.07	0.47
	H03	302	0.14	0.09	0.05	0.61	63	0.17	0.10	0.06	0.49
	H04	302	0.12	0.08	0.04	0.54	63	0.15	0.09	0.05	0.44
	H05	302	0.12	0.07	0.04	0.44	63	0.14	0.08	0.05	0.37
	H06	302	0.14	0.06	0.05	0.42	63	0.15	0.07	0.06	0.34
	H07	302	0.21	0.07	0.08	0.50	63	0.17	0.07	0.07	0.38
	H08	302	0.24	0.07	0.10	0.54	63	0.16	0.07	0.08	0.38
	H09	302	0.23	0.07	0.10	0.50	63	0.16	0.07	0.07	0.40
	H10	302	0.21	0.08	0.08	0.49	63	0.13	0.07	0.03	0.37
	H11	302	0.19	0.08	0.06	0.46	63	0.07	0.08	-0.15	0.30
	H12	302	0.16	0.09	0.00	0.45	63	0.03	0.10	-0.32	0.25
	H13	302	0.13	0.09	-0.09	0.46	63	-0.03	0.15	-0.55	0.20
	H14	302	0.10	0.11	-0.22	0.42	63	-0.11	0.19	-0.80	0.16
	H15	302	0.07	0.12	-0.27	0.40	63	-0.14	0.22	-0.85	0.15
	H16	302	0.07	0.11	-0.28	0.35	63	-0.14	0.22	-0.81	0.14
	H17	302	0.09	0.10	-0.22	0.34	63	-0.11	0.19	-0.74	0.15
	H18	302	0.11	0.08	-0.11	0.36	63	-0.06	0.14	-0.52	0.14
	H19	302	0.13	0.07	-0.01	0.38	63	0.02	0.09	-0.27	0.18
	H20	302	0.16	0.07	0.05	0.45	63	0.08	0.06	-0.05	0.26
	H21	302	0.17	0.07	0.07	0.49	63	0.10	0.05	0.01	0.29
	H22	302	0.19	0.08	0.08	0.50	63	0.13	0.05	0.04	0.30
	H23	302	0.19	0.08	0.08	0.49	63	0.14	0.05	0.06	0.29
	H24	302	0.19	0.08	0.07	0.51	63	0.15	0.06	0.07	0.34
Roadside Traffic Elasticities	H01	301	0.33	0.11	0.11	0.89	62	0.33	0.12	0.17	0.68
	H02	301	0.35	0.14	0.11	1.02	62	0.39	0.16	0.19	0.86
	H03	301	0.33	0.14	0.11	0.92	62	0.41	0.20	0.19	0.98
	H04	301	0.30	0.13	0.10	0.97	62	0.39	0.19	0.17	0.92
	H05	301	0.29	0.11	0.10	0.84	62	0.36	0.17	0.17	0.79
	H06	301	0.29	0.08	0.12	0.62	62	0.32	0.12	0.18	0.67
	H07	301	0.30	0.07	0.14	0.55	62	0.33	0.10	0.21	0.64
	H08	301	0.15	0.06	0.01	0.37	62	0.32	0.09	0.19	0.56
	H09	301	0.07	0.06	-0.10	0.24	62	0.26	0.09	0.14	0.52
	H10	302	0.10	0.06	-0.04	0.27	62	0.18	0.09	0.04	0.43
	H11	302	0.07	0.07	-0.11	0.25	62	0.01	0.11	-0.29	0.25
	H12	302	0.05	0.08	-0.18	0.22	62	-0.02	0.13	-0.34	0.28
	H13	302	0.04	0.10	-0.29	0.26	62	-0.12	0.17	-0.64	0.18
	H14	302	-0.01	0.11	-0.40	0.19	62	-0.22	0.18	-0.67	0.11
	H15	302	-0.05	0.12	-0.43	0.18	62	-0.24	0.20	-0.82	0.09
	H16	302	-0.05	0.11	-0.39	0.21	62	-0.24	0.20	-0.71	0.09
	H17	302	-0.04	0.10	-0.33	0.19	62	-0.21	0.18	-0.71	0.08
	H18	302	-0.03	0.09	-0.31	0.18	62	-0.18	0.16	-0.63	0.07
	H19	302	0.00	0.08	-0.28	0.19	62	-0.06	0.11	-0.34	0.16
	H20	302	0.08	0.07	-0.14	0.30	62	0.08	0.09	-0.08	0.32
	H21	302	0.16	0.06	0.03	0.35	62	0.12	0.08	0.01	0.34
	H22	302	0.20	0.06	0.07	0.38	62	0.17	0.07	0.05	0.37
	H23	302	0.23	0.06	0.09	0.47	62	0.23	0.07	0.09	0.44
	H24	302	0.28	0.08	0.10	0.69	62	0.31	0.09	0.14	0.63

Table H.7 Hourly elasticities w.r.t. the solar radiation variable in the NO_2 models

Variable	Hour	Weekdays					Sunday				
		N	Mean	Std.	Min	Max	N	Mean	Std.	Min	Max
Background Solar Radiation Elasticities	H01	302	0.00	0.00	0.00	0.00	63	0.00	0.00	-0.01	0.00
	H02	302	0.00	0.00	0.00	0.00	63	0.00	0.00	0.00	0.00
	H03	302	0.00	0.00	0.00	0.00	63	0.00	0.00	0.00	0.00
	H04	302	0.00	0.00	0.00	0.00	63	0.00	0.00	0.00	0.00
	H05	302	0.00	0.00	0.00	0.00	63	0.00	0.00	0.00	0.00
	H06	302	0.00	0.00	0.00	0.02	63	0.00	0.01	-0.03	0.00
	H07	302	0.00	0.00	-0.01	0.01	63	0.00	0.01	-0.04	0.00
	H08	302	-0.01	0.01	-0.06	0.00	63	-0.01	0.01	-0.07	0.00
	H09	302	-0.02	0.03	-0.16	0.00	63	-0.03	0.04	-0.21	0.00
	H10	302	-0.05	0.06	-0.41	0.00	63	-0.08	0.08	-0.53	0.00
	H11	302	-0.11	0.12	-0.79	0.00	63	-0.17	0.16	-0.92	-0.02
	H12	302	-0.19	0.21	-1.23	0.00	63	-0.28	0.27	-1.47	-0.03
	H13	302	-0.30	0.32	-1.72	0.00	63	-0.44	0.42	-2.21	-0.04
	H14	302	-0.41	0.42	-2.21	0.00	63	-0.59	0.54	-2.81	-0.04
	H15	302	-0.46	0.45	-2.30	0.00	63	-0.69	0.62	-2.92	-0.04
	H16	302	-0.44	0.43	-2.16	0.00	63	-0.66	0.60	-2.71	-0.04
	H17	302	-0.35	0.34	-1.89	0.00	63	-0.55	0.50	-2.21	-0.04
	H18	302	-0.24	0.24	-1.45	0.00	63	-0.39	0.34	-1.59	-0.04
	H19	302	-0.15	0.14	-0.85	0.00	63	-0.23	0.20	-1.00	-0.02
	H20	302	-0.08	0.07	-0.42	0.00	63	-0.13	0.12	-0.60	-0.01
	H21	302	-0.03	0.04	-0.24	0.00	63	-0.07	0.07	-0.42	0.00
	H22	302	-0.01	0.02	-0.11	0.00	63	-0.03	0.04	-0.24	0.00
	H23	302	0.00	0.01	-0.04	0.00	63	-0.01	0.02	-0.11	0.00
	H24	302	0.00	0.00	-0.01	0.00	63	0.00	0.01	-0.03	0.00
Roadside Solar Radiation Elasticities	H01	301	0.00	0.00	0.00	0.01	62	0.00	0.00	0.00	0.00
	H02	301	0.00	0.00	0.00	0.00	62	0.00	0.00	0.00	0.00
	H03	301	0.00	0.00	0.00	0.00	62	0.00	0.00	0.00	0.00
	H04	301	0.00	0.00	0.00	0.00	62	0.00	0.00	0.00	0.00
	H05	301	0.00	0.00	0.00	0.00	62	0.00	0.00	0.00	0.00
	H06	301	0.00	0.01	0.00	0.05	62	0.00	0.01	0.00	0.04
	H07	301	0.00	0.01	0.00	0.05	62	0.00	0.01	0.00	0.03
	H08	301	0.01	0.01	0.00	0.07	62	0.01	0.01	0.00	0.03
	H09	301	0.01	0.02	-0.02	0.11	62	0.01	0.01	-0.01	0.04
	H10	302	0.01	0.03	-0.05	0.20	62	0.00	0.02	-0.05	0.06
	H11	302	0.01	0.05	-0.14	0.22	62	-0.01	0.04	-0.15	0.07
	H12	302	0.01	0.06	-0.23	0.24	62	-0.03	0.06	-0.22	0.09
	H13	302	0.01	0.09	-0.39	0.34	62	-0.05	0.08	-0.31	0.08
	H14	302	0.00	0.10	-0.46	0.30	62	-0.07	0.10	-0.38	0.08
	H15	302	-0.01	0.11	-0.46	0.29	62	-0.08	0.11	-0.38	0.08
	H16	302	-0.01	0.10	-0.40	0.25	62	-0.08	0.10	-0.37	0.09
	H17	302	0.00	0.09	-0.31	0.23	62	-0.07	0.08	-0.26	0.06
	H18	302	0.01	0.07	-0.21	0.20	62	-0.05	0.06	-0.19	0.05
	H19	302	0.02	0.06	-0.15	0.21	62	-0.02	0.04	-0.11	0.06
	H20	302	0.02	0.04	-0.08	0.19	62	0.00	0.03	-0.06	0.08
	H21	302	0.02	0.03	-0.04	0.15	62	0.00	0.02	-0.03	0.06
	H22	302	0.02	0.02	-0.01	0.12	62	0.00	0.01	-0.01	0.04
	H23	302	0.01	0.01	0.00	0.08	62	0.00	0.01	0.00	0.03
	H24	302	0.00	0.01	0.00	0.05	62	0.00	0.00	0.00	0.01

Table H.8 Hourly elasticities w.r.t. the wind speed variable in the NO_2 models

Variable	Hour	Weekdays					Sunday				
		N	Mean	Std.	Min	Max	N	Mean	Std.	Min	Max
Background Wind Speed Elasticities	H01	302	0.006	0.007	0.000	0.061	63	0.007	0.008	0.000	0.044
	H02	302	0.007	0.009	0.000	0.074	63	0.008	0.009	0.000	0.043
	H03	302	0.008	0.011	0.000	0.076	63	0.009	0.012	0.000	0.050
	H04	302	0.009	0.011	0.000	0.080	63	0.009	0.012	0.000	0.056
	H05	302	0.008	0.010	0.000	0.080	63	0.009	0.010	0.000	0.050
	H06	302	0.008	0.009	0.000	0.073	63	0.008	0.010	0.000	0.045
	H07	302	0.007	0.007	0.000	0.041	63	0.008	0.009	0.000	0.042
	H08	302	0.006	0.005	0.000	0.034	63	0.008	0.008	0.000	0.040
	H09	302	0.007	0.005	0.000	0.039	63	0.008	0.008	0.001	0.043
	H10	302	0.008	0.007	0.000	0.049	63	0.009	0.008	0.001	0.041
	H11	302	0.009	0.008	0.001	0.047	63	0.010	0.010	0.001	0.046
	H12	302	0.010	0.009	0.000	0.050	63	0.012	0.009	0.001	0.040
	H13	302	0.012	0.010	0.000	0.070	63	0.013	0.010	0.001	0.051
	H14	302	0.012	0.010	0.000	0.058	63	0.013	0.009	0.000	0.041
	H15	302	0.013	0.009	0.000	0.063	63	0.015	0.009	0.000	0.037
	H16	302	0.012	0.009	0.001	0.056	63	0.014	0.008	0.000	0.033
	H17	302	0.011	0.008	0.001	0.053	63	0.013	0.008	0.000	0.030
	H18	302	0.010	0.006	0.000	0.049	63	0.011	0.007	0.002	0.028
	H19	302	0.008	0.006	0.000	0.040	63	0.009	0.006	0.000	0.024
	H20	302	0.007	0.006	0.000	0.043	63	0.008	0.005	0.000	0.024
	H21	302	0.007	0.006	0.000	0.035	63	0.007	0.006	0.000	0.024
	H22	302	0.007	0.006	0.000	0.036	63	0.006	0.005	0.000	0.026
	H23	302	0.006	0.007	0.000	0.049	63	0.006	0.006	0.000	0.029
	H24	302	0.006	0.007	0.000	0.051	63	0.006	0.005	0.000	0.021
Roadside Wind Speed Elasticities	H01	N/A	N/A	N/A	N/A	N/A	N/A	N/A	N/A	N/A	N/A
	H02	N/A	N/A	N/A	N/A	N/A	N/A	N/A	N/A	N/A	N/A
	H03	N/A	N/A	N/A	N/A	N/A	N/A	N/A	N/A	N/A	N/A
	H04	N/A	N/A	N/A	N/A	N/A	N/A	N/A	N/A	N/A	N/A
	H05	N/A	N/A	N/A	N/A	N/A	N/A	N/A	N/A	N/A	N/A
	H06	N/A	N/A	N/A	N/A	N/A	N/A	N/A	N/A	N/A	N/A
	H07	N/A	N/A	N/A	N/A	N/A	N/A	N/A	N/A	N/A	N/A
	H08	N/A	N/A	N/A	N/A	N/A	N/A	N/A	N/A	N/A	N/A
	H09	N/A	N/A	N/A	N/A	N/A	N/A	N/A	N/A	N/A	N/A
	H10	N/A	N/A	N/A	N/A	N/A	N/A	N/A	N/A	N/A	N/A
	H11	N/A	N/A	N/A	N/A	N/A	N/A	N/A	N/A	N/A	N/A
	H12	N/A	N/A	N/A	N/A	N/A	N/A	N/A	N/A	N/A	N/A
	H13	N/A	N/A	N/A	N/A	N/A	N/A	N/A	N/A	N/A	N/A
	H14	N/A	N/A	N/A	N/A	N/A	N/A	N/A	N/A	N/A	N/A
	H15	N/A	N/A	N/A	N/A	N/A	N/A	N/A	N/A	N/A	N/A
	H16	N/A	N/A	N/A	N/A	N/A	N/A	N/A	N/A	N/A	N/A
	H17	N/A	N/A	N/A	N/A	N/A	N/A	N/A	N/A	N/A	N/A
	H18	N/A	N/A	N/A	N/A	N/A	N/A	N/A	N/A	N/A	N/A
	H19	N/A	N/A	N/A	N/A	N/A	N/A	N/A	N/A	N/A	N/A
	H20	N/A	N/A	N/A	N/A	N/A	N/A	N/A	N/A	N/A	N/A
	H21	N/A	N/A	N/A	N/A	N/A	N/A	N/A	N/A	N/A	N/A
	H22	N/A	N/A	N/A	N/A	N/A	N/A	N/A	N/A	N/A	N/A
	H23	N/A	N/A	N/A	N/A	N/A	N/A	N/A	N/A	N/A	N/A
	H24	N/A	N/A	N/A	N/A	N/A	N/A	N/A	N/A	N/A	N/A

Table H.9 Hourly elasticities w.r.t. the temperature variable in the NO_2 models

Variable	Hour	Weekdays					Sunday				
		N	Mean	Std.	Min	Max	N	Mean	Std.	Min	Max
Background Temperature Elasticities	H01	302	0.04	0.05	-0.12	0.24	63	0.05	0.05	-0.13	0.19
	H02	302	0.05	0.06	-0.15	0.29	63	0.06	0.07	-0.14	0.24
	H03	302	0.06	0.07	-0.16	0.34	63	0.07	0.08	-0.14	0.28
	H04	302	0.06	0.08	-0.17	0.36	63	0.07	0.08	-0.14	0.30
	H05	302	0.06	0.08	-0.16	0.37	63	0.07	0.08	-0.13	0.32
	H06	302	0.05	0.06	-0.13	0.33	63	0.06	0.07	-0.13	0.29
	H07	302	0.04	0.05	-0.10	0.25	63	0.06	0.06	-0.11	0.27
	H08	302	0.04	0.05	-0.08	0.21	63	0.05	0.06	-0.11	0.26
	H09	302	0.04	0.04	-0.08	0.20	63	0.06	0.06	-0.10	0.26
	H10	302	0.05	0.05	-0.08	0.20	63	0.08	0.08	-0.13	0.29
	H11	302	0.05	0.05	-0.09	0.20	63	0.10	0.10	-0.15	0.37
	H12	302	0.06	0.05	-0.08	0.20	63	0.12	0.12	-0.17	0.57
	H13	302	0.07	0.06	-0.08	0.22	63	0.14	0.15	-0.17	0.74
	H14	302	0.07	0.06	-0.08	0.23	63	0.16	0.16	-0.16	0.79
	H15	302	0.07	0.05	-0.07	0.23	63	0.17	0.17	-0.15	0.83
	H16	302	0.07	0.05	-0.06	0.22	63	0.17	0.17	-0.13	0.83
	H17	302	0.06	0.05	-0.06	0.22	63	0.15	0.15	-0.11	0.76
	H18	302	0.05	0.04	-0.05	0.19	63	0.12	0.12	-0.09	0.58
	H19	302	0.05	0.04	-0.05	0.17	63	0.09	0.09	-0.08	0.45
	H20	302	0.04	0.04	-0.06	0.17	63	0.07	0.07	-0.09	0.36
	H21	302	0.04	0.04	-0.07	0.17	63	0.06	0.06	-0.09	0.32
	H22	302	0.04	0.04	-0.08	0.19	63	0.05	0.06	-0.07	0.25
	H23	302	0.04	0.04	-0.09	0.20	63	0.05	0.05	-0.06	0.21
	H24	302	0.04	0.04	-0.10	0.21	63	0.05	0.05	-0.06	0.20
Roadside Temperature Elasticities	H01	301	0.00	0.00	0.00	0.00	62	-0.06	0.06	-0.24	0.08
	H02	301	0.00	0.00	0.00	0.00	62	-0.07	0.07	-0.31	0.11
	H03	301	0.00	0.00	0.00	0.00	62	-0.08	0.09	-0.39	0.12
	H04	301	0.00	0.00	0.00	0.00	62	-0.09	0.10	-0.41	0.14
	H05	301	0.00	0.00	0.00	0.00	62	-0.09	0.10	-0.40	0.11
	H06	301	0.00	0.00	0.00	0.00	62	-0.07	0.07	-0.28	0.08
	H07	301	0.00	0.00	0.00	0.00	62	-0.06	0.06	-0.21	0.06
	H08	301	0.00	0.00	0.00	0.00	62	-0.05	0.06	-0.20	0.07
	H09	301	0.00	0.00	0.00	0.00	62	-0.05	0.06	-0.21	0.05
	H10	302	0.00	0.00	0.00	0.00	62	-0.05	0.06	-0.21	0.05
	H11	302	0.00	0.00	0.00	0.00	62	-0.05	0.05	-0.21	0.04
	H12	302	0.00	0.00	0.00	0.00	62	-0.05	0.05	-0.21	0.03
	H13	302	0.00	0.00	0.00	0.00	62	-0.05	0.05	-0.20	0.03
	H14	302	0.00	0.00	0.00	0.00	62	-0.05	0.05	-0.19	0.02
	H15	302	0.00	0.00	0.00	0.00	62	-0.05	0.05	-0.22	0.02
	H16	302	0.00	0.00	0.00	0.00	62	-0.05	0.05	-0.21	0.02
	H17	302	0.00	0.00	0.00	0.00	62	-0.05	0.05	-0.19	0.02
	H18	302	0.00	0.00	0.00	0.00	62	-0.05	0.05	-0.20	0.02
	H19	302	0.00	0.00	0.00	0.00	62	-0.05	0.05	-0.18	0.02
	H20	302	0.00	0.00	0.00	0.00	62	-0.05	0.05	-0.20	0.03
	H21	302	0.00	0.00	0.00	0.00	62	-0.05	0.05	-0.18	0.04
	H22	302	0.00	0.00	0.00	0.00	62	-0.05	0.05	-0.18	0.04
	H23	302	0.00	0.00	0.00	0.00	62	-0.05	0.05	-0.18	0.03
	H24	302	0.00	0.00	0.00	0.00	62	-0.05	0.05	-0.22	0.04

Table H.10 Hourly elasticities w.r.t. the humidity variable in the NO_2 models

Variable	Hour	Weekdays					Sunday				
		N	Mean	Std.	Min	Max	N	Mean	Std.	Min	Max
Background Humidity Elasticities	H01	302	-0.04	0.02	-0.15	-0.01	63	0.32	0.39	-0.73	1.64
	H02	302	-0.04	0.02	-0.17	-0.01	63	0.39	0.48	-0.78	2.04
	H03	302	-0.03	0.02	-0.18	-0.01	63	0.48	0.59	-0.76	2.31
	H04	302	-0.03	0.02	-0.16	-0.01	63	0.53	0.65	-0.77	2.60
	H05	302	-0.03	0.02	-0.13	-0.01	63	0.55	0.65	-0.72	2.72
	H06	302	-0.03	0.02	-0.11	-0.01	63	0.48	0.58	-0.72	2.36
	H07	302	-0.06	0.02	-0.15	-0.02	63	0.40	0.48	-0.59	2.07
	H08	302	-0.07	0.03	-0.19	-0.01	63	0.36	0.44	-0.63	1.98
	H09	302	-0.06	0.03	-0.21	0.00	63	0.34	0.42	-0.53	1.99
	H10	302	-0.03	0.04	-0.20	0.09	63	0.34	0.42	-0.57	1.82
	H11	302	0.00	0.05	-0.17	0.20	63	0.34	0.41	-0.54	1.60
	H12	302	0.02	0.07	-0.16	0.28	63	0.35	0.41	-0.52	1.46
	H13	302	0.05	0.08	-0.14	0.41	63	0.35	0.41	-0.50	1.46
	H14	302	0.07	0.10	-0.14	0.45	63	0.34	0.39	-0.42	1.46
	H15	302	0.08	0.10	-0.13	0.44	63	0.35	0.40	-0.38	1.54
	H16	302	0.08	0.09	-0.13	0.41	63	0.35	0.39	-0.37	1.44
	H17	302	0.07	0.08	-0.13	0.37	63	0.33	0.36	-0.35	1.34
	H18	302	0.04	0.07	-0.13	0.30	63	0.31	0.35	-0.33	1.26
	H19	302	0.02	0.06	-0.14	0.22	63	0.30	0.34	-0.35	1.16
	H20	302	0.00	0.04	-0.15	0.12	63	0.29	0.33	-0.41	1.21
	H21	302	-0.02	0.03	-0.15	0.07	63	0.28	0.34	-0.45	1.28
	H22	302	-0.04	0.03	-0.14	0.03	63	0.29	0.33	-0.40	1.18
	H23	302	-0.04	0.02	-0.14	-0.01	63	0.29	0.33	-0.38	1.12
	H24	302	-0.05	0.02	-0.15	-0.01	63	0.31	0.35	-0.34	1.15
Roadside Humidity Elasticities	H01	301	-0.08	0.03	-0.26	-0.02	62	0.05	0.04	0.00	0.22
	H02	301	-0.07	0.03	-0.21	-0.02	62	0.03	0.05	-0.07	0.25
	H03	301	-0.06	0.03	-0.22	-0.01	62	0.01	0.06	-0.16	0.25
	H04	301	-0.05	0.03	-0.19	-0.01	62	-0.01	0.07	-0.22	0.26
	H05	301	-0.05	0.02	-0.17	-0.01	62	-0.02	0.07	-0.24	0.19
	H06	301	-0.05	0.02	-0.13	-0.02	62	-0.01	0.05	-0.11	0.15
	H07	301	-0.09	0.03	-0.17	-0.03	62	0.02	0.03	-0.05	0.13
	H08	301	-0.11	0.04	-0.26	-0.03	62	0.04	0.03	-0.02	0.16
	H09	301	-0.09	0.05	-0.30	-0.02	62	0.06	0.03	0.02	0.14
	H10	302	-0.05	0.05	-0.27	0.08	62	0.08	0.03	0.03	0.17
	H11	302	-0.02	0.06	-0.24	0.14	62	0.10	0.04	0.04	0.23
	H12	302	0.00	0.07	-0.22	0.21	62	0.11	0.04	0.04	0.21
	H13	302	0.03	0.08	-0.21	0.28	62	0.12	0.04	0.04	0.24
	H14	302	0.05	0.08	-0.20	0.31	62	0.12	0.04	0.06	0.24
	H15	302	0.06	0.08	-0.21	0.29	62	0.13	0.04	0.05	0.26
	H16	302	0.05	0.08	-0.20	0.31	62	0.13	0.04	0.04	0.25
	H17	302	0.05	0.08	-0.21	0.32	62	0.12	0.04	0.05	0.23
	H18	302	0.03	0.08	-0.21	0.25	62	0.12	0.03	0.05	0.21
	H19	302	0.00	0.07	-0.20	0.17	62	0.12	0.03	0.05	0.20
	H20	302	-0.02	0.06	-0.22	0.11	62	0.10	0.03	0.04	0.17
	H21	302	-0.04	0.05	-0.20	0.06	62	0.09	0.03	0.03	0.16
	H22	302	-0.06	0.04	-0.20	0.01	62	0.08	0.03	0.03	0.16
	H23	302	-0.07	0.03	-0.18	-0.01	62	0.07	0.03	0.02	0.14
	H24	302	-0.08	0.03	-0.17	-0.02	62	0.05	0.03	0.00	0.12

Table H.11 Hourly elasticities w.r.t. the traffic variable in the CO models

Variable	Hour	Weekdays					Sunday				
		N	Mean	Std.	Min	Max	N	Mean	Std.	Min	Max
Background Traffic Elasticities	H01	302	0.13	0.07	0.03	0.50	63	0.07	0.05	0.01	0.22
	H02	302	0.07	0.05	0.01	0.35	63	0.05	0.04	0.01	0.17
	H03	302	0.04	0.03	-0.01	0.24	63	0.04	0.03	0.00	0.14
	H04	302	0.02	0.03	-0.02	0.16	63	0.03	0.02	0.00	0.11
	H05	302	0.02	0.02	-0.02	0.12	63	0.02	0.02	0.00	0.09
	H06	302	0.04	0.03	-0.01	0.15	63	0.03	0.02	-0.01	0.10
	H07	302	0.19	0.09	0.05	0.52	63	0.04	0.04	0.00	0.15
	H08	302	0.43	0.18	0.11	1.12	63	0.05	0.05	-0.04	0.20
	H09	302	0.45	0.19	0.12	1.16	63	0.05	0.08	-0.15	0.26
	H10	302	0.36	0.17	0.09	1.06	63	0.01	0.12	-0.37	0.28
	H11	302	0.31	0.20	-0.17	1.05	63	-0.05	0.20	-0.72	0.32
	H12	302	0.22	0.25	-0.55	1.15	63	-0.15	0.27	-0.99	0.29
	H13	302	0.08	0.32	-0.95	0.97	63	-0.26	0.37	-1.42	0.31
	H14	302	0.02	0.39	-1.37	1.13	63	-0.37	0.44	-1.67	0.31
	H15	302	-0.02	0.43	-1.44	1.27	63	-0.43	0.47	-1.81	0.31
	H16	302	-0.01	0.43	-1.42	1.13	63	-0.42	0.48	-1.83	0.31
	H17	302	0.06	0.38	-1.28	0.97	63	-0.36	0.44	-1.81	0.30
	H18	302	0.17	0.31	-0.95	0.98	63	-0.24	0.35	-1.35	0.32
	H19	302	0.26	0.24	-0.41	1.09	63	-0.12	0.25	-0.93	0.33
	H20	302	0.28	0.19	-0.13	1.10	63	-0.03	0.16	-0.55	0.26
	H21	302	0.27	0.15	-0.01	0.92	63	0.03	0.12	-0.35	0.27
	H22	302	0.29	0.14	0.07	0.86	63	0.06	0.09	-0.18	0.27
	H23	302	0.27	0.13	0.08	0.74	63	0.07	0.07	-0.04	0.25
	H24	302	0.21	0.10	0.06	0.58	63	0.06	0.05	0.00	0.20
Roadside Traffic Elasticities	H01	301	0.20	0.09	0.04	0.59	62	0.10	0.06	0.02	0.31
	H02	301	0.12	0.07	0.02	0.47	62	0.09	0.05	0.02	0.32
	H03	301	0.07	0.05	0.01	0.32	62	0.08	0.04	0.03	0.25
	H04	301	0.05	0.04	0.00	0.23	62	0.07	0.03	0.02	0.20
	H05	301	0.04	0.04	0.00	0.19	62	0.07	0.03	0.02	0.18
	H06	301	0.09	0.05	0.01	0.27	62	0.08	0.03	0.03	0.19
	H07	301	0.32	0.10	0.11	0.66	62	0.10	0.05	0.03	0.34
	H08	301	0.64	0.18	0.21	1.36	62	0.11	0.06	0.03	0.37
	H09	301	0.69	0.21	0.26	1.62	62	0.15	0.08	0.02	0.44
	H10	302	0.61	0.19	0.21	1.28	62	0.19	0.10	0.01	0.49
	H11	302	0.65	0.21	0.19	1.42	62	0.26	0.14	0.00	0.66
	H12	302	0.73	0.25	0.18	1.66	62	0.33	0.19	0.00	0.95
	H13	302	0.83	0.30	0.21	2.28	62	0.42	0.23	0.01	1.05
	H14	302	1.02	0.40	0.24	3.22	62	0.48	0.27	0.02	1.03
	H15	302	1.06	0.40	0.27	2.50	62	0.52	0.31	0.02	1.40
	H16	302	1.04	0.38	0.28	2.62	62	0.50	0.29	0.02	1.20
	H17	302	0.98	0.34	0.26	2.10	62	0.46	0.26	0.02	1.05
	H18	302	0.93	0.31	0.24	1.91	62	0.37	0.21	0.01	0.92
	H19	302	0.84	0.24	0.24	1.79	62	0.29	0.17	0.00	0.77
	H20	302	0.71	0.20	0.19	1.52	62	0.22	0.13	0.01	0.58
	H21	302	0.57	0.16	0.15	1.20	62	0.17	0.11	0.00	0.45
	H22	302	0.50	0.15	0.13	1.09	62	0.14	0.09	0.00	0.38
	H23	302	0.42	0.13	0.10	0.87	62	0.11	0.08	0.01	0.32
	H24	302	0.32	0.11	0.08	0.84	62	0.10	0.06	0.02	0.26

Table H.12 Hourly elasticities w.r.t. the solar radiation variable in the CO models

Variable	Hour	Weekdays					Sunday				
		N	Mean	Std.	Min	Max	N	Mean	Std.	Min	Max
Background Solar Radiation Elasticities	H01	302	0.00	0.00	-0.01	0.00	63	0.00	0.00	-0.01	0.00
	H02	302	0.00	0.00	0.00	0.00	63	0.00	0.00	0.00	0.00
	H03	302	0.00	0.00	0.00	0.00	63	0.00	0.00	0.00	0.00
	H04	302	0.00	0.00	0.00	0.00	63	0.00	0.00	0.00	0.00
	H05	302	0.00	0.00	0.00	0.00	63	0.00	0.00	0.00	0.00
	H06	302	0.00	0.01	-0.03	0.00	63	0.00	0.01	-0.02	0.00
	H07	302	-0.01	0.01	-0.05	0.00	63	-0.01	0.01	-0.04	0.00
	H08	302	-0.03	0.03	-0.17	0.00	63	-0.02	0.02	-0.08	0.00
	H09	302	-0.07	0.07	-0.40	0.00	63	-0.05	0.05	-0.20	0.00
	H10	302	-0.13	0.11	-0.54	0.00	63	-0.11	0.08	-0.33	0.00
	H11	302	-0.21	0.15	-0.84	0.00	63	-0.20	0.13	-0.64	-0.03
	H12	302	-0.28	0.19	-1.12	0.00	63	-0.23	0.18	-0.86	0.06
	H13	302	-0.29	0.25	-1.26	0.42	63	-0.26	0.28	-1.16	0.59
	H14	302	-0.30	0.33	-1.57	0.90	63	-0.27	0.38	-1.35	0.96
	H15	302	-0.30	0.37	-1.72	1.04	63	-0.25	0.46	-1.48	1.30
	H16	302	-0.31	0.36	-1.63	0.98	63	-0.25	0.48	-1.36	1.41
	H17	302	-0.33	0.30	-1.48	0.69	63	-0.27	0.41	-1.19	1.14
	H18	302	-0.33	0.22	-1.15	0.21	63	-0.26	0.27	-0.89	0.72
	H19	302	-0.28	0.16	-0.79	0.00	63	-0.21	0.15	-0.63	0.25
	H20	302	-0.19	0.11	-0.51	0.00	63	-0.15	0.09	-0.40	0.01
	H21	302	-0.11	0.07	-0.32	0.00	63	-0.10	0.06	-0.25	0.00
	H22	302	-0.06	0.05	-0.24	0.00	63	-0.05	0.05	-0.20	0.00
	H23	302	-0.02	0.03	-0.15	0.00	63	-0.02	0.02	-0.12	0.00
	H24	302	-0.01	0.01	-0.05	0.00	63	-0.01	0.01	-0.04	0.00
Roadside Solar Radiation Elasticities	H01	301	0.00	0.00	-0.01	0.00	62	0.00	0.00	-0.01	0.00
	H02	301	0.00	0.00	0.00	0.00	62	0.00	0.00	0.00	0.00
	H03	301	0.00	0.00	0.00	0.00	62	0.00	0.00	0.00	0.00
	H04	301	0.00	0.00	0.00	0.00	62	0.00	0.00	0.00	0.00
	H05	301	0.00	0.00	0.00	0.00	62	0.00	0.00	0.00	0.00
	H06	301	0.00	0.01	-0.03	0.00	62	0.00	0.01	-0.03	0.00
	H07	301	0.00	0.00	-0.03	0.00	62	0.00	0.01	-0.04	0.00
	H08	301	0.00	0.00	-0.02	0.01	62	-0.01	0.02	-0.09	0.00
	H09	301	0.00	0.01	-0.04	0.02	62	-0.03	0.03	-0.18	0.00
	H10	302	-0.02	0.02	-0.11	0.01	62	-0.06	0.05	-0.23	0.00
	H11	302	-0.05	0.04	-0.29	0.01	62	-0.08	0.07	-0.28	0.00
	H12	302	-0.09	0.08	-0.33	0.02	62	-0.12	0.10	-0.45	0.00
	H13	302	-0.16	0.14	-0.71	0.02	62	-0.15	0.14	-0.56	0.00
	H14	302	-0.20	0.18	-0.91	0.04	62	-0.15	0.17	-0.68	0.04
	H15	302	-0.21	0.20	-1.16	0.06	62	-0.16	0.19	-0.72	0.06
	H16	302	-0.20	0.19	-0.87	0.05	62	-0.15	0.19	-0.80	0.15
	H17	302	-0.16	0.15	-0.74	0.05	62	-0.14	0.17	-0.63	0.06
	H18	302	-0.11	0.11	-0.55	0.03	62	-0.09	0.11	-0.45	0.02
	H19	302	-0.06	0.07	-0.37	0.02	62	-0.08	0.08	-0.28	0.01
	H20	302	-0.05	0.05	-0.24	0.02	62	-0.07	0.06	-0.25	0.00
	H21	302	-0.03	0.03	-0.18	0.01	62	-0.04	0.04	-0.21	0.00
	H22	302	-0.01	0.02	-0.10	0.00	62	-0.02	0.02	-0.16	0.00
	H23	302	-0.01	0.01	-0.06	0.00	62	-0.01	0.01	-0.08	0.00
	H24	302	0.00	0.00	-0.02	0.00	62	0.00	0.01	-0.03	0.00

Table H.13 Hourly elasticities w.r.t. the wind speed variable in the CO models

Variable	Hour	Weekdays					Sunday				
		N	Mean	Std.	Min	Max	N	Mean	Std.	Min	Max
Background Wind Speed Elasticities	H01	302	0.005	0.011	-0.039	0.082	63	0.013	0.017	0.000	0.087
	H02	302	0.006	0.011	-0.042	0.078	63	0.015	0.017	0.000	0.083
	H03	302	0.007	0.012	-0.038	0.069	63	0.017	0.021	0.000	0.106
	H04	302	0.008	0.012	-0.034	0.075	63	0.016	0.019	0.000	0.103
	H05	302	0.008	0.012	-0.027	0.065	63	0.015	0.015	0.000	0.073
	H06	302	0.008	0.013	-0.020	0.079	63	0.016	0.017	0.000	0.096
	H07	302	0.008	0.011	-0.021	0.056	63	0.017	0.019	-0.003	0.101
	H08	302	0.006	0.010	-0.020	0.059	63	0.016	0.019	-0.023	0.096
	H09	302	0.005	0.010	-0.030	0.053	63	0.014	0.019	-0.026	0.096
	H10	302	0.004	0.010	-0.027	0.055	63	0.014	0.016	-0.009	0.080
	H11	302	0.005	0.011	-0.020	0.055	63	0.015	0.016	0.000	0.087
	H12	302	0.008	0.012	-0.036	0.074	63	0.020	0.017	0.000	0.075
	H13	302	0.013	0.014	-0.027	0.115	63	0.025	0.018	0.001	0.087
	H14	302	0.018	0.018	-0.022	0.113	63	0.030	0.022	0.000	0.111
	H15	302	0.023	0.021	-0.012	0.132	63	0.036	0.025	0.000	0.110
	H16	302	0.023	0.021	-0.012	0.128	63	0.035	0.022	0.001	0.088
	H17	302	0.021	0.020	-0.012	0.108	63	0.033	0.022	0.000	0.100
	H18	302	0.018	0.017	-0.010	0.110	63	0.029	0.018	0.004	0.095
	H19	302	0.013	0.014	-0.012	0.099	63	0.024	0.016	0.001	0.082
	H20	302	0.009	0.013	-0.029	0.111	63	0.021	0.016	0.000	0.074
	H21	302	0.007	0.011	-0.025	0.063	63	0.017	0.016	0.000	0.068
	H22	302	0.005	0.013	-0.042	0.100	63	0.014	0.015	0.000	0.061
	H23	302	0.005	0.012	-0.044	0.103	63	0.013	0.015	-0.002	0.057
	H24	302	0.005	0.011	-0.039	0.073	63	0.012	0.015	-0.010	0.060
Roadside Wind Speed Elasticities	H01	301	-0.012	0.011	-0.077	0.000	62	-0.013	0.011	-0.053	0.000
	H02	301	-0.013	0.012	-0.072	0.000	62	-0.014	0.012	-0.049	0.000
	H03	301	-0.013	0.013	-0.070	0.000	62	-0.015	0.015	-0.075	0.000
	H04	301	-0.014	0.013	-0.087	0.000	62	-0.014	0.014	-0.067	0.000
	H05	301	-0.015	0.013	-0.065	0.000	62	-0.015	0.013	-0.055	0.000
	H06	301	-0.015	0.014	-0.068	0.000	62	-0.014	0.013	-0.066	0.000
	H07	301	-0.014	0.012	-0.078	0.000	62	-0.015	0.015	-0.089	0.000
	H08	301	-0.012	0.009	-0.057	0.000	62	-0.016	0.014	-0.073	0.000
	H09	301	-0.012	0.009	-0.055	0.000	62	-0.016	0.014	-0.074	-0.002
	H10	302	-0.012	0.009	-0.055	0.000	62	-0.017	0.011	-0.065	-0.002
	H11	302	-0.013	0.009	-0.049	-0.002	62	-0.019	0.012	-0.064	-0.002
	H12	302	-0.015	0.011	-0.056	-0.001	62	-0.021	0.014	-0.070	-0.002
	H13	302	-0.018	0.013	-0.069	0.000	62	-0.022	0.013	-0.049	-0.002
	H14	302	-0.021	0.014	-0.100	0.000	62	-0.022	0.013	-0.058	0.000
	H15	302	-0.021	0.014	-0.084	0.000	62	-0.024	0.015	-0.094	0.000
	H16	302	-0.021	0.014	-0.090	-0.002	62	-0.023	0.013	-0.066	-0.001
	H17	302	-0.019	0.013	-0.097	-0.001	62	-0.022	0.013	-0.054	0.000
	H18	302	-0.018	0.011	-0.066	0.000	62	-0.020	0.011	-0.049	-0.003
	H19	302	-0.016	0.010	-0.053	0.000	62	-0.018	0.011	-0.044	-0.001
	H20	302	-0.015	0.012	-0.069	0.000	62	-0.017	0.011	-0.048	0.000
	H21	302	-0.015	0.011	-0.067	0.000	62	-0.016	0.011	-0.045	-0.001
	H22	302	-0.014	0.011	-0.087	0.000	62	-0.013	0.010	-0.038	0.000
	H23	302	-0.013	0.012	-0.075	0.000	62	-0.012	0.010	-0.042	0.000
	H24	302	-0.013	0.012	-0.063	0.000	62	-0.011	0.009	-0.034	0.000

Table H.14 Hourly elasticities w.r.t. the temperature variable in the CO models

Variable	Hour	Weekdays					Sunday				
		N	Mean	Std.	Min	Max	N	Mean	Std.	Min	Max
Background Temperature Elasticities	H01	302	-0.10	0.13	-0.66	0.00	63	-0.13	0.15	-0.67	0.00
	H02	302	-0.11	0.15	-0.78	0.00	63	-0.14	0.17	-0.79	0.00
	H03	302	-0.12	0.16	-0.90	0.00	63	-0.15	0.19	-0.89	0.00
	H04	302	-0.13	0.17	-0.98	0.00	63	-0.16	0.20	-1.00	0.00
	H05	302	-0.13	0.17	-0.92	0.00	63	-0.16	0.21	-1.07	0.00
	H06	302	-0.12	0.15	-0.89	0.00	63	-0.15	0.18	-0.91	0.00
	H07	302	-0.09	0.12	-0.75	0.01	63	-0.14	0.17	-0.82	0.00
	H08	302	-0.07	0.09	-0.49	0.03	63	-0.14	0.17	-0.84	0.00
	H09	302	-0.05	0.08	-0.45	0.05	63	-0.13	0.16	-0.74	0.01
	H10	302	-0.05	0.09	-0.40	0.08	63	-0.11	0.15	-0.65	0.02
	H11	302	-0.04	0.10	-0.42	0.14	63	-0.08	0.14	-0.58	0.05
	H12	302	-0.02	0.11	-0.46	0.22	63	-0.06	0.15	-0.57	0.16
	H13	302	0.01	0.14	-0.51	0.30	63	-0.02	0.16	-0.47	0.32
	H14	302	0.04	0.16	-0.50	0.43	63	0.02	0.17	-0.40	0.38
	H15	302	0.06	0.17	-0.48	0.49	63	0.03	0.19	-0.40	0.42
	H16	302	0.06	0.16	-0.45	0.53	63	0.03	0.19	-0.41	0.41
	H17	302	0.04	0.15	-0.43	0.47	63	0.02	0.17	-0.36	0.38
	H18	302	0.02	0.12	-0.37	0.35	63	0.00	0.13	-0.33	0.25
	H19	302	-0.01	0.09	-0.30	0.17	63	-0.04	0.11	-0.34	0.14
	H20	302	-0.03	0.08	-0.28	0.08	63	-0.06	0.10	-0.37	0.06
	H21	302	-0.05	0.08	-0.31	0.04	63	-0.07	0.09	-0.38	0.02
	H22	302	-0.07	0.09	-0.41	0.02	63	-0.09	0.10	-0.38	0.01
	H23	302	-0.08	0.10	-0.48	0.01	63	-0.10	0.11	-0.53	0.01
	H24	302	-0.09	0.11	-0.57	0.01	63	-0.11	0.13	-0.58	0.00
Roadside Temperature Elasticities	H01	301	-0.07	0.07	-0.34	0.08	62	-0.07	0.07	-0.26	0.08
	H02	301	-0.07	0.07	-0.34	0.09	62	-0.08	0.08	-0.28	0.10
	H03	301	-0.07	0.08	-0.40	0.10	62	-0.09	0.09	-0.37	0.10
	H04	301	-0.08	0.09	-0.42	0.10	62	-0.09	0.10	-0.41	0.10
	H05	301	-0.09	0.09	-0.44	0.11	62	-0.10	0.11	-0.43	0.11
	H06	301	-0.08	0.09	-0.43	0.09	62	-0.10	0.10	-0.42	0.10
	H07	301	-0.07	0.08	-0.39	0.08	62	-0.09	0.09	-0.36	0.12
	H08	301	-0.06	0.06	-0.29	0.07	62	-0.09	0.09	-0.35	0.12
	H09	301	-0.05	0.05	-0.21	0.05	62	-0.09	0.09	-0.38	0.10
	H10	302	-0.05	0.04	-0.21	0.04	62	-0.08	0.08	-0.36	0.08
	H11	302	-0.05	0.04	-0.19	0.04	62	-0.08	0.08	-0.38	0.06
	H12	302	-0.05	0.04	-0.27	0.04	62	-0.08	0.08	-0.35	0.06
	H13	302	-0.06	0.05	-0.21	0.04	62	-0.08	0.07	-0.26	0.05
	H14	302	-0.06	0.05	-0.26	0.04	62	-0.07	0.06	-0.26	0.04
	H15	302	-0.06	0.05	-0.23	0.03	62	-0.07	0.06	-0.23	0.04
	H16	302	-0.06	0.05	-0.26	0.03	62	-0.08	0.07	-0.31	0.04
	H17	302	-0.06	0.05	-0.25	0.03	62	-0.07	0.06	-0.28	0.04
	H18	302	-0.06	0.05	-0.23	0.05	62	-0.07	0.07	-0.30	0.05
	H19	302	-0.05	0.05	-0.20	0.06	62	-0.08	0.07	-0.28	0.05
	H20	302	-0.06	0.05	-0.21	0.06	62	-0.07	0.07	-0.25	0.07
	H21	302	-0.06	0.06	-0.22	0.06	62	-0.07	0.07	-0.28	0.06
	H22	302	-0.06	0.06	-0.25	0.06	62	-0.07	0.07	-0.24	0.07
	H23	302	-0.06	0.06	-0.23	0.06	62	-0.07	0.07	-0.26	0.07
	H24	302	-0.06	0.06	-0.29	0.06	62	-0.07	0.07	-0.24	0.06

Table H.15 Hourly elasticities w.r.t. the humidity variable in the CO models

Variable	Hour	Weekdays					Sunday				
		N	Mean	Std.	Min	Max	N	Mean	Std.	Min	Max
Background Humidity Elasticities	H01	302	-0.03	0.05	-0.19	0.12	63	-0.02	0.05	-0.18	0.12
	H02	302	-0.04	0.06	-0.25	0.13	63	-0.02	0.05	-0.18	0.08
	H03	302	-0.04	0.06	-0.36	0.13	63	-0.03	0.06	-0.19	0.14
	H04	302	-0.05	0.07	-0.35	0.12	63	-0.04	0.07	-0.24	0.13
	H05	302	-0.05	0.07	-0.30	0.10	63	-0.05	0.08	-0.28	0.09
	H06	302	-0.05	0.06	-0.30	0.11	63	-0.05	0.07	-0.23	0.11
	H07	302	-0.04	0.06	-0.24	0.10	63	-0.04	0.07	-0.18	0.13
	H08	302	-0.03	0.05	-0.18	0.09	63	-0.03	0.06	-0.18	0.16
	H09	302	-0.01	0.04	-0.15	0.09	63	-0.01	0.06	-0.15	0.13
	H10	302	0.00	0.04	-0.16	0.12	63	0.00	0.06	-0.22	0.11
	H11	302	0.01	0.04	-0.13	0.15	63	0.01	0.07	-0.22	0.12
	H12	302	0.02	0.05	-0.16	0.15	63	0.02	0.06	-0.22	0.12
	H13	302	0.02	0.05	-0.16	0.16	63	0.03	0.07	-0.16	0.15
	H14	302	0.03	0.05	-0.17	0.15	63	0.03	0.06	-0.14	0.14
	H15	302	0.03	0.05	-0.16	0.15	63	0.03	0.06	-0.13	0.15
	H16	302	0.03	0.05	-0.15	0.15	63	0.03	0.06	-0.14	0.12
	H17	302	0.02	0.05	-0.16	0.16	63	0.03	0.06	-0.15	0.13
	H18	302	0.02	0.05	-0.15	0.12	63	0.02	0.06	-0.11	0.12
	H19	302	0.01	0.04	-0.13	0.11	63	0.01	0.06	-0.13	0.11
	H20	302	0.00	0.04	-0.14	0.14	63	0.00	0.05	-0.11	0.10
	H21	302	-0.01	0.04	-0.17	0.11	63	-0.01	0.05	-0.14	0.09
	H22	302	-0.01	0.04	-0.16	0.11	63	-0.01	0.05	-0.16	0.09
	H23	302	-0.02	0.05	-0.18	0.12	63	-0.02	0.05	-0.15	0.10
	H24	302	-0.02	0.05	-0.20	0.12	63	-0.02	0.05	-0.15	0.09
Roadside Humidity Elasticities	H01	301	-0.06	0.07	-0.34	0.08	62	-0.07	0.07	-0.26	0.08
	H02	301	-0.07	0.07	-0.34	0.09	62	-0.08	0.08	-0.28	0.10
	H03	301	-0.07	0.08	-0.40	0.10	62	-0.09	0.09	-0.37	0.10
	H04	301	-0.08	0.09	-0.42	0.10	62	-0.09	0.10	-0.41	0.10
	H05	301	-0.09	0.09	-0.44	0.11	62	-0.10	0.11	-0.43	0.11
	H06	301	-0.08	0.09	-0.39	0.09	62	-0.09	0.09	-0.38	0.10
	H07	301	-0.07	0.08	-0.35	0.08	62	-0.08	0.08	-0.32	0.12
	H08	301	-0.05	0.06	-0.25	0.07	62	-0.07	0.08	-0.29	0.12
	H09	301	-0.03	0.04	-0.18	0.06	62	-0.06	0.08	-0.31	0.11
	H10	302	-0.01	0.04	-0.17	0.09	62	-0.03	0.07	-0.29	0.11
	H11	302	0.01	0.04	-0.15	0.11	62	0.01	0.08	-0.29	0.17
	H12	302	0.03	0.05	-0.14	0.15	62	0.04	0.09	-0.29	0.26
	H13	302	0.05	0.07	-0.15	0.21	62	0.07	0.10	-0.22	0.31
	H14	302	0.07	0.08	-0.14	0.50	62	0.09	0.10	-0.17	0.25
	H15	302	0.08	0.08	-0.17	0.34	62	0.10	0.10	-0.14	0.28
	H16	302	0.08	0.08	-0.23	0.36	62	0.10	0.11	-0.13	0.29
	H17	302	0.08	0.08	-0.22	0.33	62	0.08	0.10	-0.13	0.24
	H18	302	0.06	0.07	-0.21	0.28	62	0.06	0.09	-0.14	0.21
	H19	302	0.04	0.06	-0.18	0.18	62	0.04	0.08	-0.18	0.18
	H20	302	0.01	0.05	-0.16	0.14	62	0.01	0.07	-0.20	0.16
	H21	302	-0.01	0.05	-0.17	0.09	62	-0.02	0.06	-0.21	0.10
	H22	302	-0.04	0.05	-0.19	0.08	62	-0.05	0.06	-0.21	0.08
	H23	302	-0.05	0.05	-0.20	0.06	62	-0.06	0.06	-0.23	0.07
	H24	302	-0.06	0.06	-0.27	0.06	62	-0.07	0.07	-0.24	0.06

Table H.16 Hourly elasticities w.r.t. the traffic variable in the SO_2 models

Variable	Model	Weekdays					Sunday				
		N	Mean	Std.	Min	Max	N	Mean	Std.	Min	Max
Background Traffic Elasticities	H01	302	0.08	0.06	0.00	0.31	63	0.08	0.06	0.00	0.00
	H02	302	0.06	0.04	0.00	0.27	63	0.06	0.04	0.00	0.00
	H03	302	0.04	0.03	0.00	0.19	63	0.04	0.03	0.00	0.00
	H04	302	0.03	0.03	0.00	0.15	63	0.03	0.02	0.00	0.00
	H05	302	0.03	0.02	0.00	0.14	63	0.03	0.02	0.00	0.00
	H06	302	0.04	0.03	-0.01	0.18	63	0.03	0.02	0.00	0.06
	H07	302	0.08	0.06	0.00	0.37	63	0.04	0.03	0.00	0.06
	H08	302	0.13	0.09	-0.01	0.56	63	0.05	0.04	0.00	0.07
	H09	302	0.16	0.11	0.00	0.68	63	0.05	0.06	-0.01	0.08
	H10	302	0.18	0.11	-0.01	0.67	63	0.02	0.08	-0.06	0.11
	H11	302	0.20	0.12	0.00	0.74	63	-0.04	0.12	-0.15	0.14
	H12	302	0.22	0.13	0.01	0.74	63	-0.11	0.17	-0.25	0.29
	H13	302	0.23	0.14	0.01	0.72	63	-0.20	0.23	-0.34	0.43
	H14	302	0.25	0.16	0.00	0.82	63	-0.30	0.30	-0.54	0.43
	H15	302	0.26	0.17	0.00	0.83	63	-0.35	0.32	-0.62	0.52
	H16	302	0.26	0.16	0.01	0.80	63	-0.36	0.34	-0.60	0.76
	H17	302	0.25	0.16	0.00	0.89	63	-0.33	0.31	-0.50	0.55
	H18	302	0.23	0.15	-0.01	0.91	63	-0.25	0.25	-0.41	0.35
	H19	302	0.21	0.14	-0.01	1.01	63	-0.15	0.18	-0.27	0.28
	H20	302	0.19	0.12	-0.01	0.88	63	-0.06	0.14	-0.11	0.29
	H21	302	0.16	0.10	0.00	0.71	63	0.01	0.10	-0.04	0.19
	H22	302	0.14	0.09	0.00	0.61	63	0.05	0.08	-0.01	0.10
	H23	302	0.13	0.09	0.00	0.48	63	0.08	0.06	0.00	0.06
	H24	302	0.11	0.07	0.00	0.38	63	0.07	0.05	0.00	0.03
Roadside Traffic Elasticities	H01	301	0.26	0.11	0.06	0.71	62	0.13	0.08	0.00	0.00
	H02	301	0.25	0.10	0.07	0.66	62	0.18	0.08	0.00	0.00
	H03	301	0.22	0.09	0.06	0.59	62	0.18	0.07	0.00	0.00
	H04	301	0.19	0.08	0.05	0.56	62	0.17	0.07	0.00	0.00
	H05	301	0.18	0.07	0.05	0.46	62	0.15	0.06	0.00	0.00
	H06	301	0.20	0.08	0.06	0.51	62	0.14	0.06	0.00	0.01
	H07	301	0.20	0.10	0.03	0.74	62	0.14	0.06	0.00	0.02
	H08	301	0.07	0.12	-0.29	0.51	62	0.13	0.06	-0.01	0.02
	H09	301	0.04	0.13	-0.54	0.42	62	0.08	0.09	-0.04	0.03
	H10	302	0.12	0.12	-0.47	0.52	62	0.03	0.13	-0.12	0.04
	H11	302	0.15	0.14	-0.35	0.65	62	-0.06	0.16	-0.25	0.08
	H12	302	0.18	0.15	-0.32	0.74	62	-0.04	0.17	-0.40	0.14
	H13	302	0.23	0.16	-0.15	1.01	62	-0.06	0.18	-0.53	0.18
	H14	302	0.23	0.17	-0.16	0.96	62	-0.12	0.22	-0.69	0.28
	H15	302	0.22	0.18	-0.23	0.98	62	-0.13	0.23	-0.80	0.32
	H16	302	0.20	0.17	-0.29	0.93	62	-0.15	0.23	-0.68	0.32
	H17	302	0.18	0.16	-0.38	0.87	62	-0.16	0.23	-0.55	0.29
	H18	302	0.14	0.15	-0.39	0.80	62	-0.20	0.23	-0.39	0.29
	H19	302	0.11	0.14	-0.40	0.70	62	-0.15	0.19	-0.25	0.21
	H20	302	0.14	0.13	-0.20	0.64	62	-0.06	0.15	-0.13	0.15
	H21	302	0.17	0.12	-0.03	0.70	62	-0.04	0.14	-0.08	0.11
	H22	302	0.18	0.12	0.01	0.69	62	-0.02	0.13	-0.04	0.06
	H23	302	0.19	0.11	0.03	0.62	62	0.04	0.10	-0.02	0.03
	H24	302	0.23	0.11	0.05	0.73	62	0.12	0.07	0.00	0.01

Table H.17 Hourly elasticities w.r.t. the solar radiation variable in the SO_2 models

Variable	Hour	Weekdays					Sunday				
		N	Mean	Std.	Min	Max	N	Mean	Std.	Min	Max
Background Solar Radiation Elasticities	H01	302	0.00	0.00	0.00	0.00	63	0.00	0.00	0.00	0.00
	H02	302	0.00	0.00	0.00	0.00	63	0.00	0.00	0.00	0.00
	H03	302	0.00	0.00	0.00	0.00	63	0.00	0.00	0.00	0.00
	H04	302	0.00	0.00	0.00	0.00	63	0.00	0.00	0.00	0.00
	H05	302	0.00	0.00	0.00	0.00	63	0.00	0.00	0.00	0.00
	H06	302	0.00	0.00	-0.02	0.01	63	0.00	0.01	0.00	0.06
	H07	302	0.00	0.00	-0.02	0.01	63	0.01	0.01	0.00	0.06
	H08	302	0.00	0.01	-0.05	0.02	63	0.01	0.02	0.00	0.07
	H09	302	-0.01	0.02	-0.10	0.03	63	0.02	0.02	-0.01	0.08
	H10	302	-0.03	0.04	-0.22	0.03	63	0.03	0.03	-0.06	0.11
	H11	302	-0.05	0.06	-0.36	0.03	63	0.02	0.05	-0.15	0.14
	H12	302	-0.07	0.09	-0.47	0.08	63	0.03	0.09	-0.25	0.29
	H13	302	-0.08	0.12	-0.71	0.19	63	0.04	0.12	-0.34	0.43
	H14	302	-0.08	0.14	-0.80	0.22	63	0.04	0.15	-0.54	0.43
	H15	302	-0.08	0.16	-0.93	0.29	63	0.05	0.17	-0.62	0.52
	H16	302	-0.07	0.16	-0.94	0.29	63	0.06	0.18	-0.60	0.76
	H17	302	-0.06	0.15	-0.80	0.24	63	0.05	0.16	-0.50	0.55
	H18	302	-0.05	0.12	-0.68	0.21	63	0.04	0.12	-0.41	0.35
	H19	302	-0.04	0.08	-0.39	0.18	63	0.05	0.08	-0.27	0.28
	H20	302	-0.03	0.06	-0.26	0.09	63	0.06	0.07	-0.11	0.29
	H21	302	-0.02	0.03	-0.18	0.04	63	0.03	0.04	-0.04	0.19
	H22	302	-0.01	0.02	-0.12	0.02	63	0.02	0.02	-0.01	0.10
	H23	302	0.00	0.01	-0.07	0.01	63	0.01	0.01	0.00	0.06
	H24	302	0.00	0.00	-0.02	0.01	63	0.00	0.01	0.00	0.03
Roadside Solar Radiation Elasticities	H01	301	0.00	0.00	0.00	0.00	62	0.00	0.00	0.00	0.00
	H02	301	0.00	0.00	0.00	0.00	62	0.00	0.00	0.00	0.00
	H03	301	0.00	0.00	0.00	0.00	62	0.00	0.00	0.00	0.00
	H04	301	0.00	0.00	0.00	0.00	62	0.00	0.00	0.00	0.00
	H05	301	0.00	0.00	0.00	0.00	62	0.00	0.00	0.00	0.00
	H06	301	0.00	0.00	-0.01	0.01	62	0.00	0.00	0.00	0.01
	H07	301	0.00	0.00	0.00	0.01	62	0.00	0.00	0.00	0.02
	H08	301	0.00	0.01	-0.04	0.02	62	0.00	0.01	-0.01	0.02
	H09	301	0.00	0.01	-0.10	0.03	62	0.00	0.01	-0.04	0.03
	H10	302	-0.01	0.03	-0.18	0.06	62	-0.01	0.03	-0.12	0.04
	H11	302	-0.02	0.05	-0.28	0.13	62	-0.02	0.06	-0.25	0.08
	H12	302	-0.03	0.08	-0.45	0.21	62	-0.03	0.09	-0.40	0.14
	H13	302	-0.04	0.12	-0.74	0.29	62	-0.04	0.12	-0.53	0.18
	H14	302	-0.05	0.15	-0.92	0.25	62	-0.05	0.16	-0.69	0.28
	H15	302	-0.05	0.16	-1.03	0.25	62	-0.05	0.18	-0.80	0.32
	H16	302	-0.05	0.15	-0.98	0.22	62	-0.04	0.17	-0.68	0.32
	H17	302	-0.04	0.13	-0.81	0.21	62	-0.04	0.14	-0.55	0.29
	H18	302	-0.03	0.10	-0.67	0.17	62	-0.03	0.11	-0.39	0.29
	H19	302	-0.02	0.07	-0.54	0.20	62	-0.01	0.07	-0.25	0.21
	H20	302	-0.01	0.04	-0.28	0.10	62	-0.01	0.04	-0.13	0.15
	H21	302	-0.01	0.03	-0.14	0.06	62	0.00	0.03	-0.08	0.11
	H22	302	0.00	0.01	-0.07	0.05	62	0.00	0.02	-0.04	0.06
	H23	302	0.00	0.01	-0.04	0.03	62	0.00	0.01	-0.02	0.03
	H24	302	0.00	0.00	-0.01	0.01	62	0.00	0.00	0.00	0.01

Table H.18 Hourly elasticities w.r.t. the wind speed variable in the SO_2 models

Variable	Hour	Weekdays					Sunday				
		N	Mean	Std.	Min	Max	N	Mean	Std.	Min	Max
Background Wind Speed Elasticities	H01	302	0.008	0.009	-0.052	0.051	63	0.008	0.008	-1.24	0.32
	H02	302	0.008	0.010	-0.070	0.061	63	0.008	0.007	-1.35	0.31
	H03	302	0.009	0.009	-0.055	0.067	63	0.009	0.008	-1.41	0.31
	H04	302	0.010	0.010	-0.043	0.071	63	0.009	0.008	-1.23	0.33
	H05	302	0.010	0.010	-0.037	0.069	63	0.009	0.008	-0.95	0.31
	H06	302	0.010	0.010	-0.043	0.065	63	0.009	0.007	-0.89	0.29
	H07	302	0.010	0.010	-0.026	0.060	63	0.009	0.007	-0.88	0.29
	H08	302	0.009	0.009	-0.029	0.059	63	0.008	0.009	-0.99	0.26
	H09	302	0.008	0.011	-0.040	0.059	63	0.007	0.009	-0.99	0.22
	H10	302	0.007	0.011	-0.057	0.062	63	0.007	0.007	-0.84	0.22
	H11	302	0.008	0.010	-0.040	0.073	63	0.008	0.007	-0.73	0.20
	H12	302	0.010	0.011	-0.049	0.067	63	0.011	0.009	-0.76	0.23
	H13	302	0.013	0.013	-0.082	0.056	63	0.014	0.010	-0.75	0.26
	H14	302	0.018	0.013	-0.023	0.084	63	0.018	0.012	-0.91	0.28
	H15	302	0.021	0.015	-0.026	0.101	63	0.021	0.014	-0.90	0.28
	H16	302	0.021	0.015	-0.019	0.089	63	0.023	0.015	-1.03	0.25
	H17	302	0.020	0.015	-0.068	0.097	63	0.021	0.014	-1.01	0.32
	H18	302	0.019	0.012	-0.017	0.068	63	0.020	0.012	-0.99	0.28
	H19	302	0.015	0.012	-0.058	0.066	63	0.017	0.011	-0.78	0.31
	H20	302	0.011	0.012	-0.091	0.065	63	0.015	0.010	-0.73	0.29
	H21	302	0.009	0.010	-0.049	0.048	63	0.011	0.009	-0.77	0.29
	H22	302	0.007	0.010	-0.067	0.048	63	0.009	0.009	-0.78	0.28
	H23	302	0.007	0.010	-0.064	0.046	63	0.008	0.009	-0.82	0.27
	H24	302	0.007	0.009	-0.044	0.056	63	0.009	0.010	-0.82	0.33
Roadside Wind Speed Elasticities	H01	301	0.008	0.008	0.000	0.057	62	-0.012	0.010	-0.74	0.07
	H02	301	0.015	0.015	0.000	0.111	62	-0.008	0.008	-0.94	0.06
	H03	301	0.019	0.020	0.000	0.180	62	-0.001	0.019	-0.91	0.04
	H04	301	0.023	0.022	0.000	0.170	62	0.001	0.017	-0.96	0.04
	H05	301	0.023	0.022	0.000	0.168	62	0.001	0.011	-1.09	0.03
	H06	301	0.018	0.017	0.000	0.123	62	0.000	0.013	-1.00	0.02
	H07	301	0.002	0.003	0.000	0.024	62	-0.005	0.014	-0.96	0.03
	H08	301	-0.013	0.012	-0.074	0.000	62	-0.008	0.013	-0.72	0.04
	H09	301	-0.019	0.016	-0.110	0.000	62	-0.015	0.011	-0.64	0.06
	H10	302	-0.016	0.014	-0.101	0.000	62	-0.023	0.013	-0.64	0.08
	H11	302	-0.018	0.014	-0.097	-0.003	62	-0.029	0.015	-0.64	0.13
	H12	302	-0.019	0.014	-0.081	-0.001	62	-0.031	0.018	-0.64	0.31
	H13	302	-0.018	0.013	-0.090	0.000	62	-0.034	0.017	-0.61	0.57
	H14	302	-0.022	0.015	-0.090	-0.001	62	-0.038	0.022	-0.71	0.74
	H15	302	-0.025	0.017	-0.113	0.000	62	-0.039	0.024	-0.54	0.89
	H16	302	-0.025	0.016	-0.106	-0.002	62	-0.040	0.021	-0.49	0.89
	H17	302	-0.024	0.017	-0.097	-0.002	62	-0.038	0.020	-0.56	0.78
	H18	302	-0.025	0.016	-0.137	0.000	62	-0.041	0.021	-0.53	0.74
	H19	302	-0.023	0.016	-0.136	0.000	62	-0.035	0.019	-0.49	0.40
	H20	302	-0.017	0.014	-0.104	0.000	62	-0.028	0.015	-0.55	0.20
	H21	302	-0.010	0.008	-0.044	0.000	62	-0.026	0.014	-0.49	0.10
	H22	302	-0.008	0.007	-0.047	0.000	62	-0.022	0.015	-0.51	0.07
	H23	302	-0.005	0.005	-0.041	0.000	62	-0.017	0.013	-0.58	0.07
	H24	302	0.001	0.001	-0.002	0.013	62	-0.013	0.009	-0.70	0.06

Table H.19 Hourly elasticities w.r.t. the temperature variable in the SO_2 models

Variable	Hour	Weekdays					Sunday				
		N	Mean	Std.	Min	Max	N	Mean	Std.	Min	Max
Background Temperature Elasticities	H01	302	0.04	0.15	-0.84	0.30	63	0.03	0.20	-1.24	0.32
	H02	302	0.05	0.15	-0.82	0.32	63	0.03	0.21	-1.35	0.31
	H03	302	0.06	0.16	-0.87	0.33	63	0.04	0.22	-1.41	0.31
	H04	302	0.06	0.16	-0.92	0.39	63	0.05	0.20	-1.23	0.33
	H05	302	0.06	0.17	-1.06	0.38	63	0.06	0.17	-0.95	0.31
	H06	302	0.06	0.17	-1.01	0.37	63	0.06	0.17	-0.89	0.29
	H07	302	0.05	0.17	-1.14	0.34	63	0.05	0.17	-0.88	0.29
	H08	302	0.02	0.16	-1.00	0.32	63	0.02	0.17	-0.99	0.26
	H09	302	0.00	0.14	-0.90	0.33	63	-0.01	0.18	-0.99	0.22
	H10	302	-0.02	0.15	-0.71	0.34	63	-0.03	0.17	-0.84	0.22
	H11	302	-0.05	0.17	-0.61	0.30	63	-0.06	0.19	-0.73	0.20
	H12	302	-0.07	0.20	-0.63	0.28	63	-0.08	0.21	-0.76	0.23
	H13	302	-0.09	0.22	-0.75	0.31	63	-0.09	0.23	-0.75	0.26
	H14	302	-0.11	0.24	-0.80	0.32	63	-0.11	0.26	-0.91	0.28
	H15	302	-0.11	0.25	-0.93	0.32	63	-0.12	0.27	-0.90	0.28
	H16	302	-0.10	0.23	-0.80	0.30	63	-0.11	0.28	-1.03	0.25
	H17	302	-0.09	0.23	-0.84	0.32	63	-0.10	0.26	-1.01	0.32
	H18	302	-0.06	0.21	-0.82	0.29	63	-0.07	0.25	-0.99	0.28
	H19	302	-0.04	0.19	-0.83	0.32	63	-0.04	0.22	-0.78	0.31
	H20	302	-0.01	0.16	-0.95	0.31	63	-0.01	0.20	-0.73	0.29
	H21	302	0.01	0.15	-0.83	0.34	63	0.00	0.19	-0.77	0.29
	H22	302	0.02	0.14	-0.94	0.30	63	0.01	0.18	-0.78	0.28
	H23	302	0.02	0.14	-0.98	0.31	63	0.02	0.18	-0.82	0.27
	H24	302	0.03	0.14	-1.12	0.31	63	0.03	0.18	-0.82	0.33
Roadside Temperature Elasticities	H01	301	-0.12	0.17	-0.72	0.07	62	-0.15	0.19	-0.74	0.07
	H02	301	-0.14	0.19	-0.78	0.06	62	-0.18	0.23	-0.94	0.06
	H03	301	-0.16	0.20	-0.87	0.05	62	-0.21	0.26	-0.91	0.04
	H04	301	-0.16	0.21	-0.83	0.05	62	-0.22	0.26	-0.96	0.04
	H05	301	-0.16	0.20	-0.80	0.05	62	-0.21	0.26	-1.09	0.03
	H06	301	-0.13	0.18	-0.85	0.06	62	-0.18	0.23	-1.00	0.02
	H07	301	-0.07	0.13	-0.83	0.10	62	-0.15	0.21	-0.96	0.03
	H08	301	-0.03	0.12	-1.04	0.15	62	-0.15	0.19	-0.72	0.04
	H09	301	-0.01	0.10	-0.90	0.17	62	-0.12	0.17	-0.64	0.06
	H10	302	-0.01	0.11	-0.86	0.21	62	-0.10	0.16	-0.64	0.08
	H11	302	0.00	0.11	-0.80	0.27	62	-0.05	0.16	-0.64	0.13
	H12	302	0.03	0.13	-0.71	0.38	62	-0.03	0.18	-0.64	0.31
	H13	302	0.05	0.15	-0.76	0.47	62	0.02	0.20	-0.61	0.57
	H14	302	0.09	0.18	-0.90	0.58	62	0.06	0.23	-0.71	0.74
	H15	302	0.10	0.19	-0.83	0.72	62	0.08	0.24	-0.54	0.89
	H16	302	0.10	0.17	-0.67	0.60	62	0.08	0.24	-0.49	0.89
	H17	302	0.09	0.17	-0.83	0.58	62	0.07	0.22	-0.56	0.78
	H18	302	0.07	0.15	-0.80	0.51	62	0.05	0.20	-0.53	0.74
	H19	302	0.05	0.13	-0.77	0.47	62	0.01	0.15	-0.49	0.40
	H20	302	0.02	0.11	-0.57	0.26	62	-0.04	0.15	-0.55	0.20
	H21	302	-0.02	0.11	-0.68	0.15	62	-0.06	0.14	-0.49	0.10
	H22	302	-0.04	0.12	-0.73	0.14	62	-0.09	0.15	-0.51	0.07
	H23	302	-0.06	0.12	-0.71	0.11	62	-0.11	0.16	-0.58	0.07
	H24	302	-0.08	0.14	-0.86	0.09	62	-0.14	0.19	-0.70	0.06

Table H.20 Hourly elasticities w.r.t. the humidity variable in the SO_2 models

Variable	Hour	Weekdays					Sunday				
		N	Mean	Std.	Min	Max	N	Mean	Std.	Min	Max
Background Humidity Elasticities	H01	302	-0.33	0.18	-1.26	-0.03	63	-0.31	0.15	-0.76	-0.06
	H02	302	-0.30	0.16	-1.06	-0.02	63	-0.27	0.13	-0.64	-0.05
	H03	302	-0.28	0.15	-0.96	-0.02	63	-0.26	0.12	-0.57	-0.04
	H04	302	-0.27	0.15	-0.92	-0.01	63	-0.24	0.11	-0.56	-0.03
	H05	302	-0.27	0.15	-0.89	-0.01	63	-0.24	0.11	-0.49	-0.04
	H06	302	-0.31	0.15	-0.89	-0.04	63	-0.25	0.11	-0.56	-0.04
	H07	302	-0.43	0.20	-1.26	-0.07	63	-0.29	0.14	-0.65	-0.04
	H08	302	-0.48	0.25	-1.50	-0.05	63	-0.27	0.15	-0.61	0.01
	H09	302	-0.40	0.27	-1.45	-0.04	63	-0.23	0.16	-0.57	0.06
	H10	302	-0.28	0.26	-1.47	0.04	63	-0.18	0.18	-0.61	0.11
	H11	302	-0.19	0.26	-1.42	0.20	63	-0.13	0.21	-0.73	0.24
	H12	302	-0.12	0.27	-1.29	0.32	63	-0.07	0.24	-0.69	0.42
	H13	302	-0.04	0.28	-1.11	0.47	63	-0.02	0.26	-0.72	0.53
	H14	302	-0.01	0.29	-1.13	0.57	63	0.00	0.29	-0.74	0.59
	H15	302	0.01	0.30	-1.02	0.63	63	0.02	0.30	-0.77	0.64
	H16	302	0.01	0.30	-1.03	0.57	63	0.01	0.31	-0.73	0.68
	H17	302	-0.03	0.30	-1.03	0.54	63	-0.03	0.33	-0.97	0.65
	H18	302	-0.10	0.29	-1.19	0.48	63	-0.10	0.32	-0.92	0.57
	H19	302	-0.18	0.28	-1.25	0.32	63	-0.17	0.31	-1.10	0.45
	H20	302	-0.24	0.25	-1.32	0.17	63	-0.22	0.29	-1.18	0.37
	H21	302	-0.29	0.23	-1.23	0.07	63	-0.28	0.24	-1.13	0.21
	H22	302	-0.33	0.21	-1.10	0.00	63	-0.33	0.22	-1.11	0.07
	H23	302	-0.35	0.19	-1.12	-0.02	63	-0.36	0.19	-1.11	-0.04
	H24	302	-0.35	0.18	-1.10	-0.03	63	-0.33	0.18	-1.11	-0.06
Roadside Humidity Elasticities	H01	301	-0.06	0.14	-0.60	0.35	62	-0.15	0.26	-0.90	0.21
	H02	301	-0.03	0.14	-0.47	0.41	62	-0.13	0.25	-0.79	0.25
	H03	301	0.00	0.13	-0.46	0.44	62	-0.12	0.26	-0.85	0.24
	H04	301	0.02	0.13	-0.44	0.46	62	-0.12	0.26	-0.76	0.26
	H05	301	0.02	0.13	-0.39	0.40	62	-0.13	0.26	-0.79	0.42
	H06	301	-0.02	0.12	-0.47	0.35	62	-0.14	0.24	-0.84	0.42
	H07	301	-0.14	0.15	-0.94	0.18	62	-0.18	0.27	-0.98	0.39
	H08	301	-0.21	0.19	-1.27	0.08	62	-0.15	0.27	-1.01	0.49
	H09	301	-0.18	0.19	-1.28	0.09	62	-0.12	0.30	-1.29	0.45
	H10	302	-0.09	0.18	-1.21	0.21	62	-0.06	0.31	-1.39	0.48
	H11	302	-0.04	0.18	-1.02	0.32	62	-0.02	0.30	-0.99	0.53
	H12	302	-0.01	0.18	-0.82	0.40	62	0.02	0.32	-0.99	0.55
	H13	302	0.03	0.18	-0.69	0.50	62	0.03	0.34	-1.01	0.54
	H14	302	0.04	0.19	-0.68	0.44	62	0.04	0.37	-1.14	0.57
	H15	302	0.05	0.18	-0.74	0.46	62	0.04	0.39	-1.45	0.60
	H16	302	0.04	0.19	-0.82	0.36	62	0.01	0.39	-1.29	0.61
	H17	302	0.02	0.18	-0.92	0.33	62	-0.01	0.37	-1.12	0.59
	H18	302	-0.02	0.18	-0.88	0.28	62	-0.05	0.38	-1.30	0.63
	H19	302	-0.06	0.18	-0.81	0.24	62	-0.10	0.35	-1.33	0.54
	H20	302	-0.08	0.17	-0.85	0.21	62	-0.14	0.34	-1.18	0.43
	H21	302	-0.09	0.16	-0.76	0.23	62	-0.16	0.31	-1.02	0.38
	H22	302	-0.11	0.15	-0.64	0.23	62	-0.20	0.31	-1.15	0.33
	H23	302	-0.10	0.14	-0.61	0.21	62	-0.21	0.30	-1.19	0.27
	H24	302	-0.09	0.13	-0.57	0.24	62	-0.17	0.27	-1.04	0.30

Table H.21 Hourly elasticities w.r.t. the traffic variable in the PM10 models

Variable	Hour	Weekdays					Sunday				
		N	Mean	Std.	Min	Max	N	Mean	Std.	Min	Max
Background Traffic Elasticities	H01	302	0.03	0.05	-0.24	0.24	63	0.04	0.06	-0.14	0.39
	H02	302	0.02	0.04	-0.16	0.18	63	0.03	0.04	-0.12	0.29
	H03	302	0.02	0.03	-0.11	0.19	63	0.02	0.03	-0.11	0.18
	H04	302	0.02	0.03	-0.09	0.17	63	0.02	0.02	-0.05	0.13
	H05	302	0.02	0.03	-0.09	0.17	63	0.02	0.02	-0.04	0.10
	H06	302	0.02	0.04	-0.12	0.24	63	0.02	0.02	-0.07	0.10
	H07	302	0.04	0.07	-0.24	0.43	63	0.02	0.03	-0.12	0.14
	H08	302	0.06	0.10	-0.42	0.72	63	0.03	0.04	-0.16	0.15
	H09	302	0.05	0.11	-0.49	0.83	63	0.03	0.05	-0.21	0.20
	H10	302	0.04	0.10	-0.46	0.72	63	0.03	0.07	-0.28	0.25
	H11	302	0.04	0.10	-0.36	0.68	63	0.04	0.08	-0.36	0.29
	H12	302	0.04	0.10	-0.38	0.77	63	0.04	0.08	-0.31	0.30
	H13	302	0.04	0.10	-0.38	0.91	63	0.04	0.08	-0.34	0.32
	H14	302	0.05	0.11	-0.44	1.14	63	0.05	0.09	-0.35	0.32
	H15	302	0.05	0.11	-0.44	1.19	63	0.05	0.09	-0.39	0.31
	H16	302	0.05	0.11	-0.47	1.21	63	0.05	0.08	-0.30	0.30
	H17	302	0.05	0.10	-0.44	0.97	63	0.05	0.07	-0.25	0.28
	H18	302	0.05	0.10	-0.39	1.07	63	0.05	0.08	-0.26	0.30
	H19	302	0.05	0.10	-0.32	1.08	63	0.05	0.08	-0.25	0.29
	H20	302	0.05	0.09	-0.25	0.97	63	0.04	0.06	-0.21	0.28
	H21	302	0.05	0.08	-0.20	0.81	63	0.04	0.06	-0.18	0.29
	H22	302	0.05	0.08	-0.21	0.80	63	0.04	0.07	-0.18	0.32
	H23	302	0.04	0.07	-0.24	0.67	63	0.04	0.06	-0.18	0.29
	H24	302	0.04	0.07	-0.28	0.58	63	0.03	0.05	-0.16	0.24
Roadside Traffic Elasticities	H01	301	0.22	0.14	0.04	0.97	62	0.14	0.09	0.02	0.46
	H02	301	0.19	0.14	0.04	0.94	62	0.18	0.12	0.02	0.58
	H03	301	0.17	0.13	0.03	1.01	62	0.18	0.13	0.02	0.63
	H04	301	0.14	0.11	0.03	0.67	62	0.17	0.12	0.02	0.59
	H05	301	0.14	0.10	0.03	0.68	62	0.17	0.14	0.03	0.99
	H06	301	0.16	0.11	0.03	0.67	62	0.17	0.12	0.03	0.79
	H07	301	0.22	0.13	0.05	0.69	62	0.16	0.10	0.02	0.57
	H08	301	0.22	0.12	0.05	0.66	62	0.14	0.07	0.03	0.39
	H09	301	0.21	0.11	0.04	0.70	62	0.08	0.05	0.01	0.22
	H10	302	0.22	0.12	0.04	0.66	62	0.02	0.04	-0.10	0.13
	H11	302	0.23	0.12	0.04	0.81	62	-0.09	0.09	-0.36	0.02
	H12	302	0.25	0.12	0.04	0.71	62	-0.08	0.08	-0.40	0.04
	H13	302	0.26	0.14	0.04	0.83	62	-0.12	0.10	-0.49	0.04
	H14	302	0.27	0.15	0.04	0.88	62	-0.18	0.13	-0.61	0.01
	H15	302	0.27	0.14	0.04	0.94	62	-0.19	0.13	-0.66	0.00
	H16	302	0.26	0.14	0.04	0.78	62	-0.20	0.16	-0.91	0.00
	H17	302	0.26	0.13	0.04	0.85	62	-0.21	0.17	-1.12	-0.01
	H18	302	0.25	0.12	0.04	0.88	62	-0.23	0.18	-1.22	-0.02
	H19	302	0.24	0.12	0.04	0.94	62	-0.16	0.14	-0.86	0.01
	H20	302	0.23	0.12	0.03	0.85	62	-0.05	0.07	-0.36	0.09
	H21	302	0.23	0.12	0.03	1.01	62	-0.04	0.07	-0.32	0.10
	H22	302	0.24	0.13	0.03	0.96	62	-0.01	0.05	-0.23	0.12
	H23	302	0.24	0.14	0.03	0.86	62	0.05	0.04	-0.01	0.19
	H24	302	0.23	0.13	0.04	0.86	62	0.13	0.08	0.04	0.34

Table H.22 Hourly elasticities w.r.t. the solar radiation variable in the PM10 models

Variable	Hour	Weekdays					Sunday				
		N	Mean	Std.	Min	Max	N	Mean	Std.	Min	Max
Background Solar Radiation Elasticities	H01	302	0.00	0.00	0.00	0.00	63	0.00	0.00	0.00	0.00
	H02	302	0.00	0.00	0.00	0.00	63	0.00	0.00	0.00	0.00
	H03	302	0.00	0.00	0.00	0.00	63	0.00	0.00	0.00	0.00
	H04	302	0.00	0.00	0.00	0.00	63	0.00	0.00	0.00	0.00
	H05	302	0.00	0.00	0.00	0.00	63	0.00	0.00	0.00	0.00
	H06	302	0.00	0.00	-0.02	0.00	63	0.00	0.00	-0.02	0.00
	H07	302	0.00	0.00	-0.03	0.00	63	0.00	0.00	-0.02	0.00
	H08	302	-0.01	0.01	-0.07	0.00	63	-0.01	0.01	-0.05	0.00
	H09	302	-0.02	0.03	-0.19	0.00	63	-0.02	0.02	-0.11	0.00
	H10	302	-0.04	0.05	-0.38	0.00	63	-0.04	0.04	-0.22	0.00
	H11	302	-0.07	0.08	-0.54	0.00	63	-0.08	0.08	-0.33	0.00
	H12	302	-0.12	0.12	-0.70	0.00	63	-0.12	0.12	-0.45	0.00
	H13	302	-0.16	0.16	-1.06	0.00	63	-0.18	0.17	-0.63	-0.01
	H14	302	-0.20	0.21	-1.46	0.00	63	-0.22	0.21	-0.76	-0.01
	H15	302	-0.22	0.22	-1.45	0.00	63	-0.25	0.23	-0.90	0.00
	H16	302	-0.21	0.21	-1.34	0.00	63	-0.24	0.22	-0.91	0.00
	H17	302	-0.18	0.17	-1.06	0.00	63	-0.20	0.19	-0.71	0.00
	H18	302	-0.14	0.12	-0.78	0.00	63	-0.15	0.13	-0.53	0.00
	H19	302	-0.09	0.08	-0.53	0.00	63	-0.10	0.09	-0.44	0.00
	H20	302	-0.06	0.05	-0.27	0.00	63	-0.06	0.06	-0.25	0.00
	H21	302	-0.03	0.03	-0.18	0.00	63	-0.03	0.03	-0.17	0.00
	H22	302	-0.01	0.02	-0.13	0.00	63	-0.02	0.02	-0.11	0.00
	H23	302	-0.01	0.01	-0.06	0.00	63	-0.01	0.01	-0.07	0.00
	H24	302	0.00	0.00	-0.02	0.00	63	0.00	0.00	-0.03	0.00
Roadside Solar Radiation Elasticities	H01	301	0.00	0.00	0.00	0.00	62	0.00	0.00	0.00	0.00
	H02	301	0.00	0.00	0.00	0.00	62	0.00	0.00	0.00	0.00
	H03	301	0.00	0.00	0.00	0.00	62	0.00	0.00	0.00	0.00
	H04	301	0.00	0.00	0.00	0.00	62	0.00	0.00	0.00	0.00
	H05	301	0.00	0.00	0.00	0.00	62	0.00	0.00	0.00	0.00
	H06	301	0.00	0.00	-0.01	0.00	62	0.00	0.00	-0.02	0.00
	H07	301	0.00	0.00	-0.02	0.00	62	0.00	0.00	-0.02	0.00
	H08	301	0.00	0.01	-0.04	0.01	62	0.00	0.01	-0.04	0.01
	H09	301	-0.01	0.02	-0.12	0.01	62	-0.01	0.02	-0.11	0.01
	H10	302	-0.02	0.03	-0.17	0.02	62	-0.02	0.04	-0.20	0.03
	H11	302	-0.04	0.06	-0.32	0.06	62	-0.05	0.07	-0.30	0.04
	H12	302	-0.07	0.09	-0.50	0.07	62	-0.08	0.11	-0.50	0.08
	H13	302	-0.11	0.14	-0.78	0.14	62	-0.12	0.17	-0.74	0.12
	H14	302	-0.14	0.18	-1.03	0.12	62	-0.15	0.21	-1.04	0.13
	H15	302	-0.15	0.21	-1.32	0.14	62	-0.16	0.23	-1.12	0.15
	H16	302	-0.14	0.19	-1.09	0.14	62	-0.15	0.21	-0.87	0.17
	H17	302	-0.12	0.16	-0.92	0.18	62	-0.13	0.18	-0.69	0.20
	H18	302	-0.09	0.12	-0.60	0.13	62	-0.10	0.14	-0.50	0.17
	H19	302	-0.06	0.08	-0.41	0.11	62	-0.06	0.09	-0.33	0.10
	H20	302	-0.04	0.05	-0.22	0.09	62	-0.04	0.05	-0.22	0.06
	H21	302	-0.02	0.03	-0.14	0.06	62	-0.02	0.03	-0.12	0.05
	H22	302	-0.01	0.01	-0.09	0.03	62	-0.01	0.01	-0.06	0.04
	H23	302	0.00	0.01	-0.05	0.02	62	0.00	0.01	-0.04	0.02
	H24	302	0.00	0.00	-0.01	0.01	62	0.00	0.00	-0.02	0.00

Table H.23 Hourly elasticities w.r.t. the wind speed variable in the PM10 models

Variable	Hour	Weekdays					Sunday				
		N	Mean	Std.	Min	Max	N	Mean	Std.	Min	Max
Background Wind Speed Elasticities	H01	302	0.005	0.011	-0.016	0.074	63	0.006	0.012	-0.019	0.055
	H02	302	0.005	0.010	-0.015	0.099	63	0.007	0.014	-0.012	0.080
	H03	302	0.005	0.011	-0.012	0.127	63	0.006	0.013	-0.032	0.060
	H04	302	0.005	0.011	-0.011	0.128	63	0.005	0.013	-0.029	0.068
	H05	302	0.005	0.011	-0.011	0.143	63	0.005	0.010	-0.021	0.051
	H06	302	0.005	0.012	-0.013	0.113	63	0.004	0.010	-0.028	0.050
	H07	302	0.005	0.011	-0.011	0.092	63	0.005	0.012	-0.030	0.065
	H08	302	0.006	0.012	-0.014	0.107	63	0.006	0.012	-0.026	0.053
	H09	302	0.007	0.012	-0.013	0.087	63	0.007	0.013	-0.030	0.051
	H10	302	0.008	0.013	-0.010	0.095	63	0.008	0.013	-0.033	0.057
	H11	302	0.009	0.013	-0.012	0.105	63	0.010	0.014	-0.032	0.068
	H12	302	0.011	0.014	-0.011	0.109	63	0.011	0.015	-0.027	0.070
	H13	302	0.012	0.014	-0.020	0.093	63	0.012	0.016	-0.018	0.085
	H14	302	0.013	0.015	-0.015	0.105	63	0.013	0.017	-0.026	0.088
	H15	302	0.014	0.015	-0.016	0.098	63	0.013	0.015	-0.020	0.064
	H16	302	0.013	0.016	-0.010	0.108	63	0.013	0.017	-0.016	0.092
	H17	302	0.012	0.015	-0.016	0.118	63	0.012	0.019	-0.018	0.106
	H18	302	0.011	0.015	-0.013	0.136	63	0.012	0.018	-0.016	0.108
	H19	302	0.010	0.015	-0.011	0.158	63	0.010	0.018	-0.017	0.110
	H20	302	0.008	0.014	-0.013	0.129	63	0.009	0.015	-0.011	0.077
	H21	302	0.007	0.013	-0.017	0.116	63	0.007	0.014	-0.021	0.082
	H22	302	0.006	0.011	-0.018	0.084	63	0.006	0.011	-0.009	0.068
	H23	302	0.006	0.011	-0.020	0.078	63	0.006	0.012	-0.007	0.074
	H24	302	0.006	0.012	-0.019	0.110	63	0.005	0.012	-0.017	0.059
Roadside Wind Speed Elasticities	H01	301	0.025	0.037	0.000	0.224	62	0.029	0.046	0.000	0.201
	H02	301	0.030	0.046	0.000	0.384	62	0.035	0.058	0.000	0.295
	H03	301	0.034	0.060	0.000	0.716	62	0.041	0.069	0.000	0.377
	H04	301	0.038	0.056	0.000	0.524	62	0.038	0.063	0.000	0.308
	H05	301	0.038	0.055	0.000	0.556	62	0.038	0.059	0.000	0.367
	H06	301	0.036	0.059	0.000	0.489	62	0.036	0.062	0.000	0.359
	H07	301	0.023	0.038	0.000	0.272	62	0.031	0.045	0.000	0.212
	H08	301	0.013	0.025	-0.005	0.176	62	0.029	0.044	0.000	0.246
	H09	301	0.012	0.026	-0.006	0.188	62	0.024	0.035	0.000	0.157
	H10	302	0.013	0.026	-0.007	0.227	62	0.021	0.026	0.000	0.138
	H11	302	0.014	0.024	-0.007	0.140	62	0.021	0.027	-0.001	0.117
	H12	302	0.017	0.029	-0.008	0.183	62	0.024	0.029	-0.002	0.122
	H13	302	0.021	0.037	-0.009	0.293	62	0.023	0.025	-0.005	0.104
	H14	302	0.023	0.036	-0.013	0.272	62	0.023	0.028	-0.006	0.105
	H15	302	0.024	0.035	-0.013	0.270	62	0.027	0.036	-0.004	0.165
	H16	302	0.024	0.039	-0.013	0.312	62	0.027	0.039	-0.005	0.227
	H17	302	0.023	0.042	-0.011	0.336	62	0.029	0.043	-0.006	0.234
	H18	302	0.021	0.040	-0.011	0.375	62	0.025	0.030	-0.005	0.145
	H19	302	0.020	0.040	-0.010	0.334	62	0.023	0.029	-0.003	0.143
	H20	302	0.021	0.043	-0.006	0.295	62	0.027	0.036	-0.001	0.173
	H21	302	0.019	0.035	-0.003	0.328	62	0.026	0.038	0.000	0.191
	H22	302	0.020	0.034	-0.004	0.306	62	0.021	0.032	0.000	0.167
	H23	302	0.020	0.035	-0.004	0.247	62	0.024	0.044	0.000	0.282
	H24	302	0.022	0.039	-0.001	0.341	62	0.025	0.039	0.000	0.231

Table H.24 Hourly elasticities w.r.t. the temperature variable in the PM10 models

Variable	Hour	Weekdays					Sunday				
		N	Mean	Std.	Min	Max	N	Mean	Std.	Min	Max
Background Temperature Elasticities	H01	302	0.04	0.10	-0.43	0.66	63	0.03	0.10	-0.32	0.38
	H02	302	0.05	0.11	-0.42	0.64	63	0.04	0.10	-0.39	0.47
	H03	302	0.06	0.12	-0.40	0.76	63	0.05	0.12	-0.52	0.54
	H04	302	0.07	0.13	-0.45	0.82	63	0.06	0.13	-0.48	0.73
	H05	302	0.07	0.14	-0.45	0.91	63	0.07	0.14	-0.48	0.75
	H06	302	0.07	0.14	-0.48	0.92	63	0.07	0.13	-0.47	0.65
	H07	302	0.05	0.11	-0.37	0.70	63	0.06	0.12	-0.43	0.52
	H08	302	0.02	0.09	-0.35	0.65	63	0.05	0.12	-0.44	0.58
	H09	302	0.01	0.08	-0.25	0.52	63	0.02	0.11	-0.47	0.45
	H10	302	0.00	0.08	-0.26	0.35	63	0.01	0.11	-0.48	0.43
	H11	302	0.00	0.08	-0.27	0.31	63	0.00	0.11	-0.42	0.36
	H12	302	0.00	0.08	-0.37	0.27	63	0.01	0.11	-0.44	0.34
	H13	302	0.01	0.09	-0.49	0.36	63	0.02	0.11	-0.39	0.34
	H14	302	0.02	0.09	-0.50	0.43	63	0.03	0.11	-0.39	0.38
	H15	302	0.03	0.10	-0.36	0.53	63	0.03	0.11	-0.33	0.47
	H16	302	0.03	0.09	-0.30	0.49	63	0.04	0.11	-0.34	0.43
	H17	302	0.03	0.09	-0.27	0.45	63	0.04	0.10	-0.28	0.49
	H18	302	0.03	0.08	-0.29	0.44	63	0.04	0.11	-0.27	0.51
	H19	302	0.03	0.08	-0.25	0.53	63	0.04	0.11	-0.30	0.49
	H20	302	0.03	0.08	-0.26	0.53	63	0.04	0.10	-0.34	0.46
	H21	302	0.03	0.08	-0.26	0.52	63	0.03	0.11	-0.39	0.50
	H22	302	0.02	0.08	-0.26	0.48	63	0.03	0.11	-0.37	0.49
	H23	302	0.02	0.08	-0.26	0.54	63	0.03	0.12	-0.38	0.51
	H24	302	0.03	0.09	-0.28	0.62	63	0.03	0.12	-0.44	0.50
Roadside Temperature Elasticities	H01	301	-0.08	0.21	-1.34	0.41	62	-0.10	0.21	-0.87	0.15
	H02	301	-0.08	0.21	-1.07	0.40	62	-0.11	0.24	-1.08	0.16
	H03	301	-0.07	0.22	-1.20	0.41	62	-0.10	0.23	-1.19	0.19
	H04	301	-0.07	0.22	-1.29	0.58	62	-0.09	0.21	-0.91	0.19
	H05	301	-0.06	0.22	-1.21	0.48	62	-0.09	0.23	-1.07	0.25
	H06	301	-0.05	0.18	-0.89	0.39	62	-0.08	0.22	-0.99	0.23
	H07	301	-0.05	0.15	-0.68	0.28	62	-0.07	0.18	-0.85	0.21
	H08	301	-0.06	0.14	-0.64	0.33	62	-0.08	0.19	-1.00	0.22
	H09	301	-0.07	0.14	-0.79	0.21	62	-0.11	0.20	-0.89	0.14
	H10	302	-0.08	0.15	-0.71	0.20	62	-0.13	0.24	-0.91	0.14
	H11	302	-0.08	0.17	-0.73	0.19	62	-0.13	0.27	-1.28	0.15
	H12	302	-0.08	0.18	-0.89	0.25	62	-0.12	0.27	-1.18	0.16
	H13	302	-0.07	0.20	-1.18	0.29	62	-0.11	0.29	-1.21	0.23
	H14	302	-0.05	0.20	-0.98	0.33	62	-0.09	0.29	-1.14	0.33
	H15	302	-0.04	0.21	-1.14	0.39	62	-0.08	0.28	-1.20	0.34
	H16	302	-0.04	0.21	-1.03	0.39	62	-0.07	0.26	-0.94	0.28
	H17	302	-0.04	0.20	-1.34	0.34	62	-0.07	0.25	-0.95	0.24
	H18	302	-0.05	0.19	-1.38	0.33	62	-0.08	0.24	-0.84	0.24
	H19	302	-0.05	0.17	-1.01	0.27	62	-0.08	0.23	-0.79	0.22
	H20	302	-0.05	0.15	-0.82	0.21	62	-0.08	0.22	-0.88	0.26
	H21	302	-0.06	0.15	-0.74	0.25	62	-0.08	0.21	-0.82	0.35
	H22	302	-0.07	0.16	-0.86	0.22	62	-0.09	0.21	-0.79	0.37
	H23	302	-0.07	0.16	-0.80	0.22	62	-0.09	0.23	-0.95	0.54
	H24	302	-0.07	0.17	-0.91	0.23	62	-0.10	0.24	-1.10	0.40

Table H.25 Hourly elasticities w.r.t. the humidity variable in the PM10 models

Variable	Hour	Weekdays					Sunday				
		N	Mean	Std.	Min	Max	N	Mean	Std.	Min	Max
Background Humidity Elasticities	H01	302	0.19	0.42	-0.48	2.90	63	0.19	0.35	-0.33	1.61
	H02	302	0.20	0.42	-0.46	2.49	63	0.19	0.34	-0.39	1.67
	H03	302	0.22	0.44	-0.44	2.98	63	0.21	0.38	-0.50	1.81
	H04	302	0.23	0.45	-0.44	3.29	63	0.23	0.42	-0.46	2.33
	H05	302	0.23	0.45	-0.42	3.44	63	0.23	0.41	-0.46	2.29
	H06	302	0.24	0.46	-0.42	3.86	63	0.23	0.41	-0.43	1.91
	H07	302	0.22	0.41	-0.35	2.73	63	0.24	0.42	-0.39	1.91
	H08	302	0.20	0.40	-0.34	2.49	63	0.23	0.46	-0.40	2.24
	H09	302	0.19	0.37	-0.35	2.73	63	0.22	0.45	-0.46	2.21
	H10	302	0.19	0.36	-0.35	2.77	63	0.25	0.50	-0.46	2.59
	H11	302	0.20	0.36	-0.26	2.21	63	0.29	0.58	-0.40	2.86
	H12	302	0.21	0.35	-0.22	2.02	63	0.30	0.59	-0.39	3.17
	H13	302	0.23	0.37	-0.21	1.84	63	0.31	0.57	-0.33	2.59
	H14	302	0.24	0.36	-0.19	1.74	63	0.34	0.59	-0.30	2.63
	H15	302	0.25	0.37	-0.15	1.62	63	0.34	0.57	-0.25	2.70
	H16	302	0.26	0.39	-0.15	2.00	63	0.33	0.57	-0.22	2.64
	H17	302	0.25	0.40	-0.15	2.51	63	0.29	0.52	-0.21	2.81
	H18	302	0.24	0.41	-0.17	2.73	63	0.31	0.59	-0.23	3.31
	H19	302	0.22	0.41	-0.20	3.04	63	0.30	0.57	-0.28	3.06
	H20	302	0.20	0.38	-0.26	2.81	63	0.26	0.46	-0.34	2.21
	H21	302	0.19	0.37	-0.28	2.55	63	0.23	0.47	-0.38	2.39
	H22	302	0.18	0.37	-0.30	2.60	63	0.23	0.50	-0.42	2.73
	H23	302	0.18	0.36	-0.31	2.47	63	0.23	0.47	-0.43	2.40
	H24	302	0.18	0.39	-0.32	2.62	63	0.22	0.44	-0.47	2.27
Roadside Humidity Elasticities	H01	301	0.09	0.20	-0.33	1.72	62	0.11	0.19	-0.17	0.77
	H02	301	0.12	0.23	-0.30	1.40	62	0.15	0.24	-0.23	1.13
	H03	301	0.15	0.27	-0.33	1.59	62	0.17	0.27	-0.22	1.36
	H04	301	0.17	0.28	-0.35	1.94	62	0.19	0.27	-0.17	1.34
	H05	301	0.17	0.28	-0.33	2.05	62	0.22	0.35	-0.21	2.18
	H06	301	0.14	0.24	-0.31	1.55	62	0.19	0.31	-0.18	1.62
	H07	301	0.06	0.16	-0.41	0.86	62	0.14	0.24	-0.15	1.18
	H08	301	0.01	0.13	-0.43	0.59	62	0.12	0.20	-0.21	0.96
	H09	301	0.02	0.12	-0.32	0.59	62	0.11	0.18	-0.19	0.79
	H10	302	0.06	0.13	-0.24	0.55	62	0.14	0.20	-0.17	0.91
	H11	302	0.09	0.14	-0.19	0.67	62	0.16	0.21	-0.11	0.92
	H12	302	0.12	0.15	-0.16	0.66	62	0.19	0.22	-0.08	0.84
	H13	302	0.16	0.17	-0.12	0.89	62	0.22	0.22	-0.04	0.85
	H14	302	0.18	0.18	-0.09	0.98	62	0.24	0.23	-0.05	0.89
	H15	302	0.19	0.18	-0.09	0.87	62	0.25	0.23	-0.03	0.87
	H16	302	0.19	0.17	-0.07	0.85	62	0.24	0.21	-0.03	1.01
	H17	302	0.17	0.17	-0.09	0.88	62	0.22	0.23	-0.05	1.30
	H18	302	0.15	0.16	-0.17	0.86	62	0.21	0.23	-0.09	1.24
	H19	302	0.12	0.15	-0.33	0.76	62	0.18	0.21	-0.13	1.03
	H20	302	0.10	0.15	-0.37	0.82	62	0.15	0.21	-0.17	0.87
	H21	302	0.08	0.14	-0.31	0.65	62	0.12	0.19	-0.18	0.86
	H22	302	0.06	0.14	-0.36	0.71	62	0.09	0.19	-0.26	0.89
	H23	302	0.06	0.14	-0.40	0.75	62	0.09	0.19	-0.25	0.71
	H24	302	0.06	0.15	-0.37	0.68	62	0.10	0.19	-0.23	0.83

Appendix I. Results of Fixed Effects Regression Models

Table I.1 Results of fixed effects O_3 models w.r.t. space and time during the Spring season

One-way fixed effects regression model w.r.t. Space					One-way fixed effects regression model w.r.t. Time				
Regressors	Par.	Std. Error	t Value	Pr > | t |	Regressors	Par.	Std. Error	t Value	Pr > | t |
α1	1.60	0.94	1.70	0.090	α1	-0.14	1.01	-0.14	0.892
α2	2.19	0.93	2.35	0.019	α2	0.09	1.02	0.09	0.926
α3	1.99	0.99	2.02	0.044	α3	-0.07	1.04	-0.07	0.945
α4	3.59	0.93	3.85	0.000	α4	-0.39	1.05	-0.37	0.709
α5	8.40	1.17	7.18	<.0001	α5	-0.79	1.05	-0.75	0.454
α6	7.66	0.92	8.34	<.0001	α6	-1.96	1.03	-1.90	0.058
α7	3.99	0.92	4.35	<.0001	α7	-1.41	1.00	-1.41	0.160
α8	1.03	0.93	1.10	0.271	α8	0.47	1.02	0.46	0.644
α9	5.93	0.92	6.47	<.0001	α9	2.74	1.04	2.64	0.008
α10	4.16	0.92	4.52	<.0001	α10	5.38	1.02	5.25	<.0001
α11	6.68	0.91	7.31	<.0001	α11	9.70	1.02	9.48	<.0001
α12	3.69	1.05	3.51	0.001	α12	14.55	1.02	14.27	<.0001
α13	4.21	1.04	4.06	<.0001	α13	18.62	1.01	18.41	<.0001
α14	-0.59	1.12	-0.53	0.598	α14	21.82	1.02	21.46	<.0001
α15	2.31	1.00	2.31	0.021	α15	23.65	1.02	23.19	<.0001
α16	4.65	0.91	5.10	<.0001	α16	23.80	1.02	23.31	<.0001
α17	-1.20	0.98	-1.23	0.219	α17	22.21	1.02	21.71	<.0001
α18	4.08	0.94	4.35	<.0001	α18	18.92	1.03	18.41	<.0001
α19	0.36	1.21	0.30	0.764	α19	14.23	1.03	13.79	<.0001
α20	2.63	0.98	2.67	0.008	α20	7.96	1.02	7.80	<.0001
α21	0.95	0.96	0.99	0.321	α21	3.79	1.01	3.76	0.000
α22	5.77	0.91	6.33	<.0001	α22	2.14	1.01	2.13	0.034
α23	2.93	1.03	2.86	0.004	α23	0.86	1.00	0.86	0.391
α24	2.49	0.98	2.56	0.011	Intercept	17.02	1.02	16.64	<.0001
α25	1.55	0.93	1.67	0.095	WVKT_R5500	-1.01	0.11	-9.40	<.0001
α26	3.56	1.15	3.10	0.002	ComDD	-16.71	4.18	-4.00	<.0001
α27	0.68	1.01	0.68	0.500	Res_R5000	-4.07	3.48	-1.17	0.243
α28	0.94	0.91	1.03	0.306	Ind_R4500	-2.69	1.52	-1.77	0.077
α29	-3.07	0.91	-3.35	0.001	NDVI_R1000	4.82	4.67	1.03	0.302
α30	-3.29	0.92	-3.57	0.000					
α31	-0.82	0.95	-0.86	0.390					
α32	-1.30	0.91	-1.42	0.156					
α33	-1.08	0.91	-1.18	0.239					
Intercept	25.44	8.77	2.90	0.004					
WVKT_R5500	-1.33	0.12	-10.68	<.0001					
Solar radiation	12.57	1.10	11.40	<.0001					
WS	0.73	1.12	0.65	0.516					
Temp	-0.41	0.40	-1.03	0.305					
Hum	-0.16	0.08	-2.09	0.037					
F-test for No Fixed Effects	F-value	19.5	Pr > F	<.0001	F-test for No Fixed Effects	F-value	126.4	Pr > F	<.0001
R^2	0.89				R^2	0.82			

Appendix J. First-Order Autoregressive Parameters in Panel Models

Table J.1 First-order autoregressive parameters in the O_3 models

AQM	O_3 Model			
	Spring	Summer	Autumn	Winter
1	0.92	0.76	0.79	0.99
2	0.76	0.95	0.92	0.90
3	0.91	0.79	0.79	0.82
4	0.80	0.76	0.42	0.58
5	0.93	0.82	0.71	0.94
6	0.93	0.82	0.96	0.87
7	0.64	0.87	0.94	0.72
8	0.92	0.86	0.95	0.94
9	0.91	0.89	0.83	0.89
10	0.75	0.75	0.65	0.90
11	0.92	0.80	0.66	0.82
12	0.95	0.89	0.92	0.69
13	0.88	0.92	0.87	0.60
14	0.86	0.27	0.45	0.89
15	0.78	0.81	0.92	0.82
16	0.88	0.90	0.59	0.83
17	0.99	0.87	0.75	0.89
28	0.94	0.76	0.86	0.77
29	0.94	0.85	0.94	0.67
30	0.94	0.58	0.71	0.71
31	0.91	0.80	0.63	0.81
32	0.91	0.67	0.76	0.94
33	0.90	0.83	0.81	0.91
34	0.92	0.92	0.89	0.74

Table J.2 First-order autoregressive parameters in the NO_2 models

AQM	SO_2 Model			
	Spring	Summer	Autumn	Winter
1	0.87	0.71	0.99	0.81
2	0.92	0.68	1.00	0.99
3	0.86	0.88	0.93	0.74
4	0.89	0.77	0.78	0.39
5	0.92	0.79	0.91	0.54
6	0.88	0.87	0.95	0.64
7	0.97	0.93	0.87	0.93
8	1.00	0.84	0.96	0.84
9	0.86	0.49	0.95	0.63
10	0.82	0.68	0.87	0.86
11	0.97	0.80	0.84	0.86
12	0.94	0.94	0.99	0.73
13	0.91	0.71	0.86	0.90
14	0.75	0.14	0.75	0.80
15	0.95	0.96	0.99	0.95
16	0.95	0.84	1.00	0.94
17	1.00	0.98	0.95	0.91
28	0.98	0.64	0.98	0.85
29	0.91	0.96	1.00	0.75
30	0.84	0.83	0.98	0.62
31	0.96	0.93	0.93	0.91
32	0.96	0.80	0.95	0.99
33	0.98	0.75	0.93	0.93
34	0.82	0.84	0.79	0.76

Table J.3 First-order autoregressive parameters in the CO models

AQM	CO Model			
	Spring	Summer	Autumn	Winter
1	0.81	0.95	0.97	0.71
2	0.97	0.91	0.86	0.99
3	0.88	0.98	0.90	0.77
4	0.96	0.93	0.83	0.98
5	0.74	0.98	0.80	0.71
6	0.85	0.90	0.75	0.56
7	0.96	0.91	0.99	0.77
8	0.97	0.93	0.90	0.91
9	0.74	0.62	0.88	0.68
10	0.78	0.92	0.92	0.68
11	0.60	0.95	0.78	0.59
12	0.88	0.96	0.96	0.79
13	0.94	0.89	0.86	0.83
14	0.99	0.98	0.72	0.93
15	0.65	0.75	0.90	0.97
16	0.98	0.99	0.95	0.99
17	0.80	0.81	0.92	0.49
28	0.92	0.96	0.89	0.94
29	0.93	0.95	0.99	0.51
30	0.85	0.86	1.00	0.89
31	0.98	0.97	0.99	0.99
32	0.94	0.73	0.99	0.94
33	0.99	0.99	0.99	0.99
34	0.97	0.99	0.97	0.94

Table J.4 First-order autoregressive parameters in the SO_2 models

AQM	SO_2 Model			
	Spring	Summer	Autumn	Winter
1	0.99	0.83	0.92	0.95
2	0.94	0.97	0.99	1.00
4	0.87	0.97	0.94	0.97
5	0.88	0.89	0.96	1.00
6	0.95	0.83	0.92	0.90
7	0.97	0.98	0.97	0.93
8	0.97	0.89	0.95	0.98
9	0.87	0.98	0.72	1.00
10	0.93	0.70	0.94	0.97
11	0.61	0.18	0.64	0.85
12	0.82	1.00	0.82	0.87
13	0.92	0.90	0.85	0.84
16	0.95	0.89	0.97	0.98
17	0.99	0.99	0.99	0.96
18	0.74	0.92	0.89	0.96
19	0.93	0.93	0.95	0.94
20	0.91	0.99	0.98	0.94
21	0.93	0.95	0.95	1.00
28	0.88	0.98	0.99	0.94
29	0.97	0.98	0.96	0.98
30	0.79	0.98	0.97	0.93
32	0.85	0.98	0.99	0.91
33	0.83	0.97	0.84	0.81
34	0.74	1.00	0.93	0.96

Table J.5 First-order autoregressive parameters in the PM10 models

AQM	PM10 Model			
	Spring	Summer	Autumn	Winter
1	0.86	0.87	0.93	0.93
3	0.99	0.96	0.96	0.97
4	0.97	0.95	0.79	0.83
5	0.96	0.96	0.93	0.89
6	0.92	0.92	0.91	0.95
7	0.91	0.86	0.99	0.95
8	0.97	0.93	0.89	0.95
9	0.93	0.40	0.77	0.62
10	0.78	0.79	0.98	0.98
11	0.97	0.83	0.85	0.71
12	0.92	0.90	0.92	0.89
13	0.85	0.84	0.94	0.81
14	0.93	0.93	0.95	0.95
15	0.81	0.83	0.91	0.76
16	0.90	0.99	0.86	0.97
18	0.98	0.68	0.98	0.88
20	0.89	0.84	0.79	0.86
28	0.94	0.75	0.69	0.47
29	0.99	0.69	0.79	0.94
30	0.94	0.79	0.82	0.69
31	0.93	0.98	0.94	0.73
32	0.57	0.87	0.70	0.91
33	0.94	0.94	0.86	0.65
34	0.93	0.95	0.95	0.85

Appendix K. Descriptive Statistics of Elasticities: Air Quality Panel Models

Table K.1 Hourly elasticities w.r.t. WVKT in the O_3 panel models

Variable	Model	Background WVKT Elasticities					Roadside WVKT Elasticities				
		N	Mean	Std.	Min	Max	N	Mean	Std.	Min	Max
Spring	H01	17	-0.27	0.12	-0.47	-0.04	7	-0.26	0.07	-0.39	-0.20
	H02	17	-0.18	0.07	-0.27	-0.02	7	-0.16	0.04	-0.22	-0.10
	H03	17	-0.14	0.06	-0.20	-0.02	7	-0.12	0.03	-0.17	-0.08
	H04	17	-0.11	0.04	-0.16	-0.01	7	-0.09	0.02	-0.12	-0.06
	H05	17	-0.11	0.05	-0.17	-0.01	7	-0.09	0.02	-0.12	-0.07
	H06	17	-0.18	0.08	-0.30	-0.02	7	-0.16	0.03	-0.22	-0.13
	H07	17	-0.45	0.20	-0.74	-0.05	7	-0.41	0.12	-0.59	-0.28
	H08	17	-0.73	0.34	-1.16	-0.10	7	-0.59	0.18	-0.85	-0.42
	H09	17	-0.58	0.26	-0.96	-0.08	7	-0.50	0.16	-0.78	-0.36
	H10	17	-0.40	0.17	-0.61	-0.06	7	-0.40	0.14	-0.67	-0.24
	H11	17	-0.28	0.12	-0.43	-0.05	7	-0.34	0.15	-0.63	-0.16
	H12	17	-0.21	0.08	-0.32	-0.04	7	-0.28	0.13	-0.52	-0.11
	H13	17	-0.16	0.07	-0.26	-0.03	7	-0.23	0.11	-0.43	-0.09
	H14	17	-0.15	0.06	-0.24	-0.03	7	-0.22	0.10	-0.42	-0.10
	H15	17	-0.15	0.06	-0.23	-0.03	7	-0.22	0.10	-0.39	-0.10
	H16	17	-0.15	0.06	-0.24	-0.03	7	-0.22	0.09	-0.36	-0.11
	H17	17	-0.16	0.06	-0.24	-0.03	7	-0.23	0.09	-0.37	-0.11
	H18	17	-0.19	0.07	-0.29	-0.03	7	-0.26	0.09	-0.39	-0.13
	H19	17	-0.24	0.10	-0.37	-0.04	7	-0.31	0.08	-0.44	-0.18
	H20	17	-0.32	0.13	-0.46	-0.05	7	-0.36	0.08	-0.51	-0.25
	H21	17	-0.38	0.18	-0.64	-0.05	7	-0.37	0.08	-0.53	-0.31
	H22	17	-0.42	0.18	-0.66	-0.06	7	-0.40	0.11	-0.58	-0.31
	H23	17	-0.48	0.22	-0.82	-0.06	7	-0.46	0.14	-0.69	-0.33
	H24	17	-0.42	0.19	-0.73	-0.05	7	-0.39	0.12	-0.61	-0.29
Summer	H01	17	-0.31	0.14	-0.56	-0.04	7	-0.18	0.06	-0.29	-0.13
	H02	17	-0.20	0.09	-0.31	-0.03	7	-0.11	0.04	-0.19	-0.08
	H03	17	-0.13	0.06	-0.21	-0.02	7	-0.08	0.03	-0.13	-0.05
	H04	17	-0.10	0.04	-0.17	-0.01	7	-0.06	0.02	-0.08	-0.04
	H05	17	-0.09	0.04	-0.15	-0.01	7	-0.05	0.01	-0.08	-0.04
	H06	17	-0.15	0.06	-0.25	-0.02	7	-0.09	0.03	-0.14	-0.07
	H07	17	-0.37	0.16	-0.62	-0.05	7	-0.23	0.07	-0.38	-0.17
	H08	17	-0.61	0.28	-1.07	-0.09	7	-0.35	0.12	-0.60	-0.25
	H09	17	-0.27	0.12	-0.48	-0.04	7	0.13	0.04	0.08	0.22
	H10	17	-0.19	0.08	-0.33	-0.03	7	0.10	0.03	0.07	0.16
	H11	17	-0.13	0.05	-0.22	-0.03	7	0.08	0.02	0.06	0.11
	H12	17	-0.09	0.04	-0.15	-0.02	7	0.06	0.01	0.04	0.08
	H13	17	-0.07	0.03	-0.10	-0.02	7	0.05	0.01	0.03	0.06
	H14	17	-0.06	0.02	-0.09	-0.01	7	0.04	0.01	0.03	0.06
	H15	17	-0.06	0.02	-0.09	-0.01	7	0.04	0.01	0.03	0.05
	H16	17	-0.06	0.02	-0.09	-0.01	7	0.04	0.01	0.03	0.05
	H17	17	-0.06	0.02	-0.09	-0.01	7	0.05	0.00	0.04	0.05
	H18	17	-0.08	0.03	-0.11	-0.02	7	0.06	0.01	0.05	0.07
	H19	17	-0.10	0.04	-0.15	-0.02	7	0.07	0.01	0.06	0.09
	H20	17	-0.14	0.06	-0.23	-0.02	7	0.09	0.02	0.08	0.12
	H21	17	-0.17	0.08	-0.32	-0.02	7	0.11	0.03	0.08	0.17
	H22	17	-0.22	0.11	-0.41	-0.03	7	0.13	0.05	0.09	0.20
	H23	17	-0.52	0.26	-1.01	-0.07	7	-0.34	0.14	-0.58	-0.21
	H24	17	-0.47	0.23	-0.88	-0.07	7	-0.30	0.11	-0.49	-0.21

Continued

Continued Table K.1

Variable	Model	Background WVKT Elasticities					Roadside WVKT Elasticities				
		N	Mean	Std.	Min	Max	N	Mean	Std.	Min	Max
Autumn	H01	17	-0.45	0.22	-0.89	-0.06	7	-0.28	0.06	-0.36	-0.22
	H02	17	-0.31	0.16	-0.66	-0.04	7	-0.20	0.04	-0.26	-0.16
	H03	17	-0.22	0.11	-0.45	-0.03	7	-0.14	0.03	-0.18	-0.12
	H04	17	-0.17	0.08	-0.31	-0.02	7	-0.11	0.02	-0.14	-0.09
	H05	17	-0.17	0.08	-0.31	-0.03	7	-0.11	0.02	-0.13	-0.09
	H06	17	-0.28	0.14	-0.51	-0.04	7	-0.19	0.04	-0.25	-0.14
	H07	17	-0.85	0.47	-1.74	-0.11	7	-0.51	0.17	-0.77	-0.32
	H08	17	-1.60	0.98	-3.77	-0.22	7	-0.77	0.27	-1.10	-0.46
	H09	17	-1.20	0.73	-2.86	-0.17	7	-0.46	0.13	-0.59	-0.28
	H10	17	-0.71	0.39	-1.48	-0.11	7	-0.33	0.07	-0.41	-0.22
	H11	17	-0.46	0.22	-0.83	-0.08	7	-0.24	0.05	-0.31	-0.18
	H12	17	-0.30	0.13	-0.51	-0.06	7	-0.19	0.03	-0.24	-0.15
	H13	17	-0.21	0.09	-0.33	-0.05	7	-0.14	0.02	-0.17	-0.11
	H14	17	-0.19	0.07	-0.28	-0.04	7	-0.14	0.03	-0.19	-0.10
	H15	17	-0.18	0.07	-0.28	-0.04	7	-0.13	0.02	-0.17	-0.10
	H16	17	-0.18	0.07	-0.29	-0.04	7	-0.14	0.02	-0.17	-0.12
	H17	17	-0.21	0.09	-0.36	-0.05	7	-0.16	0.02	-0.18	-0.13
	H18	17	-0.29	0.12	-0.50	-0.06	7	-0.20	0.02	-0.23	-0.18
	H19	17	-0.49	0.22	-0.82	-0.09	7	-0.29	0.06	-0.39	-0.23
	H20	17	-0.63	0.30	-1.07	-0.11	7	-0.32	0.08	-0.43	-0.24
	H21	17	-0.63	0.30	-1.04	-0.11	7	-0.32	0.09	-0.46	-0.22
	H22	17	-0.72	0.35	-1.38	-0.11	7	-0.34	0.11	-0.51	-0.22
	H23	17	-0.86	0.47	-1.79	-0.10	7	-0.51	0.18	-0.78	-0.30
	H24	17	-0.70	0.35	-1.29	-0.09	7	-0.44	0.11	-0.60	-0.31
Winter	H01	17	-0.34	0.16	-0.58	-0.05	7	-0.19	0.04	-0.25	-0.15
	H02	17	-0.22	0.10	-0.36	-0.03	7	-0.12	0.02	-0.15	-0.10
	H03	17	-0.16	0.07	-0.26	-0.02	7	-0.09	0.01	-0.11	-0.07
	H04	17	-0.13	0.05	-0.21	-0.02	7	-0.07	0.01	-0.08	-0.06
	H05	17	-0.14	0.06	-0.23	-0.02	7	-0.07	0.01	-0.09	-0.06
	H06	17	-0.25	0.10	-0.38	-0.04	7	-0.13	0.03	-0.18	-0.09
	H07	17	-0.75	0.39	-1.54	-0.09	7	-0.31	0.11	-0.45	-0.20
	H08	17	-1.73	1.35	-5.68	-0.16	7	-0.52	0.19	-0.77	-0.30
	H09	17	-1.58	1.33	-6.09	-0.16	7	-0.39	0.13	-0.59	-0.24
	H10	17	-0.89	0.47	-2.05	-0.10	7	-0.31	0.07	-0.42	-0.21
	H11	17	-0.61	0.30	-1.31	-0.08	7	-0.26	0.05	-0.34	-0.19
	H12	17	-0.45	0.20	-0.83	-0.07	7	-0.22	0.03	-0.26	-0.18
	H13	17	-0.32	0.13	-0.57	-0.05	7	-0.18	0.02	-0.21	-0.14
	H14	17	-0.28	0.11	-0.48	-0.05	7	-0.17	0.02	-0.21	-0.14
	H15	17	-0.27	0.11	-0.47	-0.05	7	-0.17	0.02	-0.21	-0.14
	H16	17	-0.28	0.12	-0.46	-0.05	7	-0.18	0.02	-0.22	-0.15
	H17	17	-0.33	0.15	-0.58	-0.06	7	-0.21	0.03	-0.25	-0.17
	H18	17	-0.47	0.23	-1.00	-0.07	7	-0.25	0.04	-0.33	-0.19
	H19	17	-0.65	0.34	-1.34	-0.09	7	-0.30	0.06	-0.40	-0.22
	H20	17	-0.69	0.33	-1.21	-0.10	7	-0.29	0.06	-0.35	-0.21
	H21	17	-0.60	0.29	-1.13	-0.09	7	-0.25	0.04	-0.30	-0.19
	H22	17	-0.60	0.30	-1.14	-0.09	7	-0.25	0.05	-0.32	-0.19
	H23	17	-0.64	0.31	-1.16	-0.09	7	-0.32	0.07	-0.40	-0.23
	H24	17	-0.55	0.26	-0.94	-0.08	7	-0.28	0.08	-0.44	-0.20

Table K.2 Hourly elasticities w.r.t. solar radiation in the O_3 panel models

Variable	Model	Background Solar Elasticities					Roadside Solar Elasticities				
		N	Mean	Std.	Min	Max	N	Mean	Std.	Min	Max
Spring	H01	17	0.00	0.00	0.00	0.00	7	0.00	0.00	0.00	0.00
	H02	17	0.00	0.00	0.00	0.00	7	0.00	0.00	0.00	0.00
	H03	17	0.00	0.00	0.00	0.00	7	0.00	0.00	0.00	0.00
	H04	17	0.00	0.00	0.00	0.00	7	0.00	0.00	0.00	0.00
	H05	17	0.00	0.00	0.00	0.00	7	0.00	0.00	0.00	0.00
	H06	17	0.00	0.00	0.00	0.00	7	0.00	0.00	0.00	0.00
	H07	17	0.04	0.01	0.02	0.06	7	0.02	0.01	0.02	0.03
	H08	17	0.21	0.05	0.11	0.28	7	0.12	0.03	0.08	0.15
	H09	17	0.45	0.10	0.25	0.68	7	0.29	0.07	0.23	0.40
	H10	17	0.66	0.14	0.38	0.91	7	0.49	0.12	0.39	0.73
	H11	17	0.78	0.16	0.51	1.13	7	0.69	0.23	0.43	1.15
	H12	17	0.86	0.15	0.63	1.23	7	0.83	0.32	0.45	1.39
	H13	17	0.92	0.15	0.70	1.25	7	0.95	0.38	0.52	1.60
	H14	17	0.96	0.14	0.72	1.28	7	1.05	0.41	0.64	1.74
	H15	17	0.98	0.14	0.73	1.29	7	1.09	0.41	0.65	1.69
	H16	17	0.97	0.14	0.72	1.27	7	1.08	0.36	0.69	1.55
	H17	17	0.94	0.13	0.68	1.20	7	1.02	0.33	0.64	1.45
	H18	17	0.91	0.14	0.62	1.17	7	0.93	0.27	0.61	1.23
	H19	17	0.87	0.14	0.55	1.13	7	0.84	0.16	0.65	1.04
	H20	17	0.86	0.15	0.49	1.05	7	0.72	0.08	0.65	0.90
	H21	17	0.71	0.15	0.39	1.02	7	0.53	0.08	0.43	0.66
	H22	17	0.43	0.09	0.23	0.58	7	0.31	0.06	0.23	0.40
	H23	17	0.20	0.05	0.09	0.31	7	0.13	0.03	0.09	0.18
	H24	17	0.04	0.01	0.02	0.07	7	0.03	0.01	0.02	0.04
Summer	H01	17	0.04	0.01	0.02	0.06	7	0.03	0.01	0.02	0.04
	H02	17	0.00	0.00	0.00	0.00	7	0.00	0.00	0.00	0.00
	H03	17	0.00	0.00	0.00	0.00	7	0.00	0.00	0.00	0.00
	H04	17	0.00	0.00	0.00	0.00	7	0.00	0.00	0.00	0.00
	H05	17	0.00	0.00	0.00	0.00	7	0.00	0.00	0.00	0.00
	H06	17	0.08	0.02	0.04	0.11	7	0.06	0.02	0.04	0.09
	H07	17	0.20	0.05	0.11	0.28	7	0.15	0.05	0.10	0.23
	H08	17	0.52	0.13	0.31	0.76	7	0.36	0.11	0.24	0.55
	H09	17	0.86	0.20	0.55	1.39	7	0.60	0.17	0.36	0.91
	H10	17	1.10	0.25	0.75	1.75	7	0.85	0.21	0.54	1.21
	H11	17	1.19	0.24	0.85	1.76	7	1.02	0.17	0.78	1.25
	H12	17	1.16	0.19	0.88	1.63	7	1.08	0.13	0.93	1.25
	H13	17	1.15	0.16	0.90	1.56	7	1.13	0.12	0.97	1.29
	H14	17	1.12	0.14	0.88	1.47	7	1.12	0.12	0.97	1.26
	H15	17	1.13	0.14	0.90	1.44	7	1.15	0.12	1.00	1.28
	H16	17	1.13	0.15	0.91	1.52	7	1.17	0.11	1.00	1.36
	H17	17	1.16	0.16	0.89	1.50	7	1.22	0.11	1.07	1.35
	H18	17	1.17	0.16	0.89	1.44	7	1.26	0.14	1.06	1.47
	H19	17	1.20	0.15	0.90	1.43	7	1.26	0.16	0.92	1.37
	H20	17	1.30	0.22	0.81	1.66	7	1.28	0.23	0.93	1.52
	H21	17	1.24	0.26	0.67	1.77	7	1.16	0.30	0.82	1.55
	H22	17	0.99	0.24	0.48	1.43	7	0.82	0.28	0.54	1.18
	H23	17	0.59	0.17	0.29	0.89	7	0.46	0.17	0.28	0.73
	H24	17	0.22	0.06	0.13	0.35	7	0.16	0.05	0.11	0.25

Continued

Continued Table K.2

Variable	Model	Background Solar Elasticities					Roadside Solar Elasticities				
		N	Mean	Std.	Min	Max	N	Mean	Std.	Min	Max
Autumn	H01	17	0.00	0.00	0.00	0.00	7	0.00	0.00	0.00	0.00
	H02	17	0.00	0.00	0.00	0.00	7	0.00	0.00	0.00	0.00
	H03	17	0.00	0.00	0.00	0.00	7	0.00	0.00	0.00	0.00
	H04	17	0.00	0.00	0.00	0.00	7	0.00	0.00	0.00	0.00
	H05	17	0.00	0.00	0.00	0.00	7	0.00	0.00	0.00	0.00
	H06	17	0.00	0.00	0.00	0.00	7	0.00	0.00	0.00	0.00
	H07	17	0.00	0.00	0.00	0.00	7	0.00	0.00	0.00	0.00
	H08	17	0.09	0.04	0.05	0.20	7	0.04	0.01	0.02	0.05
	H09	17	0.34	0.14	0.19	0.75	7	0.14	0.04	0.08	0.19
	H10	17	0.59	0.19	0.35	1.05	7	0.28	0.07	0.18	0.37
	H11	17	0.71	0.19	0.45	1.09	7	0.38	0.07	0.27	0.46
	H12	17	0.75	0.15	0.53	0.99	7	0.46	0.05	0.37	0.52
	H13	17	0.77	0.14	0.57	1.02	7	0.51	0.04	0.46	0.57
	H14	17	0.80	0.13	0.59	1.04	7	0.57	0.10	0.48	0.77
	H15	17	0.82	0.13	0.59	1.07	7	0.60	0.08	0.51	0.76
	H16	17	0.81	0.11	0.59	1.00	7	0.61	0.06	0.54	0.72
	H17	17	0.80	0.13	0.57	1.07	7	0.60	0.06	0.51	0.66
	H18	17	0.85	0.15	0.58	1.14	7	0.59	0.06	0.51	0.67
	H19	17	0.97	0.21	0.62	1.31	7	0.59	0.14	0.43	0.75
	H20	17	0.82	0.20	0.54	1.15	7	0.44	0.13	0.29	0.58
	H21	17	0.48	0.11	0.33	0.68	7	0.25	0.08	0.16	0.34
	H22	17	0.22	0.05	0.13	0.31	7	0.10	0.04	0.07	0.15
	H23	17	0.06	0.02	0.03	0.10	7	0.03	0.01	0.02	0.04
	H24	17	0.02	0.00	0.01	0.02	7	0.01	0.00	0.01	0.01
Winter	H01	17	0.00	0.00	0.00	0.00	7	0.00	0.00	0.00	0.00
	H02	17	0.00	0.00	0.00	0.00	7	0.00	0.00	0.00	0.00
	H03	17	0.00	0.00	0.00	0.00	7	0.00	0.00	0.00	0.00
	H04	17	0.00	0.00	0.00	0.00	7	0.00	0.00	0.00	0.00
	H05	17	0.00	0.00	0.00	0.00	7	0.00	0.00	0.00	0.00
	H06	17	0.00	0.00	0.00	0.00	7	0.00	0.00	0.00	0.00
	H07	17	0.00	0.00	0.00	0.00	7	0.00	0.00	0.00	0.00
	H08	17	0.00	0.00	0.00	0.00	7	0.00	0.00	0.00	0.00
	H09	17	0.05	0.03	0.02	0.17	7	0.00	0.00	0.00	0.00
	H10	17	0.16	0.06	0.07	0.32	7	-0.01	0.00	-0.01	-0.01
	H11	17	0.25	0.08	0.13	0.49	7	-0.02	0.00	-0.02	-0.01
	H12	17	0.33	0.09	0.19	0.54	7	-0.02	0.00	-0.03	-0.02
	H13	17	0.36	0.08	0.23	0.52	7	-0.03	0.00	-0.03	-0.02
	H14	17	0.40	0.08	0.26	0.52	7	-0.03	0.00	-0.04	-0.03
	H15	17	0.44	0.08	0.30	0.58	7	-0.04	0.01	-0.05	-0.03
	H16	17	0.45	0.09	0.30	0.64	7	-0.04	0.01	-0.06	-0.03
	H17	17	0.46	0.11	0.29	0.72	7	-0.04	0.01	-0.06	-0.03
	H18	17	0.49	0.16	0.28	0.95	7	-0.04	0.01	-0.07	-0.03
	H19	17	0.47	0.15	0.26	0.89	7	-0.03	0.01	-0.06	-0.02
	H20	17	0.33	0.08	0.19	0.52	7	-0.02	0.01	-0.03	-0.01
	H21	17	0.16	0.04	0.09	0.23	7	-0.01	0.00	-0.02	-0.01
	H22	17	0.06	0.01	0.03	0.08	7	0.00	0.00	-0.01	0.00
	H23	17	0.01	0.00	0.00	0.01	7	0.00	0.00	0.00	0.00
	H24	17	0.00	0.00	0.00	0.00	7	0.00	0.00	0.00	0.00

Table K.3 Hourly elasticities w.r.t. WVKT in the NO_2 panel models

Variable	Model	Background WVKT Elasticities					Roadside WVKT Elasticities				
		N	Mean	Std.	Min	Max	N	Mean	Std.	Min	Max
Spring	H01	17	0.08	0.02	0.04	0.11	7	0.14	0.03	0.10	0.17
	H02	17	0.07	0.02	0.04	0.09	7	0.12	0.02	0.09	0.15
	H03	17	0.06	0.02	0.03	0.08	7	0.10	0.02	0.07	0.12
	H04	17	0.05	0.01	0.02	0.06	7	0.08	0.02	0.06	0.11
	H05	17	0.05	0.01	0.03	0.06	7	0.08	0.02	0.06	0.10
	H06	17	0.06	0.02	0.03	0.09	7	0.10	0.02	0.06	0.12
	H07	17	0.12	0.04	0.06	0.18	7	0.17	0.03	0.11	0.21
	H08	17	0.17	0.05	0.07	0.27	7	0.25	0.04	0.15	0.28
	H09	17	0.17	0.05	0.07	0.28	7	0.25	0.05	0.14	0.29
	H10	17	0.16	0.05	0.07	0.23	7	0.23	0.05	0.13	0.26
	H11	17	0.17	0.05	0.07	0.23	7	0.22	0.04	0.14	0.26
	H12	17	0.18	0.05	0.07	0.26	7	0.22	0.04	0.14	0.27
	H13	17	0.19	0.06	0.07	0.27	7	0.21	0.04	0.13	0.26
	H14	17	0.20	0.06	0.08	0.29	7	0.22	0.05	0.12	0.27
	H15	17	0.20	0.06	0.09	0.30	7	0.22	0.05	0.13	0.28
	H16	17	0.20	0.05	0.08	0.27	7	0.21	0.04	0.13	0.27
	H17	17	0.19	0.05	0.08	0.26	7	0.21	0.05	0.12	0.27
	H18	17	0.18	0.05	0.08	0.25	7	0.22	0.05	0.13	0.27
	H19	17	0.17	0.05	0.08	0.24	7	0.22	0.04	0.14	0.27
	H20	17	0.14	0.04	0.07	0.20	7	0.20	0.04	0.13	0.25
	H21	17	0.12	0.03	0.06	0.16	7	0.18	0.03	0.11	0.22
	H22	17	0.12	0.03	0.06	0.16	7	0.18	0.04	0.11	0.21
	H23	17	0.12	0.03	0.06	0.16	7	0.18	0.03	0.11	0.21
	H24	17	0.10	0.03	0.05	0.14	7	0.16	0.03	0.10	0.20
Summer	H01	17	0.11	0.03	0.05	0.17	7	0.20	0.03	0.14	0.24
	H02	17	0.10	0.03	0.05	0.14	7	0.17	0.04	0.12	0.22
	H03	17	0.08	0.03	0.04	0.13	7	0.15	0.03	0.11	0.20
	H04	17	0.07	0.02	0.04	0.11	7	0.13	0.03	0.09	0.17
	H05	17	0.08	0.02	0.04	0.11	7	0.13	0.03	0.09	0.17
	H06	17	0.10	0.03	0.05	0.15	7	0.15	0.04	0.09	0.23
	H07	17	0.18	0.06	0.08	0.26	7	0.26	0.07	0.15	0.38
	H08	17	0.25	0.08	0.10	0.37	7	0.35	0.09	0.21	0.49
	H09	17	0.29	0.09	0.11	0.42	7	0.39	0.10	0.23	0.53
	H10	17	0.27	0.08	0.10	0.37	7	0.35	0.07	0.22	0.46
	H11	17	0.26	0.08	0.10	0.37	7	0.33	0.07	0.22	0.44
	H12	17	0.27	0.08	0.10	0.39	7	0.32	0.07	0.21	0.44
	H13	17	0.26	0.08	0.10	0.39	7	0.29	0.06	0.20	0.39
	H14	17	0.28	0.09	0.11	0.43	7	0.30	0.06	0.20	0.39
	H15	17	0.28	0.09	0.11	0.41	7	0.29	0.06	0.19	0.37
	H16	17	0.28	0.09	0.11	0.41	7	0.29	0.06	0.19	0.37
	H17	17	0.26	0.08	0.11	0.37	7	0.28	0.06	0.18	0.36
	H18	17	0.26	0.08	0.10	0.34	7	0.29	0.06	0.19	0.37
	H19	17	0.24	0.07	0.10	0.33	7	0.30	0.06	0.19	0.39
	H20	17	0.20	0.06	0.09	0.29	7	0.28	0.05	0.19	0.36
	H21	17	0.18	0.05	0.08	0.25	7	0.26	0.05	0.17	0.34
	H22	17	0.17	0.05	0.08	0.25	7	0.26	0.05	0.17	0.34
	H23	17	0.15	0.04	0.07	0.21	7	0.23	0.05	0.15	0.31
	H24	17	0.14	0.04	0.06	0.19	7	0.22	0.04	0.15	0.27

Continued

Continued Table K.3

Variable	Model	Background WVKT Elasticities					Roadside WVKT Elasticities				
		N	Mean	Std.	Min	Max	N	Mean	Std.	Min	Max
Autumn	H01	17	0.16	0.05	0.07	0.25	7	0.21	0.05	0.15	0.26
	H02	17	0.13	0.04	0.06	0.20	7	0.17	0.04	0.12	0.22
	H03	17	0.11	0.04	0.05	0.17	7	0.15	0.04	0.10	0.19
	H04	17	0.09	0.03	0.04	0.15	7	0.12	0.03	0.08	0.17
	H05	17	0.09	0.03	0.04	0.15	7	0.12	0.03	0.08	0.17
	H06	17	0.12	0.05	0.05	0.20	7	0.15	0.05	0.10	0.24
	H07	17	0.23	0.09	0.09	0.39	7	0.26	0.09	0.17	0.43
	H08	17	0.33	0.13	0.12	0.57	7	0.38	0.10	0.24	0.57
	H09	17	0.38	0.14	0.14	0.62	7	0.42	0.11	0.25	0.60
	H10	17	0.34	0.12	0.13	0.53	7	0.39	0.10	0.25	0.53
	H11	17	0.34	0.11	0.14	0.50	7	0.38	0.10	0.26	0.50
	H12	17	0.35	0.11	0.14	0.50	7	0.38	0.09	0.26	0.49
	H13	17	0.34	0.11	0.13	0.49	7	0.35	0.09	0.24	0.47
	H14	17	0.36	0.12	0.13	0.51	7	0.36	0.10	0.23	0.50
	H15	17	0.36	0.12	0.13	0.51	7	0.36	0.10	0.23	0.48
	H16	17	0.34	0.11	0.14	0.51	7	0.35	0.10	0.22	0.48
	H17	17	0.33	0.11	0.13	0.50	7	0.35	0.10	0.22	0.47
	H18	17	0.31	0.11	0.12	0.49	7	0.36	0.10	0.23	0.47
	H19	17	0.29	0.10	0.12	0.47	7	0.36	0.10	0.23	0.47
	H20	17	0.26	0.09	0.11	0.43	7	0.33	0.08	0.22	0.43
	H21	17	0.24	0.08	0.10	0.40	7	0.29	0.07	0.19	0.39
	H22	17	0.23	0.08	0.10	0.38	7	0.29	0.06	0.20	0.39
	H23	17	0.21	0.07	0.09	0.33	7	0.26	0.06	0.18	0.35
	H24	17	0.19	0.07	0.08	0.30	7	0.23	0.05	0.17	0.30
Winter	H01	17	0.13	0.05	0.06	0.24	7	0.23	0.03	0.19	0.30
	H02	17	0.10	0.04	0.05	0.20	7	0.19	0.03	0.16	0.24
	H03	17	0.08	0.03	0.04	0.16	7	0.15	0.02	0.13	0.19
	H04	17	0.07	0.03	0.03	0.13	7	0.13	0.02	0.11	0.16
	H05	17	0.06	0.03	0.03	0.13	7	0.12	0.02	0.09	0.15
	H06	17	0.08	0.03	0.04	0.18	7	0.14	0.03	0.10	0.18
	H07	17	0.16	0.06	0.07	0.32	7	0.25	0.05	0.17	0.29
	H08	17	0.22	0.08	0.10	0.42	7	0.35	0.08	0.22	0.43
	H09	17	0.23	0.08	0.10	0.41	7	0.36	0.09	0.22	0.46
	H10	17	0.22	0.07	0.09	0.35	7	0.33	0.08	0.20	0.43
	H11	17	0.21	0.06	0.09	0.34	7	0.33	0.08	0.22	0.45
	H12	17	0.21	0.07	0.09	0.34	7	0.33	0.08	0.20	0.43
	H13	17	0.21	0.07	0.09	0.32	7	0.32	0.07	0.20	0.41
	H14	17	0.23	0.08	0.09	0.37	7	0.34	0.09	0.21	0.47
	H15	17	0.24	0.08	0.10	0.36	7	0.36	0.09	0.21	0.48
	H16	17	0.23	0.08	0.09	0.36	7	0.35	0.09	0.21	0.46
	H17	17	0.23	0.08	0.09	0.36	7	0.35	0.09	0.21	0.47
	H18	17	0.22	0.07	0.09	0.36	7	0.35	0.08	0.21	0.46
	H19	17	0.22	0.07	0.09	0.37	7	0.36	0.08	0.23	0.47
	H20	17	0.21	0.07	0.09	0.37	7	0.34	0.07	0.23	0.43
	H21	17	0.19	0.07	0.08	0.36	7	0.31	0.07	0.21	0.39
	H22	17	0.19	0.07	0.08	0.38	7	0.31	0.07	0.20	0.38
	H23	17	0.18	0.07	0.08	0.38	7	0.29	0.06	0.21	0.36
	H24	17	0.16	0.06	0.07	0.32	7	0.27	0.04	0.20	0.32

Table K.4 Hourly elasticities w.r.t. solar radiation in the NO_2 panel models

Variable	Model	Background Solar Elasticities					Roadside Solar Elasticities				
		N	Mean	Std.	Min	Max	N	Mean	Std.	Min	Max
Spring	H01	17	0.00	0.00	0.00	0.00	7	0.00	0.00	0.00	0.00
	H02	17	0.00	0.00	0.00	0.00	7	0.00	0.00	0.00	0.00
	H03	17	0.00	0.00	0.00	0.00	7	0.00	0.00	0.00	0.00
	H04	17	0.00	0.00	0.00	0.00	7	0.00	0.00	0.00	0.00
	H05	17	0.00	0.00	0.00	0.00	7	0.00	0.00	0.00	0.00
	H06	17	0.00	0.00	0.00	0.00	7	0.00	0.00	0.00	0.00
	H07	17	-0.01	0.00	-0.02	-0.01	7	-0.01	0.00	-0.01	-0.01
	H08	17	-0.06	0.01	-0.08	-0.04	7	-0.03	0.00	-0.04	-0.03
	H09	17	-0.16	0.03	-0.21	-0.11	7	-0.09	0.01	-0.11	-0.07
	H10	17	-0.32	0.05	-0.40	-0.21	7	-0.18	0.03	-0.21	-0.14
	H11	17	-0.55	0.08	-0.68	-0.35	7	-0.29	0.04	-0.36	-0.24
	H12	17	-0.84	0.11	-1.03	-0.58	7	-0.42	0.07	-0.54	-0.34
	H13	17	-1.21	0.16	-1.57	-0.87	7	-0.56	0.10	-0.73	-0.44
	H14	17	-1.48	0.22	-1.89	-1.02	7	-0.66	0.12	-0.84	-0.48
	H15	17	-1.58	0.24	-2.00	-1.04	7	-0.70	0.14	-0.92	-0.53
	H16	17	-1.50	0.23	-1.91	-1.03	7	-0.66	0.12	-0.86	-0.52
	H17	17	-1.31	0.20	-1.62	-0.91	7	-0.59	0.12	-0.79	-0.44
	H18	17	-1.03	0.16	-1.24	-0.70	7	-0.50	0.09	-0.65	-0.39
	H19	17	-0.73	0.12	-0.89	-0.48	7	-0.38	0.06	-0.48	-0.31
	H20	17	-0.45	0.08	-0.57	-0.30	7	-0.26	0.04	-0.33	-0.21
	H21	17	-0.27	0.05	-0.34	-0.18	7	-0.16	0.03	-0.20	-0.13
	H22	17	-0.14	0.03	-0.18	-0.10	7	-0.09	0.02	-0.11	-0.07
	H23	17	-0.06	0.01	-0.08	-0.04	7	-0.04	0.01	-0.04	-0.03
	H24	17	-0.01	0.00	-0.02	-0.01	7	-0.01	0.00	-0.01	-0.01
Summer	H01	17	-0.01	0.00	-0.01	0.00	7	0.00	0.00	0.00	0.00
	H02	17	0.00	0.00	0.00	0.00	7	0.00	0.00	0.00	0.00
	H03	17	0.00	0.00	0.00	0.00	7	0.00	0.00	0.00	0.00
	H04	17	0.00	0.00	0.00	0.00	7	0.00	0.00	0.00	0.00
	H05	17	0.00	0.00	0.00	0.00	7	0.00	0.00	0.00	0.00
	H06	17	-0.02	0.01	-0.03	-0.02	7	-0.01	0.00	-0.01	-0.01
	H07	17	-0.04	0.01	-0.06	-0.03	7	-0.01	0.00	-0.02	-0.01
	H08	17	-0.08	0.02	-0.13	-0.06	7	-0.03	0.00	-0.03	-0.02
	H09	17	-0.15	0.03	-0.23	-0.11	7	-0.05	0.01	-0.06	-0.04
	H10	17	-0.26	0.05	-0.38	-0.18	7	-0.08	0.01	-0.10	-0.07
	H11	17	-0.40	0.08	-0.56	-0.27	7	-0.12	0.01	-0.14	-0.10
	H12	17	-0.55	0.10	-0.76	-0.38	7	-0.15	0.02	-0.20	-0.13
	H13	17	-0.74	0.14	-1.04	-0.50	7	-0.19	0.03	-0.24	-0.16
	H14	17	-0.87	0.17	-1.29	-0.60	7	-0.21	0.03	-0.26	-0.18
	H15	17	-0.92	0.19	-1.37	-0.63	7	-0.22	0.03	-0.26	-0.18
	H16	17	-0.90	0.18	-1.33	-0.63	7	-0.22	0.03	-0.26	-0.18
	H17	17	-0.79	0.16	-1.17	-0.53	7	-0.20	0.03	-0.24	-0.16
	H18	17	-0.66	0.13	-0.97	-0.45	7	-0.17	0.02	-0.20	-0.15
	H19	17	-0.48	0.10	-0.70	-0.33	7	-0.14	0.02	-0.17	-0.12
	H20	17	-0.33	0.07	-0.49	-0.23	7	-0.11	0.01	-0.12	-0.09
	H21	17	-0.22	0.04	-0.32	-0.16	7	-0.07	0.01	-0.09	-0.06
	H22	17	-0.13	0.03	-0.20	-0.10	7	-0.05	0.01	-0.06	-0.04
	H23	17	-0.07	0.01	-0.10	-0.05	7	-0.02	0.00	-0.03	-0.02
	H24	17	-0.03	0.00	-0.04	-0.02	7	-0.01	0.00	-0.01	-0.01

Continued

Continued Table K.4

Variable	Model	Background Solar Elasticities					Roadside Solar Elasticities				
		N	Mean	Std.	Min	Max	N	Mean	Std.	Min	Max
Autumn	H01	17	0.00	0.00	0.00	0.00	7	0.00	0.00	0.00	0.00
	H02	17	0.00	0.00	0.00	0.00	7	0.00	0.00	0.00	0.00
	H03	17	0.00	0.00	0.00	0.00	7	0.00	0.00	0.00	0.00
	H04	17	0.00	0.00	0.00	0.00	7	0.00	0.00	0.00	0.00
	H05	17	0.00	0.00	0.00	0.00	7	0.00	0.00	0.00	0.00
	H06	17	0.00	0.00	0.00	0.00	7	0.00	0.00	0.00	0.00
	H07	17	0.00	0.00	0.00	0.00	7	0.00	0.00	0.00	0.00
	H08	17	-0.01	0.00	-0.01	-0.01	7	0.00	0.00	0.00	0.00
	H09	17	-0.03	0.01	-0.05	-0.02	7	-0.01	0.00	-0.02	-0.01
	H10	17	-0.09	0.02	-0.11	-0.06	7	-0.03	0.01	-0.04	-0.02
	H11	17	-0.16	0.03	-0.22	-0.12	7	-0.06	0.02	-0.08	-0.04
	H12	17	-0.26	0.05	-0.34	-0.19	7	-0.10	0.02	-0.13	-0.07
	H13	17	-0.38	0.06	-0.49	-0.27	7	-0.13	0.03	-0.17	-0.09
	H14	17	-0.46	0.07	-0.59	-0.34	7	-0.16	0.04	-0.21	-0.11
	H15	17	-0.49	0.07	-0.61	-0.37	7	-0.18	0.04	-0.23	-0.12
	H16	17	-0.46	0.07	-0.55	-0.35	7	-0.16	0.04	-0.22	-0.11
	H17	17	-0.37	0.05	-0.46	-0.29	7	-0.14	0.04	-0.19	-0.09
	H18	17	-0.27	0.04	-0.35	-0.21	7	-0.11	0.03	-0.14	-0.07
	H19	17	-0.18	0.03	-0.23	-0.14	7	-0.08	0.02	-0.10	-0.05
	H20	17	-0.11	0.02	-0.14	-0.08	7	-0.05	0.01	-0.06	-0.04
	H21	17	-0.06	0.01	-0.07	-0.04	7	-0.02	0.00	-0.03	-0.02
	H22	17	-0.02	0.00	-0.03	-0.02	7	-0.01	0.00	-0.01	-0.01
	H23	17	-0.01	0.00	-0.01	0.00	7	0.00	0.00	0.00	0.00
	H24	17	0.00	0.00	0.00	0.00	7	0.00	0.00	0.00	0.00
Winter	H01	17	0.00	0.00	0.00	0.00	7	0.00	0.00	0.00	0.00
	H02	17	0.00	0.00	0.00	0.00	7	0.00	0.00	0.00	0.00
	H03	17	0.00	0.00	0.00	0.00	7	0.00	0.00	0.00	0.00
	H04	17	0.00	0.00	0.00	0.00	7	0.00	0.00	0.00	0.00
	H05	17	0.00	0.00	0.00	0.00	7	0.00	0.00	0.00	0.00
	H06	17	0.00	0.00	0.00	0.00	7	0.00	0.00	0.00	0.00
	H07	17	0.00	0.00	0.00	0.00	7	0.00	0.00	0.00	0.00
	H08	17	0.00	0.00	0.00	0.00	7	0.00	0.00	0.00	0.00
	H09	17	0.00	0.00	-0.01	0.00	7	0.00	0.00	0.00	0.00
	H10	17	-0.02	0.00	-0.03	-0.02	7	-0.01	0.00	-0.02	-0.01
	H11	17	-0.05	0.01	-0.07	-0.04	7	-0.03	0.01	-0.04	-0.02
	H12	17	-0.09	0.01	-0.12	-0.07	7	-0.05	0.01	-0.06	-0.04
	H13	17	-0.13	0.02	-0.20	-0.11	7	-0.07	0.01	-0.10	-0.06
	H14	17	-0.18	0.03	-0.24	-0.14	7	-0.09	0.02	-0.13	-0.07
	H15	17	-0.20	0.03	-0.27	-0.16	7	-0.11	0.02	-0.16	-0.08
	H16	17	-0.20	0.03	-0.26	-0.16	7	-0.11	0.02	-0.15	-0.08
	H17	17	-0.17	0.02	-0.22	-0.14	7	-0.09	0.02	-0.13	-0.07
	H18	17	-0.13	0.02	-0.17	-0.10	7	-0.07	0.01	-0.10	-0.06
	H19	17	-0.09	0.01	-0.12	-0.07	7	-0.05	0.01	-0.07	-0.04
	H20	17	-0.06	0.01	-0.08	-0.04	7	-0.03	0.01	-0.04	-0.03
	H21	17	-0.03	0.01	-0.04	-0.02	7	-0.02	0.00	-0.02	-0.01
	H22	17	-0.01	0.00	-0.02	-0.01	7	-0.01	0.00	-0.01	0.00
	H23	17	0.00	0.00	0.00	0.00	7	0.00	0.00	0.00	0.00
	H24	17	0.00	0.00	0.00	0.00	7	0.00	0.00	0.00	0.00

Continued

Table K.5 Hourly elasticities w.r.t. WVKT in the CO panel models

Variable	Model	Background WVKT Elasticities					Roadside WVKT Elasticities				
		N	Mean	Std.	Min	Max	N	Mean	Std.	Min	Max
Spring	H01	17	0.05	0.02	0.02	0.07	7	0.18	0.08	0.09	0.27
	H02	17	0.04	0.01	0.02	0.06	7	0.13	0.06	0.07	0.21
	H03	17	0.03	0.01	0.02	0.05	7	0.11	0.05	0.05	0.18
	H04	17	0.02	0.01	0.01	0.04	7	0.10	0.05	0.05	0.16
	H05	17	0.02	0.01	0.01	0.04	7	0.10	0.05	0.05	0.15
	H06	17	0.03	0.01	0.02	0.06	7	0.13	0.06	0.06	0.21
	H07	17	0.06	0.02	0.04	0.11	7	0.24	0.10	0.11	0.35
	H08	17	0.09	0.03	0.05	0.16	7	0.30	0.11	0.15	0.45
	H09	17	0.10	0.03	0.05	0.17	7	0.31	0.10	0.16	0.48
	H10	17	0.11	0.03	0.06	0.16	7	0.28	0.09	0.14	0.45
	H11	17	0.12	0.03	0.06	0.18	7	0.27	0.08	0.15	0.41
	H12	17	0.13	0.04	0.07	0.20	7	0.28	0.09	0.16	0.44
	H13	17	0.14	0.04	0.07	0.21	7	0.30	0.10	0.14	0.46
	H14	17	0.14	0.04	0.07	0.23	7	0.33	0.11	0.16	0.44
	H15	17	0.15	0.04	0.07	0.24	7	0.33	0.11	0.15	0.49
	H16	17	0.15	0.05	0.07	0.24	7	0.31	0.10	0.15	0.44
	H17	17	0.15	0.05	0.07	0.24	7	0.32	0.10	0.15	0.46
	H18	17	0.15	0.05	0.06	0.24	7	0.32	0.10	0.15	0.42
	H19	17	0.14	0.04	0.06	0.21	7	0.30	0.09	0.14	0.41
	H20	17	0.11	0.03	0.05	0.18	7	0.28	0.09	0.14	0.42
	H21	17	0.10	0.03	0.05	0.15	7	0.27	0.11	0.13	0.48
	H22	17	0.09	0.03	0.05	0.14	7	0.26	0.12	0.13	0.49
	H23	17	0.08	0.02	0.04	0.12	7	0.24	0.09	0.13	0.40
	H24	17	0.06	0.02	0.03	0.10	7	0.22	0.10	0.12	0.38
Summer	H01	17	0.00	0.00	0.00	0.00	7	0.15	0.07	0.08	0.28
	H02	17	0.00	0.00	0.00	0.00	7	0.12	0.06	0.06	0.23
	H03	17	0.00	0.00	0.00	0.00	7	0.10	0.05	0.05	0.20
	H04	17	0.00	0.00	0.00	0.00	7	0.09	0.05	0.04	0.18
	H05	17	0.00	0.00	0.00	0.00	7	0.10	0.06	0.04	0.20
	H06	17	0.00	0.00	0.00	0.00	7	0.14	0.07	0.05	0.26
	H07	17	0.00	0.00	0.00	0.00	7	0.24	0.10	0.10	0.38
	H08	17	0.00	0.00	0.00	0.00	7	0.29	0.12	0.13	0.44
	H09	17	0.06	0.02	0.04	0.10	7	0.31	0.11	0.16	0.47
	H10	17	0.06	0.02	0.04	0.10	7	0.26	0.09	0.15	0.42
	H11	17	0.06	0.02	0.04	0.11	7	0.25	0.09	0.16	0.39
	H12	17	0.07	0.02	0.04	0.12	7	0.25	0.08	0.16	0.39
	H13	17	0.07	0.02	0.04	0.11	7	0.29	0.10	0.16	0.39
	H14	17	0.07	0.02	0.04	0.12	7	0.32	0.12	0.17	0.42
	H15	17	0.07	0.02	0.04	0.12	7	0.31	0.11	0.16	0.42
	H16	17	0.08	0.02	0.04	0.13	7	0.29	0.09	0.16	0.38
	H17	17	0.08	0.02	0.04	0.12	7	0.28	0.10	0.15	0.40
	H18	17	0.07	0.02	0.05	0.12	7	0.30	0.11	0.16	0.47
	H19	17	0.07	0.02	0.04	0.10	7	0.29	0.10	0.15	0.40
	H20	17	0.06	0.01	0.03	0.08	7	0.30	0.14	0.14	0.53
	H21	17	0.05	0.01	0.03	0.07	7	0.29	0.17	0.14	0.64
	H22	17	0.05	0.01	0.03	0.07	7	0.29	0.17	0.13	0.61
	H23	17	0.00	0.00	0.00	0.00	7	0.23	0.12	0.11	0.43
	H24	17	0.00	0.00	0.00	0.00	7	0.20	0.11	0.10	0.40

Continued

Continued Table K.5

Variable	Model	Background WVKT Elasticities					Roadside WVKT Elasticities				
		N	Mean	Std.	Min	Max	N	Mean	Std.	Min	Max
Autumn	H01	17	0.08	0.03	0.04	0.12	7	0.21	0.10	0.10	0.33
	H02	17	0.06	0.02	0.03	0.10	7	0.17	0.09	0.08	0.33
	H03	17	0.05	0.02	0.03	0.08	7	0.15	0.09	0.06	0.30
	H04	17	0.04	0.01	0.02	0.07	7	0.12	0.07	0.05	0.25
	H05	17	0.05	0.02	0.02	0.07	7	0.13	0.08	0.05	0.26
	H06	17	0.07	0.02	0.03	0.11	7	0.18	0.10	0.07	0.36
	H07	17	0.12	0.04	0.06	0.20	7	0.32	0.16	0.13	0.59
	H08	17	0.17	0.06	0.08	0.26	7	0.40	0.17	0.16	0.67
	H09	17	0.20	0.07	0.10	0.32	7	0.42	0.17	0.18	0.69
	H10	17	0.20	0.07	0.10	0.32	7	0.36	0.12	0.17	0.47
	H11	17	0.23	0.07	0.12	0.36	7	0.35	0.11	0.18	0.49
	H12	17	0.26	0.08	0.13	0.42	7	0.37	0.12	0.20	0.51
	H13	17	0.27	0.09	0.13	0.46	7	0.42	0.18	0.20	0.69
	H14	17	0.29	0.10	0.14	0.47	7	0.47	0.21	0.21	0.78
	H15	17	0.30	0.09	0.15	0.43	7	0.46	0.21	0.21	0.78
	H16	17	0.30	0.10	0.15	0.48	7	0.46	0.20	0.19	0.73
	H17	17	0.30	0.10	0.15	0.48	7	0.42	0.16	0.18	0.63
	H18	17	0.26	0.09	0.13	0.41	7	0.41	0.16	0.18	0.60
	H19	17	0.22	0.07	0.11	0.36	7	0.43	0.18	0.18	0.65
	H20	17	0.19	0.06	0.09	0.32	7	0.41	0.23	0.17	0.83
	H21	17	0.16	0.05	0.08	0.25	7	0.39	0.23	0.16	0.82
	H22	17	0.15	0.05	0.08	0.23	7	0.37	0.23	0.15	0.84
	H23	17	0.11	0.04	0.06	0.18	7	0.32	0.20	0.13	0.70
	H24	17	0.10	0.03	0.05	0.16	7	0.29	0.19	0.12	0.66
Winter	H01	17	0.12	0.05	0.06	0.23	7	0.26	0.11	0.11	0.41
	H02	17	0.09	0.04	0.05	0.17	7	0.19	0.08	0.09	0.29
	H03	17	0.07	0.03	0.04	0.14	7	0.15	0.06	0.07	0.23
	H04	17	0.06	0.02	0.03	0.12	7	0.12	0.05	0.06	0.18
	H05	17	0.06	0.02	0.03	0.13	7	0.12	0.05	0.05	0.19
	H06	17	0.07	0.03	0.04	0.17	7	0.17	0.07	0.07	0.25
	H07	17	0.14	0.05	0.07	0.25	7	0.31	0.13	0.12	0.52
	H08	17	0.18	0.06	0.09	0.28	7	0.37	0.13	0.17	0.58
	H09	17	0.22	0.07	0.11	0.34	7	0.40	0.12	0.19	0.57
	H10	17	0.21	0.06	0.12	0.34	7	0.36	0.11	0.18	0.53
	H11	17	0.23	0.07	0.13	0.39	7	0.38	0.12	0.18	0.54
	H12	17	0.26	0.09	0.14	0.43	7	0.40	0.12	0.18	0.54
	H13	17	0.28	0.09	0.14	0.46	7	0.47	0.18	0.19	0.71
	H14	17	0.32	0.12	0.15	0.55	7	0.58	0.27	0.20	0.88
	H15	17	0.36	0.15	0.16	0.68	7	0.57	0.24	0.21	0.87
	H16	17	0.37	0.15	0.17	0.64	7	0.57	0.24	0.19	0.84
	H17	17	0.37	0.15	0.18	0.65	7	0.55	0.22	0.19	0.80
	H18	17	0.35	0.13	0.17	0.59	7	0.52	0.20	0.19	0.78
	H19	17	0.33	0.12	0.16	0.58	7	0.53	0.21	0.19	0.78
	H20	17	0.30	0.12	0.14	0.54	7	0.51	0.23	0.20	0.89
	H21	17	0.27	0.11	0.13	0.56	7	0.49	0.26	0.19	0.96
	H22	17	0.26	0.12	0.12	0.62	7	0.47	0.24	0.18	0.86
	H23	17	0.18	0.09	0.08	0.45	7	0.36	0.18	0.14	0.61
	H24	17	0.16	0.08	0.07	0.40	7	0.34	0.18	0.13	0.64

Table K.6 Hourly elasticities w.r.t. solar radiation in the CO panel models

Variable	Model	Background Solar Elasticities					Roadside Solar Elasticities				
		N	Mean	Std.	Min	Max	N	Mean	Std.	Min	Max
Spring	H01	17	0.00	0.00	0.00	0.00	7	0.00	0.00	0.00	0.00
	H02	17	0.00	0.00	0.00	0.00	7	0.00	0.00	0.00	0.00
	H03	17	0.00	0.00	0.00	0.00	7	0.00	0.00	0.00	0.00
	H04	17	0.00	0.00	0.00	0.00	7	0.00	0.00	0.00	0.00
	H05	17	0.00	0.00	0.00	0.00	7	0.00	0.00	0.00	0.00
	H06	17	0.00	0.00	0.00	0.00	7	0.00	0.00	0.00	0.00
	H07	17	-0.01	0.00	-0.01	0.00	7	0.00	0.00	-0.01	0.00
	H08	17	-0.03	0.00	-0.04	-0.02	7	-0.01	0.01	-0.03	-0.01
	H09	17	-0.08	0.01	-0.10	-0.06	7	-0.04	0.01	-0.07	-0.02
	H10	17	-0.17	0.03	-0.21	-0.11	7	-0.07	0.03	-0.14	-0.05
	H11	17	-0.32	0.06	-0.42	-0.22	7	-0.11	0.04	-0.20	-0.07
	H12	17	-0.52	0.10	-0.69	-0.36	7	-0.17	0.07	-0.32	-0.11
	H13	17	-0.74	0.14	-0.96	-0.49	7	-0.25	0.11	-0.47	-0.16
	H14	17	-0.88	0.16	-1.17	-0.62	7	-0.30	0.10	-0.46	-0.20
	H15	17	-0.96	0.18	-1.27	-0.68	7	-0.32	0.11	-0.48	-0.20
	H16	17	-0.95	0.19	-1.24	-0.69	7	-0.30	0.09	-0.44	-0.20
	H17	17	-0.85	0.18	-1.11	-0.58	7	-0.28	0.09	-0.40	-0.17
	H18	17	-0.69	0.16	-0.96	-0.45	7	-0.23	0.08	-0.37	-0.14
	H19	17	-0.48	0.10	-0.67	-0.33	7	-0.16	0.05	-0.24	-0.11
	H20	17	-0.30	0.06	-0.40	-0.20	7	-0.11	0.03	-0.15	-0.08
	H21	17	-0.17	0.03	-0.22	-0.11	7	-0.07	0.02	-0.10	-0.05
	H22	17	-0.09	0.01	-0.12	-0.07	7	-0.04	0.01	-0.06	-0.03
	H23	17	-0.03	0.01	-0.05	-0.03	7	-0.02	0.01	-0.03	-0.01
	H24	17	-0.01	0.00	-0.01	-0.01	7	0.00	0.00	-0.01	0.00
Summer	H01	17	-0.01	0.00	-0.01	-0.01	7	0.00	0.00	-0.01	0.00
	H02	17	0.00	0.00	0.00	0.00	7	0.00	0.00	0.00	0.00
	H03	17	0.00	0.00	0.00	0.00	7	0.00	0.00	0.00	0.00
	H04	17	0.00	0.00	0.00	0.00	7	0.00	0.00	0.00	0.00
	H05	17	0.00	0.00	0.00	0.00	7	0.00	0.00	0.00	0.00
	H06	17	-0.03	0.01	-0.04	-0.02	7	-0.02	0.01	-0.03	-0.01
	H07	17	-0.05	0.01	-0.08	-0.04	7	-0.03	0.01	-0.05	-0.02
	H08	17	-0.11	0.02	-0.18	-0.08	7	-0.05	0.02	-0.09	-0.03
	H09	17	-0.21	0.04	-0.33	-0.15	7	-0.09	0.03	-0.13	-0.06
	H10	17	-0.36	0.07	-0.55	-0.26	7	-0.13	0.04	-0.22	-0.09
	H11	17	-0.59	0.13	-0.82	-0.41	7	-0.20	0.08	-0.37	-0.12
	H12	17	-0.84	0.19	-1.19	-0.55	7	-0.27	0.09	-0.43	-0.17
	H13	17	-1.12	0.25	-1.64	-0.76	7	-0.42	0.15	-0.70	-0.26
	H14	17	-1.34	0.30	-2.09	-0.93	7	-0.51	0.19	-0.83	-0.32
	H15	17	-1.46	0.33	-2.37	-1.03	7	-0.51	0.15	-0.75	-0.35
	H16	17	-1.49	0.36	-2.52	-1.05	7	-0.49	0.13	-0.69	-0.35
	H17	17	-1.36	0.33	-2.31	-0.98	7	-0.44	0.16	-0.78	-0.30
	H18	17	-1.12	0.26	-1.87	-0.76	7	-0.40	0.17	-0.77	-0.26
	H19	17	-0.81	0.19	-1.35	-0.59	7	-0.30	0.10	-0.50	-0.21
	H20	17	-0.54	0.11	-0.84	-0.40	7	-0.25	0.10	-0.42	-0.15
	H21	17	-0.34	0.06	-0.52	-0.25	7	-0.18	0.08	-0.31	-0.10
	H22	17	-0.20	0.04	-0.30	-0.14	7	-0.11	0.05	-0.20	-0.06
	H23	17	-0.10	0.02	-0.15	-0.07	7	-0.06	0.03	-0.11	-0.03
	H24	17	-0.04	0.01	-0.05	-0.03	7	-0.02	0.01	-0.04	-0.01

Continued

Continued Table K.6

Variable	Model	Background Solar Elasticities					Roadside Solar Elasticities				
		N	Mean	Std.	Min	Max	N	Mean	Std.	Min	Max
Autumn	H01	17	0.00	0.00	0.00	0.00	7	0.00	0.00	0.00	0.00
	H02	17	0.00	0.00	0.00	0.00	7	0.00	0.00	0.00	0.00
	H03	17	0.00	0.00	0.00	0.00	7	0.00	0.00	0.00	0.00
	H04	17	0.00	0.00	0.00	0.00	7	0.00	0.00	0.00	0.00
	H05	17	0.00	0.00	0.00	0.00	7	0.00	0.00	0.00	0.00
	H06	17	0.00	0.00	0.00	0.00	7	0.00	0.00	0.00	0.00
	H07	17	0.00	0.00	0.00	0.00	7	0.00	0.00	0.00	0.00
	H08	17	-0.01	0.00	-0.02	-0.01	7	-0.01	0.00	-0.01	0.00
	H09	17	-0.06	0.01	-0.08	-0.04	7	-0.03	0.01	-0.05	-0.02
	H10	17	-0.16	0.03	-0.23	-0.12	7	-0.07	0.02	-0.11	-0.05
	H11	17	-0.34	0.06	-0.49	-0.27	7	-0.14	0.04	-0.21	-0.09
	H12	17	-0.60	0.11	-0.82	-0.45	7	-0.22	0.06	-0.32	-0.16
	H13	17	-0.90	0.17	-1.24	-0.61	7	-0.36	0.13	-0.55	-0.24
	H14	17	-1.15	0.22	-1.55	-0.71	7	-0.47	0.19	-0.71	-0.29
	H15	17	-1.27	0.21	-1.68	-0.77	7	-0.50	0.18	-0.77	-0.32
	H16	17	-1.23	0.20	-1.62	-0.77	7	-0.49	0.20	-0.74	-0.28
	H17	17	-1.04	0.19	-1.34	-0.60	7	-0.39	0.15	-0.60	-0.23
	H18	17	-0.71	0.12	-0.88	-0.45	7	-0.29	0.11	-0.45	-0.17
	H19	17	-0.42	0.06	-0.51	-0.28	7	-0.21	0.09	-0.36	-0.12
	H20	17	-0.23	0.04	-0.29	-0.16	7	-0.13	0.06	-0.22	-0.08
	H21	17	-0.11	0.02	-0.15	-0.09	7	-0.07	0.04	-0.13	-0.04
	H22	17	-0.04	0.01	-0.06	-0.03	7	-0.03	0.01	-0.05	-0.02
	H23	17	-0.01	0.00	-0.02	-0.01	7	-0.01	0.00	-0.01	0.00
	H24	17	0.00	0.00	0.00	0.00	7	0.00	0.00	0.00	0.00
Winter	H01	17	0.00	0.00	0.00	0.00	7	0.00	0.00	0.00	0.00
	H02	17	0.00	0.00	0.00	0.00	7	0.00	0.00	0.00	0.00
	H03	17	0.00	0.00	0.00	0.00	7	0.00	0.00	0.00	0.00
	H04	17	0.00	0.00	0.00	0.00	7	0.00	0.00	0.00	0.00
	H05	17	0.00	0.00	0.00	0.00	7	0.00	0.00	0.00	0.00
	H06	17	0.00	0.00	0.00	0.00	7	0.00	0.00	0.00	0.00
	H07	17	0.00	0.00	0.00	0.00	7	0.00	0.00	0.00	0.00
	H08	17	0.00	0.00	0.00	0.00	7	0.00	0.00	0.00	0.00
	H09	17	-0.01	0.00	-0.01	0.00	7	0.00	0.00	-0.01	0.00
	H10	17	-0.03	0.00	-0.04	-0.02	7	-0.02	0.01	-0.03	-0.01
	H11	17	-0.08	0.01	-0.10	-0.05	7	-0.05	0.02	-0.08	-0.03
	H12	17	-0.15	0.03	-0.22	-0.11	7	-0.08	0.03	-0.13	-0.05
	H13	17	-0.25	0.04	-0.36	-0.17	7	-0.15	0.06	-0.25	-0.08
	H14	17	-0.35	0.06	-0.50	-0.24	7	-0.23	0.11	-0.40	-0.11
	H15	17	-0.44	0.09	-0.66	-0.30	7	-0.26	0.10	-0.39	-0.13
	H16	17	-0.45	0.11	-0.77	-0.31	7	-0.26	0.11	-0.41	-0.12
	H17	17	-0.40	0.09	-0.64	-0.28	7	-0.22	0.08	-0.34	-0.11
	H18	17	-0.29	0.05	-0.40	-0.21	7	-0.16	0.06	-0.25	-0.08
	H19	17	-0.19	0.03	-0.26	-0.14	7	-0.11	0.05	-0.19	-0.06
	H20	17	-0.11	0.02	-0.16	-0.08	7	-0.07	0.03	-0.11	-0.04
	H21	17	-0.06	0.01	-0.09	-0.04	7	-0.04	0.02	-0.07	-0.02
	H22	17	-0.02	0.01	-0.04	-0.01	7	-0.01	0.01	-0.02	-0.01
	H23	17	0.00	0.00	-0.01	0.00	7	0.00	0.00	0.00	0.00
	H24	17	0.00	0.00	0.00	0.00	7	0.00	0.00	0.00	0.00

Table K.7 Hourly elasticities w.r.t. WVKT in the SO_2 panel models

Variable	Model	Background WVKT Elasticities					Roadside WVKT Elasticities				
		N	Mean	Std.	Min	Max	N	Mean	Std.	Min	Max
Spring	H01	18	0.06	0.02	0.03	0.10	6	0.14	0.02	0.12	0.17
	H02	18	0.04	0.01	0.02	0.08	6	0.11	0.02	0.10	0.15
	H03	18	0.03	0.01	0.02	0.07	6	0.09	0.02	0.08	0.12
	H04	18	0.03	0.01	0.01	0.05	6	0.07	0.02	0.06	0.10
	H05	18	0.03	0.01	0.01	0.05	6	0.07	0.02	0.06	0.11
	H06	18	0.04	0.01	0.02	0.07	6	0.09	0.02	0.07	0.12
	H07	18	0.07	0.02	0.03	0.13	6	0.15	0.03	0.12	0.20
	H08	18	0.10	0.03	0.04	0.17	6	0.22	0.03	0.19	0.27
	H09	18	0.10	0.04	0.04	0.18	6	0.23	0.02	0.20	0.25
	H10	18	0.09	0.03	0.04	0.17	6	0.21	0.02	0.19	0.24
	H11	18	0.09	0.03	0.04	0.17	6	0.22	0.02	0.19	0.25
	H12	18	0.09	0.03	0.04	0.18	6	0.22	0.03	0.19	0.26
	H13	18	0.09	0.03	0.05	0.18	6	0.21	0.03	0.18	0.25
	H14	18	0.10	0.03	0.06	0.18	6	0.23	0.03	0.20	0.27
	H15	18	0.10	0.03	0.06	0.19	6	0.23	0.03	0.19	0.27
	H16	18	0.10	0.03	0.06	0.19	6	0.22	0.03	0.18	0.25
	H17	18	0.10	0.03	0.07	0.18	6	0.22	0.03	0.19	0.26
	H18	18	0.11	0.03	0.07	0.19	6	0.23	0.02	0.21	0.28
	H19	18	0.11	0.03	0.07	0.20	6	0.25	0.04	0.21	0.31
	H20	18	0.11	0.03	0.07	0.19	6	0.23	0.03	0.19	0.29
	H21	18	0.09	0.02	0.07	0.16	6	0.21	0.04	0.17	0.27
	H22	18	0.09	0.02	0.06	0.16	6	0.20	0.04	0.16	0.26
	H23	18	0.08	0.02	0.05	0.14	6	0.18	0.03	0.16	0.24
	H24	18	0.07	0.02	0.04	0.12	6	0.16	0.02	0.15	0.20
Summer	H01	18	0.06	0.02	0.03	0.10	6	0.12	0.04	0.08	0.18
	H02	18	0.05	0.01	0.02	0.08	6	0.10	0.04	0.06	0.17
	H03	18	0.04	0.01	0.02	0.06	6	0.08	0.04	0.05	0.14
	H04	18	0.03	0.01	0.02	0.05	6	0.07	0.03	0.04	0.11
	H05	18	0.03	0.01	0.02	0.05	6	0.07	0.03	0.04	0.11
	H06	18	0.04	0.01	0.02	0.06	6	0.08	0.04	0.05	0.13
	H07	18	0.08	0.02	0.04	0.12	6	0.15	0.06	0.10	0.23
	H08	18	0.12	0.04	0.05	0.19	6	0.21	0.08	0.14	0.33
	H09	18	0.12	0.04	0.05	0.21	6	0.22	0.08	0.15	0.36
	H10	18	0.12	0.04	0.05	0.20	6	0.20	0.07	0.14	0.32
	H11	18	0.12	0.04	0.05	0.20	6	0.19	0.06	0.13	0.31
	H12	18	0.13	0.05	0.05	0.24	6	0.19	0.06	0.12	0.29
	H13	18	0.12	0.05	0.05	0.25	6	0.18	0.06	0.11	0.28
	H14	18	0.13	0.06	0.05	0.28	6	0.19	0.06	0.12	0.28
	H15	18	0.13	0.06	0.06	0.30	6	0.19	0.06	0.12	0.26
	H16	18	0.13	0.05	0.06	0.26	6	0.19	0.06	0.12	0.26
	H17	18	0.13	0.05	0.06	0.27	6	0.19	0.06	0.12	0.24
	H18	18	0.13	0.05	0.06	0.23	6	0.19	0.06	0.12	0.26
	H19	18	0.13	0.04	0.06	0.21	6	0.20	0.06	0.12	0.27
	H20	18	0.12	0.04	0.06	0.17	6	0.18	0.06	0.12	0.26
	H21	18	0.11	0.03	0.05	0.15	6	0.17	0.05	0.11	0.24
	H22	18	0.10	0.03	0.05	0.14	6	0.16	0.05	0.11	0.23
	H23	18	0.09	0.02	0.05	0.14	6	0.16	0.05	0.11	0.21
	H24	18	0.08	0.02	0.04	0.12	6	0.14	0.04	0.09	0.20

Continued

Continued Table K.7

Variable	Model	Background WVKT Elasticities					Roadside WVKT Elasticities				
		N	Mean	Std.	Min	Max	N	Mean	Std.	Min	Max
Autumn	H01	18	0.08	0.03	0.04	0.16	6	0.11	0.03	0.09	0.16
	H02	18	0.07	0.02	0.03	0.14	6	0.09	0.04	0.07	0.16
	H03	18	0.05	0.02	0.03	0.11	6	0.08	0.03	0.05	0.13
	H04	18	0.04	0.02	0.02	0.09	6	0.06	0.03	0.04	0.11
	H05	18	0.05	0.02	0.02	0.09	6	0.06	0.02	0.04	0.10
	H06	18	0.06	0.02	0.03	0.13	6	0.08	0.03	0.05	0.13
	H07	18	0.12	0.04	0.05	0.24	6	0.15	0.04	0.10	0.21
	H08	18	0.17	0.06	0.07	0.36	6	0.21	0.06	0.14	0.30
	H09	18	0.17	0.06	0.06	0.34	6	0.22	0.07	0.15	0.36
	H10	18	0.16	0.06	0.06	0.32	6	0.20	0.06	0.13	0.32
	H11	18	0.16	0.06	0.06	0.32	6	0.20	0.06	0.14	0.32
	H12	18	0.16	0.06	0.07	0.33	6	0.20	0.05	0.16	0.31
	H13	18	0.16	0.06	0.08	0.32	6	0.20	0.06	0.15	0.31
	H14	18	0.17	0.06	0.09	0.34	6	0.21	0.05	0.15	0.31
	H15	18	0.18	0.07	0.10	0.36	6	0.21	0.05	0.16	0.31
	H16	18	0.18	0.07	0.10	0.37	6	0.21	0.06	0.15	0.32
	H17	18	0.18	0.07	0.10	0.36	6	0.21	0.06	0.14	0.31
	H18	18	0.18	0.06	0.10	0.35	6	0.21	0.06	0.15	0.31
	H19	18	0.17	0.06	0.09	0.35	6	0.21	0.05	0.14	0.28
	H20	18	0.15	0.05	0.08	0.30	6	0.19	0.05	0.13	0.27
	H21	18	0.13	0.04	0.07	0.25	6	0.17	0.05	0.13	0.25
	H22	18	0.13	0.04	0.07	0.24	6	0.16	0.04	0.13	0.23
	H23	18	0.12	0.04	0.06	0.23	6	0.15	0.03	0.11	0.21
	H24	18	0.10	0.03	0.05	0.19	6	0.14	0.03	0.10	0.19
Winter	H01	18	0.10	0.03	0.05	0.18	6	0.20	0.04	0.15	0.25
	H02	18	0.08	0.03	0.04	0.15	6	0.16	0.03	0.12	0.19
	H03	18	0.06	0.02	0.03	0.11	6	0.13	0.03	0.09	0.15
	H04	18	0.05	0.02	0.02	0.08	6	0.10	0.02	0.07	0.12
	H05	18	0.04	0.02	0.02	0.08	6	0.09	0.02	0.07	0.12
	H06	18	0.06	0.02	0.03	0.11	6	0.12	0.02	0.10	0.14
	H07	18	0.12	0.04	0.06	0.20	6	0.21	0.04	0.16	0.26
	H08	18	0.17	0.05	0.08	0.28	6	0.29	0.06	0.22	0.38
	H09	18	0.17	0.05	0.07	0.27	6	0.29	0.05	0.23	0.38
	H10	18	0.14	0.05	0.06	0.23	6	0.26	0.04	0.21	0.33
	H11	18	0.13	0.05	0.06	0.24	6	0.25	0.03	0.21	0.31
	H12	18	0.12	0.05	0.06	0.26	6	0.24	0.04	0.22	0.31
	H13	18	0.12	0.05	0.06	0.26	6	0.23	0.04	0.20	0.30
	H14	18	0.13	0.05	0.07	0.26	6	0.25	0.04	0.21	0.31
	H15	18	0.13	0.05	0.07	0.28	6	0.25	0.04	0.19	0.31
	H16	18	0.14	0.06	0.08	0.29	6	0.25	0.04	0.19	0.31
	H17	18	0.15	0.06	0.08	0.31	6	0.26	0.04	0.21	0.33
	H18	18	0.16	0.06	0.09	0.32	6	0.28	0.03	0.24	0.33
	H19	18	0.17	0.06	0.09	0.33	6	0.29	0.04	0.25	0.35
	H20	18	0.16	0.06	0.09	0.34	6	0.28	0.04	0.24	0.34
	H21	18	0.15	0.06	0.08	0.32	6	0.26	0.04	0.22	0.31
	H22	18	0.14	0.05	0.08	0.30	6	0.26	0.04	0.22	0.30
	H23	18	0.14	0.05	0.07	0.30	6	0.24	0.04	0.20	0.28
	H24	18	0.12	0.04	0.06	0.24	6	0.22	0.04	0.18	0.27

Table K.8 Hourly elasticities w.r.t. solar radiation in the SO_2 panel models

Variable	Model	Background Solar Elasticities					Roadside Solar Elasticities				
		N	Mean	Std.	Min	Max	N	Mean	Std.	Min	Max
Spring	H01	18	0.00	0.00	0.00	0.00	6	0.00	0.00	0.00	0.00
	H02	18	0.00	0.00	0.00	0.00	6	0.00	0.00	0.00	0.00
	H03	18	0.00	0.00	0.00	0.00	6	0.00	0.00	0.00	0.00
	H04	18	0.00	0.00	0.00	0.00	6	0.00	0.00	0.00	0.00
	H05	18	0.00	0.00	0.00	0.00	6	0.00	0.00	0.00	0.00
	H06	18	0.00	0.00	0.00	0.00	6	0.00	0.00	0.00	0.00
	H07	18	0.00	0.00	0.00	0.00	6	0.00	0.00	0.00	0.00
	H08	18	-0.01	0.00	-0.01	-0.01	6	0.00	0.00	-0.01	0.00
	H09	18	-0.02	0.01	-0.04	-0.02	6	-0.01	0.00	-0.02	-0.01
	H10	18	-0.04	0.01	-0.06	-0.03	6	-0.03	0.00	-0.03	-0.02
	H11	18	-0.07	0.02	-0.10	-0.05	6	-0.04	0.01	-0.06	-0.04
	H12	18	-0.11	0.03	-0.16	-0.08	6	-0.07	0.01	-0.08	-0.05
	H13	18	-0.16	0.04	-0.23	-0.10	6	-0.09	0.02	-0.11	-0.07
	H14	18	-0.20	0.05	-0.28	-0.12	6	-0.11	0.02	-0.14	-0.09
	H15	18	-0.21	0.06	-0.33	-0.13	6	-0.11	0.02	-0.15	-0.09
	H16	18	-0.21	0.06	-0.31	-0.13	6	-0.11	0.02	-0.13	-0.09
	H17	18	-0.19	0.05	-0.26	-0.12	6	-0.10	0.02	-0.12	-0.08
	H18	18	-0.16	0.04	-0.22	-0.10	6	-0.08	0.02	-0.11	-0.06
	H19	18	-0.13	0.03	-0.18	-0.07	6	-0.07	0.01	-0.09	-0.05
	H20	18	-0.09	0.02	-0.14	-0.06	6	-0.05	0.01	-0.06	-0.04
	H21	18	-0.05	0.01	-0.09	-0.03	6	-0.03	0.01	-0.04	-0.02
	H22	18	-0.03	0.01	-0.04	-0.02	6	-0.02	0.00	-0.02	-0.01
	H23	18	-0.01	0.00	-0.02	-0.01	6	-0.01	0.00	-0.01	0.00
	H24	18	0.00	0.00	0.00	0.00	6	0.00	0.00	0.00	0.00
Summer	H01	18	0.00	0.00	0.00	0.00	6	0.00	0.00	0.00	0.00
	H02	18	0.00	0.00	0.00	0.00	6	0.00	0.00	0.00	0.00
	H03	18	0.00	0.00	0.00	0.00	6	0.00	0.00	0.00	0.00
	H04	18	0.00	0.00	0.00	0.00	6	0.00	0.00	0.00	0.00
	H05	18	0.00	0.00	0.00	0.00	6	0.00	0.00	0.00	0.00
	H06	18	0.00	0.00	-0.01	0.00	6	0.00	0.00	0.00	0.00
	H07	18	-0.01	0.00	-0.01	0.00	6	0.00	0.00	0.00	0.00
	H08	18	-0.02	0.00	-0.02	-0.01	6	0.00	0.00	0.00	0.00
	H09	18	-0.03	0.01	-0.05	-0.02	6	0.00	0.00	0.00	0.00
	H10	18	-0.05	0.02	-0.09	-0.03	6	-0.01	0.00	-0.01	0.00
	H11	18	-0.08	0.03	-0.13	-0.04	6	-0.01	0.00	-0.01	-0.01
	H12	18	-0.11	0.05	-0.22	-0.06	6	-0.01	0.00	-0.01	-0.01
	H13	18	-0.15	0.06	-0.29	-0.07	6	-0.01	0.00	-0.02	-0.01
	H14	18	-0.17	0.07	-0.35	-0.09	6	-0.02	0.01	-0.02	-0.01
	H15	18	-0.19	0.08	-0.38	-0.10	6	-0.02	0.01	-0.02	-0.01
	H16	18	-0.18	0.07	-0.35	-0.09	6	-0.02	0.01	-0.02	-0.01
	H17	18	-0.17	0.07	-0.34	-0.09	6	-0.02	0.01	-0.02	-0.01
	H18	18	-0.15	0.06	-0.31	-0.08	6	-0.01	0.00	-0.02	-0.01
	H19	18	-0.12	0.04	-0.23	-0.06	6	-0.01	0.00	-0.02	-0.01
	H20	18	-0.08	0.03	-0.16	-0.05	6	-0.01	0.00	-0.01	0.00
	H21	18	-0.06	0.02	-0.12	-0.03	6	-0.01	0.00	-0.01	0.00
	H22	18	-0.03	0.01	-0.06	-0.02	6	0.00	0.00	0.00	0.00
	H23	18	-0.02	0.01	-0.03	-0.01	6	0.00	0.00	0.00	0.00
	H24	18	-0.01	0.00	-0.01	0.00	6	0.00	0.00	0.00	0.00

Continued

Continued Table K.8

Variable	Model	Background Solar Elasticities					Roadside Solar Elasticities				
		N	Mean	Std.	Min	Max	N	Mean	Std.	Min	Max
Autumn	H01	18	0.00	0.00	0.00	0.00	6	0.00	0.00	0.00	0.00
	H02	18	0.00	0.00	0.00	0.00	6	0.00	0.00	0.00	0.00
	H03	18	0.00	0.00	0.00	0.00	6	0.00	0.00	0.00	0.00
	H04	18	0.00	0.00	0.00	0.00	6	0.00	0.00	0.00	0.00
	H05	18	0.00	0.00	0.00	0.00	6	0.00	0.00	0.00	0.00
	H06	18	0.00	0.00	0.00	0.00	6	0.00	0.00	0.00	0.00
	H07	18	0.00	0.00	0.00	0.00	6	0.00	0.00	0.00	0.00
	H08	18	-0.01	0.00	-0.01	-0.01	6	0.00	0.00	-0.01	0.00
	H09	18	-0.03	0.01	-0.05	-0.02	6	-0.02	0.00	-0.03	-0.01
	H10	18	-0.09	0.02	-0.13	-0.05	6	-0.05	0.01	-0.07	-0.04
	H11	18	-0.16	0.04	-0.26	-0.10	6	-0.10	0.02	-0.13	-0.08
	H12	18	-0.26	0.07	-0.44	-0.15	6	-0.16	0.03	-0.20	-0.11
	H13	18	-0.37	0.10	-0.63	-0.22	6	-0.23	0.05	-0.29	-0.15
	H14	18	-0.47	0.13	-0.75	-0.26	6	-0.28	0.06	-0.35	-0.18
	H15	18	-0.53	0.14	-0.80	-0.30	6	-0.31	0.08	-0.41	-0.19
	H16	18	-0.51	0.14	-0.77	-0.31	6	-0.30	0.07	-0.36	-0.18
	H17	18	-0.45	0.11	-0.66	-0.27	6	-0.25	0.06	-0.31	-0.15
	H18	18	-0.34	0.08	-0.49	-0.20	6	-0.19	0.04	-0.23	-0.12
	H19	18	-0.22	0.05	-0.34	-0.14	6	-0.13	0.03	-0.16	-0.08
	H20	18	-0.13	0.03	-0.19	-0.09	6	-0.08	0.02	-0.09	-0.05
	H21	18	-0.07	0.02	-0.09	-0.05	6	-0.04	0.01	-0.05	-0.03
	H22	18	-0.03	0.01	-0.04	-0.02	6	-0.02	0.00	-0.02	-0.01
	H23	18	-0.01	0.00	-0.01	0.00	6	0.00	0.00	-0.01	0.00
	H24	18	0.00	0.00	0.00	0.00	6	0.00	0.00	0.00	0.00
Winter	H01	18	0.00	0.00	0.00	0.00	6	0.00	0.00	0.00	0.00
	H02	18	0.00	0.00	0.00	0.00	6	0.00	0.00	0.00	0.00
	H03	18	0.00	0.00	0.00	0.00	6	0.00	0.00	0.00	0.00
	H04	18	0.00	0.00	0.00	0.00	6	0.00	0.00	0.00	0.00
	H05	18	0.00	0.00	0.00	0.00	6	0.00	0.00	0.00	0.00
	H06	18	0.00	0.00	0.00	0.00	6	0.00	0.00	0.00	0.00
	H07	18	0.00	0.00	0.00	0.00	6	0.00	0.00	0.00	0.00
	H08	18	0.00	0.00	0.00	0.00	6	0.00	0.00	0.00	0.00
	H09	18	0.00	0.00	0.00	0.00	6	0.00	0.00	0.00	0.00
	H10	18	0.00	0.00	-0.01	0.00	6	-0.01	0.00	-0.01	-0.01
	H11	18	-0.01	0.00	-0.01	-0.01	6	-0.02	0.00	-0.02	-0.02
	H12	18	-0.02	0.00	-0.03	-0.01	6	-0.03	0.00	-0.04	-0.03
	H13	18	-0.03	0.01	-0.04	-0.02	6	-0.05	0.01	-0.06	-0.04
	H14	18	-0.04	0.01	-0.06	-0.03	6	-0.07	0.01	-0.08	-0.06
	H15	18	-0.04	0.01	-0.07	-0.03	6	-0.08	0.01	-0.09	-0.06
	H16	18	-0.04	0.01	-0.07	-0.03	6	-0.08	0.01	-0.09	-0.06
	H17	18	-0.04	0.01	-0.06	-0.03	6	-0.07	0.01	-0.08	-0.06
	H18	18	-0.03	0.01	-0.05	-0.02	6	-0.06	0.01	-0.07	-0.05
	H19	18	-0.02	0.01	-0.04	-0.02	6	-0.04	0.01	-0.05	-0.03
	H20	18	-0.02	0.00	-0.02	-0.01	6	-0.03	0.00	-0.03	-0.02
	H21	18	-0.01	0.00	-0.01	-0.01	6	-0.01	0.00	-0.02	-0.01
	H22	18	0.00	0.00	0.00	0.00	6	0.00	0.00	-0.01	0.00
	H23	18	0.00	0.00	0.00	0.00	6	0.00	0.00	0.00	0.00
	H24	18	0.00	0.00	0.00	0.00	6	0.00	0.00	0.00	0.00

Table K.9 Hourly elasticities w.r.t. humidity in the SO_2 panel models

Variable	Model	Background Humidity Elasticities					Roadside Humidity Elasticities				
		N	Mean	Std.	Min	Max	N	Mean	Std.	Min	Max
Spring	H01	18	-1.60	0.33	-2.17	-1.04	6	-1.07	0.26	-1.44	-0.79
	H02	18	-1.69	0.36	-2.34	-1.10	6	-1.20	0.33	-1.72	-0.89
	H03	18	-1.80	0.35	-2.42	-1.27	6	-1.27	0.36	-1.85	-0.95
	H04	18	-1.88	0.42	-2.66	-1.27	6	-1.35	0.44	-2.09	-0.99
	H05	18	-1.93	0.43	-2.68	-1.28	6	-1.38	0.48	-2.27	-1.00
	H06	18	-1.91	0.41	-2.60	-1.23	6	-1.22	0.36	-1.90	-0.88
	H07	18	-1.78	0.37	-2.52	-1.16	6	-1.02	0.25	-1.51	-0.78
	H08	18	-1.49	0.33	-2.34	-1.01	6	-0.88	0.17	-1.19	-0.71
	H09	18	-1.19	0.29	-1.81	-0.79	6	-0.75	0.11	-0.91	-0.64
	H10	18	-1.05	0.24	-1.51	-0.73	6	-0.69	0.11	-0.86	-0.59
	H11	18	-0.97	0.22	-1.36	-0.70	6	-0.65	0.11	-0.81	-0.54
	H12	18	-0.98	0.23	-1.34	-0.65	6	-0.63	0.11	-0.80	-0.52
	H13	18	-1.02	0.26	-1.45	-0.60	6	-0.63	0.13	-0.82	-0.52
	H14	18	-1.03	0.27	-1.50	-0.63	6	-0.64	0.12	-0.83	-0.53
	H15	18	-1.05	0.29	-1.61	-0.62	6	-0.62	0.13	-0.81	-0.50
	H16	18	-1.07	0.30	-1.60	-0.65	6	-0.61	0.12	-0.76	-0.49
	H17	18	-1.12	0.27	-1.54	-0.73	6	-0.64	0.13	-0.81	-0.50
	H18	18	-1.18	0.26	-1.64	-0.76	6	-0.69	0.14	-0.89	-0.52
	H19	18	-1.29	0.29	-1.82	-0.78	6	-0.77	0.17	-1.06	-0.58
	H20	18	-1.43	0.32	-2.29	-0.94	6	-0.83	0.18	-1.15	-0.66
	H21	18	-1.45	0.36	-2.32	-0.91	6	-0.85	0.20	-1.23	-0.64
	H22	18	-1.42	0.30	-1.90	-0.95	6	-0.87	0.21	-1.26	-0.65
	H23	18	-1.44	0.32	-2.02	-0.96	6	-0.87	0.21	-1.25	-0.66
	H24	18	-1.49	0.31	-2.06	-1.02	6	-0.92	0.20	-1.24	-0.74
Summer	H01	18	-0.29	0.08	-0.45	-0.17	6	-0.32	0.11	-0.43	-0.20
	H02	18	-0.30	0.09	-0.46	-0.16	6	-0.36	0.14	-0.52	-0.21
	H03	18	-0.31	0.10	-0.48	-0.16	6	-0.40	0.18	-0.66	-0.21
	H04	18	-0.31	0.09	-0.48	-0.18	6	-0.41	0.19	-0.69	-0.22
	H05	18	-0.32	0.10	-0.51	-0.19	6	-0.42	0.20	-0.72	-0.23
	H06	18	-0.31	0.10	-0.51	-0.17	6	-0.38	0.17	-0.64	-0.21
	H07	18	-0.29	0.08	-0.47	-0.18	6	-0.32	0.12	-0.48	-0.20
	H08	18	-0.26	0.08	-0.44	-0.15	6	-0.29	0.10	-0.41	-0.19
	H09	18	-0.24	0.07	-0.43	-0.14	6	-0.26	0.08	-0.34	-0.18
	H10	18	-0.23	0.07	-0.41	-0.12	6	-0.23	0.07	-0.31	-0.17
	H11	18	-0.23	0.08	-0.39	-0.13	6	-0.22	0.07	-0.31	-0.15
	H12	18	-0.24	0.10	-0.47	-0.12	6	-0.21	0.07	-0.30	-0.14
	H13	18	-0.24	0.10	-0.48	-0.12	6	-0.22	0.07	-0.30	-0.13
	H14	18	-0.24	0.10	-0.49	-0.12	6	-0.22	0.07	-0.30	-0.13
	H15	18	-0.24	0.11	-0.50	-0.13	6	-0.21	0.08	-0.30	-0.13
	H16	18	-0.24	0.09	-0.46	-0.12	6	-0.22	0.08	-0.30	-0.12
	H17	18	-0.24	0.10	-0.49	-0.13	6	-0.21	0.08	-0.30	-0.12
	H18	18	-0.25	0.10	-0.52	-0.13	6	-0.22	0.08	-0.31	-0.13
	H19	18	-0.26	0.10	-0.51	-0.14	6	-0.23	0.08	-0.34	-0.14
	H20	18	-0.26	0.09	-0.50	-0.14	6	-0.24	0.08	-0.33	-0.15
	H21	18	-0.27	0.10	-0.55	-0.14	6	-0.24	0.08	-0.34	-0.16
	H22	18	-0.26	0.09	-0.48	-0.15	6	-0.25	0.08	-0.36	-0.16
	H23	18	-0.26	0.08	-0.43	-0.16	6	-0.27	0.09	-0.39	-0.17
	H24	18	-0.27	0.08	-0.40	-0.16	6	-0.28	0.09	-0.38	-0.18

Continued

Continued Table K.9

Variable	Model	Background Humidity Elasticities					Roadside Humidity Elasticities				
		N	Mean	Std.	Min	Max	N	Mean	Std.	Min	Max
Autumn	H01	18	-0.36	0.08	-0.48	-0.23	6	-0.12	0.02	-0.14	-0.09
	H02	18	-0.38	0.10	-0.60	-0.23	6	-0.13	0.04	-0.19	-0.09
	H03	18	-0.41	0.10	-0.61	-0.27	6	-0.15	0.05	-0.21	-0.10
	H04	18	-0.44	0.11	-0.67	-0.27	6	-0.16	0.05	-0.23	-0.10
	H05	18	-0.47	0.13	-0.70	-0.27	6	-0.16	0.06	-0.25	-0.11
	H06	18	-0.47	0.12	-0.69	-0.29	6	-0.15	0.06	-0.26	-0.10
	H07	18	-0.43	0.11	-0.64	-0.30	6	-0.14	0.04	-0.21	-0.10
	H08	18	-0.38	0.09	-0.59	-0.27	6	-0.12	0.03	-0.16	-0.08
	H09	18	-0.31	0.07	-0.46	-0.20	6	-0.10	0.02	-0.13	-0.07
	H10	18	-0.28	0.07	-0.42	-0.17	6	-0.09	0.02	-0.12	-0.07
	H11	18	-0.27	0.07	-0.43	-0.17	6	-0.09	0.02	-0.11	-0.07
	H12	18	-0.26	0.07	-0.44	-0.16	6	-0.08	0.02	-0.11	-0.06
	H13	18	-0.26	0.07	-0.44	-0.16	6	-0.08	0.02	-0.11	-0.06
	H14	18	-0.26	0.07	-0.42	-0.14	6	-0.08	0.02	-0.10	-0.05
	H15	18	-0.27	0.07	-0.40	-0.15	6	-0.08	0.02	-0.11	-0.05
	H16	18	-0.27	0.07	-0.41	-0.16	6	-0.08	0.02	-0.10	-0.05
	H17	18	-0.29	0.07	-0.42	-0.17	6	-0.08	0.02	-0.10	-0.05
	H18	18	-0.30	0.07	-0.43	-0.18	6	-0.09	0.02	-0.11	-0.05
	H19	18	-0.29	0.07	-0.44	-0.19	6	-0.09	0.02	-0.11	-0.05
	H20	18	-0.30	0.07	-0.42	-0.20	6	-0.09	0.02	-0.11	-0.06
	H21	18	-0.30	0.07	-0.43	-0.21	6	-0.10	0.02	-0.12	-0.06
	H22	18	-0.31	0.07	-0.43	-0.20	6	-0.10	0.02	-0.11	-0.07
	H23	18	-0.32	0.07	-0.43	-0.18	6	-0.10	0.02	-0.12	-0.07
	H24	18	-0.33	0.08	-0.45	-0.20	6	-0.11	0.02	-0.13	-0.08
Winter	H01	18	-2.30	0.46	-3.30	-1.69	6	-2.23	0.42	-2.72	-1.70
	H02	18	-2.42	0.49	-3.44	-1.82	6	-2.42	0.50	-3.03	-1.84
	H03	18	-2.46	0.47	-3.34	-1.86	6	-2.52	0.61	-3.37	-1.84
	H04	18	-2.47	0.45	-3.29	-1.85	6	-2.57	0.61	-3.36	-1.87
	H05	18	-2.43	0.46	-3.24	-1.77	6	-2.47	0.58	-3.29	-1.87
	H06	18	-2.38	0.45	-3.19	-1.76	6	-2.17	0.47	-2.98	-1.69
	H07	18	-2.29	0.44	-3.13	-1.69	6	-1.92	0.36	-2.57	-1.56
	H08	18	-2.12	0.38	-2.90	-1.58	6	-1.76	0.28	-2.21	-1.46
	H09	18	-1.79	0.29	-2.43	-1.36	6	-1.52	0.19	-1.79	-1.30
	H10	18	-1.37	0.22	-1.81	-0.99	6	-1.25	0.15	-1.43	-1.03
	H11	18	-1.16	0.19	-1.63	-0.91	6	-1.10	0.13	-1.26	-0.90
	H12	18	-1.09	0.19	-1.71	-0.90	6	-1.04	0.12	-1.18	-0.88
	H13	18	-1.08	0.21	-1.78	-0.92	6	-1.02	0.11	-1.16	-0.89
	H14	18	-1.06	0.20	-1.66	-0.84	6	-1.01	0.12	-1.17	-0.86
	H15	18	-1.07	0.22	-1.71	-0.83	6	-0.99	0.15	-1.16	-0.77
	H16	18	-1.12	0.24	-1.79	-0.82	6	-1.00	0.16	-1.20	-0.77
	H17	18	-1.28	0.28	-2.02	-0.89	6	-1.12	0.17	-1.29	-0.89
	H18	18	-1.47	0.32	-2.21	-1.04	6	-1.26	0.18	-1.48	-1.03
	H19	18	-1.59	0.35	-2.33	-1.09	6	-1.34	0.18	-1.57	-1.12
	H20	18	-1.70	0.40	-2.67	-1.12	6	-1.44	0.18	-1.70	-1.23
	H21	18	-1.83	0.45	-2.97	-1.19	6	-1.57	0.22	-1.90	-1.32
	H22	18	-1.90	0.43	-2.92	-1.28	6	-1.66	0.24	-2.03	-1.41
	H23	18	-1.95	0.46	-3.17	-1.36	6	-1.66	0.29	-2.12	-1.37
	H24	18	-1.99	0.44	-3.02	-1.44	6	-1.82	0.29	-2.22	-1.46

Table K.10 Hourly elasticities w.r.t. WVKT in the PM10 panel models

Variable	Model	Background WVKT Elasticities					Roadside WVKT Elasticities				
		N	Mean	Std.	Min	Max	N	Mean	Std.	Min	Max
Spring	H01	17	0.03	0.02	0.01	0.07	7	0.09	0.03	0.06	0.15
	H02	17	0.02	0.01	0.01	0.06	7	0.07	0.02	0.05	0.11
	H03	17	0.02	0.01	0.01	0.05	7	0.06	0.02	0.04	0.09
	H04	17	0.02	0.01	0.01	0.04	7	0.05	0.02	0.03	0.08
	H05	17	0.01	0.01	0.01	0.03	7	0.05	0.02	0.03	0.08
	H06	17	0.02	0.01	0.01	0.05	7	0.06	0.02	0.03	0.10
	H07	17	0.04	0.02	0.01	0.09	7	0.11	0.05	0.06	0.20
	H08	17	0.06	0.03	0.02	0.13	7	0.16	0.07	0.10	0.30
	H09	17	0.07	0.03	0.02	0.15	7	0.17	0.07	0.10	0.32
	H10	17	0.06	0.03	0.02	0.14	7	0.16	0.06	0.09	0.28
	H11	17	0.06	0.03	0.02	0.14	7	0.16	0.06	0.10	0.27
	H12	17	0.06	0.03	0.02	0.14	7	0.16	0.06	0.09	0.26
	H13	17	0.06	0.03	0.02	0.13	7	0.15	0.05	0.10	0.24
	H14	17	0.06	0.03	0.02	0.15	7	0.17	0.05	0.11	0.27
	H15	17	0.06	0.03	0.03	0.16	7	0.17	0.06	0.10	0.28
	H16	17	0.07	0.04	0.02	0.15	7	0.17	0.05	0.10	0.27
	H17	17	0.06	0.04	0.02	0.16	7	0.17	0.06	0.10	0.27
	H18	17	0.07	0.04	0.03	0.16	7	0.18	0.06	0.10	0.28
	H19	17	0.07	0.04	0.03	0.16	7	0.19	0.06	0.11	0.29
	H20	17	0.06	0.04	0.02	0.15	7	0.17	0.06	0.11	0.27
	H21	17	0.05	0.03	0.02	0.13	7	0.15	0.05	0.09	0.25
	H22	17	0.05	0.03	0.02	0.13	7	0.15	0.05	0.09	0.24
	H23	17	0.05	0.03	0.02	0.11	7	0.14	0.05	0.09	0.22
	H24	17	0.04	0.02	0.02	0.10	7	0.12	0.04	0.08	0.20
Summer	H01	17	0.02	0.01	0.01	0.04	7	0.15	0.06	0.09	0.25
	H02	17	0.01	0.01	0.00	0.03	7	0.12	0.04	0.07	0.18
	H03	17	0.01	0.01	0.00	0.02	7	0.10	0.04	0.06	0.15
	H04	17	0.01	0.01	0.00	0.02	7	0.08	0.03	0.05	0.13
	H05	17	0.01	0.00	0.00	0.02	7	0.08	0.04	0.05	0.14
	H06	17	0.01	0.01	0.00	0.02	7	0.10	0.04	0.06	0.18
	H07	17	0.02	0.01	0.01	0.04	7	0.19	0.08	0.11	0.34
	H08	17	0.03	0.02	0.01	0.08	7	0.28	0.13	0.17	0.54
	H09	17	0.04	0.02	0.01	0.09	7	0.30	0.14	0.18	0.57
	H10	17	0.04	0.02	0.01	0.08	7	0.29	0.13	0.17	0.53
	H11	17	0.04	0.02	0.01	0.09	7	0.30	0.12	0.17	0.50
	H12	17	0.04	0.02	0.01	0.09	7	0.30	0.11	0.18	0.48
	H13	17	0.04	0.02	0.01	0.09	7	0.28	0.10	0.17	0.43
	H14	17	0.04	0.02	0.01	0.09	7	0.30	0.10	0.18	0.45
	H15	17	0.04	0.02	0.01	0.09	7	0.30	0.10	0.19	0.43
	H16	17	0.04	0.02	0.01	0.09	7	0.30	0.09	0.19	0.43
	H17	17	0.04	0.02	0.01	0.10	7	0.30	0.10	0.17	0.45
	H18	17	0.04	0.02	0.01	0.10	7	0.30	0.10	0.17	0.44
	H19	17	0.04	0.02	0.01	0.09	7	0.30	0.10	0.17	0.43
	H20	17	0.03	0.02	0.01	0.09	7	0.28	0.09	0.16	0.41
	H21	17	0.03	0.02	0.01	0.07	7	0.25	0.09	0.14	0.40
	H22	17	0.03	0.02	0.01	0.07	7	0.24	0.09	0.14	0.38
	H23	17	0.03	0.02	0.01	0.07	7	0.22	0.08	0.12	0.35
	H24	17	0.02	0.01	0.01	0.05	7	0.19	0.07	0.11	0.32

Continued

Continued Table K.10

Variable	Model	Background WVKT Elasticities					Roadside WVKT Elasticities				
		N	Mean	Std.	Min	Max	N	Mean	Std.	Min	Max
Autumn	H01	17	0.03	0.02	0.01	0.06	7	0.12	0.04	0.08	0.19
	H02	17	0.02	0.01	0.01	0.05	7	0.10	0.03	0.06	0.14
	H03	17	0.02	0.01	0.01	0.04	7	0.08	0.02	0.05	0.11
	H04	17	0.01	0.01	0.00	0.03	7	0.06	0.02	0.04	0.10
	H05	17	0.01	0.01	0.00	0.03	7	0.07	0.02	0.04	0.10
	H06	17	0.02	0.01	0.01	0.04	7	0.09	0.03	0.05	0.14
	H07	17	0.04	0.02	0.01	0.09	7	0.17	0.06	0.10	0.27
	H08	17	0.06	0.03	0.02	0.13	7	0.24	0.09	0.14	0.39
	H09	17	0.06	0.04	0.02	0.15	7	0.24	0.10	0.14	0.42
	H10	17	0.06	0.03	0.02	0.15	7	0.23	0.09	0.12	0.38
	H11	17	0.06	0.04	0.02	0.15	7	0.22	0.08	0.12	0.36
	H12	17	0.06	0.04	0.02	0.15	7	0.24	0.09	0.12	0.39
	H13	17	0.06	0.03	0.02	0.14	7	0.24	0.08	0.14	0.37
	H14	17	0.07	0.04	0.02	0.15	7	0.26	0.09	0.16	0.40
	H15	17	0.07	0.04	0.03	0.16	7	0.27	0.09	0.16	0.40
	H16	17	0.07	0.04	0.03	0.16	7	0.26	0.08	0.15	0.38
	H17	17	0.07	0.04	0.02	0.17	7	0.25	0.08	0.15	0.36
	H18	17	0.06	0.04	0.02	0.17	7	0.25	0.08	0.15	0.36
	H19	17	0.06	0.04	0.02	0.17	7	0.24	0.07	0.15	0.35
	H20	17	0.05	0.03	0.02	0.15	7	0.22	0.07	0.13	0.33
	H21	17	0.05	0.03	0.01	0.13	7	0.19	0.06	0.12	0.29
	H22	17	0.04	0.03	0.02	0.12	7	0.18	0.06	0.12	0.29
	H23	17	0.04	0.03	0.01	0.10	7	0.17	0.06	0.11	0.27
	H24	17	0.04	0.02	0.01	0.09	7	0.15	0.05	0.10	0.24
Winter	H01	17	0.05	0.03	0.02	0.12	7	0.14	0.04	0.08	0.20
	H02	17	0.03	0.02	0.01	0.09	7	0.10	0.03	0.06	0.15
	H03	17	0.03	0.02	0.01	0.07	7	0.08	0.02	0.05	0.12
	H04	17	0.02	0.01	0.01	0.05	7	0.07	0.02	0.04	0.10
	H05	17	0.02	0.01	0.01	0.05	7	0.06	0.02	0.04	0.10
	H06	17	0.03	0.02	0.01	0.07	7	0.08	0.03	0.05	0.13
	H07	17	0.05	0.03	0.02	0.14	7	0.16	0.05	0.09	0.24
	H08	17	0.08	0.05	0.03	0.21	7	0.22	0.07	0.13	0.34
	H09	17	0.08	0.05	0.03	0.21	7	0.22	0.07	0.13	0.34
	H10	17	0.07	0.04	0.03	0.18	7	0.20	0.06	0.11	0.30
	H11	17	0.07	0.04	0.03	0.17	7	0.19	0.06	0.10	0.29
	H12	17	0.07	0.04	0.03	0.17	7	0.19	0.06	0.11	0.28
	H13	17	0.07	0.03	0.03	0.15	7	0.19	0.05	0.12	0.27
	H14	17	0.07	0.04	0.03	0.16	7	0.20	0.06	0.12	0.29
	H15	17	0.07	0.04	0.03	0.17	7	0.21	0.07	0.13	0.31
	H16	17	0.07	0.04	0.03	0.17	7	0.21	0.07	0.13	0.31
	H17	17	0.07	0.04	0.03	0.18	7	0.21	0.06	0.14	0.31
	H18	17	0.08	0.04	0.03	0.19	7	0.22	0.06	0.14	0.31
	H19	17	0.08	0.05	0.03	0.20	7	0.23	0.07	0.14	0.33
	H20	17	0.08	0.04	0.03	0.19	7	0.21	0.07	0.13	0.32
	H21	17	0.07	0.04	0.03	0.17	7	0.20	0.06	0.12	0.29
	H22	17	0.07	0.04	0.02	0.17	7	0.19	0.06	0.11	0.28
	H23	17	0.06	0.04	0.02	0.16	7	0.18	0.05	0.11	0.27
	H24	17	0.06	0.03	0.02	0.14	7	0.16	0.05	0.09	0.24

Table K.11 Hourly elasticities w.r.t. solar radiation in the PM10 panel models

Variable	Model	Background Solar Elasticities					Roadside Solar Elasticities				
		N	Mean	Std.	Min	Max	N	Mean	Std.	Min	Max
Spring	H01	17	0.00	0.00	0.00	0.00	7	0.00	0.00	0.00	0.00
	H02	17	0.00	0.00	0.00	0.00	7	0.00	0.00	0.00	0.00
	H03	17	0.00	0.00	0.00	0.00	7	0.00	0.00	0.00	0.00
	H04	17	0.00	0.00	0.00	0.00	7	0.00	0.00	0.00	0.00
	H05	17	0.00	0.00	0.00	0.00	7	0.00	0.00	0.00	0.00
	H06	17	0.00	0.00	0.00	0.00	7	0.00	0.00	0.00	0.00
	H07	17	0.00	0.00	0.00	0.00	7	0.00	0.00	0.00	0.00
	H08	17	-0.01	0.00	-0.02	-0.01	7	-0.01	0.00	-0.01	-0.01
	H09	17	-0.04	0.01	-0.05	-0.03	7	-0.03	0.01	-0.04	-0.03
	H10	17	-0.08	0.01	-0.11	-0.06	7	-0.06	0.01	-0.08	-0.05
	H11	17	-0.13	0.02	-0.19	-0.10	7	-0.11	0.02	-0.13	-0.09
	H12	17	-0.19	0.03	-0.25	-0.16	7	-0.16	0.02	-0.19	-0.13
	H13	17	-0.26	0.04	-0.31	-0.20	7	-0.22	0.04	-0.29	-0.17
	H14	17	-0.32	0.04	-0.37	-0.24	7	-0.27	0.06	-0.39	-0.23
	H15	17	-0.34	0.05	-0.40	-0.26	7	-0.29	0.07	-0.43	-0.24
	H16	17	-0.34	0.05	-0.42	-0.26	7	-0.28	0.07	-0.43	-0.23
	H17	17	-0.30	0.04	-0.38	-0.23	7	-0.26	0.06	-0.38	-0.20
	H18	17	-0.25	0.03	-0.31	-0.19	7	-0.22	0.05	-0.33	-0.18
	H19	17	-0.19	0.03	-0.24	-0.14	7	-0.17	0.04	-0.25	-0.15
	H20	17	-0.13	0.02	-0.18	-0.10	7	-0.12	0.02	-0.16	-0.10
	H21	17	-0.08	0.01	-0.11	-0.06	7	-0.07	0.01	-0.09	-0.06
	H22	17	-0.04	0.01	-0.06	-0.03	7	-0.04	0.01	-0.05	-0.03
	H23	17	-0.02	0.00	-0.02	-0.01	7	-0.02	0.00	-0.02	-0.01
	H24	17	0.00	0.00	-0.01	0.00	7	0.00	0.00	0.00	0.00
Summer	H01	17	0.00	0.00	0.00	0.00	7	0.00	0.00	0.00	0.00
	H02	17	0.00	0.00	0.00	0.00	7	0.00	0.00	0.00	0.00
	H03	17	0.00	0.00	0.00	0.00	7	0.00	0.00	0.00	0.00
	H04	17	0.00	0.00	0.00	0.00	7	0.00	0.00	0.00	0.00
	H05	17	0.00	0.00	0.00	0.00	7	0.00	0.00	0.00	0.00
	H06	17	0.00	0.00	0.00	0.00	7	0.00	0.00	0.00	0.00
	H07	17	-0.01	0.00	-0.01	-0.01	7	-0.01	0.00	-0.01	0.00
	H08	17	-0.02	0.00	-0.02	-0.01	7	-0.01	0.00	-0.02	-0.01
	H09	17	-0.04	0.01	-0.05	-0.03	7	-0.02	0.00	-0.03	-0.02
	H10	17	-0.07	0.01	-0.09	-0.05	7	-0.04	0.01	-0.05	-0.03
	H11	17	-0.10	0.02	-0.13	-0.08	7	-0.07	0.01	-0.08	-0.06
	H12	17	-0.14	0.03	-0.20	-0.11	7	-0.09	0.01	-0.11	-0.07
	H13	17	-0.19	0.03	-0.25	-0.14	7	-0.12	0.01	-0.14	-0.11
	H14	17	-0.22	0.03	-0.27	-0.17	7	-0.14	0.02	-0.19	-0.12
	H15	17	-0.23	0.03	-0.29	-0.18	7	-0.15	0.03	-0.20	-0.13
	H16	17	-0.23	0.03	-0.28	-0.17	7	-0.15	0.03	-0.20	-0.13
	H17	17	-0.20	0.03	-0.24	-0.16	7	-0.14	0.03	-0.19	-0.12
	H18	17	-0.17	0.02	-0.21	-0.14	7	-0.12	0.02	-0.16	-0.10
	H19	17	-0.13	0.02	-0.16	-0.11	7	-0.09	0.02	-0.14	-0.08
	H20	17	-0.09	0.01	-0.12	-0.07	7	-0.07	0.02	-0.10	-0.06
	H21	17	-0.06	0.01	-0.08	-0.05	7	-0.05	0.01	-0.07	-0.04
	H22	17	-0.04	0.01	-0.05	-0.03	7	-0.03	0.00	-0.04	-0.02
	H23	17	-0.02	0.00	-0.02	-0.01	7	-0.01	0.00	-0.02	-0.01
	H24	17	-0.01	0.00	-0.01	0.00	7	0.00	0.00	-0.01	0.00

Continued

Continued Table K.11

Variable	Model	Background Solar Elasticities					Roadside Solar Elasticities				
		N	Mean	Std.	Min	Max	N	Mean	Std.	Min	Max
Autumn	H01	17	0.00	0.00	0.00	0.00	7	0.00	0.00	0.00	0.00
	H02	17	0.00	0.00	0.00	0.00	7	0.00	0.00	0.00	0.00
	H03	17	0.00	0.00	0.00	0.00	7	0.00	0.00	0.00	0.00
	H04	17	0.00	0.00	0.00	0.00	7	0.00	0.00	0.00	0.00
	H05	17	0.00	0.00	0.00	0.00	7	0.00	0.00	0.00	0.00
	H06	17	0.00	0.00	0.00	0.00	7	0.00	0.00	0.00	0.00
	H07	17	0.00	0.00	0.00	0.00	7	0.00	0.00	0.00	0.00
	H08	17	-0.01	0.00	-0.01	-0.01	7	-0.01	0.00	-0.01	-0.01
	H09	17	-0.04	0.01	-0.05	-0.03	7	-0.03	0.00	-0.03	-0.03
	H10	17	-0.10	0.02	-0.12	-0.08	7	-0.08	0.01	-0.09	-0.06
	H11	17	-0.20	0.03	-0.24	-0.16	7	-0.15	0.01	-0.16	-0.12
	H12	17	-0.33	0.06	-0.41	-0.25	7	-0.24	0.03	-0.30	-0.20
	H13	17	-0.48	0.09	-0.62	-0.33	7	-0.35	0.04	-0.42	-0.30
	H14	17	-0.61	0.11	-0.80	-0.43	7	-0.45	0.05	-0.55	-0.41
	H15	17	-0.67	0.12	-0.87	-0.48	7	-0.50	0.05	-0.58	-0.45
	H16	17	-0.64	0.11	-0.82	-0.46	7	-0.47	0.06	-0.57	-0.41
	H17	17	-0.52	0.07	-0.64	-0.40	7	-0.39	0.04	-0.46	-0.34
	H18	17	-0.37	0.05	-0.44	-0.31	7	-0.30	0.04	-0.36	-0.26
	H19	17	-0.24	0.03	-0.28	-0.19	7	-0.21	0.03	-0.26	-0.17
	H20	17	-0.14	0.02	-0.17	-0.11	7	-0.12	0.02	-0.15	-0.11
	H21	17	-0.07	0.01	-0.08	-0.06	7	-0.06	0.01	-0.07	-0.05
	H22	17	-0.03	0.00	-0.03	-0.02	7	-0.02	0.00	-0.03	-0.02
	H23	17	-0.01	0.00	-0.01	-0.01	7	-0.01	0.00	-0.01	-0.01
	H24	17	0.00	0.00	0.00	0.00	7	0.00	0.00	0.00	0.00
Winter	H01	17	0.00	0.00	0.00	0.00	7	0.00	0.00	0.00	0.00
	H02	17	0.00	0.00	0.00	0.00	7	0.00	0.00	0.00	0.00
	H03	17	0.00	0.00	0.00	0.00	7	0.00	0.00	0.00	0.00
	H04	17	0.00	0.00	0.00	0.00	7	0.00	0.00	0.00	0.00
	H05	17	0.00	0.00	0.00	0.00	7	0.00	0.00	0.00	0.00
	H06	17	0.00	0.00	0.00	0.00	7	0.00	0.00	0.00	0.00
	H07	17	0.00	0.00	0.00	0.00	7	0.00	0.00	0.00	0.00
	H08	17	0.00	0.00	0.00	0.00	7	0.00	0.00	0.00	0.00
	H09	17	0.00	0.00	0.00	0.00	7	0.00	0.00	0.00	0.00
	H10	17	-0.01	0.00	-0.01	-0.01	7	-0.01	0.00	-0.01	0.00
	H11	17	-0.02	0.00	-0.02	-0.01	7	-0.01	0.00	-0.01	-0.01
	H12	17	-0.03	0.00	-0.04	-0.02	7	-0.02	0.00	-0.03	-0.02
	H13	17	-0.04	0.01	-0.06	-0.03	7	-0.03	0.01	-0.04	-0.03
	H14	17	-0.06	0.01	-0.07	-0.04	7	-0.04	0.00	-0.05	-0.04
	H15	17	-0.07	0.01	-0.08	-0.05	7	-0.05	0.01	-0.06	-0.05
	H16	17	-0.07	0.01	-0.08	-0.05	7	-0.05	0.01	-0.06	-0.05
	H17	17	-0.06	0.01	-0.07	-0.05	7	-0.05	0.01	-0.06	-0.04
	H18	17	-0.05	0.01	-0.05	-0.04	7	-0.04	0.01	-0.05	-0.03
	H19	17	-0.03	0.00	-0.04	-0.02	7	-0.03	0.00	-0.03	-0.02
	H20	17	-0.02	0.00	-0.02	-0.01	7	-0.02	0.00	-0.02	-0.01
	H21	17	-0.01	0.00	-0.01	-0.01	7	-0.01	0.00	-0.01	-0.01
	H22	17	0.00	0.00	0.00	0.00	7	0.00	0.00	0.00	0.00
	H23	17	0.00	0.00	0.00	0.00	7	0.00	0.00	0.00	0.00
	H24	17	0.00	0.00	0.00	0.00	7	0.00	0.00	0.00	0.00

Appendix L. Specifications of the Total R^2 and the Regression R^2 in Autoregressive Time-series Models

Let the first-order autoregressive error model as follows:

$$Y_t = a + bX_t + v_t \quad (1)$$

$$v_t = \rho v_{t-1} + \varepsilon_t \quad (2)$$

These two equations are estimated simultaneously and the total R^2 is calculated with:

$$R^2_{tot} = 1 - \frac{SSE}{SST} \quad (3)$$

where,

$SST = \sum(Y_t - Y_m)^2$, Y_m is the mean of Y,

$SSE = \sum(\varepsilon_t)^2$.

Once ρ is estimated, Eq. (1) can be transformed as:

$$Y_t^* = a(1-\rho) + bX_t^* + \varepsilon_t \quad (4)$$

where,

$Y_t^* = Y_t - \rho Y_{t-1}$,

$X_t^* = X_t - \rho X_{t-1}$.

$$R^2_{reg} = 1 - \frac{TSSE}{TSST} \quad (5)$$

where,

TSST is the total sum of squares of the transformed response variable corrected for the transformed intercept,

TSSE is the error sum of squares for this transformed regression problem.